BOOK OF ABSTRACTS

of the Second International Conference on the Application of Physical Modelling to Port and Coastal Protection (CoastLab08)

Bari, Italy, July 2-52008

edited by
Leonardo Damiani and Michele Mossa

Nuova Bios

ISBN: 978-88-6093-046-0

Via A. Rendano, 25 – 87040 Castrolibero (CS)
Casella postale 449 – Tel. 0984 854149 – Fax 0984 854038
www.edibios.it – e-mail: info@edibios.it

Coastlab08

Second International Conference
on the Application of Physical Modelling to Port and Coastal Protection

Organizing Committee

L. Damiani
P. Aminti
M. Calabrese
L. Das Neves
P. De Girolamo
E. Foti
L. Franco
C. George
G. Iglesias
A. Mancinelli
M. Mossa
E. Pugliese Carratelli
L. Rabaudengo Landò
P. Ruol
F. Taveira Pinto
G.R. Tomasicchio
P. Troch
F. Veloso Gomes
P. Veltri

Scientific Advisory Committee

A.F. Petrillo
E. Benassai
P. Boccotti
T. Darlymple
P. Davies
P.L. - F Liu
G. Frega
J. Gruene
N. Kobayashi
G. Matteotti
A. Noli
P. Prinos
A. Sanchez Arcillia
G. Scarsi
C.E. Synolakis
F. Veloso Gomes

CONTENTS

RECENT ADVANCEMENT IN NUMERICAL MODELING OF OCEAN WAVE PROPAGATION

Philip L-F. LIU

Professor, School of Civil and Environmental Engineering, Cornell University, Ithaca, NY, 14853, USA. E-mail: pll3@cornell.edu

Abstract

In recent years significant advancement has been made in developing theories and numerical methods modelling ocean wave propagation from open coast, wave-structure interactions and sediment transport processes in coastal region. In this paper we shall only focus on some of the work that has been achieved at Cornell University.

1. Depth-Integrated wave propagation models

Since early 1970's Boussinesq equations have been used to model wave propagation in an open coast from fairly shallow water to very shallow water. The Boussinesq equations were originally derived for weakly nonlinear and weakly dispersive waves with the specific assumption that $O(a/h) \approx O(2\pi h/l)^2 \ll O(1)$ where a is the characteristic wave amplitude, h the water depth and l the wavelength. It has been shown that the accuracy of the traditional Boussinesq equation models diminishes when $O(2\pi h/l) > 1.0$. Furthermore, as the water depth decreases wave amplitude increases and so does the nonlinearity parameter a/h. Therefore, the traditional Boussinesq equation models, strictly speaking, can only be applied in a relative small region in coastal zones.

In the last fifteen years much of the development in Boussinesq-type modelling has been focused on extending the applicability of the depth-integrated wave equations into deeper water (or shorter waves). Many successful models have been developed, which extended the applicability of these models to relatively deep water. Fully nonlinear models have also been developed. For example, Lynett and Liu (2004) introduced a multi-layer Boussinesq-type wave model, in which the water column is divided into several layers and the Boussinesq approximation is employed. Within each layer the horizontal velocity is assumed to be a quadratic polynomial and the matching conditions are required along the interface of two adjacent layers. Invoking the conservation of mass and momentum in each layer yields a set of model equations in which the highest order of derivatives remains three. Lynett and Liu (2004) showed that the limits of application are $2\pi h/l \approx 8$, 17, 30 for 2, 3, and 4 layer model, respectively.

In this paper we shall discuss different approaches for improving the properties of frequency dispersion and shoaling of Boussinesq-type wave models such that these models can be used in very deeper water depth. Moreover, in these approaches the order of derivatives in the depth-Integrated wave equations as low as possible to avoid difficulties in specifying boundary conditions. We will show that some of these models can be applied to water as deep as $2\pi h/l \approx 8$.

2. 2D and 3D free surface Navier-Stokes equations models

In the surf zone, wave breaking is a dominating feature and is a driving force for many dynamic processes, such as coastal currents and sediment transport. However, it is a non-trivial task to model wave breaking because of the complex mechanisms involved in turbulence generation and the fragmentation of free surface. In the existing models (e.g., Lin and Liu 1998) most commonly adopted approach is to solve the Reynolds Averaged Navier-Stokes (RANS) equations with a coupled turbulent closure model, such as the $k\varepsilon-$model. The Large Eddy Simulation (LES) method has also been developed. In both methods severe concerns on the treatment of free surface and the associated boundary

conditions on turbulence remain unresolved.

In this paper we discuss a newly developed free surface tracking method: polygonal area mapping (PAM) method (Zhang and Liu 2008). We will demonstrate that PAM method is non-diffusive and is much accurate than the Volume of Fluid (VOF) method. The PAM method has been coupled to a two-step projection method to form a hybrid continuum-particle model for two-dimensional incompressible two-phase free surface flows. Additional algorism is developed to deal with free surface fragmentation. Physical problems such as the droplet impacts and dam-break waves will be used to illustrate the new model.

3. Two-phase flow modelling of sediment transport

Granular sediment transport mechanisms include saltation, collisional suspension, turbulent suspension, and advection. To understand these processes under periodic waves, Hsu, Jenkins and Liu (2004) adopted a sediment transport model based on the two-phase equations for mass, momentum, and energy, formulated these equations for a turbulent flow, and proposed closures to the higher correlations. To account for the fluid flow turbulence at high Reynolds numbers, the Favre-averaging was applied to these equations. A two-equation turbulence model for the fluid-phase and proposed closures for the fluid-fluid and fluid-particle correlations associated with the Favre averaging was derived. The exchange of momentum and energy between particles was assumed to result from collisions, a balance equation that included contributions from fluid-particle interactions was introduced for the particle fluctuation energy, and the lower part of the bed load was modeled as a very viscous fluid moving above a stationary bed whose location was determined by a yield condition. Because of the periodicity in both time and horizontal direction, the model is essentially one-dimensional.

In this paper we will discuss the extension of the one-dimensional model to two dimensions. The resulting models can be used to investigate two-dimensional scouring problems.

Acknowledgment

The research presented here has been supported by National Science Foundation, Office of Navy Research and Sea Grant program through grants and projects to Cornell University.

References

Hsu, T-J., Jenkins, J.T. and Liu, P. L.-F. (2004) “Two-phase sediment transport: Sheet flow of massive particles.” *Proc. Roy. Soc. London,* A, 460: 2223-2250.

Lin, P. and Liu, P. L.-F. (1998) “A numerical study of breaking waves in the surf zone.” *J. Fluid Mech.*, 359: 239-264.

Lynett, P. J. and Liu, P. L.-F. (2004) “A two-layer approach to wave modeling.” *Proc. Roy. Soc. London,* A, 460: 2637-2669.

Zhang, Q. and Liu, P. L.-F. (2008) “A new interface tracking method: the polygonal area mapping method.” *J. Computational Physics*, 227, 4063-4088.

MOBILE-BED HYDRAULIC TESTS. THE SANDS PROJECT WITHIN HYDRALAB-III

Agustin SANCHEZ-ARCILLA [(1)] & Ivan CACERES [(2)]

[(1)] *Prof., Maritime Eng. Lab (LIM/UPC), Universitat Politècnica de Catalunya, Jordi Girona, 1-3, D1, 08034 Barcelona, Spain. agustin.arcilla@upc.edu*

[(2)] *Dr., ., Maritime Eng. Lab (LIM/UPC), Universitat Politècnica de Catalunya, Jordi Girona, 1-3, D1, 08034 Barcelona, Spain. i.caceres@upc.edu*

Abstract

Mobile bed testing still presents a number of important uncertainties. They refer to 1) scaling, 2) flume performance, 3) sediment dynamics, 4) instrument limitations and 5) processing and interpretation.

Basic questions such as the sediment scaling, the predominance of bed or suspended load or even the definition of the actual sea-bed level remain an open scientific question. And yet mobile bed experiments must be used in many research and consultancy projects where numerical models or state of art formulations present errors which may exceed one order of magnitude.

This paper will address mobile bed modelling in a critical manner based on the results of the ongoing European Union research project Hydralab-SANDS. The SANDS project (Scaling and Analysis and New instrumentation for Dynamic bed TestS) analyses the full sequence of steps involved in hydraulic modelling with a mobile bed. It covers from the design stage to the result analysis and interpretation. The emphasis is on i) the compatibility and repeatability of experiments and ii) the observation potential offered by the new developments in optic and acoustic technologies.

SANDS includes the execution of 3 carefully designed series of experiments in the Hannover (GWK), Barcelona (CIEM UPC) and Delft flumes (figure 1). It also deals with novel optical techniques for bed mapping, swash zone fluxes and high resolution and accuracy particle tracking methods (figure 2).

Finally SANDS also includes the development of a new acoustic probe (figure 3) which is able to provide measurements of water/sediment fluxes, sediment characteristics and sea-bed levels.

This combination of elements, supported by conventional advanced observational equipment (ADVs, ABSs, ECMs, etc.) is expected to provide a scientific breakthrough in mobile bed modelling. The paper will end with some preliminary conclusions and remarks since the SANDS project is still very much ongoing.

Partner	Scale	d50 (µm)	Hm0 (m)	h0 (m)	bed level
Hannover	1	300	1	3.2	1.0
Barcelona	1.9	246	0.53	1.76	0.7
Delft	6	130	0.167	0.5	0.2

Figure 1. The three flumes involved in the SANDS intercomparison experiments.

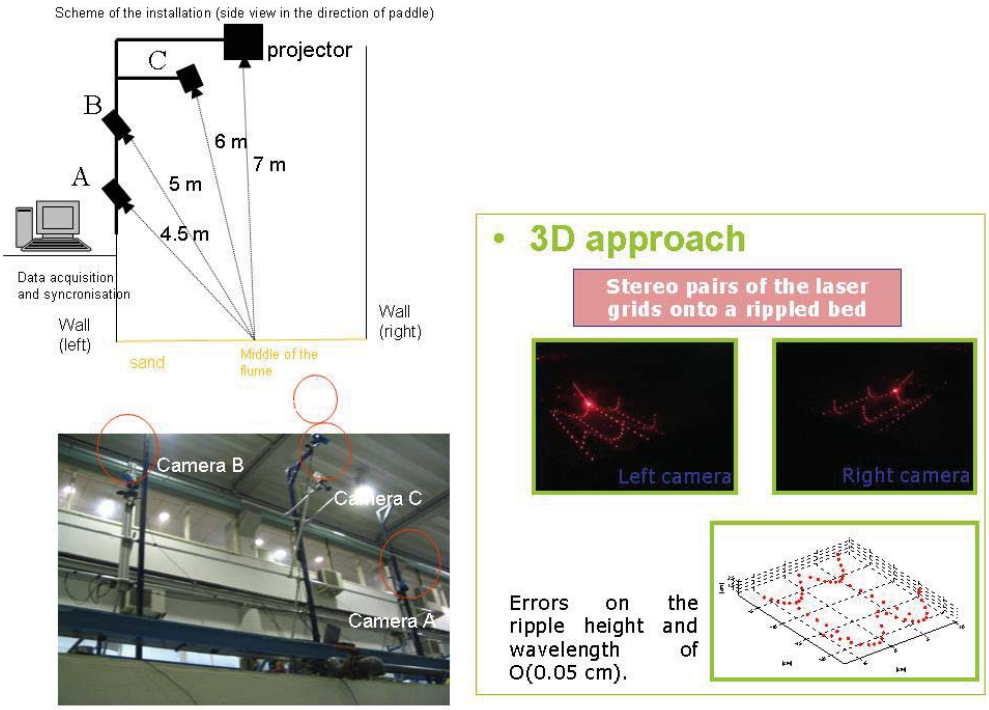

Figure 2. Illustration of the optical techniques used for bed-mapping and swash-zone fluxes in SANDS.

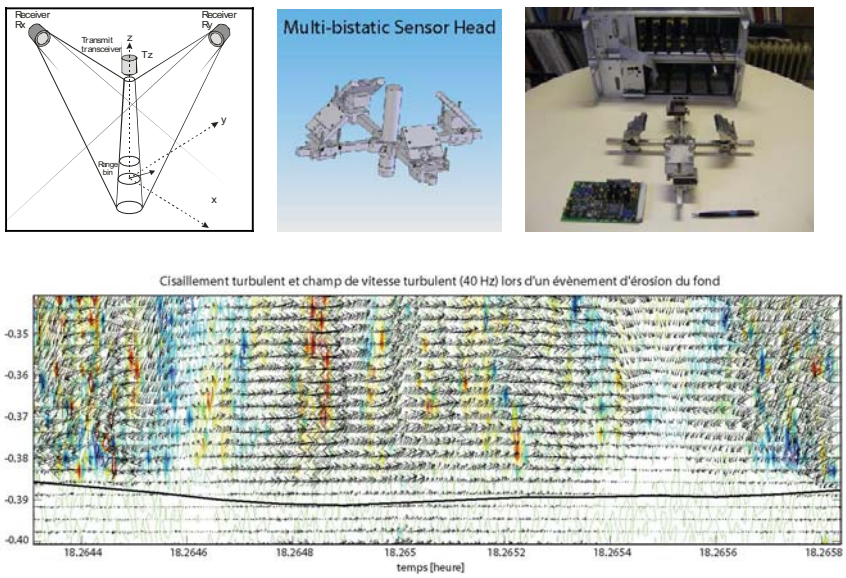

Figure 3. Illustration of the new acoustic equipment developed within SANDS.

2D AND 3D EXPERIMENTAL ANALYSIS ON FORCES AND PERFORMANCE OF FLOATING BREAKWATERS

Piero RUOL [(1)], Luca MARTINELLI [(2)] , Barbara ZANUTTIGH [(2)]

[(1)] *Prof., IMAGE, University of Padova, Via Ognissanti 39, Padova, 35129, piero.ruol@unipd.it*

[(2)] *PhD, DISTART Idraulica, University of Bologna, V.le Risorgimento 2, Bologna, 40136, Italy, luca.martinelli@mail.ing.unibo.it, barbara.zanuttigh@unibo.it*

Abstract

Objective of this contribution is to assess forces and performance of a typical floating breakwater (FB) with particular attention at evaluating the 3D effects on the experimental results. Tests have been carried out at the University of Padova both in the wave flume and in the wave basin on the same FB under irregular wave attacks. 2D and 3D measurements of incident and transmitted waves, mooring and link forces as well as FB motions will be presented and compared where possible. Considerations on measuring techniques will be also drawn.

1. Introduction

FBs are an alternative solution to conventional fixed breakwaters in coastal areas with mild wave conditions. FBs have many advantages compared to the fixed ones, e.g. lower environmental impact, flexibility of future extensions, lower cost and ability of a short time transportation and installation.

Several papers present experimental investigations focussing on the FB performance, which in most case is carried out in wave flumes, among the others Cox and Beach (2007), Koftis and Prinos (2007). The wave basin is used more rarely, apart from specific designs which are too difficult to generalize, such as the Port of Brownsville Marina in Washington State (Allyn et al., 2004). Recently, Ruol and Martinelli (2007) and Martinelli et al. (2007) examined respectively in a wave flume and in a wave basin the load acting on mooring system in case of snapping in presence of simple and complex layouts under irregular waves. These investigations lead to the following questions: are the results obtained by means of 2D tests really representative of prototype conditions? It is at least expected that under perpendicular waves the performance in the basin and in the flume are alike, but is this assumption really verified in practice?

3. Experimental Investigation

Physical model tests were carried out in the 33x1.0x1.4m wave flume and in the 6.0x20.6x0.8 m wave basin of the Maritime Laboratory of the University of Padova.

In the 2D experiments (Fig. 1), the floating elements are about 20m long, 2-3m high, around 4m wide and have typically a core in polystyrene, covered by a thin concrete shield. They have been reproduced in geometrical scales 1:12 (extensive testing) and 1:20 (few tests). Irregular waves were generated using an active wave absorption device. Significant wave heights are in the range 0.4-1.0m (prototype scale), and wave steepness in the range 1%-7%. Four types of moorings were examined: a pair of piles to which the floating body is connected and a system of 4 diverging chains characterized by 3 initial stresses. Measurements were performed using: some wave gauges (4 in front and 3 behind the FB) to assess the incident, transmitted and reflected waves; 4 force transducers (placed along the connections or along the piles) to evaluate the forces; 3 displacement transducers to study the rigid body motions and response.

In the 3D tests (Fig. 2), irregular long-crested waves were generated with heights again in the range 0.4-1.0 m and steepness between 1%-7%. The FB is composed by 3 aligned elements, identical to those used in the flume tests, in scale 1:20.

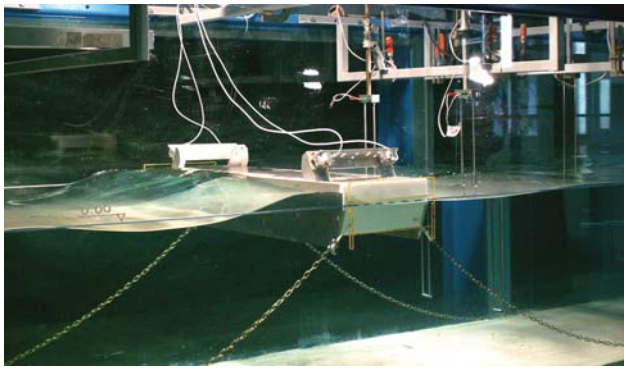

Figure 1. View of the experimental set-up in the wave flume.

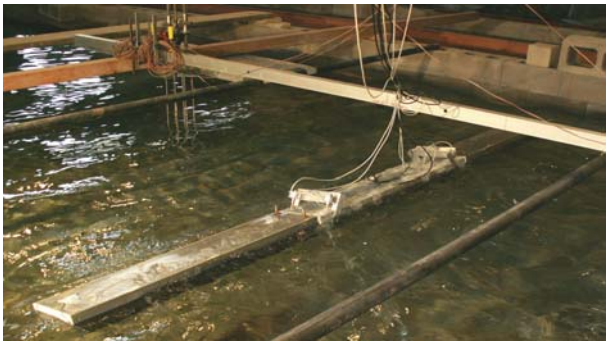

Figure 2. Tests under way in the wave basin.

Incident and transmitted wave conditions were measured using several wave gauges in front and behind the structures. Mooring forces and link forces between modules were assessed by means of suitable load cells.

4. Results

The main result of the experimental investigations is the assessment of wave transmission and structure solicitation in wave flume and in wave basin for the same structure geometry under the same incident wave conditions. Specifically for the 2D case, measurements of the rigid body movements and floating performance for the 4 different mooring systems will be presented.

References

Allyn N., E. Watchorn, W. Jamieson and Y. Gang, 2001. Port of Brownsville Floating Breakwater, *Proc. Ports Conference*.

Cox R. and D. Beach, 2007. Floating breakwater performance – wave transmission and reflection, energy dissipation, motions and restraining forces, *Proc. Coastlab06*, 371-381.

Koftis T. and P. Prinos, 2007. Experimental study on wave overtopping of floating breakwaters, *Proc. Coastlab06*, 351-362.

Martinelli, L, Zanuttigh, B. and P. Ruol, 2007. Effect of layout on floating breakwater performance: results of wave basin experiments, *Proc. Coastal Structures'07*, Venice, in press.

Oliver J.G, Aristaghes P., Cederwall K., Davidson D., De Graaf F., Thackery M. and A. Torum, 1994. Floating Breakwaters-A practical guide for design and construction. PIANC Rep. 13, Belgium.

Ruol P., Martinelli, L. 2007: Wave flume investigation on different mooring systems for floating breakwaters. *Proc. Coastal Structures'07*, Venice, in press.

PHYSICAL MODELLING STUDY OF THE HYDRAULIC EFFICIENCY OF VERTICAL PERFORATED QUAY WALLS

H. GUEDES LOPES [(1)], P. ROSA SANTOS [(2)], F. VELOSO GOMES [(3)], F. TAVEIRA PINTO [(4)] & E. BRÓGUEIRA DIAS [(5)]

[(1)] PhD Candidate, Faculty of Engineering of the University of Porto, Rua Dr. Roberto Frias s/n, Porto, 4200-465, Portugal, hglopes@fe.up.pt

[(2)] PhD Candidate, Faculty of Engineering of the University of Porto, Rua Dr. Roberto Frias s/n, Porto, 4200-465, Portugal, pjrs@fe.up.pt

[(3)] Full Professor, Faculty of Engineering of the University of Porto, Rua Dr. Roberto Frias s/n, Porto, 4200-465, Portugal, vgomes@fe.up.pt

[(4)] Assistant Professor, Faculty of Engineering of the University of Porto, Rua Dr. Roberto Frias s/n, Porto, 4200-465, Portugal, fpinto@fe.up.pt

[(5)] Administrator of the APDL ,APDL –Administration of the Douro and Leixões Harbours, SA ,Av. da Liberdade s/n, Leça da Palmeira, 4451-851, Portugal, brogueira.dias@apdl.pt

Abstract

The new multipurpose terminal, in construction on the inner side of the Leixões south breakwater, Fig. 1, is composed by three new berths. For this terminal a solution based on the use of innovative blocks was chosen, with the aim of reducing the wave reflection. Even thought they have been used on a small fishing harbour, their hydraulic efficiency in terms of wave reflection has never been analysed.
In the paper, the results of the hydraulic efficiency of the quay in terms of wave reflection are going to be presented for the tested configurations.

Figure 1. New multipurpose terminal.

1. The multipurpose terminal

The structural solution in construction will be materialized by pre-made concrete blocks called NOREF (Non Reflection Blocks). These patented blocks allow building a vertical perforated berth, less reflective than traditional continuous quay walls and therefore improving wave conditions on the inner area of the harbour. With this solution, the Port Authority was looking for the less reflective solution in order to offer better navigation, operational and safety conditions.

2. The laboratory tests

In order to study the behaviour of these blocks, and because they have never been tested before, physical modelling tests were performed on the wave tank of the Hydraulics Laboratory of the Faculty of Engineering of the University of Porto. The wave tank is 28,0 m long, 12,0 m wide and 1,2 m in depth.
The tests were made at a 1:30 scale in order to analyse the influence of the wave period (T), the wave height (H), and the wave steepness (H/L) on the hydraulic efficiency to reflection of the blocks. For the tests, two different quay walls lengths were built inside the wave tank, Fig. 2: the first one 2,0 m wide (60,0 m on the prototype); and the other 0,5 m wide (15,0 m on the prototype).

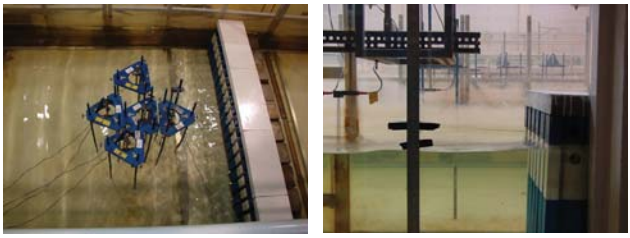

Figure 2. Quay walls lengths used in the physical modelling tests.

The experimental work included two tide levels: 1,9 m (half tide) and 3,8 m (high tide), four significant wave heights (irregular waves): 0,50 m, 0,75 m, 1,0 m, 1,50 m; and four wave periods: 3 s, 4 s, 5 s and 6 s.

3. Results

The results obtained on both channels, for different test conditions, were analysed. As an example, Fig. 3 presents the comparison of the results obtained for the two tested quay walls lengths, for a wave period of 3 s and half tide.

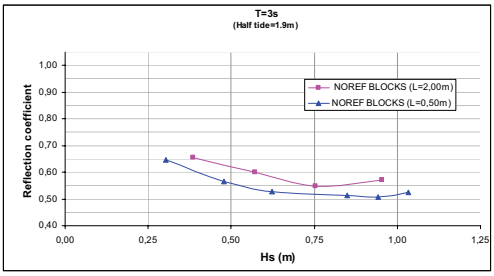

Figure 3. Results obtained for T = 3 s, half tide.

In the paper cross relations between several parameters will be discussed, and global hydraulic efficiency in terms of wave reflection will be presented.

References

Hughes, S.A. (1995). "Physical Models and Laboratory Techniques in Coastal Engineering", Advanced series on Ocean Engineering – Volume 7, World Scientific, Singapore.

IHRH, 2004. Estudo Sobre as Condições de Operacionalidade no Terminal Petroleiro do Porto de Leixões, Relatório de Modelação Física, Volumes 1 a 3, Porto, Portugal. (in Portuguese).

Taveira Pinto, F. (2002). Análise das Oscilações e dos Campos de Velocidade nas Proximidades de Quebramares Submersos, sob a Acção da Agitação Marítima, FEUP. Tese de Doutoramento. (in Portuguese).

EXPERIMENTAL RESULTS OF LOADING CONDITIONS DUE TO VIOLENT WAVE IMPACTS ON COASTAL STRUCTURES WITH CANTILEVER SURFACES

Dogan KISACIK [(1)], Philippe Van BOGAERT [(1)], Peter TROCH [(1)], Joost Van SLYCKEN [(2)], Patricia VERLEYSEN [(2)]

[(1)] *Ghent University, Department of Civil Engineering, Technologiepark 904, Ghent, 9052, Belgium. Dogan.Kisacik@UGent.be, Philippe.VanBogaert@UGent.be, Peter.Troch@UGent.be*

[(2)] *Ghent University, Department of Mechanical construction and production, Sint-Pietersnieuwstraat 41, Ghent, 9000, Belgium. Joost.VanSlycken@UGent.be, Patricia.Verleysen@UGent.be*

Abstract

Port and coastal structures protect land from sea actions like high water levels and waves. Constructions with vertical walls are frequently used both in “coastal engineering” and “offshore engineering” applications. These constructions have to be designed to resist quasi-static loads as well as short but intense violent wave impacts that are distributed in time and space.

Because of sea level rise, rougher sea states and stricter regulations for tolerable wave overtopping, vertical walls would be dimensioned higher and higher. Therefore, coastal engineers provide vertical walls more and more with a return crown wall or even a completely horizontal cantilever slab: this strongly reduces the wave overtopping. Yet, the wave impacts on horizontal decks (or return crown walls) cause an important uplifting force. In the design, these forces cannot be substituted by a static equivalent value. A description of the space and time distribution of the wave impacts is necessary.

The qualitative and quantitative determination of wave loads on vertical walls has already been examined intensively in the past decades (e.g. Oumeraci et al., 2001). Uplift loads below horizontal decks are examined at present in several research projects (e.g. McConnell et al., 2003).

In opposition to a single vertical or horizontal wall, structures consisting of both vertical parapets and horizontall cantilever slabs have scarcely been considered. A consensus on the necessary approach for the research of this type of structures lacks completely (Okamura 1993). Due to the special geometry, involving closed angles, which do not allow incident waves to dissipate, the wave kinematics differ fundamentally from the preceding situations.

Hence, larger wave impact and divergent response of the structures is expected, as it depends heavily on structural stiffness and interaction. The behaviour of cantilever structures above sea level may be regarded as similar to a bridge deck, since the incident loads vary strongly with time and space.

An example structure for wave impacts on a vertical wall with an overhanging horizontal cantilever slab is the Pier of Blankenberge (see fig. 1) located along the Belgian coast. During high tide, the sea flows freely under the building what makes the structure vulnerable for wave impacts. The wave impacts are caused by waves running up against the vertical wall of the extended cylindrical structure, successively slamming against the horizontal slabs. During the winter season of 2002-2003 and 2007-2008 the structure was damaged, due to violent wave impacts as a result of heavy storms. In Cherlet et al. (2006) a description of the field monitoring equipment, installed on the pier for measuring wave loading and structural response has been provided.

Figure 1. The renovated Pier of Blankenberge, Belgium. Picture taken during low tide.

Taking into account the problem description above, the general objective is to bring a new design tool to estimate violent water wave impacts on a vertical wall with an overhanging horizontal cantilever slab, based on the correlation between the kinematics of breaking waves, aeration level due to the breaking and the height, distribution, duration and characteristics of the violent wave impacts. On the other hand, the structural response, the generation and proceeding of wave induced vibrations, comfort conditions for use and the structural safety will be analysed under the defined hydrodynamic conditions. For achieving the above aims, small scale physical model tests are planned. Experimental results will be compared with the prototype measurements of the Blankenberge Pier.

Physical model tests are carried out in the wave flume (30 m x 1 m x 1.2 m) of Ghent University, on a scale of 1/15. The model is located 18m away from the wave paddle on a uniform slope with thickness of 45 cm at the structure. The foreshore slope is 1/10. The scale model is 40 cm in height and the horizontal part is 80 cm in length (see fig. 2). The physical model is instrumented with 10 pressure sensors to register wave impact pressures and related forces both on the vertical and horizontal parts. Free surface profile and aeration level in front of the structure are measured from the high speed camera recordings on a light sheet created with an infrared laser beam. Nine wave gauges have been installed for active wave absorption, wave reflection and breaking wave height near the structure, respectively.

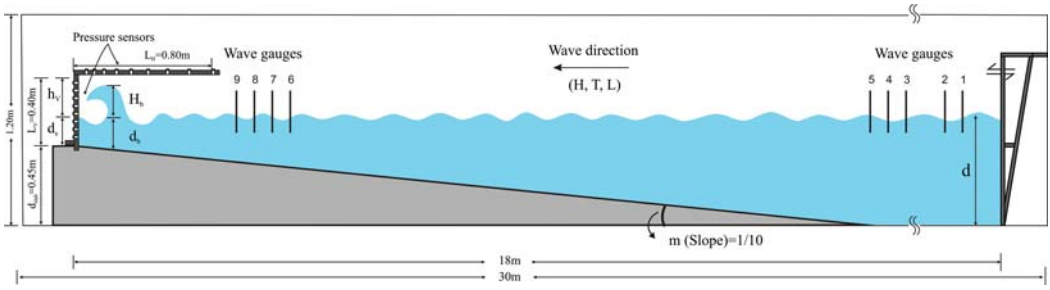

Figure 2. Small-scale model set up.

In the model tests, the wave period, wave height and water depth are considered as variable input parameters. For a range of values of these parameters, physical parameters like peak pressure characteristics (magnitude, duration and rising time), aeration level in front of the structure, reflection coefficient due to the structure, breaking wave height and depth are measured in time and space.

As an example, the pressure record of one sensor located at the water level (d_s=19 cm) is shown in Figure 3 on a time interval which shows several associated impacts, for regular waves with wave period T=1.6 s, incident wave height H=22.3 cm and sampling frequency 20 kHz. The peak pressure of 87 kPa

is the highest recorded pressure for this particular set-up. As it is well known in the literature, the variations in the peak pressure values are high and not repeatable.

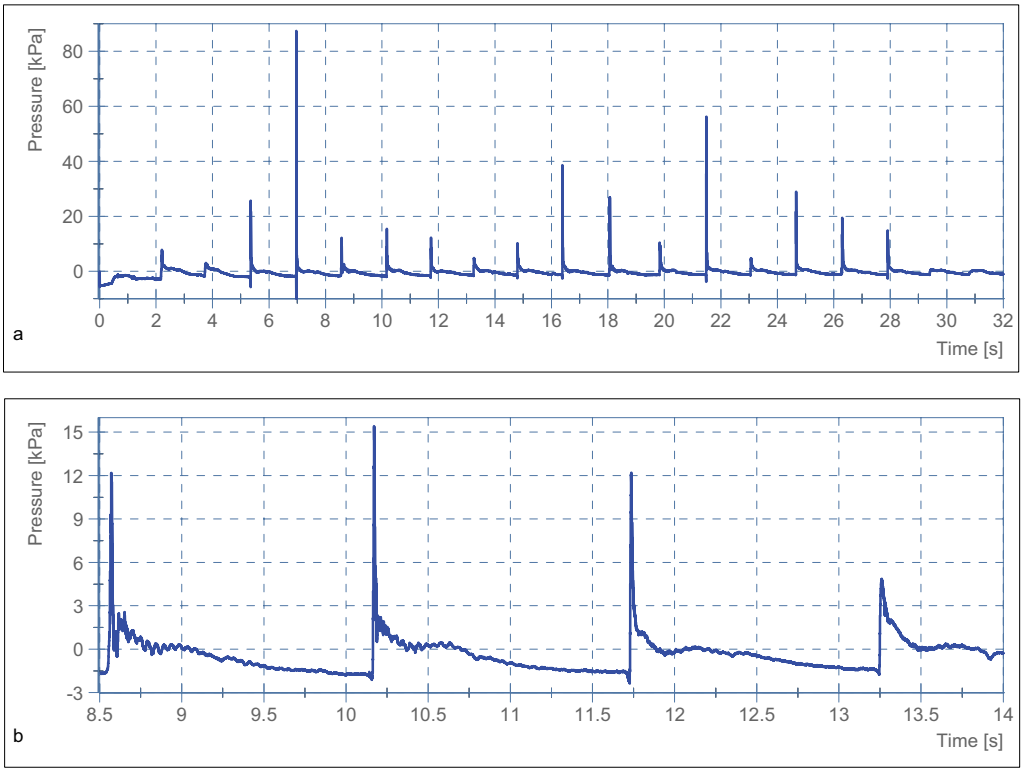

Figure 3. Time series of the pressure record for the pressure sensor located at the water level (d_s=19 cm, H=22.3 cm and T=1.6 s). a) Time window of 32 s, b) detail showing of 4 consecutive impacts.

This paper will describe the set up of the small scale model tests in the wave flume including scaling of the model, installed instruments, data acquisition system and will discuss the analysis and the first results.

Acknowledgments

This study has been supported by the Special Research Fund by Ghent University (BOF). The support of funding for new instruments by Research Foundation-Flanders (FWO) is also gratefully acknowledged.

References

Cherlet, J; Boone, C; Verhaeghe, H; Troch, P; De Rouck, J; Awouters, J; Ockier, M; Devos, G 2006, 'Prototype monitoring of wave loads on concrete structure in intertidal zone', *Book of Abstracts First Int. Conf. on the Application of Physical Modelling to Port and Coastal Protection,* Porto

McConnell, K.J; Allsop, N.W.H; Cuomo, G; and. Cruickshank, I.C, 2003, 'New guidance for wave forces on jetties in exposed locations', *Paper to Conf. COPEDEC VI*, Colombo, Sri Lanka 20 pp

Okamura, M, 1993. 'Impulsive pressure due to wave impact on an inclined plane wall', *Fluid Dynamics Research*, volume 12, issue 4, pp. 215-228.

Oumeraci, H; Kortenhaus, A; Allsop, W; de Groot, M; Crouch, R; Vrijling, H; Voortman, H, 2001, 'Probabilistic Design Tools for Vertical Breakwaters', *Balkema Publishers*, New York.

METHOD FOR IDENTIFYING OF BREAKING WAVE-WALL-CONTACTING MEDIUM

Jordan MARINSKI [(1)], Gergana DROUMEVA [(2)], Rumen MARINOV [(3)]

[(1)] Senior Researcher, Bulgarian Academy of Sciences, Institute of Water Problems, Akad. G. Bonchev St., Bl.1, Sofia 1113, Bulgaria. E-mail: marinski@bas.bg

[(2)] Scientific Researcher, Bulgarian Academy of Sciences, Institute of Water Problems, Akad. G. Bonchev St., Bl.1, Sofia 1113, Bulgaria. E-mail: droumeva@iwp.bas.bg

[(3)] Scientific Researcher, Bulgarian Academy of Sciences, Institute of Water Problems, Akad. G. Bonchev St., Bl.1, Sofia 1113, Bulgaria. E-mail: rummarin@yahoo.com

1. Introduction

The nature of the impact pressures and forces induced by breaking waves upon the wall has been studied in many experimental works, but still there is no generally accepted and comprehensive physical explanation of it (Kamel, 1970; Oumeraci H. et al., 1993; Hull & Müller, 2002; Peregrine, 2003; Bullock et al., 2005). Their generation mechanism could be clarified if direct data are available, showing the wave-wall-contacting medium at pressure peak occurrence. With that end in view experiments have been cried out in the Large Wave Flume (CIEM) at the Maritime Engineering Laboratory (LIM), Research Center of the Catalonia University of Technology (UPC), Barcelona, under quite close to natural conditions: negligible scale effects and at irregular wave regime (Big-VOWS project coordinating by Prof. W. Allsop).

2. Methodology

The kind of medium at the wall boundary at the moment of pressure peak occurrence was precisely identified by means of water sensor tool, Fig. 1.

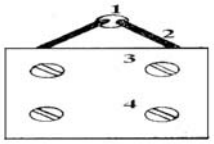

Figure 1. Water sensor

The water sensors were located on the wall, in the immediate vicinity of the pressure transducers, Fig. 2.

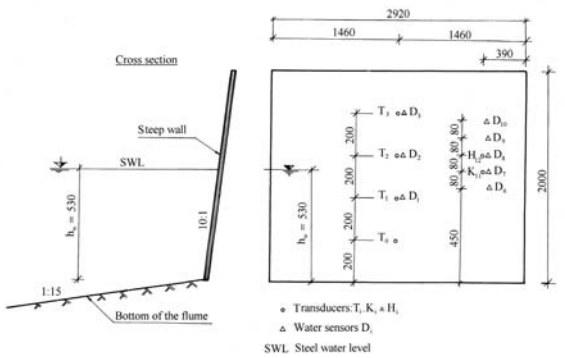

Figure 2. Location of the pressure transducers and water sensors on the steep wall

Thus, when the water particles touched the water sensors, the electric signal was recorded simultaneously with the pressure fluctuations.

The water sensor signals are time-domain signals presented in time/voltage coordinates (Fig. 3). When the water or air-water mixture comes in touch with the wall, the voltage signal is deflected and fixes the start of the contact. An unstable record indicates that air-water mixture gets in touch with the wall, whereas fast deflection suggests a water-wall contact.

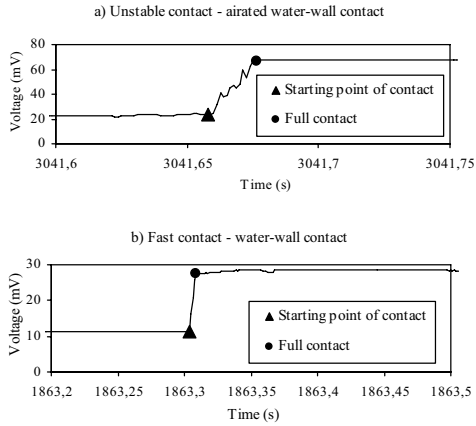

Figure 3. Identification of the wave-wall-contacting medium by water sensor records.

The synchronization between pressure and water sensor records allows identifying the physical medium at the wall boundary in the moment of pressure peak occurrence (Fig. 4).

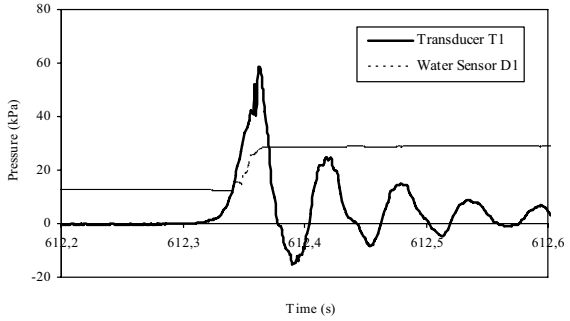

Figure 4. Synchronized records of pressure transducer and water sensor

Almost all impulsive pressure peaks have been recorded at full water-wall contact and only 2% of pressure peaks – before full contact, but after the starting point of contact. No case of impact pressure peaks before the starting point of water-wall contact has been registered and this means that the air compression should not be considered as a unique reason for impulse pressure origin.

5. Conclusion

Studying the kind of wave-wall-contacting medium (liquid, air or air-water mixture) through water sensors, when peaks of maximum pressures occur at wave impacts allows for more solid conclusions to be drawn about their origin and physical nature.

Acknowledgments

The investigations were carried out within the Big-VOWS project Contract № HPRI-CT-1999-0006. The financial support from the Access to Large Scale Facilities Programme (TMR-EU) is gratefully acknowledged.

References

Bullock G., A. Crawford, P. Hewson, M. Walkden, P. Bird, 2001. The influence of air and scale on wave impact pressures, Coastal Engineering, vol. 42, pp. 291- 312.

Bullock G., C. Obhrai, G. Müller, G. Wolters, H. Peregrine, H. Bredmose, 2005. Advances in the understanding of wave impact forces, Proc. ICE Conf.: "Coastlines, Structures and Breakwaters", Thomas Telford, London, pp. 111-120.

Hull P., G. Müller, 2002, Breaker shape and impact pressures, Ocean Engineering, vol. 29, 1, pp. 59-79.

Kamel A., 1970, Shock pressures caused by waves breaking against on coastal structures, Proc. ASCE, Journal of Waterways and Harbor Division, vol. 96, 3, pp. 689-699.

Oumeraci H., P. Klammer, H. Partenscky, 1993. Classification of breaking wave impact loads on vertical structure, Proc. ASCE, Journal of Waterway, Port, Coastal and Ocean Engineering, vol. 119, 4, pp. 381-397.

Peregrine D., 2003. Water-wave impact on walls, Ann. Rev. Fluid Mech., vol. 35, pp. 23-43.

HYDRAULIC CHARACTERISTICS OF VERTICAL PERFORATED SEA WALL

Androcec VLADIMIR[(1)], Carevic DALIBOR[(2)] & Pusic VELIMIR[(3)]

[(1)] *Ph.d. University of Zagreb, Faculty of Civil Engineering, Water Research Department, Savska 16, Zagreb, 10000, Croatia, androcec@grad.hr*

[(2)] *C.E. University of Zagreb, Faculty of Civil Engineering, Water Research Department, Savska 26, Zagreb, 10000, Croatia, car@grad.hr*

[(3)] *Nav.Arch. University of Zagreb, Faculty of Civil Engineering, Water Research Department, Savska 16, Zagreb, 10000, Croatia, pusic@grad.hr*

Keywords: perforated construction, reflection coefficient, wave force, upper board

1. Introduction

Experimental tests of vertical perforated construction were conducted on two models at the scales of 1:25 and 1:40, respectively. On the model at the scale of 1:25, optimum porosity n (%) of perforated wall was tested, which gives the minimum coefficients of reflection. The larger scale model was chosen for testing of reflection characteristics of the construction to avoid the influence of the scale in dissipation effects within the construction chamber. On the same model the pressure at point 7 (Fig. 2.) was also measured, to assess the influence of the model scale on measured pressures, and to assess the influence of porosity of the perforated wall on pressures in the chamber. On the other physical model at the scale of 1:40 (and optimal porosity 32%), pressures were tested at 9 points of the front side of the perforated wall and within the chamber (Fig. 2.). The pressure gauges 7, 8, and 9 are situated on the upper board, within the chamber. The results of measurements of the pressure gauges 1, 5, and 6 are not presented in this paper.

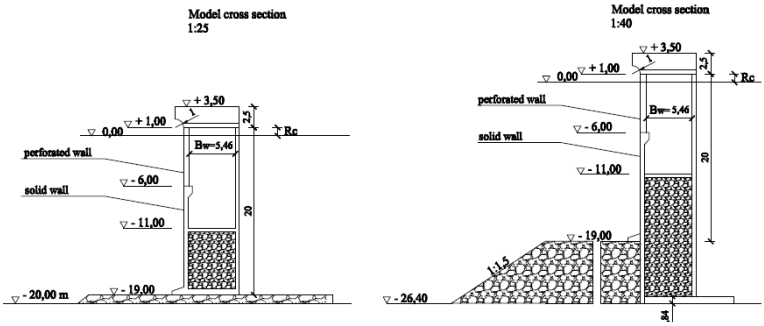

Figure 1. Cross-sections of models of vertical perforated structure

Measurings were done in the canal 1 m wide and 1.5 m deep.The piston-type wave generator (DHI, Denmark) was used to generate regular and irregular wave fields in the canal. Measuring of the reflection coefficient was done by capacitive probes, and incoming and reflected waves were separated by the method (Goda and Suzuki, 1976)

As already mentioned, one construction was tested on two models, at two different scales. The model 1:40 was used to test porosities n = 0, 24, 32 and 40 %, and the model 1:25 for testing of porosity

n = 32 %, as this porosity showed the best reflection characteristics. Testing on both models was done by regular (Stokes) and irregular (Jonswap) waves, for sea level altitudes 0.00m and +0.50 m.

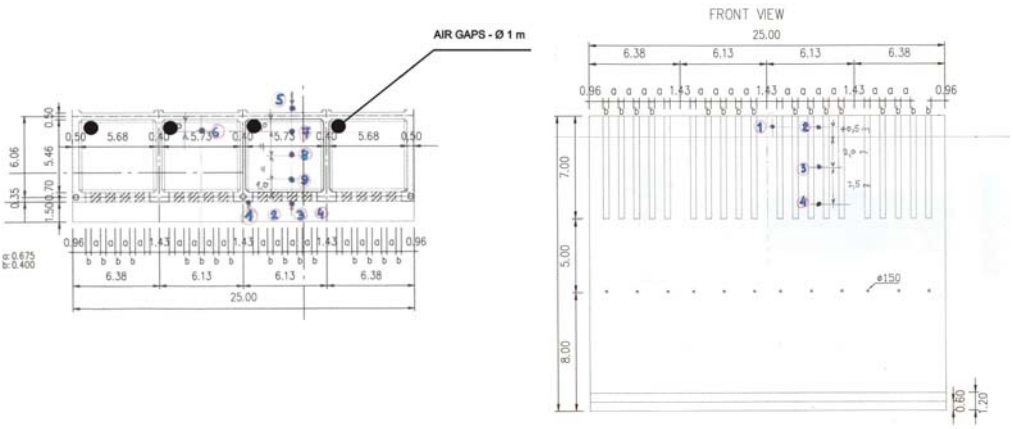

Figure 2. Ground plan and front side view of the perforated structure, porosity n = 32%, layout of pressure gauge probes (1 through 9).

2. Physical model I (scale 1:25)

Testing on the scale 1:25 model was done by means of regular and irregular waves, according to the testing program in the table 1. Periods T [s] i T_p [s] are determined according to different values of wave steepness L/H_i i L_p/H_{si}. For the purpose of this paper, steepnesses were used as reciprocal values of the conventional parameter of steepness H/L.

Table 1. Program of testing by regular (Stokes) and irregular (Jonswap) waves on 1:25 model.

WL [0m,+0.5m]		L/H_i (reg.) and		L_p/H_{si} (irreg.)		M 1:25 Bw=5,46m
n = [0,24,32,40%]		10	15	20	30	
H_{si} [m] (irreg.) H_i [m] (reg.)	0,5	1,8	2,2	2,5	3,1	T [s] (reg.) T_p [s] (irreg.)
	1	2,5	3,1	3,6	4,4	
	1,5	3,1	3,8	4,4	5,4	
	2	3,6	4,4	5,1	6,2	
	2,5	4,0	4,9	5,7	6,9	

Tests were performed on vertical perforated walls of various porosities (n= 0, 24, 32 and 40 %), measuring the coefficient of reflection from each wall, as a function of the wave steepness parameter. For regular waves, the reflection coefficient (C_r) is defined as $C_r = H_r / H_i$, where H_i = incoming wave height, and H_r, reflected wave height. For irregular waves, the reflection coefficient (C_r) is defined as $C_r = H_{sr} / H_{si}$, where H_{si} = significant incoming wave height, and H_{sr} significant reflected wave height.

Results of the analysis are shown in Fig. 3.

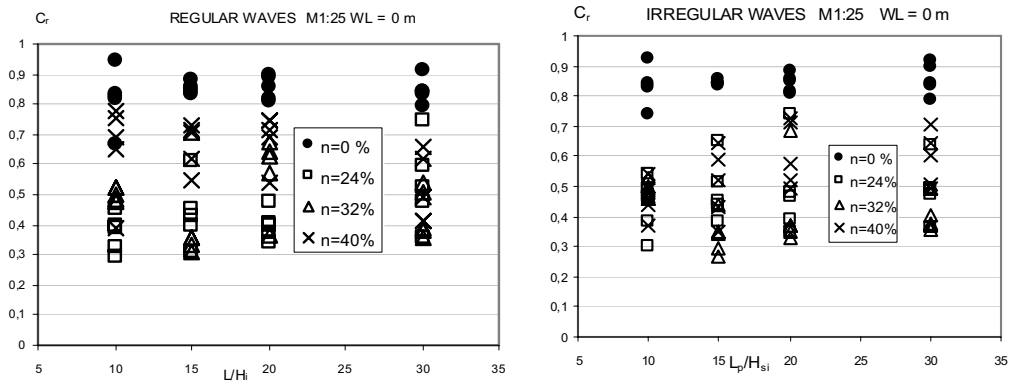

Figure 3. Reflection coefficient (C_r), as function of wave steepness (L/H_i, L_p/H_{si}) and porosity of the perforated wall (n), for regular waves and irregular waves, water level WL=0m.

It may be seen in Fig. 3, that the values of the reflection coefficient are the lowest for porosities n = 24 % ($L/H_i=L_p/H_s=10$) and n = 32 % ($L/H_i=L_p/H_s=15$). Dependence of reflection coefficients on wave steepness or wave length is not clear expressed.

Mechanisms of energy dissipation in the construction chamber without the upper board are the resonance mechanism, which makes the reflection coefficient dependent on the period of incoming waves, and the mechanism of dissipation in the chamber through turbulence. As the chamber upper board is situated very close to the water level (WL), the resonance mechanism is excluded, and the reflection coefficient is independent from frequency of incoming waves, and energy dissipation occurs only through turbulence in the chamber. For the above reasons reflection coefficient minimums for regular waves occur around the value of 0.3, while for perforated constructions without upper board the minimum is around 0.1 (Suh, 2006). For irregular waves, minimum values of reflection coefficient match the values for partially perforated constructions without upper boards, about 0.3 (Suh, 2006).

The same model was used to test the influence of wall porosity on the pressures on the upper board of the chamber (in pressure gauge 7, Fig. 2). The influence of porosity is shown in Fig. 4 with very clear tendency.

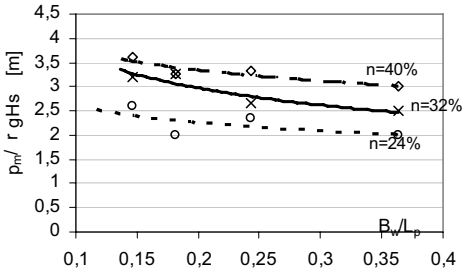

Figure 4. Maximum measured pressures (p_m/rg), in gauge 7, as function of parameter B_w/L_p, for different porosities of perforated wall (n), for irregular waves.

3. Physical model II (scale 1:40)

The second model was made primarily for testing of pressures and forces on the perforated construction, with and without air gaps on the upper board, for optimal porosity n=32%. The air gaps are 1 m in diameter, situated on the upper board as shown in Fig. 3. Measurings on the second model were done for regular and irregular waves, only for steepness $L/H_i = L_p/H_{si} = 15$, according to the test program in table 2.

Table 2. Program of testing by regular (Stokes) and irregular (Jonswap) waves on scale 1:40 model.

WL [0m,+0.5m] n = [32%]		T_p [s] (irreg.)	M 1:40 B_w=5,46m	WL [0m,+0.5m] n = [32%]		T [s] (reg.)	M 1:40 B_w=5,46m
H_{si} [m] (irreg.)	2	4,4	L_p/H_{si} =15	H_i [m] (reg.)	1,5	3,8	L/H_i =15
	2,5	4,9			2,5	4,9	
	3,4	5,7	with and without air gaps		3,5	5,8	
	4	6,2			4,5	6,6	
					5,5	7,3	with and without air gaps
					6,8	8,1	

By integrating the measured pressure diagrams, the forces on the perforated wall bollard (width 0.675 m) and on the upper board of the chamber (per m of board length) were determined. The pressure diagrams were extrapolated prior to integrating, and they encompass the entire height of the bollard and the entire width of the board of the perforated construction.

Maximum forces were calculated, on the bollard without air gaps F_B [kN], and with air gaps F_{BO} [kN] and maximum forces on the upper board without air gaps F_{UB} [kN/m'] and with air gaps F_{UBO} [kN/m'].

The influence of air gaps on reduction of forces on the upper board and the bollard of the perforated construction is evident (Fig. 5).. The level of reduction of the forces is analyzed through the ratio of forces with and without air gaps: F_{BO}/F_B and F_{UBO}/F_{UB}

The influence of the model scale was analyzed in measuring point 7, on both models (1:25 and 1:40). From Fig. 6 it may be concluded that for regular waves there are no significant differences in measured pressures, for the area $B_w/H_i > 2.0$. With irregular waves, differences become higher at larger wave heights, $B_w/H_{si} < 2.0$.

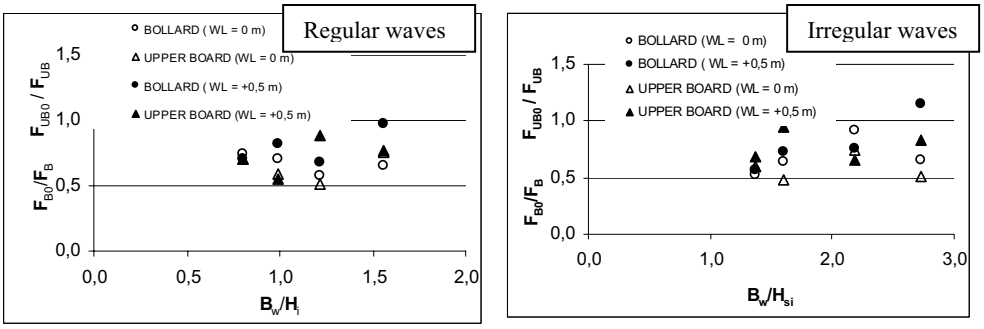

Figure 5. Ratios of forces on the bollard, with and without air gaps (F_{BO}/F_B) and ratios of forces on the upper board with and without air gaps (F_{UBO}/F_{UB}), for water levels WL=0 and 0,5m, for regular waves and irregular waves.

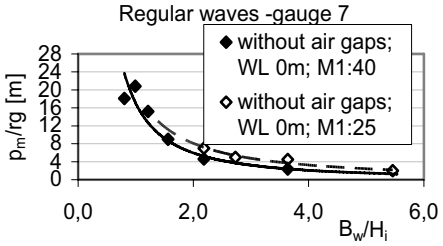

Figure 6. Influence of model scale (1:25 and 1:40) for measured pressures at point 7, without air gaps, water level WL = 0 m, for regular and irregular waves.

4. Conclusion

On the basis of mentioned analyses it may be concluded that the upper board of the partially perforated construction adversely affects the reflection characteristics, increasing reflection from the wall. It has also been confirmed that minimum reflection coefficients occur at front wall porosity of approximately 30 %. Pressures on the upper board of the chamber are dependent on the porosity of the front wall, and decrease with decreased porosity. Air gaps on the upper board of the construction reduce forces on the bollards of the front wall and on the upper board by up to 50 % for larger waves. The model scale doesn't influence measured pressures.

Bibliography

S. A. Hughes, 1993., 'Phisical models and laboratory techniques in coastal engineering'; Advanced Series on Ocean Engineering, World Scientific ,Volume 7,

K.J. McCinnell, D.M. Ethelston, N.W.H. Allsop, 1998., 'Development of new structures and aplication in Hong Kong', Coastlines, structures and breakwaters, T. Telford, London, [2]

H. Oumeraci et al., 2001., 'Probabilistic design tools for vertical breakwaters', Lisse: A.A. Balkema publishers, Netherland, ISBN 9058092488,

K. D. Suh, J. K. Park, W. S. Park, 2006., 'Wave reflection from partially perforated-wall caisson breakwater'; Ocean Engineering 33, 264-280. [6]

V. Androcec, V. Pusic, R. Dolovcak, M. Markovic, 2006., Rijeka Port, Model experiments of vertical quay with disipation chamber, Faculty of Civil Engineering, Water Research Department.

PHYSICAL MODEL TESTS OF THE WAVE ENERGY CONVERTER WAVECAT

Gregorio IGLESIAS [(1)], Alberte CASTRO [(2)], Rodrigo CARBALLO [(2)], Fernando VARELA [(3)] & Hernán FERNANDEZ [(3)]

[(1)] *Assoc. Prof., Univ. of Santiago de Compostela, Dep. Agr. Eng., Campus Univ., Lugo, 27002, Spain. iglesias@usc.es*

[(2)] *Assoc. Res., Univ. of Santiago de Compostela, Dep. Agr. Eng., Campus Univ., Lugo, 27002, Spain. albertecastro@udc.es, rcarba@usc.es*

[(3)] *Assist. Res., Univ. of Santiago de Compostela, Dep. Agr. Eng., Campus Esteiro, Ferrol, 15403, Spain. fernando.varela@rai.usc.es, hernan.fernandez@rai.usc.es*

Abstract

A 1:30 physical model of a hull of the WAVECAT, a new wave energy converter, is tested in a wave flume. The model allows to vary the key design parameters (freeboard, draft, hull convergence angle), so that different configurations can be tested until their optimum values — those that maximise the amount of overtopping and the height above mean sea level at which it is collected — are found. The refined design resulting from these tests will be used to build a large-scale model (possibly 1:5) which will be tested in a wave tank and in the sea.

1. Introduction

The use of carbon-emitting energy sources and its effects on the global climate is a reason for serious concern, hence the importance of shifting to renewable energy sources. Among these, wave energy is currently emerging as one of the sources with the greatest potential for countries with coastlines submitted to an energetic wave climate (Carbon Trust, 2006). Its late development relative to other renewable sources is due to the technological challenges that it poses. Nowadays there are a number of devices to exploit wave energy, in different stages of development. According to their interaction with the incoming wave, they are classified as point-absorber devices, attenuators, and terminators. WAVECAT is a wave energy converter of the terminator type. It can be described as a sort of catamaran, its hulls forming an angle when seen from above (Figure 1).

2. WAVECAT Operation

When in operation, WAVECAT is moored with its centreline aligned in the direction of the waves. As a wave crest advances between both hulls, their convergence causes the wave height to increase, until eventually the hull boards are overtopped. The overtopping volume is collected in tanks above the mean sea level. These tanks discharge through a turbine system into the sea, so that the higher water level in the tanks is used to drive the turbines and generators coupled to them.

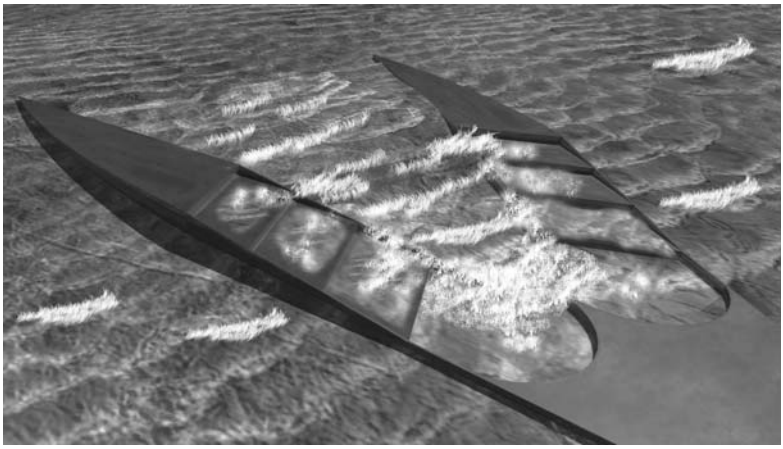

Figure 1. The WAVECAT wave energy converter.

Overtopping has been extensively studied in conventional breakwaters (e. g. Van der Meer et al., 1994) and also in low crest structures. However, the nature of overtopping occurring at the WAVECAT is different for several reasons. First, the wave energy converter, being a floating craft, moves under wave action. Second, the vertical walls on which the waves impinge have a limited draft, in addition to a low freeboard. Third, waves act on these walls at a high obliquity. Therefore it is necessary to study the overtopping in this case by means of ad hoc tests.

3. Physical Model Tests

With this purpose, a model of one of the hulls at a scale 1:30 is tested in the wave flume of the University of Santiago de Compostela, with dimensions of 20 m (length) x 0.9 m (height) x 0.65 m (width). The model allows to modify the key design parameters: freeboard, draft, and hull convergence angle. A number of configurations are tested with different values of these parameters, under various wave conditions representative of the sea states offshore the Galician coast (NW Spain), where the first deployment of the WAVECAT is planned. The overtopping rates for each configuration are measured. The aim is to determine the values of the design parameters conducive to the highest overtopping rate and height above mean sea level at which the water is collected, hence to the greatest potential for power production. The complete tests results will be presented at the Conference. The refined design achieved through these small-scale tests will be constructed at a larger scale (possibly 1:5) by a shipyard, and tested in a wave tank and at sea.

References

Carbon Trust, 2006. ‘Future Marine Energy’, Eds. Callaghan J. and Boud R. Available from: http://www.carbontrust.co.uk/technology/technologyaccelerator/marine_energy.htm

Van der Meer, J. W., and Janssen, J. P. F. M. 1994. 'Wave Run-up and Wave Overtopping at Dikes'. In: Kobayashi, N. and Demirbilek, Z., (eds) Wave Forces on inclined and vertical wall structures, pp 1-27, ASCE. Also Delft hydraulics, Publ. No 487.

The design wave for coastal structures

Giuseppe Barbaro [(1)], Maria Chiara Martino [(2)]

[(1)] *Professor, Department of Mechanics and Materials, "Mediterranea" University of Reggio Calabria, Loc. Feo di Vito, 89100, Reggio Calabria, Italy, giuseppe.barbaro@unirc.it*

[(2)] *Researcher, Department of Mechanics and Materials, "Mediterranea" University of Reggio Calabria, Loc. Feo di Vito, 89100, Reggio Calabria, Italy, chiara.martino@unirc.it*

Abstract

In the design of coastal facilities, it is customary to estimate parameters of a design sea state corresponding to a specified return period or annual risk, and then develop an estimate of the expected largest individual wave height within that sea state. In the paper, the design wave produced by wind generated waves on coastal structures (rubble mound breakwaters, groins, ports) will be obtained.
To this aim, the expressions proposed by the Technical Instructions for the Planning of Maritime Breakwaters (1995) will be used and applied at the Italian location.

1. The design wave for wind generated waves

Let us consider the design wave to calculate the maximum force produced by wind generated waves on coastal structures. The design wave has an height *h(R)* that has a given probability *P* of being exceeded in the lifetime *L* of the structure.

The upright breakwater must be able to withstand the design sea state with same dictated safety factors. The rubble mound breakwaters must be able to withstand the design sea state, suffering at the most damages contained within a prescribed level. So, it is necessary to fix the design lifetime *L* of the structure and the probability that the wave height, in *L*, exceeds a fixed threshold.

Tables 1-2 give the minimum lifetime *L* and maximum encounter probability *P* indicated in the Italian Technical Instructions for the Planning of Maritime Breakwaters (1995).

Table 1. Minimum lifetime L (years).

Safety level → / **Structure type** ↓		**1**	**2**	**3**
General use		25	50	100
Special use		15	25	50

Table 2. Maximum encounter probability *P*.

Economic consequence in case of failure		**Risk for human life**	
		Small	**High**
Low		0.20	0.15
Average		0.15	0.10
High		0.10	0.05

An additional verification is required for the rubble mound breakwaters.

Specifically, the structure must be able to withstand, with practically no damage, a sea state that has a relatively high encounter probability (see Table 3).

Table 3. Maximum encounter probability *P* (second verification of rubble mound breakwaters).

Economic consequence in case of failure		Risk for human life	
		Small	High
Low		0.50	0.30
Average		0.30	0.20
High		0.25	0.15

Once the values of *L* and *P* have been fixed, it is possible to derive the return period *R(L,P)* that, in the hypothesis of Poisson process, is equal to:

$$R(L,P)=\frac{L}{\ln\left(\frac{1}{1-P}\right)}. \qquad [1]$$

When the return period *R* is known, using the series proposed by Boccotti (2000), we can derive the significant height that corresponds to such a return period. The series can be written in the form:

$$x_i = A + u\ln x_{i-1}, \qquad [2]$$

with:

$$A \equiv 1 + u\ln\left(\frac{R}{B}\right),\ x \equiv \frac{B}{R}\exp\left(\frac{h}{w}\right)^u.$$

As a first attempt value *B* can be assumed equal to b_{10} (mean value of the bases of the equivalent triangular sea storms recorded in *N* years - Boccotti, 2000). The series [2] converges quickly, so that it is possible to derive easily *x* and therefore *h(R)* through the expression:

$$h(R)=w\left[\ln\left(\frac{R}{B}x\right)\right]^{\frac{1}{u}}. \qquad [3]$$

Following the Technical Instructions for rubble mound breakwaters, in the hypothesis of total destruction or incipient damage, and for coastline defence works the design wave has an height $H_s=h(R)$ and a period T_p that, in the hypothesis of JONSWAP spectrum, is:

$$T_p = 8.5\pi\sqrt{\frac{h(R)}{4g}}. \qquad [4]$$

Furthermore, for vertical breakwaters, the design wave have an height equal to $H_{20}=1.4h(R)$ and a period T_h equal to the average period of a wave in a sea state with the significant height equal to *h*. Using the expression of Rice (1945), for wind waves in the JONSWAP spectrum hypothesis, it results equal to:

$$T_h = 0.92T_p. \qquad [5]$$

The calculation scheme proposed in the paper is applicable for any defence work located near the shoreline.

Tables 4-6 indicate the design wave for different kinds of port defences and coastline structures. The results are referred to the locations were, currently, are located the wave metric buoys managed by the Italian Wave Metric Net of the Agency for the Environmental and Territory (APAT) (see Fig. 1). We obtained theses results considering the most serious conditions foreseen by the Normative for the different kinds of maritime structures. From Tab. 5 we can deduce, for instance, that the design wave of a vertical breakwater at Alghero, characterized by the strongest sea of Italy, can be assumed equal to $H_{20}=19.74$ *mt* and $T_h=14.72$ *sec*. At the same location, the design wave of a coastline defence structure is equal to $H_s=10.93$ *mt* and $T_p=14.08$ *sec*.

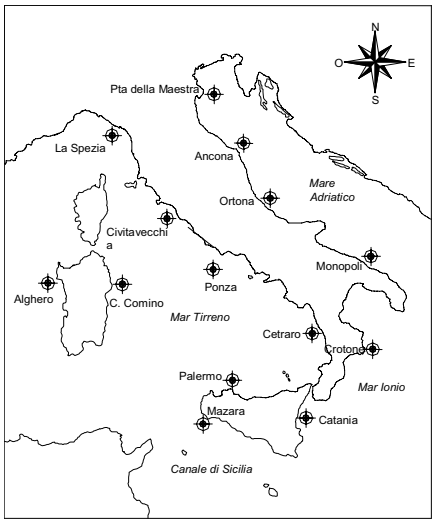

Figure 1. Location of the Italian wave metric buoys managed by the APAT.

Table 4. Design wave for rubble mound breakwaters.

Location	Rubble mound breakwater			
	Incipient damage *(L=50years,P=0.5)*		Total destruction *(L=50years,P=0.1)*	
	H_{10} *(mt)*	T_p *(sec)*	H_{10} *(mt)*	T_p *(sec)*
Alghero	14.76	14.52	17.07	15.62
Catania	10.10	12.01	12.27	13.24
Crotone	9.86	11.87	11.66	12.91
La Spezia	10.48	12.24	12.38	13.30
Mazara del Vallo	9.24	11.50	10.50	12.25
Monopoli	7.90	10.63	9.18	11.45
Pescara	9.78	11.83	11.62	12.89
Ponza	9.71	11.78	11.20	12.65

Table 5 Design wave for vertical breakwaters.

Location	Vertical breakwater *(L=100years,P=0.1)*	
	H_{20} *(mt)*	T_h *(sec)*
Alghero	19.74	14.72
Catania	14.42	12.58
Crotone	13.57	12.20
La Spezia	14.42	12.58
Mazara del Vallo	12.07	11.51
Monopoli	10.63	10.80
Pescara	13.55	12.19
Ponza	12.94	11.92

Table 6. Design wave for coastline defence structures.

Location	Coastline defence structure *(L=25years,P=0.5)*	
	H_s *(mt)*	T_p *(sec)*
Alghero	10.93	14.08
Catania	7.33	11.54
Crotone	7.24	11.46
La Spezia	7.70	11.82
Mazara del Vallo	6.90	11.19
Monopoli	5.85	10.30
Pescara	7.17	11.41
Ponza	7.20	11.43

Otherwise, it is possible to use the directional probability of exceedance. Let us consider the probability $P(H_s>h;\ \theta_1<\theta<\theta_2)$ (see curve on the right in Fig. 1) that the significant wave height, at a given location, exceeds a fixed threshold h, with the dominant direction within a fixed sector (θ_1,θ_2). Directional probability must be less than equal to omnidirectional probability that often can be fitted by:

$$P(H_s > h) = \exp\left[-\left(\frac{h}{w}\right)^u\right]. \qquad [6]$$

This is a Weibull distribution whose parameters u and w depend on the special location under examination (see curve on the left in Fig. 1). While $P(H_s>h;\ \theta_1<\theta<\theta_2)$ can be expressed as a difference between two Weibull forms (Boccotti, 2000):

$$P(H_s > h;\theta_1 < \theta < \theta_2) = \exp\left[-\left(\frac{h}{w_\alpha}\right)^u\right] - \exp\left[-\left(\frac{h}{w_\beta}\right)^u\right], \qquad [7]$$

where the non negative parameters w_α and w_β generally vary from one sector to another, while u takes on the same value as in the omnidirectional probability of exceedance $P(H_s > h)$. Parameter w_α must be greater than w_β, otherwise the probability would take on same negative values and must be smaller than or equal to and w (the parameter of $P(H_s > h)$). For plotting the data we shall use:

$$X \equiv 100\ln\left(2.5h(R)\right),\ Y \equiv 100\ln\ln\left(\frac{1}{P}\right). \qquad [8]$$

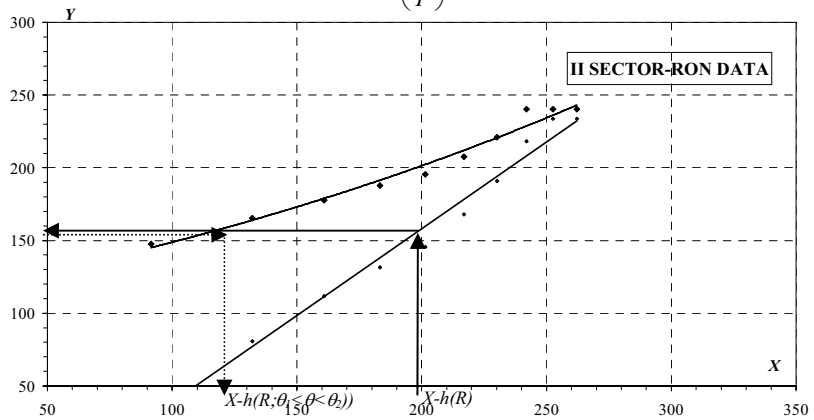

Figure 2. The probabilities $P(H_s>h)$ and $P(H_s>h;\ \theta_1<\theta<\theta_2)$ at Crotone (Italy) in the Jonian Sea (Southern of Mediterranean).

Calculated $h(R)$, it is possible to obtain the design wave $h(R;\ \theta_1<\theta<\theta_2)$ for a fixed sector of wave advance. It is necessary to enter in the abscissa of Figure 2, with the value of X calculated (see eq.ns [3] and [8]) and to draw, in ordinate, the value Y whose corresponds, in abscissa, $h(R;\ \theta_1<\theta<\theta_2)$.

References

Boccotti, P. 2000. 'Wave Mechanics for Ocean Engineering', Elsevier Science, Oxford.

Hasselmann, K., Barnett, T.P., Bouws, et al., 1973. 'Measurements of wind wave growth and swell decay during the Joint North Sea Wave Project (JONSWAP)', *Deut. Hydrogr. Zeit.*, A8, pp. 1-95.

Rice, S. O., 1945. 'mathematical analysis of random noise'. *Bell Syst. Tech. J.* 24, pp. 46-156.

STABILITY OF ARMOUR BLOCK FOR RUBBLE-MOUND BREAKWATERS

YOUNG-TAEK KIM [(1)] & JONG-IN LEE [(2)]

[(1)] *Senior Researcher, Korea Institute of Construction Technology, 2311 Daehwa-dong Ilsanseo-gu Goyang Gyeonggi-do, 411-712, Republic of KOREA. ytkim@kict.re.kr*

[(2)] *Research Fellow, Korea Institute of Construction Technology, 2311 Daehwa-dong Ilsanseo-gu Goyang Gyeonggi-do, 411-712, Republic of KOREA. jilee@kict.re.kr*

Abstract

The rubble-mound breakwaters have been most widely used in Korea. Recently, serious damages for the rubble-mound breakwaters are reported frequently and they are concentrated on the head and curved sections of breakwaters. In general, the breakwater head and curved sections are one of the most important part in a whole breakwater. Therefore these parts are designed to locate the heavier blocks rather than trunk section. In this study, the stability of the breakwater heads covered by tetrapods are investigated with the hydraulic model tests.

1. Introduction

The types of breakwaters could be classified into the rubble mound, the vertical caisson or cell block and the composite type *etc*. In Korea, about 70% of total lengths of breakwaters are rubble mound type breakwaters and the tetrapods are most widely used armour blocks. The total lengths of breakwaters mean the summation of each length of all breakwaters which are constructed in Korea.

It is well known that many typhoons generated near the Guam and Philippines in the Pacific Ocean move to the north-east Asia. In the north-ease Asia, Korea is neighbored by China and Japan and its southern coastal zone faces the Pacific Ocean. At least two or three typhoons almost every year have caused significant damages on the southern coast of Korea. These typhoons rotated counterclockwise and pass through the Korea peninsula or the Straits of Korean between Korea and Japan. Because the typhoons turn round, the direction of waves are very important. That is, since the breakwaters are designed to the normally incident waves, the obliquely incident waves could brought about the unexpected damages.

In this study, the damage from the oblique incident wave onto the breakwater heads are investigated by the series of hydraulic model experiments.

2. Experimental Setup

In this study, a series of stability tests for the rubble-mound breakwaters has been carried out in an elaborately controlled laboratory facility. The basin is 42m long and 36m wide. A uni-directional spectral wave generator is installed in one end of the basin and is used to generate irregular waves with equivalent significant wave heights and wave periods. The width of wave generator is 20m.

Figure 1 and Figure 2 show the schematic sketch of wave basin and model setup for experiments. The length of breakwater which is tested in this study is 4m long and the water depth at the toe of breakwater is 0.45m. The height of superstructure is 0.9m. The main armour blocks are the tetrapods (T.T.P) and the weights of them are 211g and 271g for head part of breakwater. The breakwater has the slope of 1:1.5. The unidirectional irregular waves with Bretschneider-Mitsuyasu spectrum were used and the wave condition

was non-breaking or partially breaking at the toe of the structures. Table 1 shows the summaries of test condition.

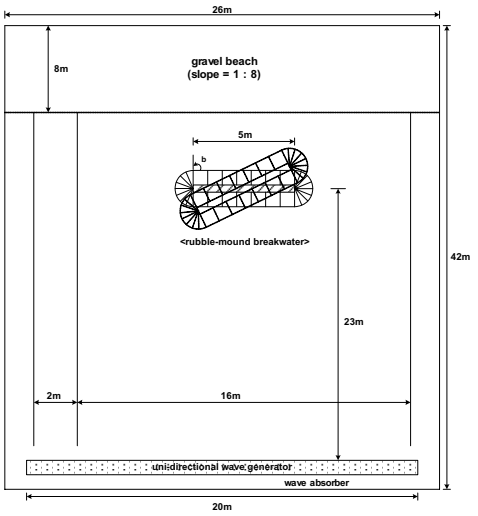

Figure 1. Wave basin and model setup

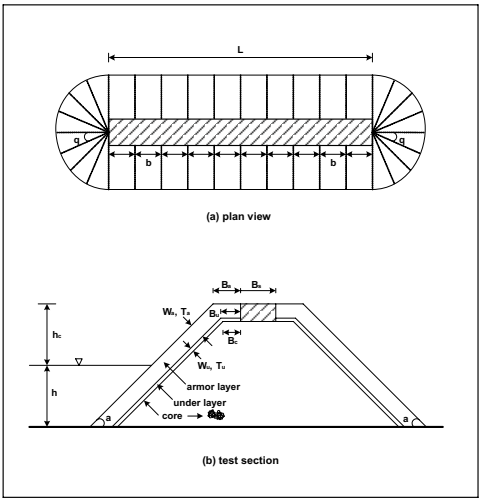

Figure 2. Top and cross section views of breakwater

Table 1. Summary of test conditions in the model

Wave height (cm)	Wave period (sec)	Water Depth	Weigh of Armour	Number of wave	Δβ
7, 8, 9, 10, 11, 12 13, 14, and 15	1.0, 1.2, 1.4, 1.6, 1.8, and 2.0	45cm	T.T.P : 211g and 271g	1,000	15° (β =0° ~ 90°)

3. Analysis of Stability

Analysis of stabilty for breakwater is investigated in detail with respect to the change of wave heights, wave periods, and incident angles of waves. When analysing the stability of breakwaters, N_s, the stability number in the Hudson's empirical formula is applied. The empirical formula suggested by Hudson is as followings (CEM, 2002).

$$M = \frac{\rho H^3}{N_s^{\ 3}(S_r - 1)^3}, \quad N_s = (K_D \cot\alpha)^{1/3} \qquad [1]$$

In equation (1), M is mass of armour unit, ρ is mass density of armor unit, H is wave height, $S_r = \rho / \rho_{water}$, N_s is stability coefficient and α is angle of structure slope($\cot\alpha$ = 1.5).

The breakwater head and trunk is divided by several sections and the stability number, N_s is tested and measured for each section from the experiments (Figure 3).

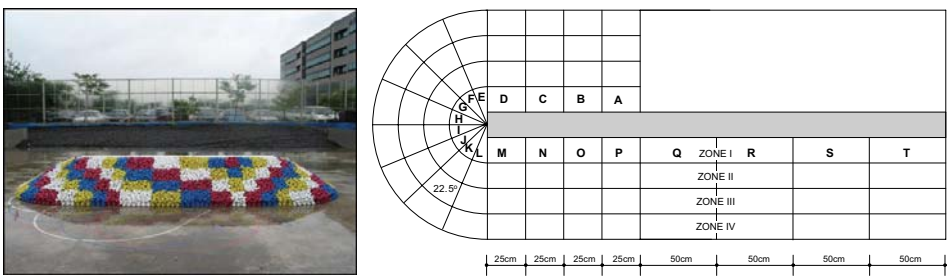

Figure 3. Model setup (left) and test section division (right)

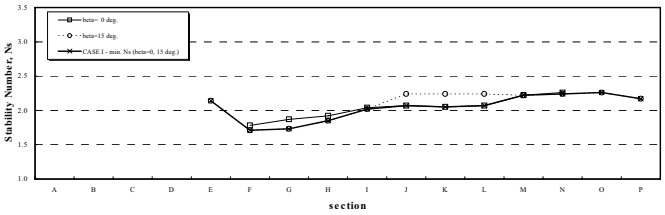

Figure 4. Stability number for CASE (β=0° and 15°)

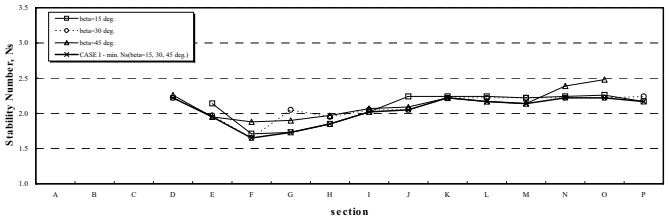

Figure 5. Stability number for CASE (β=15°, 30° and 45°)

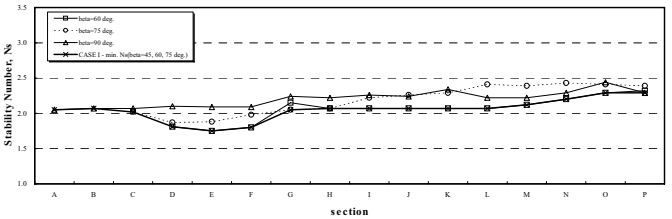

Figure 6. Stability number for CASE (β=60°, 75° and 90°)

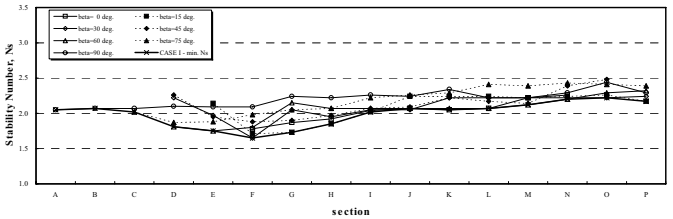

Figure 7. Comparison of stability number for CASE

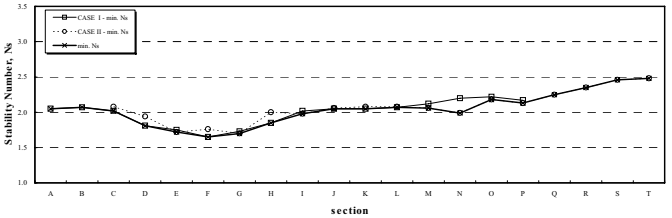

Figure 8. Mimimum stability number for all test conditions

The damage rate of breakwater was calculated by the following 2 methods. The one is the total damage ratio, that is, the ratio of the number of dislocated armour blocks to that of the originally covered total blocks and the other is the partial damage rate, that is, when the damage is concentrated on the special area,

the partial damage rate is applied. As the Hudson formula was used for evaluating the stabilty, the damage rate for 0%~5% ranges are investigated.

4. Results and Discussion

The stability number is investigated using the hydraulic model experiments and the test results is analised with Hudson forumula. In this study, the stability for 2 kinds of T.T.Ps are investigated. The weight of T.T.P for CASE □is 271g and CASE□ is 211g. Figure 4 ~ Figure 6 are the results of CASE □ for eache wave direction, Figure 7 is the comparison with all directions for CASE□ and Figure 8 is the comparsion with the minimum stability number for CASE□ and CASE□.

Figure 4 ~ Figure 6 show that as the incident angle(β) is changed, the stability number is also varied. Figure 7 is the result for the comparison with minimum stability number for each incident angle and shows that as the incident angle become larger, the stability number increased and the main damaged area is shifted into the inner harbor area. The stability number for θ=112.5°~157.5° is relatively small rather than other area, that is, this part is most vulnerable area among the several section of breakwater head.

Figure 8 shows that the stability numbers from CASE□and CASE□ are similar and the area for below 2.0 is around θ=90°~180°. The stability of head parts is more vulnerable than the trunk parts.

References

US Army Corps of Engineers. ‘Coastal Engineering Manual’, EM 1110-2-1100.

3D HYDRAULIC MODEL STUDY TO THE BREAKWATER DESIGN FOR COLOMBO SOUTH HARBOUR

D.M.D.T.B. DASSANAYAKE[(1)], S. KUMUTHINI[(2)], D. WOOTTON[(3)] & M. MENDIS[(4)]

[(1)] Mr, Research Engineer, Lanka Hydraulic Institute, Moratuwa, Sri Lank. darshana@lhi.lk , darshana.dassanayake@gmail.com

[(2)] Ms, Former Senior Research Engineer, Lanka Hydraulic Institute, Moratuwa, Sri Lank. kumuthini.k@gmail.com

[(3)] Mr, Technical Director, Scott Wilson, UK, don.wootton@scottwilson.lk

[(4)]Mr, Chief Executive / Director, Lanka Hydraulic Institute, Moratuwa, Sri Lank. malith.mendis@lhi.lk

Abstract

This paper includes findings from two model tests to cover the Main Breakwater head and the Main Breakwater root. A Single layer of CORE-LOC^{TM} units was used as the primary armour layer for the breakwater. Stability of the primary armour layer with CORE-LOC^{TM} armour units, stability of the CORE-LOC^{TM} armour units at the breakwater round head, degree of scouring in front of the toe, wave overtopping and impacts of wave overtopping on lee side armour layer were studied. Results were compared with the current state-of-the-art design formulae and the results are described in the paper.

1. Introduction

The Port of Colombo, one of the few deepwater ports in the Indian subcontinent, is strategically placed along the main shipping route.. The current depth of the Colombo port is insufficient to accommodate mega-carriers coming into service. With the demand for container throughput expected to exceed Colombo's capacity in the near future, the Government of Sri Lanka has recognized the need to increase Colombo's capacity to maintain its hub status in South Asia. Lanka Hydraulic Institute Ltd. (LHI) carried out field investigations, numerical modelling and physical modelling to optimise the functional and operational efficiency of the newly developed harbour layouts.

This paper presents the results of the hydraulic model investigations (three dimensional physical model tests) conducted to optimize the breakwater head and the breakwater alignment at the root.

2. Model Set-Up and Testing Procedure

Since the size of the model basin is not large enough to accommodate the full harbour layout, two separate layouts were tested. Main breakwater root was covered in the first layout (South Layout) while main breakwater head (see Figure 1) and small boat harbour were covered in the second layout (North Layout) A total of 80 model test runs were performed on the aforementioned breakwater layouts at LHI laboratory basin, which is 35m long, 25m wide and 1.0m deep. The main concern when testing model structures is to ensure that the wave structure interaction is correctly represented without the results being biased by scale effects. Hence after considering number of factors such as size of the flume and available sizes of model CORE-LOC^{TM} units, the final geometrical scale was chosen as 1:83 using Froude's similarity.

The method of placing armour units was random, similar to prototype, in order to ensure that correct packing density was achieved. The designed prototype CORE-LOC^{TM} unit size of 19.74 MT which approximately corresponds to model unit weighing 34g with a specific gravity of 2.35 (at the selected scale of 1:83).

The model testing of the breakwater layouts was carried out at a water level of +1.2m LWOST (Low Water Ordinary Spring Tide) The model testing was carried out for the two different wave systems characterizing the wave climate at Colombo (Swell Wave Conditions, and Overall (Combined) Wave Conditions). These transformed wave conditions were used as input wave conditions at the up wave boundary (near the paddle) of the coastal profile for the two-dimensional flume testing. A JONSWAP spectrum was used to generate the required wave conditions. The generalized test path followed during each test series was 0.1year, 1year, 10 year, 50 year, 100 year, 200 year, and 200 year+20%. 200+20% year was to establish a factor of safety on the stability of the CORE-LOC^{TM}. Two wave directions were used for South Layout (225^0 & 265^0) and three wave directions were used for North Layout (265^0, 285^0 & 385^0).

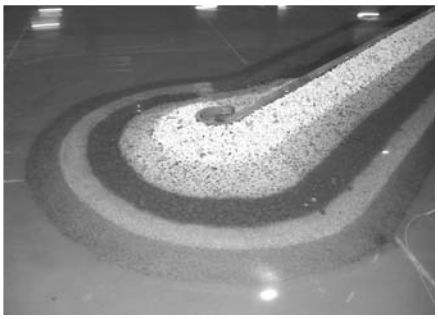

Figure 1: Main breakwater head model at LHI 3D wave basin

3. Discussion of Results

The Principal aim of these model tests was to assess the stability of the armour units including CORE-LOC^{TM} units and the wave overtopping at the head and along the truck when the structure was subjected to oblique wave attack. The final design showed good stability against even for the 20% higher wave heights (Hs=7.7m and Tp=17s) than the design storm conditions (Design Conditions are 200 Year Return Period; Hs=6.4m and Tp=16.0 at 15m Water Depth).

Percentage damage of the Toe armour (8-12 ton) was well below the acceptable damage levels. However lee side armours (3-6 ton) were damaged severely during design wave conditions with 285^0 direction. Severe damage was mainly observed near the breakwater head. Then the amour size was increased until acceptable damage level was reached.

Severe damage due to significant wave overtopping was observed at the main breakwater root during 50 year wave condition with 285^0 direction. To reduce the wave overtopping several options were tested with different alignments and different crown wall heights. Final alignment, the most seaward option and to tie the root to near by rocky headland. This arrangement reduced the focusing of waves in the bay formed at the root in previous alignments. Also crown wall was moved away from the marine drive which leads to different overtopping criteria. Based on the wave overtopping measurements and the amour stability results from the model study, the alignment of breakwater, the crest level of crown wall and sizes of armour unites were optimized.

This paper will contain the important findings from the model tests. These findings will enhance the general understanding of breakwaters with artificial armour units. Improvements resulting from the model tests will be presented during the presentation with comparison of results with current design practices.

References

Kumuthini S, Dassanayake D.M.D.T.B,.2005. Colombo port efficiency and expansion project, Physical Modelling 3D Stability (Basin) Model, LHI report 1826;

MELBY, J. A. AND TURK, G.F. (1997), Core-Loc concrete armour unites: Technical guidelines, Technical Report, CHL-97-4, US Army Corps of Engineer Research and Development Centre, Vicksburg, MS

3D PHYSICAL MODELLING OF AN EXTENDED BREAKWATER UNDER OBLIQUE WAVE ATTACK

Osanne PAIREAU [(1)], Melanie GRECO [(2)], Luc HAMM [(3)], Guy OLLIVER [(4)] & John WALLACE [(5)]

[(1)] Engineer, SOGREAH,
6 rue de Lorraine, Echirolles, 38130, France. osanne.paireau@sogreah.fr

[(2)] Engineer, SOGREAH,
6 rue de Lorraine, Echirolles, 38130, France. melanie.greco@sogreah.fr

[(3)] Technical Director, SOGREAH,
6 rue de Lorraine, Echirolles, 38130, France. luc.hamm@sogreah.fr

[(4)] Senior Engineer, PETER FRARNKLE & PARTNERS LTD,
South House, 21-37 South Street, Dorking, Survey, RH4 2JZ, United Kingdom. gf0@fraenkle.co.uk

[(5)] Chief Executive, PETERHEAD PORT AUTHORITY,
Harbour Office, West Pier, Peterhead AB42 1DW, Scotland. jewallace@peterheadport.co.uk

Abstract

This paper describes the 3D physical modelling performed during the design phase of the Smith Embankment Development planned to be built inside Peterhead Bay Harbour in north east Scotland. This development designed by Peter Fraenkel & Partners Ltd comprises in particular a 100m long rock rubble mound extension to the existing Albert Quay Breakwater with a wave wall, to protect a new general purpose quay along its inside. The extension also protects a further 200m long quay and reclamation which will be mainly dedicated to fishing activities.

1. Context of the Study

Sogreah has been subcontracted by Peterhead Port Authority to investigate the structural response of this extension to the breakwater when subjected to oblique wave attack inside the harbour and to measure its impact on the wave disturbance at other facilities around the harbour.

Three-dimensional wave tank model tests were required to check the stability of the new breakwater extension, to compare overtopping with that at the existing Albert Quay, and to optimise the structure of the rubble mound breakwater and the wave wall with regard to stability, overtopping and economy of the design.

2. Location and Description of the structure

The main armour on the breakwater extension is rock to tone in with that on the existing Albert Quay Breakwater. The breakwater extension has been angled off to the North-West to limit the effects of waves reflected towards facilities in the southern part of the harbour. The reflection coefficients of the extension, under oblique wave attack from the main harbour entrance, are uncertain. The 3D physical model of the area local to the extension was thus an appropriate tool to make direct wave measurements in front of the structures and within the harbour in order to provide data from which a numerical wave penetration model could determine these coefficients.

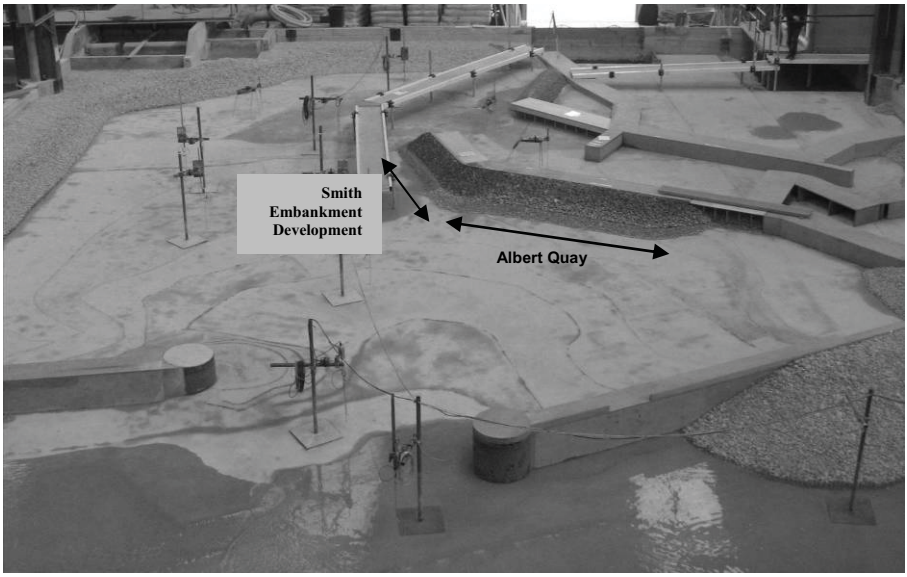

Figure 1. Top view of the physical model including the development at Smith Embankment

3. Description and results of the 3D model tests

The agreed approach consisted in performing initial wave tests on the existing harbour structures (without the extension), and then secondly with the extension to the Albert Quay Breakwater (Fig 1). This strategy allowed an assessment to be made on the influence of the extension to wave agitation inside the harbour. The typical set of wave tests consisted of a series of wave conditions including storms up to once in 200 years.

One of the objectives of these 3D wave tank tests was to measure the impact of the breakwater extension on wave disturbance, and particularly on operational wave conditions, with storms having a one in 10-year return period. The results showed that the impact of the extended breakwater was very limited in terms of wave agitation. The maximum increase was observed at only one point, located in the rear side of a future dredged area, and is less than 10%.

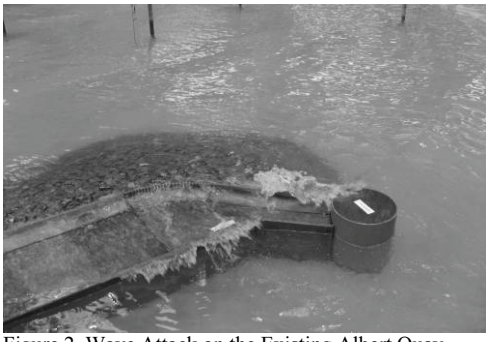

Figure 2. Wave Attack on the Existing Albert Quay

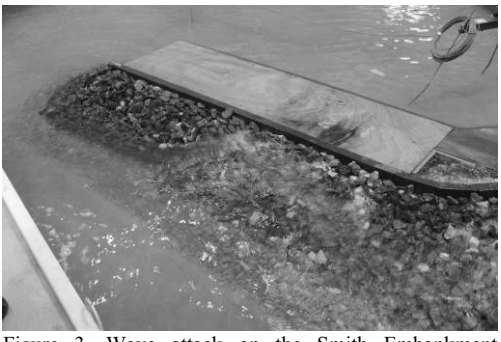

Figure 3. Wave attack on the Smith Embankment extension

Another objective of the tests was to check the stability of the new breakwater extension and to compare overtopping with that at the existing Albert Quay.

Therefore, this 3D physical modelling was important to assess how the stability of the rock armour layer was increased under the oblique wave attack. Indeed, due to the complexity of the wave attack inside the harbour (i.e. wave obliquity, reflection from the existing structures, diffraction around the harbour main entrance, etc), such result was difficult to anticipate.

For the same level of damages observed on both structures, the existing Albert Quay is armoured with 20 - 25 t rocks, with a slope from 2.3H:1V to 5H:1V. The Smith Embankment extension is armoured with 10 - 16 t rocks, with a slope from 2.3H:1V on the elbow (to the junction with the existing part and, because the wave attack was stronger around this elbow) to 1.3H:1V on the second part of the trunk section.

It was also found in the model that the stability of the rock toe berm was enhanced under oblique waves. The first version of the design included a 1 - 3 t rock toe berm levelled to -7.2 m CD. Finally, the stability of the 1 - 3 t rock toe berm levelled to -6.2 m CD was confirmed, even for the 200-year wave conditions. All these results allowed the design to be optimised significantly.

Regarding wave overtopping, the Smith Embankment extension wave wall was regularly overtopped. Moreover, the water that overtopped the wave wall on the Albert Quay breakwater side of the elbow ran along the Smith Embankment deck, which increased the total volume of overtopping reaching the rear side of the extension (Fig 4).

Consequently, the wave wall height was increased, particularly at the junction. The overtopping discharge was larger close to the beginning of the extension than at its end, because of the loss of energy induced by the waves running along this extension.

Figure 4. Snapshot of an overtopping event on the extended breakwater (during a one in 10-year wave test)

Conclusions

With the final design, the new structures are found to be stable and the extended breakwater has a minimal impact on the wave agitation. It was also shown that vessels could safely stay at berth along the inner side of the extension with their equipment including under storms of a severity up to a 1 in 10 year return period.

The results of the wave measurements showed that the impact of the extended breakwater on its immediate area is very limited with a mean increase of wave disturbance of about 2-3% and a maximum of 8%. Although these are small in the context of the relatively high waves at the extension, the reflected waves propagate into more sheltered areas, such as the marina and berths in the southern part of the Bay Harbour. Even a small increase from reflected waves could result in downtime into these areas.

Numerical modelling which was performed by HR Wallingford was calibrated against the measurements in the physical model. The calibration was achieved through adjustments to the reflection and transmission coefficients of the breakwater extension. The best fit values of these coefficients have been derived and taken on to further studies.

The various properties of the extension under oblique wave attack have been compared with theoretical estimates of the properties under normal wave attack.

VELOCITY SPECTRA EVALUATION NEAR SUBMERGED BREAKWATERS DUE TO IRREGULAR WAVE ACTION

A. C. NEVES [(1)], F. VELOSO GOMES [(2)], F.TAVEIRA PINTO [(3)]

(1) PhD Researcher, FEUP, Rua Dr. Roberto Frias, s/n 4200-465 Porto, Portugal, acneves@fe.up.pt

(2) Full Professor, IHRH, FEUP, Rua Dr. Roberto Frias, s/n 4200-465 Porto, Portugal, vgomes@fe.up.pt

(3) Assistant Professor, IHRH, FEUP, Rua Dr. Roberto Frias, s/n 4200-465 Porto, Portugal, fpinto@fe.up.pt

Abstract

Two dimensional physical experiments were conducted in the Hydraulics Laboratory of the Faculty of Engineering of Porto in order to investigate the wave-induced velocity and turbulence field around a submerged breakwater model. The tests were performed with incident irregular waves, with a significant wave height equal to 0.065 m and a peak period equal to 1.5 s. The submerged breakwater model was built with a geometric scale equal to 1/40 and its cross-section is represented in Figure 1.

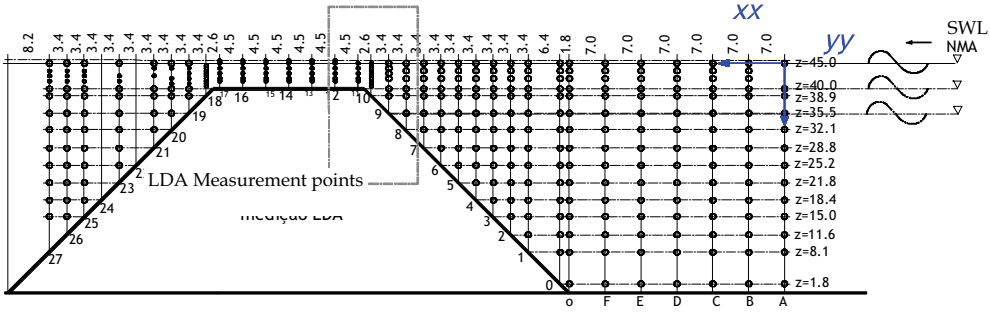

Figure 1. Cross-section of the model and location of the measuring points.

The tests were conducted with two water depths, leading to a 0 and a -5 cm freeboard (F). Horizontal and vertical velocity components were measured using a Laser Doppler Anemometry optical system. These measurements were taken in different locations successively nearer the breakwater and in the seaward and landward slopes, as indicated in Figure 1. Wave probes, placed in the section where the horizontal/vertical velocity component was measured, recorded simultaneously the instantaneous water surface elevation.

Pressure and velocity acting on the surface of the model were also recorded simultaneously for points located at the seaward and leeward slope.

The velocity, water surface elevation and pressure spectra were calculated and analysed for each one of the measurements. Figure 2 represents some of the results obtained for the F=-5cm case. The figure respects to velocity spectra obtained for points located in the seaward and in the leeward slopes.

Considerable differences in the shape and magnitude of the spectra, according to the location of the measured point were noticed. An attenuation of the velocity spectra for the points located in the leeward slope is clearly seen, though the energy associated to the peak frequency observed in the upper part of the leeward slope is still very significant.

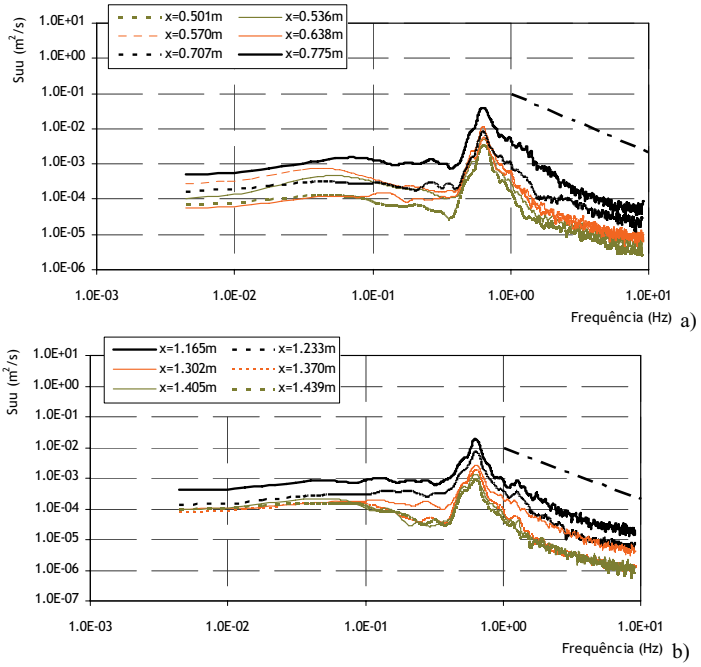

Figure 2. Velocity spectra at the surface of the submerged breakwater model, F=-5cm, a) seaward slope, b) leeward slope.

Figure 3 illustrates the role of these structures in the reduction of the significant wave heights. Spectral changes in the water surface elevation spectra, besides the decrease in magnitude, were observed. The broadening of the spectrum and the formation of a second peak frequency in the points located in the leeward of the model (as referred in previous studies) were observed. None of these changes occurred in the pressure spectra, though this variable is directly dependent of the water surface elevation value.

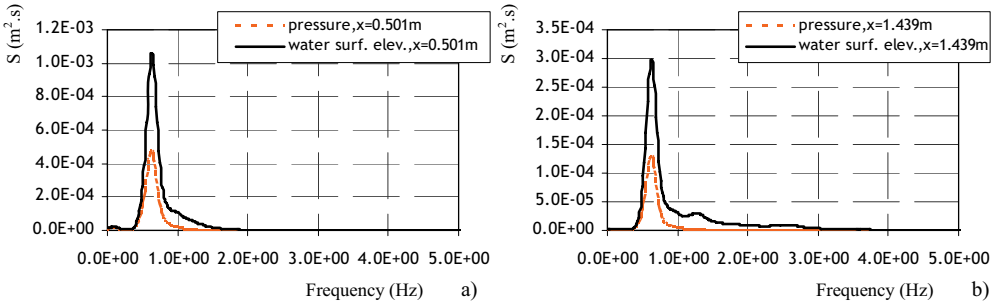

Figure 3. Water surface elevation and pressure spectra for different locations of the submerged breakwater, F=-5cm, a) seaward slope, b) leeward slope.

An analysis of the effect of the submergence of the breakwater model was also performed, through the comparison between the results obtained for the two different water depths. After a comparison between the results predicted by other authors, who performed similar experiments, a detailed investigation of the velocity and turbulence field around these structures was done, in order to understand the hydrodynamics and characteristics of the flow around these structures.

A LABORATORY AND NUMERICAL STUDY OF A WAVE SCREEN BREAKWATER

D. STAGONAS.[1] , G. MÜLLER [2], Th. KARMBAS [3], D. WARBRICK, T.ZARKADAS, G. VALAIS

(1)Phd student, Dep. of Civil Eng. University of Southampton, Highfield Campus, Southampton, SO17 1BJ, UK,.ds204@soton.ac.uk
(2) Senior Lectured, Dep. of Civil Eng. Uni. of Southampton, Highfield Campus, Southampton, SO17 1BJ, UK, g.muller@soton.ac.uk
(3) A. professor, , Department of Marine Sciences, University of the Aegean ,Mytilini, 81100, Greece, Karambas@marine.aegean.gr

Abstract

A wave screen like breakwater located in the entrance of a small recreational/fishery harbour was reaching the end of it's life. The structure was reported to sufficiently reduce the incoming wave height and allow navigability for almost 100 years. Laboratory experiments were conducted to explore the hydraulic performance of a section of the structure, and two different numerical models were employed to investigate both the linear and non-linear effects of local bathymetry. Results indicate that the performance of the structure strongly depends upon the adjacent topographical features and that scale effects are very important for the laboratory investigation of this type of structures. Finally results from the use of a so-called micro-model provide fertile ground for a discussion concerning drug coefficient losses in the lab due to small Reynolds numbers.

1. Introduction

Vertical permeable walls, or 'wave screens' could provide a soft engineering solution to reduce the wave energy entering a sheltered area while maintaining a large degree of the littoral drift, and onshore-offshore sediment movement. Such structures potentially have several advantages over conventional breakwaters; smaller footprint, smaller loading forces, cost effective. A number of researchers have investigated non-perforated pile breakwaters in the past (Mani and Pranesh; 1986, Rao et al, 1998) but to the authors knowledge, a study involving the performance of an already existed breakwater has rarely been reported.

Consequently the present work involves the study of a timber, wave screen like, existed breakwater with an element ratio (W) of 0.2; the hydraulic performance of the structure is explored through the use of two different numerical models and laboratory experiments.

2. Methods

Physical modeling

Initially a 1/40 scale section of the structure was installed into a 12meters long wave flume, to assess the effects of incident wave angle and conditions. Three different angles of approach were tested, 45°, 60°, 75° (90° was normal to the wave propagation) for wave steepness ranging between 0.01 and 0.06, and periods between 0.8-1sec.

In an attempt to minimize the pronounced side wall effects of the wave flume a 1/80 scale section of the structure was introduced in a small wave basin, 1.8m long and 0.8m wide. The same incident angles were adopted, for wave steepness ranging between 0.04-0.14, and periods of 0.04-0.06sec; no breaking waves were generated.

Numerical modeling

Two different numerical models were selected to investigate the effects of local topography to wave refraction, shoaling and breaking. The spectral wave model of MIKE 21 package (DHI) was chosen along with a highly non-linear numerical to better describe wave transformations in shallow waters (Karambas and Koutitas 2003). Three different scenarios were investigated (existed wave screen structure, solid breakwater, no breakwater) for wave heights between 1.7-3.2m and periods ranging from 5 to 8sec.

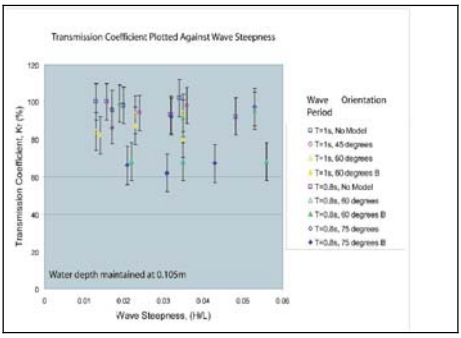

Figure 1: Transmission coefficient against wave steepness

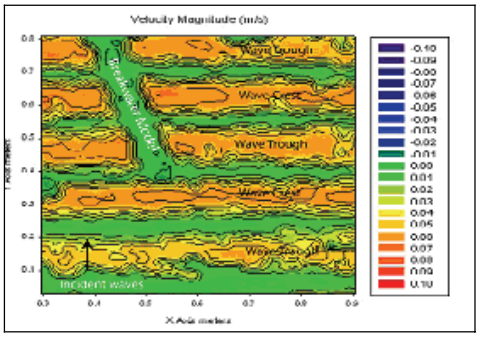

Figure 2: Horizontal particle velocities inside the small wave tank; breakwater model installed at 15degrees

3. Results

Physical model

Wave tank results are presented first (Fig. 1); the transmission coefficient is plotted against the wave steepness for a series of two experimental set-ups A and B. Micro-model results are cited here as well but only in the form of a 2D visualization of surface particle velocities (Fig.2).

Numerical models

For briefness sake, only a single result from MIKE21 model is included here. Wave height reduction due to topography effects and interactions with structure follows (Fig. 3)

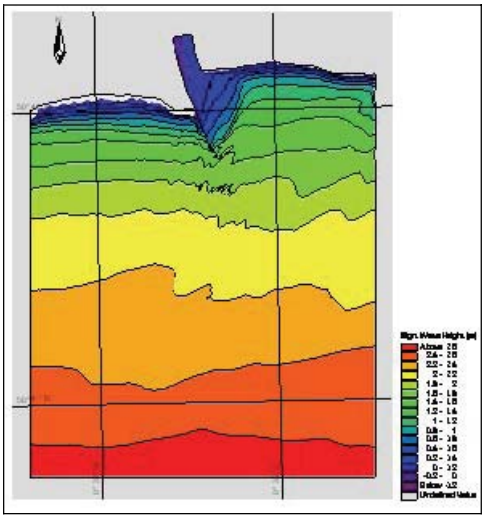

Figure 3: Simulation result for initial wave height 2.7meters and the wave screen structure

4. Discussion and Conclusions

- 1/40 scale testing indicates an average transmission coefficient between 70%-90%. Smaller scale (1/80) results indicate a larger range in the transmission coefficient and a large dependence on water depth and incident wave angle. Both results do not directly coincide with the Harbor's master testimony, but they are in relatively good agreement with already published data (Rao et al, 1998).
- Both numerical models revealed the significant effect of local topography to the overall wave height deduction. They also resulted to a wave height reduction due to the structure of almost 50% but for already broken waves. However the non-linear model was able to more accurately describe nearshore wave transformations.

References

Karambas Th. and Koutitas C. (2002), 'Surf and Swash Zone Morphology Evolution Induced by nonlinear Waves' *J. Wtrwy., Port, Coast., and Oc. Eng.*, Vol. 128, Issue 3, pp. 102-113

Mani, J.S. and Pranesh, M.R., (1986) Pile breakwater floating barrier interaction. *Proceedings of 3rd Indian National Conference on Ocean Engineering, Department of Civil Engineering*, IIT, Bombay, India, pp. B217-B228.

Rao S., Rao N.B.S, Sathyanarayana V.S. (1998), Laboratory investigation on wave transmission through two rows of perforated hollow piles, *Ocean Engineering*, vol. 26, pp. 675-699

Stagonas, D., & Muller, G., (2007), 'Wave Field Mapping and Particle Image Velocimetry', *Ocean Engineering* vol. 34, pp 1781-1785

PROBABILISTIC DISTRIBUTIONS OF SEA WAVE PARAMETERS IN THE DIAGNOSIS OF RUBBLE-MOUND BREAKWATERS

João Alfredo SANTOS [(1)], Rui CAPITÃO [(2)] & Isaac Almeida de SOUSA [(3)]

[(1)] *Research Officer, LNEC, Av. do Brasil, 101, 1700-066 Lisboa, Portugal. jasantos@lnec.pt*

[(2)] *Research Officer, LNEC, Av. do Brasil, 101, 1700-066 Lisboa, Portugal. rcapitao@lnec.pt*

[(3)] *Research grant holder, LNEC, Av. do Brasil, 101, 1700-066 Lisboa, Portugal. isousa@lnec.pt*

Abstract

The probabilistic procedure to simulate armour layer evolution under wave attack is presented. Such a procedure can be used to design the armour layer of rubble-mound breakwaters and to help in scheduling repair and / or maintenance works in these structures. This paper focuses on one of the key issues in this simulation: the selection of the most adequate distributions for the wave heights and periods to be used in the armour damage evolution formulations. An example of the application of such procedures to the breakwater that protects the fishing harbour of Sines (Portugal) is presented and discussed.

1. Introduction

The design of the armour layer of rubble-mound breakwaters, as well as the decision-making process on the schedule of the repair and / or maintenance works in the same armour layer, can now be based upon a probabilistic approach.

In fact, using the formula proposed by Melby and Kobayashi (1999) for the armour layer damage evolution,

$$\left[S(t)\right]^4 = \left[S(t_n)\right]^4 + \left(0{,}011\, N_s^5\right)^4 \frac{t - t_n}{T_m} \qquad [1]$$

where, $S(t)$ is the damage at time t contained in the interval $\left[t_n, t_{n+1}\right]$, during which it can be assumed that wave conditions are constant (i.e. significant wave height, H_s, and average zero up-crossing period, T_m, do not change) and $N_s = H_s / (\Delta D_{n50})$ is the stability number, Δ being the submerged density of the armour layer material and D_{n50} the median nominal diameter of the same material, it is possible to simulate the armour layer response to any sequence of sea-waves incident on it. If one uses a large number of samples made of sequences of waves with a given duration, one may estimate the probability of the damage at the end of that period reaching a pre-set level.

For the design of the armour layer, the simulation period should be the desired structure life-span and the structure initial status should be the one expected after its construction, whereas for scheduling of repair and / or maintenance works on the structure, the structure's initial status should be the one measured in the last survey of the armour layer envelope and the simulation period should go from that instant up to the next expected survey.

From the above, it is clear that one of the key points in the use of Melby and Kobayashi formula is the correct simulation of the sea-state parameters' sequences. This paper illustrates the use of that formula in the simulation of the damage evolution of the armour layer of Sines fishing harbour, Figure 1. This breakwater was chosen instead of the Sines west breakwater because the Melby and Kobayashi formula was developed for armour layers made of rock and not of artificial elements. For these, new coefficients, or a new formula, still have to be defined.

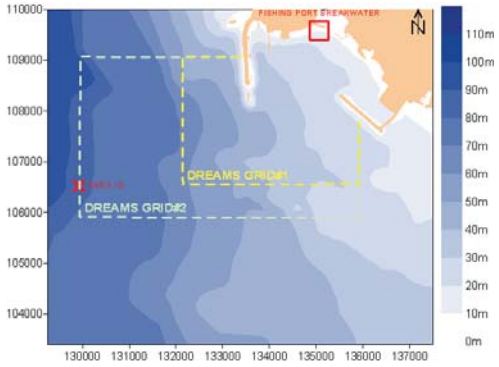

Figure 1. The breakwater of Sines fishing harbour

The port of Sines is located on the west coast of Portugal some 100 km to the south of Lisbon. The armour layer of the fishing harbour breakwater is made of rocks whose average weight is 45kN and which were randomly placed in two layers in a slope of 1:2 (V:H). Considering a density of 29 kN/m^3 the rocks' D_{n50} is 1.16 m. The water depth at the structure's toe is enough to avoid waves to break before hitting the structure.

2. Damage evolution simulations

The first problem to be addressed in the damage evolution simulations is the unrealistic continuous damage increase predicted by equation [1] for very low energy sea-states that may last for long periods. Sousa (2007) solved that problem by using the critical stability number concept presented in Smith et al. (1999). Then equation [1] becomes

$$S(t) = \left(\left[S(t_n) \right]^4 + \left(0{,}011\, N_s^5 \right)^4 \frac{t - t_n}{T_m} \right)^{0.25} \quad \text{if } N_s > N_c$$

$$S(t) = S(t_n) \quad \text{if } N_s \le N_c \qquad [2]$$

So, when the stability number, N_s, falls below the critical value, N_c, there is no damage increase. This critical stability number depends on the armour layer porosity and slope as well as on the wave slope at the structure location. It is not difficult to infer from the above equation that the damage increase at the end of any period is independent from the order by which the sea-states acted on the structure during that period. This somewhat simplifies the simulation procedure.

By transferring the wave characteristics measured offshore with a directional waverider buoy deployed at the SINES 1D location (Figure 1) up to the breakwater location, Sousa (2007) determined the three-hourly time series of significant wave heights, H_s, and of average zero up-crossing periods, T_m. Probability distributions were fitted to these variables and so using those distributions and a sampling procedure, several sequences of significant wave heights and of average zero up-crossing periods were produced and the damage evolution curves for five of those sequences as well as the average of the results for the one hundred sequences generated are presented in Figure 2.

This figure shows that the damage increment occurs at discrete events. It is particularly remarkable that most of the damage is the result of outstanding events. It can be also seen in that figure, specially in the average curve, that there is a trend for the damage to slow down as the armour layer becomes damaged. This can be interpreted as approaching an equilibrium state that, however, is never attained.

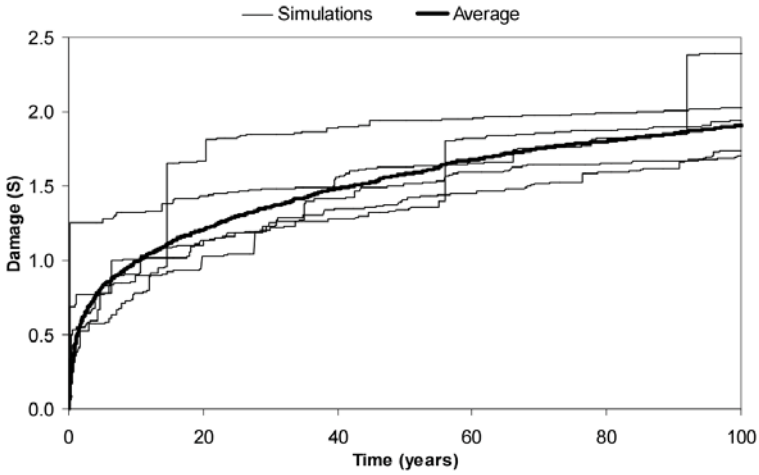

Figure 2. Damage evolution in five 100-year simulations and average of the 100 simulations performed with an armour layer made of 45 kN rock elements.

3. Distribution fitting

The above referred probability distributions that were fitted to H_s and T_m assumed absence of any correlation between wave periods and the wave heights, something that is not always true. Actually, there usually exists some degree of dependency between wave heights and wave periods - the greater the wave height the greater the wave period (positive correlation). Therefore, the use of bivariate probability distributions based on the adopted univariate (marginal) distributions of both variables will be investigated in order to enable a better description of the correlation that usually exists between H_s and T_m.

4. Results

In the final paper results from the investigation on the use of other threshold definitions for that sea-wave energy in the damage evolution for shorter time periods, which are better suited to the diagnosis procedure, will be presented. More realistic simulations of sea state characteristics produced for a large number of intervals between inspections (whose length ranges from one up to five years) are being obtained by trying out and fitting selected univariate and/or bivariate probability distributions of wave heights and periods.

References

Melby, J. A.; Kobayashi, N. 1999. 'Damage Progression and variability on´breakwaters trunks', *Proc. Coastal Structures '99*, pp. 309-315.

Smith, W. G.; Kobayashi, N.; Kaku, S. 1992. 'Profile Changes of Rock Slopes by Irregular Waves', *Proc. 23rd Coastal Engineering Conference*, Volume 2, pp. 1559-1572.

Sousa, I.A. 2007. 'Damage progression of rubble-mound breakwaters armour layer. Evaluation using level III probabilistic methods' (in Portuguese), Instituto Superior Técnico, Lisboa.

EVALUATING SCALE EFFECTS ON EXPERIMENTAL STUDIES OF NONLINEAR UNSTEADY FLOW REGIMES THROUGH RUBBLE MOUND BREAKWATERS

Sadaf NEZAFATKHOH[(1)] & Habib O. BAYAT[(2)]

[(1)] *Post graduate Student, Civil Eng. Dept., Amirkabir University of Technology, 424 Hafez Ave., Tehran, 15914, Iran.*
sadafnez@yahoo.com

[(2)] *Associate Professor, Civil Eng. Dept. Amirkabir University of Technology, 424 Hafez Ave., Tehran, 15914, Iran*

byatt@aut.ac.ir

Abstract

Nowadays rubble mounds have become a key issue in designing inshore structures due to their economic superiority over other types of maritime structures and ease of construction. However, the rubble mound's core stability characteristic in reality is controlled by a variety of uncertainties [1] and may become a source of concern in design and analyses. In other words, as the core material's geotechnical parameters in rubble mound breakwaters do affect the armours stability, it is commonly necessary to study a scaled model of a proposed structure [2]. The scaled models in hydraulic engineering, in turn, must be based on similarity principles and usually leads to concerns over scale effects when related hydraulic model observations are to be interpreted [3]. This paper describes findings of an analytical evaluation of unsteady transitional flow regimes through coarse porous media in an attempt to develop a modelling law based on similarities between hydraulic behaviours of model and prototype. A non-linear analysis approach based on the so-called modified Forsch-Hiemer equation has been employed in developing necessary equations needed for the scale effects assessments.

Based on the Hudson equation [4] for rubble mound stability analyses, the severity of damage to the armour layer in a scaled model is assumed to be the same in model and prototype for a given set of wave characteristics. Such characteristics are commonly introduced to the model by means of either Reynolds number or Froude number. However, It has been postulated that [3], due to transitional flow regime dominating through porous core materials, viscous forces may be relatively greater and cause dissimilarities between laboratory observations and prototype performance. Therefore, the so-called scale effect should be given thorough importance when interpreting laboratory findings.

Some investigators [5 & 2] have introduced a critical Reynolds number to describe such conditions and have stated that due to relatively low permeability of the core materials, a sort of down rush flow from the inside of the structure with a Reynolds number lower than critical one may occur. That means that a relatively different wave transmission and reflection coefficient may be involved in the model, in comparison with those occurring at prototype [6 & 7].

On the other hand at very large Reynolds numbers exceeding 30'000, simulation principals in scaled model studies should be based on the Froude number criterion due to the fact that gravitational forces are dominant in the media [7]. But it was later argued that the so called critical Reynolds number might exceed 40'000 [8].

In this investigation a distribution factor – K'; based on the assumption proposed by Le'Mehaut (1965) and Keulgan (1973) [2] – has been employed to determine the grain diameter of model material in relation with that values given for the prototype. Then, flow characteristics could be simulated by means of Reynolds number and a scaling law was consequently developed. Findings indicate that besides grain diameter, other characteristics of porous media such as porosity, tortuosity and the pore shape factor do not affect the developed scaling law, in Reynolds numbers greater than 10. However at smaller Reynolds numbers, they have to be scaled with the mathematical relations proposed in this investigation.

The extent of validity of the developed scaling law has been examined using available data published by previous researchers [10, 11, 16 and 15] in the field of rubble mound structures and /or porous media.

Keywords: Scale effect, unsteady non-linear flow, Rubble mound breakwaters

References

Quinn, A. DeF.,(1972), "Design and Construction of Ports and Marine Structures", Mc Graw Hill book company,2nd Edition, USA

Hughes S. A.,(1993), "Physical Models and Laboratory Techniques In Coastal Engineering", Coastal Engineering Research Center, Waterway Experiment Station , USA, World Scientific

Hudson, R. Y., Herrmann, F. A., Sager, R. A., Whalin, R.W., Keulegan G. H., Chatham, C. E., and Hales, L. Z. (1979). "Coastal Hydraulic Models", Special Report No.5, US Army Engineer Waterways Experiment Station, Vicksburg, Mississippi

Hudson, R. Y., (1959) "Laboratory Investigation of Rubble Mound Breakwaters", Journal of Waterways and Harbourd Division, ASCE, Vol. 85, No. WW3, pp. 93-121

Dai, Y. B., and Kamel, A. M.,(1969) "Scale effect Tests for Rubble Mound Breakwaters; Hydraulic Model Investigation", Research Report H-69-2, US Army Engineer Waterways Experiment Station, Vicksburg, Mississippi

Oumeraci. H. (1984). "Scale Effects in Coastal Hydraulic Models", Symposium on Scale Effects in Modeling Hydraulic Structures, ed. H. Kobus, International Association for Hydraulic Research, pp7.10-1-7.10-7

Wilson, K.W., and Cross, R.H.(1972), "Scale Effects in Rubble Mound Breakwaters", Proceeding of the 13th Coastal Engineering Conference, ASCE, Vol. 3, pp 1873-1884

Shimada, A., Toshimi, F., Saito, S., Sakakiyama, T.,(1986) "Scale Effects on Stability and Wave Reflection Regarding Armour Units", Proceeding of the 20th Coastal Engineering Conference, ASCE, Vol.3, pp 2238-2252

Abhabhirama, A. M., Antonio A. Dinoy,(1973) "Friction Factor and Reynolds Number in Porous Media Flow", Journal Hydraulic Division, Proceedings of the ASCE, Vol. 99, No. HY6

Hannoura, A., A., Mc. Corquodale, A.,(1978) "Virtual Mass of Coarse Granular Media" Journal of Waterway, Port, Coastal and Ocean Division, ASCE, Vol. 104, No. WW2

Ahmed, N. and Sunada, D. K., (1969), Nonlinear flow in porous media, J. Hyd. Div. Proc. ASCE Vol. 95, No. HY6

Kevin R. Hall, (1991)" Trends in Phreatic Surface Motion in Rubble-Mound Breakwaters" Journal of Waterway, Port, Coastal and Ocean Engineering, Vol. 117, No. 2, , pp. 179-187

Barends, F. B. J., Holscher, P.,(1988) "Modeling Interior Process In Breakwaters"

Shokri, M., (2005),"Effective Parameters on Unsteady Nonlinear Flow in Porous Media", MSc. thesis, Amirkabir University of Tehran, Tehran, Iran

Ghasemi, A., (2006), "Hydraulic Diameter and Friction factor Evaluation in Unsteady Nonlinear Flow in Porous Media", MSc thesis, Amirkabir University of Tehran, Iran

HYDRAULIC STABILITY OF ANTIFER CUBES ON RUBBLE MOUND BREAKWATERS. STUDY ON A 3D PHYSICAL MODEL

Cristina AFONSO [(1)], M. Graça NEVES [(2)] , L. Gabriel SILVA[(2)] & A. TRIGO-TEIXEIRA[(3)]

[(1)] *WW - Consultores de Hidráulica e Obras Marítimas, S.A., Av. Conselheiro Ferreira Lobo, 23, Laveiras, 2760-032 Caxias, Portugal, cafonso@wwsa.pt*

[(2)] *LNEC - Laboratório Nacional de Engenharia Civ l, Av. do Brasil, 101,1700-066 Lisboa, Portugal, gneves@lnec.pt, lgsilva@lnec.pt*

[(3)] *Instituto Superior Técnico, Av . Rovisco Pais, 1049-001 Lisboa, Portugal. trigo.teixeira@civil.ist.utl.pt*

Abstract

Most rubble mound breakwaters have an armour of concrete blocks. The Antifer cube is generally used as a two layer of units and can be considered as randomly placed, however a pattern for the placement is followed. The first layer of units lays directly over the underlayer on a regular grid with the cube faces parallel to the slope. The second layer goes on top, either in an even (parallel to the first layer) or in an irregular jagged way. In both modes of placement the packing density can be made to vary.

First, 3D physical model tests were performed to investigate the influence of wave direction, mode of placement and packing density on stability of Antifer cubes. The head and a trunk segment of a breakwater were built in the model at a linear scale 1:50. Two wave directions were tested: orthogonal and to an angle of 50º. In total, 107 tests were completed.

Test results are discussed for the trunk and the head of the structure and compared with those obtained using empirical stability formulae. In the trunk of the breakwater and for waves orthogonal to the structure, the mode of placement has a larger influence than the packing density. However, for waves to an angle the packing density seems to play a more important role on stability than the mode of placement. On the head of the structure, the packing density appears to be the most important factor controlling stability independently of the wave direction and the mode of placement. Finally, the conclusions of the study and suggestions for further testing are presented.

1. Introduction

In very exposed areas, cubes of the Antifer type are being used to replace the more slender units in design and when maintenance is required. The Antifer is made of unreinforced concrete and shows great structural integrity. The mode of placement and packing density are key issues on hydraulic stability and armour units show different behaviour in the head and the trunk of the structure. Most of the stability tests are conducted in wave flumes which imply wave directions orthogonal to the structure. Fewer results are available for waves at an angle, since more expensive 3D model tests must be completed. Burcharth (1993) using Dolos and rock armour layers tested the head of a breakwater for waves at an angle between 45º and 135º, to conclude that the area which suffered more damage was located in a sector defined by angles between 90º and 150º, see Figure 1. This shows clearly the need for a better understanding of the stability of blocks used as armour in breakwaters in particular the Antifer cube in places that could be "thought as sheltered" in the head.

2. Model tests and model setup

Physical model tests were performed in a 3D basin to study the stability of Antifer cubes. Two modes of placement (even and jagged), two packing densities and two wave angles were considered (0º and 50º).

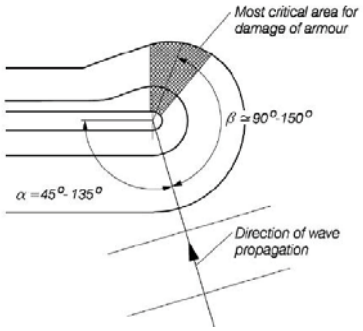

Figure 1. Illustration of critical areas for damage in the head (Burchard 1993).

A JONSWAP spectrum was taken with peak periods of T_p=1.2, 1.7 and 2.2s. Wave heights were in the range between 0,06m and 0,14m and tests were conducted with increasing wave height without model reconstruction. Figure 2 shows a plan of the experimental setting in a tank with an area of (14m × 20m). On the same picture, the two modes of placement: even and jagged are also presented. Two packing densities were considered for the even mode of placement. Four probes to measure the water level were installed: one close to the wave maker and three others in the vicinity of the structure.

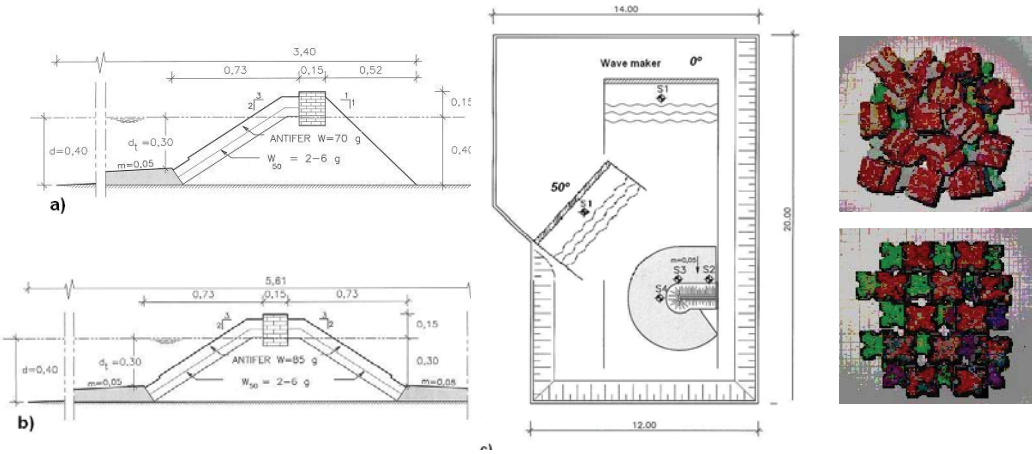

Figure 2. a) Trunk cross section b) Head cross section c) Physical model setting and Jagged and even mode of placement for block units.

Figure 3 shows the percentage of block units falling as a function of the stability number for the head and an orthogonal wave attack, where: H_s = significant wave height, Δ = relative mass density, D_n = nominal diameter. Model tests show a greater stability for the even mode of placement and higher packing density with little influence of the wave period.

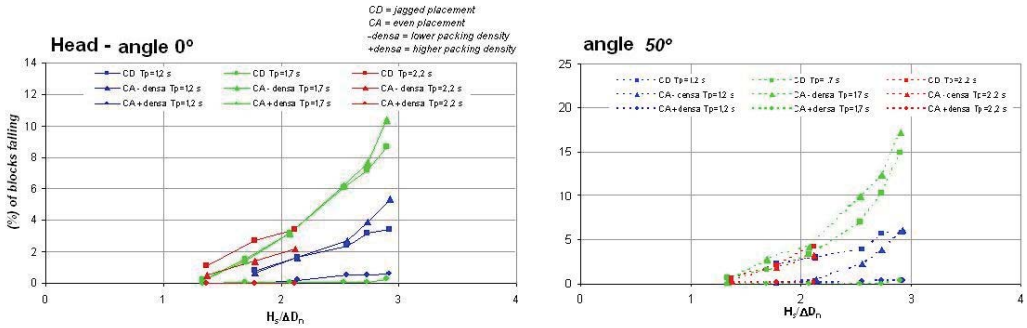

Figure 3. Percentage of antifer block units falling in the head as a function of the stability number. Set of tests for angles of 0º and 50º.

The full set of results for the trunk will be presented in the final paper, but some general conclusions can be drawn. Stability decreases when waves are at an angle. In the head stability is controlled mainly by the packing density. In the trunk, stability is controlled by the mode of placement for orthogonal wave attack and by the packing density for waves at an angle of 50º.

3. Damage and stability

It is clear from the tests performed that the damage increases for waves at an angle when compared with a frontal attack. This is mainly due to the displacement of the breaker zone to a different location. The problem is that most of the conceptual design for rubble mound breakwaters is made using semi-empirical equations deduced for waves in flumes, which means frontal attack to the structure. Figure 4 shows the comparison between the zones damaged in the head during the physical model tests and the results previously published by Burcharth (1993). Attack angles are of 0º and 50º, which correspond to angles α_1 of 90º and 140º as measured by Burcharth.

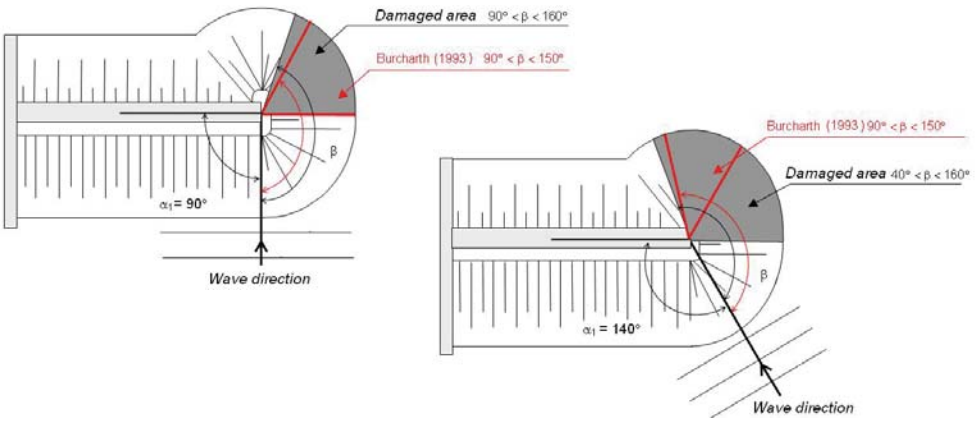

Figure 4. Damaged area in the head. Set of tests for angles of 0º and 50º. Comparison with Burcharth (1993) results.

When compared with Burcharth (1993) tests, for a frontal attack (α_1 =90º) the damaged area in the head nearly overlaps. However, for an angle (α_1 =140º) the tests show damage in a narrower sector in the leeside of the head.

Figure 5 shows an example of stability in the trunk when compared with results of Van der Meer (1999)

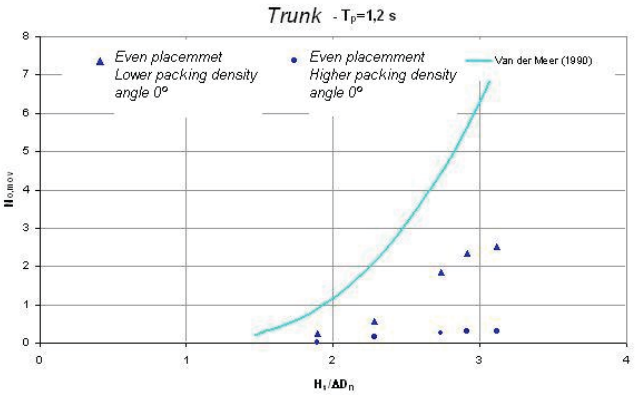

Figure 5. Model tests and results from Van der Meer (1999) for the trunk, frontal attack, even mode of placement and two packing densities.

4. Conclusions

In the conceptual design of rubble mound breakwaters using Antifer cubes in the armour layer and according to the model tests performed two main conclusions may be drawn: a) If moderate overtopping may be permitted and the highest waves attack the structure head-on the regular mode of placement shall be used in the trunk of the structure; b) If the highest waves may attack the structure from various angles an higher packing density shall be used and the mode of placement (either regular or jagged) decided based upon the overtopping permitted.

References

Brucharth, H. F., 1993. The design of breakwaters. Department of Civil Engineering, Aalborg University, Denmark.

CEM, 2006, "Coastal Engineering Manual. Chapter 5 - Fundamentals of Design. Part VI. U

Van der Meer, J.W., 1999. Design of concrete armour layers, Proc. Coastal Structures 1999, Santander, Spain. Losada (ed.), Balkema, Rotterdam, pp. 213-221.

Afonso, C., Neves, M. G., Silva L., Trigo-Teixeira, A., 2007. Influência da Obliquidade da Agitação e da Densidade de Colocação dos Blocos Antifer na Estabilidade de Obras Marítimas de Talude. 5as Jornadas Portuguesas de Engenharia Costeira e Portuária. Lisboa.

GEOTEXTILE SAND CONTAINERS USED FOR SUBMERGED BREAKWATER: SCALING EFFECTS AND STABILITY

Enrica MORI [(1)], Claudia D'ELISO [(2)] & Pier Luigi AMINTI [(3)]

[(1)] Ph.D. Student, Department of Civil and Environmental Engineering, University of Florence, Via S. Marta 3, Florence, 50139, Italy. enrica.mori@dicea.unifi.it

[(2)]Ph.D., Department of Civil and Environmental Engineering, University of Florence, Via S. Marta 3, Florence, 50139, Italy. cldelis@dicea.unifi.it

[(3)] Professor, Department of Civil and Environmental Engineering, University of Florence, Via S. Marta 3, Florence, 50139, Italy. aminti@dicea.unifi.it

Abstract

Stability of Geotextile Sand Containers has been studied through 2D laboratory tests, with attention to scale effects regarding textile features. The tests performed provide results on the influence of size of containers and textile in breakwaters made of geotextile sand containers under wave attacks.

1. Introduction, objective and methodology

Stability of geotextile sand containers (GSCs) depends on several factors, more than classic rubble mound structures. In fact, the bags can be made with various shapes, different textiles, and they vary their shape during wave attacks (Recio & Oumeraci, 2007). Moreover, for GSCs long period field experiences are not available (Lawson, 2006). As a consequence, in order to investigate the stability of this kind of structures a large amount of experiments are needed.

The objective of the set of experiments presented in this work is therefore to investigate the stability of submerged breakwaters made with GSCs compared with rubble mound ones, and to understand scaling effects related to the textile.

In a near full scale, the weakest textile on the market can be used, but with small scale (1/20÷ 1/30) scaling effects could be relevant.

2. Laboratory tests on Geotextile Sand Containers

The laboratory tests have been performed in the wave-current flume of the Civil and Environmental Engineering Department of the University of Florence, which is 50 m long, 0.8 m wide and 0.8 m deep. The upper limit of the generated wave heights is approximately 0.20 m at 1 Hz frequency. Peak periods up to 2 s can be reproduced in the flume.

Two different fabrics (Tab. 1) are used in each test, with half channel (40 cm wide) with bags made of fabric 1 and the other of fabric 2. Three different breakwaters have been built: barrier A made of bags 380g weigh, barrier B made of bags 250g weigh, and barrier C made of rocks with D_{50}=225 mm.

Each barrier is tested with 9 wave attacks combining 3 significant wave heights ($H_{s,0}$ = 6.0/11.0/16.0 cm) and 3 wave steepnesses ($H_{s,0}/L_0$ = 0.02/0.04/0.06).

The tests are lasting 2 hours. After each test the structure is reshaped at its initial geometry. Measurements during the tests include: (i) water levels at different locations along the wave flume by using 10 common wave gauges, (ii) displacement of bags over time recorded every 60 s by a camera and (iii) initial and final shape of the structure using three cameras and a profiler.

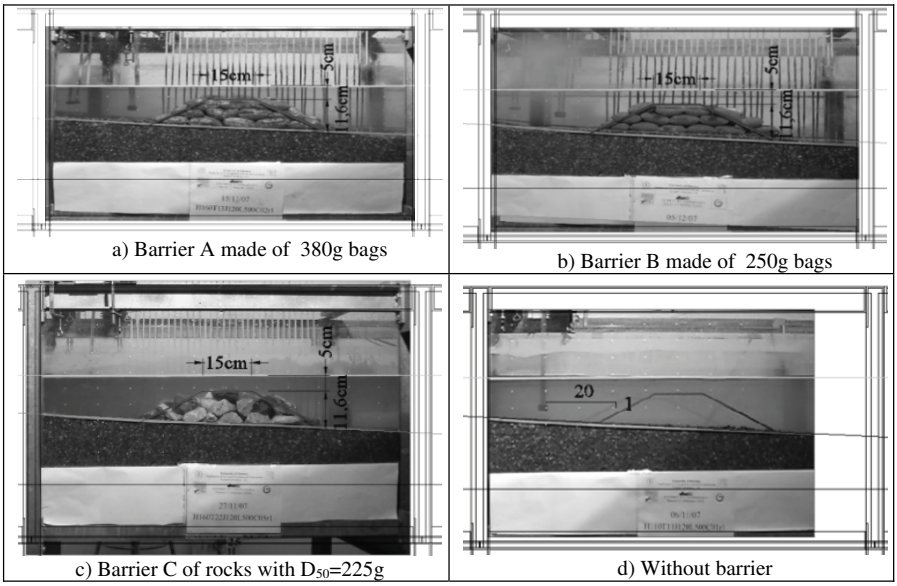

a) Barrier A made of 380g bags

b) Barrier B made of 250g bags

c) Barrier C of rocks with D_{50}=225g

d) Without barrier

Figure 1. The four tested configurations in the wave flume.

Table 1. Technical values of the two used textile: MD= machine direction CMD= cross machine direction .

	Mass per unit area [g/m²]	Max tensile strength (MD) [KN/m]	Max tensile strength (CMD) [KN/m]	Elongation at max tensile strength (MD) [%]	Elongation at max tensile strength (CMD) [%]
Type 1	30	0.8	0.3	35	40
Type 2	150	6.0	10.0	60	40

3. Data analysis and preliminary results

The test plan has been successfully set up in order to investigate: (i) influence of wave height and period on GSCs stability, (ii) differences between traditional rubble mound structures and GSCs in terms of wave transmission and set-up, (iii) importance of scaling effect of textile on the stability (Fig. 2). Preliminary analysis of collected data indicates that the performed tests are consistent, reproducing stable structures under the lower wave attacks, and instable ones under the higher wave attacks.

In figure 3.a), as an example, the amount of displaced bags during the 2 hr of test are depicted, with highest wave attack H_s =16cm and T_P =2.2s at the generation depth (50 cm). In figure 3.b) wave transmission over the barrier for the same wave attack is plotted over time.

Sand bag stability is strongly related with their weight (Figure 3a). Therefore, after instability has taken place, the transmission coefficient becomes sensibly lower in the test with the heavier than with the lighter sand bags (around 10%),while at the beginning of the test they almost assume the same value (0.5). Despite the amount of unstable bags (60%) the protection level of the barrier is not totally compromised (Figure 3b).

The instability process is divided in three phases (Figure 3a): the percentage of displaced bags firstly increases more than linearly (t=0-20 minutes), in a second phase almost linearly (t=20-80 minutes) and finally remains constant (t>80 minutes).

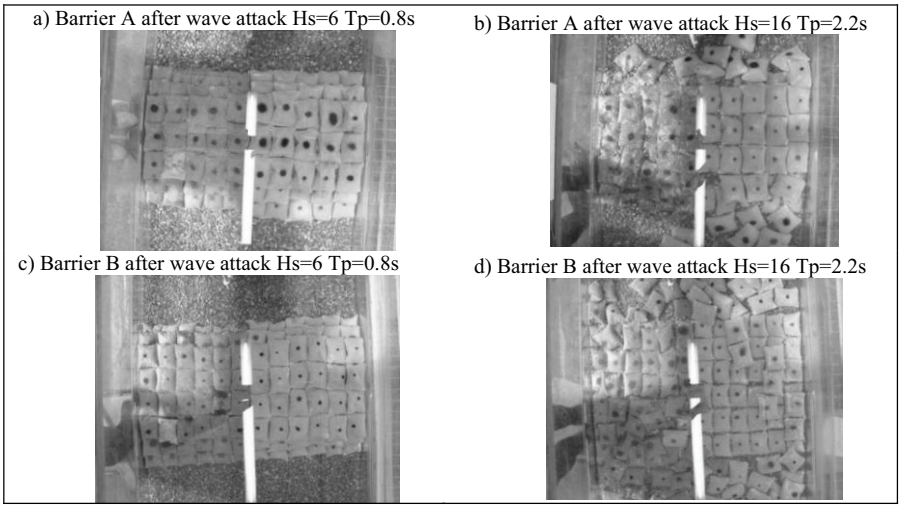

Figure 2. Comparison of final shape of the two barriers with the highest and the lowest wave attack after 2 hr of test. H_s and T_P are measured at the generation depth (50 cm).

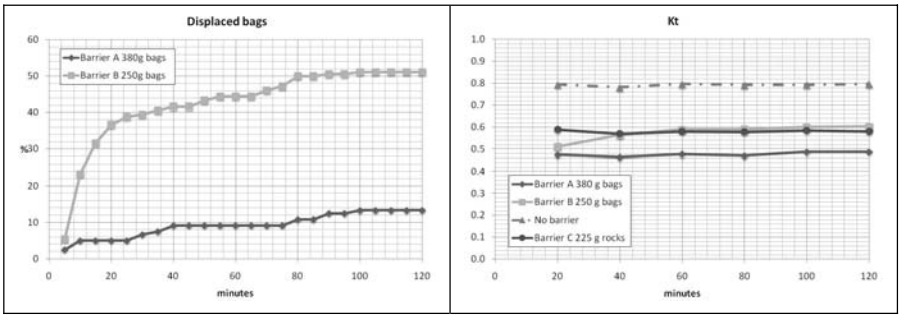

Figure 3. On the left, a) ratio between the percentage of bags displaced during the test and the highest wave attack. On the right, b) the related transmission coefficients.

4. Concluding remarks

The tests performed provide a consistent data set in order to investigate the influence of different breakwaters made of geotextile sand containers under wave attacks.

References

C. R. Lawson 2006. 'Geotextile containment for hydraulic and environmental engineering'. *8th International Conference on Geosynthetics*, YOKOHAMA, Millpress.

Recio J. and Oumeraci H. 2007. 'Effect of deformations on the hydraulic stability of coastal structures made of geotextile sand containers', *Geotextiles and Geomembranes*, Volume 25, Issues 4-5, August-October 2007, Pages 278-292.

A MULTI LAYER COASTAL STRUCTURE TO CAP CONTAMINATED MATERIAL

V. CAMPANARO[(1)], G.R. TOMASICCHIO[(2)], F. D'ALESSANDRO[(3)]

[(1)] *Technical Director, Enviromental Office of the Town of Bari, v.campanaro@comune.bari.it*

[(2)] *Full professor, University of Salento, via per Monteroni, Lecce, 73100, Italy. roberto.tomasicchio@unile.it*

[(3)] *PhD, University of Salento, via per Monteroni, Lecce, 73100, Italy. dalessandro@dds.unical.it*

1. Introduction

Contamination of coastal areas due to industrial activities represents an ongoing threat for the environment. This is very frequent in the case of the industrialized regions of the world; in fact, contaminated spots have been often identified at several locations along industrialized coastlines.

The paper presents aspects related to the design and verification of a contaminated material capping project along a shoreline. The coastline of interest is called Torre Quetta and is located just south of the urbanized area of Bari, along the Adriatic coast of Italy.

This unique project has been started in order to obtain a recreational area where a contaminated area exists. The end of construction of the new beach is scheduled by the end of spring 2008. The coastal area has been contaminated by the land disposal of asbestos from the residuals of a factory producing concrete pipelines for aqueducts. The factory stopped its activity at the end of seventies. After that time, the consciousness about the presence of pollution at Torre Quetta went lost. In fact, the contaminated area was rehabilitated with a nourishment project and officially opened to the recreational use of public in 2000 (Fig. 1). After an initial use by the inhabitants, the detection of the contaminated material was clear and the area was immediately closed to the public.

The present public administration intends to re-open the beach area to the public by the summer 2008.

Figure 1. Photograph of the coastal area Torre Quetta (2000)

2. Design and verification

During the sixties, Torre Quetta was the scene of industrial activities which generated contamination along the coastline. When the pollution was detected, the area was classified as a site of potential risk to

human health and to the environment. In fact, asbestos waste generating pulmonary cancer was found both in the terrestrial and in the near-shore sea environment.

Following an extensive research program and several design alternatives, the Office for the Environment of the town of Bari has selected the in-situ material capping method together with a beach nourishment intervention in order to remediate the asbestos and to preserve the recreational use of the area.

The capping structure has a longitudinal extension of 2.5 km. The coastline will be seaward advanced for about 30 m. The capping structure will have cross-shore a submerged extension from 10 to 20 m depending on the local bathymetry. The design includes a series of detached submerged breakwaters to make stable the new beach material.

Preliminary extensive field investigation program and research and design process have been carried out with the purpose of identifying the particularities of the hydrodynamic field and sediment transport for various combinations of incident waves and water levels.

The design process has considered the wave induced circulation and morpho-dynamic studies conducted by means of numerical models for different scenarios. In fact, the main goals to be reached have been to ensure water quality characteristics for bathing of human beings and to obtain an acceptable lifetime of the future beach.

The project has been carried for the following aspects: (1) the contaminated materials are located in shallow water - 0 to 3.0 m water depth - along the shoreline, both inside and outside of the surfzone; (2) the project area is subjected to the combined action of waves and currents; (3) given the future use of the area, the capping structure and the beach material must allow the recreational and bathing use to the town inhabitants; (4) the structure of the multi-layer cap has to perfectly seal and prevent the migration of dangerous materials.

The design process has included various armouring options for the upper layer of the composite capping structure, depending on the dominant hydrodynamic forces. The final design includes: (1) a reinforced geo textile installed directly on the contaminated material at the bottom; (2) about 30 cm layer of sand and gravel; (3) a protective rubble mound submerged toe at a water depth of about 2 m; (4) a series of protective submerged detached rubble mound breakwaters to reduce the wave action and to avoid large loss of the new beach material.

3. CONCLUSIONS

The paper intends to describe the details of the problem encountered and the solutions that have been proposed through the time. In particular, the results from different adopted design scenarios will be discussed. Reference to the studies with numerical models will be given.

The paper aims to represent a source of experience for designers and researchers who will face similar problems in the future.

Keywords
Contaminated material, Beach nourishment, Capping structure, Detached submerged breakwaters

A NEW 2D STRATEGY FOR MEASURING THE EVOLUTION OF A SANDY BOTTOM

L. CAVALLARO [(1)], A. MARINI[(2)], R. E. MUSUMECI[(2)] & G. PARATORE[(3)]

[(1)] University of Messina - Dept. of Civil Engineering, C.da di Dio – 98166 Messina, Italy. E-mail lcavallaro@ingegneria.unime.it

[(2)] University of Catania - Dept of Civil and Environmental Engineering, V.le A. Doria 6 – 95125 Catania, Italy. E-mail rmusume@dica.unict.it

[(3)] University of Reggio Calabria - Dept of Mechanic and Material, via Graziella, loc. Feo di Vito – 89060 Reggio Calabria, Italy. E-mail giovanni_paratore@hotmail.it

Abstract

In this paper a non-invasive measurement system for determining sandy bottom evolution forced by wave flows is presented. To overcome some limits of previous contactless techniques, a laser sheet is produced directly within the flow by bringing the laser beam under the undisturbed water level. This new strategy has been here applied in order to obtain a contactless and dynamic measure of the evolution of a sand pit induced by waves. The results of the preliminary tests carried out in the wave flume of the Hydraulic Laboratory of Catania (Italy) are also presented.

1. Introduction

The analysis of a sandy bottom evolution in a wave dominated flow has been usually conducted by focusing the attention on the equilibrium profile or, due to the difficulties in performing non-invasive measurements, gathering data only at discrete time steps. Indeed, bottom data have been previously gathered by using mechanical profilers or traditional hydrometers, which are able to provide only a coarse and discrete resolution in time and space.

Some previous works tried to face such a problem by using structured light coupled with an acquisition system (Faraci et al 2000, Faraci & Foti 2001). In the mentioned works a laser sheet was generated outside a wave tank and projected onto the bottom through a glass window. Though useful results were obtained, the proposed technique seemed to introduce some unwanted refraction problems. To overcome such limits the present work shows the results concerning a sandy bottom evolution obtained by generating the laser sheet directly within the flow, i.e. by bringing the laser beam under the undisturbed water level.

The present contribution shows the preliminary results of an experimental campaign on the morphodynamics of a trench.

2. Measurement technique

The problem of the investigation of the evolution of a sandy bottom is here solved by using a computer vision system and a suitable lighting source. Such an approach appears to be particularly appropriate when contactless measurements are required as in the case being. Arbitrary selection of a light source often gives rise to unsuitable results due to poor contrast, undesired shadows or unpredictable reflections. Among other source, here ‘structured light’ has been chosen. Indeed, a flat sheet of laser light projected onto an object produces a reflected light that follows the contour of the object itself and that can be suitably used for various measurements.

Such a procedure is here applied in order to obtain a contactless and dynamic measure of the

evolution of a sand pit as induced by waves. The experiments were carried out in a flume with a cohesionless horizontal bottom in which a pit is obtained by using an appropriate mould.

The light sheet optically slices the pit creating a cross-sectional image that can be recorded through a video camera and then analyzed to obtain the desired dimensions. In order to do that, suitable image processing procedures must be performed. In particular the correspondence between the "image units" and the object dimensions must be preliminary stated. This calibration process was carried out by means of a tool created on purposely. Figure 1 shows an example of the "structured light" projected over a sand pit section. From the image, it can be noticed that small bed perturbation are generated by wave motion, and though quite small, O(1÷5 cm), are accurately recovered by the measuring system.

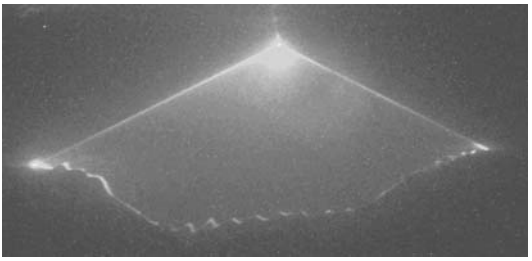

Figure 1. The laser sheet projected over trasversal section of a pit.

To solve the unwanted refraction problems a new approach has been adopted in order to match two needs, i.e.: (i) to leave the laser source outside the flume and (ii) to bring the beam under the undisturbed water level. Precisely a new waterproof pipe equipped with a cylindrical lens at one end was developed. To put the camera under water level a waterproof box was used. Figure 2 shows the experimental setup and Figure 3 shows some details of the waterproof pipe system.

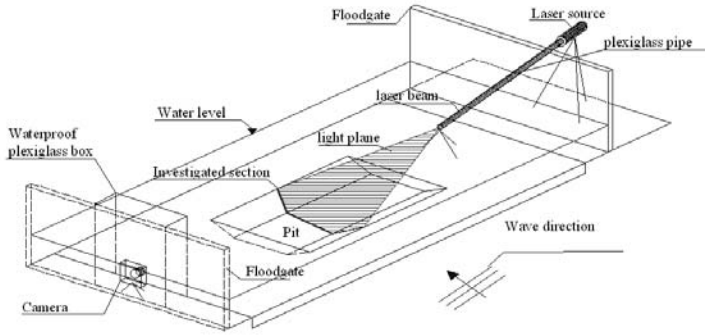

Figure 2. Setup of the experimental apparatus.

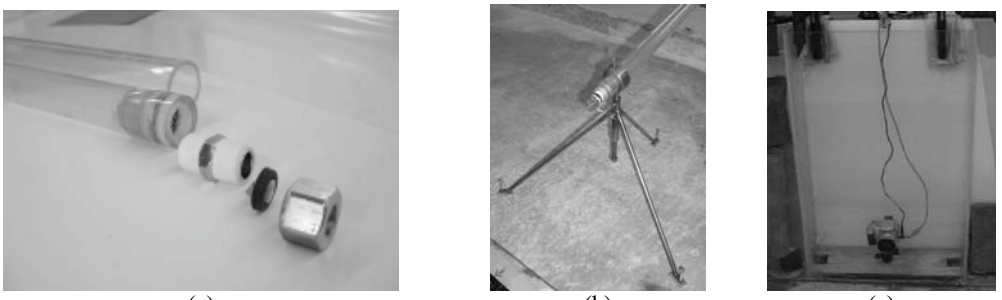

(a) (b) (c)

Figure 3. (a) Components of the pipe system; (b) Particular of the pipe system; (c) Waterproof box for the camera

In order to convert the acquired data from image units to spatial units a calibration procedure is required. Figure 4 shows the adopted calibration tool which reproduces the shape of the initial bottom profile.

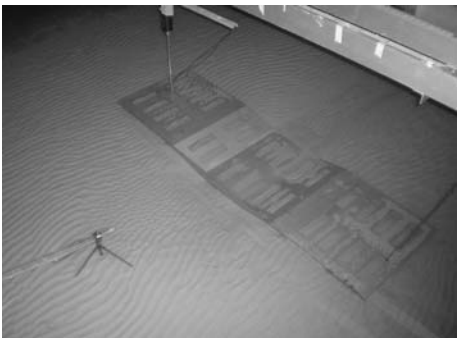

Figure 4. The adopted calibration tool.

3. Experimental results

All the experiments have been performed in the wave flume of the Hydraulics Laboratory of the University of Catania (Italy) which is 3.6 wide, 18 m long and 0.8 m deep, showed in Figure 5. The new setup, showed in Figure 2, gives a measuring section longer than 1 m, whereas such types of techniques have been usually applied to section much smaller, O(30 cm). The bottom of the tank is covered by a quartz sand with a diameter D_{50}=0.25 mm.

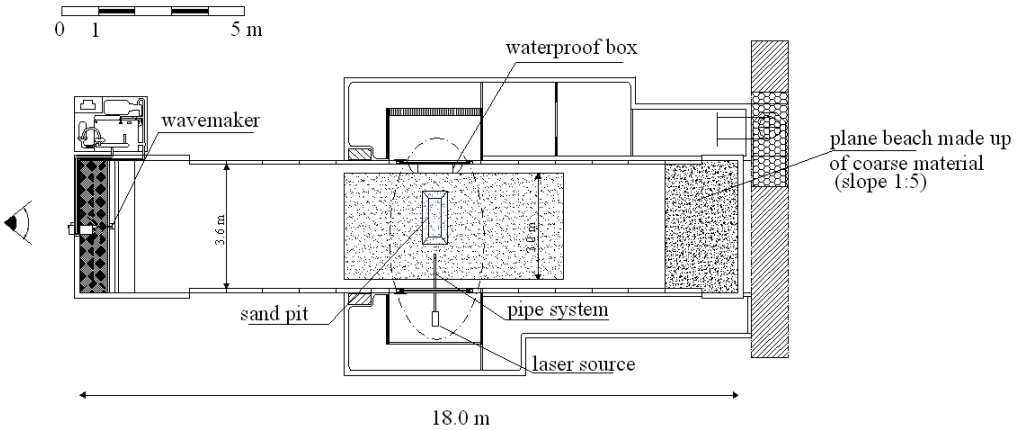

Figure 5. The wave flume of the Hydraulic Laboratory of the University of Catania (Italy).

Preliminary tests have been performed with different values of water depth and wave height in order to evaluate the accuracy of the proposed technique in different conditions of sediment transport. More in details, Table 1 shows the average water depth h, the wave height H, the wave period T and the duration d of each experiment.

Figure 6 shows the bottom profile at different time steps obtained during test n. 3. Even though during such an experiment the bottom evolution was very fast the proposed technique allows to reproduce the profile with adequate accuracy.

Table 1. Control hydrodynamic parameters: average water depth h, wave height H, wave period T and duration d of each experiments.

Exp. n°	h	H	T	d
	[cm]	[cm]	[s]	[min]
1	25	5,73	1	150
2	30	8,09	1	230
3	28	12,96	1	185
4	28	10,30	1	360

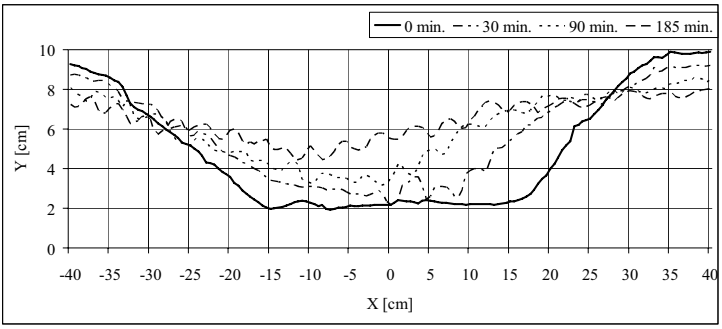

Figure 6. Bottom evolution as obtained by using the proposed measurements technique.

4. Conclusion

An innovative, non-invasive and accurate measurements technique aimed at evaluating the morphodynamics of a sandy bottom has been presented.

The proposed technique is based on computer vision methodologies and allows to reproduce the bottom evolution within short time steps.

To light up the bottom profile a laser sheet is created directly inside the water by bringing the laser beam beneath the undisturbed under water level through a waterproof pipe. This simple and economical solution allows to avoid unwanted refraction problems.

Such a technique has been here applied to evaluate the wave induced morphodynamics of sand pit.

The results obtained from the preliminary tests carried out in the wave flume of the University of Catania (Italy) have shown that the proposed technique allows to reproduce the bottom evolution with adequate accuracy, both in space and time.

Acknowledgments

This work has been partly founded by SIGMA s.r.l (Contract inside the framework of POR Sicilia-Misura 3.14) and by the HYDRALAB-III in the framework of the Joint Research Activity SANDS (contract no. 0224411(RII3)).

References

Faraci C., Foti E., Baglio S. 2000, 'Measurements of sandy bed scour processes in an oscillating flow by using structured light', *Measurements*, 28, 159-174.

Faraci C., Foti E. 2001, 'Evolution of small scale regular patterns generated by waves propagating over a sandy bottom', *Physics of fluids*, 13, 6, 1624-1634.

Large-scale laboratory measurements of suspended sand concentration induced by non-breaking waves with acoustic backscatter technique

ALIREZA AHMARI [(1)], JOACHIM GRUENE [(2)] & HOCINE OUMERACI [(3)]

(1) *Coastal Research Centre (FZK) of Leibniz University Hannover and Technical University Braunschweig, Merkurstrasse 11, 30419 Hannover, Germany, ahmari@fzk.uni-hannover.de*

(2) *Coastal Research Centre (FZK) of Leibniz University Hannover and Technical University Braunschweig, Merkurstrasse 11, 30419 Hannover, Germany, gruene@fzk.uni-hannover.de*

(3) *Coastal Research Centre (FZK) of Leibniz University Hannover and Technical University Braunschweig, Merkurstrasse 11, 30419 Hannover, Germany, h.oumeraci@tu-bs.de*

Abstract

Experiments with movable sand bed were carried out recently in the Large Wave Channel (GWK) of the Coastal Research Centre (FZK) to measure the suspended sediment concentrations (SSC) under non breaking waves using multi frequency acoustic backscatter sensors (ABS), optical sensors (OBS) and transverse suction system (TSS) as shown in Fig. 1. First experiments are performed by different participants of the Joint Research Activity SANDS of the EC-supported Integrated Infrastructure Initiative HYDRALAB-III, further experiments are performed within the BMBF supported project ModPro. The proposed paper focuses on recording and estimation of vertical distribution of temporal-spatial fluctuation of suspended sediment concentration using a multi frequency acoustic backscatter sensors (ABS) and includes a comparison of vertical sediment distribution measured by ABS with collecting profiles of time-averaged suspended sediment concentration using the transverse suction system (TSS).

1. Introduction

Measuring of suspended sand concentration is continuously increasing in recent years. There is a strong requirement to record and analyse the suspended sand transport as the major part of estimating the total sediment load due to waves, which is important for several coastal engineering topics along the coastlines. New measuring devices (e.g. acoustic backscatter sensors) are able to measure both vertical distribution of sediment concentration and particle size in time and space where the traditional devices (e.g. suction systems and carousel sampler) are based on time- or depth-averaged principle.

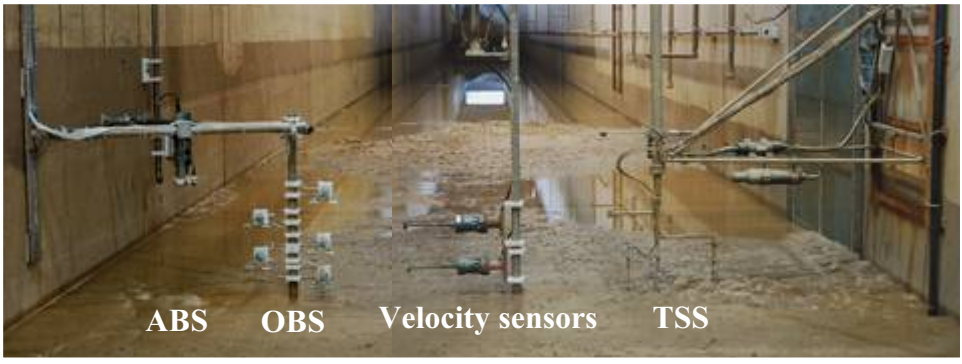

Figure 1. Sensors installed in the GWK for measuring the suspended sand concentration

The objective of using acoustic backscatter sensors is to measure the vertical distribution of suspended sediment concentration and size with sufficient spatial and temporal resolution to study the turbulence and intra-waves processes, which, coupled with the bed form morphology observations, would provide new measuring capabilities to advance the understanding of sediment entrainment and transport (Thorne and Hanes, 2002).

In the work, described in this paper the main focus was on ABS data, recorded with an "Aquascat" - sensor. This multi frequency acoustic backscatter sensor (ABS) uses three acoustic transducers operating at 1.0, 2.0 and 4.0 MHz, which were mounted on the mounting bracket at 0.68 m above the sand bottom. As the acoustic signals are omitted down towards to the bed, suspended particles backscatter a part of the acoustic energy and the bed generally returns a strong echo.

The system operates in a monostatic mode, which means that both transmitting and receiving occur on the same transducer. The three transducers were interleaved with the frequency of 128 Hz (Profile rate) and the backscattered signals were averaged over 32 profiles (profiles per average), which provided a temporal resolution of 0.25 s. The number of bins was 100 and the operating range 1.0 m, which provided the spatial resolution of 0.01 m.

To calculate the particle size and concentration *Kt*-value (system constant) has to be known for each frequency, which requires a system calibration. The calibration takes place in a calibration tank (Ø 0.4 m by 2.1m), where water and sediment are re-circulated and the transducers are positioned in the centre of the tank pointing downwards.

To compare the recorded values of suspended sediment concentrations by ABS a Transverse Suction System (TSS) was also used to measure simultaneously the time-averaged concentration values. The system consists of four suction tubes, which were mounted at different levels. Principle is based on sucking samples through the intake nozzles in a direction normal to the ambient flow. Table 1 shows instrumentation and sampling summary used in tests.

Table 1: Instrumentation and sampling summary for tests

Parameter	Instrument	Remark
Velocity	Electro-magnetic (NSW) current meter	Sampling rate range: 40 Hz
Particle size and concentration	ABS: 1 MHz, 2.0 MHz, 4.0 MHz	Number of bins: 100 Spatial resolution: 0.01 m Temporal-resolution: 0.25 s
	TSS	Extraction of water and sediment: 30 minutes. The nozzle speed: 1.5 m/s.
Waves	Wave gauges	Analog output, amplification about 1.3 Volts/m. Sampling rate range: 40 Hz

Results from one performed experiment (irregular waves from Jonswap-spectra; SWL = 3.5 m above sea bottom, Hs = 1.2 m, Tp = 6.5 s) are shown exemplarily in Fig. 2, where the time histories for a time section of 1500 seconds are plotted for the free surface elevation (h), the cross-shore horizontal velocity (vx) at 20 cm above bottom and the suspended sediment concentrations at 10, 20, 45 and 60 cm above sea bottom. Furthermore the time-averaged concentrations from the simultaneously used suction system (TSS) at two levels above bottom are plotted for comparison. Fig. 3 shows exemplarily the temporal changes of vertical profile of suspended sand concentration above sea bottom for a time period of 9 s.

References

P. D., Thorne, D. M. Hanes, 2002. "A review of acoustic measurement of small-scale sediment processes" *Continental Shelf Research, Volume 22, Issue 4*, Elsevier Science Ltd., 603–632

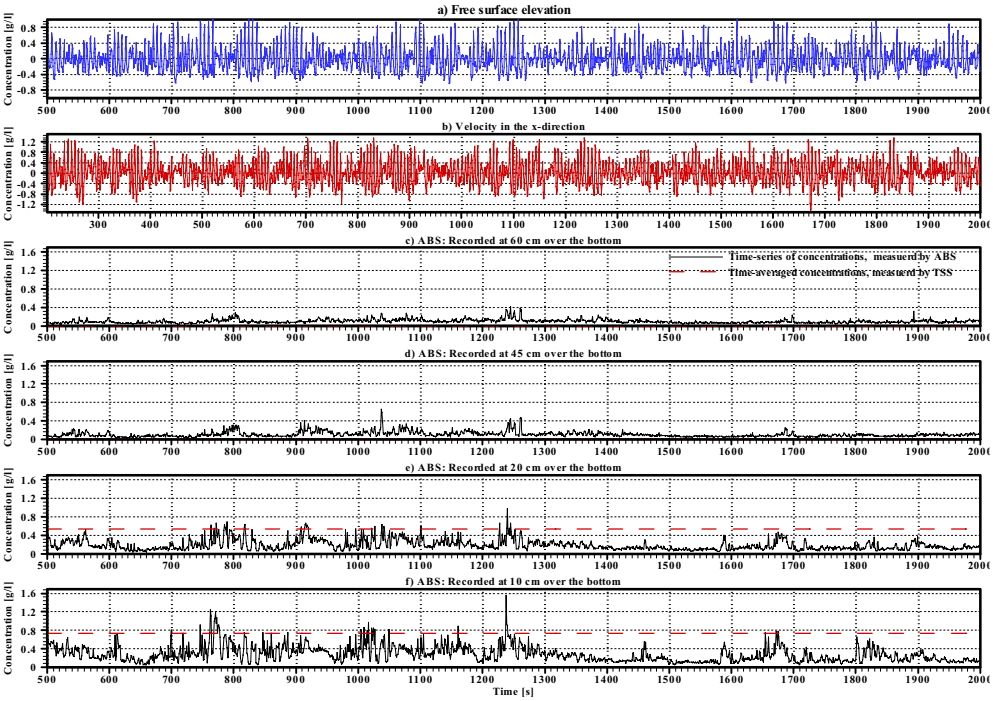

Figure 2. Time-series measurements of the following: (a) free surface elevations (h), (b) cross-shore horizontal velocity (vx) at 20 cm above bottom and (c, d, e and f) suspended sediment concentrations at 10, 20, 45 and 60 cm above the sand bed including time-averaged concentrations recorded by TSS at 10 and 20 cm above bottom.

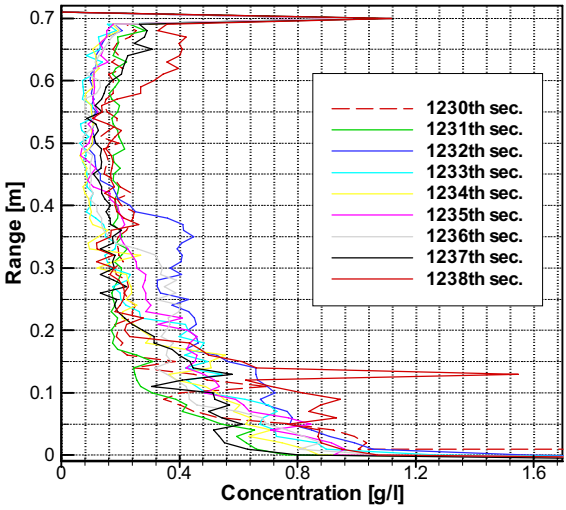

Figure 2. Vertical distribution of suspended sand concentration above sea bottom averaged during 9 s

CROSS-SHORE BEACH EVOLUTION LARGE-SCALE LABORATORY TESTS WITH IRREGULAR WAVES

Joachim Grüne [(1)], Reinold Schmidt-Koppenhagen [(2)] & Zeya Wang [(3)]

[(1)] *Dipl.-Ing., Coastal Research Centre (FZK) of Leibniz University Hannover and Technical University Braunschweig, Merkurstrasse 11, 30419 Hannover, Germany, E-Mail: gruene@fzk.uni-hannover.de*

[(2)] *Dipl.-Ing., Coastal Research Centre (FZK) of Leibniz University Hannover and Technical University Braunschweig, Merkurstrasse 11, 30419 Hannover, Germany, E-Mail: sk@fzk.uni-hannover.de*

[(3)] *M.-Ing., Coastal Research Centre (FZK) of Leibniz University Hannover and Technical University Braunschweig, Merkurstrasse 11, 30419 Hannover, Germany, E-Mail: wang@fzk.uni-hannover.de*

Abstract

The paper describes large scale laboratory tests on beach evolution due to erosive irregular wave climate. The tests are part of an investigation on scaling results from different laboratory scales from 1:1 to 1:6 in different wave facilities.

1. Model set-up and test programme

Scaling of results from physical models dealing with beach erosion still is a complicated procedure due to strong scale effects both from breaking wave impacts and from simulating the beach material. One of the goals of the Joint Research Activity project SANDS in the EC-supported Integrated Initiative HYDRALAB-III is to improve the scaling procedure by comparing test results performed in different scales.

One of the test series is being performed in three European laboratories, in each with same boundary conditions but with different scales: based on tests in the Large Wave Channel GWK as prototype scale 1:1 at CIEM/UPC in scale 1:1.9 and at Deltares (former Delft Hydraulics) in scale 1:6. The waves in all laboratories were generated as identical time histories adapted to each scale. The proposed paper focuses on the tests performed in the GWK of the FZK. The longitudinal section of the installed sand bed and beach is shown in Fig.1 and Fig. 2 gives an image of the beach after the tests

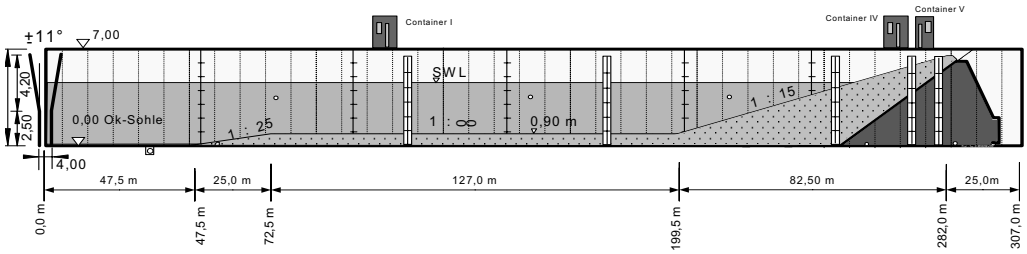

Fig. 1 Longitudinal section of installed sand bed and beach in the GWK for beach erosion tests

Fig. 2 Photo of the beach after the erosion tests

2. First results

The tests with a uniform slope of 1:15 at the beginning were carried out with the wave parameters H1/3 = 1.0 m and Tp = 5.6 s and a still water level SWL = 3.2 m above horizontal sand bed. Fig. 3 shows the beach profiles recorded in time intervals from starting with uniform slope until reaching a certain equilibrium beach profile after 23450 waves, which correspond to a total duration of 32,5 hours.

In Fig. 4 some parameters for schematizing the beach profile during the evolution process are defined. The time depending evolution is shown exemplarily with some significant parameters of the bar in Fig. 5 and 6. In Fig. 5 the horizontal positions (distance of bar to juncture of SWL and original uniform slope) of the crest of the bar (delta l bar) and the foot section of the bar are plotted versus the duration of the wave attack.

The vertical position of the crest of the bar is plotted in Fig. 6 versus the duration of the wave attack, both as crest level below the still water level SWL (delta z bar) and as crest height above the original uniform beach profile. More detailed analysis will be presented and discussed in the final paper.

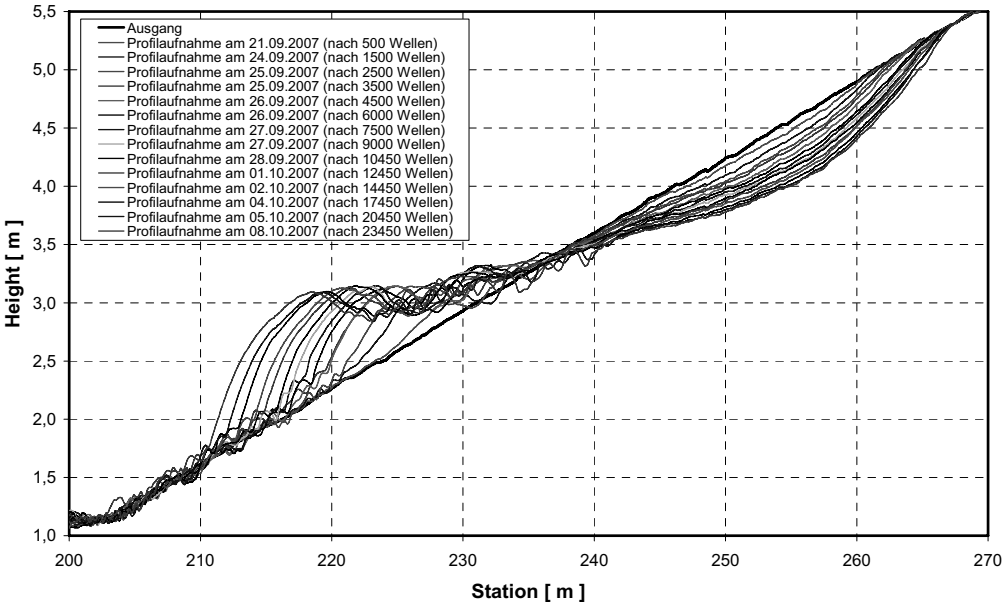

Fig. 3 Beach profiles recorded during the erosion tests in the GWK of a total duration of 32,5 hours

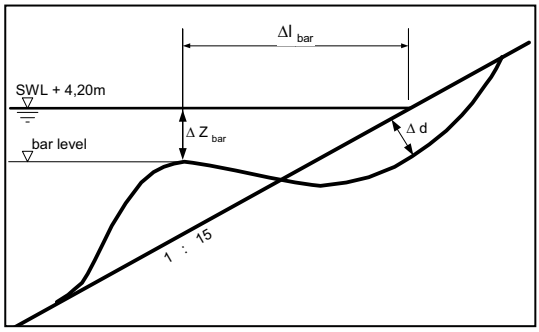

Fig.4 Definition of parameters for schematizing the beach profile

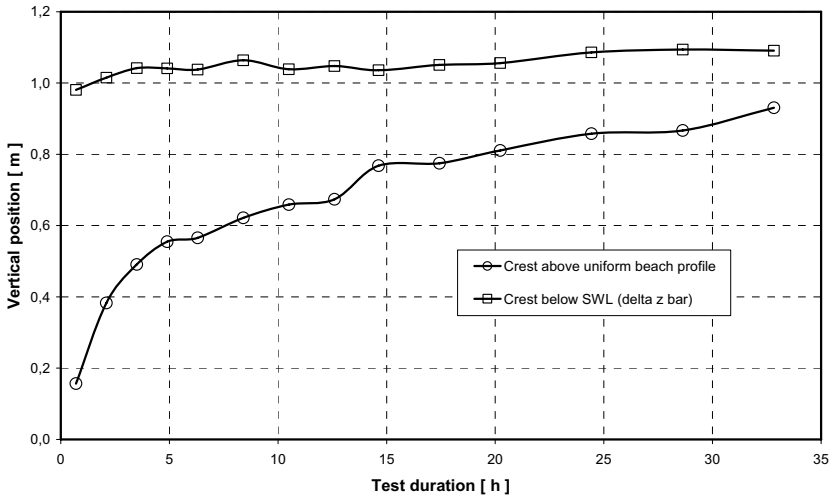

Fig. 5 Vertical positions of bar crest during the beach evolution

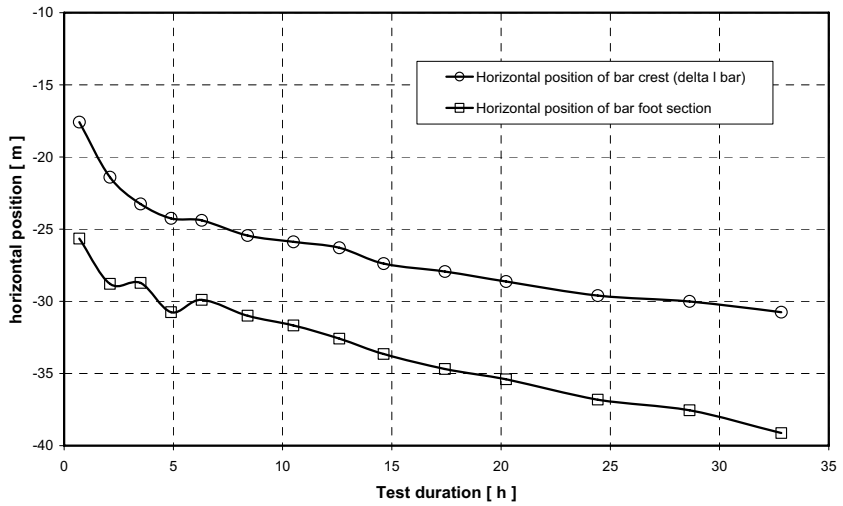

Fig. 5 Horizontal positions of bar crest and bar foot section during the beach evolution

Acknowledgment

The work described in this publication was supported by the European Community's Sixth Framework Programme through the grant to the budget of the Integrated Infrastructure Initiative HYDRALAB III, Contract no. 022441 (RII3)

MOBILE-BED TESTS. THE SANDS EXPERIMENTS PERFORMED AT THE CIEM

Cáceres, I.[1], Alsina, J.M.[2], Sánchez-Arcilla, A.[1]

[1] *Laboratori d'Enginyeria Marítima, Universitat Politècnica de Catalunya. c/Jordi Girona 1-3, D1, Campus Nord. 08034 Barcelona (Spain). email: i.caceres@upc.edu, agustin.arcilla@upc.edu*
[2] *Coastal Engineering Research Center, The University of Queensland. St. Lucia, Queensland, 4072. email: josealsina@uq.edu.au*

1. Introduction

Present mobile bed tests are designed using scaling laws which are only valid for a "part" of the physical problem (Hughes, 1993) as it is virtually impossible to ensure that the relative magnitudes of all dominant processes are the same in the model and prototype. Consequently results obtained from a scaled physical model may not compare well with reality. Nevertheless, physical modelling remains a useful qualitative tool in understanding the dominant forces and response mechanisms of sediment. Moreover, there is still many important features in the sediment transport process which the state-of-art equipment are not able to observe, such as turbulent and intra-wave fluid-sediment interactions over the entire boundary layer. Most of the available observational equipment disturbs the water and sediment fluxes, has limited accuracy and limited efficiency. Because of this the actual uncertainties in hydraulic experiments lead to results which are poorly constrained and contain unquantified errors. Large-scale facilities are better suited (due to smaller scale effects and covering better the suspended transport regime) for morphodynamic tests although requiring further scientific and engineering advancement and experiencing limitations from an instrumentation standpoint.

Within this context the paper will present the acquired data in the CIEM flume within the SANDS project. SANDS is a Joint Research Activity within the EC Framework 6 Integrated Infrastructure Initiative, HYDRALAB-III (http://www.hydralab.eu). Among the objectives of this project the next aims can be found:

- Improve the scaling and analysis procedures and achieve more "repeatable" and compatible movable bed tests (with known error bounds).
- Innovate data capture and analysis using advanced optical and acoustic non intrusive probes.
- Develop new protocols for the design and interpretation of the movable bed test results.

To achieve these goals a set of experiments are being performed in the LARGE WAVE CHANNEL (GWK) of the Coastal Research Centre (FZK) in Hannover, in the Large Wave Flume CIEM of the Maritime Engineering Laboratory (UPC) in Barcelona and in the Scheldt flume of DELFT Hydraulics in Delft.

This paper deals with the analysis of the data obtained within the SANDS experiments performed in the CIEM flume focused to improve the morphodynamic measuring system and to gain a better understanding in the mobile bed experiments repeatability and performing protocols. In these experiments several equipment (two PIV system, two optic equipment to recover the sediment transport within the swash zone plus high amount of conventional gear) is recovering information regarding the sediment transport under erosive (Hs 0.53 m and Tp of 4.14 s) and accretive wave conditions (Hs 0.32 m and Tp of 5.44 s) at scale of 1:1.9 regarding Hannover (used as prototype in the SANDS project).

2. Mobile-bed tests

Within the planned experiments two different profiles (Figure 1) are being done in the CIEM flume (100 m length, 3 m wide and 5 m depth). The sand characteristics are controlled by measuring the sediment

size (d_{50}=250μ), fall velocity and density. The sediment transport is being measured by using a standard profiler while the advanced and under development equipment is being tested mainly in the swash zone and in the flat part of the profile.

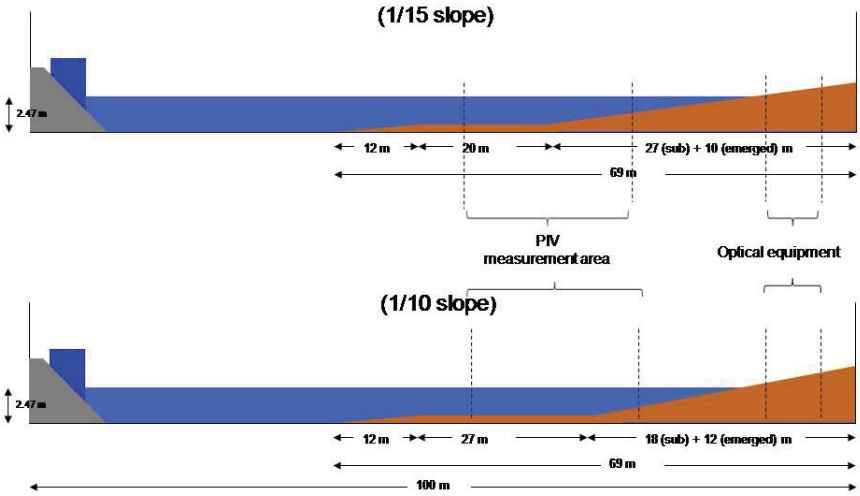

Figure 1. Slopes being tested in the CIEM flume

The paper provides a wide description of the acquired bottom bed evolution data and the time evolution of the bar formation under the reproduced erosive wave conditions (Fig 2). A wide range of parameters: bar position, height, slopes of the bar, position of the trough, depth, final slope … are being analysed and their evolution in time should give us a piece of the physics controlling this sediment transport. The erosive wave conditions were run for 47 consecutive tests (500 waves per test with Jonswap spectrum) simulating a total amount of 33 hours at prototype.

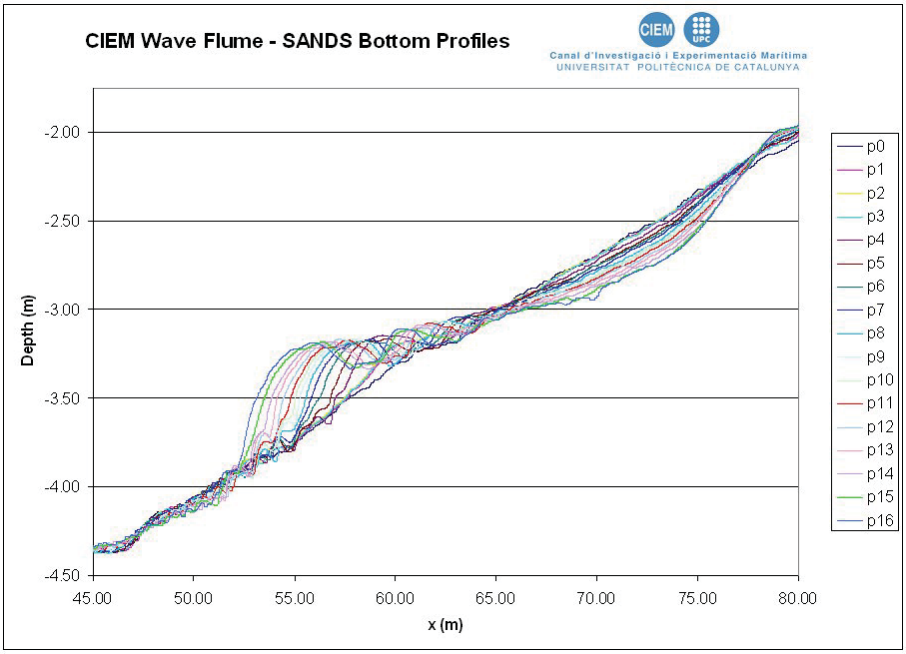

Figure 2. Bottom profile evolution under erosive wave conditions (1/15 slope)

The reproduced accretive conditions started from the final erosive profile (no reprofiling). 35 tests of accretive wave conditions (500 waves per test, Jonswap spectrum) representing 32 hours at prototype were done. In the measured profile (Figure 3) there is a clear shoreward sediment transport of the formed bar, but no movement of the shoreline was measured.

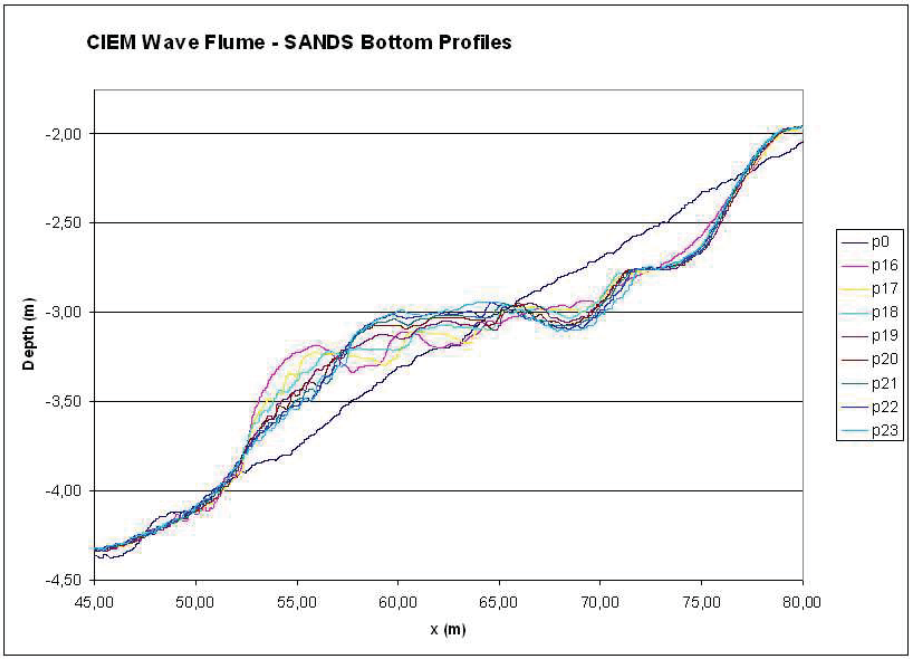

Figure 3. Bottom profile evolution under accretive wave conditions (1/15 slope)

Moreover the acquired bottom profiles, other standard equipment was deployed in order to measure the sediment transport and velocities in the swash-zone. A set of seven ADV and OBS was placed following three different configurations in order to recover the maximum information while there is a clear profile erosion in the study area. This equipment was checked every morning to be at depths ranging between the minimum of 9 cm and a maximum of 20 cm from the bottom. The ADV were placed at the right side of the flume while the OBS were placed at the left side of the flume, both systems followed the same pattern distribution in order to link the measured velocities and the sediment concentration measurements.

The wave height data was measured with the use of resistance and acoustic wave gauges. The information acquired from all these probes is being analysed in order to recover information related to the wave height at the toe of the initial slope, along the flat part of the profile, along the final slope and also it's evolution through the changing profile.

References

Hughes, S.A., 1993. Physical models and laboratory techniques in coastal engineering: World Scientific, 588p

A Sheet Flow Model to Estimate the Sediment Transport Rate for Beaches Protected by Seawalls

S.A. Lashteh Neshaei [(1)], M.A. Mehrdad [(2)], M. Arabani [(3)], M. Shakeri Majd [(4)]

[1] *Assistant Professor, Department of Civil Engineering, Guilan University, 41635, Rasht, Iran, e-mail: maln@guilan.ac.ir*

[2] *Assistant Professor, Department of Civil Engineering, Guilan University, 41635, Rasht, Iran, e-mail: mehrdad_gu@yahoo.com*

[3] *Assistant Professor, Department of Civil Engineering, Guilan University, 41635, Rasht, Iran, e-mail: M_Arabani@yahoo.com*

[4] *Lecturer, Department of Civil Engineering, Islamic Azad University-Anzali, 43145-1451, Anzali, Iran, Email: mortezashakeri@yahoo.com*

Abstract:

To consider the effect of reflective structures on coastal sediment transport and beach morphology, experiments have been performed at laboratory model scale on a partially reflective seawall located in the surf zone. Based on the results obtained from experiments, a simple sheet flow model is developed to estimate the short – term response of a beach to a partially reflective seawall located in the surf zone. The main conceptual innovation of the model is taking the probability density functions of the near – bed horizontal velocities into account and integrating them to calculate the sediment displacements across the profile using a threshold criterion for initiation of sediment motion.

1. Introduction

Although there exist advanced models which predict the sediment transport rate for natural beaches, there are still insufficient theoretical work and measured data on hydrodynamics of the surf zone and the associated sediment transport for the beaches protected by seawalls. In the present study, based on the results obtained from experiments, a new approach is used to develop a semi – empirical model for the calculation of sediment transport and beach profile evolution in the vicinity of a partially reflective seawall. The main input to the model is a driving function in the form of a probability density function (PDF) of the near – bed horizontal velocity.

2. Structure of the model

As described by Asano (1995) and Hoque et al (2001), the sheet flow occurs under high shear stress where ripples are washed out. It is assumed that the sediment in the top layer of the bed moves at the fluid velocity when the threshold velocity for initiation of sediment motion (u_{Cr}) is exceeded. Referring to Figure 1, the negative, positive and net displacements of the sediment for a given location during a period of time (T) can be derived as:

$$neg\ .dis\ . = \int_{t_1}^{t_2} u dt \qquad pos\ .dis\ . = \int_{t_3}^{t_4} u dt \tag{1}$$

$$net\ .dis\ . = \sum_{t=0}^{T} (pos\ .dis\ .) - \sum_{t=0}^{T} (neg\ .dis\ .) \tag{2}$$

Where,

$$u(t_1)=u(t_2)=-u_{Cr} \quad u(t_3)=u(t_4)=+u_{Cr} \tag{3}$$

In the present study, by transferring the problem to the probability domain, an alternative approach based on the PDF of the near- bed horizontal velocity is introduced to avoid the difficulties associated with time series calculations. As discussed by Neshaei (1997), the displacement of a particle in motion can be derived simply as the product of its velocity and the duration of the time in which the particle is in motion. Therefore, the positive, negative and net displacements can be given, respectively, as:

$$pos\ .dis\ . = \int_{u_{Cr}}^{u_{\max}} up\ (u)du \tag{4}$$

$$neg\ .dis\ . = \int_{u_{\min}}^{-u_{Cr}} up\ (u)du \tag{5}$$

$$net\ .dis\ . = pos\ .dis\ . - neg\ .dis \tag{6}$$

Figure 2 shows a typical shape of the function $up\ (u)$ which is the first moment of the probability density function of the sediment velocity at the top of the mobile layer. Figure 3 shows the displacements calculated over a number of points across the profile for different wave conditions used in the experiments. A numerical method was applied to calculate the area under the $up\ (u)$ curve, which corresponds to the sediment displacement per unit time (Mehrdad and Neshaei, 2004). As can be seen in this figure, in most cases, inside the surf zone the positive displacements (towards the shoreline) are dominant, resulting in onshore transport and building a berm profile in front of the seawall. These results are in agreement with the experimental observations. In the experimental program , four water depths in front of the seawall were selected (0,50,100 and 150 mm) and the changes in bed elevation were measured for three different wave conditions (S1,S2 and S3) summarized in Table 1 using two different sizes of sediments (fine sand , D50 = 0.5 mm and coarse sand , D50 =1.5 mm) . The experimental program is explained in detail by Holmes and Neshaei (1996).

Finally, by solving the continuity equation, bed level changes in front of the seawall is calculated. Figure 4 shows a comparison between predicted and measured bed level changes for a particular wave condition indicating a good agreement.

Table 1. Descriptions of spectra. (Hs= Significant wave height, Tz= Zero – crossing period)

Spectrum	Hs (m)	Tz (S)
S1	0.074	1.24
S2	0.088	1.46
S3	0.095	1.67

3. Conclusion

A sheet flow model is developed to calculate sediment displacements across the profile based on integrating the product of the near -bed horizontal velocities and their probability density functions. Having calculated the sediment displacements, the bed level changes have been estimated based on mass balance at a series of location across the profile. The validity of this approach is shown by comparison of the predicted results with those obtained from the experiments. The probabilistic mature employed in the

present study is one of the most important advantages of the proposed model. Noting that existing beach morphology models are essentially deterministic, in that they describe the deterministic morphological processes in response to deterministic inputs, the stochastic approach adapted in the present work is an essential contribution to existing knowledge and to the state of the art in modeling coastal morphology.

References

Asano T. (1995). *'Sediment Transport under Sheet – Flow Conditions'*, *Journal* of *Waterway*, port, Coastal and Ocean Engineering, Vol. 121, ASCE, No. 5, PP.239 – 246.

Holmes, P. and Neshaei, M .A. L (1996),*'The Effect of Seawalls on Coastal Morphology*', proceedings of the Ecohydraulics 2000, Vol. A., pp. 525 – 530.

Hoque, M.A. & Asano, T. & Lashteh Neshaei, M.A (2001). '*Effect of Reflective Structures on Undertow Distribution.*' proceeding of the Fourth International Symposium Waves 2001-California-USA, Vol. 2 ,pp 1042-1051.

Mehrdad, M.A, and Neshaei, M.A.L. (2004). *'Hydrodynamics of the Surface in the Vicinity of a Partially Reflective Seawall*', *International Journal of Civil Engineering*, Vol.2, No.3, Iran University of Science and Technology.

Neshaei, M. A. L. (1997). *'A Semi – Empirical Model for Beach Profile Evolution in front of a Partially Reflective Structure'*, Proceeding of the XXVII IAHR Congress, ASCE, pp.31-36.

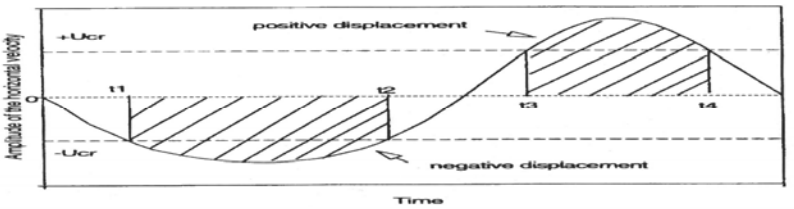

Figure 1: Calculation of sediment displacements based on the time series of horizontal velocity.

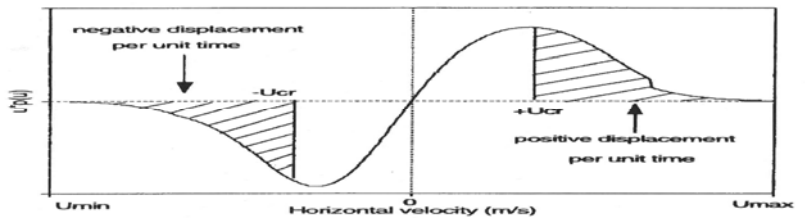

Figure 2: Calculation of sediment displacements based on the probability density function of horizontal velocity.

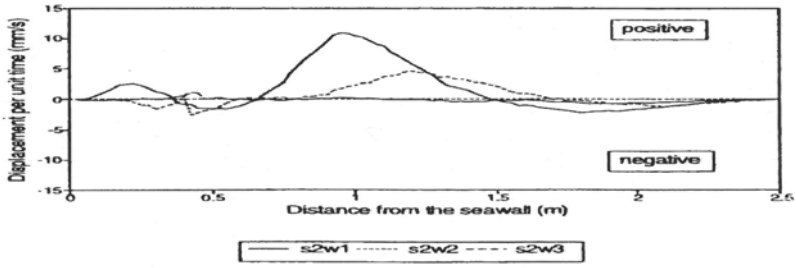

Figure 3 .Calculated net sediment Displacements across the profile for different Wave conditions used in the experiments. w1, w2 and w3 represent 0.05, 0.1 and 0.15 m, Water depths at the wall, respectively.

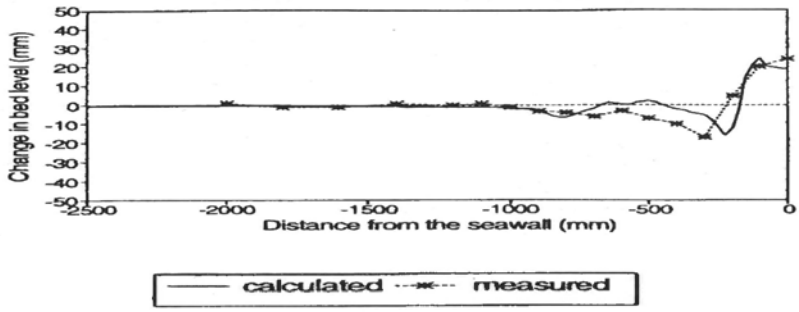

Figure 4.Comparison between predicted and measured bed level changes in front of the partially reflective seawall using a particular Wave condition for coarse sediment.

On the computation of longshore sediment transport in a sea state

Giuseppe Barbaro [(1)], Maria Chiara Martino [(2)], Saveria Meduri [(3)] & Felice Arena [(4)]

[(1)(4)] *Professor, Department of Mechanics and Materials, "Mediterranea" University of Reggio Calabria, Loc. Feo di Vito, 89100, Reggio Calabria, Italy, arena@unirc.it, giuseppe.barbaro@unirc.it*

[(2)(3)] *Researcher, Department of Mechanics and Materials, "Mediterranea" University of Reggio Calabria, Loc. Feo di Vito, 89100, Reggio Calabria, Italy, chiara.martino@unirc.it, saveria.meduri@unirc.it*

Abstract

Longshore sediment transport rate may be calculated using semi-empirical equations, which are based on laboratory and field data. These formulae use a bulk sediment transport method that relates longshore sediment transport to a few wave and beach parameters (see, for example, the CERC-1984 and the Kamphuis-1991 expressions). In this paper, a new approach is proposed for the computation of the longshore sediment transport in a sea state, with a given significant wave height at breaking and a given spectrum. An application is then proposed, where the results given by the new solution are compared with those achieved with the CERC and the Kamphuis formulae.

1. Introduction

Total Longshore Sediment Transport (LST) rate is one of the most commonly required quantities in coastal engineering, needed in problems such as infilling and dredged channels, dispersion of beach fills and placement of dredged material, and the morphodynamic response of coastal areas to engineering structures. Predicting coastal evolution typically requires reliable calculations of the LST. Furthermore, the design of shoreline structures and beach nourishment project relies on assessment of the impact on the shoreline that is often the result of gradients in the LST rate.

The main objective of the present study is to develop and validate a new predictive formula for the total LST rate, to be used in engineering applications. In the following, the most commonly applied formulae for calculating the LST rate are first reviewed. Finally, the new formula is compared with two other formulae, namely the CERC equation (USACE, 1984) and the Kamphuis formula (2002).

2. Existing equations for longshore sediment transport

A number of different longshore sediment transport formulae were proposed through the years, considering wave-generated currents (CERC, USACE, 1984; Kamphuis, 1991).

The most common method for calculating the total LST rate is the CERC formula (Shore Protection Manual 1977, 1984). It is based on the principle that the volume of sand in transport Q is proportional to the longshore power per unit length of the beach, it being given as

$$Q = \frac{\tilde{K}}{16}\sqrt{\frac{g}{\gamma}}H_{sb}^{\frac{5}{2}}\sin\left(2\alpha_b\right), \qquad [1]$$

with:

$$\tilde{K} \equiv \frac{K}{(1-p)(\rho_s-\rho)/\rho}. \qquad [2]$$

In Equations [1] and [2], K is an empirical coefficient, ρ the water density, ρ_s the density of the sand,

p the porosity index, g the acceleration due to gravity, H_{sb} the significant wave height at breaking, γ_b the breaker index (as a first approximation it may be considered equal to 0.78), and α_b the angle which represents the wave direction at breaking. The Shore Protection Manual (USACE, 1984) recommends a value of $K = 0.39$ that was derived from the original field study by Komar and Inman (1970) using tracers.

Kamphuis (1991) developed a relationship for estimating longshore sediment transport rates based upon dimensional analysis; he also calibrated it by using physical model experiments. His final expression (2002), which may be applicable to both field and model data, is:

$$Q_u = 2.27 H_{sb}^{2} T_p^{1.5} m_b^{0.75} D_{50}^{-0.25} \sin^{0.6}(2\alpha_b) \qquad [3]$$

in which Q_u is the transport rate of underwater mass (kg/sec), T_p is the peak wave period (sec), m_b is the beach slope from the breaker line to the shoreline (i.e. the slope over one or two wave lengths seaward of the breaker line) and D_{50} is the median grain size (mm).

The Kamphuis' formula is appealing since it includes the wave period and the beach slope, which both influence wave breaking, and the grain size, which is an important factor for the mobilization and transport of sediment.

2. The longshore sediment transport for wind generated waves

The Cartesian co-ordinates system x, y, z has the x-axis along the shoreline, the y-axis orthogonal to the x-axis and landward oriented, and the origin of the vertical z-axis on the mean water level. Let us consider the control volume extending from the breaking line up to the shoreline and delimited by two parallel vertical plans and by the bottom. To equilibrate the longshore discharge momentum $\langle I \rangle$, acting on the plan parallel to the breaking line, a force $\langle F \rangle$ is exerted by the bottom on the control volume. Following the logic proposed by Longuet-Higgins (1972) and Boccotti (2000), it is possible to obtain the longshore sediment transport $\langle Q \rangle$ that the sea is able to move along the coast by means of the shear stress $\langle F \rangle$ (note that the symbol $\langle f(t) \rangle$ represents the mean value of the function f). Therefore, for progressive and periodic waves, the formula of the longshore discharge momentum that crosses the breaking line, in the hypothesis that the contour lines are straight and x-parallel, was obtained.

In this paper, following a similar approach, a new expression is obtained for a sea state of given characteristics. For this purpose, the general theory of wind-generated waves (Longuet-Higgins, 1963; Phillips, 1967) is applied to obtain the expression of longshore discharge momentum in a sea state:

$$\langle I \rangle = \frac{1}{2} \rho g \int_0^{\infty} \int_0^{2\pi} S(\omega, \theta) \left[1 + (2\mathrm{kd}/\sinh(2\mathrm{kd}))\right] \sin\theta \cos\theta \, \mathrm{d}\theta \, \mathrm{d}\omega \qquad [4]$$

where $S(\omega, \theta)$ is the directional spectrum, k is the wave number and d is the water depth.

By defining coefficient:

$$\delta \equiv \left[\int_0^{\infty} \int_0^{2\pi} S(\omega, \theta) \left[1 + \frac{2\mathrm{kd}}{\sinh(2\mathrm{kd})} \right]_{d=d_b} \sin\theta \cos\theta \, \mathrm{d}\theta \, \mathrm{d}\omega \Big/ 64 \mathrm{sen}\alpha \cos\alpha H_s^2 \right]_{d=d_b} \qquad [5]$$

equation [4], at breaking depth d_b, becomes:

$$< I >= [\delta(\omega, \vartheta)]_{d=d_b} \rho g H_{sb}^{2} \sin(2\alpha_b) . \qquad [6]$$

The longshore sediment transport $\langle Q \rangle$ can be expressed through the mean force $\langle F \rangle$ exerted by the wave motion on the bottom (as we have already mentioned it is equal to the momentum excharge longshore $\langle I \rangle$), through the wave celerity, and through the sediment characteristics:

$$\langle Q \rangle = \frac{g \tilde{K}}{\mu} \sqrt{g d_b} < F > . \qquad [7]$$

Replacing into the eq. [7] the expression [6] for $\langle F \rangle$ ($\equiv \langle I \rangle$) we obtain the solution to calculate the longshore sediment transport in a sea state:

$$\langle Q \rangle = \delta \frac{g\tilde{K}}{\mu} \sqrt{g d_b} H_{sb}^2 \operatorname{sen}(2\alpha_b). \qquad [8]$$

In our paper the longshore sediment transport at some Italian locations is estimated, and the results given by new expression [8] is compared with the CERC (1984) (Eq. [1]) and the Kamphuis (1991) (Eq. [3]) formulae.

An example is given in Table 1, which shows the bulk longshore sediment transport rate, calculated at Cetraro (Figure 1), in the Tyrrhenian coast of Calabria (Italy) with the different expressions.

Figure 1. Cetraro (Italy): directions of wave advance.

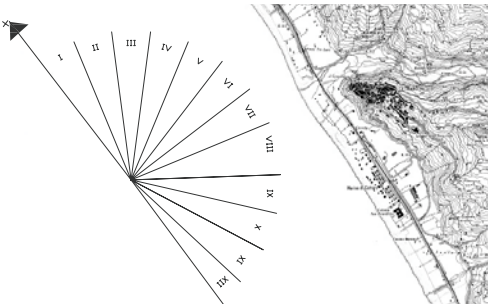

Table 1. Cetraro (Tyrrhenian Sea – Italy): bulk longshore sediment transport rate (mean value, in [m^3/year]) calculated with different expressions.

SECTOR	CERC (1994)	KAMPHUIS (1991)	NEW EXPRESSION	SECTOR	CERC (1994)	KAMPHUIS (1991)	NEW EXPRESSION
I	4 890	1 268	4 902	VII	0	0	0
II	11 182	2 667	11 211	VIII	-144 761	-41 544	-145 132
III	18 842	4 166	18 890	IX	-332 393	-76 442	-333 245
IV	30 820	6 717	30 899	X	-210 450	-45 869	-210 990
V	34 518	7 938	34 606	XI	-87 349	-19 313	-87 573
VI	25 242	7 244	25 307	XII	-36 797	-8 777	-36 892

Figure 3. Longshore sediment transport calculated trough the CERC (1994) formula.

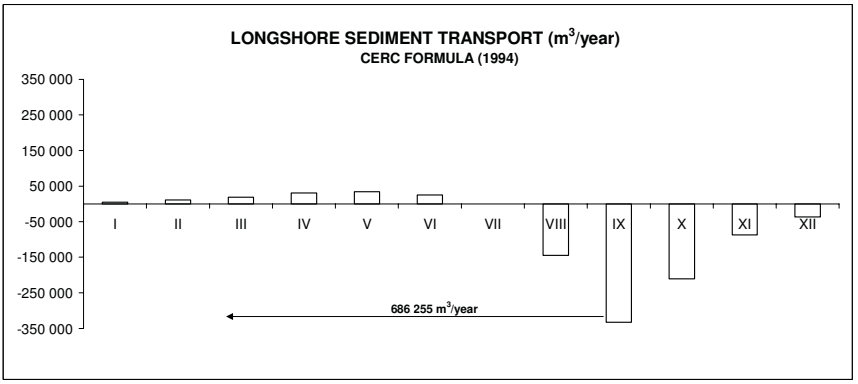

Figure 4. Longshore sediment transport calculated trough the Kamphuis (1991) formula.

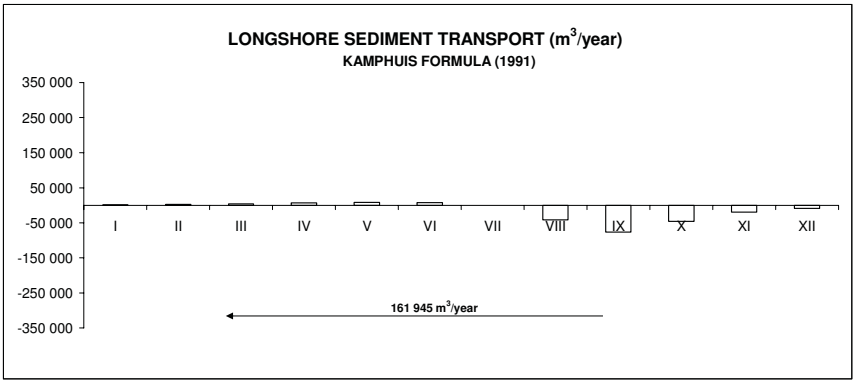

Figure 5. Longshore sediment transport calculated trough the new solution.

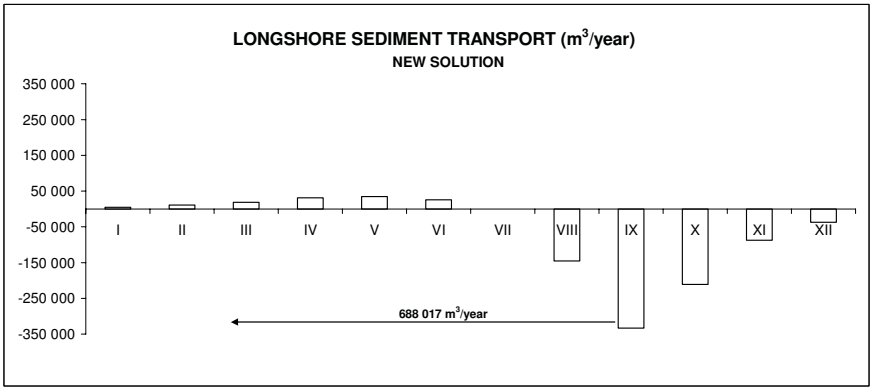

References

Boccotti, P. 2000. 'Wave Mechanics for Ocean Engineering', Elsevier Science, Oxford.

Kamphuis, J.W. 1991. 'Alongshore Sediment Transport Rate'. *J. Waterway, Port, Coastal an Ocean Eng., ASCE*, Vol. 117, pp. 624-641.

Kamphuis, J.W. , 2002, 'Alongshore transport of sand'. *Proceedings of the 28th International Conference on Coastal Engineering. ASCE*, pp. 2330-2345,

Komar, P.D. and Inman, D.L. 1970. 'Alongshore sand transport rate on the beaches', *J. Geophys*. Res. 75, pp. 5914-5927.

Longuet-Higgins, M.S. 1963. 'The effects of non linearities on statistical distributions in the theory of sea waves', J. Fluid. Mech. 17.

Longuet-Higgins, M.S. 1972. 'Recent progress in the study of longshore currents, in waves on beaches and resulting sediment transport', Academic Press, New York.

Phillips, O.M. 1976. 'The theory of wind-generated waves', *Advances in Hydroscience*, 4, pp. 119-149.

USACE, 1994. 'Shore Protection Manual'. Department of the Army, U.S. Corps of Engineers, Washington, DC 20314.

COMPOSITE MODELING OF SEDIMENT DYNAMICS FOR PROPAGATING WAVES REACHING COASTAL DEFENCES

Paula FREIRE [(1)], Francisco SANCHO[(2)] & Filipa S. B. F. OLIVEIRA [(3)]

[(1)] PhD in Geology, LNEC, Av. Brasil 101, 1700-066 Lisboa, Portugal. pfreire@lnec.pt

[(2)] PhD in Civil Engineering, LNEC, Av. Brasil 101, 1700-066 Lisboa, Portugal. fsancho@lnec.pt

[(3)] PhD in Coastal Engineering, LNEC, Av. Brasil 101, 1700-066 Lisboa, Portugal. foliveira@lnec.pt

Abstract

In this study, the beach profile evolution in front of a seawall was investigated through combining a large scale physical model and a deterministic 2D-vertical cross-shore morphodynamic numerical model. Experiments were conducted under erosive and accretive wave conditions, for two different water levels at the toe of a seawall, affecting the wave-structure interaction and beach profile evolution. The results show the importance of the wave-structure interaction determining the profile evolution. A better agreement was observed between the numerical and physical results when that interaction is considered.

1. Introduction

Under the Joint Research Activity "CoMIBBS – Composite Modelling of the Interaction between Beaches and Structures", funded by the EU "HYDRALABIII – Integrated Infrastructure Initiative" (http://www.hydralab.eu/), the work described here aims the combination of physical and numerical models in the study of beach evolution in front of alongshore structures such as seawalls/revetments.

The coastal morphodynamic process can be relatively well reproduced with large physical models. However, the costs and time associated to their use make this tool not always the most practicable one. Alternatively, small-scale physical models have several limitations reproducing the sediment dynamics as one can not satisfy all different scaling laws (Kamphuis, 1996). On the other hand, numerical models can be less expensive and more flexible but, although their capacity for modelling beach profile evolution was greatly improved in the last decades, limitations still remain, particularly in what concerns the swash zone dynamics and the onshore sediment transport. Thus, the combination of both approaches, in an integrated and balanced way exploring their individual strengths, can improve the simulation capacity of the complex processes involved in coastal problems.

In the present paper, the first results of the combined physical and numerical modelling approach to study a beach profile evolution in front of a seawall are presented.

2. Methodology

The experimental set-up is based on a field site, Buarcos beach, located in the central Atlantic west coast of Portugal. This beach has been extensively studied (Oliveira, 2002; Larangeiro et al., 2003; Freire et al., 2004) and has now a relatively complete morphological, sedimentological and wave climate characterisation. This site was selected for the present study for having characteristics suitable to be reproduced in both physical and numerical models (seawall existence, coarser grain size, suitable beach slope).

2.1 Numerical modelling

At the initial stage, the numerical model Litprof (DHI, 2007), a deterministic 2D-vertical cross-shore morphological model, was applied to assist the design of the experimental set-up. The model was used to

estimate the geometrical changes of the equilibrium profile in the prototype conditions. The results obtained for the profile change under constant shore-normal storm wave attack show the formation of a seaward bar and erosion in front of the revetment. The erosion thickness (after a certain storm duration) was considered as the minimum thickness of the sand layer to be placed in the experimental set-up at the chosen model scale. Since in the experimental set-up the nearshore profile is preceded by a platform, the numerical model was also applied to verify, in the prototype, the effect of different-length and configuration platforms on the morphological evolution of the nearshore beach. The numerical results revealed that the erosion in front of the seawall is not dependent on the offshore profile, but, in the cases with platforms the predicted outer bar features are smoother, particularly the offshore slope.

The numerical model was also applied at the physical model scale, for the beach profile configuration and wave conditions tested in the flume. Two different wave theories were considered to calculate the wave kinematic parameters, and consequently, the sediment transport and morphological evolution. They were Doering and Bowen (1995) theory and Stokes 5th-order theory (Fenton, 1985).

2.2 Physical modelling

The physical tests were performed in a large scale flume, with 73 m length, 3 m width and 0.7 m height. Two conditions were considered for the hydrodynamic scaling: the model is geometrically undistorted, i.e., the length scales are scaled in the same extent; Froude number is similar in the model and the prototype. For the sediment, the suspended-load scaling law $n_{D50}=n_h^{0.56}$ was considered, where n_{D50} and n_h are, respectively, the scaling relation of sediment median diameter (D_{50}) and of the depth. An analysis of the sediment mobility number was performed in order to verify if the scaled model tests fell in the same sediment transport/bed regime as the prototype. In Figure 1 the set-up of the physical model is presented. The scale adopted was 1:6 and the initial geometry was a planar profile with 1:20, in front of a reflective structure. The sediment used was silica sand (Sibelco) with D_{50}=400μm and geometrical deviation, defined as $(D_{80}/D_{16})^{0.5}$, of 1.35.

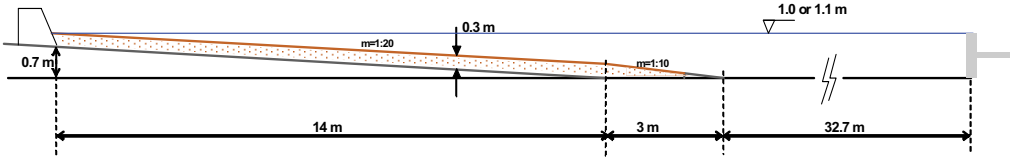

Figure 1. Set-up of the physical model.

Two series of tests, including erosive and accretive wave conditions were performed (Table 1). Test series 1 and 2 have the same wave conditions but different water levels: in the first the interaction with the structure is not simulated, as in opposite to the second. The wave characteristics were chosen based on estimates of erosive and accretive conditions, according to the dimensionless fall velocity parameter $\Omega = H_b/T\ W_s$ being larger than 2 or smaller than 1, respectively (Gourlay, 1968). The data acquired during the tests were: bed profiles, every 1 and 2 hours after erosion and accretion runs, respectively; surface elevation at 5 locations and 3D velocities at 2 locations, during the first 25 minutes of each run (of 1 or 2 hours); sediment porosity after each test; and beach profile photographies at 8 positions along the flume, every 1 or 2 hours.

Table 1. Physical tests performed.

Test series	Initial geometry	Wave conditions (Jonswap spectrum)	Duration (hours)	Water level (m)
1	1:20	Erosive (Hs=0.37; Tp=3.40)	12	1.0
	result of previous test	Accretive (Hs=0.22; Tp=3.40)	16	1.0
2	1:20	Erosive (Hs=0.37; Tp=3.40)	12	1.1
	result of previous test	Accretive (Hs=0.22; Tp=3.40)	16	1.1

3. Results and discussion

For both test series 1 and 2, the initial planar-beach profile evolved to a barred-beach profile under erosive wave conditions and then the bar moved shorewards under accretive wave conditions (Figure 2). However, different intermediate and final profiles were obtained for both test series, due to the different water levels at the toe of the structure. Based on the comparison of the results obtained for both test series (Figure 2), the waves interaction with the seawall causes: i) the displacement of a lower sand volume from the upper part of the profile; ii) the generation of a submerged bar with smoother features; iii) significant erosion of the profile at the toe of the structure; iv) less changes of the profile on the seaward side of the bar. The two first and the last remarks (i, ii and iv) can also be observed in the numerical results.

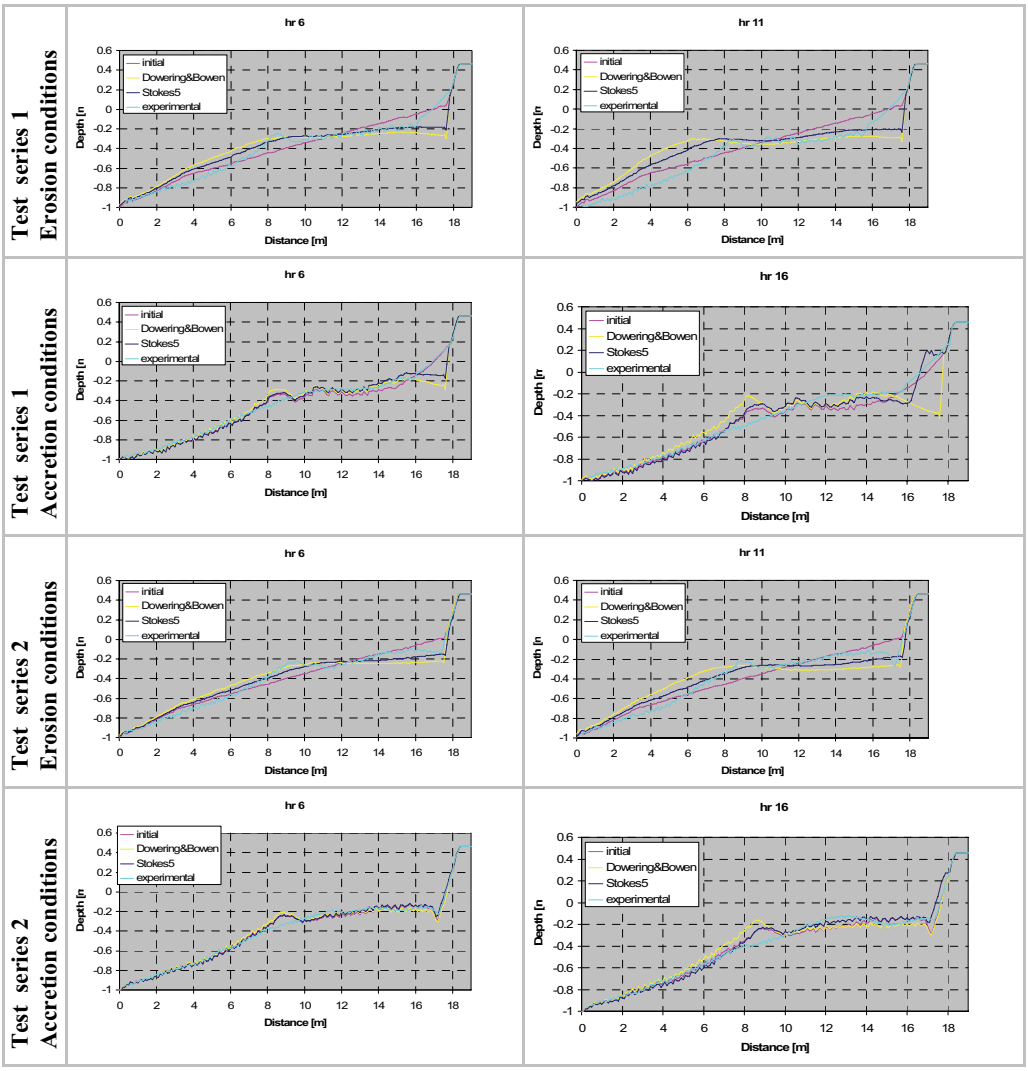

Figure 2. Numerical and experimental results of beach profile evolution for test series 1 and 2.

However, in what concerns profile erosion (iii), the numerical model always generates its location at the basis of the structure, whereas in tests series 1 we obtain experimentally a robust beach face in front of the structure and erosion occurs between this feature and the bar. The numerical results show a better agreement with the experimental results in the case of wave-structure interaction. Finally, in what

concerns the best wave theory to simulate the profile evolution under erosion conditions, the results reveal that during the first hours of the erosive event Doering and Bowen theory provides a better approximation of the profile evolution, however, even before reaching half of the event is Stokes 5th-order wave theory that yields the best results. On the overall, Doering and Bowen theory overestimates the offshore sediment transport.

Under accretive conditions, the sand accumulated at the submerged bar was transported onshore, for both test series (Figure 2). However, this phenomenon developed differently in both series. Without wave-structure interaction the sand is accumulated in front of the structure uniformly, i.e., allowing the maintenance of the slope of the beach face. However, the results of the test series 2 show that the wave-structure interaction inhibits the sand deposition/accumulation process on its base, and due to that the upper part of the beach is unable to recover the initial geometry. The numerical results show that none of the wave theories allow the correct simulation of the beach recovery process. In fact, in the absence of wave-structure interaction, during the first hours of simulation the numerical results reveal the ongoing process of scour in front of the structure. However, using Stokes 5th order theory, the model is capable of simulating onshore transport and sand accumulation at the upper beach part. This capability gives better agreement with experimental results in the case of wave-structure interaction.

4. Conclusions

Two series of beach profile evolution were performed in a large scale physical model, showing bar formation under erosive waves and beach recovery under mild wave conditions. In the test series with stronger wave-structure interaction (higher water level), strong erosion occurred in front of the seawall, which reduced the beach capability of recovery. This highlights the importance of the water level in front of a seawall in determining the profile evolution. A process-based numerical model was used in the design of the physical set-up and to simulate the experimental cases. The numerical results showed that the model reproduces qualitatively well the profile evolution under the erosive events but has limitations in reproducing beach recovery, and that the agreement between the numerical and experimental results is better in the case of higher water level.

Acknowledgments

This paper is a contribution from “"HYDRALABIII – Integrated Infrastructure Initiative" funded by European Union (contract n. 022441).

References

DHI, 2007. Litpack. Noncohesive Sediment Transport in Currents and Waves. User Guide. Danish Hydraulic Institute, Denmark.

Doering, J.C. and Bowen, A.J., 1995. Parametrization of orbital velocity asymmetries of shoaling and breaking waves using bispectral analysis. Coastal Engineering, Vol. 26, pp. 15-33.

Fenton, J., 1985. A fifth-order Stokes theory for steady waves. J. Coastal, Port. Waterway and Ocean Eng., ASCE, Vol. 111, pp. 216-234.

Freire, P., Oliveira, F.S.B.F., Capitão, R., Fortes, C. and Costa, M., 2004, Cross-shore evolution of Buarcos beach, Portugal. 29th International Conference on Coastal Engineering, ASCE, Lisboa, Portugal, pp. 2314-2326.

Gourlay, M.R., 1968. Beach and dune erosion tests. Delft Hydraulics Laboratory, Rep. No. M935/M936.

Kamphuis, J.W., 1996. Physical Modeling of Coastal Processes. Chapter in "Advances in Coastal and Ocean Engineering, Volume 2", P. Liu (Ed.), Singapore: World Scientific Press, pp. 79-114.

Larangeiro, S.H.C.D., Oliveira, F.S.B.F. and Freire, P.M.S., 2003. Longshore sediment transport along a sandy coast with hard rock outcrops, *Shore and Beach*, Vol.71, No.2, pp. 20-24.

Oliveira, F.S.B.F., 2002. Effect of the sea level variation in the offshore limit of the surf zone of Buarcos, Portugal. Littoral 2002, The changing coast. EUROCOAST/EUCC, Porto, Portugal, pp. 363-368.

ON THE SCALING OF SEDIMENT TRANSPORT DURING ONSHORE SANDBAR MIGRATION

M. HENRIQUEZ [(1)], A.J.H.M. RENIERS [(2)], B.G. RUESSINK [(3)], T.P. STANTON [(4)] & M.J.F. STIVE [(5)]

[(1)] *MSc, Delft University of Technology, P.O. Box 5048, 2600 GA, Delft, The Netherlands. m.henriquez@tudelft.nl*

[(2)] *PhD, Delft University of Technology, P.O. Box 5048, 2600 GA, Delft, The Netherlands. a.j.h.m.reniers@tudelft.nl*

[(3)] *PhD, Utrecht University, P.O. Box 80.115, 3508 TC, Utrecht, The Netherlands. g.ruessink@geo.uu.nl*

[(4)] *Prof, Naval Postgraduate School, Code OC/St, Monterey, CA 93943, USA. stanton@nps.edu*

[(5)] *Prof, Delft University of Technology, P.O. Box 5048, 2600 GA, Delft, The Netherlands. m.j.f.stive@tudelft.nl*

Abstract

This paper investigates the scaling of sediment transport processes under waves. To gain more insight in the physical processes a movable-bed wave flume experiment will be conducted. The flume will be equipped with state-of-the-art acoustic instruments and filled with artificial sediment to minimize scale effects. These detailed measurements will be compared with prototype scale measurements to gain insight in scale laws and scale effects.

1. Introduction

The physical processes responsible for onshore transport of sediment by the orbital flow under waves in the nearshore are poorly understood (Nielsen, 2006; Henderson, 2004; Hoefel & Elgar, 2003; Madsen, 1974). Field experiments and large wave flumes give the opportunity to measure the transport processes. However, both types of experiments require a great number of personal and instruments making them expensive. Relatively small wave flumes provide a solution; the flume can be operated by only one person and can be easily overseen. Also, the instrumentation can be smaller, less intrusive and easier to operate. The smaller scale gives greater control over the sediment properties since a smaller amount is needed. This allows for the use of artificial sediment. Also the water quality is better for experimental measurement techniques such as Particle Image Velocimetry (PIV). There are drawbacks such as scale effects. The small-scale physical model is only useful if the transport processes responsible for morphological change are the same in model and prototype. For example, scaling of onshore bar migration in the nearshore is challenging since various transport processes and transport modes need to be represented simultaneously (See Figure 1 for an illustration). Hence, the scaling of onshore sandbar migration in the nearshore is investigated by conducting a small-scale flume experiment and compare the acquired data to existing data of field and large wave flume experiments.

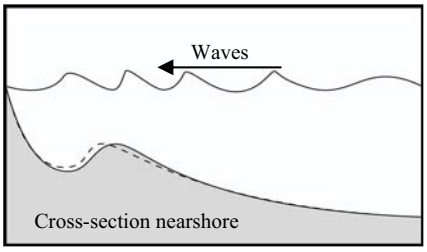

Figure 1. Onshore migration of a bar in the nearshore due to the orbital motion under waves.

2. Small-scale physical model

To scale all the dominant processes various scale laws need to be considered which can not all be satisfied simultaneously but should be approximated as much as possible. We use scale laws suggested by Kamphuis (1985), more specifically, the grain Reynolds number, the densimetric Froude number and the relative fall speed. The hydrodynamics in the model will be geometrically undistorted which leaves only two other scalable variables: the sediment grain size and density. By using artificial sediment both parameters will be used to approximate the scale laws.

Measuring the transport processes will be done with non-intrusive instruments: (1) an acoustic profiler that measures flow velocity profiles and sediment concentrations profiles close to the bottom (Thorne & Hanes, 2002; Stanton, 1996) and (2) a PIV instrument that provides a picture of the flow and sediment field over an area of ***O***(10 cm) close to the bottom (Nichols & Foster, 2006). Both instruments where deployed in large wave flumes and/or field campaigns providing data for comparison.

3. Outlook

The small wave flume experiment will provide detailed data of flow and sediment properties close to the bottom. By comparing the data with field and large wave flume data, insight is gained in scale laws and scale effects of nearshore transport processes. This knowledge is needed to interpret data from future small-scale flume experiments.

Acknowledgments

We gratefully acknowledge the financial support of the Technology Foundation STW, applied science division of NWO, in the Netherlands, under project number DCB.7908.

References

Henderson, S.M., Allen, J.S., & Newberger, P.A. 2004. Nearshore sandbar migration predicted by an eddy-diffusive boundary layer model. *Journal of Geophysical Research*, 109.

Hoefel, Fernanda, & Elgar, Steve. 2003. Wave-induced sediment transport and sandbar migration. *Science*, 299(2003/03/21).

Kamphuis, J. W. 1985. On Understanding Scale Effects in Coastal Mobile Bed Models. Pages 141–162 of: Dalrymple, R. A. (ed), Physical Modelling in Coastal Engineering. Rotterdam, The Netherlands: Balkema, A. A.

Madsen, O. S. 1974. Stability of a sand bed under breaking waves. Pages 776–794 of: 14th Int. Conf. on Coastal Engineering.

Nichols, C. S., & Foster, D. L. in review. Full-Scale Observations of Wave-Induced Vortex Generation over a Rippled Bed. Journal of Geophysical Research.

Nielsen, Pieter. 2006. Sheet flow sediment transport under waves with acceleration skewness and boundary layer streaming. Coastal Engineering, 53, 749–758.

Stanton, T.P. 1996. Probing ocean wave boundary layers with a hybrid bistatic/monostatic coherent acoustic Doppler profiler. In: Proceedings of the Microstructure sensors in the ocean workshop.

Thorne, Peter D., & Hanes, Daniel M. 2002. A review of acoustic measurement of small-scale sediment processes. Continental Shelf Research, 22, 603–632.

EXPERIMENTAL MODELING OF SAND BEACH NOURISHMENT CROSS-SHORE EVOLUTION

Iolanda LISI [(1)], Marcello DI RISIO [(2)], Paolo DE GIROLAMO[(3)], Gian-Mario BELTRAMI[(4)]

[(1)] Ph.D. Student, ICRAM, Central Institute of Marine Research, Via di Casalotti 300, I-00166 Rome, Italy, i.lisi@icram.org

[(2)] Post-Doc Researcher, University of L'Aquila, DISAT-LIAM, P.le Pontieri 1 ,67040 Monteluco di Roio, L'Aquila, Italy, mdirisio@ing.univaq.it

[(3)] Professor, University of L'Aquila, DISAT-LIAM, P.le Pontieri 1 ,67040 Monteluco di Roio, L'Aquila, Italy, padegi@ing.univaq.it

[(4)] Researcher, University of L'Aquila, DISAT-LIAM,P.le Pontieri 1 ,67040 Monteluco di Roio, L'Aquila, Italy, beltrami@ing.univaq.it

Abstract

The present paper describes new two-dimensional experiments carried out at the Environmental and Maritime Hydraulics Laboratory "Umberto Messina" (LIAM) of the University of L'Aquila (Italy) aimed at reproducing cross-shore evolution of a typical sand beach profile after nourishment activities, both in the case of unprotected and protected nourishments. Three different incident wave spectra were reproduced and free surface time series and cross shore profile were measured during the experiments. This paper intends to illustrate results of the investigation in terms of cross-shore profile evolution, cross-shore sand transport and emerged berm evolution

1. Introduction

Beach nourishment, the placement of large quantities of sand in the nearshore region to advance the shoreline seaward, is increasingly applied as a method of erosion control. It is considered as an environmentally acceptable method of shore protection and restoration for short-term emergencies, i.e. storm-induced erosion, as well as long-term issues, i.e. structural erosion and sea level rise (Hamm et al., 2002). Anyway, the nourishment induces effects on the beach system equilibrium, in relation to sediment transport processes, both alongshore and cross-shore (Dean and Yoo, 1992, 1994). Longshore sediment transport tends to smooth the planform of the shoreline that follows nourishment activities. Furthermore, the cross shore profile is steeper than equilibrium one and it tends to be smoothed too. Hence, prediction of the performance of beach-nourishment projects includes analysis of the cross-shore and longshore transport processes and it is of considerable significance to a rational evaluation of the economic benefits of the project.

The aim of this paper is to investigate the performance of a typical nourishment project by means of experimental modeling in order to reproduce cross-shore profile evolution, both in case of protected and unprotected nourishment.

2. Description of the experimental set-up

A sand beach (sediment grain size d_{50}=0.12 mm, fall velocity 2.5 cm/s) characterised by a piecewise linear initial profile with three different slopes was set into a 45.0 m long and 1.5 m wide wave flume. A PVC wall along centerline of the flume was used to reduce width of the beach to 0.75 m. The offshore beach initial slope was set to 1:110 (from -0.33 m.l.w. up to -0.17 m.l.w.), while the nearshore one to 1:7

(reproducing typical slope of sand nourishments from -0.17 m.l.w. up to +0.15 m.l.w.). The inner part of the emerged initial profile was set horizontal (+0.15 m s.l.w.). The beach profile is connected to the offshore water depth (set to 0.67 m) by means of a steel fixed ramp (slope 1:20, see Figure 1). The preceding described characteristics were selected in order to reproduce a typical beach of the middle Adriatic Sea (at a Froude scale of 1:12). In the followings, if not specified, the dimensions are reported in prototype scale.

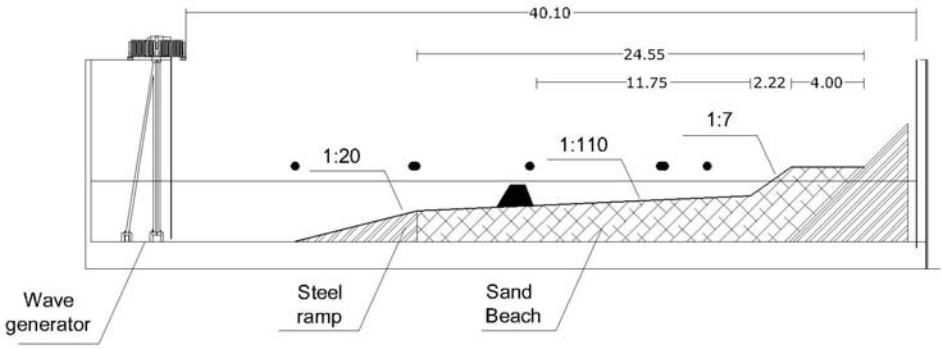

Figure 1. Sketch of initial beach profile (dark circles represent wave gauges).

Incident wave spectra were chosen in order to reproduce both erosion and accretion of sand beach (Kraus et al, 1991). In particular Jonswap spectra characterised by significant waves ranging from 2,50 m up to 3,20 m and peak period from 5,20 s up to 8,90 s were chosen to represent offshore wave conditions. Two types of wave attack were reproduced. The first one was a constant incident wave condition propagating for about 65 hours (19 hours at model scale) in order to reach stationary condition of beach profile. The second type of wave attack aimed at reproducing beach profile evolution during a storm event with a growing significative wave height in the first hours and a decreasing significative wave height in the last hours, for total storm duration of 27 hours.

Two sets of experiments were carried out. The first one aimed at measuring the evolution of cross-shore beach profile in the case of absence of any protection structure (unprotected sand nourishment). For the second set of experiments a rubble mound structures model (berm width 10,00 m, toe water depth 3,5 m, crest freeboard -1.50 m, see Figures 1 and 2) was placed into the flume (protected nourishment).

During the overall experiments elevation time series were collected by means of a series of 12 resistive wave gauges. Furthermore the initial beach profile was measured by means of a laser system (cross-shore spatial resolution equal to 0,24 m, 0,02 m in model scale) and its evolution was evaluated by stopping the waves and measuring the bottom position for 20 times during the experiment. Beach profiles were measured with increasing time step in order to observe rapid evolution at the beginning of the test (first 3 hours at model scale).

3. Preliminary results

Experimental results consist of (i) cross-shore profiles evolution, (ii) cross-shore total sediment and (iii) incident wave parameters. Figure 3, as an example of experimental results, shows the cross-shore beach profiles evolution for the three incident wave conditions and both for protected and unprotected nourishment. It has to be noted that in the case of wave conditions H_{m0}=3.12 m, T_p = 5.20 s the presence of the submerged structures induces a shoreline displacement lower if compared with the unprotected case one and in the case of lower incident wave height (right upper panel of Figure 3).

Figure 2. Pictures of the rubble mound structure taken during one of the experiments.

Acknowledgments

The research described herein was funded by "Regione Abruzzo" within the S.I.Co.R.A. project. Thanks are due to Eng. Carlo Visca and Pierluigi Caputi. Furthermore the LIAM "Umberto Messina" technicians Mr. Mario Nardi and Mr. Lucio Matergia are acknowledged.

References

Kraus, N.C., Larson, M., Kriebel, D.L., 1991. Evaluation of beach erosion and accretion predictors. Proc. Coastal Sediments '91, ASCE, Seattle, 572– 587.

Robert G. Dean, and Chui-Hee Yoo, 1992. Beach-Nourishment Performance Predictions. Journal of Waterway, Port, Coastal, and Ocean Engineering, Vol. 118, No. 6, November/December,

Robert G. Dean, and Chui-Hee Yoo, 1994. Beach Nourishment in Presence of Seawall. Journal of Waterway, Port, Coastal, and Ocean Engineering, Vol. 120, No. 3, May/June.

L. Hamma, M. Capobianco, H.H. Dette, A. Lechuga, R. Spanhoff , M.J.F. Stive, 2002. A Summary of European Experience with Shore Nourishment. Coastal Engineering 47, 237–264

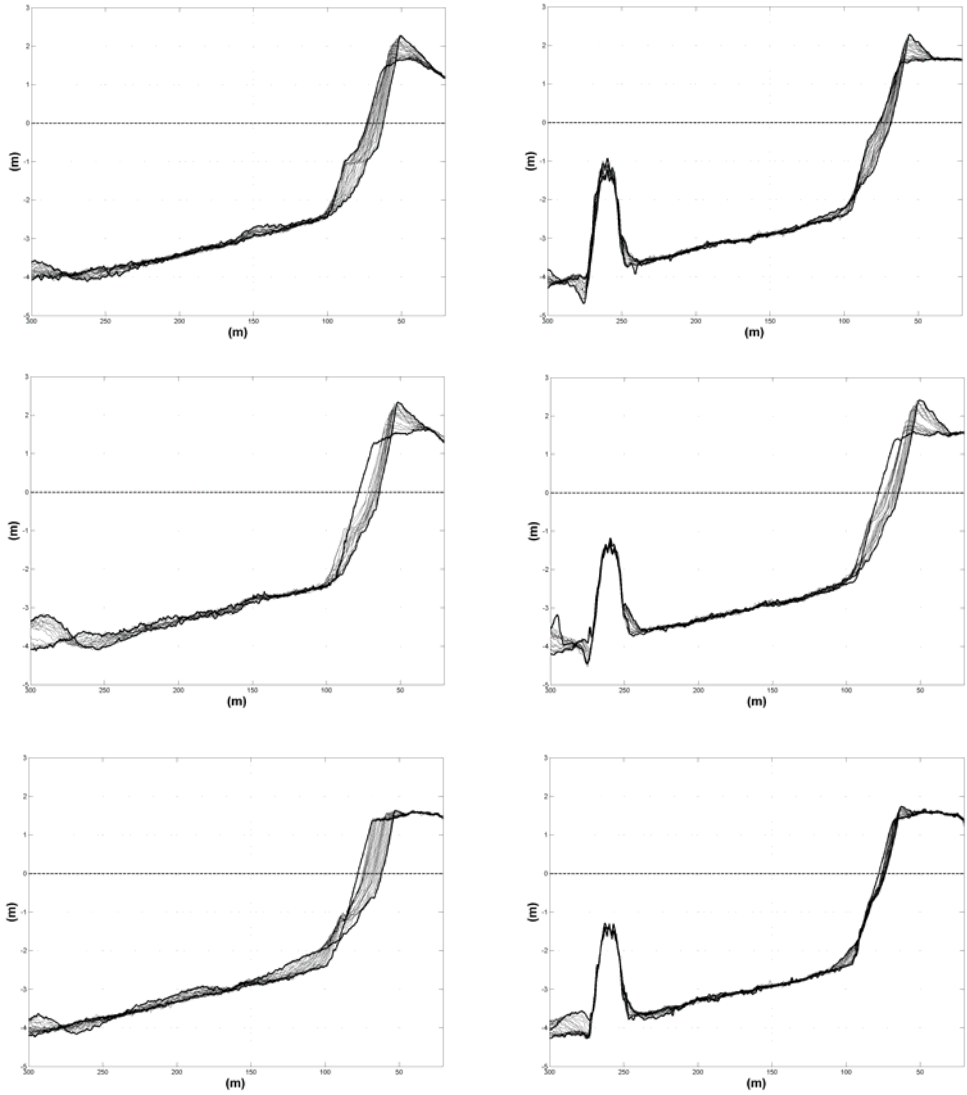

Figure 3. Cross-shore profile evolution for unprotected (left panels) and protected (right panels) for H_{m0}=2.52 m, T_p=7.90 s (upper panels), H_{m0}=3.12 m, T_p = 8.90 s (middle panels) and H_{m0}=3.12 m, T_p = 5.20 s (lower panels).

PRECISO COSTE: COASTLINE CHANGE DETECTION WITH VERY HIGH RESOLUTION IMAGERY

Andrea NAVARRA [(1)], Massimo ZOTTI[(1)]

[1]*Planetek Italia srl, Via Massaua 12, I-70123 Bari ITALY, navarra @ planetek.it*

Abstract overwiev

Preciso Coste is a service developed by Planetek Italia designed for the structured acquisition of the coastline and all the connected maritime infrastructures from Ikonos very high resolution orthorectified satellite imagery. The resulting coastline database is the basis for the successive coastline evolution analysis based on the comparison with reference cartography.

Both European Space Agency (ESA) and Italian Agency for Environmental Protection and Technical Services (APAT) are involved in the promotion of Earth Observation based products for the Coastal Dynamics Monitoring.

1. The Preciso Coste Service

Preciso Coste is a service designed for the monitoring of coastline dynamics. The service releases a series of products for the assessment and classification of coastline, port and defence works and for the monitoring of their development.

Preciso Coste provides that every stretch of coastline is classified according to type and depending on the variations (advancement, erosion or stability) over the reference coastline extracted from orthophotos IT2000 (acquired in 1998/1999).

The port works are identified and classified according to type and intended use (industrial port / commercial dock / pier, port channel, military port, etc), while the defence works are surveyed and divided by design type (emerged reefs / toll lanes are flooded with / without toll lanes, plain and thrown to the wall, brushes orthogonal emerged / submerged, armed mouth, etc).

The classification adopted by Preciso Coste is standardized and allows for the development and preparation of reports and statistical studies, including space-based, in a manner consistent with the standards.

In support of themes concerning the status and evolution of coastlines, are also given information associated with data related aspects of administrative structures from the official sector. These layers of different informative nature identify the limits of regional, provincial and municipal coastal and geographical boundaries of particular types of areas under environmental protection.

Preciso Coste products are provided in a standard GIS format, ready to allow the use of databases with every type of information system used by the client. Preciso Coste includes a detailed statistical report that showing the results obtained.

Technical specifications

The main technical specifications and features of Preciso Coste are listed in Tab 1.

Tab. 1: Technical Specifications of the product

Specifica	Tipo
Source of information	IKONOS satellite images (1m resolution) Digital color Orthophotos IT2000 (1m resolution)
Projection System	UTM32/33 Datum WGS84
Accuracy	The accuracy of the carthography realized is complyed to 1:10.000 scale.
Outcome	PersonalGeodatabase

2. The Project

2.1. Using Remotely sensed data

The first phase of the project consist of high resolution imagery collection from IKONOS satellite. This satellite has clear operational benefits, including the ability to plan and obtain such images very quickly.

This feature makes the use of IKONOS satellite data particularly suited to monitoring stretches of coastline distributed throughout the national coast.

2.2. Coastline Classification

Once the collection is made, using IKONOS high resolution satellite, Preciso Coste is processed through a photointerpretation, a video digitisation and a spatial analysis of data. The identification and classification in several sections types is made by grouping the different stretches of coastline by their characteristics and divided therefore for different types: (Natural, Artificial, Fictive).

Fig. 1: Sample classification according to the coast height and lythology

The coast of natural type is itself classified according to the morphology of the coast (height and lythology if any interpretation is possible). The coast of artificial type is itself classified according to the type of work for defence or portuale. The type of fictive coast is stated to maintain the continuity and consistency of topological representation (for example in connection of the mouth of watercourses the coastline should be connected between the

extremes of banks of watercourse) and is in turn classified depending on the type of connection.

The digitized coastline is stored in a structured archive (geodatabase). The structuring of the archive allows the creation of an information layer in which the coastline is divided into sections and classified as homogeneous parts, marked by a unique code (identifier).

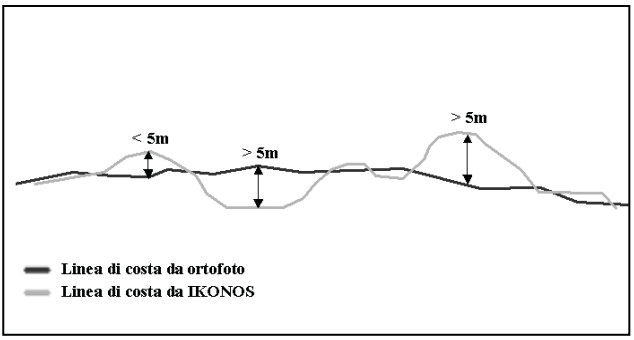

Fig. 2: Parameters for variation measurements according to the orthophoto.

2.3. Analisi delle variazioni della linea di costa

Once the coastline has been classified, it is possible to proceed with its variations analysis realized through a direct comparison between the coastline derived by the most up-to-date satellite imagery and the reference coastline derived by orthophotos IT2000 collected in the biennium 1998/99. Such analysis allows the division of the coastline into several contiguous lengths classified on the base of their variations in respect to the reference coastline (Advancement, Erosion, Stability). The variation analysis procedure consists in considering as modified (advanced/backward) all those coastline lengths, derived from Ikonos images, comprised between two continuous intersections with the reference coastline and including at least one point with a distance from the reference coastline equal to or more than 5 m. All the other lengths are considered as stable.

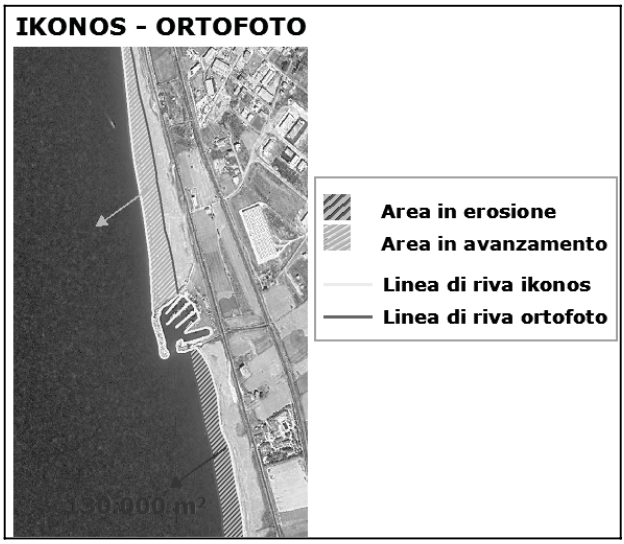

Fig. 3: Coastline erosion and advancements

In addition to the identification of the kind of variation, the mean and maximum variation entity and the lost, or acquired from the coast, area size are defined.

2.4. Statistic Reports

Based on the information contained into the database, specific report are compiled as table at different analysis scale (national, regional, provincial and per physiographic unit) containing all the information extracted from the thematic layer produced

Regione: Sicilia
Provincia: Caltanissetta Coste 33 Km

Tipo costa	Descrizione	Litologia	Lunghezza [m]	Lunghezza [%]	Opere N°	Opere [%] N°	Opere [%] Dim.
Totale			32.510	100,0			
Naturale			29.969	92,2			
	Alta		443	1,5			
	Bassa		29.526	98,5			
		Sabbiosa	28.146	95,3			
		Ciottolosa	0	0.0			
		Rocciosa	708	2,4			
		Non definito	672	2,3			
Artificiale			894	2,7	27	100,0	100,0
	Radente a gettata		894	100,0	5	18,5	36,1
	Radente a muro		0	0.0	0	0.0	0.0
	Scogliere emerse con varchi				17	63,0	63,9
	Scogliere emerse senza varchi				0	0.0	0.0
	Scogliere sommerse con varchi				0	0.0	0.0
	Scogliere sommerse senza varchi				0	0.0	0.0
	Pennelli obliqui emersi				0	0.0	0.0
	Pennelli obliqui sommersi				0	0.0	0.0
	Pennelli ortogonali emersi				0	0.0	0.0
	Pennelli ortogonali sommersi				0	0.0	0.0
	Pennelli a T emersi				0	0.0	0.0
	Pennelli a T sommersi				0	0.0	0.0
	Pennelli a Y emersi				0	0.0	0.0
	Isolotti				0	0.0	0.0
	Opere miste		0	0.0	0	0.0	
	Foci armate				2	7,4	
	Opere portuali				1	3,7	
	Altro (lidi, pontili, ecc.)		0	0.0	2	7,4	
Fittizia			1.647	5,1			
	Collegamento porto		617	37,5			
	Collegamento opera		962	58,4			
	Collegamento foce del fiume		68	4,1			

Analisi estesa a tutte le coste

	Lunghezza [m]	Lunghezza [%]
Coste	32.510	100,0
Stabili	10.136	31,2
Modificate	21.637	66,6
Non definito*	738	2,3
Coste modificate	21.637	66,6
Arretramento	9.610	29,6
Avanzamento	12.027	37,0

Analisi estesa alle coste basse

	Lunghezza [m]	Lunghezza [%]
Coste	29.526	100,0
Stabili	8.808	29,8
Modificate	20.683	70,1
Non definito*	34	0,1
Coste modificate	20.683	70,1
Arretramento	9.590	32,5
Avanzamento	11.093	37,6

Fig. 4: Example of statistic report at provincial scale

3. Conclusions

Based on satellite very high resolution imagery, Preciso Coste is a service designed for the coastline and all the connected maritime infrastructures identification. The resulting coastline is archived in a Geodatabase and is the basis for the further coastline evolution analysis.

LARGE-SCALE MODEL TESTS ON SCOUR AROUND SLENDER MONOPILE UNDER LIVE-BED CONDITION

Ulrike PREPERNAU [(1)], Joachim GRÜNE [(2),] Reinhold SCHMIDT-KOPPENHEGEN [(3),] Zeya WANG [(4)] & Houcine OUMERACI [(5)]

[(1)] Dipl-Geogr., Coastal Research Centre (FZK), Merkurstr. 11, Hannover, 30419, Germany. prepernau@fzk.uni-hannover.de

[(2)] Dipl-Ing., Coastal Research Centre (FZK), Merkurstr. 11, Hannover, 30419, Germany. gruene@fzk.uni-hannover.de

[(3)] Dipl-Ing., Coastal Research Centre (FZK), Merkurstr. 11, Hannover, 30419, Germany. sk@fzk.uni-hannover.de

[(4)] M.-Ing., Coastal Research Centre (FZK), Merkurstr. 11, Hannover, 30419, Germany. wang@fzk.uni-hannover.de

[(5)] Prof. Dr.- Ing., Coastal Research Centre (FZK), Merkurstr. 11, Hannover, 30419, Germany H.Oumeraci@tu-bs.de

Abstract

This paper presents the results of an experimental investigation on scour around monopiles exposed to irregular waves. The large-scale laboratory tests were focussed on the development of scour in time, using different intensities of wave spectra consecutively without grading the mobile bed surface around the monopile. The scour process was monitored continuously by an installed observation window and a digital camera.

1. Introduction

The proposed paper deals with a comprehensive study on scour development around a slender monopile, which is mainly used for support structures of offshore wind turbines. The large-scale laboratory tests were carried out in the Large Wave Channel (GWK) of the Coastal Research Centre (FZK) under live-bed conditions with varying intensities of spectra (Jonswap) (see test conditions in Tab. 1 and Fig. 2), as it occurs similar to a strong wind field passing a monopile location. The GWK has a width of 5 m, a height of 7 m and a length of 325 m, the sand bed (mean diameter d_{50} = 0.33 mm) had a thickness of 1 m.

Table 1. Test conditions

Parameter	Spectra 1	Spectra 2	Spectra 3	Spectra 4
Significant wave height H_s [m]	0.90	1.00	1.10	1.20
Spectral peak period T_p [s]	7.60	8.00	8.40	8.80
waterdepth above sand bed h [m]	3.20	3.20	3.20	3.20
pile diameter D [m]	0.55	0.55	0.55	0.55

2. Experimental setup

To record the development of the scour continuously during the tests, an observation window was installed at one side of the monopile (shown in Fig. 1). Inside the monopile a digital camera was fixed on a vertical lift system, which was able to monitor the sand level at the bottom of the actual scour through the observation window. The digital images taken by the camera in time steps of some minutes during the tests were transferred online by telemetric system to a computer.

Fig. 1: Photos of the observation window at the monopile and of the installed camera
(left hand and middle photo from outside of monopile)
and recorded sand level in the scour (right hand side from inside of the monopile).

In a first test series the tests were started with an even bottom around the monopile to find out the maximum scour depth and scour evolution equilibrium respectively. In a second test series the different spectra from table 1 were applied in a sequence which is schematically similar to a storm surge in the North Sea which occurs typically in winter season. Such a storm surge starts with a period of steadily increasing wave energy up to a certain maximum value and ends with a period of steadily decreasing wave energy. The test series performed in the GWK was divided in 6 parts; 4 parts with increasing and 2 parts with decreasing wave energy and each part being constant as shown in Fig. 2.

3. Results

First results are shown in Fig. 2, where the scour depth S is plotted versus the number of generated waves of a sequence of different wave spectra. The results indicate that the scour depth development in dependence of stepwise changing generated wave spectra (parameters spectral peak period T_p and significant wave height H_s) lead to surprising and not expected results.

Despite to test conditions with an even bottom at starting a test with constant wave spectra, in the test series with a sequence of different spectra after changing to a spectra with higher energy the scour depth S firstly decreases with increasing wave energy and then after a while increases again up to a higher value compared to that before with a lower wave energy spectra. A similar effect was observed after changing the wave spectra to a lower one as before, firstly the scour depth S decreases as generally expected, but after a certain period the scour depth increases again.

A more detailed analysis on the test results and the sand transport at the scour bottom will be presented and discussed in the final paper.

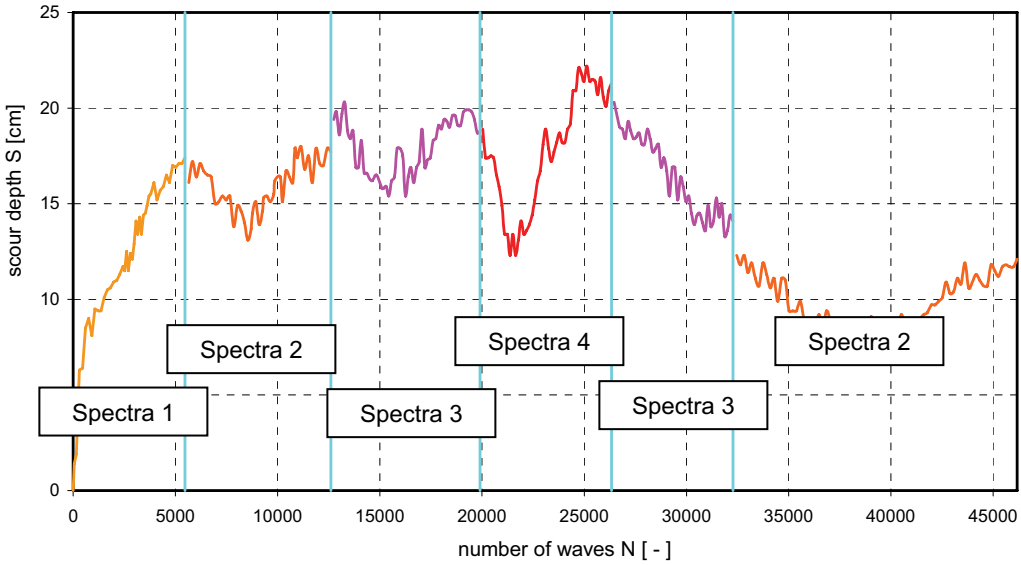

Fig. 2: Measured scour depth S at monopile versus number of generated waves

Acknowledgments

The work described in this publication was supported by the European Community's Sixth Framework Programme through the grant to the budget of the Integrated Infrastructure Initiative HYDRALAB III, Contract no. 022441 (RII3) within the Joint Research Activity "CoMIBBS".

On the experimental study of scour protections around monopile foundations: profile of dynamically stable scour protection

DE VOS LEEN [(1)], DE ROUCK JULIEN [(2)] & TROCH PETER [(3)]

[(1)] *Ir., Ghent University, Technologiepark 904, Ghent, 9052, Belgium. Leen.DeVos@UGent.be*

[(2)] *Prof. Dr. Ir., Ghent University, Technologiepark 904, Ghent, 9052, Belgium. Julien.DeRouck@UGent.be*

[(3)] *Prof. Dr. Ir., Ghent University, Technologiepark 904, Ghent, 9052, Belgium. Peter.Troch@UGent.be*

Abstract

When a monopile foundation is placed offshore it changes the local flow pattern and thus induces local scour at the base of the foundation. The scour hole can reach a depth of up to 2 times the pile diameter, and can therefore seriously affect the stability and dynamical behaviour of the foundation. A riprap scour protection is therefore mostly used to prevent a scour hole to threaten the foundations stability. The goal of the scour protection is not to avoid scour completely yet to shun scour from within a certain perimeter around the foundation. The authors investigated the time evolution of the damage development of a scour protection by means of an experimental study. A combined hydrodynamical flow is studied. This paper discusses the characteristics of the damaged profile, considering the flow pattern around the monopile. The results show that different shapes develop according to the loading condition.

1. Introduction

When a monopile is placed offshore and no countermeasures are taken, the sea bottom is subject to local scour due to waves and/or currents, due to the local amplification of the velocity and the turbulence by the foundation. When the expected scour depth has too large an influence on the foundations design or is not acceptable for the structures stability, a scour protection is applied. At this moment, riprap scour protections are commonly used around offshore foundations to avoid scour in the direct vicinity of the foundation. When designing a scour protection for an offshore monopile, the general tendency is to design a statically stable scour protection, with the requirement that individual stones are not to be displaced during the design storm. The required stone size is therefore strongly depending on the maximum velocity which can occur in the vicinity of the pile. As the local amplifications of the velocity, due to the presence of the pile can be up to a factor 4, the strict "no movement-criterion" may lead to conservative designs. An alternative design approach may accept some movement of individual stones (i.e. damage), without causing failure of the protection. Such a scour protection could be termed a dynamically stable scour protection, after the dynamically stable breakwaters (van der Meer, 1988)). A dynamically stable breakwater develops an S-shaped profile. An experimental study has been performed to determine the profile which develops in a scour protection around a monopile foundation and to investigate whether such a dynamically stable scour protection is possible. Tests have been carried out with irregular waves, combined with a steady current.

2. Experimental set-up

The experiments were conducted at Ghent University. Figure 1 shows a sketch of the set-up in the wave flume, which has a total length of 30m, a width of 1m and a height of 1m. One of the flumes side walls is made of glass, to facilitate observations. A current can be produced in both directions, permitting the current to follow or oppose the waves.

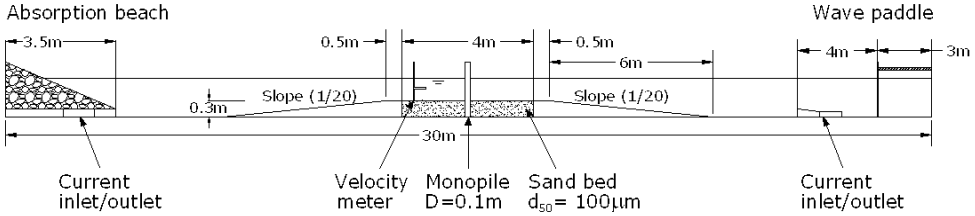

Figure 1. Side view of experimental set-up (not to scale).

A movable sand bed was installed in the middle of the flume by aids of an elevated bottom. A monopile with diameter of 0.1m was installed in the centre of the flume and represents a typical monopile foundation for offshore wind turbines in the north sea, on scale 1/50. A rip-rap scour protection with an outer diameter equal to 5 times the pile diameter is placed on top of a geotextile filter. The scour protection is constructed above the sand bottom. Figure 2 shows a picture of a scour protections placed around the monopile foundation.

The bed profiles were surveyed before and after testing with a non-contact laser profiler on a grid of 5 x 5mm. The scour protection was placed in concentric, coloured rings to allow a visual estimate of the damage as well and 4 damage levels can be distinguished after testing:

1. damage level 1: no movement of the stones
2. damage level 2: very limited movement of stones
3. damage level 3: significant movement of stones, without failure of the protection
4. damage level 4: failure of the protection

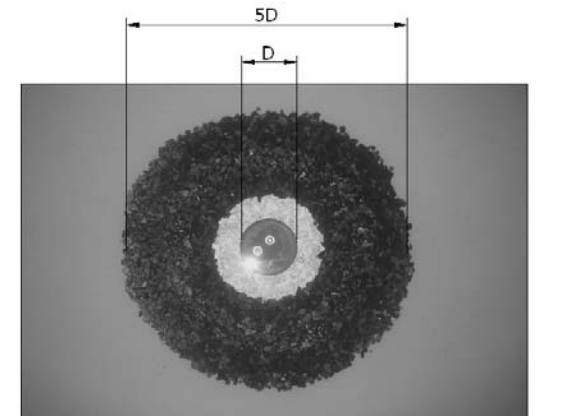

Figure 2: Example of scour protection around monopile foundation.

The range of wave and current conditions at the monopile are shown in Table 1. The irregular waves have a Jonswap spectrum with a gamma factor $\gamma = 3.3$, representing typical North Sea conditions (Goda, 2000)). The Keulegan Carpenter number KC represents the ratio of the amplitude of the orbital motion, caused by the waves and the pile diameter. The KC number is calculated according to Sumer and Fredsøe (2002) as $KC = U_m T_p/D$, with U_m a representative orbital velocity near the bottom, calculated from the spectrum of the orbital velocities S(f) as $U_m = \sqrt{2}.\sigma_u$, with $\sigma_u^2 = \int S(f)df$. For most tests, 5000 waves were generated. The bed profile was measured before each test, after 1000 waves, after 3000 waves and after 5000 waves.

Table 1. Hydraulic conditions at the pile: wave and current characteristics.

Parameter	Symbol	Range
Wave height [m]	H_s	0.05-0.168
Wave period [s]	T_p	1.13-1.7
Water depth [m]	d	0.2-0.4
Current velocity [m/s]	U_s	0-0.28
Keulegan Carpenter number [-]	KC	0.8-3.6
Pile Reynolds number [-]	Re_D	1.5-4.3 (10^4)

3. Analysis of dynamic profile

Figure 3 shows damage profiles which were deduced from the bed profiles of the scour protection. The damage is represented as the difference between the bed level before and after a test. Figure 3 represents three different loading cases, corresponding to the typical damage shapes that were measured around the monopile foundation. Waves are always travelling from bottom to top. Profile (a) represents a typical wave alone case: damage is mostly present at the sides of the pile, while a slight lowering is also found in front of the pile. Case (b) represents a typical damage profile due to a wave following a current: an area behind the pile experiences a lowering of the scour protection. Some damage is still found at the edges of the pile. Case (c) represents a typical damage profile for a wave opposing the current: the damage is now located in front of the pile (when considering the wave direction). In both cases (b) and (c) the damaged area is somewhat wider than the pile diameter. The applied current velocities were too small to obtain damage to the applied scour protections due to a steady current velocity alone.

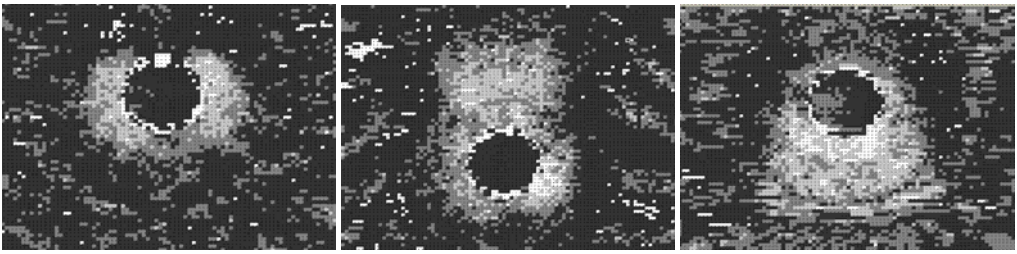

(a) (b) (c)

Figure 3. Measured elevations [mm] (erosion (< 0) and deposition (> 0)) from the bed profiles of the scour protection around the monopile. ■ : +10 < elevation ≤ 0; ■ : 0 < elevation ≤ -5; □: -5 < elevation ≤ -10; □: -10 < elevation.

For the quantitative analysis of the damage, the scour protection is divided into sub areas, as shown in Figure 4. The scour protection area is divided into 4 rings, corresponding with the 4 coloured rings in the set-up. Each ring has a width of 0.05m, corresponding to the radius of the pile. These rings are then further divided into different sub areas, with a surface equal to the pile's area. The orientation of the zones is chosen to optimally represent the damage location and is therefore mainly based on the current direction. The damage number is calculated per sub area as the ratio of eroded volume to the surface of the sub area times the nominal stone diameter. The damage number of the total scour protection is defined as the damage number for the zone with the highest damage.

The location of the damage depends mainly on the presence and direction of the current. For very small current velocities, the damaged profile is the same as for the wave alone case, i.e. only damage at the sides of the pile is present. When the current velocity increases, damage develops in the area behind the pile. For limited current velocities, the damage is still highest at the sides of the pile. For high current velocities the damage is however highest in the area behind the pile. This is illustrated in Figure 5, where

for each of the three cases (waves only (a), waves and following current (b), waves and opposing current (c)), the location of the damage is shown. Per zone, the percentage of tests resulting in the highest damage in this zone is given.

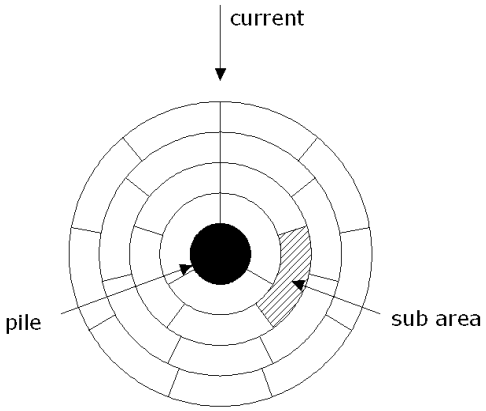

Figure 4: Division of the scour protection into sub areas.

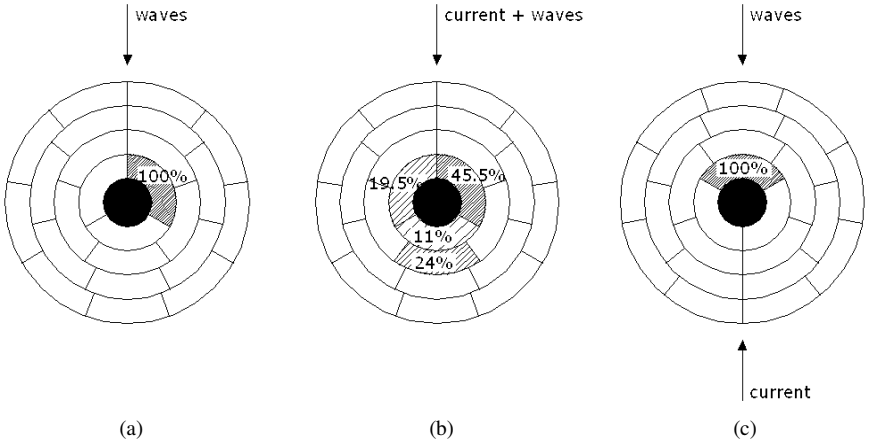

Figure 5: Location of damage and % of tests with highest damage in the zones: for waves only (a), waves and following current (b), waves and opposing current (c).

Acknowledgments

The grant for this research was provided by the Research Foundation – Flanders. The Research Foundation – Flanders is gratefully acknowledged.

References

Goda, Y., 2000. Random seas and design of maritime structures. Advanced series on ocean engineering. World scientific, Singapore, 981-02-3256-X.

Sumer, B.M. and Fredsøe, J., 2002. 'The mechanics of scour in the marine environment', Advanced series on ocean engineering, World Scientific, River Edge, NJ. 981-02-4930-6.

Van der Meer, J.W., 1988. 'Rock slopes and gravel beaches under wave attack', Delft hydraulics.

LABORATORY TESTS ON PERFORMANCE OF A COASTAL PROTECTION PROJECT IN AGROPOLI

EDOARDO BENASSAI [(1)], MARIO CALABRESE [(1)], MARIANO BUCCINO [(1)], PASQUALE DI PACE [(1)], FRANCESCO PASANISI [(2)], CARLO TEBANO [(2)] & FRANCESCO ZARLENGA[(3)]

[(1)] *University of Napoli Federico II, Dept. Hydraulic, Geotechnical, Environmental Engineering, Via Claudio 21, Napoli, 80125, Italy. benassai@unina.it, calabres@unina.it, buccino@unina.it, pdipace@unina.it*

[(2)] *ENEA, Dept. Environment, Global Changes and Sustainable Development, Portici Research Center, Località Granatello, Portici (NA), 80055, Italy. francesco.pasanisi@portici.enea.it, carlo.tebano@portici.enea.it*

[(3)] *ENEA, Dept. Environment, Global Changes and Sustainable Development, Casaccia Research Center, Via Anguillarese 301, S. Maria di Galeria (Roma), 00123, Italy. zarlenga@casaccia.enea.it*

Abstract

An experimental study was commissioned to evaluate, at design stage, the performance of a beach nourishment protected by a submerged rubble mound breakwater with gaps in Agropoli (Gulf of Salerno). Experiments were performed in the wave basin at University of Napoli Federico II. Results showed that under extreme wave conditions no significant loss of material is to be expected through the gaps of the structure. Measured post-nourishment coastline retreats due to cross-shore processes were comparable with prediction obtained using mathematical models, and were considered acceptable.

1. Overview of the project

The coast between Cape San Marco and the mouth of Testene River, in Agropoli at southern end of the Gulf of Salerno, is a straight, narrow, sandy beach, about 1.5 km long and 20-25 m wide. The littoral showed, over the last decades, a significant erosive trend, with a great concern for the safety of the coast road and other structures located landwards.

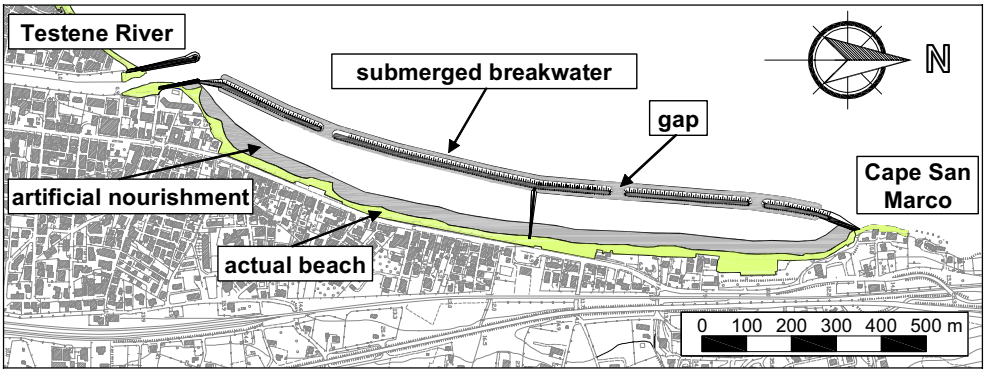

Figure 1. Plan of the coastal protection project in Agropoli

A protection measure was thus proposed, consisting of an artificial beach nourishment protected by a shore-parallel submerged rubble mound breakwater located 120m offshore (considering actual coastline), at about 3.5m depth, with a 0.70m freeboard above the crest.

Post-nourishment shoreline advance is 30.0m, with an expected 10.0m long term erosion, resulting in a planned net 20.0m advance. Three gaps are planned along the structure, 20.0m wide, to ensure water circulation and navigation. Finally, semi-submerged groins are planned at both ends and in the middle of the barrier.

In Figure 1 a plan of the protection project is reported while Figure 2 shows a cross-section of the submerged barrier.

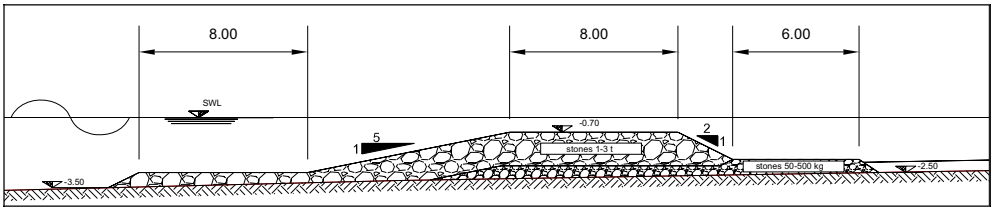

Figure 2. Cross-section of submerged breakwater

In order to verify the hydraulic performance and shoreline response to the structure, that, despite recent progresses, can be affected by dramatic uncertainties (Ranasinghe & Turner, 2006), an experimental study was commissioned to complete the design stage.

2. The physical model

Experiments were performed in the 3D wave basin at University of Napoli Federico II, Department of Hydraulic and Environmental Engineering "G. Ippolito" (Figure 3). The basin was recently equipped with HR Wallingford multi-element wavemaker and up-to-date instrumentation in the frame of a research project ENEA-University of Napoli.

Figure 3. Pictures taken during tests. Two couples of wave gauges are visible at leading side and trailing side of the submerged barrier.

A geometric 1:40 scale factor was chosen and Froude similarity was adopted. Sediment size was scaled under the criterion of conservation of fall speed parameter (Hughes, 1993).

Two different layouts were tested, corresponding to different stages of project execution:

A. Submerged barrier and actual beach;
B. Submerged barrier and beach nourishment.

Both configurations were tested under extreme design wave conditions corresponding to 30 years return period: H_s=5.14m, T_p=11.4s, storm duration=12 hours (prototype scale), direction: 275°N. Long-shore processes were not considered.

3. Summary of main results

Similarly as widely reported in literature (e.g. Loveless & MacLeod, 1999, Johnson et al., 2005), a strong current offshore directed was noticed at the gap of the barrier. Local excavation was thus observed around the heads of the barrier, with sedimentation inside the gap (Figure 3).

Figure 4. Current pattern and sediment processes at the gap of the barrier.

Beach profiles before and after wave attacks were measured using a beach profiler with touch sensitive probe along different transects.
Results for layout A (without nourishment) showed a limited beach profile erosion behind the breakwater, due to wave energy reduction at barrier. As expected, profile erosion was more evident behind the gap rather then behind current section of the breakwater.

As regards layout B, results showed a typical post-storm beach profile, characterized by high steepness, coastline retreat and sediment deposition landward (Figure 5).

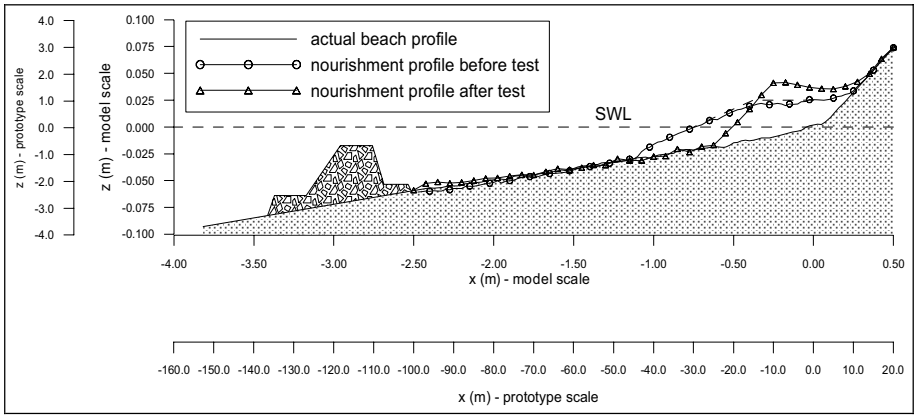

Figure 5. Beach nourishment profile modification behind the barrier under extreme waves attack

Observed profiles behind the current section of the breakwater are similar to those typically reported in laboratory and field (Figure 6) studies for this kind of structures (Sorensen & Reil, 1988, Ferrante et al. 1992).

Measured coastline retreat varies in the range 8.0-10.0 m and is comparable to what predicted at earlier design stage using mathematical models. Similar results, but with a milder beach profile, were obtained behind the gap.

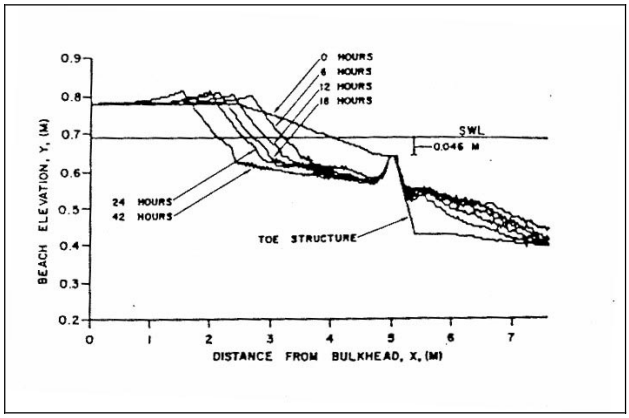

Figure 6. Evolution of the beach nourishment profile behind a barrier reported by Sorensen & Reil (1988).

Acknowledgments

Experimental study was commissioned by Autorità di Bacino Regionale Sinistra Sele.

References

Ferrante, A., Franco, L. & Boer, S., 1992. 'Modelling and Monitoring of a Perched Beach at Lido di Ostia (Rome)'. *Proc. 23rd Int. Conf. on Coastal Engineering, Venice, Italy*.

Hughes, S.A. 1993. 'Physical Models and Laboratory Techniques in Coastal Engineering'. World Scientific Publishing, Singapore. ISBN 9810215401

Johnson, H., Karambas, T.V., Avgeris, I., Zanuttigh, B., Gonzalez-Marco, D. & Caceres, I. 2005. 'Modelling of Waves and Currents Around Submerged Breakwaters', *Coastal Engineering,* 52, 949-969.

Loveless, J. & MacLeod, B. 1999. 'The Influence of Set-Up Currents on Sediment Movement Behind Detached Breakwater', *Coastal Sediments '99*, 2026-2041.

Ranasinghe, R. & Turner, I.L. 2006. 'Shoreline Response to Submerged Structures: A review', *Coastal Engineering*, 53, 65-79.

Sorensen, R. & Reil, N.J., 1988. 'Perched Beach Profile Response to Wave Action'. *Proc. 21th Int. Conf. on Coastal Engineering*, Malaga, Spain.

DUNE EROSION PREDICTION DURING STORM SURGES

Rosanna Gencarelli [(1)], Giuseppe Roberto Tomasicchio [(2)], Felice D'Alessandro[(3)], & Ferdinado Frega [(4)]

[(1)] *Post Doct ., Soil Conservation Dept., University of Calabria, Ponte P.Bucci, Cubo 41 B, Rende, 87036,Italy.*
E-mail: rgencarelli@dds.unical.it

[(2)] *Full Professor, Engineering Dept, University of Salento, Via Per Monteroni, Lecce, 73100, Italy.*
E-mail roberto.tomasicchio@unile.it

[(3)] *Post Doct, Engineering Dept., University of Salento, Via Per Monteroni, Lecce, 73100, Italy.*
E-mail: dalessandro@dds.unical.it

[(4)] *Ass. Professor, Soil Conservation Dept., University of Calabria, Ponte P.Bucci, Cubo 41 B, Rende, 87036,Italy.*
E-mail: ferdinandofrega@dds.unical.it

Abstract

The study analyzes the dune erosion and breaching occurred on the northern Outer Banks of North Carolina in September 2003 during Hurricane Isabel. LIDAR mapping of topography collected by USGS is used to establish pre- and post- storm profiles. Isabel made landfall near the USACE Field Research Facility (FRF) at Duck, North Carolina, where high quality wave and water level measurements are available. With the use of the hydrodynamics data, the bathymetric and topography data have been analyzed to examine the degree and alongshore variability of the dune retreat and breaching as a function of the pre-storm beach and dune characteristics. In addition, the data will be used to calibrate and verify the numerical model CSHORE (Kobayashi et al., 2007) to predict the dune erosion and overwash for obliquely incident waves with longshore currents.

1. Introduction

Coastal dune reduce the extent and impact of significant wave events. Thieler and Young (1991), for instance, found that the presence of dunes before a storm reduced the damage from waves and storm surge during hurricane Hugo. Dune erosion and breaching, however, are expected to occur more frequently as sea level rise and hurricane intensity accelerate due to rising temperatures. At present, no reliable method exists to predict dune erosion and breaching due to the lack of comprehensive field data and to the limited capability of predicting cross-shore sand transport. Only few studies have been developed to predict the dune erosion.

The investigation of cross-shore sediment transport, that has been an increasingly important topic as coastlines around the world continue to change (Jimènez and Sànchez-Arcilla, 2004), is complex due to the variability of factors contributing to sediment motion. Cross-shore sediment transport on beaches has been investigated extensively, however an accurate prediction of beach erosion and accretion, even for the idealized case of alongshore uniformity, normally-incident waves and uniform sediment, is still not possible.

Kobayashi et al. (2007b) conducted small-scale physical model tests on a fine sand beach in order to obtain a new data set and to calibrate the numerical model CSHORE (2007d) for cross-shore sediment transport. The model predicts dune erosion and overwash-induced effects on the cross-shore profile evolution after an extreme storm event. This model will be analyzed and verified in order to predict the effects due to the impact of hurricane Isabel along the North Carolina coastline.

2. Hurricane Isabel

Hurricane Isabel made landfall on September 18, 2003 near Ocracoke, Outer Banks (Fig 1), in North Carolina as a Category 2 hurricane (Saffir-Simpson Hurricane scale,1969).

Figure 1. Outer Banks, North Carolina

Hydrodynamic forces information about hurricane were collected by the Field Research Facility (FRF) at Duck, North Carolina. It's an internationally recognized coastal observatory founded in 1977 by U.S Army Corps of Engineers. Central element of the observatory is a 560 meter long pier and specialized equipments that record constantly changing of waves, wind, tide and currents. The maximum values of significant wave height, H_{mo}, measured during the hurricane have been 8.12 m.

A NOS (National Ocean Service) acoustic tide gauge is used to collect water level every 6 minutes throughout the day. This gauge is at the seaward end of the FRF pier. The maximum value of the observed tide is equal to 2 m referenced to the National Geodetical Vertical Datum of 1929 (NGVD) system.

3. Dune erosion and beach profiles evolution during Hurricane Isabel

Waves and currents interacting with the bottom sediments produce changes in the beach and nearshore bathymetry. These changes can occur very rapidly in response to storms or slowly as a result of persistent but less forceful seasonal variations in waves and currents. In the case of hurricane Isabel, information about profiles and dunes evolution have been assembled using LIDAR data and FRF survey data.

The LIDAR system sampled laser altimetry data before and after extreme storms to quantify amount of coastal change. The LIDAR system cold not penetrate deep enough into turbid water to identify the sub-aqueous profiles; for this reason LIDAR data, in the Isabel analysis, have been used only to analyze the dune erosion and breaching.

The eroded area, A, and average vertical change, d, have been calculated for each LIDAR dune profiles. The alongshore variation of the dune area eroded ($A < 0$) during Isabel is a function of the distance to the point where the hurricane made landfall. Mean value of the eroded area is close to 20 m^2/m, which corresponds to a 10-year event according to the empirical formula proposed by Hallermeier and Rhodes (1988). The new breach opened near the point where Isabel made landfall.

Since 1981, the FRF has been conducting detailed surveys of beach profiles. These data set allow to quantify the dynamic evolution of the nearshore zone during storms when changes are most rapid.

Bathymetry at the FRF is characterized by regular shore-parallel contours, moderate slope and barred surf zone. This pattern is interrupted in the immediate vicinity of the pier. Profile configuration is typically single-barred with the most active zone extending from the base of the dune to about 6 meters water depth. Maximum vertical change occurs just seaward of the shoreline.

29 FRF survey profiles were collected before and after hurricane Isabel to quantify the area erosion and vertical change due to the impact of hurricane . Pre Isabel profiles were observed the 8th August, 2003; post Isabel profiles were observed the 21th September, 2003. The values of A have been analyzed as a function of alongshore distance to the FRF pier.

4. The numerical model CSHORE

The numerical model CSHORE (Kobayashi et al., 2007d) is an extension of the time averaged model

developed by Kobayashi et al. (2007a) on the basis of laboratory tests by Reniers and Battjes (1997) and Ruessink et al (2001). The time-averaged continuity, cross-shore momentum, longshore momentum and wave energy equations are used to predict the cross-shore variation of the mean free surface elevation, $\overline{\eta}$, above SWL, the free surface standard deviation, σ_η, the depth-averaged cross-shore, $\overline{U}$, and longshore, $\overline{V}$, current.

The combined wave and current model predicts the cross-shore variation of the hydrodynamics variables used in the transport model for given beach profile, water level and seaward wave condition.

The bottom sediment is assumed to be uniform and characterized by mean diameter, d_{50}, sediment fall velocity, w_f, sediment specific gravity, s, and porosity of bottom, n_p.

The cross-shore variation of the degree of sediment suspension is estimated using the experimental findings of Kobayashi et al (2005) showing that the turbulent velocities measured in the vicinity of the bottom are related to the energy dissipation rate due to bottom friction.

The cross-shore and longshore suspended sediment transport rates, q_{sx} and q_{sy}, are given as

$$q_{sx} = a\ \overline{U}V_s \quad ; \quad q_{sy} = \overline{V}V_s \qquad \textbf{[1]}$$

where $a = 0.2$ is an empirical suspended load parameter and V_s is a suspended sediment volume per unit horizontal bottom area (Kobayashi and Johnson, 2001).

The formulae for the cross-shore and longshore bedload transport rate, q_{bx} and q_{by}, are determined somewhat intuitively because in the surf zone they have never been observed. The proposed beadload formulae are written as

$$\begin{aligned} q_{sx} &= \frac{bP_s}{g(s-1)}\sigma_T^3\left(1 + U_*V_*^2 + 2F_m\sin\theta\right)G_s \\ q_{sy} &= \frac{bP_s}{g(s-1)}\sigma_T^3\left(V_*\left(1 + U_*^2 + V_*^2\right) - 2r_m\sin\theta\right) \end{aligned} \qquad \textbf{[2]}$$

where the empirical bedload parameter, b, is equal to 0.002, and G_s is the bottom slope function introduced by Kobayashi et al.(2007) to account for the effect of the steep cross-shore slope, S_b, on the bedload transport rate.

5. Comparison with the data

The numerical model CSHORE has been tested and verified using the FRF survey profiles before and after Isabel. The information about wave, tide value and wind velocity and direction are given by FRF gauges. The FRF profiles are characterized by mean sediment diameter, d_{50}, equal to 0.20 mm, by sediment fall velocity, w_f, equal to 0.025 m/s and specific gravity of sediment equal 2.60.

Results have been obtained about the measured and computed temporal (7 days during September 15-21) variation of the free surface standard deviation at the seaward end of the FRF pier (gauge 625) for the empirical breaker ratio parameter γ= 0.7, used in the previous laboratory test comparison by Kobayashi et al (2007a,b,c), and 0.6. A better agreement has been found for γ=0.6.

Figure 2 shows the computed cross-shore and longshore transport rate.

The cross-shore variation of bedload, q_{bx}, transport rate is positive, whereas the cross-shore suspended sand transport rate, q_{sx}, is negative. The absolute values of q_{bx} and q_{sx} are larger in the breaker zone. The computed total sand transport rate, $q_x = (q_{bx} + q_{sx})$, is positive except in the zone close to the shoreline.

The longshore bedload transport, q_{by}, rate is small in comparison with the longshore suspended sand transport rate, q_{sy}.

In general, the longshore sand transport, q_y, exceeds the cross-shore transport rate, q_x.

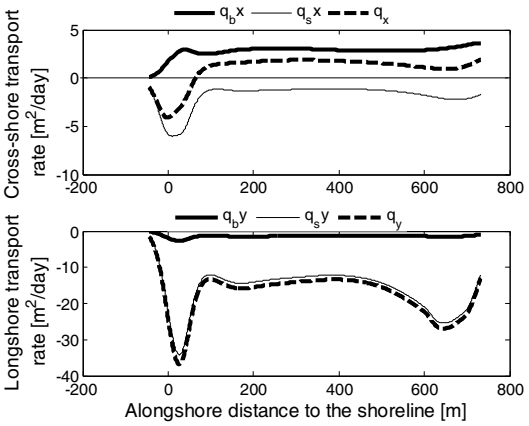

Figure 2. Measured cross-shore and longshore transport rate component

References

Agarwal, A., Kobayashi, N., Johnson, B.D., 2006. Longshore suspended sediment transport in surf and swash zone. *Proc. 30th Coastal Engineering Conf.,* Word Scientific, Singapore.

Battjes, J.A., and Stive, M.J.F., 1985. Calibration and verification of a dissipation model for random breaking waves. *J. Geophys. Res.,* 90 (C5) 9159-9167.

Hallermeier, R.J., Rhodes, P.E., 1988. Generic treatment of dune erosion for 100-year event. *Proc., 21st Int. Conf. on Coastal Engineering*, ASCE, New York, 1197–1211.

Jimenez, J.A. and Sànchez-Arcilla, A., 2004. A long term (decadal) evolution model for microtidal barrier system. *Coastal Engineering*, 51, 749-764.

Kobayashi, N. 1987. Analytical solution for dune erosion by storm. *J.Waterway, Port, Coastal, Ocean Eng.*, 113(4), 401-418.

Kobayashi, N., Johnson, B.D., 2001. Sand suspension, storage, advection and settling in surf and swash zones. J. Geophys. Res., 106(C5), 9363-9376.

Kobayashi, N., Agarwal, A., Johnson, B.D., 2007a. Longshore current and sediment transport on beaches. *J. Waterway, Port, Coastal, Ocean Eng*., 133(4) 296-306.

Kobayashi, N., Payo, A., Schmied, L. D., 2007b.Cross-shore suspended sand and bedload transport on the beaches. *J. Geophys. Res*., (submitted).

Kobayashi, N., de los Santos, F.J., 2007c. Irregular wav seepage and overtopping of permeable slopes. *J.Waterway, Port, Coastal, Ocean Eng.*, 133(4), 245-254.

Kobayashi, N., Payo, A., Johnson, B.D., 2007d. Suspended sand and bedload transport on beaches. *Handbook of coastal and ocean engineering*, Word Scientific Singapore (will be published).

Ruessink, B.G., Miles, J.R., Feddersen, F., Guza, R.T., Elgar, S., 2001. Modeling the alongshore current on barred beaches. *J. Geophys. Res.* 106, 22451-22463.

van Gent, M.R.A., Coeveld, E.M., Walstra, D.J.R., van de Graaff, J., Steetzel, H.J. and Boers, M., 2006. Dune erosion tests to study the influence of wave periods. *Proceedings of the 30th International Conference of Coastal Engineering*, ASCE, 3, 2779-2791.

Thieler, E.R., and Young, R. S. 1991. *"Quantitative evaluation of coastal geomorphic changes in South Carolina After Hurricane Hugo*" In: Finkl, C.W. and Pilkey, O.H. (eds.), Impacts of Hurricane Hugo: September 10-22, 1989, J. Coast. Res. #**8**: 187-200.

EVOLUTION OF AN UNPROTECTED BEACH UNDER OBLIQUE WAVE ATTACKS

M.G. Molfetta[1], A.F. Petrillo[1], L. Pratola[1], A. Rinaldi[1]

(1) *Department of Water Engineering and Chemistry – Research and Experimentation Laboratory for Coastal Defense (LIC) - Polytechnic University of Bari - Italy*

*e-mail: m.molfetta@poliba.it, petrillo@poliba.it, l.pratola@poliba.it, a.rinaldi@poliba.*it

Keywords: longshore currents, beach nourishment, shoreline evolution.

Abstract

Some of most important factors responsible for the morphodynamic evolution of a sandy beach are incident wavy motion features and duration, grain size and character of the sand and the bathymetry and slope of the beach. For a sandy beach with nourishment and without artificial protection structures, the shore creates natural defences against attacks by waves, currents and storms. The first of these defences is the sloping nearshore bottom that causes waves to break offshore, dissipating their energy over the surf zone. The process of breaking often creates an offshore bar in front of the beach that helps to trip following waves. The broken waves re-form to break again, and may do this several times before finally rushing up the beach foreshore with specific features. These features produce alterations to the shoreline due to accretion and/or erosion patterns. Littoral transport, defined as the movement of sediment in the nearshore zone by waves and currents, is divided into two general classes: transport parallel to the shore (longshore transport) and transport perpendicular to the shore (cross-shore transport). Cross-shore transport is determined primarily by wave steepness, sediment size, and beach slope. In general, high steep waves move material offshore and low steepness waves move material onshore. Longshore transport is a result of the stirring up of sediment by the breaking wave and the movement of this sediment by both the component of the wave energy in an alongshore direction and the longshore current generated by the breaking wave. The direction and the rate of longshore transport is directly related to the direction of wave approach and the angle between the breaking waves and the shoreline. An increase in the angle produces an increase in the longshore transport rate.

In the present study, experimental surveys were carried out on a 3D physical model with a mobile bottom, and were analysed in order to investigate the morphodynamic evolution of a sandy beach without coastal protection structures under oblique wavy attacks.

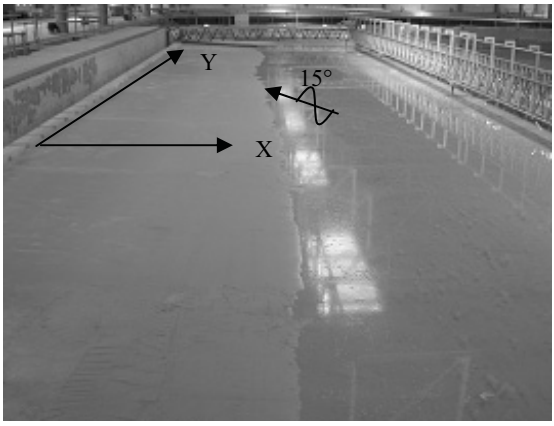

Figure 1. View of the model.

The study was conducted in a 3D physical model (Fig. 1) at the Coastal Engineering Laboratory of the Water Engineering and Chemistry Department of the Technical University of Bari – Italy. A stretch of Italian coastline was reconstructed characterized by a sandy beach with nourishment but without artificial protection structures.

The basin (90m long, 50m wide and 1.2m deep) was equipped with a wave maker which was able to generate waves with different characteristics along a wavefront of 28.8m. The model was built at 1/15th scale using a Froude analogy,

while a Dean analogy was used to reproduce the sand transport; Dean analogy foresees the conservation of the parameter H/(wT), where H and T are the height and the period of the significant wave respectively, while w is the fall velocity of sediments. The sand grains used for the bed were silica sand characterized by a very narrow granulometric distribution curve of D_{50}=0.129mm and a fall velocity of w = 1.91cm/s, measured in the laboratory using a pipe with continuous methodology (G. Ranieri, 2002).

Wavy attacks were generated in the model with a JONSWAP spectrum, at a depth of 0.9m (13.5m in prototype), with only one direction at an inclined angle of 15°.

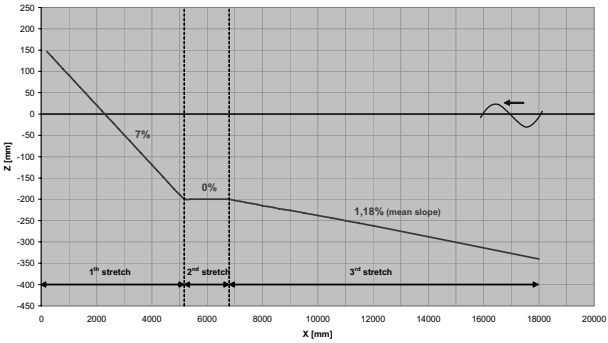

Figure. 2. Initial generic profile.

The initial bathymetric configuration was characterized by a profile with three different stretches: the first, from the emerged beach to -0.2m depth (3m in prototype scale) with 7% slope; the second, on the final depth of the previous stretch, 1.6m wide (24m in prototype) and horizontal; the last with a 1.18% mean slope, arriving at the closing ramp with a depth of -0.34m (5.1m in prototype). In figure 2 the initial profile is reproduced in deformed scale, as described before.

In the model, different wave attacks were generated with a JONSWAP spectrum. In table 1, significant height, peak period and duration indications of the wave attacks are reported.

Test n.	H_s [cm]	T_p [s]	Duration [h]	Surveys
				Depth D_0 Shoreline S_0
1a	3.0	1.20	0.75	
1b	6.0	1.20	0.33	
1c	9.0	1.20	3.00	Shoreline S_1
2	9.0	1.20	9.50	Shoreline S_2
3	9.0	1.20	4.00	Shoreline S_3
4	5.0	1.78	5.00	Shoreline S_4
5	7.6	1.50	3.00	Shoreline S_5
6	15.7	1.80	2.00	Shoreline S_6
7	5.0	1.78	5.00	Shoreline S_7
8	7.6	1.50	4.00	Shoreline S_8
9	15.7	1.80	2.00	Depth D_9 Shoreline S_9

Table 1. Tests and surveys.

For each of them, a number of topographical surveys (shown in the same table) were performed at the end. The two depth surveys, carried out just before the first wavy attack (Depth D_0) and at the end of the last one (Depth D_9), were performed on the emerged and submerged beach by means of a total station. They was conducted along initial shoreline perpendicular transepts, with a 0.2m acquisition step as far as X=9m, 0.5m between X=9m and X=12m and 1m for the remaining length (see figure 3 for the reference frame XY). Transepts were spaced 2m from each other.

Initially, a series of three different wavy attacks were generated (tests 1a, 1b, 1c) in order to shape the beach with a natural pattern. For this reason, shoreline surveys were conducted only at the end of the last of the previous tests (Shoreline S1). For the remaining tests, they were conducted at the end of each one. Shoreline surveys were carried out with a 1m step alongshore (Y direction). Depth surveys analysis shows a strong scour along the shoreline strip for low values of Y direction, and a considerable store for high values. This is a clear effect of the longshore sediment transport towards increasing Y values, due to the inclination of incident waves. As an example, in figure 3 the superimposition of the generic initial profile and the final one conducted in a central zone of the model (precisely at Y=18m) is reproduced. It is possible to observe the above mentioned erosion in the shoreline zone, which caused a moving back of the shoreline as far as Y=25÷26m (for higher values of Y, the shoreline moved forward). Moreover, a rise of the bed is clearly visible between the first and second initial stretch (from X=3,5m to X=7,5m for the profile in figure 3).

For greater depth, fluctuations of the bed were characterized by long undulations near the initial profile, with the formation of bars (visible on the graph).

To understand global sediment transport occurred in the model, an analysis was conducted by subtracting from final to initial bed elevations.

Interpolating the resulting values, it was possible to draw the bed elevation change map (figure 4). This map shows sediment erosion areas (negative values) and store areas (positive values) with a colour scale. Initial and final shorelines have been drawn with clear and dark curves respectively.

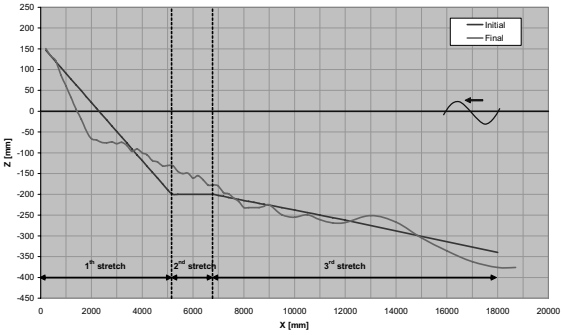

Fig. 3. Initial and final profile (at Y=18m).

To fill the triangular area over Y=28m where there are no bed elevation data, the same profile as that at Y=28m (on the corresponding X values) was assigned to the right boundary. In this way, assigned elevation data are undervalued. From figure 4, it is possible to understand the importance of sediment erosion on the emerged and submerged beach near the shoreline on the left side of the model, where scour amounts maximum value equal to 160mm, corresponding to 2.4m in the prototype scale. It is important to consider the fact that this effect is so strong due to the lack of nourishment from the left side.

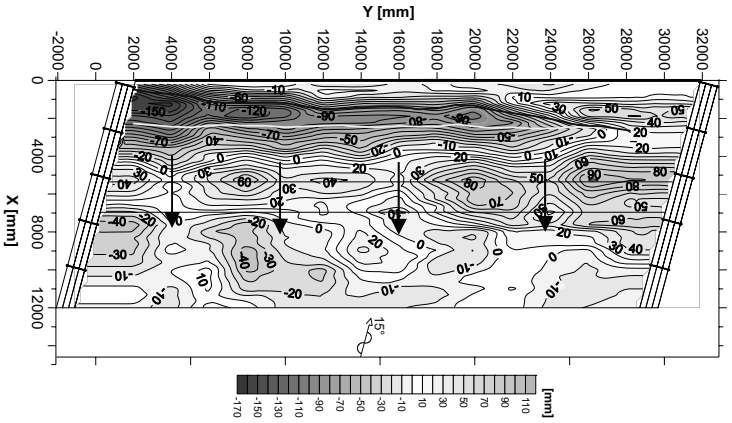

Fig. 4 Bed elevations change map

On the right side of the model, the vast area of sediment store is evident, with a maximum increase of 90mm (1.35m in prototype scale) at Y=26÷28m between the first and the second stretch of the initial profile (X=5.2m). In this zone, longshore sediment transport found an impermeable barrier due to the presence of the right boundary. This generates a circulation current which is bound for the offshore direction along the boundary. Thus, it produces the sediment store which is so visible in figure 4. In the same figure, a succession of sediment store areas along the line between the first and the second stretch of the initial profile is also clearly visible. This succession is a clear sign of rip currents generation (arrows in figure 4).

In addition to bed elevation surveys, for each test shoreline surveys were carried out. Figure 5 shows the sequence of the shorelines in a deformed scale graph. In the legend, a list of shoreline surveys with relative last wavy attack information (significant height and duration) is shown.

The moving back of the shoreline at low values of Y is evident (about 1.8m corresponding to 27m in prototype scale, at Y=2m). On the right side of the graph, curves intersected because of the moving forward of the shoreline at high values of Y, even if it is not so evident in the graph due to the lack of surveys for Y values higher than 28.18m, as mentioned above.

To evaluate shoreline evolution, the emerged beach area was calculated for the initial one (as the area between shoreline and X=0). Dividing this by 26.18m (the length of the surveyed shoreline), an initial position reference value, X_0, was obtained coming from a rectangular area. This procedure was carried out for each shoreline; thus every X_i value was compared with X_0, using a X_i/X_0 ratio which was correlated with the wave energy flux evaluated at the generation zone (figure 6).

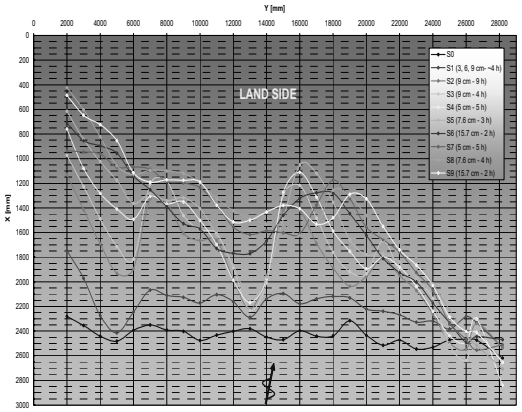

Figure 5. Sequence of shorelines.

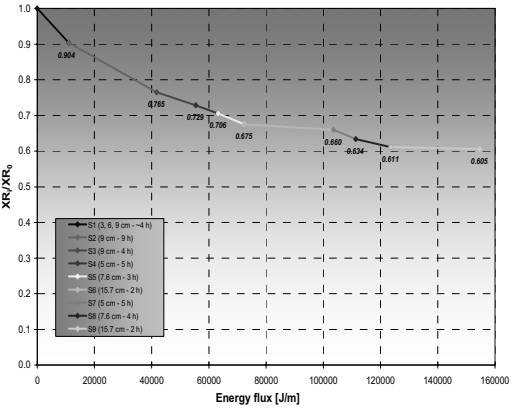

Figure 6. Shoreline evolution correlated with the energy flux.

The graph in figure 6 shows the progressive moving back of the shoreline, which is rapid in the first tests due to the non-natural initial bed configuration. In later tests, the shoreline evolution slowed down until it reached a condition near to equilibrium.

The curve ended with X_i/X_0=0.605 corresponding a 39.5% decrease of the distance between the shoreline and the Y axis. From figure 5 the progressive clockwise rotation of the shoreline is also clear which tends to assume a parallel to the incident wave direction.

Finally, our analysis allows us to deduce that in a 3D model, the shoreline of an initial profile in a "non-equilibrium condition" under oblique wave attacks reaches a condition of "quasi-equilibrium" fairly rapidly due to longshore currents. A comparison with a 2D model presented in literature showed that, with an equal energy flux, the condition of equilibrium of the shoreline is reached more slowly due to the absence of longshore currents in 2D models.

References

Chiaia G., Damiani L., Petrillo A.F. (1992). "Evolution of a beach with and without a submerged breakwater: experimental investigation", *XXIII International Conference on Coastal Engineering*, Venezia Italy, Oct. 1992.

H. Hanson and M. Larson (2004). "Implications of morphodynamic time scale for coastal protection", *Coastal Engineering*, 2620:2632.

Kriebel D.L., Dally W.R., Dean R.C. (1986). "Undistorted Froude model for surf zone sediment transport", *Coastal Eng. Proc.*, Taipei – Nov. 9-14.

Nishimura H., Sunamura T. (1986). "Numerical simulation of beach profile changes", *Coastal Eng. Proc.*, Taipei – Nov. 9-14.

Larson M. (1988). "Quantification of beach profile change", *Lund Sweden.*

Ranieri, G. (2002). "A standard method for measuring the average fall velocity of natural sands", *Proc. Hydraulic Measurements and Experimentation Conference*. Estes Park, Colorado, USA.

INVESTIGATION ON MORPHOLOGICAL EFFECTS OF DETACHED BREAKWATERS AT TRANI

Maria Francesca BRUNO [(1)], Antonio GIULIANI [(2)]

[(1)] *Eng., Research and Experimentation Laboratory for Coastal defense (LIC) - Technical University of Bari,* V. Orabona,4*, Bari, 70125, Italy. f.bruno@poliba.it*

[(2)] *Prof., Department of Water Engineering and Chemistry –- Technical University of Bari,* V. Orabona,4*, Bari, 70125, Italy.a.giuliani@poliba.it*

Introduction

Since 1975, the Trani coast south of Capo Colonna has been subject to erosion and cliff collapse due to anthropic activity along its shoreline, together with the more general problems of disappearing coastline.

The beaches along this shoreline have shown a marked tendency towards erosion to the point where they are so reduced in size as to threaten both their use as bathing areas as well as their important role in protecting the cliffs overlooking the beaches from wave attack.

As a result of the clear damage being caused, a decision was made to realize a system of ten breakwater barriers parallel to the coastline, joining another two barriers which had been realized ten years previously in front of Lido Colonna.

The present work deals with the morphological response of shoreline and sea bottom in the nearshore region to a system of emerged breakwaters.

1. Field results

In a first phase, five emerged breakwater barriers were constructed in the southernmost area of the zone. The 80m long barriers rose to 0.5m above sea level and had 30m gaps between them. They were built on a seabed depth of 3m at a distance of approximately 150m from the coastline (Fig. 1). The seabed offshore the shoreline under study, according to morphological readings using a sidescan sonar, is characterised by sand sediment with fine to medium granulometry on a substrate of calcareous rock.

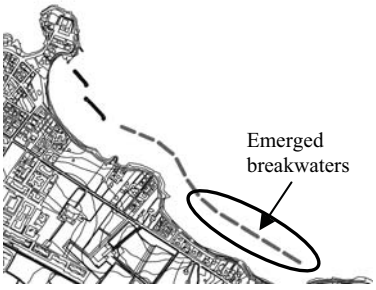

Figure 1. Planimetric layout of the protection barriers.

The seabed offshore the shoreline under study, according to morphological readings using a sidescan sonar, is characterised by sand sediment with fine to medium granulometry on a substrate of calcareous rock.

The barriers were built in order to reduce the wave force on the cliffs, thus reducing instability and helping create a sandy shore to add to the protection of the cliffs.

Building work on the first five structures was completed in November 2002, while the second phase of five barriers was carried out in 2004.

The effects of the five emerged barriers on the shoreline were studied in detail using GPS topographical surveys in 2001 (immediately before work started) and again in 2003, 2006 and 2007 after work was completed.

In the period prior to barrier construction there was a near total absence of beach area to the point where 2001 saw the beach reduced to two strips of sand divided by the sea, each with a length of approximately 100m and a width of approximately 10 metres.

Following the breakwater construction, the shoreline showed a gradual but continuous improvement; by 2005, the two small beaches had advanced by 20m (east beach) and 10m (west beach) respectively. In 2007 this progress continued and the two beaches are now joined by a strip of sand. The advancing coastline registered between 2001 and 2007 can be observed in figure 2.

An analysis of sand samples taken from the beach during a sedimentological study in 2006 shows that from a granulometric point of view, the sediment shows a fairly regular distribution with medium value diameters indicating the presence of prevalently medium sized sand grains.

The evolution of the seabed was studied comparing bathymetry levels acquired with a Multibeam Reson Seabat 8125 sonar over the work period from 2001 (before work started) and in 2003, 2006 and 2007 after work was completed.

Before the barrier work was carried out, the seabed showed a fairly regular trend with slopes of around 1%. However, in 2003 at the end of the work phase, the first substantial changes to the seabed could be seen. In the course of studies carried out in 2006, following a significant rise in the seabed level, it was not possible to carry out the planned navigation route near the barriers as the minimum seabed level needed for the craft carrying the sonar equipment had been exceeded. Indeed, comparing the results of 2001 and those of 2006 (Fig. 2), a significant accumulation of sand immediately beneath the barrier can be observed with a rise in the seabed of between 1.5 to 2 metres.

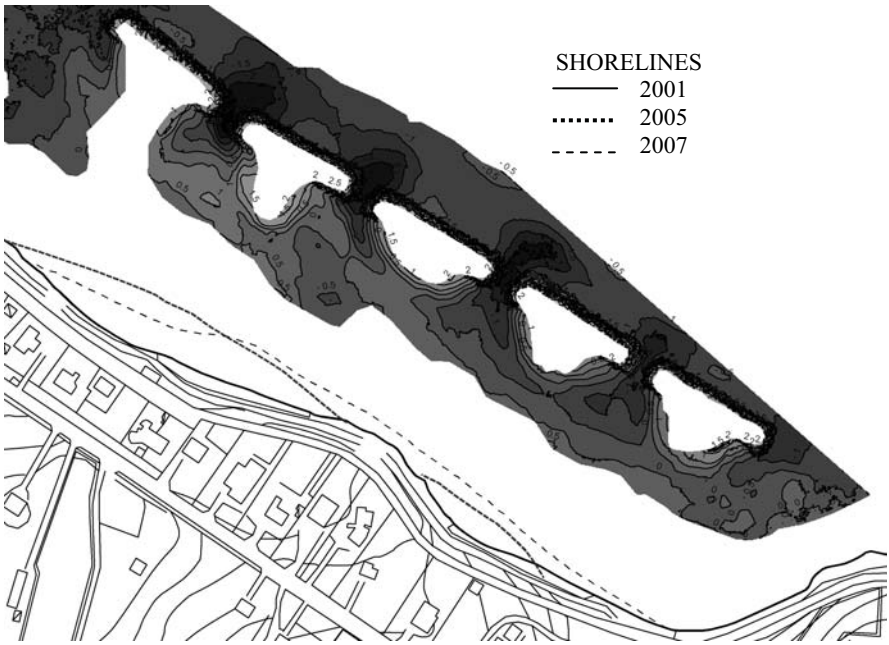

Figure 2. Comparison between bathymetric results carried out between 2001 and 2006 showing the advancing coastline

Furthermore, the presence of typical morphological phenomena caused by the surface barriers are highlighted. Indeed, one can note the presence of erosion trenches with a typical flame shape at the gaps between the breakwaters, where the seabed dropped by nearly 3m, reaching a rocky substrate which reached a depth of nearly 6m in that area. The fact that the rocky bed is reached is confirmed when comparing the results of 2006 with those of 2007 which show stability in the seabed between the gaps. The results also highlighted the localised erosion caused by particularly intense currents on the barrier heads (typically crescent-shaped erosion) and in the area offshore the structures.

The seabed in the protected zone, on the other hand, showed a general rise. It should be underlined that the sand has a medium to fine granulometry with ϕ of between 1.6 and 3.

A "natural" relationship between medium grain dimensions and depth can be noted; indeed, the largest sediment particles were present on the beach and on the shoreline while, moving towards deeper zones, sediment particles of smaller dimensions were found, always showing variations within the parameters of medium and fine sand (fig 3 a-b).

Figure 3a. Location of samples

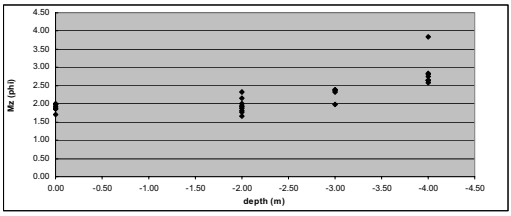

Figure 3b. Relationship between depths and ϕ

2. Empirical relationship

Moreover, the present study applied methods referred to in literature such as those used by Suh and Dalrymple (1987), Pope and Dean (1986), and Dally and Pope (1986), in order to evaluate the morphological behaviour of the breakwaters to verify their capacity in reproducing the results of the analysed shoreline. Particular attention was paid to the development of the beach.

In 1987 Suh and Darlymple carried out studies on physical models and compared their results with prototypes in order to develop a model to predict the salient Xs. These are as follows:

$$Xs / X = 14.8 Lg\, X / Ls^2 \exp(-2.83\, (LgX/Ls^2)^{0.5})$$

where:
Xs = distance from the shoreline without the breakwater to the tip of the salient
X = distance from the shoreline without the breakwater to the breakwater
Lg = gap length between adjacent breakwaters
Ls = breakwater length
Table 1 shows input values in the model and the predicted value Xs.

Table 1. Suh and Dalrymple model input and output

X (m)	L (m)	LG (m)	Xs (m)
150	80	30	145.48

Pope and Dean (1986) suggested that beach response to a segmented breakwater field is a function of two dimensionless parameters: the structure length to gap ratio (Ls/Lg) and the effective distance offshore to depth at the structure ratio (Y/Ds). The breakwaters in exam belong to the salients region, as it can be seen in figure 4.

Dally and Pope (1986) suggested that beach response to a multi-segmented breakwater field is a function of four variables: the structure length Ls, distance offshore Y, gap width Lg, and the wavelength Lw at the structure. The distance offshore is the distance between the mean high water shoreline and the seaward toe of the structure. The wavelength at the structure is a function of the water depth at the structure, Ds, and the average wave period.

Dally and Pope stated that a tombolo will form behind a segmented breakwater if $Ls/Y > 1.5$ and $Lw \leq Lg \leq Ls$ and a salient will form if $0.5 \leq Ls/Y \leq 0.67$. Uniform beach protection is predicted if $Ls/Y \leq 0.125$. In this case the ratio Ls/Y (Table 2) is included in the range of salients.

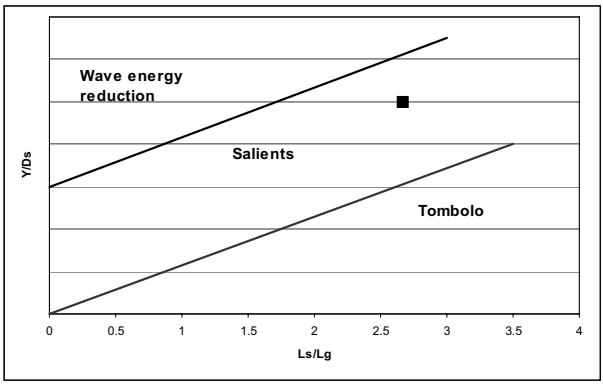

Figure 4. Pope and Dean segmented breakwater relationship

Table 2. Dally and Pope model input and output

Y (m)	Ls (m)	Ls/Y
150	**80**	**0.53**

The examined breakwaters have resulted in a significant sand accumulation forming a salients in their lee and the applied theories agree that this should be the predicted response.

References

Dally, W.R. and Pope, J., 1990 , "Detached Breakwaters for Shore Protection", Coastal Engineering Research Center, *Technical Report CERC-86-1*, U.S. Army Engineer Waterways Experiment Station, Vicksburg, MS.

Pope, J. and Dean, J.L., 1986 , "Development of Design Criteria for Segmented Breakwaters", *Proc. Of the 20th Coastal Engineering Conference*, Taipei, Taiwan, pp. 2144-58.

Suh, K. and Dalrymple, R.A., 1987, "Offshore Breakwaters in Laboratory and Field", *Journal of Waterway, Port, Coastal and Ocean Engineering*, ASCE, Vol. 113, No. 2, March, pp 105-121.

USACE (U.S. Army Corps of Engineers), 1997. "Wave Information Studies". *Coastal Engineering Data Retrieval System (CEDRS)*, Coastal and Hydraulics Laboratory. http://frf.usace.army.mil/wis/

USACE (U.S. Army Corps of Engineers), 2002. "Coastal Engineering Manual". Washington, D.C.: Engineer Manual 1110-2-1100, U.S. Army Corps of Engineers, (in 6 volumes).

EVOLUTION OF A COASTAL SYSTEM PROTECTED BY SUBMERGED NATURAL STRUCTURES: THE SHORELINE OF ERICE (WESTERN SICILY)

Maria Francesca BRUNO[(1)], Stefania LANZA[(2)], Biagio NOBILE[(3)], Antonio Felice PETRILLO[(4)], Giovanni RANDAZZO[(5)]

[(1)] *Eng., Research and Experimentation Laboratory for Coastal defense (LIC) - Technical University of Bari,* V. Orabona,4*, Bari, 70125, Italy. f.bruno@poliba.it*

[(2)] *Dr., Università degli Studi di Messina - Dipartimento di Scienze della Terra, Salita Sperone, 31 - Messina, 98166, Italy .lanzas@unime.it*

[(3)] *Eng., Research and Experimentation Laboratory for Coastal defense (LIC) - Technical University of Bari,* V. Orabona,4*, Bari, 70125, Italy.*

[(4)] *Prof., Department of Water Engineering and Chemistry –- Technical University of Bari,* V. Orabona,4*, Bari, 70125, Italy petrillo@poliba.it*

[(5)] *Prof., Università degli Studi di Messina - Dipartimento di Scienze della Terra, Salita Sperone, 31 - Messina, 98166, Italy. grandazzo@unime.it*

Introduction

The objective of this contribution is to present and discuss the medium-term morphological evolution of the shoreline of Erice, that has undergone a remarkable regression between 1960 and 1980 because of human interference on the shoreline.

The area which was examined, is situated in the western part of the Sicily, immediately North of Trapani (Fig.1).

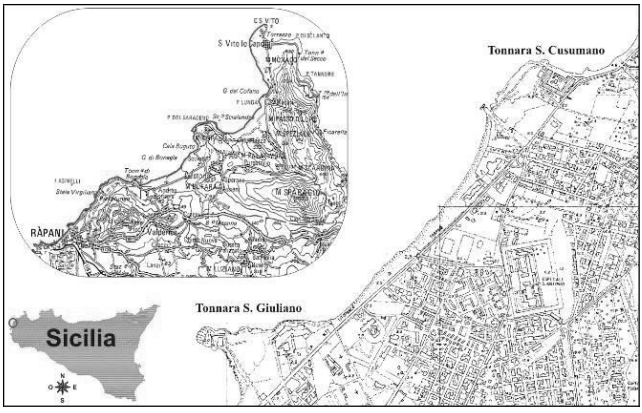

Figure 1 - Geographic location of the coastline of Erice, showing Sicily, the whole western sector and the studied stretch limited by the two headlands and the provincial road.

The studied stretch, oriented N – S, extends for approximately 1,4 km and it is limited by two headlands on which in a recent past, two tonnare (deposits for the boats and working place for fishermen of tuna fish) were present: to the North the Tonnara of San Cusumano and to the South by Punta Tonnara San Giuliano; the included beach, which is mostly sandy gets narrower from South to North, reducing

itself from about 70 to 20 meters, it is limited landward by the Provincial Road No.77 (SP 77), that has taken the place of the humid areas and the existing dunes, eliminated to create it.

The submerged beach shows a sandy bottom that slopes regularly downwards to approximately - 4 m; here a non continuous series of rocky pavements outcrop is present reaching a depth of approximately -8 m, except in the northern part of the coastline, where the bottom profile is characterized by a greater slope that denotes its erosive condition. A thick Posidonia field is present along the whole area at a depth of approximately 13 - 15 m.

The analysis is based on the outcomes of the study of the wave climate and solid load and the qualitative analysis of the evolution of the shoreline from 1840 till now.

1. Wave climate and sediment transport analysis

For the elaboration of the wave climate both the wind data set of the Station of Trapani - Birgi, using an indirect method (Hasselmann, 1973; Leenknecht, 1992), and the available wave data set (from 2004) by the buoy of Capo Gallo (Palermo), belonging to the Rete Ondametrica Nazionale (RON), characterized by a wave movement exposure very similar to the one of the coast of Erice, being exposed to sea storms from the IV and the I quadrants, have been analyzed.

The use of these two sources has allowed a reconstruction of the historical sequence of the waves appearing on the shoreline for a very remarkably period from a statistical point of view.

The frequency analysis of reconstructed sea storms showed that the waves beating against the coastal area actually come from the IV quadrant, with a slight dominance of waves from WNW, characterized by a high intensity, rather than an elevated regularity. In order to determine the characteristics of transformations from off shore waves to coastal waves, the REFDIF1 v3.0 model was used (Kirby et al., 2005) allowing the simulation of the diffraction processes; this model was ran using the values of energetically equivalent wave height with a time return of 50 years.

The information regarding off shore depths was taken, from the nautical maps of the area produced by Hydrographic Institute of Marine (IIM) in 1988 and in 1992, for a detailed analysis of the bathymetry of the area closer to the shoreline (up to a depth of -15m) a specific bathymetric survey was carried out by single - beam echo sounder associated to a positioning system GPS/RTK (the study was funded from Sviluppo Italia S.p.A. to the University of Messina in April 2006). Using the same GPS/RTK the survey of the emerged beach was carried out too.

A first evaluation of the morphodynamic behaviour of the examined shoreline was carried out by a mathematical model that estimated the solid load showing that the long shore capacity was concentrated in the surf zone and depended on the flow of a parallel energy to the coastline.

The example was applied to energetically equivalent wave, with the consequence that the flow of energy that determines transportation, did not refer to every single sea storm that had really hit the coastal area but to average annual values. Keeping in mind how often the wave movement occurs because of its different directions, the application of the model clearly shows that the longitudinal transportation of sediments is directed towards SW, with a reversal of the current just North of the Tonnara San Giuliano. This seems to be a sedimentation point.

The information, collected during the survey confirms the results, showing a sedimentation in the submerged beach in the South part of the stretch, shifting towards the bathymetric of - 5 m (Fig. 2). This evidence due both to the dynamics of the shoreline and to the geomorphology of the on shore bottom, shows that a great quantity of sediments eroded from the emerged beach, is in fact deposited in this area.

2 Shoreline evolution

The evolution of the coastline was estimated by comparing the historical sequence of some cartographies which were available of the area (Fig. 3). Starting from the first historical reference of the shoreline, since the 40s no erosive phenomenon had been evidenced. A deterioration of the coastline had been observed in the subsequent years with an increase of the erosive phenomenon from 1970 to 1994.

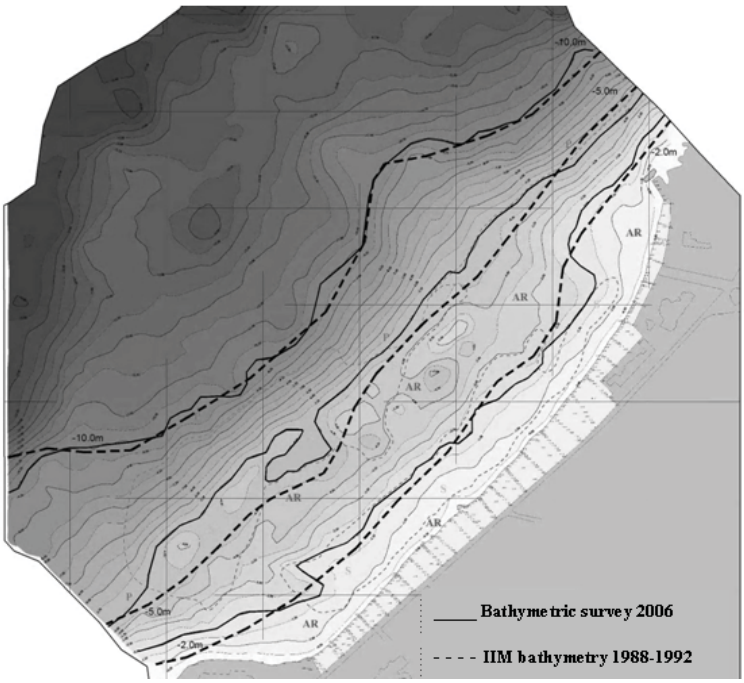

Figure 2 - Digitised map of the coastal area of Erice, based upon two different bathymetric maps, published between 1988 and in 1992 obtained from I.I.M. was compared with the survey realised in 2006.

During that period, the beach had retreated approximately 50 meters in the southern part and approximately 70 meters in the central and northern part, with an average retreat of approximately 2.5 meters per year.

The beach which is being eroded, as shown by the vibracore, that have not reached the substrate, is formed of a consisting sediment package that testifies the substantial stability of the system.

Furthermore the submerged coastal system is also characterized by the presence of submerged natural stiff structures placed respectively between -2 and -5 meters that have contributed in the damping of the incoming waves, limiting the trend of regression of the shoreline. In the past, the system has got worse because of the morphological conditions which have been narrowed between a low carbonate cliff and the sea.

These sediments shift towards South, but they cannot be stable in the southern part sheltered by Capo San Giuliano, as the strong winds of the IV quadrant and, mainly those of approximately 300°, exceed the natural submerged structure of protection and move towards the open sea. In the South area, instead, the sediments are held up by rocky surfaces and do not dissolve towards the open sea. Therefore the presence of Posidonia field and the shoreline, continue to occupy a range of roles belonging to a seasonal change. In this system which is strongly influenced by man interference, it is possible to see how the Posidonia field, has actively contributed in limiting the dispersal of sediments towards off shore, creating a sedimentary cell limited also by the two headlands and the beach itself.

At the moment, as is shown by the geomorphologic survey carried out during this research, the progressive trend of the beach is erosive, even though it has eroded less than during the past years.

In fact, even though it is possible to find an erosive phenomenon that has interested the sandy coast above all in the northern part, the major part of the coastal territory was lost because the human occupation of the land rather than because the erosion of the shoreline itself. Following the survey carried out along the shoreline, soft protection interventions were proposed (nourishment without protection or with a slight protection).

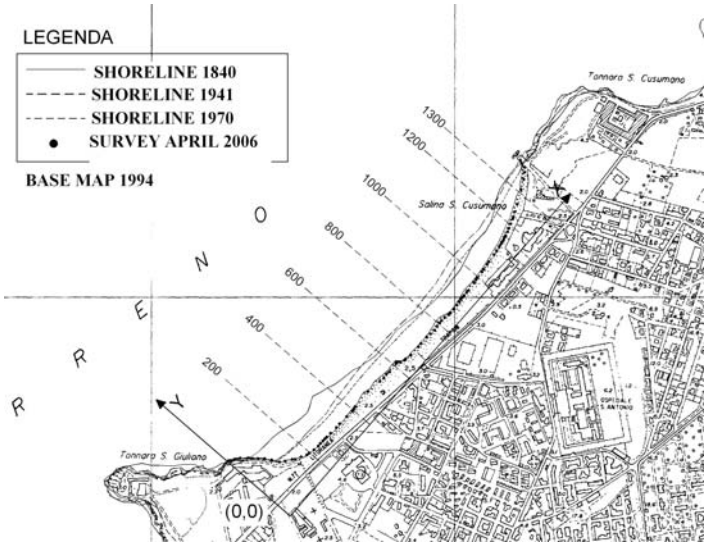

Figure 3 – Recent shoreline evolution of the studied stretch.

Considering this particular system, it would be absolutely positive if the administration refused to take part in any system of passive defence and activate a system of annual management, favouring a limited nourishments of a few thousand mc of material at the beginning of the bathing season. These, within a long-term monitoring and management program. could determine in an improvement of the actual structure of the beach leading to an irrelevant environmental impact.

The main critical point of the system is placed on the North end. Here a gap in the system of natural protection gives rise to a longshore tractive current towards South that erodes and transports the sediments in that direction. To limit the existing northern current towards south, an "artificial consolidation" of the submerged natural barrier could be created using cycloptic rocks from the nearby quarry of Custunaci (area leader in Sicily for lime stones quarries).

This protective system, inline with the standard defence systems, with a low environmental impact and above all a strong interest on behalf of the local administration , would give the present situation stability, but could certainly still not be defined as strategies of “adaptation" as learnt during the lessons held by European programs (EUROSION, 2004; M.E.S.S.I.N.A., 2006) and engaged by politics, considering the Global Climate Change.

References

EUROSION (2004) Living with coastal erosion.

M.E.S.S.I.N.A. (2006) Managing European Shorelines and Sharing Information on Near shore Areas

K. Hasselmann, (1973) “Measurement of wind wave growth and swell decay during the Joint North Sea Wave Project”, Technical Report, Deut. Hydr. Inst, Hamburg

D. Leenknecht, (1992). “Automated Coastal Engineering System: users guide”, Coastal Eng. Research Center

Kirby, J. T., Dalrymple, R. A. and Shi, F., 2005, ``Combined refraction/diffraction model REF/DIF 1, Version 3.0. Documentation and user's manual", Research Report, Centre for Applied Coastal Research, University of Delaware

COAST ACCRETION RESORTING TO SEA SANDPITS

Rodolfo M. A. NAPOLI [(1)], Daniele PANZA [(2)]

[(1)] *SEED, Sanitary Environmental Engineering Division, Department of Environmental Science, University of Naples "Parthenope", Centro Direzionale Isola C-4, 80100 Napoli. university@rodolfonapoli.it*

[(2)] *SEED, Sanitary Environmental Engineering Division, Department of Civil Engineering, University of Salerno, via Ponte don Melillo, 84084 Fisciano (SA). dpanza@unisa.it*

Abstract

The present study identifies and in short discusses technical and environmental aspects related to coast accretion by means of sea sandpits. Particularly, characteristics of sea sandpits and dredging systems were analyzed in depth. Moreover, environmental impacts were identified with regard to sand extraction and transport for coast accretion.

1. Sea sandpits and coast accretion

Coastline withdrawal derives from an interaction between sea and land physical factors producing erosion or submersion of wide coastal areas. These variables can be defined mainly as wave motion, sea level rise, subsidence, sediment supply decrease. Particularly, shores are the most critical and vulnerable coastal system due to progressive change of sediments balance; besides, the sediment lack is also enhanced by existing anthropic facilities and activities as well as economic importance of shores.

Accretion is a technical option for coast protection consisting in beach reconstruction by means of suitable materials. These materials can come from riverbeds, seaboards or sea sandpits. Accretion is characterized by a lot of advantages from an environmental and economical point of view, in comparison with other technical solutions (Benassai, 2001; APAT, 2007).

Nevertheless, coast accretion needs great quantities of sand cheaply. Besides, restrictions and poor availability of materials from quarries and riverbeds have involved identification of alternative supplying sources. As a result, sea sandpits seem to be a possible solution of the problem. Particularly, the European Project SANDPIT explains that massive mining of sand from the middle and lower shoreface in large-scale mining and borrow pits/areas will be required in future in many European countries. For example, around the North Sea and the Mediterranean Sea, mining of sand will be required to feed beaches and coastal dunes so to face coastal erosion for sea level rise. Moreover, restoration of land and realization of artificial islands (for industrial purposes such as ports and airports) in coastal seas are other activities that require substantial quantities of sand for relative construction. As a result, European Project SANDPIT specifies that the volume of sand required in the near future (10 to 20 years) will fluctuate between 100 and 1,000 million m^3 per country surrounding the North Sea. That is, existing and new sea sandpits have to be explored, characterized and exploited.

Sea sandpits are sedimentary deposits lying on the continental shelf until to depth equal to 100 m. Their main requirements are (Nicoletti et al., 2006; APAT, 2007):

- thickness > 3 – 4 m;
- suitable granulometry;
- depth between 30 and 70 m, less than 100 m anyway;
- significant areal extent;
- available cubage (also more than 3,000,000 m^3);
- surface without encrustations;
- closeness to beach.

Two dredging systems can be identified: cutter suction dredger and trailing hopper suction dredger.

The first one allows sand extraction realizing hollows with sub-circular shape, depth in the range 2 – 20 m, diameter between 20 – 100 m; the second one is characterized by formation of parallel gullies with depth of 0.5 – 2 m and width of 1 – 5 m.

Sand nourishment can be carried out either directly from dredger (pumping a mix of water and sand) or by means of specific sand pipeline.

During dredging and accretion phases, the main environmental problems are related to morphological and bathymetric changes of sea bottom and coastline, turbidity (formation of turbidity plume) and sediment loss, impacts on benthos (due to burial for example), impacts on economic activities such as fishing.

2. Conclusive remarks

With regard to the growing problem of costal erosion , accretion resorting to sea sandpits seem to be an alternative solution for beach reformation. Application of this option has to take in account some aspects, such as environmental impact, costs, social factors, life of protection system. Particularly, sea sandpits research calls for specific bathymetric investigation in order to assess the real and suitable applicability of this solution.

With regard to the massive future mining of sand and the relative impacts, the mining areas need to be situated in the offshore shoreface zone to minimize the effects of nearshore coastal erosion (APAT, 2007). Besides, sandpit mining will be progressively more expensive at greater distances from the shore. As a result, further studies are necessary in order to find the optimum and suitable solution between effect on the coast and mining costs and impacts.

At last, significant attention has to be focused on siting of new sea sandpit with regard to legal sea uses, such as protected sea areas, facilities (offshore constructions, pipelines), anthropic activities (mariculture), special area (military zone). So a preliminary in-depth cartographical analysis is necessary (Nicoletti et al., 2006).

References

APAT (2007), Atlante delle opere di sistamzione costiera, 44/2007.

Benassai E. (2001), Vulnerabilità dell'ambiente ed interventi sui litorali, Notiziario Ordine Ingegneri di Napoli, Gennaio - Maggio 2001, pp. 10-16.

European Project SANDPIT, Sand transport and morphology of offshore sand mining pits.

Nicoletti L., Paganelli D., Gabellini M., Aspetti ambientali del dragaggio di sabbie relitte a fini di ripascimento: proposta di un protocollo di monitoraggio, Quaderno ICRAM n.5: 159 pp.

A SELECTION OF A GEO-INDICATORS SET FOR THE COASTAL EROSION RISK EVALUATION

Roberto FRANCIOSO[(1)], Antonio Felice PETRILLO [(2)], Gennaro RANIERI [(3)]

[(1)] *Chemistry and Water Engineering Department - Polytechnic of Bari, via Orabona n. 4, Bari, 70125, Italy - r.francioso@poliba.it*

[(1)] *Chemistry and Water Engineering Department - Polytechnic of Bari, via Orabona n. 4, Bari, 70125, Italy - petrillo@poliba.it*

[(1)] *Chemistry and Water Engineering Department - Polytechnic of Bari, via Orabona n. 4, Bari, 70125, Italy - g.ranieri@poliba.it*

Abstract

It is possible to define the risk as a function of the probability of a harmful situation occurs in a zone and in a defined range of time (hazard concept), of the ability of a territory to resist to the event (vulnerability concept) and of the damages suffered by the territory itself:

$$R = H*E*V$$

where,

R = Risk, possibility of a loss

H = Hazard; probability of occurring of an event

V = Vulnerability; possibility of an object to suffer damage by an event

E = Economic loss; economic, human, environmental value assessment for the potentially involved territory.

According to the literature (Arcilla et al., 2000, De Girolamo et al., 2000) the evaluation of Coastal Erosion risk is possible through the analysis of a multidisciplinary geo-indicators set, in the aim of describing the physical, environmental and socio-economic factors participating to the definition of "V" and "E".

Before stating the "R" assessment, it is necessary to define the territorial extension, both for determining the "scale factor" and, above all, for individuating the UTO (Homogeneous Territorial Unit from a geo-morphologic point of view).. As concerning coastal erosion risk assessment, the evaluation of "H" leads the determination of the coastal dynamic mechanisms acting on the analyzed territory, taking into account of physical characteristics of the coast and the wave motion mechanism, both indispensable to know the homogeneous sectors in which the examined zone should be subdivided.

A first analysis aims to understand the constrain entity (Hazard), represented by the meteo-marine condition insisting on the territory; secondly the vulnerability (V) evaluation is to calculate utilizing the geo-indicators. Among the geo-indicators used to determine the "V" factor, those containing the information exploited during the coastal dynamic analysis will be also included.

Among the "V" geo-indicators you find the indicators defining the "E" factor which , as explained before, consider the socio-economic and environmental components for evaluating the economic loss. You could also consider those as "socio-economic vulnerability" indicators. There is a slight difference between the geo-indicators used to determine the morphologic vulnerability "V" and the socio-economical ones used to determine "E"; in fact, for evaluating the coastal erosion vulnerability you should introduce a set of geo-indicators spreading to various parameters even different to those that strictly concern the morphological aspects from a physical point of view (beach slope, sand composition,

etc.), but aimed to analyze the cause-effect relationship of human activities and the consequent variations of coastal morphodynamic equilibrium.

A similar problem will be faced when you should define the geo-indicators set for evaluating the "H" factor; they deal with the same topic of the indicators that treat the morphologic vulnerability.

The paper reports an application of the method applied to a sector of coast located in Puglia (Italy) between the municipalities of Barletta and Margherita di Savoia.

The set of geo-indicators has been defined starting from those found in literature. Through a tough and long selection, the number of potential indicators has been reduced, by a combination of those with a similar meaning and deleting others not really useful on the purpose. The final set has been carried out by adopting a classification criteria which takes into account of the fundamental proprieties that make the indicators useful for the calculation of the risk of coastal erosion.

Acknowledgments

This work has been carried out in the framework of the research project "Integrated Monitoring of Coastal Areas (IMCA)", funded by the Italian Ministry of Education, University and Scientific Research.

References

Arcilla, A., Jimenez, J.A., Valdemoro, H.I., (2000). "Assesing vulnerability on low-lying coastal areas". Proceeding of SURVAS Expert Workshop on European Vulnerability and Adaptation to impacts af Accelerated Sea-Level Rise (ASLR), Hamburg, Germany, 19th-21st June 2000.

De Girolamo, P; Noli, A.; Contini, P.; Mondini, F.; Beltrami, G.M.; Franco, L.; (2000). Risk analisys in coastal systems. Planning and management. Excerpta, vol.14, pp.257-271.

SELECTING INDICATORS TO CALCULATE THE RISK OF COASTAL EROSION

Leonardo DAMIANI[(1)], Giancarlo CHIAIA [(2)] & Gennaro RANIERI [(3)]

[(1)] Chemistry and Water Engineering Department - Polytechnic of Bari, via Orabona n. 4, Bari, 70125, Italy - l.damiani@poliba.it

[(2)] Chemistry and Water Engineering Department - Polytechnic of Bari, via Orabona n. 4, Bari, 70125, Italy g.chiaia@poliba.it

[(3)] Chemistry and Water Engineering Department - Polytechnic of Bari, via Orabona n. 4, Bari, 70125, Italy - g.ranieri@poliba.it

Abstract

This work was carried out under the auspices of a research project funded by the Italy-Albania INTERREG IIIA programme which also involved analysing the coastal dynamics along selected stretches of the Albanian coast, especially between Cape Rodoni and Bishti i Pallës just north of Durrës (Fig.1).

Figure 1: geographical location of the sites

The feature of particular interest which drove the authors to analyse this site in greater depth lies in the striking similarity between this stretch of coastline with another in Apulia which they had previously studied, lying between the towns of Barletta and Margherita di Savoia (Damiani et al., 2001; Magnaldi et al. 1997; Ranieri, 2006). Both coasts feature a mainly sandy shoreline with very similar grain sortings, as well as featuring the mouth of a sizeable river. Further to that, the two coastlines are almost opposite each other, with very similar sea states, and so are practically mirror images of each other (Figs. 2a and 2b).

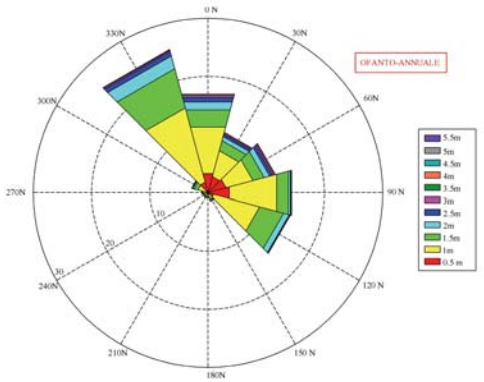

Figure 2a: Polar diagram of annual sea-state conditions off the mouth of the Ofanto River

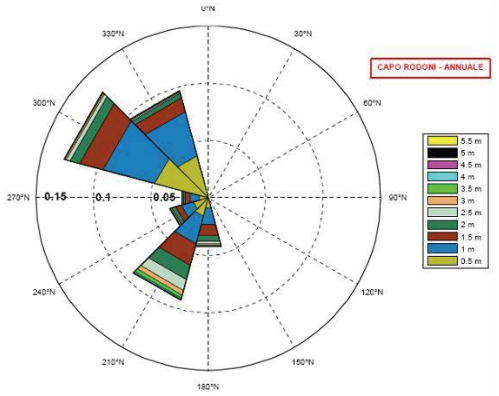

Figure 2b: Polar diagram of annual sea-state conditions off Capo Rodoni.

Over the last century, the stretch of Apulian coastline where the Ofanto meets the sea has undergone constant transformation, having been subjected to massive intervention on the part of Man. The main transformations include enlarging the harbours of both towns, and works carried out in the Ofanto basin, constructing numerous weirs along the main stem of the river and its tributaries and transforming its banks. Add to that the intense urbanisation of the coastal strip.

The most obvious consequence of these works has been widespread instability caused by the erosion process (Figs. 3a and 3b), both along the seafront road between Barletta and the river mouth as well as close to the nearby coastal settlements. Dealing with the problem has involved numerous and costly defence works, which given the lack of proper planning and management, have not had the desired effect. Moreover, considerable nourishment has occurred in areas adjacent to the harbours.

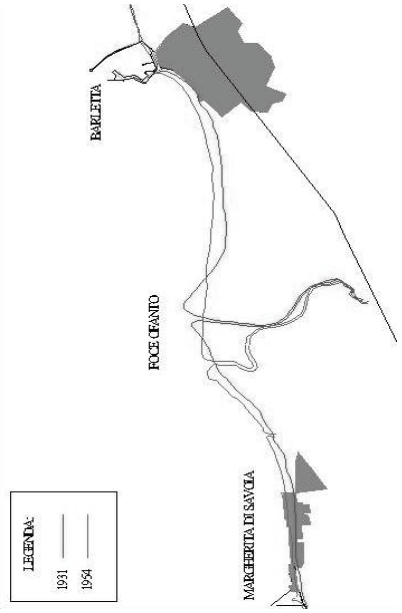

Figure 3a. The coastline between Barletta and Margherita di Savoia, 1931- 1954

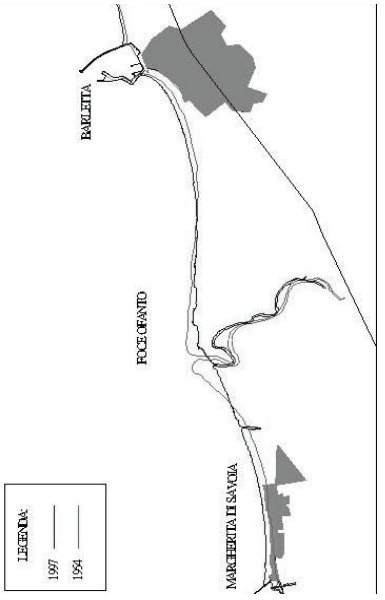

Figure 3b. The coastline between Barletta and Margherita di Savoia, 1954-1997

A similar phenomenon has occurred along the Albanian coast at the mouth of the Erzen river. The mouth has already migrated leewards in a similar way to that observed for the Ofanto between 1950 and 1970, and later the erosion process began in earnest , with the 1990s seeing significant retraction of both river mouths - the Ofanto by around 500m, and the Erzen by no less than 850m (Fig. 4). Furthermore it has been observed that the erosion phenomenon is still ongoing.

Despite the relative lack of historic cartographic materials, due in part to the difficulty of purchasing documents from the national archives, the coastlines for 1952, 1978, 1985 and 2005 have been acquired. Also, a campaign of bathymetric surveys has been carried out in order to learn about the recent evolution of the underwater terrain, and a number of satellite images have been acquired in order to understand the current status of the coastline. Characterisation of the sea state off the Bay of Lalzi was carried out using recordings from 13 years of observations, covering the period between January 9th 1992 and 31st December 2004, as reconstructed by the Dutch company ARGOSS (www.argoss.nl).

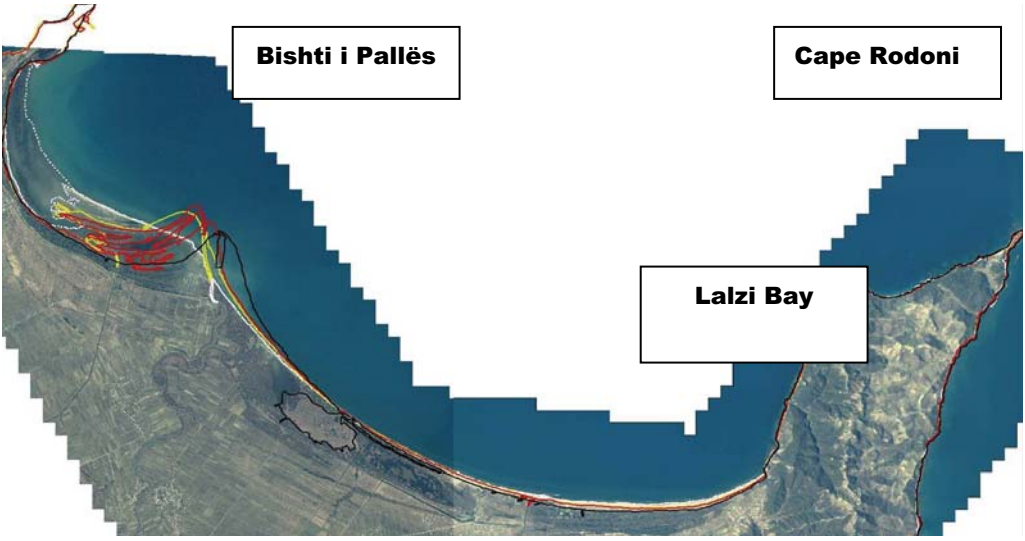

Figure 4: evolution of the mouth of the river Erzen in the Bay of Lalzi - the coastline in 1952, 1978, 1985 and 2005

The similarities between the two sites make it possible to carry out a morphodynamic analysis of the Albanian coast, helped by the previous analyses from Apulia, and with the aid of one-line models.

The model used, known as "Genesis" is an application of the "Nemos" model, which uses the CEDAS software (ver. 4.03) licensed from Very-Tech Inc.

As mentioned, the software was first calibrated by analysing the coastal dynamics along the stretch between Barletta and Margherita di Savoia. For this site, the evolution over time of the river mouth had been properly simulated using the "Beachplan" model from the Seawork software package created by H R Wallingford Ltd (Oxon, UK). Analysis led to an interesting comparison of the use of these two software packages, highlighting both their advantages and their drawbacks.

The simulation over time of the trends affecting the Albanian coastline was on one hand facilitated by this calibration work using the Italian case study as a model, but by contrast it also suffered from a lack of data, such as those regarding the transport of river sediment. In any case, we managed to analyse both coastlines, demonstrating their considerable behavioural similarities.

Acknowledgments

This work was carried out under the auspices of Project GECO (Ecocompatible Management of coastal

settlements in Albania), in which the Water Engineering and Chemistry Department is a partner, funded by the Apulian Regional administration's INTERREG IIIA Italy-Albania programme. The authors would like to take the opportunity to thank Emanuela Caravella for her excellent technical support.

References

Damiani L., Petrillo A. F., Ranieri G. (2001) Alcune considerazioni sulla tutela delle aree costiere nella Pianificazione e Gestione territoriale. Il caso dell'evoluzione della costa compresa fra Trani e Manfredonia - Convegno " LA TUTELA DELL'AMBIENTE NATURALE NELLA PIANIFICAZIONE TERRITORIALE Esperienza in Puglia" . Bari, 1 giugno 2001

Magnaldi S., Grimaldi S., Ranieri G., Greco M.; 1997. - Studio del trasporto torbido del fiume Ofanto - Atti del Convegno "Giornate di studio in onore del prof. E.Orabona nel centenario della nascita".

Ranieri G. (2006) La vulnerabilità della costa compresa tra Margherita di Savoia e Barletta: analisi degli effetti delle attività antropiche sui dinamismi costieri Giornata di studio in onore del Prof. E.Benassai Guardia Piemontese (CS)

ASSESSING WIND FIELDS BY MEANS OF REMOTE SENSING TECHNIQUES ON COASTAL ZONES

Maria ADAMO[1,2], Giacomo DE CAROLIS[2] & Guido PASQUARIELLO[2]

[1] *University of Bari, Department of Physics, via Amendola 173, Bari, 70126, Italy. adamo@ba.issia.cnr.it*

[2] *Italian National Research Council, Institute of Intelligent Systems for Automation, via Amendola 122/O, Bari, 70126, Italy. [decarolis, pasquariello]@ba.issia.cnr.it*

Abstract

The aim of this work is to assess the potential and limits of SAR procedures for the retrieval of wind fields in marine coastal areas. Two coastal sites in the Mediterranean Sea offshore Puglia (Italy) region were instrumented to collect marine and environmental parameters, including the wind speed and direction. Co-located C-VV high resolution radar images gathered by the Advanced Synthetic Aperture Radar (ASAR) onboard the European ENVISAT satellite during 2007 were analyzed to retrieve wind vectors.

1. Introduction

In the past years microwave scatterometry of the marine surface had greatly contributed to develop reliable semi-empirical forward scattering models that relate the normalized radar cross (NRCS) of the sea surface to the horizontal surface wind speed and direction 10 m above the sea level. Among others, the model called CMOD-4 (Stoffelen and Anderson, 1997, 1997a), developed by ESA, was found to perform with high accuracy in predicting the C-VV NRCS given the wind vector as input. Inversion of this model allowed wind field estimation with accuracy of ±2 m/s for the velocity and ±20° for the direction over a spatial scale of about 50 by 50 Km (Stoffelen and Anderson, 1993). When applied to SAR data, inversion of CMOD-4 gave similar results after spatial average of 25 km for backscatter (Wackerman et al., 1996; Fetterer et al., 1998). These values are relevant to deep water, open sea areas, well far from shorelines.

In this paper we exploit the SAR NRCS from coastal, shallow waters areas in order to compare the retrieved wind speed and direction from standard inversion technique with co-located wind vector measurements. Due to the vicinity of the coast, the selected SAR windows were limited to a few Km.

The objective is to evaluate SAR capability to estimate wind fields in conditions far from open sea environment.

2. The SAR Wind Inversion Procedure

The CMOD-4 backscatter formulation is based on the following functional expression (Moore and Fung, 1979; Stoffelen and Anderson, 1997):

$$\sigma_O = b_O(W_{10},\theta)[1 + b_1(W_{10},\theta)\cos(\phi) + b_2(W_{10},\theta)\cos(2\phi)]^{1.6} \quad [1]$$

where σ_O is the NRCS and (W_{10},ϕ) is the neutral wind vector 10 m above the sea surface; the wind direction, ϕ, is measured from up-wind with respect to the radar antenna; the parameters b_i depend on W_{10}, the frequency and the polarization of the incident radiation and the incidence angle of the radar beam θ.

Wind maps obtained by SAR imagery are the result of the inversion of the CMOD model. The scheme utilized in this work to invert the CMOD's is based on a Bayesian approach which minimizes the

following cost function, as originally proposed by Portabella et al. (Portabella et al., 2002):

$$J = \left(\frac{\sigma^o_{SAR} - \sigma^o_{MODEL}}{\Delta\sigma^o_{SAR}} \right)^2 + \left(\frac{U_{ECMWF} - U_{TRIAL}}{\Delta U_{ECMWF}} \right)^2 + \left(\frac{V_{ECMWF} - V_{TRIAL}}{\Delta V_{ECMWF}} \right)^2 \quad [2]$$

where σ^o_{SAR} is the NRCS measured on the SAR image and σ^o_{MODEL} is the NRCS predicted by the CMOD model being used with the trial wind components (U_{TRIAL},V_{TRIAL}) as input. The error $\Delta\sigma^o_{SAR}$ represents the average NRCS variability within the selected SAR window. The ECMWF wind components (U_{ECMWF},V_{ECMWF}) are used as guess input after assigning them the uncertainty ΔU_{ECMWF} = ΔV_{ECMWF} = 1.73 m/s. As the above uncertainty is believed realistic for points located well far from the shorelines up to about 15 Km, it should be considered in this study as the lower bound limits for ECMWF wind speed accuracy.

3. The Dataset

The inversion procedure was applied to SAR imagery gathered over two marine test sites offshore Puglia (Italy) coasts that were instrumented to collect on a continuous basis physical and chemical marine and atmospheric parameters, which include waves, currents, water and air temperature, wind speed and direction, air pressure. The test sites are located in the Ionian Sea offshore Taranto (TA) and in the Adriatic Sea offshore Margherita di Savoia (MS). The buoys were placed in shallow waters of depth about 17 m for TA site and 13 m for MS site at a distance from the coast of approximately 3 Km.

The wind fields estimation was carried out on 59 ASAR images acquired by the sensor onboard the ESA ENVISAT satellite during 2007 starting from February.

In particular, Image Mode (IM) and Wide Swath (WS) images, characterized respectively by a pixel size of 12.5 m and 75 m, were considered. The whole dataset consists of 15 IM and 19 WS for TA and 12 IM and 13 WS for MS.

Wind speeds measured by the anemometers were collected every hour at the height of 8 m for TA site and 2.5 m for MS site, respectively. In order to compare with corresponding ASAR estimated wind vectors, the measured wind speeds were converted into neutral winds at 10 m height with the LKB algorithm (Tang and Liu, 1996) and then linearly interpolated in time in order to report at the ASAR acquisition time.

The ECMWF 10 m wind vectors were available every 6 hours at spatial resolution of 0.1°×0.1°. In order to make them suitable as first guess input to the inversion scheme, they were interpolated in space to the buoy location and in time to the correspondent ASAR overpass.

Finally, the ASAR wind vector estimation was carried out after selecting image portions of 2.5 by 2.5 Km centred on the pixels corresponding to buoy locations.

4. Results and Discussion

The scatter diagrams of Figure 1 show the correlations between the ASAR estimated wind speeds and directions vs. the corresponding in situ measurements using CMOD-4. The inversion procedure was initialized using both the ECMWF winds (Fig. 1b) and buoy winds (Fig. 1c) as well in order to assess the sensitivity of the inversion scheme to the quality of the guess.

As can be seen in Fig. 1a, the two selected first guess inputs are quite dispersed. Although the root mean square error (RMSE) of wind speed is reasonable (2.03 m/s), the wind direction shows a very large scatter of about 85.17° (see the first row of Table I and II, respectively). This was expected because ECMWF winds were interpolated both in space (~5 Km) and in time (~3 hr) in order to collocate them to the buoy position and the ASAR time overpass. In contrast, buoy data differ no more than half an hour in time with ASAR acquisition time.

When applied as first guess to the ASAR inversion procedure, the results show that microwave

information provided by ASAR hardly corrects the ECMWF guess input. Indeed, ASAR inverted wind vectors resulted more dispersed with respect to buoy winds (compare RMSE of second row in Table 1and 2).

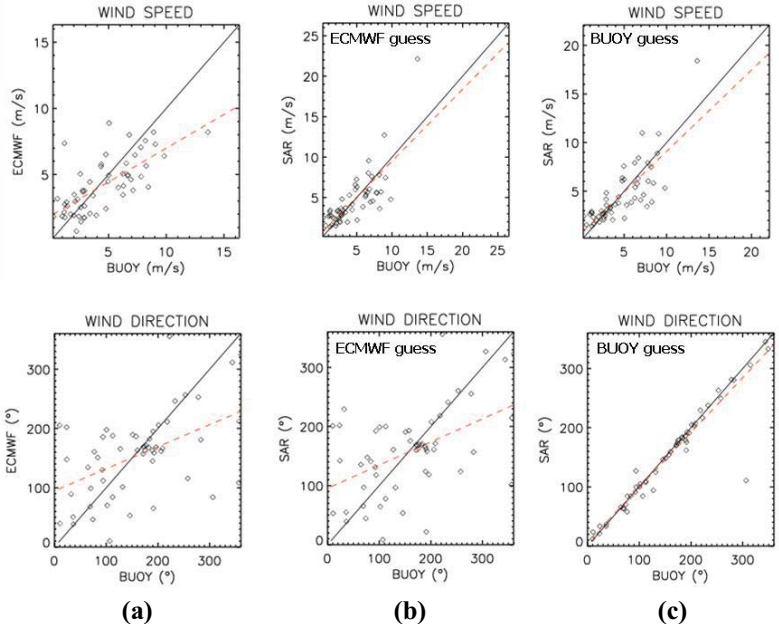

Figure 1. Scatter plots representing: the relative dispersion of the ECMWF and buoy wind speeds and directions used as guess input to the SAR inversion procedure (a); the ASAR retrieved wind speeds and directions with CMOD-4 vs corresponding buoy measurements using ECMWF data (b) and buoy data (c) as first guess input. Regression lines (dashed) and bisectors (continuous) are also represented.

It can be concluded that minimization of cost function given by [2] is strongly dependent on the initial guess. Assuming buoy data as representative of the actual atmospheric conditions during ASAR overpasses, the corresponding wind retrievals resulted reliable and accurate within CMOD-4 capability to account for backscatter. With reference to the values of Tables 1 and 2, comparison with ECMWF wind data showed that both the wind speed RMSE and the mean bias error (MBE) slightly decreased from 2.08 m/s and –0.13 m/s to values of 1.85 m/s and +0.02 m/s. Finally, there is only a slight improvement of the correlation coefficient r^2. On the other hand, the decrease of wind direction RMSE to ~28° from ~87° (and the corresponding increase of r^2) could be assigned to the fact that wind directions from buoys were used as first guess. The latter result may be explained by considering that the forward scattering model shows a greater sensitivity to adjust the wind speed rather than the wind direction in order to allow the cost function to get a minimum.

Furthermore, the accuracy of both wind speed and wind direction retrievals compare well with the values reported in the literature (Wackerman et al., 1996; Fetterer et al., 1998; Kerbaol et al., 2007).

Table 1. Statistical analysis of wind speed retrievals using ECMWF data (second row) and buoy data (third row) as first guess. The first row shows the representativeness of the ECMWF and buoy wind data considered as reference data

WIND SPEED	RMSE (m/s)	MBE (m/s)	*q*	*m*	r^2
ECMWF – Buoy	2.03	+0.31	1.88	0.51	0.50
ASAR – Buoy (ECMWF guess)	2.08	-0.13	0.64	0.89	0.60
ASAR – Buoy (Buoy guess)	1.85	+0.02	0.73	0.84	0.63

Table 2. As for Table I, but relevant to wind direction retrievals.

WIND DIRECTION	RMSE (°)	MBE (°)	*q*	*m*	r^2
ECMWF - Buoy	85.17	+7.68	94.73	0.37	0.25
ASAR – Buoy (ECMWF guess)	86.82	+3.78	95.44	0.39	0.24
ASAR – Buoy (Buoy guess)	27.97	+5.56	6.28	0.93	0.91

5. Conclusions

A recent SAR wind vector retrieval method based on a Bayesian inversion approach (Portabella et al., 2002) was applied to calibrated ENVISAT ASAR C-VV imagery for assessment in coastal zones. The validation analysis was carried out using wind measurements collected in shallow waters by two anemometers mounted on buoys offshore Puglia (Italy) coasts. Results show a good agreement between retrieved ASAR wind vectors and in situ data, in accord with literature (Kerbaol et al., 2007). In contrast, the inversion procedure showed that the retrievals were strongly dependent on the quality of the wind vector used to initialize the procedure. However, this is a promising starting point to provide accurate wind circulation map over wide coastal areas with acceptable spatial resolution.

Acknowledgments

This work was carried out in the framework of the research project “Integrated Monitoring of Coastal Areas (IMCA)”, funded by the Italian Ministry of Education, University and Scientific Research. The authors acknowledge the Department of Zoology, University of Bari, for supplying the buoy data used for this study. The ENVISAT ASAR images used were provided by ESA within the CAT-1 project 4795 “Validation of ocean geophysical parameters from ERS2 SAR and ENVISAT ASAR images with in situ data”.

References

Fetterer F., D. Generis and C. Wackerman, 1998, ‘Validating a scatterometer wind algorithm for ERS-1 SAR’, IEEE Trans. Geosci. Remote Sens., 36 (2), pp. 479-492

Kerbaol V. et al., 2007, ‘Improved bayesian wind vector retrieval scheme using ENVISAT ASAR data: principles and validation results’, Proc. ENVISAT Symposium

Moore R.K. and A.K. Fung, 1979, ‘Radar determination of winds at sea’, *Proc. IEEE*, 67, pp. 1504-1521

Portabella M., A. Stoffelen and J.A. Johannessen, 2002, ‘Toward an optimal inversion method for synthetic aperture radar wind retrieval’, *J. Geophys. Res.*, 107, 10.1029/2001JC000925

Stoffelen A. and D.L.T. Anderson, 1997, ‘Scatterometer data interpretation: derivation of the ransfer function CMOD-4’, *J. Geophys. Res.*, 102, C3, pp. 5767-5780

Stoffelen A., and D.L.T. Anderson, 1997a, ‘Scatterometer data interpretation: measurement space and inversion’, *J. Atm. and Ocean. Techn*., vol. 14(6), pp. 1298-1313

Stoffelen A. and D.L.T. Anderson, 1993, ‘ERS-1 scatterometer data and characteristics and wind retrieval skills’, Proceeding of first ERS-1 Symposium, ESA SP-359, pp. 41-47

Tang W. and W.T. Liu, 1996, ‘Equivalent neutral wind’, JPL Publication, pp. 96-17

Wackerman C., C. Rufenach, R. Schuchman, J. Johannessen and D. Davidson, 1996, ‘Wind vector retrieval using ERS-1 synthetic aperture radar imagery’, IEEE Trans. Geosci. Remote Sens., 34, pp. 1343-1352.

IMCA: INTEGRATED MANAGEMENT OF COASTAL AREAS

Claudio LA MANTIA[(1)]

[1]*Planetek Italia srl, Via Massaua 12, I-70123 Bari ITALY, lamantia @ planetek.it*

Abstract overwiev

IMCA (Integrated Monitoring of Coastal Areas) service is realized by a multidisciplinary consortium lead by Planetek Italia, supported by specialized private companies and Universities (IMCA partners).

IMCA is a service providing specific products for coastal conservation planning and water quality monitoring. The products are based on the integration of remotely sensed data, mathematical models and in-situ observations.

IMCA WebGIS was projected to pilot system to be able to distribute sample products providing essential information for the coastal zone management.

1. The studied areas

The project was realized in some areas of Puglia region, Italy. They are coastal areas of Isole Tremiti, Margherita di Savoia, Salento and Taranto (see fig. 1). In this areas the sensible sea parameter are controlled.

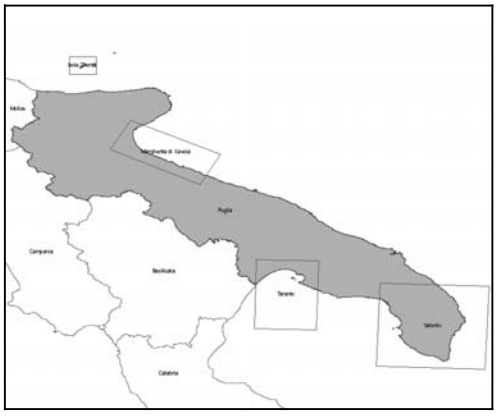

Figure 1. IMCA Studied areas

2. Material and methods

2.1. Used instruments

To supply sea parameters, same instruments are used. There are:

- four buoys located in the areas of Isole Tremiti (2 buoys), Margherita di Savoia and Taranto that transfer in real time the acquired data to IMCA database;
- other manual instruments that are used during the monitoring campaign by IMCA partners (Satlantic Profiler II, Microtops II Sunphotometer, Directional Waverider DWR-Mklll, AWAC Nortek Profiler, "Misuratore" CTD).

Data that are supplied by this instruments are, for example:

- Water Temperature
- Conductivity
- Conductivity Ratio
- Salinity
- Density
- Wind speed
- Wind direction
- Air pressure
- Air temperature
- Relative humidity
- Net solar radiation
- and so on.

2.2. Used Software Platform

The software platform used by IMCA system is the following:

- IMCA DATA SERVER

It contain IMCA database, IMCA geodatabase and the raster date repository. The server has the next system configuration:

  - S.O. MS Windows 2003 ITA
  - MS Database SQL server 2000
  - ESRI ArcSDE

- IMCA APPLICATION/WEB SERVER

It is the Server where data and imagines processing modules execute their operations. The used software are:

  - S.O MS Windows2003 ITA
  - MS IIS 6.0
  - ESRI ArcIMS

- IMCA CLIENT

Client machine used by the backoffice operator and by IMCA users. The used software are:

  - S.O Windows XP/2000
  - MS IE 6.0

2.3. Used Hardware Platform

- DATA SERVER:
  - SERVER - Proliant ML370 Tower G4 (Cod. 379906-421)
  - HARD DISK - 6*145.6GB U320 10KRPM UNIVER. HOTPLUG (Cod. 286716-B22) (total 870 GB nominal)
- APPLICATION/WEB SERVER:
  - HP 2GB REG PC2-3200 2X1GB MEMORY (Cod. 343056-B21)
  - ML370G4/DL380G4 - XEON 3.0/2MB L2 (Cod. 378748-B21)

2.4. IMCA Data Model

IMCA system uses a relational database (RDBMS) that:

- provides development objects and resources as stored procedures and triggers
- ensures a transaction management mechanism on the data.

The communication of the elaborated data, the new input data and the relative results take place according to an information flow managed by the central system that provides to unambiguously identify the elements of IMCA system.

The data model application domain that is associate to the system involves:

- products/services information management;
- users sensitive information management;
- back office information management.

The system uses MS SQL Server and so allows to store the front and back office information. Besides, the system allows to file the ancillary data for the single products.

A series of tables serves to establish the order of use of the data in the various phases and inside the system of elaboration.

Analysing the structural project status, it's derived the need to make conform the data model design to the national environmental technical specifications of APAT (Agenzia per la Protezione Ambiente e Territorio).

So, all the acquired data are stored into IMCA database that use an OST Model. This type of database can represent every territorial object or structure that is relative to every environmental theme and problem.

Furtherly, OST Model can store a large quantity of data that arrives very quickly. In this way, the inside database to the system IMCA allows to insert the data related to: Buoys, Monitoring campaign, Ancillari data, Satellite data.

To show data, IMCA WebGIS uses a geodatabase in which there are three feature class described in the following table:

Table 1. Feature Classes

Name	**Format**	**Description**
Buoys	Point	The point identify the buoy and its salient characteristics
Monitoring stations	Point	The point identify a monitored area, the used instrument and its characteristics
Studied areas	Polygon	The polygon identify an IMCA studied area

IMCA database can be updated by external users or by internal system operators.

3. Results

To provide coastal conservation and water quality, IMCA partners produce specific map using the in-situ and the automatic observation. In fact, with the support of their algorithms, they are able to graphically represent the data supplied by the instruments. The produced maps are published on the IMCA Website where IMCA users can read and download the data and the maps. IMCA WebGIS has an homepage in which there is a briefly description of IMCA project and same links useful to access to the IMCA Services.

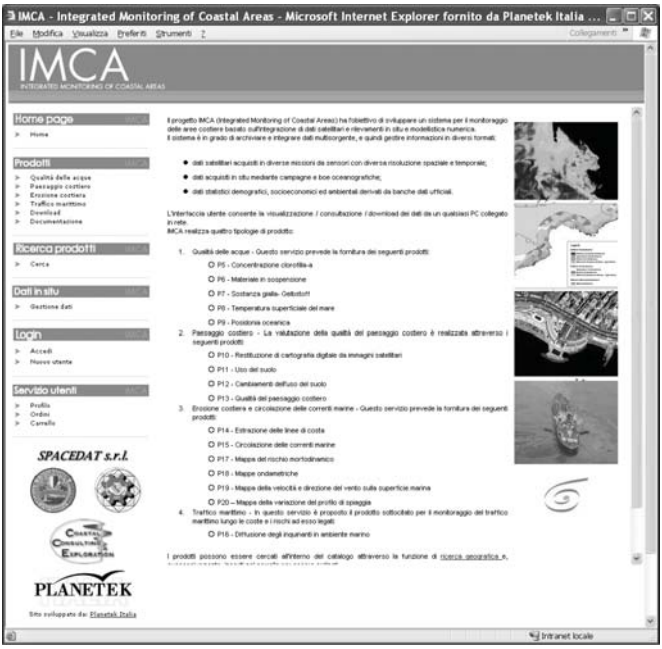

Figure 2. IMCA WebGIS homepage

On the left of the homepage there are the mentioned link. In the "Prodotti" section are present the link to access to the IMCA products description, to the download of same applications useful to manage raster data and to the User Manual ("Documentazione"). From the "Ricerca prodotti" section it's possible to access to the IMCA Service that is useful to supply maps to the users.

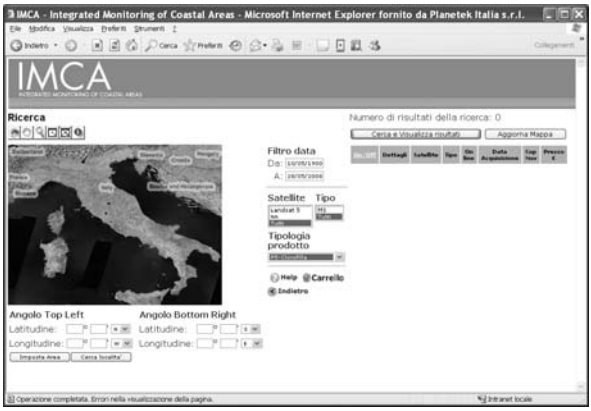

Figure 3. IMCA "Ricerca prodotti" service

The "Dati in situ" section lets you to access to the monitoring area in which it is possible to read the data related to the monitoring campaign and to the automatic surveyed buoys data. IMCA System can receive in "real time" the buoys data and so IMCA users can view and download them to implement every type of study.

The data can be displayed on the screen or can be downloaded in Excel file.

MARCOAST: WATER QUALITY SERVICES FOR THE EUROPEAN SEAS

Giulio CERIOLA[(1)], Paolo MANUNTA[(1)], Daniela IASILLO[(1)], Monique VIEL[(1)], Antonio BUONAVOGLIA[(1)]

[1]*Planetek Italia srl, Via Massaua 12, I-70123 Bari ITALY, manunta @ planetek.it*

Abstract overwiev

MarCoast is a 3 year project funded by the European Space Agency (ESA) with the aim of establishing a durable network of marine and coastal information services from remote sensing data, integrated with in-situ measurement, in close cooperation with national and regional authorities. The Water Quality Services (WQS) is addressed to users in charge of operational implementation of international, EU and national environmental policies, such as regional seas conventions (e.g. OSPAR, Barcelona Conventions), the EU Water Framework Directive (WFD), ICZM recommendations, etc. The current users are National Authorities (Belgium, Finland, Germany, Italy, Norway), Regional Authorities (France, Germany) or Research institutes (Finland, France, Germany). The services covered for the first two years:

- North sea, and Baltic sea and The Channel,
- Atlantic: Bay of Biscay,
- Mediterranean Sea: Western (French) and Central (Italian) Mediterranean coasts,
- Black sea.

Water Quality (Ocean color) products (Chlorophyll-a, Water Transparency, TSM, Turbidity, Gelbstoff absorption/yellow substance) are derived from MERIS or MERIS/MODIS Aqua data duly processed. Products are mainly delivered with a resolution of 1 km.

Planetek Italia srl is coordinator for the WQS line for European sea areas and service provider for the Adriatic, Tyrrhenian and Ligurian seas for APAT (Agenzia per la Protezione dell'Ambiente e per i Servizi Tecnici).

One of the main goals of WQS is to create an operational core of services to deliver near real time data from earth observation (EO) to monitoring the water quality of the European coasts. The scientific side includes the validation of EO data and their processing algorithms, using in situ data provided by the user and an attempt of regionalisation of the products.

1. The water quality service (s3)

The products provided by the WQS concern the monitoring of the water quality through a series of physical parameters as:

- Chlorophyll-a (Chl) concentration, the main parameter for the quality of water (WFD),
- Total suspended matter (TSM),
- Yellow substance concentration (YSC),
- Water Transparency (WT),
- Sea Surface Temperature (SST), a parameter involved in all the bio-physical processes of the sea.

Most of the data provided by the S3 service providers are based on the data generated by the Met-Ocean (S6) service from EO data processing. The S6 processing chain starts with the procurement of the EO data, then the data are processed and delivered to all the MarCoast services that use them. The portfolio of data available ranges from near real time observations (e.g. ocean colour, SST) to analysis and forecasts produced by oceanographic or atmospheric models (e.g. winds, waves, currents, 3D ocean

temperature). The service providers so have the role of organizing this data for making them accessible by the users via web, through queries of date, type, geographical location and so on.

Other data providers implemented their own processing chain from the acquisition of the satellite data, to the generation of the products and to the delivery via web sites.

Both the S6 service and those providers aimed to create a continuous processing chain able to guarantee a continuous and often also Near Real Time (NRT) service for supporting the assessment and monitoring of the water quality in the European waters. That was achieved by finding innovative solutions for:

- exploiting the satellite ground systems & archives to get a.s.a.p. in NRT the acquired data;
- exploiting the physical value of EO data from MERIS/MODIS/AVHRR satellite sensors, for gathering the Ocean Colours parameters of interest, both using the standard algorithms (ESA/NASA/NOAA) and in finding alternative ones for the regionalisation of the products;
- using the state-of-the-art technologies to make the products generated available via web and webGIS portals to the user community;
- performing the validation of the parameters gathered from the EO data with in-situ measurements provided by the users.

2. The PLANETEK ITALIA Service

2.1. The Service Chain process

For the first 2 years Planetek Italia provided the following products for the Italian coasts:

Adriatic Service for 2006 and 2007: **daily WT** (Secchi Depth, m) from MERIS Level 3 data; **daily Chl** (mg/m^3) from MERIS/MODIS (ENVISAT/Aqua satellite) Level 3 data (1km).; **Daily SST** (°C) from AVHRR Level 2 data (1km) taken from the EOWEB repository (http://eoweb.dlr.de: 8080/index.html).

Daily WT and Chl were delivered by ACRI (www.acri-st.fr), in the framework of the MarCoast S6 service. MERIS data were processed using standard atmospheric correction algorithms applied by ESA, Case 1 algorithm, and Case 2 algorithms for the coastal areas, using appropriate flags [ref. 3,4]. MODIS data were processed using the standard NASA OC3M algorithm for Case 1 waters (http://oceancolor.gsfc.nasa.gov/PRODUCTS/chlo.html)

Tyrrhenian and Ligurian sea for 2007: **daily Chl** (mg/m^3) from MERIS/MODIS Level 2 data (1km) data acquired from the ESA and NASA Rolling Archives; **daily SST** (°C) from AVHRR Level 2 data (1km) taken from the EOWEB repository; **daily Chl** (mg/m^3) from MERIS Level 1 Full Resolution data (300m) acquired from the ESA Rolling Archived and processed using the C2R (www.brockmann-consult.de/beam/plugins.html) atmospheric algorithm and chlorophyll calculation, using appropriate flags [ref. 3,4].

In particular this service was the first NRT continuous service using the MERIS Full Resolution data, and for this reason the C2R algorithm was chosen: it is an evolution of the standard ESA one and is code-free so it is possible to calibrate it using in-situ measurements.

Then 10-days, monthly Chl, WT and SST products were subsequently processed by Planetek Italia. All products are geo-referenced maps stored on a WebGIS portal (http://cartanetimca .planetek.it/MarcoastHome.asp), based on Cart@net® WebGIS solution developed by Planetek Italia, which offers extensive queries capabilities to find and select products by date, area, type of parameters and so on. The whole WebGIS is accessible from all the community, while the geophysical referenced maps are available download to the user.

For the third year of the MarCoast project (2008) the Greek seas are going to be covered with the following products: **daily SST** (°C) from AVHRR Level 2 data (1km) taken from the EOWEB repository; **daily Chl** (mg/m^3) **and WT** from MERIS Level 1 Full Resolution data (300m) acquired from the ESA Rolling Archived and processed using the C2R atmospheric algorithm and chlorophyll

calculation and an empirical algorithm for the WT, using appropriate flags [ref. 3,4]. In particular this service will be the first NRT continuous service systematically covering those sea areas and will use the MERIS Full Resolution data.

Also new users will be involved:

- the Greek Archipelagos (Institute of Marine & Environmental Research of the Aegean Sea) on behalf of the Greek Merchant Marine Ministry,
- the ARPA (Regional Agency for the Protection of the Environment) Emilia Romagna, in the view of extending the utility of the MarCoast products to regional level.

2.2. The Validation of the first year

For the Adriatic area they were available Chl, SST and WT in situ data (year 2006) acquired from the Si.Di.Mar (SIstema DIfesa MARe) Databank [ref. 5]. The Si.Di.Mar is administered by the Italian Ministry of Environment (MATTM) and stored all the monitoring data collected by the Regional Italian Authorities to respond to national and international duties (e.g. WFD, Barcelona Convention for the Mediterranean sea).

For the 2007 no Si.Di.Mar. data were available. The 2006 data covered the Adriatic areas (up to 3 km from coastline). Superficial values (0 – 0,5 m) were used for validation purpose.

Validation assessment for the Adriatic daily products was performed using statistical analysis and comparison of the annual cycle (time series) [ref. 2]; for Chl a local analysis for ten locations selected by APAT as inter-calibration stations for the Adriatic Sea in the framework of the Mediterranean GIG (Geographic Inter-calibration Group for the Mediterranean region) was performed. The ten stations are characterised by different hydrodynamic and anthropic conditions, depending on the presence or not of rivers with high nutrients loads [ref. 1].

120 coincident pairs for Chl and 91 for WT were selected from 2006 EO and in situ datasets accordingly to the selection criteria: same day and same geographic position. However, it is important to underline the intrinsic difference of the two monitoring instruments:

- Satellite and in situ data are measured at different times within the same day.
- In situ data is punctual and satellite data is obtained from the average value of the 1 x 1 km image element centered at the measurement site.
- Pixels nearest the coastline are often flagged.
- Two coastal stations could be included in the same pixel.

Validation Results are available by asking to Planetek Italia.

3. Conclusions

In the first two years the WQS of MarCoast successfully delivered products concerning the Water Quality assessment and monitoring of European sea areas. Within this framework Planetek Italia extended the area covered from the Adriatic sea (2006) to the Tyrrhenian and Ligurian sea (2007).

In the first year it took advantage of the processing chain of the Met-Ocean service, making more effort in the customizing of the high level EO derived data and in their delivery through a fully featured WebGIS.

In the second year it developed an own processing chain able to start from the acquisition of the EO low-level data, featuring also the use of the Full Resolution MERIS data, which with their 300m resolution are expected to give more information on the coastal areas. Also the choice of using an improved version of the standard MERIS algorithm, was done foreseeing the possibility of regionalisation of the products, by means of in-situ data. As a fundamental part of the project, the MarCoast Water Quality products were validated using in-situ data.

Planetek performed a validation of the water quality products (Chl, SST and WT) at 1km resolution along the Adriatic coastal area, using the available in-situ data acquired in the framework of the national coastal monitoring (Feb-Mar 2006 and Aug-Nov 2006).

The validation assessment carried out through statistical analysis and time series comparison demonstrated:

1. linear correlation statistically significant between EO & in situ data for both parameters.
2. a good consistency among time series between EO data and in situ monitoring for four specific coastal locations of the Adriatic Sea.

These first results are promising and show as EO data could be effectively used as a monitoring instrument of the water quality of coastal areas [2], in integration of in situ surveys for the Adriatic sea.

For the third year of the MarCoast project, Planetek Italia is going to maintain the current services and is going to add the coverage of the Greek seas. This will be the first systematic and continuous coverage of those sea areas with EO data, and in particular with the MERIS Full Resolution data. Finally for the third year the validation activities will have a very important role to confirm the positive results emerged for the Adriatic sea.

In particular in-situ data are expected from three different sources:

- the 2008 Si.Di.Mar. data over all the Italian coasts, from APAT;
- the regional in-situ data (even historical) for the Emilia-Romagna region, from its ARPA;
- the Aegean in-situ data, from the Archipelagos user.

Those data will be determinant to assess the accuracy of the standard MERIS/MODIS chlorophyll retrieval algorithms and to perform the first validation of the C2R algorithm on Mediterranean sea and an attempt for its regionalisation. The final scope of those validation activities will be to proper demonstrate the integrated use of EO and in situ data, for responding to the WFD obligations.

References

A.M. Cicero & Di Girolamo (eds), Metodologie Analitiche di Riferimento del Programma di Monitoraggio per il controllo dell'ambiente marino costiero (2001 – 2003). Min. Ambiente e della Tutela del Territorio, ICRAM. ICRAM, Roma 2001. **[5]**

Bacci T., Giovanardi F., Maialetti E., Mandra L., Nesti U., Russo S., Tomassetti P., Trabucco B.(2006). Relazione finale - Progetto pilota di studio e sperimentazione per la valutazione della qualità delle acque marino-costiere – Prog. di Ricerca EUWATER. Implementazione della Dir. Quadro Europea sulle Acque. ICRAM publication, 1-194. **[1]**

S.Dury, H.Hakvoort, R.Duin, H.Roberti (2006). Towards operational use of MERIS and SeaWiFS data for water quality monitoring: challenges for the end-user. EARSeL WARSAW 2006 **[2]**

MERIS Level 2 Algorithms Theoretical Basis Document – MERIS ESL PO-TN-MEL-GS-005 – ACRI ST - ESA. **[3]**

Reference model for MERIS Lev. 2 processing – MERIS ESL PO-TN-MEL-GS-0026 – ACRI ST - ESA. **[4]**

USING STEREO PHOTO MEASUREMENTS TO ANALYZE THE SURFABILITY OF SHIP INDUCED WAVES

S. DE VRIES [(1)], M.A. DE SCHIPPER [(2)], J.S.M. VAN THIEL DE VRIES [(3)], W.S.J. UIJTTEWAAL [(4)] & M.J.F. STIVE [(5)]

[(1)] *Msc, Delft University of Technology, Stevinweg 1, Delft, 2628 CN, The Netherlands. Sierd.deVries@TUDelft.nl*

[(2)] *Msc, Delft University of Technology, Stevinweg 1, Delft, 2628 CN, The Netherlands. M.A.deSchipper@TUDelft.nl*

[(3)] *Msc, Delft University of Technology, Stevinweg 1, Delft, 2628 CN, The Netherlands. J.S.M.vanThieldeVries@TUDelft.nl*

[(4)] *Msc PhD, Delft University of Technology, Stevinweg 1, Delft, 2628 CN, The Netherlands. W.S.J.Uijttewaal@TUDelft.nl*

[(5)] *Professor PhD Msc, Delft University of Technology, Stevinweg 1, Delft, 2628 CN, The Netherlands. M.J.F.Stive@TUDelft.nl*

Abstract

The objective of this paper is to demonstrate the use of Stereo Photogrammetry (SP) measuring ship generated waves and to determine under which conditions they are suitable for surfing. A physical experiment is conducted to gain insight in ship wave behavior under specific conditions. Waves are generated by a hull and are measured using SP. It is concluded that the SP technique holds great potential in laboratory use and ship waves can potentially be used for surfing purposes.

1. Introduction

The idea of generating surfable ship waves in a circular pool is patented by Australian surf board designer Greg Webber with the aim of building a surf pool. Ideally surfing waves are not influenced by currents. The angle between the wave crest and the breaker line (peel angle) is the most important surfability parameter; this angle should range between 40° to 60° (Hutt et al., 2001).

Ship waves are qualitatively described as early as 1891 by Lord Kelvin (Thomson, 1891). Ship waves can be divided in a primary and secondary wave system. The primary wave system consists of the bow and stern wave and the local water level set down due to increased water velocities beside the hull. The secondary wave system is caused by the pressure pattern due to the discontinuities in the hull. These discontinuities are found at the bow and at the stern, both of which emit waves. The emitted waves form transverse and diverging waves. Interference of these transverse and diverging waves lead to a typical wave pattern called the Kelvin wave pattern. Wave angles in the Kelvin wave pattern are generally 55°.

Using Schijf's theory (Schijf, 1949) the characteristics of the ship wave patterns can be predicted by defining sub-, trans- and super-critical regimes depending on the ship's speed and blocking percentage of the channel. When blocking and ship speeds are low, the return flow is weak and the regime is sub-critical. When blocking and ship speeds are higher and the return flow reaches a critical value the regime is trans-critical. Due to practical limitations concerning the wave pool design the super critical regime is not of interest.

A numerical model to fully predict ship induced wave characteristics is found to be not available for both sub-critical and trans-critical conditions (De Schipper, 2007). To gain insight in the generation of ship waves with respect to surface elevation and flow velocities an experiment is conducted. SP is

applied as measurement technique in the experiment. This study investigates the possibilities of SP to reconstruct water surface elevations and flow velocities. Traditional measurement devices measure surface elevation and flow velocities at one point only whereas SP shows a high resolution spatial representation of both. The obtained data can be used to verify future numerical models.

2. Experiment

The experiment is conducted in the towing tank facility of the Faculty of Mechanical, Maritime and Materials Engineering at the Delft University of Technology. The tank is 80m long and 2.75m wide. A ship's hull is towed along the sidewall of the tank generating a wave field. Ship speed and blocking percentage of the channel are varied inducing different wave fields in the sub-critical and trans-critical regime.

The generated wave field is photographed by two synchronized cameras from different positions, see figure 1. The cameras are mounted above the towing tank and photograph the wave field as the hull passes. In the measurement area floats are applied to increase contrast at the water surface.

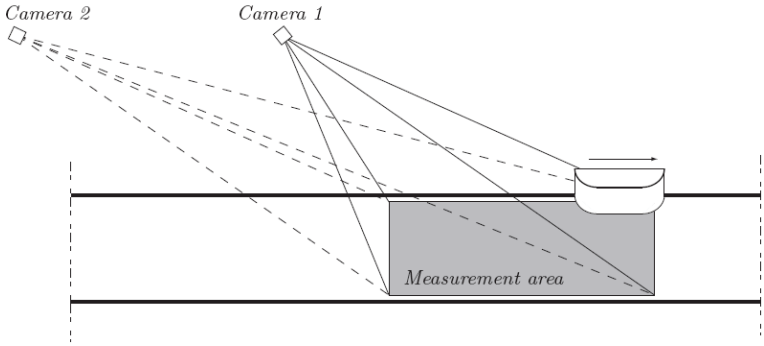

Figure 1. 3D overview of the camera setup. Arrow indicates direction of hull movement

The images from the two cameras with overlapping fields of view are used to determine a 3D presentation of the wave field in world coordinates. The procedure of stereo reconstruction is to calibrate the cameras, to correlate the two images and to reconstruct the 3D world coordinates. The method used for calibration, correlation and reconstruction is similar as the method described by Clarke et al. (in prep). In short, the calibration is done using a combination of in situ ground control points (for external camera parameters e.g. orientation) and a reference grid for internal camera parameters (e.g. distortion), the correlation is based on the principle of the epipolar constraint and triangulation is used for reconstruction. In addition to the reconstruction of the water level, Particle Tracking Velocimetry (PTV) is used to derive surface flow velocities. A time series of the images from one camera is cross correlated to determine the spatial movements of the features in the image. With the prior knowledge of the known 3D coordinates of the features in the images a 3D velocity vector is determined. With the knowledge of surface elevation, and thus the local water depth, and the flow velocities a spatial distribution of the local Froude numbers is derived.

3. Results

The experimental data processed using the SP technique results in 3D images of the surface elevations and surface flow velocities. Figure 2 shows such an image. The figure shows the dominant primary wave in the trans-critical regime. The primary wave and the return flow are clearly visible. Surface waves in the order of 5-20 cm. are measured with and estimated accuracy of 1-2 cm based on the size of the image pixel stamps in world coordinates. Velocities in the order of 0-2 m/s are measured.

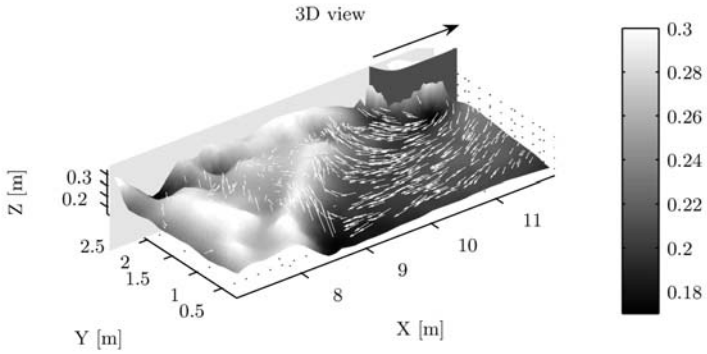

Figure 2. Image of the surface elevation of a wave field generated by a hull. The tank wall is indicated in light gray and the moving hull is depicted in black at the top right corner. The arrow indicates the direction of hull movement. Colorbar indicates water depth [m]. White vectors represent flow velocities.

A time series of the images is made at a sampling frequency of 8 Hz. A time series of the surface elevation derived by SP is generated and on specific points these surface elevations are compared with wave gauge measurements. Figure 3 shows that SP surface elevation measurements compare well with wave gauge measurements.

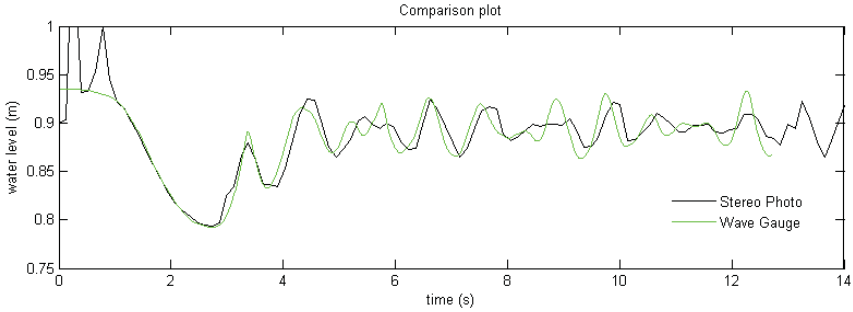

Figure 3. Comparison plot between measurements of the stereo photo technique (8Hz) and a traditional wave gauge.

Surface elevations and surface flow velocities for the different runs are analyzed. The Froude number distribution is used to identify the sub-critical and trans-critical regimes. It is found that the occurrence of sub- and trans-critical regimes can be successfully determined in accordance with Schijf's theory. The sub-critical regime accounts for a wave train and wave angles are according to the theoretical 55° with low flow velocities. The wave pattern in the trans-critical regime is dominated by an undular jump and high flow velocities. The undular jump and the high flow velocities have negative effects on the surfability of the waves.

4. Conclusions

After evaluating all images for different runs it is concluded that the new Stereo Photogrammetry technique offers great potential to measure wave characteristics. Simultaneously measuring surface elevation and flow velocity in a full 3D domain is possible.

The trans-critical regime is not suitable for surfing due to the occurrence of a dominant primary wave. This dominant primary wave involves high surface flow velocities and an undular jump. The sub-critical regime shows a dominant secondary wave field with low flow velocities. The 55° wave angle in

the sub critical regime is similar to the desired peel angles. Therefore the sub-critical regime is potentially suitable for surfing.

References

Clarke, L., Van Thiel de Vries, J.S.M., Holman, R., in preparation, 'High Resolution Morphology from Stereo Video Cameras'

De Schipper, M.A., (2007). On the generation of surfable ship waves in a circular pool, Part I: Physical background & Wave pool design. Hydraulic Engineering. Delft, TUDelft. Msc: 64.

Hutt, J. A., K. P. Black, et al. (2001). 'Classification of Surf Breaks in Relation to Surfing Skill.' Journal of Coastal Research(Special Issue): 66-81.

Schijf, J. B., 1949, 'Influence of Form and Dimensions of the Cross-Section of the Canal, of the Form, of the Speed and the Propulsion System of Vessels', *XVIIth PIANC*, section 1, subject 2, Lisbon.

Thomson W. (Lord Kelvin), 1891, 'Stochastic nonlinear shoaling of directional spectra', *Popular lectures and Addresses,* Volume III, 79-99

A VIDEO BASED TECHNIQUE FOR SHORELINE MONITORING IN ALIMINI (LE)

Leonardo DAMIANI [(1)], Matteo Gianluca MOLFETTA[(2)]

[(1)] *Prof, Technical University of Bari, Via Orabona, Bari, 70125, Italy. l.damiani@poliba.it*

[(2)] *Eng, Research and Experimentation Laboratory for Coastal Defense (LIC), Technical University of Bari, Via Orabona, 4 Bari , 70125, Italy, m.molfettta@poliba.it*

Abstract

A procedure for semi-automatic shoreline extraction from webcam images has been developed. The procedure includes images averaging, rectifying and georeferencing and shoreline extrapolation. It also includes tide correction and beach slope computing.

The procedure, developed in MATLAB environment, allows studying shoreline evolution treating a considerable number of data with a relative low cost. Thus it is possible to correlate shoreline position with wind and wave data, observing in real time the beach response to a particular sea storm and testing numerical models outputs with real phenomena.

1. Introduction

Measuring and monitoring the location of the shoreline is one of the core task of coastal researchers. In addition to scientific motivations, such as studying real effects of sea storms, there are several practical applications connected with this activity, that can include: identifying and quantifying shoreline erosion, evaluation of the real effects of coastal protection structures, etc., so that shoreline monitoring can be considered a basic input for all engineering design in the coastal zone (Aarninkhof et al., 2003)

The use of video imagery for monitoring waterline evolution offers a number of advantages compared to conventional monitoring systems, These systems, typically GPS surveys or aerial photogrammetry campaigns, consist in measurements of waterline position and its variations in time, usually with annual of biannual frequency, because of their cost. But the own peculiarities of the shoreline variations and their close dependency from all meteomarine parameters (tide, waves, wind) sometimes make these kind of surveys useless to understand the real phenomena in progress (Kroon et al, 2007, Archetti and Lamberti, 2006).

The first generation of video-based shoreline detection techniques, were based on acquisition of greyscale images and they utilized the characteristic grey-scale pixel intensities distribution, in the swash zone (Plant and Holman, 1997). Other techniques, always based on grey-scale images, were developed to study dissipative, mild sloping beaches, in which first method didn't give satisfactory results. With these techniques the location of shoreline was estimated from a characteristic feature in the correlogram of the cross-shore intensity and variance profile (Aarninkhof et al., 1997). All these methods generally needed a site-dependent correction and shoreline extraction could be complicated in some situations characterized by absence of well pronounced contrast in greyscale between sub-aerial and sub-aqueous pixels. So new methods have been developed, using additional information given by full-colour images. In all these methods, Red-Green-Blue (RGB) images were converted in Hue-Saturation-Value (HSV) Images, in which colour information (H, S) are separated by greyscale information (V). HSV intensity, suitably filtered and scaled, gives a histogram characterized by two peaks, which mark the location of dry and wet pixels. (Aarninkhof et al, 2003). The results may locally show erroneous contours of sub-aerial beach which are associated with irregular intensity characteristics of some features like water-filled, or vehicles on the beach. Applying this technique to Alimini images, with some light conditions, and especially, after a rainy day, some interpretation errors have been found because of presence of water on emerged beach. So a new approach has been attempted.

The aim of this work is to present a method to extract shoreline positions from a time averaged and

orto-rectified images of Alimini beach in Apulia region and to treat these data for studying coastline management problems.

2. Image acquisition system

The acquisition system consists in two webcams positioned on the top of a pole about ten meters high on MWL. The cameras are connected with a data logger, a pc, and a GSM modem for transmission of some selected daily images on the web (http://www.puglia-coste.it). It is possible to control by remote all acquisition parameters such as interval of acquisition, number of snap shots etc. Both cameras (CBC Europe l.t.d.-model ZC-NH255P) produce images with resolution of (1911 x 2121) and video with a duration only limited from the data logger memory.

The webcams obviously provide oblique views of the beach; transformation from two-dimensional video images to three dimensional world coordinates images requires a determination of camera geometry, typically with visually identifiable ground point control (Hathaway and Bottin, 1997)

For that reason, during installation works a topographic survey has been carried out. It has allowed determining the spatial coordinates of several points (1739) of two grids - one for every webcam - physically materialized in the portion of the beach framed by cameras by applying white markers on some pegs (Fig.1). Every vertex of this grid has been used as control point for images transformation (Holland et al., 1997).

Figure 1. Alimini beach during topographic survey; vertexes of materialized grid are visible.

Identification of shoreline using images can result a difficult operation especially in presence of waves, when the line is often obscured by swash motions and breaking phenomena; in these cases using time averaged images can be helpful (Plant and Holman, 1997). A computer based image processor has been used to produce digital images obtained by averaging a superimposed sequence of image frames. Typically every three daily hours started an acquisition event consisting in 20 snapshots for every webcam with frequency of 1 snapshot per second. After averaging operations, rectifying procedure takes place and then rectified and averaged image is transmitted on web.

3. Image post processing

The procedure that has been employed for this work is a colour-based procedure. Some Matlab routines have been developed for this study; these routines allow, first of all, obtaining a semiautomatic extraction of shoreline from an averaged and ortorectified image. A routine partially including a subroutine developed by Lau (1997) has been chosen for its better behaviour with the situation of Alimini beach. Lau's method starts at a given pixel and isolates all neighbouring pixels with values within a preset tolerance. No transformation of RGB in HSV images is required, so that the only thing asked to the operator is to identify in the picture some points on sand (or on sea) and to click on them. The operator is allowed to control in real time the results of shoreline extraction because it is possible to overlap the initial image to the extracted line. If results are not satisfactory the range of the pixel similarity colour

can be changed or other points can be clicked for including zones whose colours had been ignored before. To solve typical problem of summer images when tourists, umbrellas or vehicles presence near shoreline can make its detection very difficult, a suitable procedure has been developed. Indeed, it is possible to interpolate some selected regions in order to delete foreign objects.

The output is a binary matrix with the same size of the initial image resolution; so, knowing pixel dimensions (each pixel is about 0.06 x 0.06 meters), it is immediate to evaluate distance of shoreline from a baseline. This distance can be plotted for a number of transect that, theoretically, can be equal to the row number of the matrix - initial image - that is 1911. The evaluated shoreline can also be exported to GIS/CAD environment to overlap available cartography. In figure 2 shoreline evolution is shown on 9 representative transects during all 2006. Due to webcam system failures the time series are not complete, as can be noted.

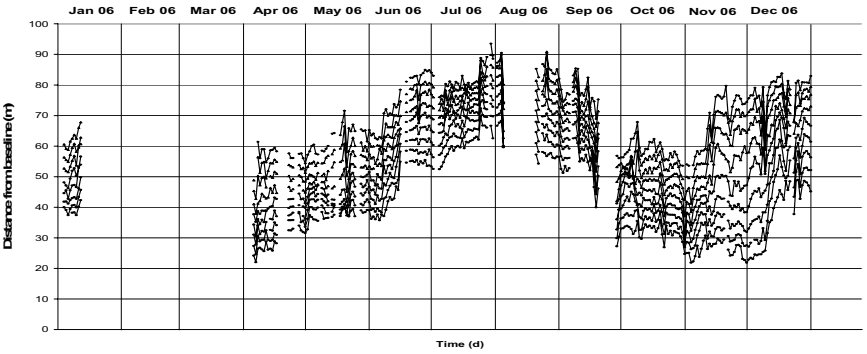

Figure 2. Shoreline evolution in 2006.

The instantaneous location of waterline is affected by offshore tidal level, storm surge, wave setup and swash oscillations. After every acquisition event the procedure identifies a beach contour that is located somewhere within the swash zone. These horizontal lines, z_{ist}, are, obviously associated to a water level that can be defined by (Aarninkhof et al, 2003):

$$z_{ist} = z_0 + \eta_{ist} + K_{osc}\frac{\eta_{osc}}{2} \qquad [1]$$

where z_o is the tide and wind offshore water level, η_{ist} is the wave setup, η_{osc} is the vertical swash height, k_{osc} is a constant, empirical coefficient.

Due to the factors that, during storms, affect sea level, as above specified, the waterlines in fig. 2 are not representative of the real shoreline position. In this study a procedure for determining beach slope in swash region in absence of wind and waves has been developed. Indeed, in these conditions, the instantaneous horizontal position of waterline can be considered as a contour if associated to a tidal level. Tidal levels are recorded from a mareograph located in Otranto, a few Km from Alimini beach. For every three consecutive acquisition events characterized by still sea, beach slope has been computed in every transect, one for each matrix column (2121), using elementary trigonometric formulas. The beach slope between two still sea states has been considered as a constant and all the waterlines detected in this slot have been related to the zero tidal level.

In first (top) panel of figure 3 tidal levels, as collected from Otranto's mareograph, are shown; in second panel shoreline evolution shown in figure 1 is now "purified" by tidal effects, as above explained, and shown for only one of the transects (continuous black line), because of shoreline trend similarity between different transects (see fig.1); in the same panel circle points represent shoreline position during still sea states, when beach slope has been calculated. Observing their position during the observation time (dashed line), it is possible to evaluate sea storms real effects (e.g. erosion or nourishment) on shoreline position; considering these points, a trend line (continuous grey line) has been traced: its shape is representative of net nourishment during 2006. In the third panel the sea states are represented in terms

of wave heights offshore Alimini. Unfortunately, wave measurements are not available in the southern Adriatic Sea, except for data collected by a buoy located about 150 km north of the examined shore, whose data, however, due to the different exposure to wave motion, are not suitable for wave hindcasting offshore Alimini beach. For this reason, the SMB method revised by the Shore Protection Manual was used to estimate the wave characteristics, using wind data acquired from an anemometer located in Otranto near the mareograph. It is important to stress that offshore Alimini higher waves come from NW, but due to the geographic exposure the shore is quit protected from mistral waves, while waves from SSE reach the shore almost undisturbed.

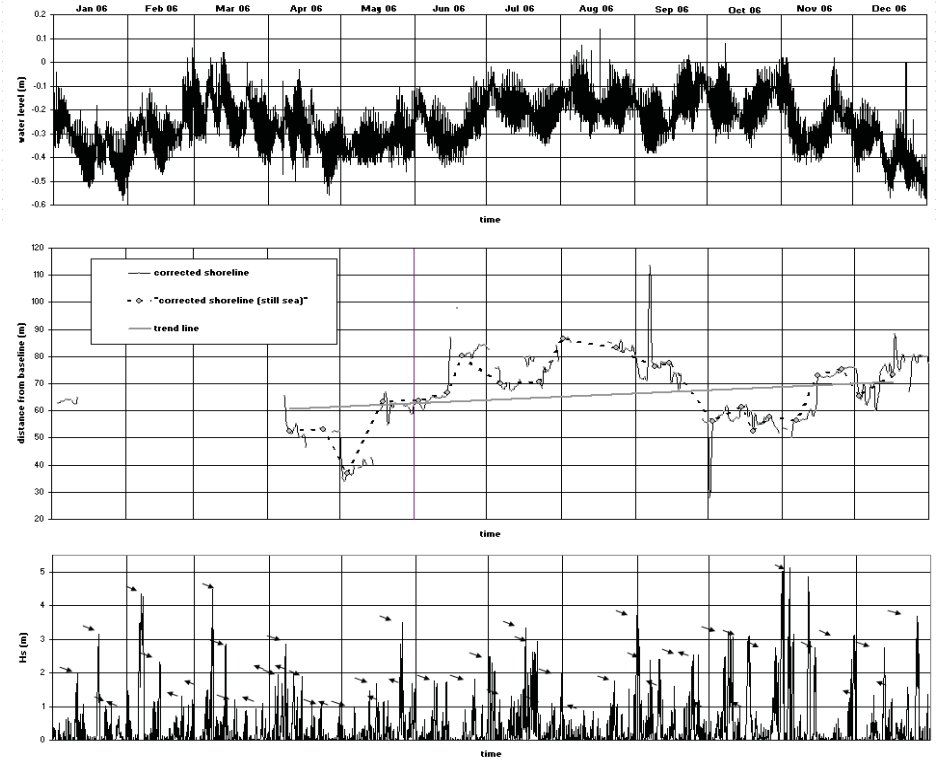

Figure 3. Tidal levels in Otranto (top panel); corrected shoreline (central panel); sea states offshore Alimini

References

Aarninkhof S.G.J., Turner I.L., Dronkers T.D.T., Calijouw M., Nipius L., 2003 'A video-based techinique for mapping intertidal beach bathymetry', *Coastal Engineering*n. 49 (pp.275-289)

Kroon A., Davidson M.A., Aarninkhof S.G.J., Archetti R., Armaroli C., Gonzales M., Medri S., Osorio A., Aagaard T., Holman R.A., Spanhoff R., 2007, 'Application of remote sensing video systems to coastline management problems', *Coastal Engineering* n. 54 (pp.493-505)

Archetti R., Lamberti L., 'Studio della evoluzione di una spiaggia protetta da opere a cresta bassa mediante video monitoraggio', proc. of XXX° convegno di Idraulica e Costruzioni Idrauliche - IDRA 2006

Plant G. N., Holman R.A., 1997, 'Intertidal beach profile estimation using video images', *Marine Geology* n. 140 (pp.1-24)

Aarninkhof S.G.J., Janssen P.C., Plant N.G., 1997, 'Quantitative estimations of bar dynamics from video images', proc. Coastal Dynamics Conference, Plymout, U.K., (pp365-374)

Hathaway K.K., Bottin R.R., 1997, 'Video measurement of wave runup on coastal structures' *Coastal Engineering Technical Note.*

Holland K.T., Holmann R.A., Lippman T.C., Stanley J., Plant N.G., 1997 'Practical use of video imagery in nearshore oceanographic field studies' *IEEE Journal of Oceanic Engineering* n. 22 (pp 81-92)

AN ARTIFICIAL VISION SYSTEM FOR PHYSICAL MODEL TESTS IN MARITIME ENGINEERING

Rodrigo CARBALLO [(1)], Óscar IBÁÑEZ [(2)], Gregorio IGLESIAS [(3)],
Alberte CASTRO [(1)] , Juan Ramón RABUÑAL[(4)] & Julián DORADO [(5)]

[(1)] Assoc. Res., Univ. of Santiago de Compostela, Dep. Ag. Eng., Campus Univ. Lugo, 27002, Spain. rcarba@usc.es, albertecastro@udc.es

[(2)] Assoc. Res.,Univ. of A Coruña, Dep. of Information &Communications Technologies. Campus Elviña, A Coruña, 15071, Spain. oibanez@udc.es

[(3)] Assoc. Prof., Univ. of Santiago, Dep. Ag. Eng. Campus Univ. Lugo, 27002, Spain. iglesias@usc.es

[(4)] Assoc. Prof., Centre of Technological Innovation in Construction and Civil Engineering (CITEEC) Campus Elviña, 15071, A Coruña, Spain. juanra@usc.es

[(5)] Assoc. Prof., Univ. of A Coruña, Dep. of Information &Communications Technologies. Campus Elviña, A Coruña, 15071, Spain. julian@udc.es

Abstract

A new measurement system for physical model tests in wave flumes has been developed. It is based on artificial vision techniques, and has a number of advantages with respect to conventional methods. The system is able to detect the free surface and to measure the displacement of floating physical models. In this work, its essential features are presented and its advantages discussed in the particular case of floating oil spill boom tests.

1. Introduction

At the present time wave gauges are the conventional method used in laboratory tests to measure the water level. These methods present numerous downsides: i) they are intrusive, meaning that a physical element must to be introduced in the fluid and its behavior can be modified; ii) they must be calibrated daily, resulting in a low time efficiency; iii) they are expensive; and last but not least, iv) they provide discrete measurements, i.e. at a single point.

Previous works based on image analysis were conducted with the aim of measuring the surface wave profile, but unfortunately they do not represent a real-time approach (García et al., 2003; Javidi and Psaltis, 1999; Zhang, 1996). Futhermore, when a floating model is tested, it is necessary to measure its displacements in order to analyze its behavior or to compare the physical results with model results. In spite of this, nowadays there is no any available technique used world-wide to this end.

Within the framework of a European research project, "Advanced tools to protect the Galician and Northern Portuguese coast against hydrocarbon spills on the high seas", a new Artificial Vision System (AVS) for laboratory tests has been developed with the aim of improving the performances of conventional methods. The system is optimized in connection with the analysis of the displacements of an oil spill boom.

2. Experimental set-up and Artificial Vision System tests

The physical tests carried out to optimize the AVS were performed in the wave and current flume of the Escuela Politécnica Superior of the University of Santiago the Compostela. The wave flume is 20 m long and 0.65 m wide with a maximum water depth of 0.8 m.

Wave conditions are generated by means of a piston-type paddle equipped with an Active Wave Absorption System (AWACS) that allows the absorption of reflected waves. Current conditions can be also generated by means of a reversible pumping system controlled by a system of valves. The general picture of the configuration of the AVS is presented in Figure 1.

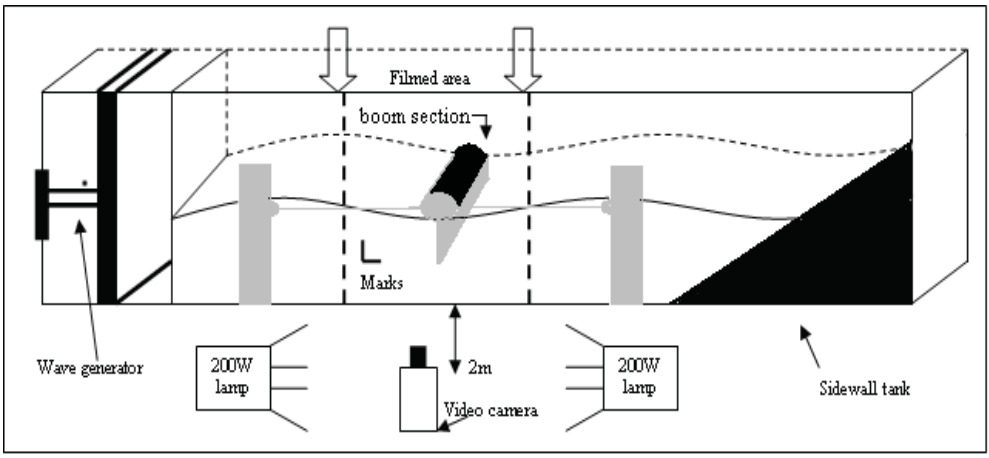

Figure 1. Laboratory set-up of the Artifical Vision System

A large number of configurations were tested in order to achieve proper results. The parameters tested were: lightning, marks on boom, camera position and camera zoom. Finally, the results were compared with those obtained by means of conventional systems. The results show a great accuracy of the system, constituting a tool which can be used worldwide in laboratory tests.

At this time, the efforts are centered in the detection of the water-contaminant interface, a key issue in the analysis of the oil spill boom performances. For this purpose, the hydrocarbon slick will be modeled in the flume by means of a substance with similar hydrodynamic properties —in terms of viscosity and density. The results will be presented in the final paper.

References

García, J., Herranz, D., Negro, V., Varela, O., Flores, J., 2003. Tratamiento por color y video. *VII Jornadas Españolas de Costas y Puertos.*

Javidi, B., Psaltis, D., 1999. 'Image sequence analysis of water surface waves in a hydraulic wind wave tank', *Proceedings of SPIE*, Vol.3804, pp. 148-158.

Zhang, X., 1996. An algorithm for calculating water surface elevations from surface gradient image data, *Experiments in Fluids*, Vol.21, No.1, Springer Berlin / Heidelberg, pp. 43-48.

DESIGN OF A MULTIDIRECTIONAL WAVE AND CURRENT BASIN FOR SHALLOW, INTERMEDIATE AND DEEP WATERS

Pedro LOMONACO[(1)], Cesar VIDAL[(2)], Inigo J. LOSADA[(3)], Raul MEDINA[(4)] & Christian KLINGHAMMER[(5)]

[(1)] *Environmental Hydraulics Institute of Cantabria (IH Cantabria), Avda de los Castros s/n, Santander, 39005, Spain.* lomonacop@unican.es

[(2)] *Environmental Hydraulics Institute of Cantabria (IH Cantabria), Avda de los Castros s/n, Santander, 39005, Spain.* vidalc@unican.es

[(3)] *Environmental Hydraulics Institute of Cantabria (IH Cantabria), Avda de los Castros s/n, Santander, 39005, Spain.* losadai@unican.es

[(4)] *Environmental Hydraulics Institute of Cantabria (IH Cantabria), Avda de los Castros s/n, Santander, 39005, Spain.* medinar@unican.es

[(5)] *Fachhochschule Jena, Carl - Zeiss - Promenade 2, Jena, 07745, Germany.* christian.klinghammer@web.de

Abstract

A new multidirectional wave basin for physical modelling in shallow, intermediate and deep water, with the added capability of current generation in any direction, has been designed and will be constructed during 2008 as part of the new premises of the Environmental Hydraulics Institute of Cantabria in Spain.

The basin is part of a three level structure formed by a 44 x 40.6 x 3.9 m sump in the lower level, a 32 x 20 x 2.5 m sub-basin aimed for the current generation system at the mid-level, and a 30 x 44 m x 4.1 m basin at the upper level, which corresponds to the main laboratory and street level (see Figure 1). The upper-level basin includes a 6 x 6 x 7 m deep pit for deepwater testing of floating structures, buoys, offshore platforms, or field instruments. Moreover, the structure of the facility will be part of a new building with offices and laboratories which will include all the necessary equipment, shops and services of the Institute. These new premises are the result of an impressive effort of the Spanish Government to create a national network of newly made singular facilities for scientific and applied research.

The design of the laboratory, in general, and of the multidirectional basin in particular, considers the application and use of state-of-the-art measuring systems, pre- and post-processing of acquired data, wave generation and dynamic control systems. The new laboratory includes the parallel application and development of a numerical mirror of the basin, providing, first, a mean to optimise the design, construction and measurement of the physical model testing, second, the testing results will be used to calibrate and validate the numerical model and, finally, it can be used to generate additional cases in support of the design of alternatives or to extend the applicability of an empirical formulation. The basin numerical mirror will be offered to internal and external researchers as part of the services provided by the new laboratory.

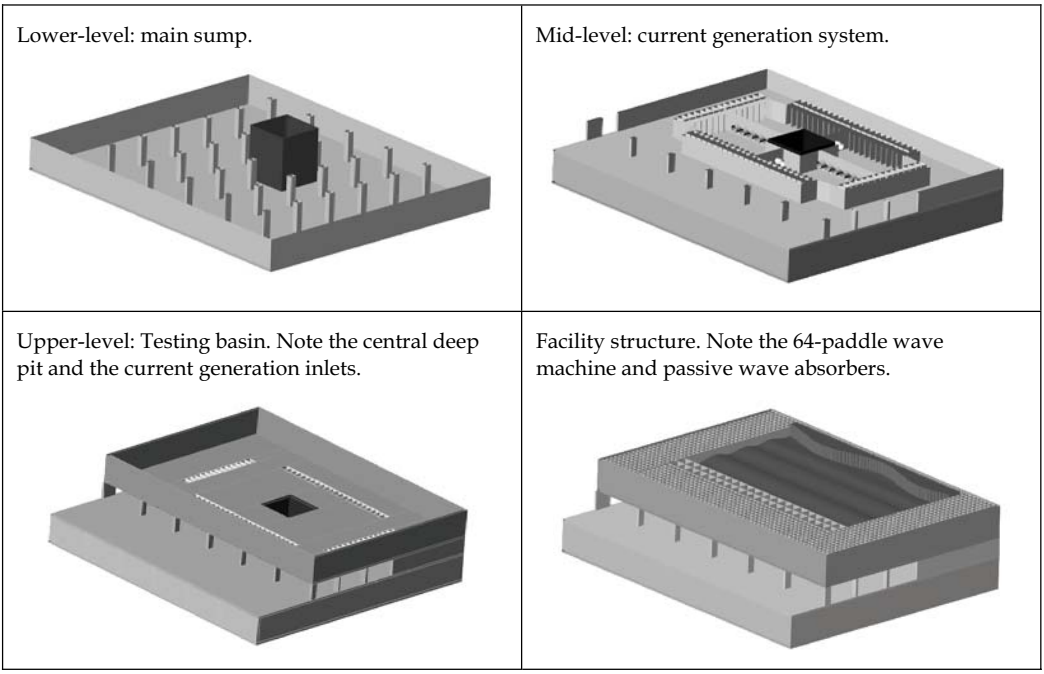

Figure 1. Configuration of the three-level structure of the new multidirectional wave basin for physical model testing in shallow, intermediate and deep waters.

Furthermore, to reduce unnecessary mobilisation of external researchers, the laboratory will be fitted with high-quality web-cams and Internet access to post-processed data, optimising the observation, monitoring and quality control of the physical model tests.

As part of the design requirements, the basin will be operational for coastal and offshore engineering studies with model scale depths ranging from 0.2 m to 3.0 m, capable of producing long- and short-crested directional regular and irregular waves in a broad range of periods and amplitudes, including the possibility of generating very long waves like seiches or tsunamis. The central 10 m deep pit includes a floating sturdy bottom for testing variable depths. A reversible current generation system will be capable of producing a uniform flow of up to 0.2 m/s over the full 3 m depth, parallel and perpendicular to the mean wave direction.

The wave machine, formed by 64 boards 0.5 m wide and 4.1 m high, portrays a maximum stroke of 2 m and will be fitted with active wave absorption. As part of the sophisticated tailor-made mechanical design, each wave board will be driven with two electrical motors enabling piston-type, hinged or combined paddle motion. Further, the secondary motor may also produce an eccentric deviation of the wave board to improve the quality of oblique wave generation. The total installed power of the wave machine is estimated to be 1.0 MW.

Figure 2 presents the theoretical performance curves of the wave board for three operational water depths. Each plot portrays the maximum individual wave height, for a range of wave periods that can be generated, considering in the computation wave breaking, power and stroke limitations. Moreover, each graph includes the performance curve for piston-mode and hinge-mode.

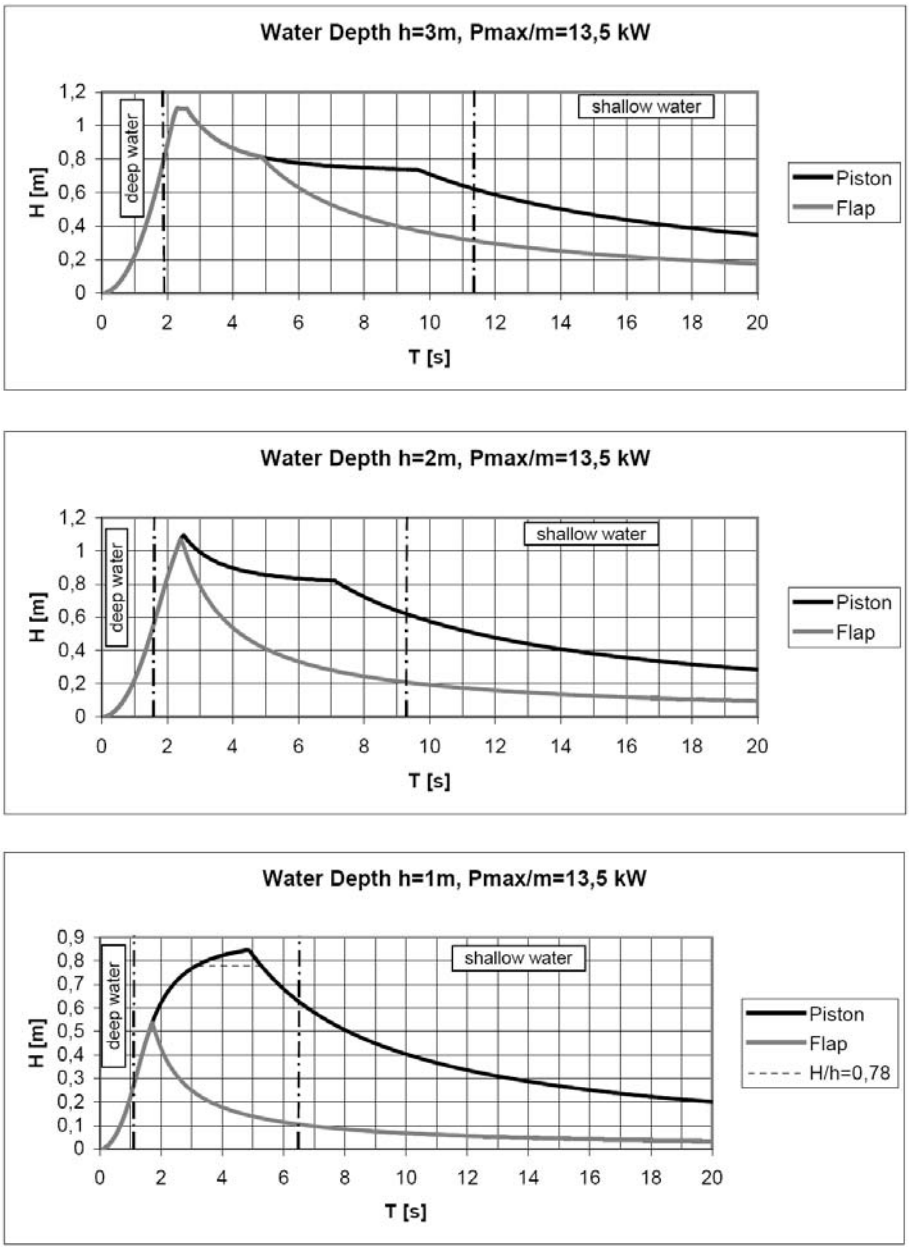

Figure 2. Theoretical performance curves for the wave machine for three water depths and for piston-mode and flap-mode. Each graph includes the limitation of wave breaking, installed power and stroke.

In Figure 3, the preliminary design of the wave boards is presented, where the frame, actuators, hinges and board are shown at “zero” position.

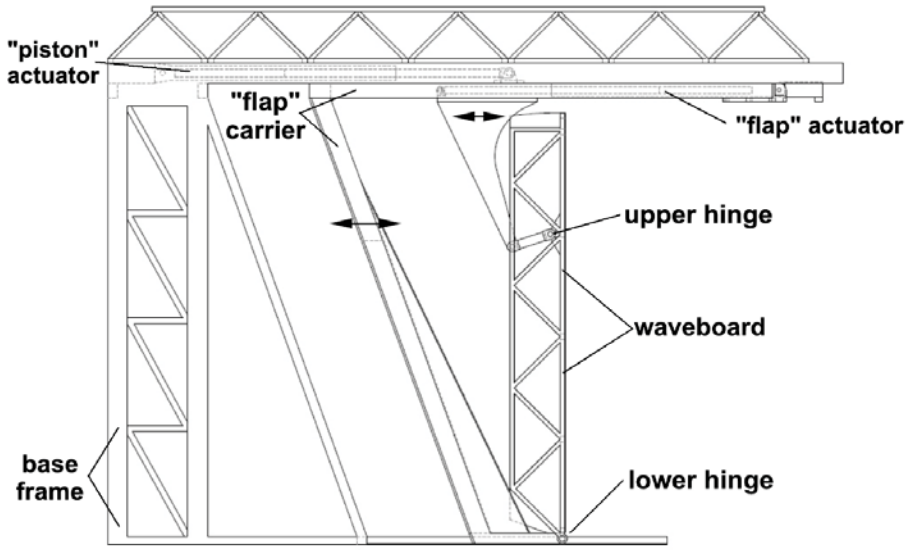

Figure 3. Preliminary design of the wave board, actuators and frame.

The current generation system is located underneath the basin, in an enclosed basin divided in four chambers interconnected by a series of 1 m diameter holes, and each will be fitted with a 22 kW thruster. The total (reversible) discharge parallel to the mean wave direction will be around 18 m^3/s and 12 m^3/s in the perpendicular direction. A total of 20 thrusters will be installed with a required power of 440 kW.

Finally, the wave basin will be surrounded by removable and floating passive wave absorbers up to 9 m wide, providing an overall testing area of circa 20 by 30 m. In the final paper, some details of the structure facility, wave machine, current generation system, numerical mirror, as well as all the environmentally friendly devices considered for the new laboratory, will be presented.

LABORATORY OBSERVATION ON MOTION AND DEFORMATION OF AQUACULTURE CAGE BY NON-INTRUSIVE STEREO IMAGING METHOD

Shu-Jing JAN [(1)], Li-An KUO [(2)],Ray-Yeng YANG [(3)], Hwung-Hweng HWUNG [(4)], Chen-Lin TENG [(5)] Hervé CAPART [(6)]

[(1)] *Postdoctoral Research Associate, Tainan Hydraulics Laboratory, Research Center of Ocean Environment and Technology, National Cheng Kung University, Tainan 709, TAIWAN. steffie@thl.ncku.edu.tw*

[(2)] *Research Assitant Tainan Hydraulics Laboratory, Research Center of Ocean Environment and Technology, National Cheng Kung University, Tainan, TAIWAN. thlkuo@mail.ncku.edu.tw*

[(3)] *Associate Director, Tainan Hydraulics Laboratory, Research Center of Ocean Environment and Technology, National Cheng Kung University, Tainan 709, TAIWAN ryyang@mail.ncku.edu.tw (corresponding author)*

[(4)] *Vice President/Director, Tainan Hydraulics Laboratory, Research Center of Ocean Environment and Technology, National Cheng Kung University, Tainan, TAIWAN. hhhwung@mail.ncku.edu.tw*

[(5)] *Research Assistant, Civil Engineering Department, National Taiwan University, Taipei 106, TAIWAN. r91521320@ntu.edu.tw*

[(6)] *Associate Professor, Civil Engineering Department, National Taiwan University, Taipei 106, TAIWAN. hcapart@yahoo.com*

Abstract

The purpose of this study is to solve this fluid-structure coupling problem with the aim of optimizing cage design and construction by laboratory observation. Utilize a 1/30-scale model of net cage to simulate and measure the motion and deformation of one in the current. Apply to the measurement method of trinocular stereo imaging that used three synchronized video cameras to follow the three-dimensional displacements of the 37 Light Emitting Diodes (LEDs) attached to the net to measure the deformation and motion of the fish net. In this study, using the method to trace the change of net and then get the place of LEDs after the net movement. The result show the motion of the collar and bottom hoop under different current velocities affected gradually the geometry of net, further calculating the tension force and the loss space of net cage.

1. Introduction

A major constraint to marine aquaculture development in Taiwan is the suitable water space. The near-shore marine aquaculture is still the drawback of the dispersion of wastes, not to expand the waters of marine aquaculture. To solve the problem, marine aquaculture is moving to deep sea, and will face some problems of which are serious in the deep-sea aquaculture. Therefore, the feasibility of extending operations into the energetic open ocean has recently been addressed. However, such a transition is not trivial because the suitable species and technologies for this energetic environment are not yet developed to a viable economics scale.

Recently, the study on near-shore marine aquaculture has brought many achievements. Bessonneau and Marical (1998) developed a mathematical method, which is an iterative method, to simulate the dynamic response of some submerged flexible reticulated surfaces. Lee and Wang (2000,2005) studied the dynamic behavior of the tension-leg platform with the net cage system and derived a set of equations of motion of a simplified two-dimensional case. Subsequently a close form solution is obtained when the

wave-structure interaction between the top platform structure and the incident wave is considered. Fredriksson (2001) physically and numerically modelled the open ocean fish cage and the mooring system dynamics. Aquaculture installations are highly flexible hydroelastic structures. Hydrodynamic forces acting on such a structure affect the shape of the structure, and then affect the hydrodynamic forces. This complex interaction between load and shape is a typical feature of hydroelastic motions. In this study, combining the digital imaging sketch that is the non-intrusive imaging method and the experimental measurement to understand the motion of net cage. The experiments of a 1:30 scale model of a flexible circular net cage with the mooring system are conducted in the circulating flume. Collar motion, Hydrodynamic force and net deformation are investigated under different uniform current.

2. Physical Model Experiment

A 1/30-scale model of net cage was composed of up and bottom hoop (or ring), nets and four buoys and four anchor blocks were moored to the tank bottom. The top of the net was mounted on the hoop so that it took the form of a cylinder with open top. The float collar system, the cage net system, the anchor system and the mooring system, all as depicted in Fig. 1. The maximum velocity of the generating uniform flow is 28cm/s.

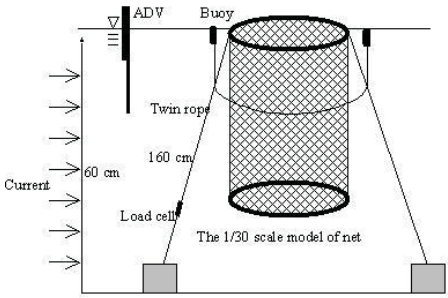

Fig. 1 The configuration of experimental setup at the circular flume tank (2.3 m×1 m×1.5 m) in the THL

In this study, it used to obtain all the net deformation (and motion), collar motion and mooring tension response to the current action (sampling at a rate of 50Hz). The measurements of the net deformation were made using a non-intrude stereo method adapted from Spinewine et al. (2003) and Douxchamps et al. (2005). Furthermore, an estimate of the net geometry was established by measuring several markers on the net. To avoid the effect of deformation and adding weight of the net cage, 37 Light Emitting Diodes (LED) were used to be the position markers. The placing and numbering of the LED markers are shown in Fig.2.

Fig. 2: The placing and numbering of LED markers on the net cage

3. Result And Discussion

In this experimental study, the imaging stereo method was utilized to measure the volume deformation of

the net cage under different current velocities. From our investigation in the experiment, the geometries of net cage under different current velocities were both the same for adding or no LED markers on the net. That proves the lightweight of LED markers does not affect the motion of net cage under current velocity. Therefore, a non-invasively experimental investigation of motion and geometry of the net cage in uniform flow is validated to be feasible. Fig.3 shows the results of two cases for v=6cm/s and v=22cm/s . Furthermore, three-dimensional deformation of the net cage for different current velocities can also be obtained from this stereo method.

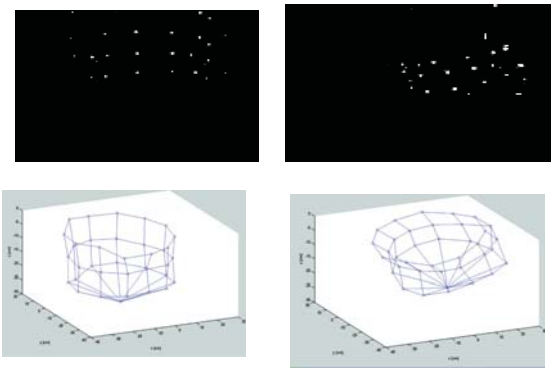

(a) v=6 cm/s (b) v=22cm/s

Fig 3. The deformation of net cage exposed to different current velocity from analysis of the stereo imaging method

While velocity of current being under 6cm/s, the collar seems maintained on the free surface, and the inclined angle(the collar on the free surface is 0°) kept not to change. However, the volume of net cage quickly decreased and responded to the increasing tension force of mooring system when the inclined angle increased with the adding current velocity. Once decreasing the volume of net cage, collar is below to the free surface. Meanwhile the living space of fish will be constricted. The result was shown in Fig.4.

The volume deformation of the net cage as it is exposed to current is qualitatively described. From these images it is clearly that the deformation increases with increasing current velocity. Both the volume and exposed area reduction show the same qualitative features. While current velocity is small, the tension force and deformation rate are small, either. That means the tension force is related to the volume changed. The effect of which the current operated on the net cage will show in the tension forces and the change of the shape of the net cage. Comparison between the tension forces and the value of the Ae*v2 is shown in the Fig.5.

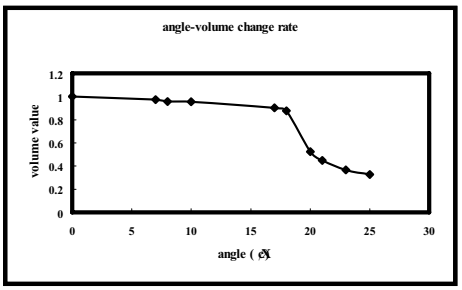

Fig. 4: The relation ship of the change of angle with collar and the projected volume of net

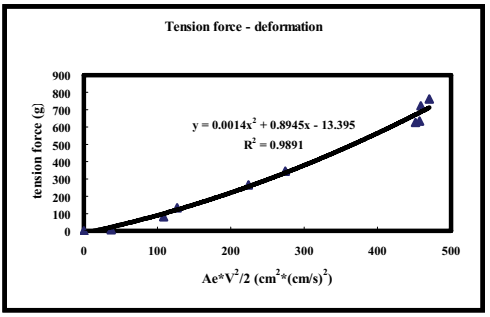

Fig. 5: The relation of the tension force and Ae*v2 as the current flows through the net cage

4. Conclusions

A non-intrusive stereo imaging measurement of the three-dimensional net geometry is established by tracing the positions of the LED markers on the net in laboratory experiment. Adding the LED but no increase the weight of the net on the net not only deduce the motion of net cage system, but also realize the physical phenomenon of the net cage. The 3D imaging method supply more specify information to consider the more complication flow, then obviously catch the motion of the net cage to get the closed the experimental results.

More convenience and detail about deformation investigation of a flexible net structure can be obtained from this study. From the experimental results, the tension force and deformation are mutually highly dependent on each other. The hydrodynamic force also appeared the impact on the stable and resistance of the net cage and collar. Understanding the dominating processes that govern fish cage and mooring system dynamics will become increasingly more important as the aquaculture industry expands into more exposed locations. Therefore, the measurement for three-dimensional geometry (or motion) of the net cage exposed to hydrodynamic force in field experiment will be developed in the near future. With this further understanding in-situ, and the use of validated analyzing techniques, future systems of the net cage can potentially be designed to better withstand the rigors of the open ocean. If the risk can be reduced, the success for many of this new marine industry in worldwide is more likely.

Acknowledgments

The NCKU-NSYSU Research Centre of Ocean Environment and Technology provided funding for this research through the research program “Improvement Study on The Structure of Marine Net Cage” The authors would like to express profound thanks for the financial support of Ministry of Education, Taiwan, on this project

References

Bessonneau, J.S., Marichal, D. 1998. Study of the dynamics of submerged supple sets (applications to trawls) *Ocean Eng.*, 25 (27):563–583.

Douxchamps D; Devriendt D; Capart H; Craeye C; Macq B; Y.Zech., 2002, “Particle-Based Imaging Method for the Characterisation of Complex Fluid Flows” *Proc of the IEEE Oceans 2000 Conf.*.

Douxchamps, D., Devriendt, D., Capart, H., Craeye, C., Macq, B. and Zech, Y. 2005, “Stereoscopic and velocimetric reconstructions of the free surface topography of antidune flows”, *Experiments in Fluids*., 39:533–551.

Fredriksson,D.W. 2001, “Open ocean fish cage abd mooring system dynamics”,Ph.D.Dissertation.The University of New Hampshire, Durham, NH.

Lee, H.H. and Wang, S.W. 2000, “Analytical solution on the surge motion of tension leg twin-platform structural system,” *Ocean Eng. -An Int. J*., 27:393–415.

Lee, H.H. and Wang, S.W. 2005, “Analytical solution on the surge motion of tension leg twin-platform structural system,” *IEEE .J. of Oceanic Engin*., 30(1):59-78.

Spinewine, B., Capart, H., Larcher, M., and Zech, Y. 2003, “Three-dimensional Voronoï imaging methods for the measurement of near-wall particulate flows”, *Experiments in Fluids*., 34(2):227–241.

LANDSLIDE GENERATED TSUNAMIS AT THE COAST OF A CONICAL ISLAND: NEW THREE-DIMENSIONAL EXPERIMENTS

Marcello DI RISIO [(1)], Giorgio BELLOTTI [(2)], Matteo G. MOLFETTA [(3)], Francesco ARISTODEMO[(4)], Andrea PANIZZO[(5)], Paolo DE GIROLAMO[(6)], Luigi PRATOLA[(3)], Antonio F. PETRILLO[(7)]

[(1)] *Post-Doc Researcher, University of L'Aquila, DISAT-LIAM, P.le Pontieri 1 ,67040 Monteluco di Roio, L'Aquila, Italy, mdirisio@ing.univaq.it*

[(2)] *Researcher, University of Rome TRE–DSIC, Via V. Volterra 62, 00146 Rome, Italy, bellotti@uniroma3.it*

[(3)] *Engineer,Technical University of Bari,LIC, Via E. Orabona 4, 70125 Bari, Italy, m.molfetta@poliba.it – l.pratola@poliba.it*

[(4)] *Post-Doc Researcher, University of Calabria-DDS, Via P.Bucci-Cubo 42B, 87036 Arcavacata di Rende, Italy, aristodemo@dds.unical.it*

[(5)] *Post-Doc Researcher,University of Roma "La Sapienza"- DITS, Via Eudossiana, 18, 00184, Rome, Italy, andrea.panizzo@uniroma1.it*

[(6)] *Professor, University of L'Aquila, DISAT-LIAM, P.le Pontieri 1 ,67040 Monteluco di Roio, L'Aquila, Italy, padegi@ing.univaq.it*

[(7)] *Professor, Technical University of Bari LIC, Via E. Orabona 4, 70125 Bari, Italy,petrillo@poliba.it*

Abstract

This paper describes new three dimensional experiments carried out at the Research and Experimentation Laboratory for Coastal Defence (LIC) of the Technical University of Bari (Italy) in cooperation with the Environmental and maritime Hydraulics Laboratory "Umberto Messina" of the University of L'Aquila (Italy). The experiments aimed at reproducing water waves generated by subaerial landslides sliding down the flank of a conical island. The generated waves in such a situation propagate both offshore and along the curvilinear shoreline.

1. Introduction

The research efforts in landslide generated waves have increased in the last decades due to events occurred around the world: the 1958 Lituya Bay event and 2002 Stromboli island one (Tinti et al., 2005), just to mention two of them. Although several researches have previously addressed landslide generated waves, the only physical model experiments involving tsunamis attacking islands are those by Briggs et al. (1995). However this first research reproduced waves attacking the island from offshore, i.e. the waves were generated elsewhere, potentially by an earthquake. In the case of the Stromboli Island, for example, the waves are generated along the coast of the island itself by a large landslide (volume of about 18Mm^3) along the flank of the volcano named "Sciara del Fuoco", and the generation-propagation-inundation phases cannot be decoupled.

The experiments described herein are therefore aimed at reproducing water waves generated directly on the flank of the conical island and at measuring both shoreline displacements and radiating waves. The experimental results can be used as benchmark for theoretical and numerical models as the landslide and the island shapes can be easily reproduced. Furthermore the experimental findings can be considered of practical interest as they allow insight about the celerity and the height of the wave run-up occurring around the island, a crucial point for the preparation of evacuation maps and for the set up of early warning systems.

2. Description of the experimental set-up

The experiments are carried out in a wave tank 30 m long, 50 m wide and 3.0 m high. The maximum water depth is 0.8 m. The conical island was made up of PVC sheets sustained by steel bars (see Figure 1). The beach slope was kept constant (1:3, 1 vertical, 3 horizontal) very similar to that of the "Sciara del Fuoco" flank of the Stromboli island. The conical island radius at the ground level is of 4.5 m. It has to be stressed that the island model can roughly represent the Stromboli Island when a scale reduction factor of about 1:1000 is applied. A series of 22 resistance wave gauges are used to measure the instantaneous surface elevation in the tank, i.e. employed in order to collect data of waves radiating offshore. Also 16 run-up gauges embedded into the PVC of the island flanks measure the displacements of the instantaneous shoreline. The landslide is represented by a rigid fibreglass elliptical body (length 0.8 m, width 0.4 m, maximum height 0.05 m) with a density of 1.83 t/m^3 and a volume of 0.0084 m^3 resulting in a total mass of 15.4 kg. The slide is equipped with an accelerometer that is used to reconstruct its motion.

Experiments were carried out by keeping constant the landslide properties (i.e. density and shape), by changing the water depth (ranging from 0.60 m up to 0.80 m) and the falling height of the body (ranging from 0.30 m up to 0.6 m, measured as the distance along the island flank between the lower part of the landslide in its initial position and the undisturbed shoreline), i.e. only aerial landslide were reproduced. It is important to stress that water depth was also varied in order to change the radius of the undisturbed shoreline that ranged from 2.10 m up to 2.6 m.

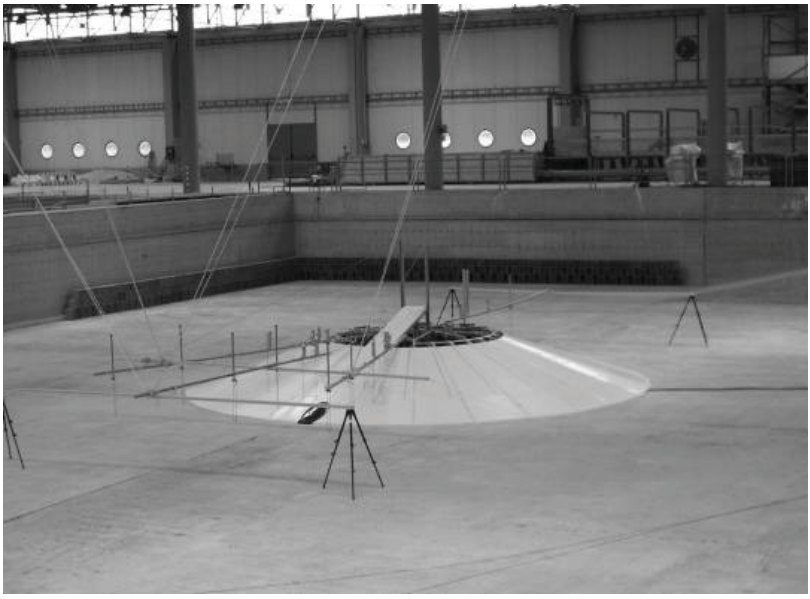

Figure 1. Picture of the conical island before water filling.

3. Results

Runup gauges and offshore wave gauges time series are analyzed in order to detect the maximum runup along the shoreline and the properties of the waves radiating towards offshore. It has to be stressed that the tank dimensions allow to measure runup before the wall reflected waves come back to the island and affect the measured time series.

Figure 2 shows an example of the measured shoreline vertical displacement. The overall results show that in the near field the wave runup grows, then at a distance larger than 2 times the landslide

width it starts to decrease. The first wave is responsible of the maximum runup only in the near field after which the trailing waves induce the maximum runup. The influence of the undisturbed shoreline radius has been observed to be important: higher the radius, higher the induced runup, whilst the falling height of the landslide (i.e. its energy) does not seem to influence the runup at the coast, at least within the experimental ranges tested here. It is important to stress that usually, in the case of landslide generated tsunami, the source type is inferred by observing if the wave front is a crest, i.e. a shoreline rising (subaerial landslide), or a depression, i.e. a shoreline receding (submerged landslide). However, also in the case of subaerial landslides (see runup time series of figure 2) the wave front is a crest so small that at some distance from the source it is hardly detected: the first evidence of the tsunami attack is then the shoreline receding given by the trough of the first wave.

On the basis of experimental data a set of empirical formulae are defined to forecast the runup induced by landslide generated waves for practical situations similar to that reproduced in the experiments described herein. Forecasting formulae suitable to reproduce the results have been selected as follows:

$$R_u^{*(1)} = 1.049\,(w^*)^{-0.470}\,(s^*)^{-2.02} \qquad R^2=0.985$$
$$R_u^{*(2)} = 0.386\,(w^*)^{-0.066}\exp[-0.116\,s^*] \qquad R^2=0.783$$
$$R_u^{*(3)} = 0.011(w^*)^{-0.945}\,\exp[0.007\,(s^*)^2] \qquad R^2=0.603$$
$$R_u^{*(4)} = 0.011(w^*)^{0.341}\,\exp[0.001\,(s^*)^2] \qquad R^2=0.525$$

where $R_u^{*(i)}$ (i=1,2,3,4) is the dimensionless wave runup induced by the i-th wave propagating alongshore ($=R_u^{(i)}/c$, c landslide thickness), w* is the dimensionless shoreline radius ($=w/r_0$, w landslide width, r_0 undisturbed shoreline radius) and s* is the dimensionless distance from generation area (=s/w, s distance from generation area along the shoreline). The coefficients presented here were obtained by inferring the 0.99 confidence level from the experimental data, so they can be used to estimate the maximum induced runup. The estimation given by the formulae is quite good for the first wave and less good for the following ones, as the first wave experimental data are less dispersed.

Acknowledgments

This work was partially funded by the Italian 368 Ministry of Research (MIUR), under the research project `Tsunami waves generated by landslides in water: mechanics of wave generation and propagation, development of forecasting tools and real-time warning systems based on tidal measurements'. Thanks are due to the LIAM "Umberto Messina" technicians Mr. Mario Nardi and Mr. Lucio Matergia and to the LIC technicians Mr. Giuseppe Intranuovo and Mr. Luciano Romanazzi.

References

Briggs, M. J., Synolakis, C. E., Harkins, G. S., Green, D.R. 1995. Laboratory experiments on Tsunami runup on a conical island. Pure and Appl. Geophys., 144 (3/4), 569-593.

Tinti S. Maramai A., Armigliato A., Graziani L., Manucci A., Pagnoni G., Zaniboni F., 2005. Observations of physical effects from tsunamis of December 30, 2002 at Stromboli volcano, southern Italy. Bulletin Of Volcanology 68 (5): 450-461.

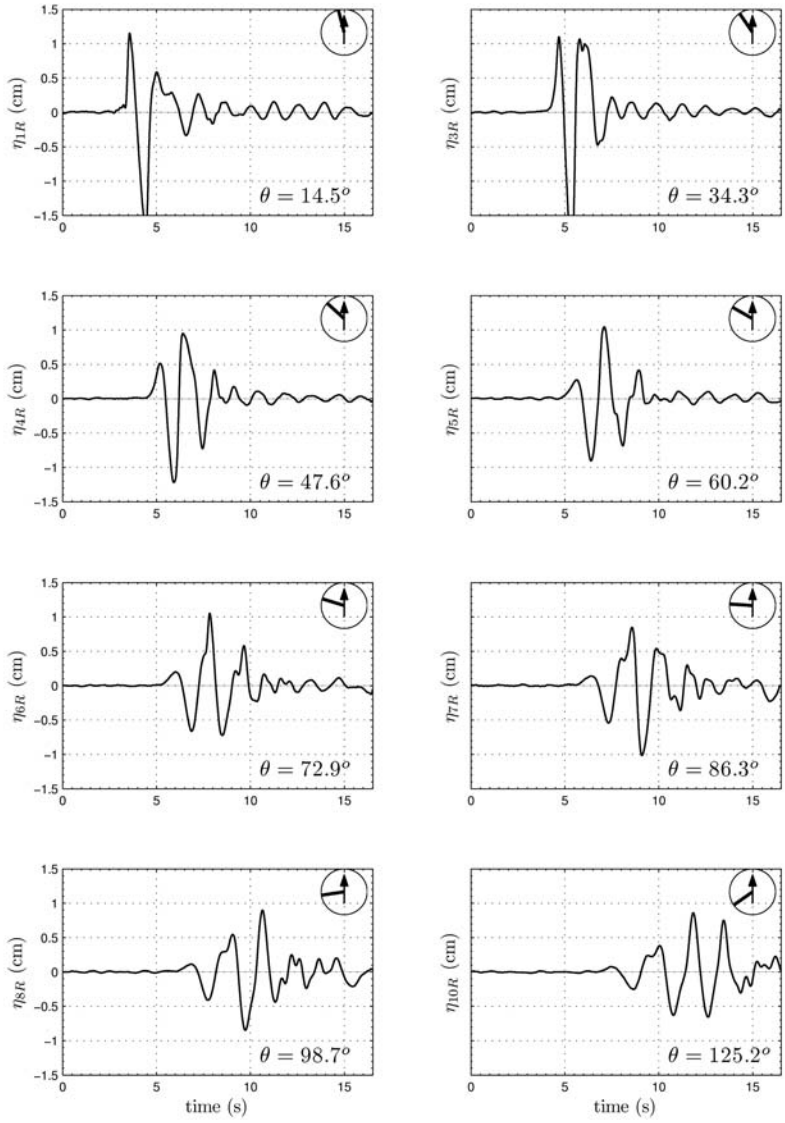

Figure 2. Runup time series measured during experiment with falling height equal to 0:50 m and undisturbed shoreline radius equal to 2:07 m. The small circle on each plot reproduces the coastline, the arrow indicates where the landslide enters into the water and the line specifies the position of the considered runup gauge

EXTREME SOLITARY WAVES AT RESTRICTED WATER DEPTH

Valeri PENCHEV

Ph.D., Black Sea Coastal Association, PO Box. 87, Varna 9003, Bulgaria, E-mail: v.penchev@bsca.bg

Abstract

Solitary wave approach is often used to study extreme waves and particularly tsunamis in shallow water, as their kinematics correspond to the case of a wave bringing tremendous amount of energy and propagating with a high speed. A system for generating 2D extreme solitary waves at restricted water depth, based on the principle of the 'collapsing water column', is presented in this paper. The system has been tested in two different experimental facilities. Tests have demonstrated abilities for simulating very high solitary waves in laboratory conditions that can be used to study extreme waves, as well as propagation of tsunamis in shallow water. A numerical model has been developed to provide a 'virtual flume' where the wave generation system was analysed and further developed. Applicability of the above approach to study extreme wave impact for prevention of flooding and protection of coasts has been demonstrated.

1. Physical Model Set-up

Solitary wave can be generated in a laboratory flume by a large single stroke of the paddle of the wave-maker. In general, this practice does not allow generation of waves close to the critical amplitude ($H_{max}=0.78h$), due to the instability and breaking of wave soon after generation (Watanabe, 2007). The so-called Scott Russel's wave generator is also used to generate solitary waves, most often to simulate tsunamis by releasing a heavy rigid box initially standing just above the water surface (Abadie, Grilli and Glockner, 2006). However, physical modelling and generation of extreme waves, especially at large scales and in restricted water depth, is still complicated, due to the physical limitations of the flumes and equipment, as well as due to a number of model and scale effects.

A 'collapsing water column' technique for generating extreme waves in a laboratory flume (a modification of the Russel's wave generator) has been developed and experimentally tested, first in the wave flume of BSHC Varna (Nicolchev and Penchev, 1997), and later in Franzius-Institute, University of Hannover (Penchev and Scheffermann 2005, and 2006). The experimental set-up is illustrated on Figure 1.

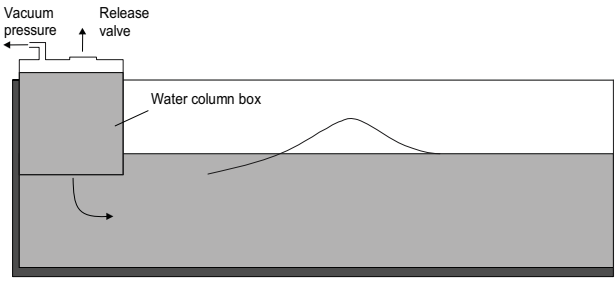

Figure 1. Sketch of the experimental set-up

Solitary wave is generated by sudden release of a large volume of water, preliminary lifted in a box using vacuum pressure. After being released the amount of water propagates along the flume and creates a large single wave.

The possibility to use this approach in order to reproduce waves bringing very high energy and propagating at very high speed (as tsunami waves do), have been demonstrated through a number of physical model tests. A series of preliminary tests have been carried out in order to optimise geometry of the box, as well as to prove other modelling techniques.

Water level variation (wave height) has been measured during the tests using 6 GHM-type wave-meters distributed along the flume. Wave crest celerity was evaluated by high-speed video recording. Orbital velocities of the wave (including bottom velocity) have been also measured using an Acoustic Doppler Velocity-meter (ADV). Special technique for fast opening and synchronization of the water-release valve has been developed.

2. Test Results

Here below some basic results from the tests carried out in Franzius-Institut, Leibniz University of Hannover in 2005 and 2006 are discussed. Physical model study has been implemented in one of the hydraulic flumes, where the above described equipment was placed. Experimental setup and the process of generation of the solitary wave are illustrated by the photographs shown on Figure 2. Some results of the measurements are presented in graphical form in Figure 3.

Tests have been repeated for several times in order to get more reliable data. Measured values have been further compared to the known theoretical values, as well as to some numerical simulation data as presented here below in section 3.

The well known relations for critical heights and celerity of a surface wave before breaking are: $H_{max}=0.78h$, and $C^2_{max}=1.56gh$. According to Fenton's theory (1972) the maximum height for a solitary wave is $H_{max}=0.85h$, and maximum propagation speed is $C^2_{max}=1.7gh$. Later studies by Longuet-Higgins (1985), Williams (1981 and 1985) suggest the limiting critical height to be $H_{max}=0.83h$ for solitary waves in shallow water with a corresponding solitary wave celerity of $C/\sqrt{gh}=1.29$ (i.e. $C^2=1.664gh$).

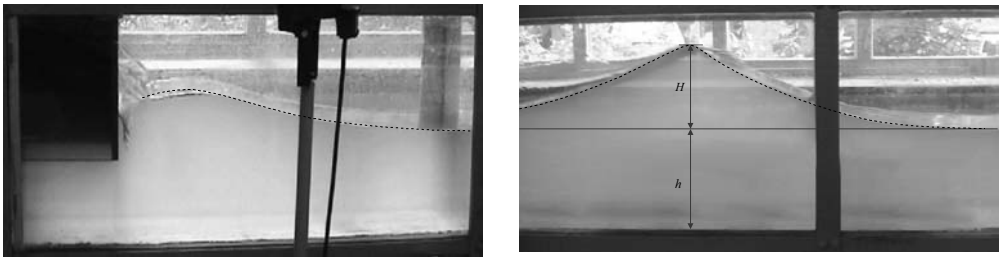

Figure 2. Photos of the model - generation and propagation of the solitary wave

During the tests a factor of relative wave height (versus water depth) from 0.78 up to 0.82 was measured at a flat horizontal bottom in the flume (Figure 3). The relative wave celerity $C/\sqrt{gh}$ observed during the tests was in the range of 1.25–1.275 (i.e. $C^2=1.56\text{-}1.63gh$).

A comparison between test measurement values and theoretical values for the maximum wave height shows a clear trend to reach limit values as indicated in the studies of Longuet-Higgins (1985) and Williams (1981 and 1985). Same conclusions were made also for the critical values of wave propagation celerity measured along the flume.

As it can be seen from Figure 3, no significant scatter of data has been detected when comparing data collected at different runs.

Results of the measurement have confirmed the appropriateness of the chosen method, and have demonstrated that very large single waves at restricted water depth can be generated using the above approach, that is otherwise impossible using traditional wave-generating methods.

3. Numerical model: Physical versus Numerical Data

A novel numerical concept has been employed to support investigations on the selected wave-generation approach. A RANSE (Reynolds-Averaged Navier-Stokes Equations) numerical model with application of VOF (Volume of Fluid) numerical technique has been developed in order to simulate the collapsing water column, and to track the discontinuous free water surface. Basic equations are conservation of mass, momentum and energy. Assuming an incompressible fluid, viscous stresses can be described with the friction approach of Newton, the continuity equation and the Navier Stokes Equations. Transposing the differential equation system to a numerical simulation system, a time averaging process results in the time-averaged continuity and the time-averaged Navier-Stokes equation.

A commercial CFD (Computational Fluid Dynamics) code was used as a basic tool. This code applies a three-dimensional RANSE-solver system widely used in fluid mechanics engineering. The relationship between time-averaged Navier-Stokes equations and Reynolds stresses is described in explicit terms, using a turbulence model. From preliminary numerical simulations the k-ε standard turbulence model was chosen. Finally, a basic 2D model representing a 'virtual test flume' was built as a numerical simulation tool.

The 'virtual test flume" has been successfully implemented to study generation of large solitary waves in shallow water, using the above described approach (Penchev & Scheffermann, 2005; Zimmermann, Penchev & Scheffermann, 2007).

A comparison of computed versus measured height of a large solitary wave at shallow water is illustrated in Figure 3.

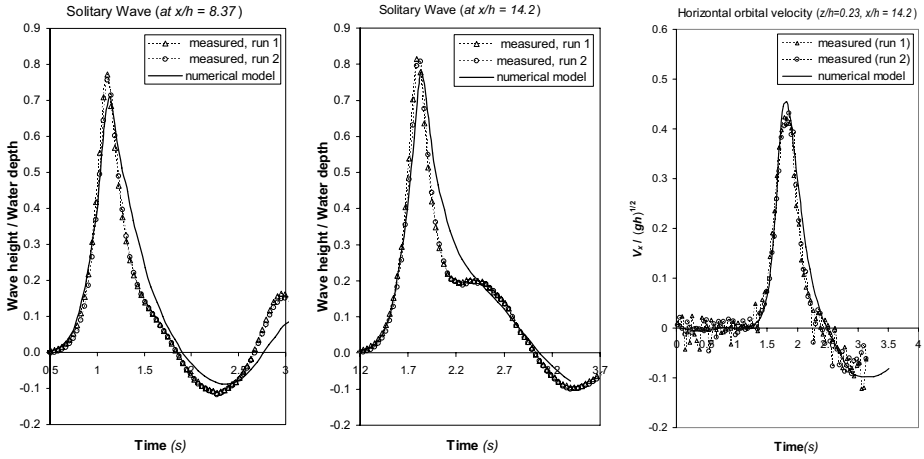

Figure 3. Computed vs measured parameters of a large solitary wave propagating at flat bottom in shallow water.

Maximum values of H_{max}/h = 0.78 have been calculated by the numerical model at a distance of approximately $15h$ from the wave generator. Velocity parameters calculated were: $u/\sqrt{gh} = 0.47$ - for the near surface orbital velocity, and $C/\sqrt{gh} = 1.28$ - for the wave celerity. These values are in good agreement to the measurements, as well as to the theoretical limits as presented above.

The comparisons between calculated and measured water surface elevations, as well as between calculated and measured orbital velocities, have shown very good correspondence. This gives reasons for further implementation of the numerical model as a tool to improve and optimise the 'collapsing water wave-generator'.

4. Conclusions

Physical model tests and computational results have shown that the above presented approach provides very good opportunities for generation of extreme solitary waves at restricted water depth in laboratory conditions. Combined use of an experimental physical model with an advanced numerical simulation tool has provided a powerful tool to study and develop the present wave-generating system. This system is highly recommended for use in hydraulic flumes to study extreme wave and tsunami impact on coasts and engineering structures.

5. Acknowledgments

The study presented in this paper was carried out with the support of the 6th and 7th Framework Programme of the Commission of the European Communities, SP-3 PEOPLE, Project EVERANS, Contract MERG-CT-2007-210085. The author expresses his sincere acknowledgments to the European Commission for providing their support to this study.

References

Abadie S., Grilli S. and Glockner S. 2006. 'A Coupled Numerical Model for Tsunamis Generated by Subaerial and Submarine Mass Failures', Proc. 30th ICCE Conference San Diego, vol. 2, pp. 1420 - 1430

Fenton, J. D. 1972. 'A Ninth-Order Solution for Solitary Waves', Journal Fluid Mech., Vol 53, pp 257-271.

Longuet-Higgins, M. S. 1985. 'A New Way to Calculate Steep Gravity Waves', The Ocean Surface, Y. Toba and H. Mitsuyasu, eds., Univ. of Tokyo Press, pp 1-15.

Nikolchev D., Penchev V. and Dragancheva D. 1991. 'Experimental Study on Submerged Permeable Structures' (in Bulgarian), Proc. of IXth Int'l Conference on Advanced Technologies for Transport Constructions, pp. 190 - 198

Penchev V. and Scheffermann J. 2005. 'Simulation of a Solitary Wave Passing a Submerged Reef', Proc. of 8th Numerical Tank Symposium (NuTTS). Varna October 2005, 26/1-26/6

Penchev V., Scheffermann J. and Zimmermann C. 2006. 'CFD Added Design of Reef Breakwaters', Proc. 30th ICCE Conference San Diego, vol. 5, pp. 4983 - 4995

Watanabe S. 2007. 'History of Soliton Experiments', Lecture Yokohama National University, http://maildbs.c.u-tokyo.ac.jp/~kuniba/psp07/Presentations/Watanabe.pdf

Williams, J. M. 1981. 'Limiting Gravity Waves in Water of Finite Depth', Phil. Trans. Roy. Soc. London, Series A, Vol 302, pp 139-188.

Zimmermann C., Penchev V., Scheffermann J. 2007. 'Modelling of Extreme Waves in Shallow Water', Proceedings Coastal Structures Conference Venice 2007, paper 1C-007

DEVELOPMENT OF A NEW TSUNAMI WAVE GENERATOR

David ROBINSON [(1)], Ingrid CHAVET [(2)], Pierre-Henri BAZIN [(3)], William ALLSOP [(4)] & Tiziana ROSSETTO [(5)]

[(1) and (3)] Engineers, [(4)] Technical Director, HR Wallingford, Howbery Park, Wallingford, OX10 8BA, UK. dir@hrwallingford.co.uk, phb@hrwallingford.co.uk and nwha@hrwallingford.co.uk, respectively

[(2)] PhD Student, [(5)] Lecturer, UCL, Civil & Env. Eng., Chadwick Building, Gower Street, London, WC1E 6BT UK, i.charvet@ucl.ac.uk and t.rossetto@ucl.ac.uk, respectively

1. Introduction

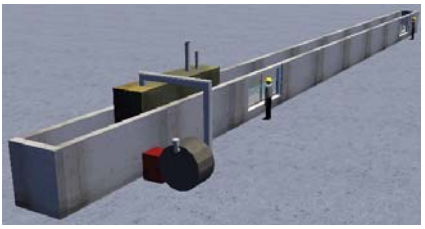

Tsunamis are water waves generated by earthquakes, underwater landslides, volcanic eruptions or major debris slides. Tsunami waves travel across oceans with quite small vertical displacements, but shoal up dramatically in coastal and nearshore depths. Generation and transformation of tsunami waves can be simulated by various numerical models (Richardson, 2006). The critical gaps in knowledge are in the propagation of tsunami waves in the nearshore region, across the shoreline, and inland. These flow processes cannot easily be simplified, and are indeed made more complex by interactions with beaches, sediment, coastal defences, and then around buildings. These processes can however be simulated in hydraulic models, but correct generation of the tsunami wave is essential, including in some instances the characteristic preceding draw-down wave. Conventional paddle generators simply do not have the stroke to reproduce the entire wavelength, which can be up to 10km at prototype scale.

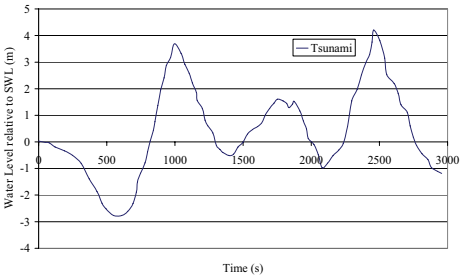

This weakness is being addressed within the EPICENTRE research initiative (EPSRC grant EP/F012179/1) through collaboration between University College London (UCL) and HR Wallingford (HRW). HRW are constructing the first Tsunami Generator that will be capable of generating a complete Tsunami wave within a hydrodynamic model by adapting the principles of HRW's pneumatic tide generators, to generate multiple waves (viz. the 3-4 peaks in the Boxing Day Tsunami), and ensure realistic wavelengths. The Tsunami Generator is being mounted within a conventional wave flume equipped to measure coastal processes, inundation and wave forces. It will generate tsunami waves which have been previously transformed from deeper water (approx -200m) to shallow water (approx -20 to -50m) using a suitable numerical model. Bathymetry in the wave flume will further shoal the tsunami waves over a representative coastal slope though the shoreline and inland, covering a suitable inland inundation area. Measurements of tsunami transformations through the nearshore region will test / validate existing numerical models. UCL and HRW researchers will then examine interactions of the tsunami with representative coastal seawalls, and test effects of tsunami waves (particularly retreating and repeated waves) with seawall and beach. These tests will then be expanded to measure wave / flow forces on representative buildings and to quantify scour potential around those buildings.

2. Preparatory Analysis

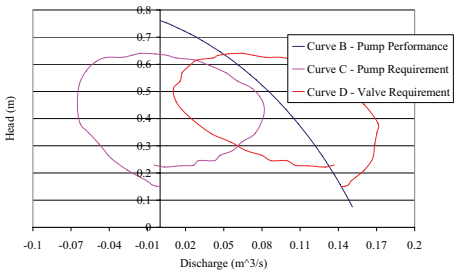

Several stages of analysis have been performed before completing construction of the Tsunami Generator, in order to ensure design success. A number of numerical models (including ANEMONE, Dodd 1998, and OXBOW, Weston 2005) are being used to model propagation of Tsunami waves from deeper water (approx -200m) to shallow water (approx -20 to -50m). These numerical models use Boussinesq and / or Non-Linear Shallow Water equations to include effects of shoaling, breaking, bottom friction, moving shoreline, partial reflection and transmission, and non linear wave-wave interaction.

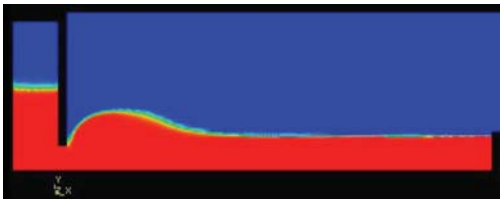

An advanced CFD modelling suite will then be used to test the performance and control strategy of the Tsunami Generator. In particular, modelling of the interactions between reduced-pressure air in the control tank, and flows between the control tank and the test flume will be shown.

3. Initial Facility Results

Construction and testing of the device being undertaken in spring 2008. The presentation to this conference will therefore present the design basis and testing plan for this unique modelling facility. The process of performance validation of the Tsunami Generator with records from the Indian Ocean Boxing day tsunami, or similar, will be shown and explained. As the UCL / HRW researchers expect to complete their tests by spring 2009, the facility will then become available for international teams to use during autumn 2009, so the presentation will describe the possibilities for such research access.

Acknowledgements

This work is being partly funded by the UK Engineering and Physical Sciences Research Council under grant EP/F012179/1, and by HR Wallingford. The authors would wish to thank Mervyn Littlewood and Dr Stephen Richardson for their support during the development of this project.

References

Dodd N. (1998) A numerical model of wave run-up, overtopping and regeneration Proc ASCE, Jo. Waterway, Port, Coast & Ocean Eng., Vol 124, No 2, pp 73-81, ASCE, New York.

Richardson, S.R. 2006 'Tsunamis - assessing the hazard for the UK and Irish coasts', *publn. Defra Flood Management Division, London*, (also reported as HRW report EX5364, HR Wallingford.) http://www.defra.gov.uk/environ/fcd/studies/tsunami/default.htm

Weston BP., A.G.L. Borthwick, P.H. Taylor, A.C. Hunt and P.K. Stansby 2005 'The performance of a hybrid Boussinesq model on wave runup and overtopping predictions for coastal structures' International Conference on Coastlines, Structures and Breakwaters 2005

A METHODOLOGY TO EVALUATE THE TSUNAMI FLOODING USING GEOMORPHOLOGIC EVIDENCES

Cosimo PIGNATELLI [(1)], Paolo SANSÒ [(2)] & Giuseppe MASTRONUZZI [(1)]

[(1)] Department of Geology and Geophysics, University of Bari, Via Orabona 4, Bari, 70125, Italy
c.pignatelli@geo.uniba.it; g.mastrozz@geo.uniba.it;

[(2)] Department of Materials Science, University of Salento, Ecotekne, 73100, Lecce, Italy, paolo.sanso@unile.it

1. Introduction

A tsunami wave can discharge its energy along the coastal areas causing wide floodings. The impact of a tsunami on rocky coasts can produce detachment of large boulders from adlitoral/intertidal zone and the successive deposit landward at different altitudes and distances from coastline (i.e.: Scheffers and Kelletat, 2005; Mastronuzzi et alii, 2007). So, the presence of boulders along the rocky coast can be used to obtain a measure of a past tsunami flooding. Aim of this study is obtain a new methodology that permit to calculate the inundation limit of palaeo-tsunami starting from the features of the boulders that testify their impact. Hydrodynamic equations have been implemented in order to calculate minimum wave height able to initiate the transport of the boulders and successive deposit inland (Nott, 2003; Noormets et alii, 2004); they take into account the size of the boulders, their density and their position prior of the transport. Generally, boulders deposits sparse along the coasts are characterised by mixed elements scattered by tsunami and/or by sea storms (i.e.: Mastronuzzi and Sansò, 2004;Hall et alii, 2006). Regarding the central basin of Mediterranean Sea, the size limit to ascribe them to tsunami or to exceptional sea storm has been calculated starting from the general features of these boulders (Mastronuzzi et alii, 2006). In fact, it is possible calculate minimum wave height necessary to move the boulders from the cliff edge using the hydrodynamic equations related to the joint bounded scenario of Nott (2003). Tsunami wave that cause inundation, discharges a water volume obtained as product of wave height, coastline perimeters and crossed sea surface; this is the water column that invades the hinterland starting from coastline. Hills and Mader (1997) introduced an experimental formula that permit to evaluate the inland limit of the wave penetration. This formula depends from Manning's number a parameter that take into account the original roughness of the surface of the flooded area.

2. Geodynamic and Geomorphologic settings

Apulia region is located in the southernmost part of Italy between Adriatic and Ionian Sea and constitute the emerged part of the foreland domain of both Apenninic and Dinaric orogens. It is placed at the centre of the Mediterranean Basin surrounded by active seismic zones, characterised by the presence of a high potential of generation of large tsunamis specially in the nearshore zone; furthermore, the Mediterranean Sea is very narrow and if generated, every tsunami can reach the Apulia in less than two hours. So these extreme events could have catastrophic effects on a local scale (Mastronuzzi et alii, 2006). Moreover, during last 600 years, about 15 tsunamis hit the coasts of Apulia (i.e.: Tinti et al., 2004) as testify by historical records and/or by geomorphologic evidences. This study has been carried out using data surveyed in the Torre Squillace locality (Fig. 1a) (Mastronuzzi and Sansò, 2000).

3. The coastal site of Torre Squillace (Lecce, Southern Italy)

Torre Squillace is placed on Ionian side of Apulia between Porto Cesareo and Gallipoli (Fig. 1a). A gently sloping rocky coast is shaped on stratified and fractured algal well cemented calcarenite. Here, isolated boulders, often imbricated, scattered between 1 m and 2 m above b.s.l. (Fig. 1b). The largest

boulder of Torre Squillace deposit is about 70 tons heavy and it is placed 40 m inland at about 1,8 m a.b.s.l. (Fig. 1c); this boulder is broken in four smaller pieces result of the transport and of the deposit of a catastrophic wave. ^{14}C age determination performed on *Lithophaga lithophaga* and historical reports seem indicate that the tsunami occurred on December 5th, 1456 likely generated by an offshore slides in the northern Ionian Sea, consequent to a strong earthquake occurred in southern Italy (Mastronuzzi and Sansò, 2000).

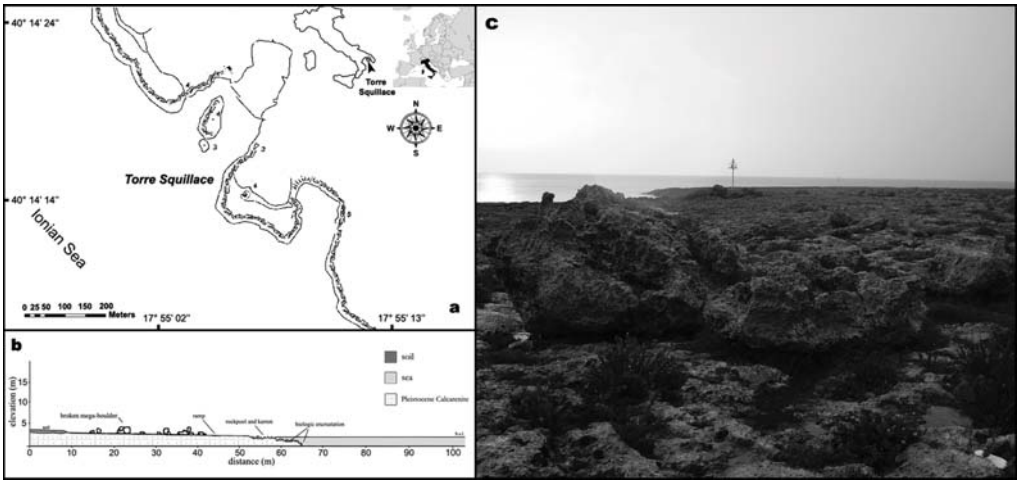

Figure 1. **a)** Topographic map of the Torre Squillace area; b) Morphological profile of the Torre Squillace terrace; **c)** the largest boulder, about 70 tonns heavy, emplaced at about 40 m and 1,8 m a.b.s.l. along the coastal sector of Torre Squillace area.

4. Evaluation of wave height and inland penetration limit

When a tsunami wave impacts a rocky coast, the detaching of the boulder from the platform edge can be summarized in two phases: a - the disjointment; b - the emplacement. These two phases are, often, continuous, but it is possible individuate at least three different scenarios in function of the initial conditions (Nott, 2003): 1 - disjointment when boulder is placed on cliff edge (joint bounded); 2 - disjointment when boulder is submerged (submerged scenario); 3 – sliding/disjointment when boulder is placed above sea level (subaerial scenario). A set of moment forces acts on a boulder: these are: ì - drag force, ìì - lift force, ìèì - inertia and restraint force (Fig. 2a). Drag and lift are mechanical forces generated by a boulder moving through a fluid (Hoerner, 1965). Restraint force consists of submerged weight of the boulder, incorporating the effect of the buoyancy. Inertia force acts in the case of the sliding of the boulder on rocky surface. Therefore, the inertia force is unimportant beyond approximately the first second after the impact (Noji et alii, 1985).

At the base of this study we use the following boulders features: a = the major axis, b = medium axis, c = minor axis), the boulders shape roughly to a parallelepiped and the mean volume weight. So, these described moment forces are reported in Fig. 2b. In Torre Squillace locality only the largest boulders can be considered result of a tsunami impact; moreover, it shows a surface with biokarstic pool that testify and intertidal provenience (Mastronuzzi and Sansò, 2000). So, we calculate wave height using this hydrodynamic equation, referred to joint bounded scenario: $H_T \geq [0.5 \cdot c \cdot (\rho_b - \rho_w / \rho_w)] / C_L$ [1]. The result is a wave height H_T = 4.94 m. This calculated wave have been introduced in the Hills and Mader (1997) formula: $Xmax = (H_{FL})1.33\ n^{-2}\ k$ [2], where: H_{FL} is wave height at the shoreline that we hypothesized as H_T; n is Manning number, k = 0.06 for many tsunami (see: Bryant, 2001). Manning's number is function of roughness degree; it was obtained empirically for different typology of surfaces; their value has been improved by mean of some post-event survey performed in numerous locality hit by December 26, 2004 tsunami (Tanaka et al., 2007). Generally, rocky coasts of algal calcarenite are

characterised by a mean value of Manning number n=0,050 (Table 1); using a buffer subdivision we have reduced Manning number variability and obtained a mean value of n=0,057 used for evaluate Torre Squillace inundation.

Table 1. Main parameters used to evaluate Manning number n in the studied area

Area description	Experimental n	n with buffers/subdivision	Tanaka (2007)
Rocky surface without vegetation	0,047-0,052	0,061	0,048
Overland surface with scarse vegetation	0,065-0,069	0,070	0,049

Furthermore, the value of n is not constant with time in the same locality due to vegetation growth and variations of flow conditions over time (Asal, 2003). As consequence, it is possible to obtain an evaluation of the present overland roughness, but it is difficult to know the roughness when the tsunami hit the coastal area. Since, there is a considerable local roughness variation, the studied area has been subdivided in buffers with constant length and inland depth; this is an approximation useful to simulate open channel flow. The Hills and Mader formula (1997) is limited to coastal area characterised by overland flat profile. The coast of Torre Squillace shows sloping overland profile; in the formula we introduce a factor cos α, where α represents the mean sloping, so [2] becomes: $Xmax = (H_{FL})1.33\ n^{-2}\ k \cos \alpha$ [3].

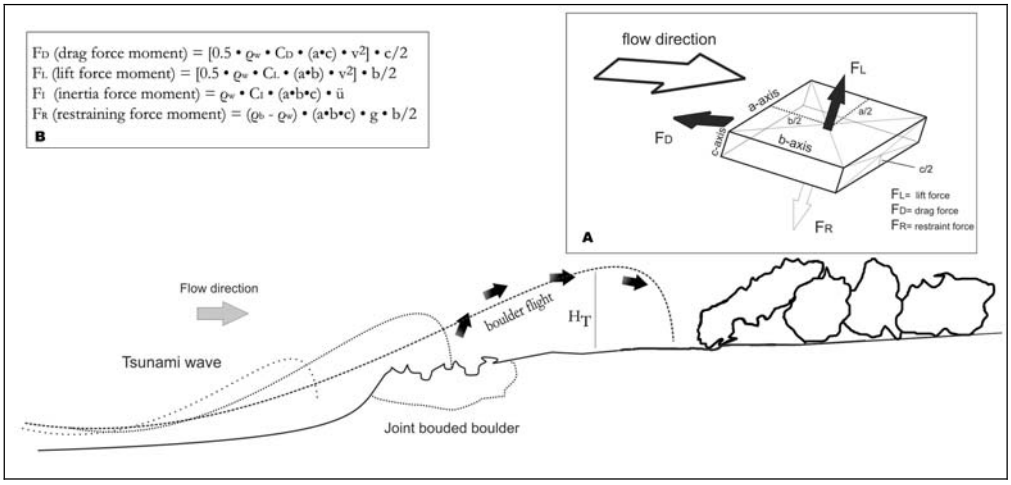

Figure 2. Hydrodynamic of tsunami wave approaching rocky coast: **A)** Moment forces schemes acting on a rocky boulders; B) Mathematical equations that represent moment forces, where ρ_w = density of the water 1.02 g/mL, ρ_b = density of the boulder (2,35 g/cm^3 for Torre Squillace), C_D = coefficient of drag = 2 (Helley, 1969), C_L = coefficient of lift = 0.178 (Einstein and El Samni, 1949), C_I = coefficient of inertia = 2 from experimental data by Noji et alii (1985), g = gravitational constant, ü = instantaneous flow acceleration, v = flow velocity, the velocity of a tsunami in deep water is $v = \sqrt{gh}$.

5. Conclusion

In the evaluation of tsunami flooding a new methodology have been implemented taking into accounts previous hydrodynamic studies and local morphological features. Adapting the first ones it has been possible obtain the height of past tsunami wave able to emplace inland large calcarenite blocks about 70 tons heavy. This boulder was recognised in the coastal sector of Torre Squillace; the weight and some morphological features testify that it is a result of a tsunami impact. The internal limit of the past tsunami flooding has been obtained applying Hills and Mader revisited formula; this, taking into account the mean slope of the overland coast, is extremely influenced by coastal roughness expressed by Manning number. The maximum flooding estimated applying the obtained equation is of about 100 m; this value

seem confirmate by the presence of a discontinuous sandy berm on which further analyses are in progress to validate the obtained value.

Aknowledgement

Study supported by MIUR-COFIN 2004/2006 Project (Nat. Coord.: S. Tinti; Res. Units: G. Mastronuzzi and P. Sansò) and by University of Bari Project 2007 (Resp.: G. Mastronuzzi).
This is an Italian contribution to the IGCP Project 495 (Leaders: A. Long, Univ. Durham, UK and Dr. S. Islam, Univ. Chittangong, Bangladesh)

References

Asal F. F. F. 2003. 'Airborne remote sensing for landscape modelling', *PhD thesis, The University of Nottingham, UK*, pp. 317.

Einstein H.A. El Samni E.A. 1949. 'Hydrodynamic forces on a rough wall', *Reviews of Modern Physics*, 21-3, 395, 520-524.

Helley E.J. 1969. 'Field measurement of the initiation of large bed particle motion in blue creek near Klamath, California', *U.S. Geological Survey Professional Paper 562-G*, 19 pp.

Hills J.G., Mader C.L. 1997. 'Tsunami producted by the impacts of the small asteroids', *Annals of the New York Accademy of Sciences*, 822, 381-394.

Hoerner S.F. 1965. 'Fluid-Dynamic Drag', *Publ. by the author, Hoerner L.A., Midland Park, NJ*, 200 pp.

Mastronuzzi G., Sansò P. 2000. 'Boulders transport by catastrophic waves along the Ionian coast of Apulia (Southern Italy)', *Marine Geology*, 170, 93-103.

Mastronuzzi G., Sanso' P. 2004. 'Large Boulder Accumulations by Extreme Waves along the Adriatic Coast of southern Apulia (Italy)'. *Quaternary International*, 120, 173-184.

Mastronuzzi G., Pignatelli C., Sansò P., 2006. 'Boulder Fields: A Valuable Morphological Indicator of Paleotsunami in the Mediterranean Sea', *Zeitschrift für Geomorphologie, Suppl.-Bd.*, 146, 173-194.

Mastronuzzi G., Pignatelli C., Sansò P., Selleri G. 2007. 'Boulder accumulations produced by the 20th February 1743 tsunami along the coast of southeastern Salento (Apulia region, Italy)', *Marine Geology*, 242, 1, 191-205.

Noji M., Imamura N. , Shuto N. 1985. 'Numerical simulation of movement of large rocks transported by tsunamis', *Proceedings of the IUGG/IOC Int.Tsunami Symposium, Wakayama, Japan*, pp. 189–197.

Noormets R, Crook K.A.W., Felton E.A. 2004. 'Sedimentology of rocky shorelines: 3. Hydrodynamics of megaclast emplacement and transport on a shore platform, Oahu, Hawaii', *Sedimentary Geology*, 172, 41-65.

Nott J. 2003. 'Waves, coastal boulders and the importance of the pre-transport setting', *Earth and Planetary Science Letters*, 210, 269-276.

Scheffers A., Kelletat D. 2005. 'Tsunami Relics On The Coastal Landscape West Of Lisbon, Portugal', *Science of Tsunami Hazards*, 23, 1, 3-16.

Tanaka N. Y., Sasaki M.I.M., Mowjood K.B. Jindasa S.N., Samang Homuchuen 2007. 'Coastal vegetation structures and their functions in tsunami protection: experience of the recent Indian Ocean tsunami', *Landscape and Ecological Engineering*, 3, 1, 33-45.

Tinti S., Maramai A., Graziani L. 2004. 'The new catalogue of Italian tsunamis', *Natural Hazards*, 33, 439-465.

NON-LINEARITY PHENOMENA IN THE EVOLUTION OF THE SEA STATES PASSING FROM DEEP TO SHALLOW WATERS

M.G. MOLFETTA[1], A.F. PETRILLO[1], L. PRATOLA[1], A. RINALDI[1]

[(1)] *Department of Water Engineering and Chemistry – Research and Experimentation Laboratory for Coastal Defense (LIC) - Polytechnic University of Bari - Italy*

e-mail: m.molfetta@poliba.it, petrillo@poliba.it, l.pratola@poliba.it, a.rinaldi@poliba.it.

Keywords: wave motion transformations, non-linearity phenomena, JONSWAP type spectrum.

Abstract

In this paper we present the results of an experimentation related to the processes through which a sea state, represented by a JONSWAP type energy spectrum, undergoes passing from the deep to intermediate and shallow waters, with particular attention paid to non-linearity phenomena.

The utilized data, in this experimental study, are the wave heigth measurements. They carried out on a 3D Physical Model of a stretch of coast (figure 1) realized in the Research and Experimentation Laboratory for Coastal Defense of the Bari Polytechnical University. The model reproduces a stretch of italian coastline characterized by the presence of rubble-mound emerged groins and a connected rubble-mound submerged breakwater between the groin heads.

Figure 1. View of the model.

The tank, 90m. long, 50m. wide and 1.2m. deep is equipped with a wave maker which is able to generate a sea state with different characteristics; the maximum wave front length is 28.8m. The model was built based on the Froude analogy with an undistorted scale of 1/30, while for the simulation of longshore drift the Dean analogy was adopted which conserves the parameter H/(wT), where H and T are the height and the period of the significant wave, and w is the sand speed fall. The sand used for the bed is siliceous, characterized by a homogeneous granulometric size distribution, with D_{50}=0.129 mm and speed fall w=1.91 cm/s measured in the laboratory using a pipe with continuous methodology (G. Ranieri, 2002). The groins and submerged breakwater were constructed with boulders of D_{50}=30÷43 mm.

In the model, the irregular waves, with JONSWAP-type spectrums, were generated from two different directions: the first with the wave front parallel to the coast line and the latter inclined at 15°. On the basic configuration shown in figure 1, a series of tests were carried out designed to examine various types of protection structures.

Water surface elevations were measured using a series of resistive wave gauges fixed on tripods. In particular, three of them were placed in front of the wave maker at appropriate distances from each other

(figure 2). In order to estimate the offshore wave height, two pairs of probes were placed in front of the offshore breakwater with the aim of determining the incident and reflection wave. Five probes were placed onshore in order to determine the transmitted wave.

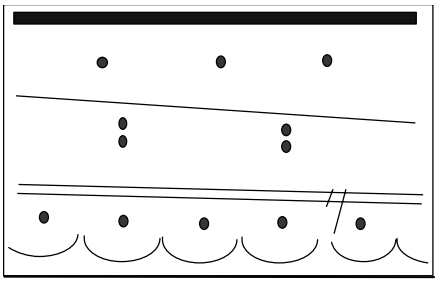

Figure 2. Wave gauge positions.

During the wave attacks, each probe acquired 4096 items of data with a sampling frequency of 20 Hz; therefore, the duration of each measurement was 205 seconds.

An analysis of the results confirmed that the Ursell number (U_r) is a significant parameter for the identification of non-linearity phenomena in the propagation of random waves, as is the case for sinusoidal waves.

In particular, the trends of parameters E_2/E_1 and E_3/E_1 vs. Ur were examined with reference to all measurements corresponding to non-breaking waves; E_1, E_2 and E_3 are the spectrum energy near the peak frequency fp, the first harmonic 2fp and the second harmonic 3fp, respectively. It was observed that for U_r less than 6, the ratio E_2/E_1 is almost constant, with a value of approximately 0.1; it subsequently increases with U_r. Similarly, the ratio E_3/E_1 is constant for U_r less than 6, with a value of approximately 0.01, it subsequently increases with U_r. This behaviour shows a rise in non-linearity phenomena, and therefore energy already transfers to higher frequencies (non-breaking conditions) from values of U_r equal to 6.

These results are in good agreement with other experimental studies, in particular with the tests carried out by A. F. Petrillo (1988), although these were carried out in different geometric and ondametric conditions and on a different type of experimental configuration (2D Physical Model).

A comparison between the data (figure 3) shows that in Petrillo's study, non-linearity phenomena near the second harmonic occur for $U_r > 10$ rather than for $U_r > 6$.

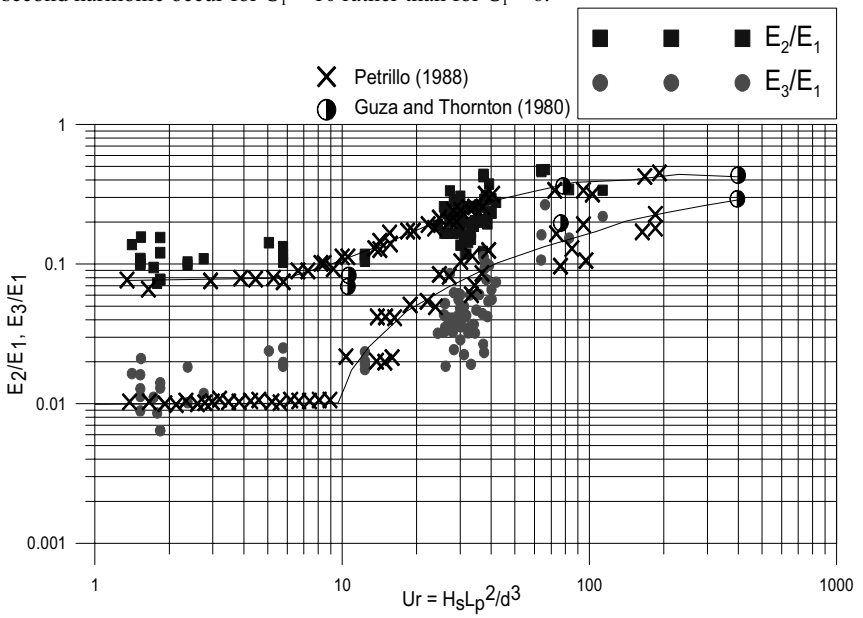

Figure 3. Trend of E_2/E_1 and E_3/E_1 vs. Ur; the experimental data are superimposed over the data of Petrillo A.F. (1988) and Guza and Thornton (1980).

Figure 4 shows the spectra of a number of examined probes for one of the sea states under study

(H_s = 15.7cm in model scale). The values between the square brackets are in prototype scale. These spectra show the changes that occur passing from deep to intermediate and shallow waters.

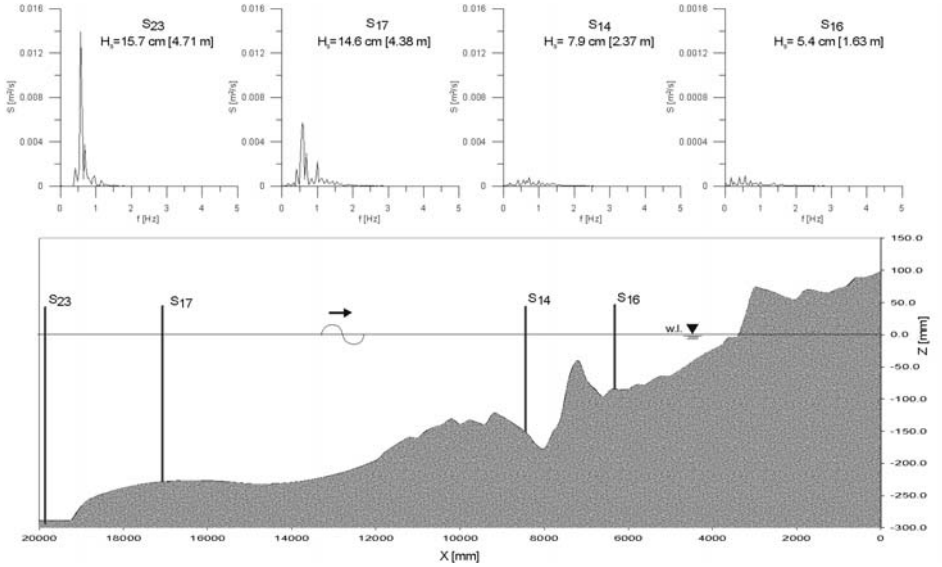

Figure 4. Spectrum evolution passing from the deep to intermediate and shallow waters.

In figure 5 the value H_S/d vs. d/L_P is plotted with reference to all the configurations studied, both breaking waves (square points) and non-breaking waves (round points). From the diagram it is possible to identify three areas of spectrum behaviour: the first, that of regular evolution, delimited above by the curve E_2/E_1=0.10; the second, transformation, and the third, breaking (for maximum wave steepness).

The diagram shows that the area of transformation is wider than the area obtained by Petrillo (1988); in fact, the spectra highlight that there is no noticeable non-linearity phenomena even when d/L_P > 0.15. On the other hand, plotting the values H/gT^2 vs. d/gT^2 in Le Mehaute's diagram with reference to all examined configurations (figure 6) for both breaking waves (square points) and non-breaking waves (round points), the points of the measurements corresponding to deep water settle in the field of validity of Stokes 2nd order theory.

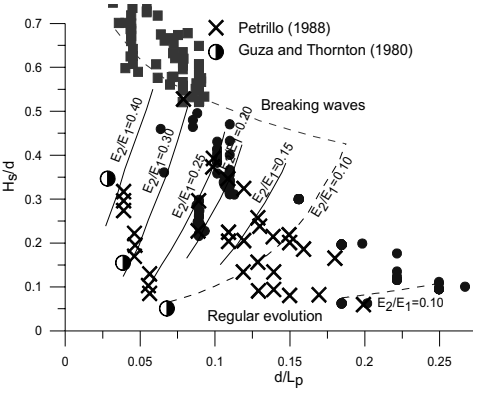

Figure 5. Trend of H/d vs. d/L; the experimental data are superimposed over data of Petrillo A.F. (1988) and Guza and Thornton (1980).

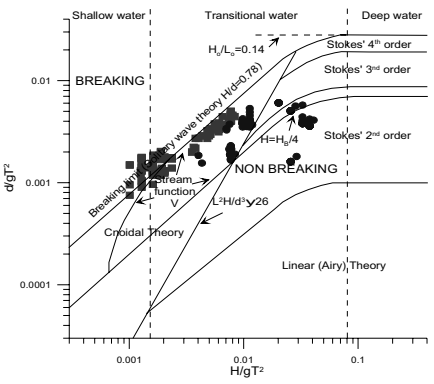

Figure 6. The experimental data are superimposed over the diagram of Le Mehaute.

In order to analyze energy transfer for both high and low frequencies in the transition from deep to intermediate and shallow waters, we considered the numbers mosx and modx; these derive from the integral density energy spectrum in the range [0, f_p] and [f_p, f_{max}], with fmax the maximum frequency spectrum.

The trends of the ratio m_{osx}/m_o ed m_{odx}/m_o vs. U_r are analysed with reference to all configurations under study, both breaking waves and non-breaking waves. The value m_o at the denominator is the local zero order moment of the spectrum.

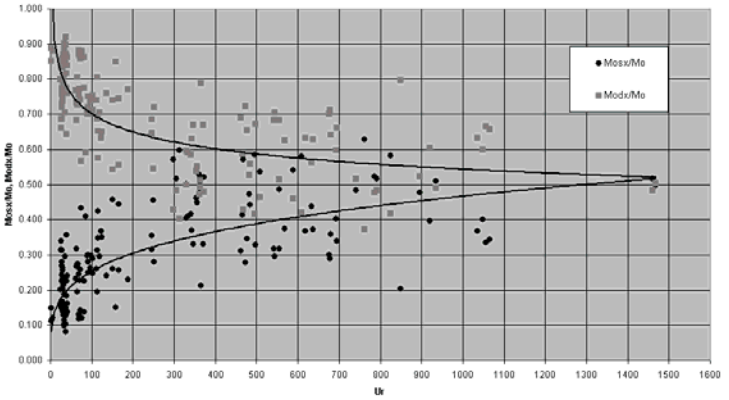

Figure 7. Diagram of m_{osx} e m_{odx} vs. Ur.

The figure shows that the values m_{odx}/m_o decrease with the increase of U_r, up to a value that is near 0.5, while the evolution of m_{osx}/m_o is the opposite, indicating that in deep water the shape of the spectrum is flattened, losing its original form.

Finally, analysis allows us to deduce that, starting from the off-shore area toward the shoreline, the sea state spectrum basically undergoes the following changes: initially, there is a decrease of energy content in correspondence to the peak frequency with energy transfers to higher frequencies; this behaviour reflects the rise of non-linearity phenomena in the propagation of the spectrum.

Moreover, there are large energy dissipations due to the breaking and transfer to low frequencies, which flatten the spectrum so that the spectrum shape is completely different with respect to the original. Indeed, the energy in correspondence to the peak frequency does not outweigh the other frequencies.

Near the shoreline, there are high energy levels at low frequencies: this justifies the slow fluctuations of the average sea level which occur in this area (surf-beat phenomenon).

References

Petrillo A.F. (1988). "Evoluzione delle onde di mare su bassi fondali sabbiosi con pendenza variabile", *IX Congresso Nazionale dell'Associazione Italiana di Meccanica Teorica ed Applicata*, atti.

Lamberti A., Petrillo A.F., Ranieri M. (1988). "Sulla generazione ed il rilievo di onde casuali in canaletta bidimensionale", *Idrotecnica*, nr. 1 gennaio-febbraio 1988.

Lamberti A., Petrillo A.F., Ranieri M. (1985). "A comparative analysis of some types of submerged barriers as beach defense structure", *XXI Congress IAHR Melbourne*, 19-23 august 1985.

Guza R.T., Thornton E. B. (1980). "Local and shoaled comparisons of sea state elevations, pressures and velocities", *Journal of Geophysical Research*, vol. 85 n. C3.

Scarsi G. (1984). "Le onde di mare. Introduzione", *Ricerche sulle onde di mare vol. 1* – Istituto di Idraulica di Genova.

Ranieri G. (2002). "A standard method for measuring the average fall velocity of natural sands", *Proc. Hydraulic Measurements and Experimentation Conference*, Estes Park, Colorado, USA.

OVERTOPPING WATER FALLING ON BREAKWATER LEESIDE

JONG-IN LEE [(1)], YONG-UK RYU [(2)] & YOUNG-TAEK KIM [(3)]

[(1)] *Research Fellow, River and Coast Research Division, Korea Institute of Construction Technology, Daehwa 2411, Goyang, Gyeonggi-Do 411-712 Korea. yuryu@kict.re.kr*

[(2)] *Postdoctoral Research Fellow, River and Coast Research Division, Korea Institute of Construction Technology, Daehwa 2411, Goyang, Gyeonggi-Do 411-712 Korea. jilee@kict.re.kr*

[(3)] *Senior Researcher, River and Coast Research Division, Korea Institute of Construction Technology, Daehwa 2411, Goyang, Gyeonggi-Do 411-712 Korea. ytkim@kict.re.kr*

Abstract

The present study investigates the behaviour of overtopping flows falling on the leeside of a rubble mound breakwater through laboratory measurements. The overtopping flows are known to mainly affect the leeside stability of the breakwater. This study focuses on not the conclusive stability but the variations of the overtopping flows depending on wave or geometry parameters. Using an image technique with shadowgraphy, the measurements of surface profiles, front velocity, and plunging distance in the leeside were carried out. Various wave and geometry parameters were tested to find how the properties of the overtopping flow change.

1. Introduction

The amount of allowable overtopping for design criteria depends on the function of a particular structure. A breakwater for protection of basins from waves may allow heavy overtopping unlike other maritime structures (e.g. low-crested breakwater). During the overtopping process, the overtopping wave crest may have extreme momentum and subsequently create a jet-like flow after the crest of a breakwater. The overtopping flow and induced falling jet flow may cause damage to exposed elements consequently influencing the leeside stability of a breakwater. Kudale and Kobayahi (1996) named the overtopping water falling on the leeside as the overtopping jet.

Most experimental studies about the leeside stability have focused on searching for the relation between resulting stability and either wave parameters or breakwater geometry. However, the behaviour of the overtopping jet has been rarely studied although the overtopping jet is considered a cause directly related to the damage. This study investigates the overtopping jet impinging on the leeside through measuring the front velocity, layer thickness, and plunging distance. The plunging distance is the distance from the rear end of the crest to the overtopping jet centre as described in figure 1. For the measurements, an image-based technique using shadowgraphy was employed to plot the interface profile and obtain the velocity.

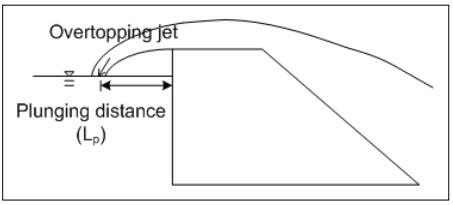

Figure 1. Overtopping jet and plunging distance.

2. Experimental Conditions

The overtopping flow was experimented for the rubble mound breakwater 1:40 scaled from a typical type. The experiments were performed in a 2D wave tank that is has a length of 50 m, a width of 1.2 m, and a height of 1.5 m equipped with a piston type wavemaker. The model of the rubble mound breakwater consists of a rectangular caisson and a 1:1.5 sloped armour layer of 32t TTP. The structure has a height of 0.6 m, a constant freeboard of 0.10 m. The wave tank was filled to a water depth of 0.50 m at the model location throughout the experiments. The deck width of the structure varied to examine the effect the structure geometry. In addition, regular wave parameters such as wave period and wave height varied in order to find the influence of the wave parameters to the overtopping jet. The wave parameters are presented in Table 1.

Table 1. Tested conditions of wave and geometry.

Wave height (cm)	Wave period (sec)	Water depth (cm)	Deck width (cm)
8, 10, 12, 14, 16	1.2, 1.5, 1.8, 2.1, 2.4	50	17, 34, 51

Since the overtopping flow is generated from large waves and tends to be aerated, difficulty consists in measuring water elevation and velocity. Water surface gages of intrusive type fail to measure interface between air and air-water mixture of a two phase flow. The interface also prevents velocimetries of various types from giving high accuracy with measuring successfully. In this study, images captured using shadowgraphy were used to plot the interface profile and to obtain the velocity using the correlation. The surface profile and interface can be obtained by intensity difference in images from air or water area. The shadowgraphy technique is described in Ryu et al. (2005). The shadowgraphy measurements were carried out by installing an acrylic sheet and light inside the tank as shown in figure 2. The images illuminated by the shadowgraphy setup were captured with a high speed camera with a high resolution.

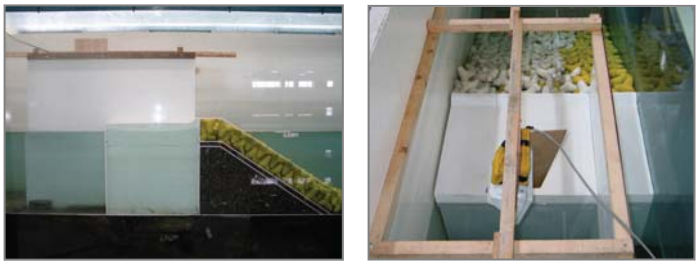

Figure 2. Experimental setup: model (left) and shadowgraphy setup(right).

3. Results and Discussion

The overtopping flows were generated from regular waves to clarify the effect of wave period and height on the behaviour of the overtopping jet. Based on the measurements, the variations of the front velocity, plunging distance, and layer thickness were analyzed depending on the parameters. In this paper, the plunging distance results of the overtopping jet are presented. The distance of the overtopping jet was determined from intercepted points of the free surface and plunging overtopping water by checking the captured images. The results were plotted in figures 3 and 4 with respect to both wave period and wave height, respectively. Although all the conditions summarized in Table 1 were tested, the cases giving a plunging jet less than 5 cm were not plotted in the figures. It is because the overtopping water with less than 5 cm plunging jet shows very small momentum. From the plotted results, the plunging distance is

found to increase with increase of the wave height and wave period. From figure 3, it is shown that the plunging distance increases linearly with wave period for the cases with wave period of 1.4 sec or larger. The distance against the wave height also shows increasing pattern as shown in figure 4. For smaller wave period cases, the increasing pattern is linear while the pattern becomes nonlinear as the wave period gets larger. The results show that the plunging jet of the overtopping water clearly depends on the wave period and wave height.

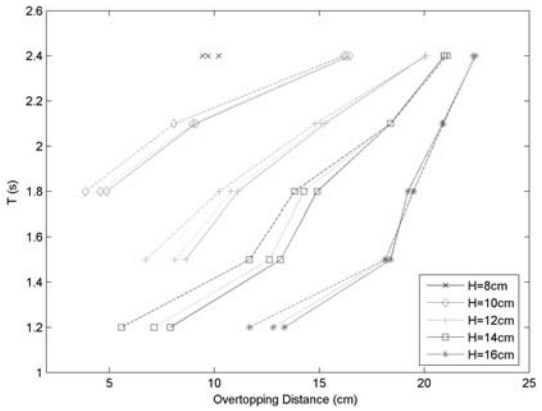

Figure 3. Plunging distance depending on wave period.

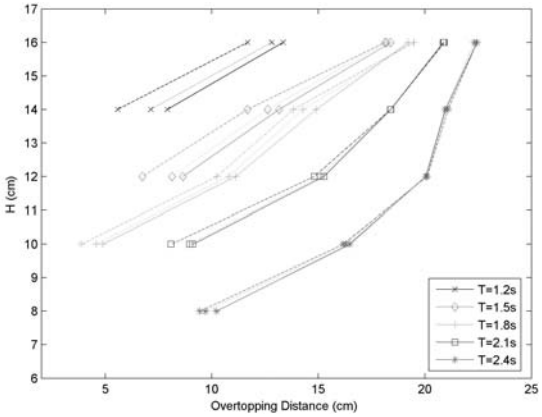

Figure 4. Plunging distance depending on wave height.

In addition, 3 different deck widths of the structure were tested to examine the geometry effect for the same wave conditions. In figures 3 and 4, the solid lines represent the deck width of 17 cm, dotted lines for 34 cm, dashed line for 51 cm, respectively. As the deck distance increases, the distance tends to decrease. Although the pattern is observed from most cases, the effect is relatively insignificant.

References

Kudale, M. D. and Kobayashi, N. (1996) "Hydraulic stability analysis of leeside slope of overtopped breakwaters." Proc. 25th Coast. Engrg. Conf., ASCE, 1721-1734.

Ryu, Y., Chang, K.-A., and Lim, H.-J. (2005) “Use of bubble image velocimetry for measurement of plunging wave impinging on structure and associated greenwater.” Measurement Science and Technology, 16, 1945-1953.

WAVE RUN-UP ESTIMATION FOR IRREGULAR DIKE PROFILES BASED ON FIELD MEASUREMENTS

Joachim GRÜNE [(1)]

[(1)] Dipl.-Ing., Coastal Research Centre (FZK) of Leibniz University Hannover and Technical University Braunschweig, Merkurstrasse 11, 30419 Hannover, Germany, E-Mail: gruene@fzk.uni-hannover.de

Abstract

The paper deals with the estimation of wave run-up on irregular dike profiles under real sea state conditions. A composite model was developed which calculates the spatial distribution of wave run-up, using a modified approach for an equivalent slope. This model was tested with results from field measurements.

1. Introduction

The safety analysis of dikes and revetments nowadays plays an important role in coastal zone management due to the discussion about increase of storm activity and increase of water level rise as consequences of global climate change. Far from all considerations with respect to probabilistic approaches the basic tool is a realistic calculation of wave run-up and overtopping. For the performance of a safety analysis, model and procedure has been developed for calculation of the decisive wave run-up and overtopping of coastal protection dikes.

This model considers the natural sea state characteristic as well as the complexity of irregular dike cross-sections in nature and are based on results from extensive wave measurements on foreshore of dykes at different places at the German North Sea coast and on results from wave run-up measurements in field at dikes with different cross-sections and sea state conditions as well as from large-scale laboratory tests and on results from long-time flotsam level field surveys.

2. Equivalent slope for dikes with irregular profile

For application on dikes with irregular profiles existing in nature an equivalent slope has to be defined which is often done by linear interpolation between two levels on the slope as defined schematically in Fig. 1. Considering the physical wave breaking process on slopes, two ranges may be distinguished between breaker point and maximum wave run-up, which is divided by point z on the slope hidden by the breaker tongue as shown in Fig. 2.

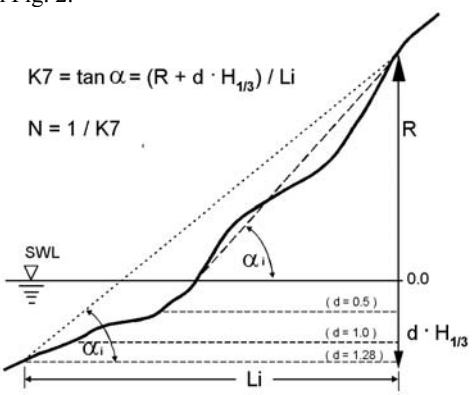

Fig. 1 Definition of equivalent slope

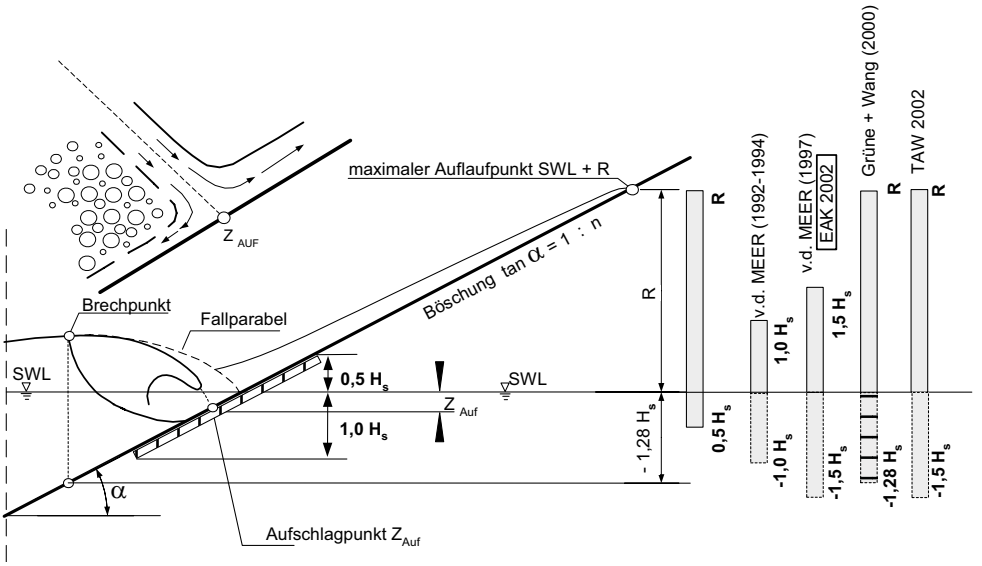

Fig. 2 Schematic sketch of geometrical interaction between wave breaking and wave run-up

Results from field measurements and large-scale laboratory tests indicate that the main level of z is at SWL – 0.5 H1/3 and the influence of slope on wave run-up is stronger for the range above z as below z. This leads to a linear interpolation between SWL – 0.5 H1/3 and R for a realistic equivalent slope. In Fig. 2 four other definitions are given which are recommended by different authors.

3. Estimation of wave run-up and comparison with field data

For performing safety analysis of coastal protection works a type of composite model was developed, which calculates the spatial distribution of wave run-up. This composite wave run-up model is based on Math-CAD and combines the extended analytical-empirical Hunt-formulae with the actual state of the art knowledge from results of small- and large scale laboratory tests and field measurements. The model is calibrated by comparison with results from synchronous field measurements of wave climate and run-up with instruments and flotsam levels.

For one field measuring location a calculation is shown in Fig. 3 exemplarily using different definitions for the equivalent slope. The run-up data, calculated with the composite model, are compared in the upper plot with those, measured with an electronic wave run-up gauge and in the lower plot with those, evaluated from flotsam level surveys. For the calculations of R_i the relation $R_{max} / R_{98} = 1.1$ has been used, as found from the field measurements and which depends on the dyke slope angle. SWL_{krit} indicates the maximum SWL before overtopping differ for both calculations consequently.

Procedures for verification and calibration of the model and applications are presented and discussed in the final paper.

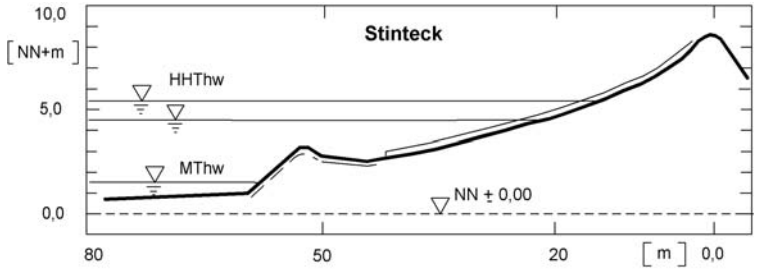

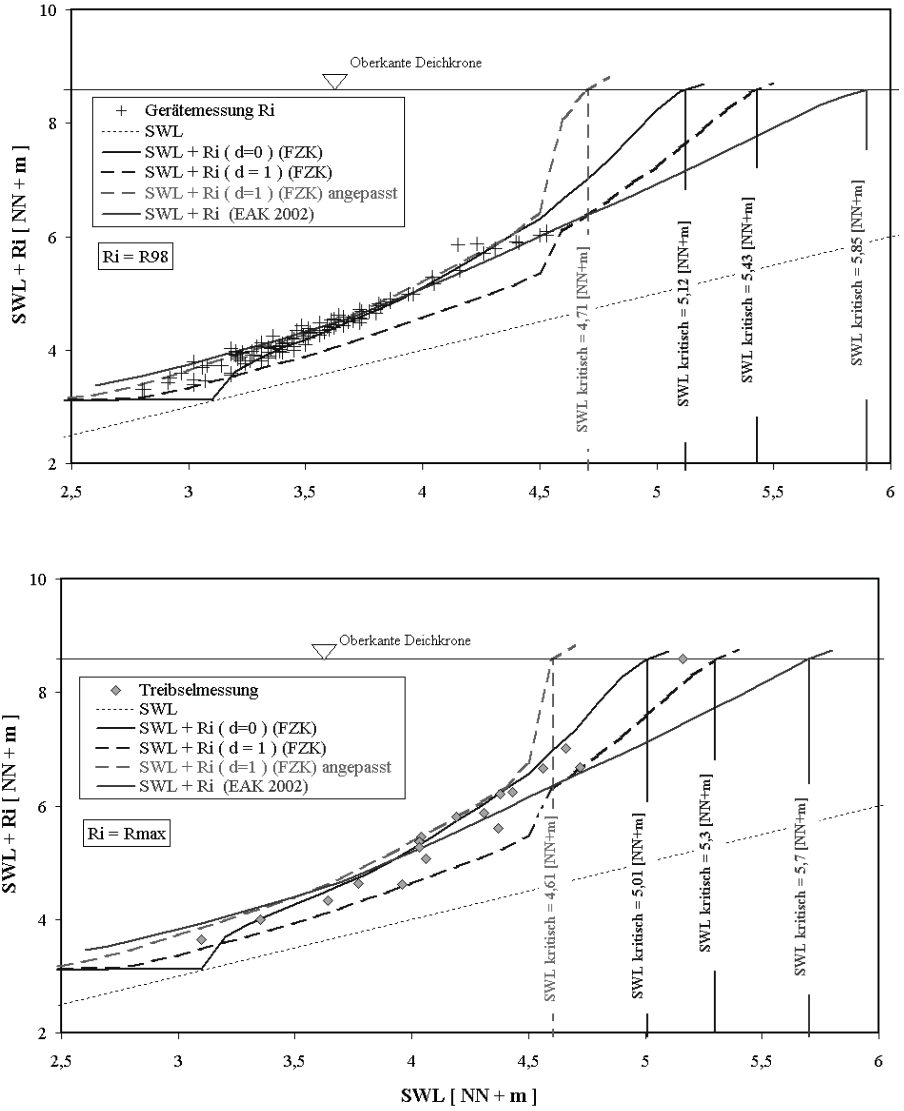

Fig. 3 Comparison of calculated wave run-up SWL + R_i with results from field measurements (gauge data in the upper plot, flotsam level data in the lower plot) measured at Stinteck location

COMPATIBILITY AND ACCURACY OF DIFFERENT APPROACHES FOR WIND WAVE MODELLING: WESTERN BLACK SEA SHELF CASE

Maria MAVROVA-GUIRGUINOVA [(1)], Nikolay VALCHEV [(2)]

[(3)]*Assoc.Prof. Dr., University of Architecture, Civil Engineering and Geodesy, Sofia, Bulgaria, margir@mbox.contact.bg*

[(2)] *Dr., Institute of Oceanology, Bulgarian Academy of Sciences, P.O. Box 152, Varna, 9000, Bulgaria, valchev@io-bas.bg*

Abstract

The paper addresses some scientific and implementation aspects of wind wave modelling and forecasting using conventional wave models based on wave theory and a relatively new tool that is artificial neural networks. Wind wave simulations are performed using the state-of-the-art third generation models WAM and SWAN forced with a coarse resolution global reanalysis wind fields. Application of different neural network architectures with supervised learning trained to establish relationships between forcing and wind wave generation are estimated.
Key words: wind forcing, wave modeling, artificial neural networks

1. Introduction

Sea state is an essential element of the coupled atmosphere - ocean system. Wind waves are one of the phenomena that determine the surface splitting these subsystems regulating the climate dynamics. Moreover, they affect many human activities such as navigation, design of hydro-technical constructions, production and transport of oil and gas, marine tourism, and are one of the main factors for environmental security in the coastal zone and shore areas.

Numerical modelling is one of the most useful tools for simulation and understanding of the wave evolution. In the study this tool is implemented using the atmospheric pressure reanalysis that is proven to give more realistic results (Davidan et al., 2006).

On the other hand, the application of neural networks method to a growing number of practical cases including environmental, financial, and engineering problems during the past ten to fifteen years is very successful. Tissot et al. (2000) carried out an application of neural networks to water level forecasting in the Gulf of Mexico. Results obtained from the neural networks by Mavrova-Guirguinova et al. (2007) can be used for the general prediction of the wind wave period and height as mean values in deep and shallow water for unlimited wind duration. The modeling philosophy applied in this paper is to train a neural network to establish relationships between forcing and wind wave generation by fitting the special features of particular wind field.

The aim of the present study is to discuss the point and accuracy of simulations using the two different methods. Obtained results are compared against in situ measurements of wind wave parameters collected in the Western Black Sea shelf. Attempt is made for a critical review of techniques limitations. The chosen period of simulation is December, 2006.

2. Wave modelling

2.1. Traditional wave modelling: concept, forcing and models

Traditional wave modelling is based on the concept of spectral models that describe the evolution of the two-dimensional wave spectrum without any assumptions on the shape of the wave spectrum. They

computes it through integration of the transport equation taking into account of all established source - sink components: wave generation by wind forcing and coupling between the air fluctuations and waves, energy transfer between wave components, and wave dissipation due to variety of processes.

Here, the wind forcing comes from the ECMWF global reanalysis with 2.5° spatial resolution. WAM (cycle 4) a third generation wave model is adopted for deep water (Komen et al., 1994). The source function is a superposition of the wind input, white capping dissipation and nonlinear transfer. SWAN, a numerical wave model designed for coastal areas, is employed for wave simulations in the Western Black Sea shelf. The source/sink terms include additionally triad wave-wave interactions, wave diffraction and wave energy dissipation due to bottom friction and wave braking (Booij et al., 1999). The wave propagation in the models is implemented on a spherical grid. Spatial resolution of WAM and SWAN simulations are 0.5° and 2 min, respectively.

2.2. Neural networks: principles and methods

Neural networks method is a computational (artificial) intelligence mathematic technique of machine learning. The concept of neural networks becomes known in the sixties as a rough emulation of the functioning of the brain. The main advantages and key characteristics of neural networks for wind waves forecasting are their non-linear modeling capability, their generic modeling capacity, their robustness to noisy data, and their ability to deal with high dimensional data (Rumelhart et al., 1995). At the heart of a neural network is the assignment of proper weights and biases to the elemental neurons of the network. Rumelheart et al. (1986) developed a type of learning algorithm to assign such a set of optimum weights and biases called Backpropagation.

The application of neural networks to wind waves forecasting consists in designing and training a network that, given a time series of wind velocity and wind direction, correctly predicts wind wave parameters. For the Galata gas exploration platform the time series data for wind velocity, wind direction and wave height for December of 2006 were analyzed. The whole data is divided into two dimensional input-output training data set (4x372), validation data set (4x185) and test data (4x186) – see neural network structure on Figure 2. The first part of the data (training data) was used for building models, the remaining data to the second part (validation and test sets) to validate the model and to check its prediction capability in unseen data. All computations are performed within the MATLAB 7.1 and the Neural Network Toolbox.

3. Results and Discussions

Davidan et al. (2006) concluded that the quality of the Black Sea products derived from the reanalysis of atmospheric pressure field satisfy the scientific requirements for reliable wave simulation.

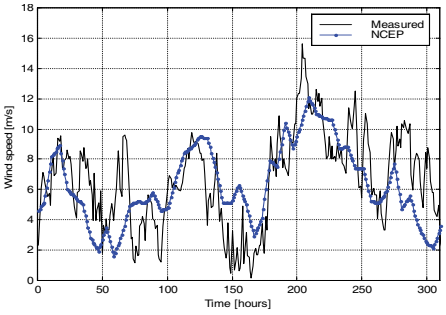

Figure 1. Global model output for the Galata shelf grid point for December, 2006 compared with available wind speed measurements.

As the quality of the forcing is key factor, Fig. 1 shows direct comparison between the wind speed computed by the downscaled global model and measured one at the Galata platform. The model output matches well the general character of the measured series. These results are logical as having a lower resolution, reanalysis fields cannot reproduce the smaller scale fluctuations.

On its turn, the neural network model is trained over one of the data set and then applied to the two other data sets to assess the model performance. The fact that a simple neural network (Fig. 2) is able to make relatively accurate wind wave predictions should not be surprising with regard to non-linear modeling capability of the neural models. The network here was not optimized and the results obtained can be estimated as preliminary after a rough modeling state.

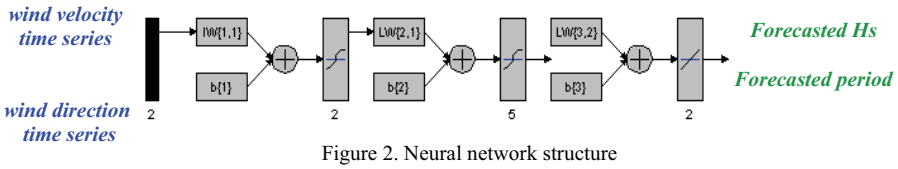

Figure 2. Neural network structure

The first output (significant wave height) seems to track the targets reasonably well, and the R–values of regression are almost 0.9. The maximum of the error in simulating of the significant wave height Hs is 0.70m (Fig. 3). Fig. 3 shows simulated and measured Hs by neural network with comparison with SWAN model output for the Galata platform grid point.

During the period SWAN with WAM boundary conditions slightly overestimates the waves with height ≤ 0.5m, while the neural network model achieves quite reasonable results. The three major windsea peaks are quite well reconstructed by both techniques; in particular the storms occurred around 12 December and during 20-22 December. As discussed earlier, the SWAN error is related mainly to the resolution of driving fields that is well discernable in Fig. 1 and 3 with respect to the largest windsea peak in the series. The neural network forecasts this peak slightly better.

a)

b)

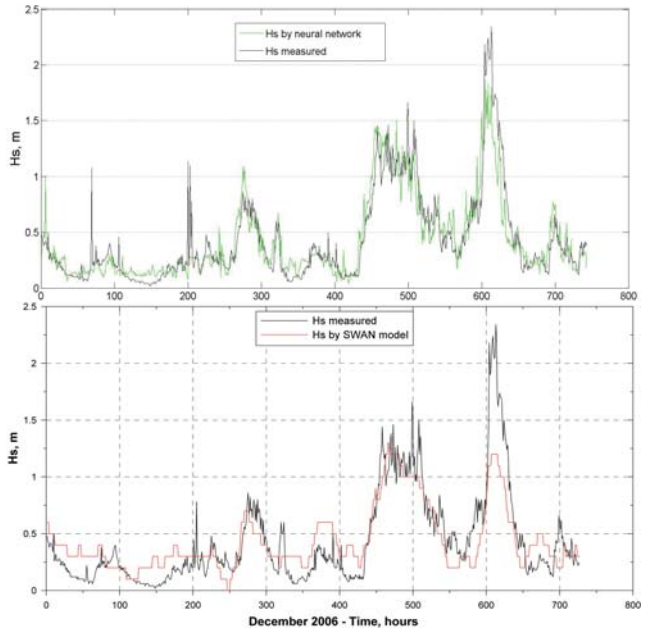

Figure 3. Comparison of simulated and measured Hs: a) by neural network model; b) by SWAN model.

The models quality is checked when the network training set was post processed by linear regression between single output by neural net A and T- the corresponding measured data output (target).

In the Fig. 4, the same is implemented for the results obtained with the conventional wave modeling technique. The scatter plots show that the neural network model forecasts slightly better the significant wave height. However, this results from the fact that the neural network model is fed directly with the measurements, while the conventional wave models are driven with estimates of the real atmospheric conditions.

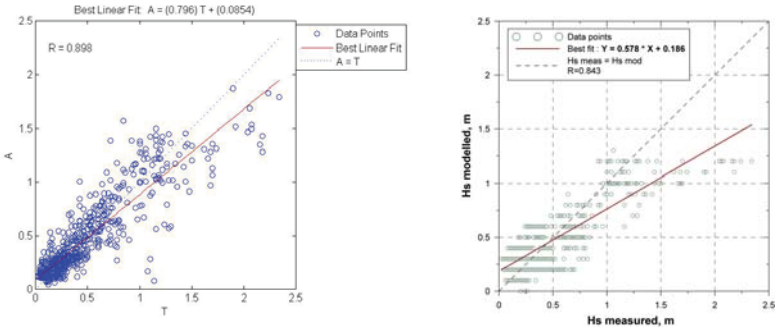

Figure 4. Scatter plots for measured and simulated significant wave height by neural network model (left) and SWAN model (right).

4. Conclusions and future challenges

It can be concluded that all models are accurate enough. Being very well developed, conventional wave models are quite sensitive to the quality of wind forcing and eventual drawbacks in their physics, such as poor parameterization of wave dissipation and insufficient resolution of the wave spectrum, have lower order of significance. Another external problem is confined accuracy of the bottom topography data that is crucial for estimation of wave transformation.

On the other hand, large amounts of observational data are required to apply neural network's technique. Increases in the performance and decreases in the cost of sensors, telecommunication and overall information processing equipment should continue for the foreseeable future and make the deployment of data driven models possible for most coastlines.

The study should be seen as a first attempt of inter comparison of the two applied modeling approaches. However, it can be already said that neural network method and conventional methods can be used in combination to further the development of wind wave modeling.

References

Booij, N., R.C. Ris, L.H. Holthuijsen (1999). A third-generation wave model for coastal regions, Part I, Model description and validation, J.Geoph.Research, 104, C4, 7649-7666.

Davidan, I., N. Valchev, Z. Belberov, N. Valcheva (2006). Assessment of the reanalyzed wind field accurateness for wave modelling purposes in the Black Sea region, Proc. of 4th Int. Conf. on EuroGOOS "European Operational Oceanography: Present and Future", 801-805.

Mavrova-Guirguinova, M., Gualev, K. 2007. 'Wind wave dimensions estimation based on ANNs', EGU – General Assembly, Vienna, Austria

Mavrova-Guirguinova, M. 2008. 'A Study of Wind Waves Forecasting in the Black Sea Shallow Waters by Neural Network Modelling', EGU – General Assembly, Vienna, Austria

Mehrotra, K., Chilukuri, K., Ranka, S., 2000. 'Elements of Artificial Neural Networks', Cambridge, The MIT Press Massachusetts Institute of Technology, Second printing

Rumelhart, D.E., Durbin, R., Golden, R., Chauvin, Y. 1995. 'Backpropagation: The Baisic Theory', Lawrence Erlbaum Associates Publishers, Hillsdale,1-34.

Tissot, P.E., Cox, D.T., Asce, M., Michaud, P. 2000 'Neural Network Forecasting of Storm Surges along the Gulf of Mexico', Ocean Wave Measurment and Analysis.

PHYSICAL MODELLING OF WAVE PROPAGATION AND BREAKING IN A FLUME USING DIFFERENT GEOMETRIC MODEL SCALES

Conceição FORTES, Rute LEMOS, Artur PALHA, Liliana PINHEIRO, Maria da Graça NEVES, João Alfredo SANTOS, Rui CAPITÃO, Isaac SOUSA & Maria Teresa REIS

Laboratório Nacional de Engenharia Civil, DHA/NPE, Av. do Brasil, 101, 1700-066 Lisboa, Portugal. E-mail: jfortes@lnec.pt, rlemos@lnec.pt, aclerigo@lnec.pt, lpinheiro@lnec.pt, gneves@lnec.pt, jasantos@lnec.pt, rcapitao@lnec.pt, isousa@lnec.pt, treis@lnec.pt

Abstract

This paper describes a set of scale model experiments carried out at the National Civil Engineering Laboratory (LNEC) to simulate, in a flume, the wave propagation along a constant slope bottom which ends on a seawall structure. This is a type of coastal defence structure quite commonly found in the Portuguese coast. Tests were undertaken using 1:10 and 1:20 physical model scales and measured data were the free surface elevation along the flume, runup levels, overtopping volumes and wave induced pressures on the structure. Statistical analyses were performed (both in the time-domain and in the frequency-domain) based upon the free surface elevation obtained along the flume. This work is the basis of a composite modelling technique, using numerical and experimental tools, to assess the influence of the physical model scale on the simulation of wave propagation up to wave breaking in front of such structures.

1. Introduction

The Composite Modelling of the Interactions between Beaches and Structures (CoMIBBs) project (a joint research activity of the European Union Integrated Infrastructure Initiative HYDRALAB III) aims at developing novel methodologies, involving both experimental and numerical techniques, by using the so-called composite modelling concept. These methodologies are meant to be applied to the interactions between hydrodynamics, structures, sediment dynamics, and beach/nearshore bed response. One of LNEC's tasks on COMIBBs focuses on developing a composite modelling methodology able to assess the influence of the physical model scale in the ability to properly simulate the wave propagation in the flume from offshore up to the wave breaking line, just in front of the coastal structures, especially when the wave breaking phenomenon plays an important role. Notice that the scale at which the physical model is built does influence the accuracy of the measurements of wave breaking quantities.

The proposed composite modelling methodology, Fortes *et al*. (2008), involves a numerical model that will help on the design of the large-scale experimental set-up and on the evaluation of its expected scale model effects. On the other hand, the physical model will provide the information needed for the calibration of the numerical model parameters.

The calibration of the numerical model was attained by evaluating the scale effects and measuring the wave conditions on wave breaking and in the vicinity of the structures of several physical model tests performed at one of LNEC's flumes. The description of the physical model tests, their results and statistical analysis are presented and discussed.

2. Prototype characteristics and experimental set-up

A physical model was constructed representing a prototype of a 1:20 beach slope ending on a 1:15 seawall. Two case conditions were selected: Case A, where the depth at the toe of the structure was 10 m or 11.5 m; and Case B, the depth at the toe of the structure was 20 m or 23 m, Figure 1. Physical model

tests were carried out at LNEC's COI2 wave flume (73 m long, 3 m wide, and 2 m deep), where generation and absorption of regular and irregular waves can be performed (Figure 1). This flume is equipped with a piston-type wave-maker controlled by the AWASYS (Troch, 2005) active wave absorption system.

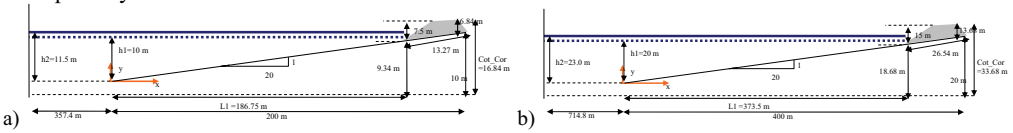

Figure 1 – Prototype: a) Case A; b) Case B.

The prototype cross sections shown in Figure 1 were reproduced in the physical model at two different scales, 1:10 and 1:20 for Cases A and B, respectively (Figure 2).

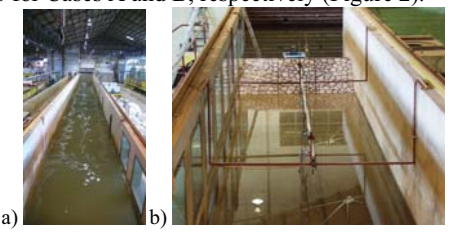

Figure 2. COI2 flume.

The considered physical model domain included the bottom profile and the seawall structure. Tests were conducted with both regular and irregular waves. For each model scale, a set of prototype test conditions were simulated: four incident wave heights (1, 2, 4 and 6 m), three wave periods (8, 12 and 14 s) and two tide levels. The flume was equipped with 6 resistive-type wave gauges to acquire sea surface elevations, 4 pressure transducers placed on the face of the structure to obtain wave induced pressures on the structure and one resistive gauge to measure run-up levels. The equipment used to collect the overtopping water was a weir located at the back of the structure, a chute to direct the water to the weir and a gauge used in the weir to measure the variation of water level within a test, allowing determination of the mean overtopping discharge.

Every test condition was repeated six times to measure the free surface elevation at 26 different locations, using six resistive gauges during each test, two of which always placed in front of the wave-maker.. Time-domain statistics were computed: root-mean-square wave heights and corresponding values of the standard deviation, skewness and kurtosis. A frequency-domain analysis was also carried out at selected points of the flume, for completeness. The measured data as well as the statistical analyses will be presented and discussed in the paper.

Acknowledgments

This work has been developed within the scope of the HYDRALAB III Project of the Research Infrastructures Program of FP6, Contract No:022441. The authors also gratefully acknowledge FCT financial sponsorship of project number POCTI/CTA/48605/2002, Portugal

References

FORTES, C. J.; NEVES, M.G.; PALHA, A.; PINHEIRO, L.; LEMOS, R., CAPITÃO, R.; SANTOS, J. A., SOUSA, I. (2008) - A methodology for the analysis of physical model scale effects on the simulation of wave propagation up to wave breaking. Preliminary physical model results. OMAE – 27th Int. Conf. Offshore Mechanics and Arctic Engineering, Estoril, Portugal, 15-20 June.

TROCH, P. (2005) - User Manual: Active Wave Absorption System. Gent University, Dep. Civil Eng.

THE GENERATION OF PERIODIC SHALLOW WATER WAVES IN A FLUME: THEORY AND MEASUREMENTS

M. CALABRESE [(1)], M. BUCCINO [(2)], F. CIARDULLI [(2)], P. DI PACE [(2)], E. BENASSAI [(1)]

[(1)] *Full Professor, Department of Hydraulic and Environmental Engineering "G.Ippolito", University of Naples "Federico II", via Claudio 21, Naples, 80125, Italy, calabres@unina.it; benassai@unina.it*

[(2)] *PhD, Department of Hydraulic and Environmental Engineering "G.Ippolito", University of Naples "Federico II", via Claudio 21, Naples, 80125, Italy, buccino@unina.it; francesco.ciardulli@unina.it; pdipace@unina.it*

1. Introduction

Despite most of experiments performed in physical modelling of coastal problems use random waves, periodic wave tests can be rather useful when a specific matter has to be studied under controlled forcing conditions. In this regard it should be noticed that many research topics refer to phenomena which take place in shallow water. Accordingly, either small water depth or long wave periods are needed. Obviously in planning the experiments the best would be generating waves under a quasi deep water condition, using a long mild slope to reach the desired water depth. Of course, it could require a rather long flume that, however, might be either not available or render the experiments too lengthy. Thus, waves are often run directly on a small depth, compared to wavelength, with wavemaker still moving as a simple sinusoid. In these cases results will be likely contaminated by the generation of secondary free waves, which travel throughout the channel and interfere with the primary oscillation. As a consequence, the resultant motion is no longer permanent and waves change their shape depending on the location across the flume. Altogether the periodic forcing which effects we wish to study, is substantially distorted by one or more high order harmonics, propagating with their own phase speed (Buhr Hansen & Svendsen 1974). Flick and Guza (1980) clearly showed them to have the same order of magnitude as the bound high harmonics of the main wave. They also showed these disturbances cannot be eliminated but adding a compensating motion to the wave-maker. For example,to properly generate a second order Stokes wave on a limited flat bottom the wavemaker should have a two component motion instead of a simple sinusoidal one.

Obviously it is of interest to predict the magnitude of spurious free waves for a given experimental condition to check in advance the reliability of measurements to be performed. This requires:

- A calculation method or formula predicting the amplitude of free waves. Hopefully it should be as simple as possible;
- A reliable technique for measuring the disturbances and validate prediction tools.

Previous points represent the core of present work. In particular the paper focuses on second order free waves, the amplitude of which can be predicted by a simple expression proposed by Madsen (1971) after a second order Stokes development of the wave-maker problem. In the following, Madsen theory is compared to results of physical model tests, conducted at the small scale flume (*SSC*) of the *LInC* Laboratory of the *Hydraulic, Geotechnical and Environmental Engineering Department (DIGA) of the University of Naples Federico II*. To experimentally measure the amplitude of the undesired disturbances, an innovative technique recently proposed by Lin & Huang, (2004) was used. It returns amplitudes and phases of different components of the wave oscillation process (either phase-locked and free and both incident and reflected) from the simultaneous recording of free surface profiles at four different locations.

On the whole the hopeful agreement between experimental and theoretical estimations will validate Madsen theory and Lin & Huang technique each other.

2. Review of Madsen Theory (1971)

Under the assumption of long waves (h/L< 0.1), Madsen faced the wave-maker problem using the Stokes perturbation technique at the second order. The author considered the paddle motion to be simply sinusoidal (Figure 1); hence the solution at the first order relates wave amplitude, *a*, and paddle stroke, ξ_0, according to the well-known expression presented in several textbooks (e.g. Dean and Darlymple, 1984):

$$a = \xi_0 \cdot \frac{\tanh(k_0 h)}{n_1}, \qquad \text{with} \qquad n_1 = \frac{1}{2}\left[1 + \frac{2k_0 h}{\sinh 2k_0 h}\right] \qquad [1]$$

where k_o obeys the linear dispersion relationship with reference to the fundamental period *T*.

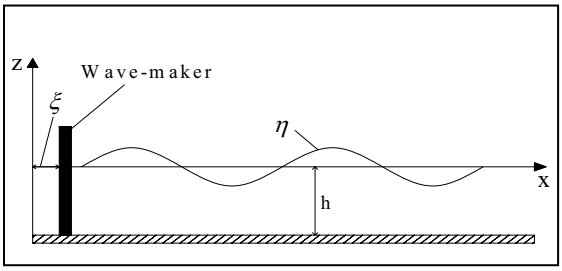

Figure 1. General scheme for wave-maker problem.

The key of Madsen work is the second order solution. By applying the Stokes perturbation method the author came to a non homogeneous system of linear differential equations, including a wave-maker boundary condition. This system can be solved by superimposing two problems. The first is given by the inhomogeneous equations where the wave-maker boundary condition is not considered. It basically gives the classical phase-locked term of second order Stokes waves. The second problem to be addressed is homogeneous and satisfies the second order wave-maker boundary condition. For the governing equations of the latter are homogeneous, free waves will be generated; they travel across the channel with their own phase speed and interact with the primary second order Stokes wave. The amplitude of these free disturbances, as obtained by Madsen, are reported below:

$$a_L^{(2)} = \frac{1}{2}a^2 \frac{\coth k_0 h}{h} \cdot \left(\frac{3}{4\sinh^2 k_0 h} - \frac{n_1}{2}\right)\frac{\tanh kh}{n_2} \qquad [2]$$

where

$$4\omega^2 = kg\tanh(kh) \quad \text{and} \quad n_2 = \frac{1}{2}\left(1 + \frac{2kh}{\sinh 2kh}\right) \qquad [3]$$

3. Experiments

Figure 2. View of *SSC*

Periodic wave experiments have been conducted at the small scale channel (*SSC*) of the *LInC Laboratory of the Hydraulic, Geotechnical and Environmental Engineering Department (DIGA) of the University of Naples Federico II. SSC* (Figure 2) is 23.50m long, 0.80m wide and 0.75m deep and is provided with a piston type wave-maker capable of generating both regular and spectral waves. An active wave absorption system is also mounted on the paddle. A spending rubble beach has been constructed at the end of the flume (opposite to the wavemaker), to minimize effects of reflection.

The beach was made up on three parts with two different slopes, namely 1:10 (inner and

seaward part) and 1:20 (middle part). The still water level has been kept constant at 31.5 cm; two wave periods were used, giving a range of relative water depth, h/L, from 0.03 to 0.05. For each wave period we have run 9 wave heights, ranging from 4 to 12 cm, to get an ensemble of 18 different tests on the whole. Wave measurements were achieved at 28 different positions.

As a preliminary check of applicability of the Madsen theory, we verified that the *Ursell number* calculated with the target wave height were much less than 32/3 π^2 which is the theoretical limit for the second order Stokes theory is accurate.

4. Lin & Huang method (2004)

The main assumption in the Lin & Huang method is that periodic waves can be described through a simple sum of an infinite number of discrete components, each with its own frequency, wave height and phase speed. Hence, taking into account the free and the phase-locked modes in the higher harmonics, the free surface elevation at whatever position in a wave flume can be expressed as follows:

$$\eta(x_m,t) = a_I \cos(kx_m - \sigma t + \phi_I) + a_R \cos(kx_m + \sigma t + \phi_R) +$$
$$+ \sum_{n\geq 2} a_{I,B}^{(n)} \cos[n(kx_m - \sigma t) + \phi_{I,B}^{(n)}] + \sum_{n\geq 2} a_{I,F}^{(n)} \cos[k^{(n)} x_m - n\sigma t + \phi_{I,F}^{(n)}] + \qquad [3]$$
$$+ \sum_{n\geq 2} a_{R,B}^{(n)} \cos[n(kx_m + \sigma t) + \phi_{R,B}^{(n)}] + \sum_{n\geq 2} a_{R,F}^{(n)} \cos[k^{(n)} x_m + n\sigma t + \phi_{R,F}^{(n)}] + e_m$$

After the Fourier transform has been applied to Equation [3] and a last squares method has been used to minimize the error caused by possible signal noise, we obtain a simple system of linear equation where the (complex) unknowns are the amplitudes and phase constants of different modes. Due to the high values of Ursell number for our experiments, the system above has been solved at the 3rd order. However for comparing measurements with Madsen theory, only 2nd order components have been analysed.

5. Experimental results

Figure 3 shows a sketch of the wave profile as acquired at two different positions along the flume. The effect of secondary waves is rather evident with shape of the waves changing with position; it is of interest that a secondary crest appears and disappears during propagation. Figure 4 shows a comparison between predictions of Madsen theory and measured amplitude of second order free waves. The agreement seems quite reasonable indicating that Ling & Huang method would work properly, at least for the hydraulic conditions here investigated. As a confirm of this, Figure 5 plots measured values of second order bound wave amplitudes vs. those given by the Stokes theory. Again the comparison is favourable apart from one point that lies very far from the perfect agreement line. However measured values are always somewhat larger than theoretical ones, giving overpredictions of 20% on average.

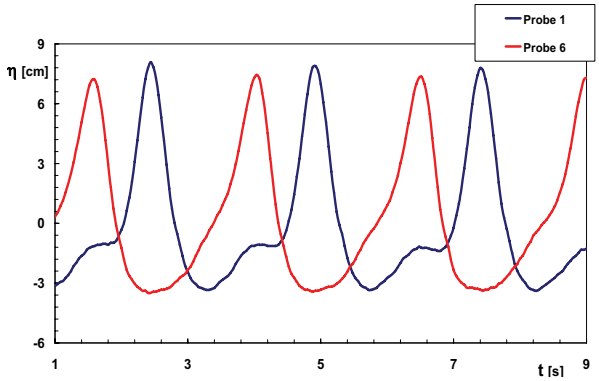

Figure 3. Example of wave profiles: H=8cm; T=2.5s.

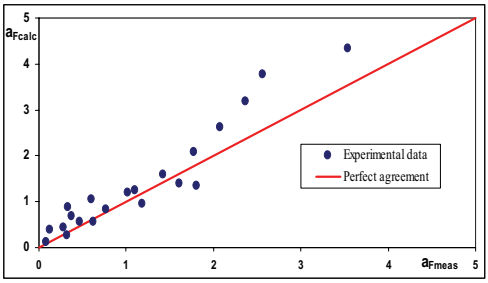

Figure 4. Measured secondary free amplitude (in cm) vs. theoretical predictions of Madsen theory.

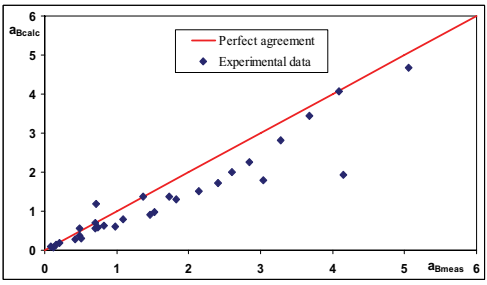

Figure 5. Measured bound wave amplitude (in cm) vs. theoretical predictions of Stokes theory

References

Buhr Hansen, J.B. and Svendsen,1974. 'Laboratory Generation of Waves of Constant Form', Proceeding, 14th International Conference on Coastal Engineering, ASCE, pp. 321-339;

Dean, R., Dalrymple, R., 1984. 'Water Wave Mechanics for engineers and Scientists', pp. 353;

Flick, R.E. and Guza, R.T., 1980. 'Paddle Generated Waves in Laboratory Channels', Journal of Waterway Port Coastal and Ocean Division, pp. 79-97;

Goda, Y. 1997. 'Recurring evolution of water waves through nonresonant interactions', Proceeding, 3rd Int. Symp. Ocean Wave Measurements and Analysis(WAVES '97), Virginia Beach, 1-23, ASCE.;

Lin, C-Y and Huang, C-J, 2004. 'Decomposition of Incident and Reflected Higher Harmonic Waves Using Four Gauges', Coastal Engineering 51, pp. 395-406;

Madsen, O.S., 1971.'On The Generation of Long Waves', Journ. of Geophy.Research vol. 76, N° 36.

APPLICATION OF NUMERICAL MODEL OF THE BALTIC SEA TO A POST-HOC ANALYSIS OF HYDRODYNAMIC CONDITIONS DURING STORM SURGES IN THE ODER MOUTH AREA

Halina KOWALEWSKA-KALKOWSKA [(1)] & Marek KOWALEWSKI [(2)]

[(1)] *Dr, Institute of Marine Sciences, University of Szczecin, Wąska 13, Szczecin, 71-415, Poland.*
halkalk@univ.szczecin.pl

[(2)] *Dr, Institute of Oceanography, University of Gdańsk, Marszałka J. Piłsudskiego 46, Gdynia, 81-378, Poland.*
ocemk@univ.gda.pl

Abstract

A pre-operational hydrodynamic model of the Baltic Sea, developed at Institute of Oceanography, University of Gdańsk was applied in post-hoc analyses of storm surges in the Oder mouth area (the southern Baltic Sea). Testing the applicability of the model on storm surge events in 2005-2007 showed a good agreement between the modelled and observed distributions of sea levels as well as water temperature and salinity. The model correctly reflected events involving high-amplitude and rapid water level fluctuations; it also generated relatively good flow simulations.

1. Introduction

The Oder mouth area (a complex structure encompassing the lower Oder branches, the Szczecin Lagoon, and the inshore Pomeranian Bay in the southern Baltic) is exposed among others to storm surges (Fig.1). They occur as a result of the passage of deep and intensive low-pressure systems over the Baltic Sea. In the Pomeranian Bay, the passages of depressions generate considerable sea level fluctuations, i.e. may produce 1.0-2.0 m high local storm surges and 0.5-1.5 m deep storm falls. During heavy storms the brackish bay water can enter the Szczecin Lagoon raising the water level in the Szczecin Lagoon and downstream reach of the Oder River. Due to strong suppression of sea level fluctuations in the straits connecting the Pomeranian Bay with the Szczecin Lagoon, water level fluctuations in the Lagoon and in the Oder channels are much weaker and follow, with a delay, changes in the sea level. The influx also affects the Lagoon's physical and chemical characteristics.

Over the recent years, the hydrodynamic regime of the Pomeranian Bay and Szczecin Lagoon has been studied with the help of numerical models by, i.a. Lass *et al.* (2001), Kałas *et al.* (2001). The hydrodynamic regime of the Oder mouth was described by, i.a., Ewertowski (1988). In this study a 3-D, pre-operational hydrodynamic model of the Baltic Sea (M3D_UG), developed at Institute of Oceanography, University of Gdańsk, was applied in post-hoc analyses of storm surges in the Oder mouth (the southern Baltic Sea). The model was based on the Princeton Ocean Model (POM), as described in detail by Blumberg and Mellor (1987). Adapting the model to the Baltic Sea required certain changes in the numerical calculation algorithm (Kowalewski, 1997). The open boundary was located between the Kattegat and the Skagerrak. A radiation boundary condition for the vertically averaged flows was applied. The solar energy input was calculated based on astronomical data and meteorological conditions (Krężel, 1997). Other components of the heat budget at the sea surface were derived from meteorological data and simulated sea surface temperatures (Jędrasik, 1997). Meteorological data were taken from the Unified Model for Poland Area (UMPL). The model takes into

account 153 riverine discharge events. Because of wind-driven water back-flow in the Lower Oder channels, a simplified operational model of the Oder discharge based on water budget in a stream channel was developed (Kowalewska-Kalkowska, Kowalewski, 2006). To obtain an adequate resolution and reliable data spatial spacing of about 1 km (0.5 nautical mile) was applied both for the Pomeranian Bay and Szczecin Lagoon.

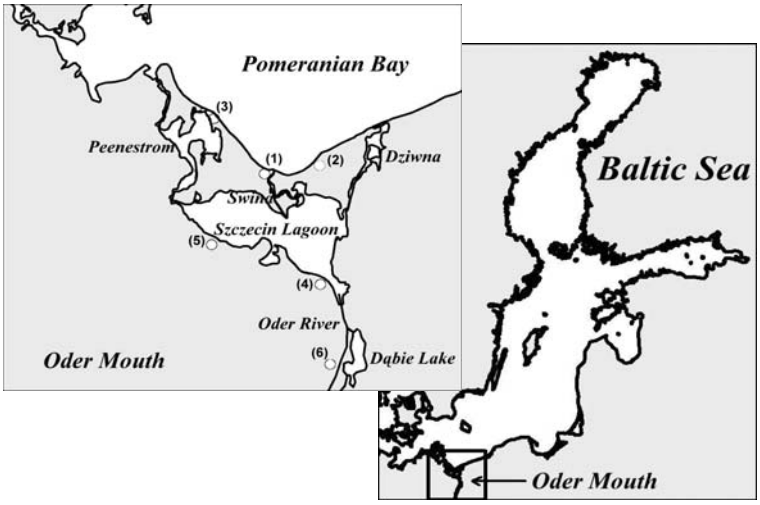

Figure 1. The Baltic Sea and the Oder Mouth with station location. Legend: Świnoujście (1), Międzyzdroje (2), Koserow (3), Trzebież (4), Ueckermünde (5), Szczecin (6).

Evaluation of the model's performance in the Pomeranian Bay and Szczecin Lagoon showed a good fit between modelled and observed distributions of data sets. The modelled water levels produced a very good fit, with correlation coefficients exceeding 0.93. A very good agreement was obtained also in water temperatures. The correlation coefficients between the empirical and numerical data sets exceeded 0.98. A somewhat poorer fit was obtained for salinities. The model correctly reflected hydrodynamic conditions and seasonal variability of the variables analysed; it also generated relatively good flow simulations.

2. Application of the model to forecasting storm surges

The good fit between the observed and the predicted data was an incentive for checking the accuracy of the model on storm surges events in 2005-2007. Temporal sea level variations in the region, as approximated by the model, may be visualized for a case involving a storm surge period that occurred in February 2007. Beginning on 31 January, the sea level began to rise as a result of the passage of deep low from the North Sea over the southern Baltic and then eastwards. The model predicted that increase in sea level fairly accurately (Fig.2). The maximum values (1.0 m above the mean sea level in Świnoujście) were also predicted with a high accuracy. Next day, the ensuing drop in the sea level was also accurately approximated by the model. For Świnoujście, some underestimates were produced only by 1 February forecast. Beginning on 2 February, the sea level began to rise again as a result of the advection of a new depression over the Bothnian Sea, to reach the maximum of 0.7 m above the MSL in Świnoujście on 3 February. That increase in sea level was slightly overestimated by the model. The ensuing drop in the sea level over the following days was accurately mimicked by the model.

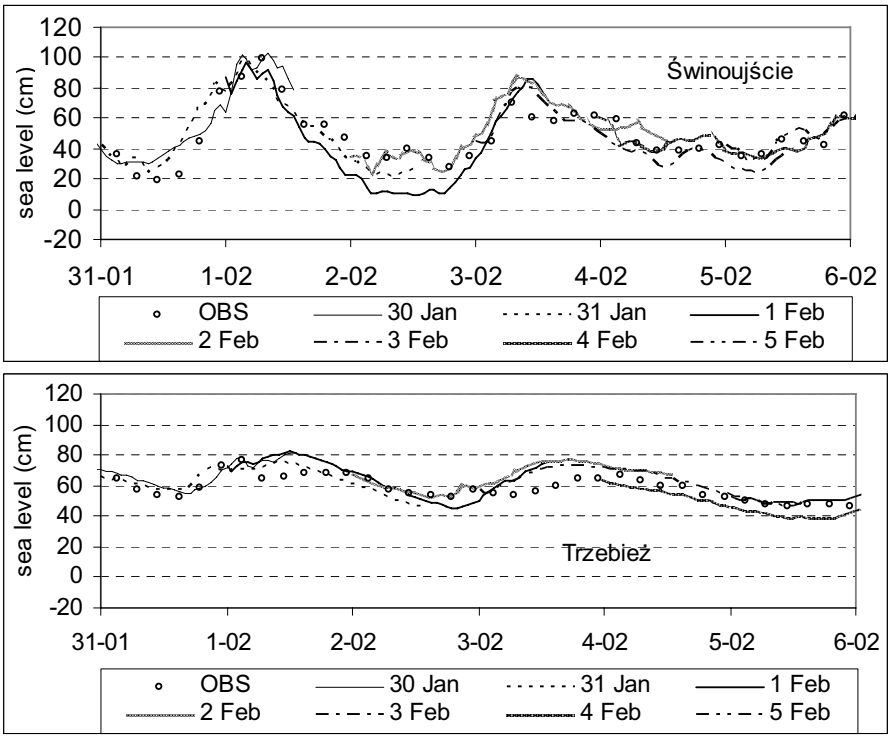

Figure 2. Observed and predicted water levels in Świnoujście and Trzebież during the storm surge in February 2007, as simulated with the M3D_UG model. Legend: forecasts from 30 January to 5 February.

During the storm surge discussed, the Szczecin Lagoon stations showed much weaker water level fluctuations. From 31 January to 1 February, a constant increase in the water level until the maximum of 0.76 m above the MSL (Trzebież) was observed (Fig.2). That increase was very accurately predicted by the model in terms of the extent, however the maximum was calculated with a delay of some hours by the 31 January and 1 February forecasts. During the next two days, the drop in the water level was recorded at first; however, the water level began to rise slowly on 3 February. Those water level fluctuations were reflected well by the model. The accuracy of the second maximum water level prediction at Trzebież was also good (0.67 m above the MSL on 4 February, with a 20-hour delay with respect to the second sea level maximum), however it was predicted to occur some hours before the real maximum. During the next few days, the slow water level drop was accurately simulated by the model.

3. Conclusions

The application of the model to forecasting of hydrodynamic conditions in the Oder mouth area during storm surges in 2005-2007 showed good agreement between the modelled and observed distributions of water levels as well as water temperature and salinity. In the cases of high-amplitude and rapid water level fluctuations as well as fast changes of physical properties of water the model reflected correctly the hydrodynamic situation. It also generated relatively good flow simulations.

A good approximation of hydrodynamic conditions in the Oder mouth area allowed to consider the model as a reliable environmental tool for forecasting and analyzing storm surges in the coastal zone of

the Pomeranian Bay as well as for studying coastal processes such as mixing of the fresh and saline waters in the Oder mouth or the spread of the Oder water in the Pomeranian Bay. A fast online access to the hydrodynamic forecast (http://model.ocean.univ.gda.pl) allows potential users to predict the day-by-day development of processes that may affect different areas of human life and activities, e.g., navigation, port operations or flood protection in coastal areas as well as estimation of the hazard of coastal pollution due to the Oder River impact.

Acknowledgments

This work was supported by the Ministry of Science and Higher Education under the research project "Impact of storm surges along the southern Baltic coast on hydrodynamic conditions in the Oder river mouth area" (grant No. N306 028 31/1644).

References

Blumberg A. F., Mellor G.L., 1987, 'A description of a three-dimensional coastal ocean circulation model', In: 'Three-dimensional coastal ocean models', N. S. Heaps, (ed.), *Am. Geophys. Union*., pp. 1–16.

Ewertowski R., 1988, 'Mathematical model of the Odra Estuary', *A.I.P.C.N.- P.I.A.N.C. Bull.*, Bruxelles, 60, pp. 95–114.

Jędrasik J., 1997, 'A model of matter exchange and flow of energy in the Gulf of Gdańsk ecosystem – overview', *Oceanol. Stud.,* 26(4), pp. 3–20.

Kałas M., Staśkiewicz A., Szefler K., 2001, 'Water level forecast for the Pomeranian Bay from the HIROMB Model', *Oceanol. Stud*., 30 (3-4), pp. 39-57.

Kowalewska-Kalkowska H., Kowalewski M., 2006, 'Hydrological forecasting in the Oder Estuary using a three-dimensional hydrodynamic model', *Hydrobiologia*, 554, pp. 47-55.

Kowalewski M., 1997, 'A three-dimensional hydrodynamic model of the Gulf of Gdańsk', *Oceanol. Stud.,* 26(4), pp. 77–98.

Krężel A., 1997, 'A model of solar energy input to the sea surface', *Oceanol. Stud.,* 26(4), pp. 21–34.

Lass H. U., Mohrholz V., Seifert T., 2001, 'On the dynamics of the Pomeranian Bight', *Cont. Shelf Res*., 21, pp. 1237–1261.

EXPERIMENTAL VERIFICATION OF THE MAXIMUM VERTICAL SPEED OF FREE SURFACE AS THE WAVE BREAKING INDEX

Takashi OKAMOTO [(1)] & Conceição FORTES [(2)]

[(1)]*Research Trainee, National Laboratory of Civil Engineering (LNEC), Av. do Brasil 101, Lisbon, 1700-066, Portugal. tokamoto@lnec.pt*

[(2)]*Research Officer, National Laboratory of Civil Engineering (LNEC), Av. do Brasil 101, Lisbon, 1700-066, Portugal. jfortes@lnec.pt*

Abstract

An adequate wave breaking index and its critical condition are required for the numerical simulation of wave breaking region. However, the critical condition of wave breaking index used in the phase-resolving type wave transformation models is not determined from the experimental data but by the numerical calibration. In this paper, we calculate the vertical speed of free surface, which is used as the wave breaking index in the FUNWAVE numerical model, from the scale model experiments with simplified bar-trough beaches, and examine the critical condition.

1. Introduction

The wave breaking is a quite important event in the nearshore area since it provides the energy to drive the nearshore phenomena, such as wave set-up/down, longshore current, etc. The phase-resolving type wave transformation models (Boussinesq equation model) are now commonly used for the analysis of the nearshore hydrodynamics. In those models, the energy dissipation due to the wave breaking is realized by adding extra momentum terms in the governing equation, and the initiation and the termination of the wave breaking are determined by an external criterion.

In FUNWAVE numerical model (Kirby et al., 1998), the vertical speed of free surface ($\partial\eta/\partial t$) is employed as the wave breaking index. The critical condition (threshold value) is controlled by three parameters, such as initiation condition, termination condition and the duration. However, the wave breaking index used in the FUNWAVE model is not determined from the experimental data but the numerical calibration. Especially, it is not clear how the termination condition of the wave breaking was determined.

Fortes et al. (2007) calculated regular waves on a simplified bar-trough shaped beach by the FUNWAVE numerical model and compared it to the physical experimental data. The agreement to the experimental data was good until slightly after the initiation of the wave breaking, but poor after that point. There are couple reasons which possibly cause the poor agreement, such as the energy dissipation intensity, the spatial distribution of breaking (roller) area, the initiation and termination of the event, and so on. Among of them, we concentrate on the critical condition of wave breaking index employed in the FUNWAVE because it is not experimentally proven. The wave tank experiments were conducted on simplified bar-trough shaped beaches. Experimental data determines the value of the vertical speed of free surface at the termination location and the change of index value during the wave breaking reveals the problem of the wave breaking mechanism employed in the FUNWAVE model.

2. Wave breaking index in the FUNWAVE

The wave breaking index in the FUNWAVE is the vertical speed of free surface. In the actual

implementation, it is calculated directly from the continuous equation. The critical condition is determined by three parameters (initiation, duration, and termination) and varies depending on the situation. The critical condition for the non-breaking wave is equal to the value of initiation parameter. Once the wave breaking begins, it decreases towards the value of termination parameter with time defined by the duration parameter. A coefficient in the eddy viscosity term is set to non-zero value while the vertical speed of the free surface exceeds the critical condition, so the momentum sink term is included in the governing equation. The initiation and termination values are given in the form of $a \times \sqrt{gd}$, where a is a constant, g is the acceleration of gravity, and d is the water depth. The value of a for the initiation is given 0.35-0.65, and for the termination, it is 0.15. According to Kirby et al. (1998), the upper limit of the initiation parameter (0.65) is for monotone sloping beaches and the lower limit (0.35) gives better agreement to bar-trough shaped beaches.

Fortes et al. (2007) calculated regular waves and compared with the experimental data. Fig.1 displays the comparison between the numerical result and the experimental data with T=1.5sec and H=10cm. It displays that the FUNWAVE does not properly calculate the wave breaking over the bar-trough shaped beach. In this example, the wave breaking initiates about 150cm before the bar crest. The wave height change agrees very well until slightly after the initiation of wave breaking (around -100cm), but the great disagreement appears after that point. The disagreement stays even after the termination of wave breaking.

The wave height is not directly connected to the vertical speed of free surface, but it is still the main factor of it. Therefore, the value of parameter calibrated in the numerical model may not agree to the actual condition due to the other causes in the numerical model.

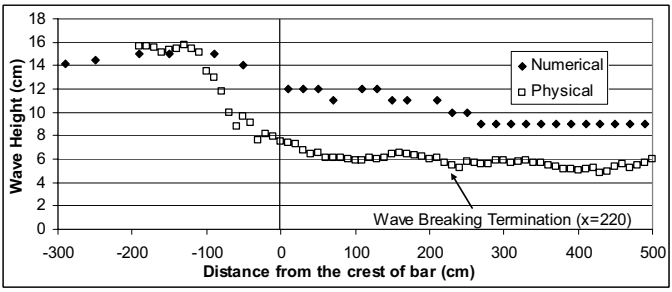

Figure 1. Comparison of wave height change between numerical calculation and experimental data (modified from Fortes et al. (2007))

3. Wave tank experiments

Wave tank experiments were carried out at LNEC. The wave flume has 32m long from the wave maker to the end of the flume and simplified bar-trough profile beaches were constructed. Slope angles of the front face of the bar and the beach section were 1:20 and the three angles of the lee side of the bar (back slope) were tested (1:20, 1:40, and 1:80). Water depth was measured at the crest of the bar. The experiments were tested with two water depths (d=10 and 15 cm). Fig.2 schematically displays the bathymetrical settings of the wave tank.

A piston-type wave maker generates regular waves with four different wave periods (T=1.1, 1.5, 2.0 and 2.5 sec). Four input wave heights (H=8, 10, 15, and 20 cm) were tested for cases with d=10 cm and two input wave heights (H=10 and 15 cm) were tested for d=15 cm. However, the wave with d=10cm, T=1.1sec, and H=20cm was broken at the wave maker due to the steepness condition, so it was discarded from the experiment. In total, sixty nine cases were tested in this experiment. In addition to the breaking waves, cases in which the wave does not break at the bar were also tested with d=10cm. The input wave

height varies on the wave period because of the limitation of the wave maker and the different shoaling rate. The input wave heights are 4.0, 3.3, 2.0, and 2.5cm for T=1.1, 1.5, 2.0 and 2.5sec, respectively.

Resistant type wave gauges were installed in the wave tank and measured the surface elevation change with the sampling rate of 100Hz. The spatial distance of the gauge is 10cm. The wave gauges were placed from 200cm before the bar crest to the bottom of the trough. So, in cases with smaller input wave heights, whole life of wave breaking was measured but the others were recorded only from the middle of the wave breaking to the termination. The duration of the record is two minutes so that the number of waves recorded is different depending on the wave period.

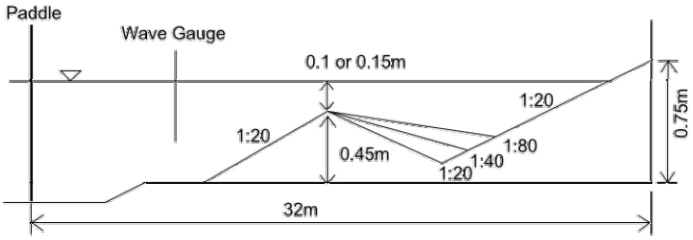

Figure 2. Wave tank setting

4. Results

The vertical speed of free surface was calculated from the wave gauge record. The maximum values in each wave period were collected and made an average. Fig.3 displays the evolution of the vertical speed of free surface with d=10cm, T=1.5sec, and H=10cm. In this case, the wave breaking initiates around 150cm before the bar crest and ceases around 220cm from the bar crest. As shown, the vertical speed of free surface decreases after the slight increase after the initiation of wave breaking. The general structure of the evolution pattern is the same as the wave height change; the rapid decrease occurs in the outer surfzone then it slows down in the inner surfzone. But, different from the wave height change, the non-linear shape change (from sinusoidal shape to saw tooth shape, or vice versa) involves in the vertical speed of free surface, so that it keeps decreasing even after the wave height gets stabilized (See Fig.1). The value at the initiation is slightly higher than the proposed value ($0.65\sqrt{gd}$) but the value at the termination is nearly equal to the proposed value ($0.15\sqrt{gd}$).

More results and the comparison with the numerical model will be presented in the Coastlab08 conference.

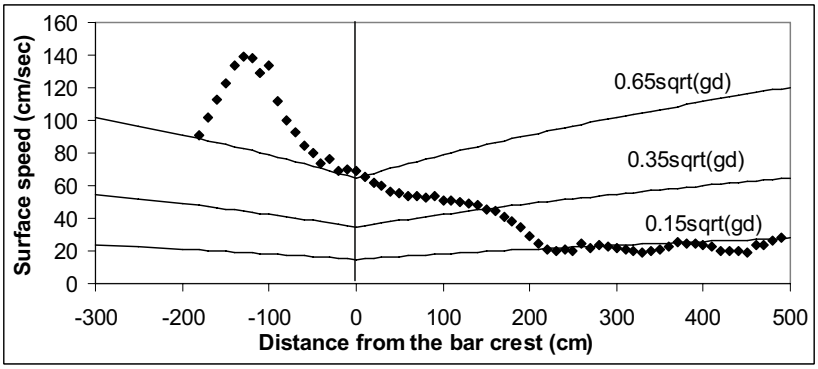

Figure 3. Maximum vertical speed of free surface (d=10cm, T=1.5sec, H=10cm)

Acknowledgments

This work is funded by FCT, the Portuguese Research Foundation, through the projects SFRH/BPD/20508/2004, POCTI/CTA/48605/2002 and PTDC/ECM/67411/2006.

References

Fortes, C.J., T. Okamoto, and A.C. Palha (2007). “Analyze of the wave breaking formulation in the FUNWAVE model”. Proc. of Portuguese Days on Port and Coastal Engineering, October (CD ROM) (in portuguese)

Kirby, J.T., G. Wei, Q. Chen, A.B. Kennedy, and R.A. Dalrymple (1998). “FUNWAVE 1.0 Fully Nonlinear Boussinesq Wave Model Documentation and User's Manual”. Res.Rep. No. CACR-98-06, Center for Applied Coastal Research, Univ. of Delaware, Newark, Delaware.

EXPERIMENTAL STUDY ON THE EFFECT OF SPUR DIKE POSITION ON THE SCORING DEPTH IN THE RIVERS BEND

A.R.MASJEDI[(1)] & A. MORADI[(2)]

[(1)] ***Assist.Prof. of Water Science Eng. Dept., Islamic Azad University, Ahvaz***

[(2)] ***MSc of Water Science Eng, Islamic Azad University, Science and research center, Ahvaz***

Abstract

Spur dikes have been used extensively for erosion control in the external wall of river bends. Experimental investigation on scoring and determination of depth of scoring are among the most important issues in spur dike designation.

One of the effective parameters on the scoring depth is the position of installing dike in the river bends. In order to investigate the effect of installing position of spur dike on scoring process some experiments carried out in a bended laboratory flume, which is made of plexiglass with 180º bending and R/B=4.7. In this research, by installing a spur dike in the position of 30, 60, 90, 120, 150 and 160 degrees the scoring phenomenon were examined under 20, 24 and 28 L/S discharging value in the limpid water with the constant water depth of 13cm.

Flume bed was fully paved by uniform granulated sand. It was found that maximum scoring depth in the river bending increases by increasing discharge and resting angle position 60º and then it faces reduction to position 120º. From 120º to 160º scoring depth increases and reaches to its maximum at position 160º.

Keywords: River bend, Scoring depth, Spur dike, Spur dike position.

1. Introduction

Spur dikes are the structures used directly or indirectly for guarding river bends. Secondary flow and erosion of external wall of bend are among the basic problems in the river bends which can be avoided by constructing spur dikes. These structures extend from riversides into the main flow and cause local contraction of flow. These structures which made in singular one or in a successive series deviate flow and prevent it from colliding with river sides. In addition eddy flow which have been taken place in downstream deposits sediments gradually and cause natural and biological development and establishment of riverside.

Scoring near dikes is one of the important factors has to be taken into consideration in spur dikes designation. Its influence on the maximum scoring depth and its efficiency in guarding riverside can be assessed by basic parameters of spur dikes.

There are many relations for scoring depth calculation around spur dikes and there are many works concerning scoring around the spur dikes in straight directions such as Miri(1995), Ahmed(1953Garde et al(1961), Ghodsian-Tehrani(2001), Gill(1972), Rajaratnam-Nwachukwa(1983).

Complication of flow pattern in the bend in companion with complication of flow around the dike, make flow pattern conditions around spur dikes in the bend more complicated. Few researches dealing with spur dike in bends are available, e.g., [5], [6],[7],[9].

Ghodsian et al [3] investigated the effect of position and length of spur dike on the scoring around the 90º bend. They found that maximum scoring depth when spur dike is installed in the first half of bend is less than second half of bend. As maximum scoring depth, scoring hole size increases when spur dike installed in the second half of bend.

In spite of extensive use of spur dikes in rivers bend, there is no enough reliable reference to invoke for designation and determination of scoring depth in rivers bend. So employing laboratory model for investigating flow behavior is inevitable.

In this research the relation between installation position and scoring hole were examined by installing single spur dike in various positions in the laboratory flume with 180º bending and constant depth and bed topographical measurements in different discharges.

2. Methodology and experimental set up

It was shown that scoring phenomenon around spur dikes is influenced by five main factors; canal geometry, spur dike specifications, sediment specifications, flow and fluid properties. In this research canal geometry, spur dike length, flow depth, bed materials properties and fluid properties kept constant and fluid discharge and angle of resting position in the bend were changed. Considering mentioned cases, following relation was presented for investigating effective parameters on the equilibrated scores:

$$\frac{dz_{maz}}{L} = f(\theta, Q) \tag{1}$$

Where:

$\theta =$ Resting position angle of spur dike in the bend

$Q =$ Flow discharge

$dz_{maz} =$ Maximum score depth in equilibrated state

$L =$ Spur dike length

Experiments were conducted in the bended plexiglass flume with 180º central angle, central radius of R=2.8 m and width of 0.6 m. relative curvature of bend was R/B = 4.7 which can be categorized in mild bends.

A straight entrance canal with the length of 9.1 m is connected to the bending part of flume (with 180º turning). This part of flume is connected to a controlling gate and an outlet tank by another straight canal with the length of 5.5 m.Figure 1 plan of bended canal and the position of installed spur dike.

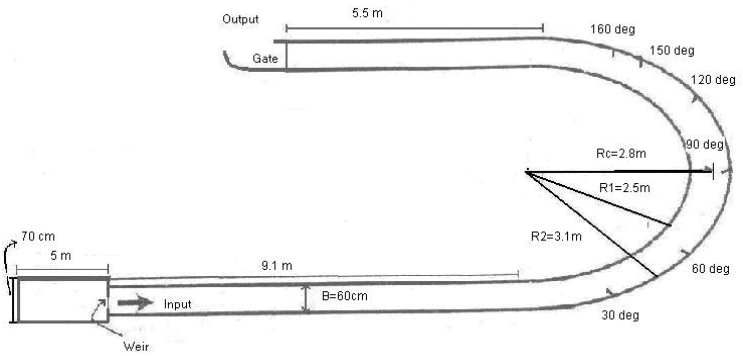

Fig. 1. Layout of flume for spur dike positions experiments

Spur dike was made from wood 3 mm thick and 11cm length. Discharging values was measured by a pre-calibrated V-notch installed in a beginning of inlet of flume. At first spur dike was installed in 6 different position in external wall of bend in the manner it made angle of 70º with upstream shore (110º with flow).then in each stage bed materials (uniform granulated river sand with 2mm average diameter and 1.3 standard deviation) scattered all over the flume by means of a movable cart. 20, 24 and 28 L/S were 3 different discharges involved in these experiments to investigate discharge effect on spur dikes in positions 30, 60, 90, 120, 150 and 160 degrees.

Equilibrium time was calculated by a long time test on spur dike in positions 30 and 160 degrees and with 20 L/s discharge. It was shown that after first 10 hr approximately more than 95% of scoring was taken placed. Considering in the first hour more than 80% of total scoring was occurred , this time (1 hr) selected as equilibrium time for all experiments.

Before switching on the pump, the end gate was closed and limpid water was conducted through flume gently. After some hours and rising up the water level and ensuring that sediments are soaked, pump switched on with low discharge and then by the main valve on the inlet pipe of still basin flow rate increased slowly to reach desired discharge value. By carefully and simultaneously adjusting main valve and downstream gate, desired discharge obtained and flow depth reached to 13cm.

After one hour, pump turned off and flume drained gently to have no effect on bed topography. After passing some hours and complete drainage, bed topography around spur dike in different positions and discharges was taken by means of 0.1mm precise point gauge.

In order to accurate assessment of changes in bed surface, data was taken from each 2cm in latitude and longitude direction. Sum of total data were taken from 18 experiments to forming a bed topographical net and other details were 20000 data.

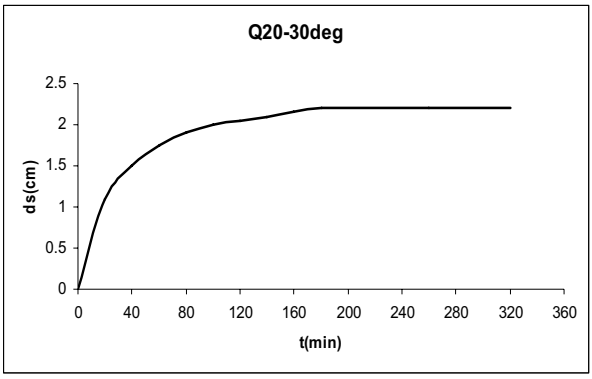

Fig. 2. Equilibrium time for 20 L/S discharge and position of 30 degrees bend

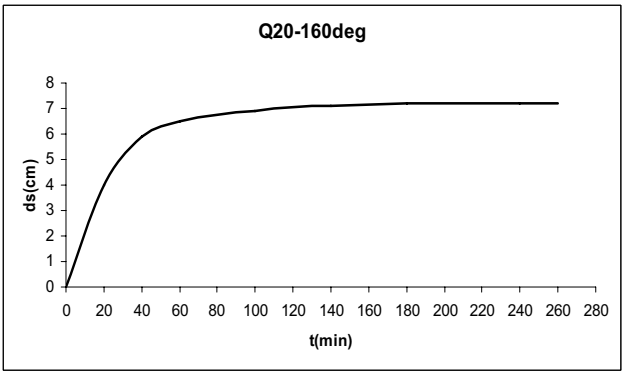

Fig. 3. Equilibrium time for 20 L/S discharge and position of 160 degrees bend

3. Conclusions and discussion

In all experiments after setting discharge and flow depth, eddy flows formed immediately in the nose of spur dike and scoring process started with high rate. Risen sediments from score hole moved towards downstream.

Some minutes after starting experiment, risen sediments of score hole come to a region that the effect of spur dike and eddy flows behind the spur dike are diminished. In this situation transferred sediments from score hole under the effect of secondary flow move toward the internal wall and cause forming two or more small dion in the internal wall. Also depends on hydraulic flow conditions, deposition occurs with minimum scoring in this area.(figure 4)

Because of presence of spur dike, some part of flow is deviated and moves faster toward internal bend and causes the rapid movement of dions and also it made them to mount on each other and create a sediment pile. In the most experiments maximum height of the pile establishes in the internal wall and downstream of the bend outlet.

Deviated flow by spur dike make a scoring in the downstream of spur dike which could be seen in all experiments but its dimensions are different for various position of spur dike. Sometimes in the downstream of spur dike this scoring hits the internal wall and causes the scoring in the bend wall and sometimes there is no hit and consequently no scoring happens but instead sedimentation occurs. It is clear that effective parameters on the size of this scoring are spur dike position and flow rate.

Fig. 4. Scoring and sedimentation in the downstream of spur dike due to deviation of flow

3.1. Effect of spur dike position on the scoring around the spur dike

Because of difference in flow patterns in various positions in the bend, installation of spur dike in different positions had remarkable influence both on bed topography and maximum scoring around the spur dike. Figure 5 shows transversal profiles of a single spur dike in the positions of 30, 60, 90, 120, 150, and 160 for discharge value of 20, 24 and 28 for maximum scoring depth. These profiles show that there is a direct relationship between scoring depth and spur dike position as scoring depth increases by increasing resting angle of spur dike.

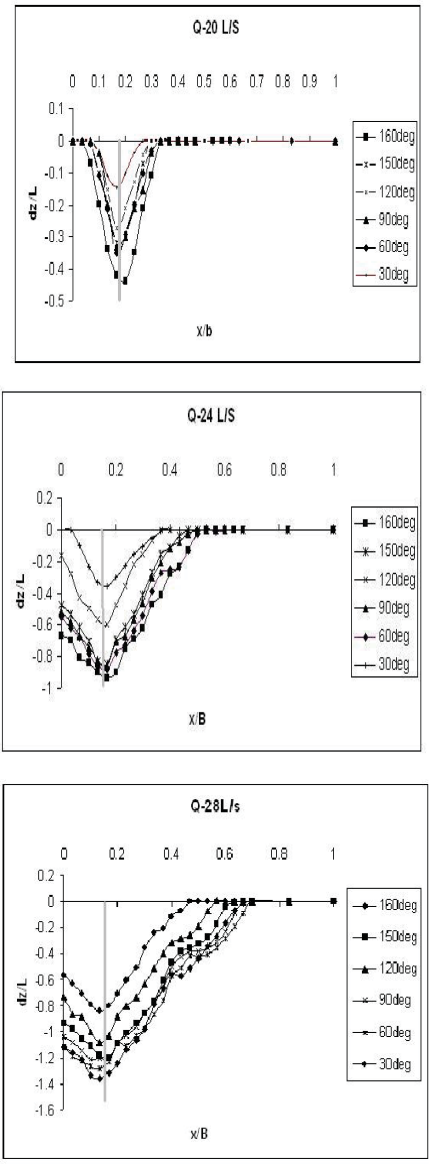

Fig. 5. Transversal profiles of maximum scoring depth in different positions and discharge value of 20, 24 and 28 L/S

3.2. Variation of scoring depth in relation with flow rate in the bending

Figure 4 shows longitudinal and transversal profiles of single spur dike in the position of 160 degrees which has the maximum scoring depth for three discharges values 20, 24 and 28 L/S. By considering figure 6 one can conclude that overall topographical shape of bed almost are as the same as each other but size and depth of scoring decreases by decreasing discharge values. Transversal profile also shows that there is a direct relation between scoring depth and discharge values and whenever discharge values increase scoring depth increase too.

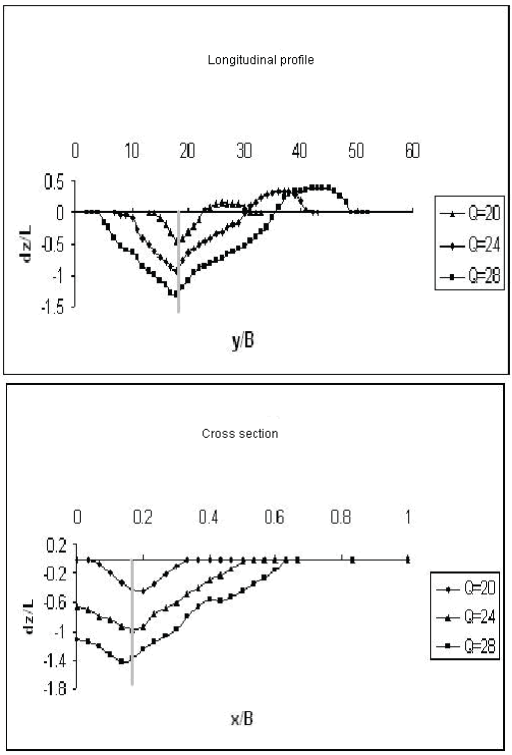

Fig. 6. Longitudinal and transversal profiles of maximum scoring depth in positions of 160 degrees with different discharges values

3.3. Variation of scoring depth in relation with flow rate and spur dike position in the bending

For investigation of effect of discharge value and spur dike position on the scoring depth in the bending simultaneously, changes of dz/l versus spur dike position in the bend is plotted for three different discharge values. Figure 7 indicates that maximum scoring depth around the spur dike has the direct relation with spur dike position and discharge values and it increases by increasing resting angle of spur dike or increasing discharge values. Also by considering the figure 7 one can conclude that maximum and minimum depth of scoring can be seen in the positions 30º and 160º respectively and after position 60º, scoring depth in comparison with position 60º decrease till position 120º, then it increases and reaches to its maximum at position 160º.

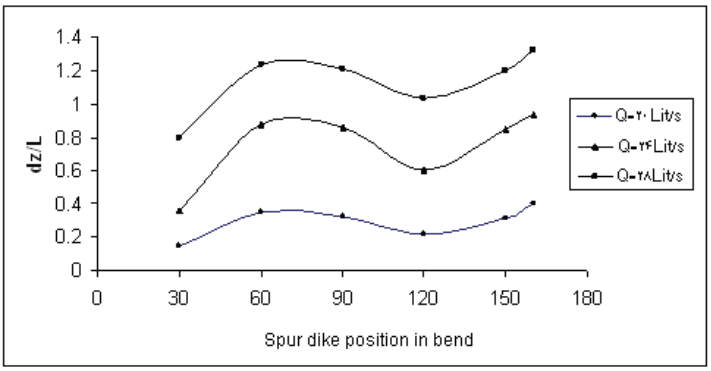

Fig.3. Variation of spur dike Positin and scoring for different discharge

References

Ahmed,M.,(1953),"Experiments on Design and Behavior of Spur dikes",Proc. Of Cong .of IAHR ,p.145

Garde,R.J.,et al, (1961),"Study of Scour Around Spur-dikes", Journal of Hydraulic Division., Vol. 87 , No .HY6.

Ghodsian,M, Tehrani,A.,(2001) ,"Scour Around Groins", International Journal. of Sediment Research V.16 N1 pp. 60-68

Gill,M.A,(1972),"Erosion of Sand Beds Around Spur dikes", Journal of Hydraulic Division., Vol. 98 , No .HY9.

Giri S.and , Shimizu Y,(2004)."Obzervation on bed variation in a meandering like flume with river training.

Mesbahi,J,(1992)"On Combined Scour Near Groynes in River Bends",M.Sc.Thesis Delft Hydraulics Report HH 132.

Przedwojski,B., Blazejewski,p.& Pilarzyk, K.W.,(1995),"River Training Techniques: Fundementals, Design and Application",Balkema, Rotterdam.

RaJaratnam,N.,& Nwachukwu, B.A, (1983), "Flow Near Groin-Like Structures", Journal of Hydraulic Engineering, ASCE , Vol:109, No3, p.463.

Soliman,M.M., Attia,K.M.,Kotb, Talaat, A.M. & Ahmed,A.F.,(1997)."Spur dike Effects on the River Nile Morphology after HighAswan Dam", Congress of the International Associaation of Hydraulic Research,IA.

PHYSICAL MODELING IN FLUME OF REGULAR AND IRREGULAR WAVE GENERATION FOR BERM BREAKWATER STUDY

Tiago ZENKER GIRELI [(1)], Paolo ALFREDINI [(2)] & Emilia ARASAKI [(3)]

[(1)] PhD, Coastal and Harbour Division of Hydraulic Laboratory of Escola Politécnica of Universidade de São Paulo , Av. Prof. Lúcio Martins Rodrigues, 120, São Paulo, 05508-900, Brazil. t_gireli@yahoo.com.br

[(2)] Associate Professor, Coastal and Harbour Division of Hydraulic Laboratory of Escola Politécnica of Universidade de São Paulo, Full Professor of Escola de Engenharia Mauá of Instituto Mauá de Tecnologia and Engineer VI of Centro Tecnológico de Hidráulica of Departamento de Águas e Energia Elétrica do Estado de São Paulo, Av. Prof. Lúcio Martins Rodrigues, 120, São Paulo, 05508-900, Brazil. alfredin@usp.br; paolo.alfredini@maua.br

[(3)] PhD Professor, Coastal and Harbour Division of Hydraulic Laboratory of Escola Politécnica of Universidade de São Paulo, Av. Prof. Lúcio Martins Rodrigues, 120, São Paulo, 05508-900, Brazil. earasaki@usp.br

1. Introduction

Considering the harbour and coastal structures significance for the Brazilian development and the complex Littoral Processes phenomena, these structures must not be designed based only on theoretical knowledge. Tools like physical models should be used to improve the project, in a way to reduce the costs of implantation and to minimize possible impacts in the environment caused by the construction.

One of these physical models is the wave flume that consists in a bidimensional model, which permits the study of sections of coastal structures under the action of waves in geometrical scales higher than 1:50. It allows scales up to 1:10 or higher, providing a more detailed study of structures like breakwaters.

In Brazil there are some wave flumes with studies related to Naval and Oceanic Engineering. However, the one of the Coastal and Harbor Division of Hydraulic Laboratory, Polytechnic School - University of São Paulo (LHEPUSP) is specifically directed to the study of ports and coastal structures by the Civil Engineering focus, which has notable importance in the development of the littoral cities of Brazil.

In 2000 the LHEPUSP asked to an important European Laboratory to sell a package to make this channel able to reproduce random waves, but due to the high cost, the LHEPUSP decided to develop its own system.

2. Purpose

This work has the purpose to develop a wave maker control system for the LHEPUSP wave fume able to generate irregular waves, based on wave energy spectra, and also, from a berm jetty case study, evaluate, from the technical point of view, the breakwater design procedure based on structure tests with design significative regular waves.

3. Materials and Methods

The LHEPUSP wave flume is prismatic and has internal dimensions of 50 m of length, 1,42m of height and 1,00 m of width. One of the flume lateral has laminated crystal, for visualization of wave dynamics and studied structures in an extension of 20 m. The wave generator consists in a piston sheet connected in its upper portion to a structure which is activated by an alternated current servomotor; a digital servo converter; a potentiometric gauge to 100cm, which is responsible for the system feedback regarding the position of the generator piston; stainless steel wire filters in beehive form are used to minimize the effect of harmonic parasites which results from the wave generation procedure; absorbing structures are

used to dissipate the wave energy in the wave flume extremes; a 500mm diameter pipeline connecting the flume extremes is used to prevent the system to piston the water, generating an uneven water surface; and a capacitive gauge for the measurement of the water level variation in the flume portion of interest. Figure 1 shows these elements that compose de LHEPUSP wave flume.

Figure 1 – Composition of elements that describe the LHEPUSP wave flume.

The wave maker control system was developed using the LabView® computational language that is a widely used tool to improve automation systems in a way to reproduce in shallow water, wave trains based on theoretical or real energy spectra. For this reason, the system uses an iterative calibration step, in which all the wave flume parameters are set.

For the case study, a section of real berm breakwater was modelled in 1:25 and studied under irregular and regular waves with the same significative height. The behaviour difference was evaluated from the berm recession and the intersection depth (PIANC, 2003). For this reason, a topo-bathimetric survey was done before and after each running, generating the profile sections M1 (averaging one), M2 (averaging two) and NS (maximum recession section).

Two runnings for each condition were done to evaluate the result repeatability. They were called R1 and R2 when referring to regular waves and I1 and I2 when referring to irregular waves. Finally, the same structure was inserted in a higher depth, which no waves broken before to reach the breakwater. These runnings were called PR1 and PR2 when referring to regular waves and PI1 and PI2 when referring to irregular waves.

4. Results

The Figure 2 shows the interface with the user and the block diagram of the software, which was developed in the LabView language to control the generation of random waves. Figure 3 presents some examples of irregular wave trains calibrated by the developed system and used during the case study runnings. Figure 4 shows an example of the profile sections obtained after the runnings.

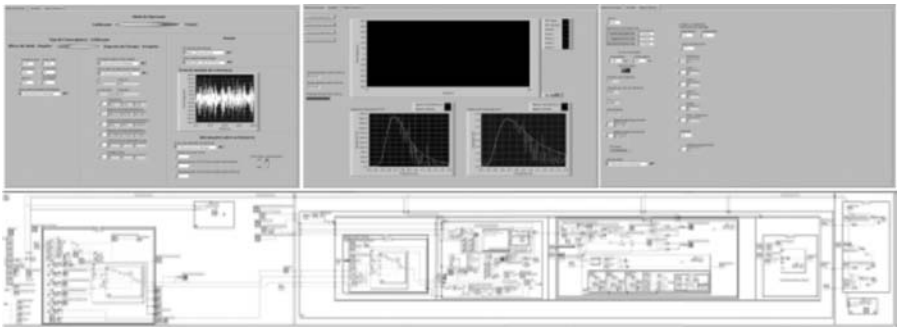

Figure 2 – Composition of elements that describe the software to control the wave generation Interface with the user and the block diagram.

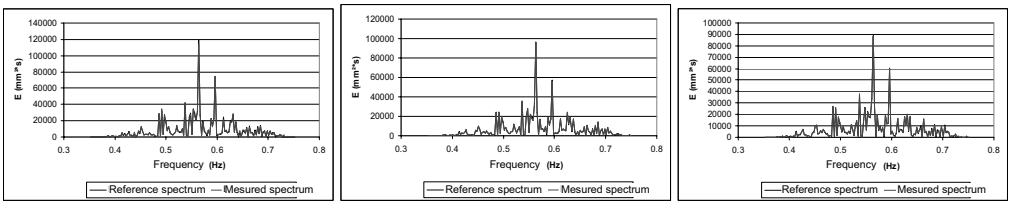

Figure 3 – Examples of irregular wave trains calibrated at LHEPUSP wave flume.

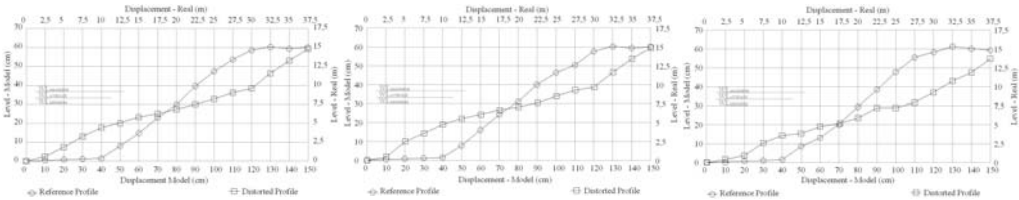

Figure 4 – Profile sections M1, M2 and 4S obtained during R1 running.

The Tables 1 until 4 present the berm recession and the intersection depth obtained during the runnings.

Table 1 – Recession and intersection depth obtained during R1 and R2 runnings

		R1-M1	R1-M2	R1-4S	R2-M1	R2-M2	R2-5S
experimental recession	**model (mm)**	317	318	403	334	343	363
	real (m)	7.91	7.94	10.07	8.35	8.56	9.08
experimental Intersection depth	**model (mm)**	73	63	127	89	79	85
	real (m)	1.83	1.57	3.16	2.22	1.97	2.13

Table 2 – Recession and intersection depth obtained during I1 and I2 runnings

		I1-M1	I1-M2	I1-6S	I2-M1	I2-M2	I2-3S
experimental recession	**model (mm)**	215	212	234	182	190	231
	real (m)	5.38	5.29	5.85	4.54	4.74	5.77
experimental Intersection depth	**model (mm)**	90	80	89	110	96	119
	real (m)	2.26	1.99	2.22	2.74	2.41	2.98

Table 3 – Recession and intersection depth obtained during PR1 and PR2 runnings

		PR1-M1	PR1-M2	PR1-9S	PR2-M1	PR2-M2	PR2-9S
experimental recession	**model (mm)**	364	374	403	344	356	368
	real (m)	9.09	9.36	10.07	8.61	8.61	9.21
experimental Intersection depth	**model (mm)**	142	156	127	126	152	137
	real (m)	3.54	3.91	344	3.15	3.79	3.42

Table 4 – Ressection and intersection depht obtainde during PI1 and PI2 runnings

		PI1-M1	PI1-M2	PI1-8S	PI2-M1	PI2-M2	PI2-3S
experimental recession	**model (mm)**	268	267	330	278	284	343
	real (m)	6.7	6.67	8.24	6.96	7.09	8.57
experimental Intersection depth	**model (mm)**	136	146	156	150	141	162
	real (m)	344	3.65	3.89	3.75	3.52	4.04

5. Discussion

About the software which was developed for the generator control it was possible to notice that the LabView programming language has shown itself very efficient, allowing the software development as planned, without surpassing the microcomputer processing capacity used in the data acquisition.

Comparing the runnings R1/R2 with I1/I2 it's perceptible that the recession presented for the structure under regular waves action was bigger than the one that it was under the action of irregular waves with same Hs. These results show that using regular waves in physical model, to design berm breakwaters, result in conservative structures when the project wave is defined by the breaking because it's used a energy higher than the one that really reaches the structure, mainly considering that some waves of the real train would break before reach the breakwater. In relation to the deep breakwater, the results obtained had shown that in average terms, the structure under action of regular waves had a recession 24% higher than the one it was under action of irregular waves. However, for the sections of maximum recession the difference was reduced to only 7.5%.

6. Conclusion

In general, the results of the tests show that the new system of wave generation of LHEPUSP was conceived successfully, providing this important tool to assist the development of coastal and port structures projects.

The case study showed, as conclusion, that the regular waves use for berm breakwaters design physical model improvement may suggest conservative results, inducing high cost structures, mainly for those ones in depths lower than 10 meters, being observed larger structural backward response differences, comparing with irregular waves action with the same significative height.

References

PIANC, 2003. State-of-the-Art of Designing and Constructing Berm Breakwaters

Taveira-Pinto, F & Neves, A. C., 2003. A Importância da Consideração do Carácter Irregular da Agitação Marítima no Dimensionamento de Quebramares de Taludes. Engenharia Civil Um, nº 16, 95 p.

U. S. ARMY/COASTAL ENGINEERING RESEARCH CENTER – CEM, 2002. Coastal Engineering Manual.

AN EXPERIMENTAL ANALYSIS OF THE HYDRODYNAMICS OF SUBMERGED STRUCTURES DISSIPATING BY MACRO-ROUGHNESS

Carlo LORENZONI [(1)], Maurizio BROCCHINI [(2)], Alessandro MANCINELLI [(3)], Luciano SOLDINI [(4)], Elisa SETA [(5)] & Matteo POSTACCHINI [(6)]

[(1)] Assistant Professor, Istituto di Idraulica e Infrastrutture viarie, Università Politecnica delle Marche, via Brecce Bianche, Ancona, 60131, Italia, c.lorenzoni@univpm.it

[(2)] Associate Professor, Istituto di Idraulica e Infrastrutture viarie, Università Politecnica delle Marche, via Brecce Bianche, Ancona, 60131, Italia, m.brocchini@univpm.it

[(3)] Full Professor, Istituto di Idraulica e Infrastrutture viarie, Università Politecnica delle Marche, via Brecce Bianche, Ancona, 60131, Italia, a.mancinelli@univpm.it

[(4)] Assistant Professor Istituto di Idraulica e Infrastrutture viarie, Università Politecnica delle Marche, via Brecce Bianche, Ancona, 60131, Italia, l.soldini@univpm.it

[(5)] Ph.D. student, Istituto di Idraulica e Infrastrutture viarie, Università Politecnica delle Marche, via Brecce Bianche, Ancona, 60131, Italia, e.seta@univpm.it

[(6)] Ph.D. student, Istituto di Idraulica e Infrastrutture viarie, Università Politecnica delle Marche, via Brecce Bianche, Ancona, 60131, Italia, m.postacchini@univpm.it

Abstract

The working features of innovative coastal defence structures, which dissipate the energy of the incoming waves by the action of large-scale bottom unevennesses (metal blades, either normal to the bottom or inclined at 45°, covering the lower half of the water depth), is investigated by means of a laboratory experimental campaign. Focus is given to characterizing the details of the flow evolution near to the structures.

1. Introduction

Various studies on the working of submerged breakwaters used to defend shorelines prone to erosion have highlighted the establishment of two mechanisms which reduce the efficiency of the structures: 1) large mean water levels gradients of the sea surface, 2) large-scale vortical structures (macrovortices) with vertical axis (Brocchini et al., 2004). The former increase the transmission of waves inshore of the breakwaters and favour, together with macrovortices, the generation of dangerous rip currents offshore directed.

In particular the Istituto di Idraulica e Infrastrutture Viarie of the Università Politecnica delle Marche of Ancona has performed a series of hydrodynamic laboratory experiences on two-dimensional physical models in reduced scale with the aim both of understanding the hydrodynamic behaviour of "dissipative structures" composed by a series of vertical or tilted blades and of quantifying the reduction of the wave motion produced by the mentioned coastal dissipative structures for their eventual use in the defence of shorelines prone to erosion. The object of the experimental campaign has been the study of the wave motion and of the main hydrodynamics features induced by the presence of the structure to characterize the influence of the various model configurations on the hydrodynamic field surrounding the structures. One further scope of the work was to verify if the use of mentioned dissipative structures would allow for the flow inversion in a typical rip-current configuration (nearby submerged structures) as suggested by Nobuoka et al.(1996).

2. Description of the Experimental Tests

The experimental tests have been made in a wave flume with a rectangular cross section, equipped with a system for the wave generation at its inside. The inside dimensions of the flume are: length 50m, width 1m, height from the bottom 1,3m. The sidewalls of the flume are glassed for the central 36m.

Focusing on the specific experiments at hand, each single element of the models is made by a steel blade soldered to a slab of the same material which serves as basis for the placement on the horizontal bottom of the flume. To the aim of realizing the various structure types to be examined, blades inclined at 45° and 90° to the horizontal have been used (Figure 1).

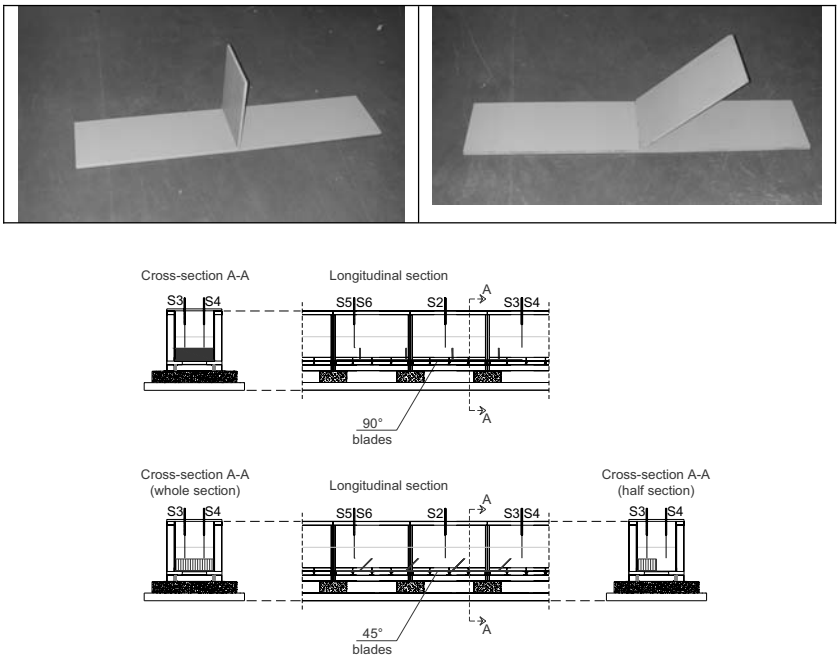

Figure 1. Elements used for the experiments with blades inclined at 90° (top left) and 45° (bottom left); longitudinal and cross-sections of the tested configurations (right).

The test configurations have been obtained by suitable assembly of the various test elements to simulate the possible configuration of coastal defence structures. For the case at hand such configuration is made by a set of four rows of submerged blades (vertical or inclined) on a depth of 60cm.

For the campaign of experimental tests the models reproduced the hypothetical field configurations with a reduction of geometric scale equal to the considerable value of 1:5 using the Froude similitude.

The tests have been performed with three configurations:

1. configuration i) blades covering the whole flume cross-section for both blade inclinations;
2. configuration ii) blades covering half of the flume cross-section along a side of the channel;
3. configuration iii) no structures at all.

The flow motion has been forced by waves, both regular than spectral, through a piston-type wavemaker. The measuring instruments used are of two types: n.8 electro-sensitive elevation gauges and n.2 three-dimensional Acoustic Doppler Velocimeters (ADVs).

The chosen position of the models guarantees undisturbed measurements for the duration of at least 20s and a minimal distance (about one wavelength) from the wavemaker.

For each of the examined configurations various experimental runs with wave cycles repeated more times of the same waves have been performed to achieve statistically-significant results.

The various regular waves are characterized by different heights. The first two regular waves, because of their large steepness, reached the model in breaking conditions, so their damping was due to both bottom friction and breaking effects. The other, smaller, input waves reached the structures without breaking, and their height reduction was arranged by frictional effects due to the steel blades.

Spectral waves were generated by using the *Jo.N.S.Wa.P.* spectrum.

3. Flow field results and discussion

Quantitative results have been obtained, both for the main synthetic parameters (wave height decay and mean water level superelevation) and for the hydrodynamic circulation induced in the vertical plane, which provide an important characterization of the working of such innovative coastal defence structures made of arrays of nearbed blades. Structures made with vertical and inclined blades provide an important and quantitatively similar wave height decay but the second typology induces lower mean water superelevations (and at times moderate setdowns inshore of the structure) compared to the other one (Lorenzoni et al., 2008).

A better characterization of the working of the structures at hand requires a more sound explanation of the wave height decay and mean water superelevation in terms of the total energy budget and by properly describing the energy removal from the wave modes. This, in turn, needs a much better description of the internal flow kinematics. To this purpose we inspected the flow by means of a non-intrusive approach which makes use of optical velocimetry methods to derive from available video images the fields characterizing the internal kinematics of the flow at hand.

Figure 2 shows two examples of the vertical flow circulation as derived from trajectories obtained by means of the FT-PTV software described in Miozzi (2004) directly from the video recordings of the experiments. Similar analyses reveal the presence of large-scale vortices with horizontal axes (macrovortices) which are believed to be responsible for much of the wave energy draining in favour of vortical features of various sizes (from the integral scale to the dissipative one). The dynamics, similar to that established at an abrupt flow expansion, is currently investigated with reference to that of a "*backward-facing step*". Obvious differences, like a) the flow unsteadiness and b) the presence of a moving boundary (i.e. the free surface), will be accounted for once some basic knowledge on the overall internal kinematics is achieved.

Simple inspection of maps like those of Figure 2 immediately allows for a first characterization of the integral-scale vortices. For example, it is clear that, each of the examined cell between two nearby blades can contain two counter-rotating vortices.

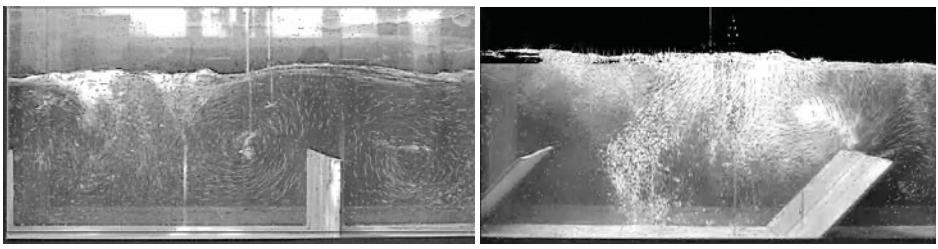

Figure 2. Description of the motion field by means of the FT-PTV software. Left: vertical blades. Right: 45° blades

Other flow features of interest are the smaller-scale edge vortices like those illustrated in Figure 3 which generated soon after the arrival of the wave crest in the form of spanwise vortices (top left panel) evolve under the action of flow perturbations in shapes similar to those of rather open hairpin vortices (top right panel) and decay once transported seaward of the blade (bottom left panel). The overall evolution is illustrated in the bottom right panel of Figure 3.

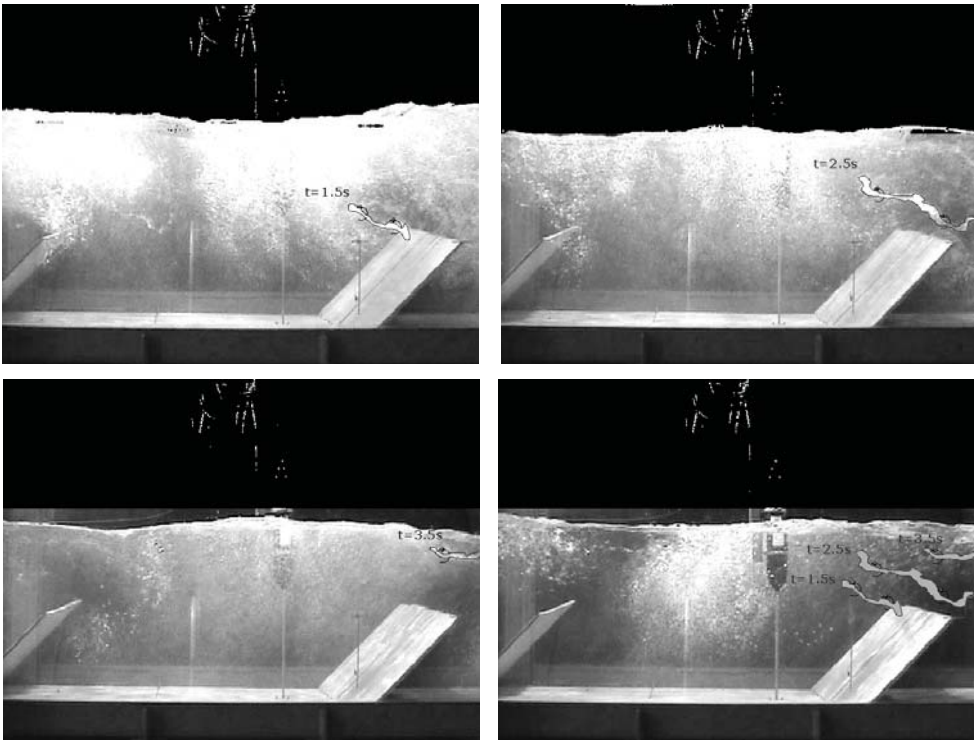

Figure 3. Schematic illustration of evolution of edge vortices elongated in the spanwise direction.

Acknowledgments

The present research has been partially financed with the contribution of the C.P.S. company (Italy).

References

Brocchini, M., Kennedy, A.B., Soldini, L. and Mancinelli, A. (2004). Topographically-controlled, breaking wave-induced macrovortices. Part 1. Widely separated breakwaters, *J. Fluid Mech.* 507: 289-307.

Lorenzoni, C., Brocchini, M., Mancinelli, A. and Soldini, L. (2008) On the working of defence coastal structures dissipating by macro-roughness. *J.W.P.C.O.E.-ASCE* (submitted for publication).

Miozzi, M., (2004). Particle image velocimetry using feature tracking and Delaunay tessellation, *Proc. 12th Int. Symp. on Appl. Laser Tech. to Fluid Mech.*

Nobuoka, H., Irie, I., Kato, H. and Mimura, N. (1996). Regulation of Nearshore Ciculation by Submerged Breakwater for Shore Protection, *Proc. 25th ICCE-ASCE,* 2394-2403.

Piattella, A. and Mancinelli, A. (2006). Idrodinamica costiera generata da "strutture dissipative". *Atti del XXX Convegno di Idraulica e Costruzioni Idrauliche*, CD-ROM, Paper N. 127, (in italian).

Soldini, L. Lorenzoni, C., Mancinelli, A. and Brocchini, M. (2007). Mitigating the impact on the nearshore hydro-morphodynamics of macrovortices generated at submerged breakwaters. *Proc. Coastal Structures'07* (in print).

STUDY OF THE WAVE DAMPING DUE TO A POROUS BED

Sara CORVARO [(1)], Alessandro MANCINELLI [(2)], Carlo LORENZONI [(3)], Elisa SETA [(4)] & Matteo POSTACCHINI [(5)]

[(1)] *Ph.D. student, Istituto di Idraulica e Infrastrutture viarie, Università Politecnica delle Marche, via Brecce Bianche, Ancona, 60131, Italia, s.corvaro@univpm.it*

[(2)] *Full Professor, Istituto di Idraulica e Infrastrutture viarie, Università Politecnica delle Marche, via Brecce Bianche, Ancona, 60131, Italia, a.mancinelli@univpm.it*

[(2)] *Assistant Professor, Istituto di Idraulica e Infrastrutture viarie, Università Politecnica delle Marche, via Brecce Bianche, Ancona, 60131, Italia, c.lorenzoni@univpm.it*

[(4)] *Ph.D. student, Istituto di Idraulica e Infrastrutture viarie, Università Politecnica delle Marche, via Brecce Bianche, Ancona, 60131, Italia, e.seta@univpm.it*

[(5)] *Ph.D. student, Istituto di Idraulica e Infrastrutture viarie, Università Politecnica delle Marche, via Brecce Bianche, Ancona, 60131, Italia, m.postacchini@univpm.it*

Abstract

In the paper are shown the first results of the experimental investigation on the damping of waves propagating over a submerged porous bed, carried on in the wave flume of the laboratory of the "Istituto di Idraulica e Infrastrutture Viarie" of the "Università Politecnica delle Marche". The presence of the rigid porous bed, made of plastic spheres filled with sand, induces an attenuation of the wave height of 20-30% larger than that due to both smooth and rough beds. The experimental results are compared to the theoretical findings of Liu and Darlymple (1984) and of Gu and Wang (1991) and confirm the experimental finding of Sawaragi and Deguchi's (1992). Interstitial pressures within the porous bed are also assessed.

1. Introduction

The present work illustrates a study of the damping of waves passing over submerged porous bed. Wave transmission and dissipation due to friction across the permeable bed are the macroscopic effects of the interaction between the external wave motion and the porous medium flow. The laboratory data, result of the dedicated laboratory campaign described In section 3, are presented and compared with literature theoretical descriptions.

Typically, laminar flows occurring in porous media can be described by Darcy's formula. For turbulent flows use of Forchheimer's equation was first proposed by Bear (1972), while for unsteady flows an extended Forchheimer equation can be used. Van Gent (1995) discussed in detail the role of the different parameters which influence the flow through permeable structures.

Karunarathna and Lin (2006) presented a two-dimensional numerical model to study the wave damping over porous seabeds. Several experiments and numerical studies were conducted on submerged permeable structures to identify the influence of the porous medium on the hydrodynamics, while few experimental tests were performed over permeable beds (e.g. Savage, 1953; Sawaragi and Deguchi, 1992). It is evident the need of studying the influence of both hydraulic and geometric properties of the porous layer on the wave damping.

2. The theoretical approach

The flow through porous media can be studied using Forchheimer's equation. The nonlinear turbulent

resistance term is, usually, replaced by a linear resistance term (Sollitt and Cross, 1972). Gu and Wang (1991) extended the model to include the effects of both inertia and turbulent resistances. They introduced a linearized resistance coefficient which is made of three resistance components (linear, turbulent and inertial) and which is evaluated by applying the "Principle of equivalent work".

Liu and Darlymple (1984) assumed that the flow bottom was irrotational above the porous bed, while they adopted the Dagan's porous flow model inside the permeable medium. For porous beds with a finite thickness, they obtained a complex wave dispersion relation:

$$\sigma^2 - gk_w \tanh k_w h = -\frac{i}{(\nu/\sigma k_p - i/n)} \tanh k_w d(gk_w - \sigma^2 \tanh k_w h) \qquad [1]$$

where h is the water depth, d is the thickness of the permeable, σ is the wave frequency, ν is the Kinematic viscosity of the fluid, n and k_p are the porosity and the intrinsic permeability of the porous medium and k_w is the wave number (k_w is a complex number whose real part k_r measures the change in wavelength, whereas the imaginary part k_i measures the damping of the wave height). In order to calculate k_w the expression needs to be solved iteratively. Gu and Wang (1991) derived a similar complex wave dispersion relationship, based on Forchheimer's equation, where both the wavenumber and the linearized friction coefficient were complex variables. The dispersion equation was solved iteratively to calculate k_w, while the linearized friction coefficient was provided through an analytical solution.

3. The experiment

The experiments were performed in the wave flume of the laboratory of the "Istituto di Idraulica e Infrastrutture Viarie" of the "Università Politecnica delle Marche" (Ancona). The channel is 50m long, 1m wide and 1.3m high and the sidewalls are glassed for the central 36m..

The water depth in the tank, over the physical model, was of 0.30m. The flow motion was forced by waves, both regular and irregular and of various steepnesses, through a piston-type wavemaker (operating maximum run of ±0.5m).. Table 1 shows characteristics of both regular (wave height H, period T and Ursell parameter Ur) and spectral Jo.N.S.Wa.P. waves (significant wave height H_s and peak period T_p).

Table 1. Waves characteristics.

	Regular Waves									Spectral Waves		
Wave	**A**	**B**	**C**	**D**	**E**	**F**	**G**	**H**	**I**	**L**	**M**	**N**
H/ Hs (cm)	3.58	3.58	5.00	10.00	10.00	10.00	15.00	15.00	20.00	10.00	10.00	15.00
T/Tp (s)	1.00	1.50	1.50	1.50	2.00	2.50	2.00	2.50	2.50	2.0	2.5	2.5
Ur	0.66	3.33	4.65	9.30	29.40	71.78	44.10	107.68	143.57			

At the opposite end of the flume a wave-absorbing mattress was placed with the function of reducing the wave reflection induced by the vertical rigid end-wall of the flume. Waves were run over three different bed configurations: i) a permeable bed, ii) a rough impermeable layer and iii) a smooth layer.

The model, which is 6m long, was placed on the horizontal bottom of the wave tank (Figure 1). The thickness of the permeable bed was of 18.2cm and the porous medium was composed of 6 layers of plastic spheres filled with sand of 3.6cm mean diameter. The rough impermeable bottom was made of a single layer of spheres.

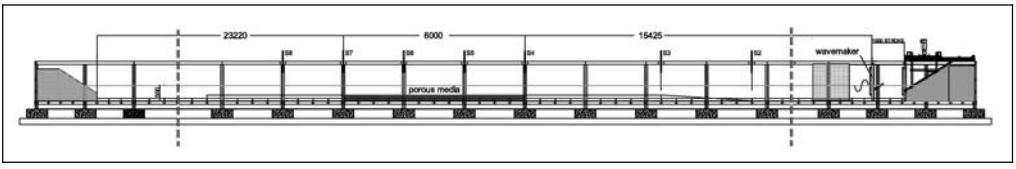

Figure 1. The physical model.

The measuring instruments used were: 8 electro-sensitive elevation gauges and 2 three-dimensional Acoustic Doppler Velocimeters (ADVs). The former gauges, used to measure the water levels, and the ADVs, employed for the measurement of the flow velocity along two verticals, were located as shown in figure 2.

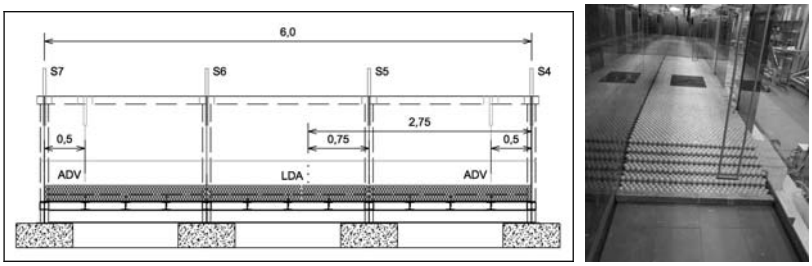

Figure 2. Instruments positions.

In order to obtain measurements with no disturbances induced by any wave reflected at the end-wall of the flume (the absorbing mattress does not provide full wave absorption), the models were placed at a sufficient distance (approximately 23m) from such an end. Undisturbed conditions were reached after a transient of about 8s during which the wave height ramped up to the regime conditions. Such a solution guarantees measurements in quasi-steady conditions for the duration of at least 15÷20s. Also a minimal distance (more than 15m, at least two wavelengths) was placed between the wavemaker and the models to allow waves to develop before reaching the region of interest.

In order to measure stresses in the area of interest 5 piezoresistive pressure transducers were fixed inside the porous media and 2 on it.

Finally both Laser Doppler Anemometry (L.D.A.) and the available F.T.-P.T.V. software (described in Miozzi, 2004) were efficiently employed to study the development of the flow turbulence in the absence of breaking.

4. Results

Preliminary results on the wave damping over the porous bed are first reported. The comparison among the three different beds (smooth, rough and porous) shows the importance of the permeable medium for the attenuation of the wave height. The damping undergone by a non-breaking wave which overpasses the porous bed is about 20-30% of the incident wave height, the influence of the porous bed being greatly reduced in the case of breaking waves (e.g. Wave I).

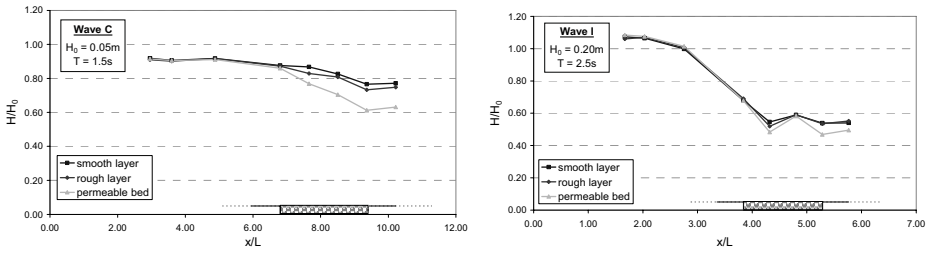

Figure 3. Experimental results of the wave damping over the porous bed (Wave C - left panel; Wave I - right panel).

The laboratory data are compared to both Liu and Darlymple's (1984) and Gu and Wang's (1991) theories. Both theoretical descriptions underpredict the observed wave attenuation.

Our experimental findings are in good agreement with Sawaragi and Deguchi's (1992) laboratory data. Two experiments conditions (e.g. wave A, wave B) were performed to compare with Sawaragi and Deguchi's (1992) (e.g. J-2 and J-6) and estimate the importance of geometric properties of the porous medium. It is found that the wave attenuation increases with the ratio *d/h*.

The pressure measurements clearly illustrate the decrease of the dynamic pressure (absolute value) due to the water flowing through the porous medium. Figure 4 shows the difference of the pressure between the linear theory and the experimental data for the case of the Wave C, which is characterized by a low value of the Ursell parameter *Ur*.

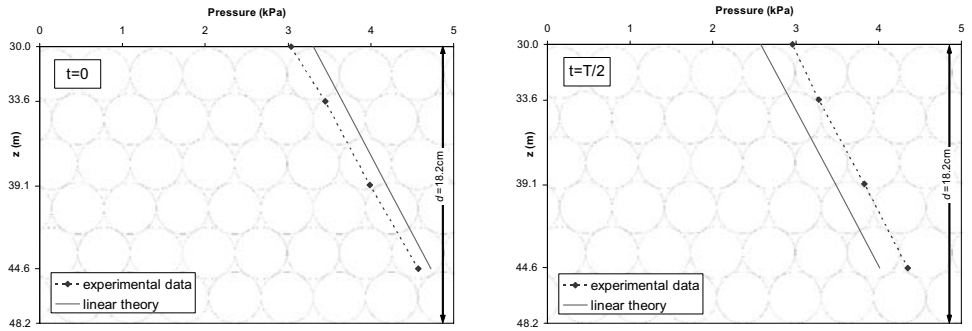

Figure 4. The difference of the pressure value between the experimental data and the linear theory for the case of the Wave C (t=0 - left panel; t=T/2 - right panel).

5. Conclusion

The preliminary results here reported confirm an influence of the porous medium on the wave damping of about 20-30%. The role of the geometric properties is also investigated. These experimental measurements provide further information about hydrodynamics quantities like the pressure inside the porous medium and the velocity over it. We are currently studying the velocity and Reynolds stresses induced by the porous bed.

Experiments are planned to be conducted over permeable beds extending up to the swash zone, with particular attention to the analysis of bed permeability effects on the hydrodynamics.

References

Bear, J. (1972). 'Dynamics of fluids in Porous Media', American Elsevier, New York.

Dagan, G. (1979). The generalization of Darcy's law for nonuniform flows, *Water Resour. Res*., 15(1), pp 1-7.

Gu, Z. & Wang, H. (1991). Gravity waves over porous bottom, *Coastal Engineering*, 15(5), 497-524.

Karunarathna, S.A. and Lin, P. (2006). 'Numerical simulation of wave damping over porous seabed', *Coastal Engineering* 53, pp 845-855.

Liu, P.L.-F and Darlymple, R.A.(1984). 'The damping of gravity waves due to percolation', *Coastal Engineering* 8, pp 33-49.

Miozzi M. Particle Image Velocimetry using Feature Tracking and Delaunay tessellation, *Proc. 12th Int. Symp. Applied Laser Techniques to Fluid Mechanics*, Lisbon 2004.

Savage, R.P. (1953). Laboratory study of energy losses by bottom friction and percolation. Beach erosion Board, *Corps of Engineers*, Technical Memorandum, 31.

Sawaragi, T. and Deguchi, I. (1992). 'Waves on permeable layers', Proc. 23rd *Coastal Engineering Conference*, ASCE, Venice, pp 1531-1544.

Sollitt, C.K. and Cross, R.H. (1972). 'Wave transmission through permeable breakwaters', *Proc. 13th Coastal Engineering Conference*, ASCE, New York, pp 1827-1846.

Van Gent, M. (1995). 'Wave interaction with Permeable Coastal Structures', Ph.D Thesis, Delft University.

Alternative methods for shear stress estimate in oscillating flows: preliminary investigations

Carla FARACI [(1)], Enrico FOTI [(2)], Romano FOTI [(2)] & Salvo BAGLIO [(3)]

[(1)] *Department of Civil Engineering, University of Messina, C.da di Dio, S. Agata (ME) 98166, Italy. faraci@ingegneria.unime.it*

[(2)] *Department of Civil and Environmental Engineering, University of Catania, v.le A. Doria, 6, Catania, 95125, Italy. efoti@dica.unict.it*

[(3)] *Department of, Electric, Electronic & System Engineering, University of Catania, v.le A. Doria, 6, Catania, 95125, Italy. sbaglio@diees.unict.it*

Abstract

In this paper innovative experimental techniques allowing for the estimate of shear stresses at the wall and within the water column of an oscillating flow are discussed. In particular, bioluminescence, i.e. the property shown by some micro-algae of emitting light under the action of shear stresses induced by the flow, has been applied to assess the stresses within the fluid flow. On the other side, ferrofluid materials, i.e. stable suspensions of colloidal ferromagnetic particles in non-magnetic carrier liquids, have been tested in order to measure the shear stresses at the wall.

1. Introduction

The estimate of the shear stress is crucial in fluid mechanics. For instance, energy losses generated by gravity waves can be estimated only in the light of the dissipations inside the boundary layers. However, their direct measurement has always been a problem absolutely non trivial. So far the instruments able to directly measure shear stresses are only hot film probes and shear plates, which can measure exclusively on smooth wall, but certainly are not able to provide measurements inside the moving fluid, where shear stresses are obtained by accurately measuring the flow velocities.

Recently Latz and Rohr (1999) observed that some micro-algae known as dinoflagellates, in the presence of a fluid flow, both laminar and turbulent, emitted short flashes of light; such a phenomenon, known in literature as bioluminescence, enhances with a monotonic law when the flow shear stress increases too. Such a growth is partly associated to a larger number of cells excited by the flow, and partly related to a brighter luminosity of the flashes when the stress increases. In particular they recognized that a monotonic response of the luminous intensity to the change in shear stresses occurred in the range between approximately 0.1 and about 2 N/m^2 (Rohr et al. 2002). Such a property can therefore be applied in order to recover shear stresses within such a range by measuring the emitted bioluminescence. Above the higher threshold, luminescence emission remains constant at increasing stress values and therefore quantitative information on shear stresses can be no longer determined, even though the luminescent response can still be adopted as a passive flow tracer.

On the other hand, ferrofluids, i.e. stable suspensions of colloidal ferromagnetic particles in non-magnetic carrier liquids, show three main properties: they stick to a magnet, they take on the 3-dimensional shape of the magnetic field that passes through it, they change their apparent density in proportion to the strength of the magnetic field that is applied to them.

In particular, apparent viscosity of ferrofluids is enhanced as external magnetic field and magnetite concentration increase (Odenbach, 2004). With the increase of the concentration the strong magnetic interaction of the particles in the magnetic field leads to the formation of chain-like structures aligned in the field direction. The breakage and formation of the chain-like structures are a result of competition

between the particle interaction and the shear flow (Zhang et al, 2005).

2. Description of the measurement strategies

2.1 Bioluminescence measurements

The idea to determine the shear stresses by analyzing the bioluminescence radiated by the micro-algae has been investigated in order to implement a reliable measurement technique able to provide shear stress measurements everywhere inside the fluid flow. The involvement of biological and optical aspects, besides the properly hydraulic features, implies an accurate procedure of instrument optimization in order to address in a suitable way the peculiarity of the investigated phenomena.

Under this perspective, the experimental set up design had to face two type of problems: on one side an hydraulic apparatus, easy to manage and which enables the performance of several experiments with small quantities of water (and, thus, dinoflagellates) and on the other side an accurate calibration of biological and optical visual instruments, was needed.

An annular cell, specifically designed for the present investigation, is constituted by a couple of coaxial cylinders, which can move simultaneously around their axis, generating an oscillating flow of fixed frequency and oscillation amplitude. The bottom of such apparatus was covered by a fixed wavy bed.

The bioluminescent dinoflagellate *Alexandrium tamarense*, 22-50 μm sized, has been adopted in order to allow bioluminescence production. The low bioluminescence intensity and duration did not enable to capture the light signal easily. It was necessary to adopt intensified photon counter systems equipped with a CMOS-APS sensor and intensified CCD video cameras.

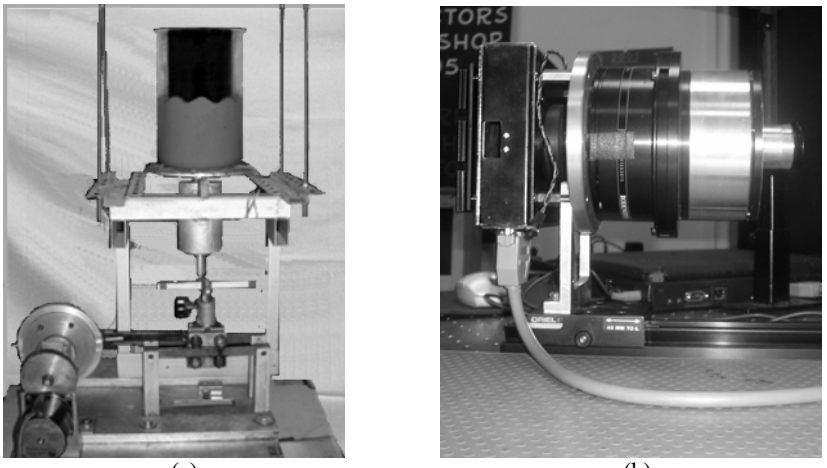

(a) (b)

Figure 1. Picture of the annular cell adopted for both bioluminescence and ferrofluid experimental campaigns (a); intensified CCD camera (b).

2.1 Ferrofluid measurements

At the walls, where the highest velocity gradients induce the strongest stresses and bioluminescence could be no longer effective due to the constant light emission, ferrofluids have been adopted. In particular, as a ferrofluid immersed in water, in the presence of an external magnetic field can exhibit spikes and chain-like structures aligned in the field direction (Figure 2a), such a property has been applied in order to recover the shear stress originated in complex flows: in particular, measuring the magnetic field and visualizing the spikes characteristics it was possible to recover the shear characteristics within the flow. The same annular cell previously described has been adopted here, by modifying the base of the cell inserting a magnet. In such a case the bed has been kept flat. An

incremental encoder, which gives a square wave with a variable frequency, has been used to recover the oscillation velocity of the annular cell. Images were gathered through a digital microcamera (Figure 2b). All the system was driven by a model developed in a Labview environment

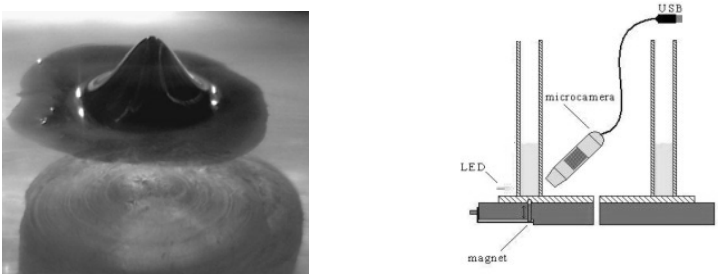

(a) (b)

Figure 2. A single spike of ferrofluid as formed within the annular cell just over the magnet (a); sketch of the annular cell application for the ferrofluid experiments (b).

3. Application of the measurement strategies

Direct observation of the flow inside the moving annular cell, showed the existence of stimulated cells which emit bioluminescence even at lower stress values than those indicated in literature. In Figure 3 two frames extracted from one of the gathered movies, obtained imposing an oscillation amplitude A of 2.4 cm and a period T of 1.7 s, are reported. In the two frames a high degree of bioluminescence emission seems to be concentrated in the lower part of the window, i.e. close to the rippled bed, where the larger shear stresses occur. Moreover it is possible to recognize the vortex structures separating at the ripple crest, thus giving a positive response to the possibility of using bioluminescence as a visualization tool.

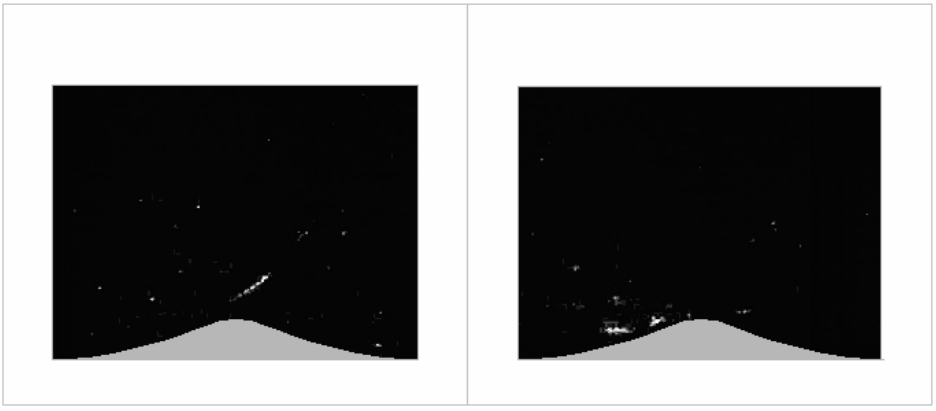

(a) (b)

Figure 3. Bioluminescence detected in the annular cell over the rippled bed (A=2.4 cm, T=1.7 s). ωt=90° (a) and ωt=270°, ω being the angular frequency. The rippled bed is qualitatively superimposed.

In order to obtain shear stress measurements starting from ferrofluid spikes, the contour of the spike is approximated with a triangle, whose top edge is projected onto its base. At rest conditions the projection coincides with the median point of the base, but when the flow oscillates the spike deforms and its edge shifts, as it can be better understood by looking at Figure 4. By knowing the displacement and the elapsed time it is thus possible to recover the spike - and thus the flow - velocity. Since the ferrofluid spikes are less than 1 mm high, this leads to the possibility of gathering velocities much closer

to the wall than typical instruments, such as ADV or LDA.

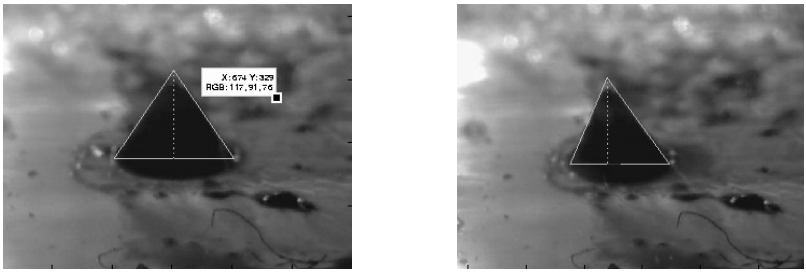

(a) (b)

Figure 4. An example of how the displacement of ferrofluid spike is estimated: a spike at rest (a), and the same spike at wt=270° of the oscillation cycle. The displacement is marked on the triangle base.

The application of both the previously mentioned techniques for the measurements of the shear stresses in the bottom boundary layer is still at a prototypal stage. However preliminary results obtained in laminar conditions (i.e. in those conditions where also analytical solutions hold) seem to confirm the reliability of the techniques and the possibility of application even to complex flows. Further developments will consider to export the application in larger facilities.

References

Latz, M.I., Rohr, J. 1999. 'Luminescent response of the red tide dinoflagellate Lingulodinium polyedrum to laminar and turbulent flow'. *Limnol. Oceanography* 44(6) pp.1423-1435.

Rohr, J., Hyman, M., Fallon, S., Latz, M.I. 2002. 'Bioluminescence flow visualization in the ocean: an initial strategy based on laboratory experiments' *Deep Sea Research I*, 49, pp. 2009-2033.

Odenbach, S. 2004. 'Recent progress in magnetic fluid research' *J. Phys. Condens. Matter* 16, pp.R1135–R1150

Zhang J. H., Xu X. F., Si M. S., Zhou Y. H, Xue D. S. 2005. 'Hydrodynamic Properties of Fe3O4 Kerosene-Based Ferrofluids with Narrow Particle Size Distribution' *Chinese Phys. Lett.* Vol. 22, No. 11, pp. 2944-2946

AERATION OF THE OVERTOPPING FLOW DUE TO BREAKING WAVES

YONG-UK RYU [(1)], KUANG-AN CHANG [(2)] & JONG-IN LEE [(3)]

[(1)] *Postdoctoral Research Fellow, River and Coast Research Division, Korea Institute of Construction Technology, Daehwa 2411, Goyang, Gyeonggi-Do 411-712 Korea. yuryu@kict.re.kr*

[(2)] *Associate Professor, Zachry Department of Civil Engineering, Texas A&M University, College Station, Texas, 77843-3136 USA. kchang@civil.tamu.edu*

[(3)] *Research Fellow, River and Coast Research Division, Korea Institute of Construction Technology, Daehwa 2411, Goyang, Gyeonggi-Do 411-712 Korea. jilee@kict.re.kr*

Abstract

The present study investigates the void fraction and velocity of an overtopping flow on a structure through laboratory measurements. The measured two-dimensional mean void fraction and velocity distributions were depth-averaged for simplicity and potential engineering applications. From the measured data, self-similarities for depth-averaged void fraction and velocity were found. The study suggests that the use of velocity data is insufficient for estimation of the flow momentum or the flow rate from comparisons with the approach using both velocity and void fraction.

1. Introduction

Breaking waves and associated flows show two phase nature of an air-water mixture flow. The aeration of breaking waves and induced flows is one of important properties in the wave breaking process. The aeration known to be pretty complicated involves strong turbulence intensity, associated energy dissipation, and density in the flows. In deep water, wave breaking acts as a main means for gas-transfer across air-water interface. Meanwhile, near shore, the aeration also plays a key role in beach processes in that wave breaking causes very turbulent flows by disturbance influencing sedimentation. In case a breaking wave event takes place near structures, aeration becomes more complex due to interactions between the breaking wave and structure. Since aeration may change the density of gas-liquid two phase flow, void fraction is considered as a factor of importance along with velocity particularly in estimating forces exerted on a structure by a breaking wave or associated flows.

This study presents investigation of velocity and void fraction of an overtopping water flow on top of a structure by a breaking wave. Velocity measurements were performed using the imaging method called bubble image velocimetry (Ryu et al., 2005) while void fraction was measured with fiber optic reflectometer (FOR) introduced by Chang et al. (2003). Instantaneous measurements of velocity and void fraction were phase-averaged to obtain mean properties. The phase average enables temporal and spatial distributions of velocity and void fraction to be presented. Volume flow rate and water volume of the overtopping water are estimated using the measured velocities and void fraction. The calculated overtopping water volume is also compared with measured volume of collected water for validation of the experiments conducted in this study. Total void fraction time-averaged from the temporal variation at a given measurement point is also discussed. Finally, depth averaged void fraction is considered and modeled with an empirical equation by applying dimensional analysis.

2. Experimental Setup

The experiments were carried out in a 50 m long, 1.2 m wide, and 1.5 m high glass-walled wave tank

equipped with a flap-type wavemaker and a 1:5.5 sloped wave absorber. A rectangular model structure was located 21.7 m away from the wavemaker. The structure is 0.31 m high and 0.37 m long (including a 0.22 m long extended deck), and spans the width of the wave tank so that it can be considered as two-dimensional. The wave tank was filled to a water depth of 0.80 m throughout the experiments and the model structure has a draft of 0.20 m so the free board is 0.11 m.

Overtopping green water was created by a plunging breaking wave that impinged on the front wall of the model structure and then overtopped the structure. The plunging breaker was generated using a wave focusing method that features a wave train with frequencies ranging from 0.7 Hz to 1.3 Hz. The breaking wave follows the same Froude scaling according to the reported maximum wave height during Hurricane Ivan (Wang et al., 2005). The plunging breaker broke at a desired location right in front of the structure.

Velocity fields of the overtopping green water flow were measured using bubble image velocimetry (BIV) that is a non-intrusive velocity measurement technique for multi-phased flows (Ryu et al., 2005). In addition to velocity measurements, void fraction in green water was also measured using a fiber optic reflectometer (FOR). Chang et al. (2003) introduced the FOR technique which is capable of measuring the time history of velocity and void fraction of a multiphase flow at a given point. The experimental setup is shown in figure 1. The image captured using the method and measurement points for void fraction are presented in figure 2.

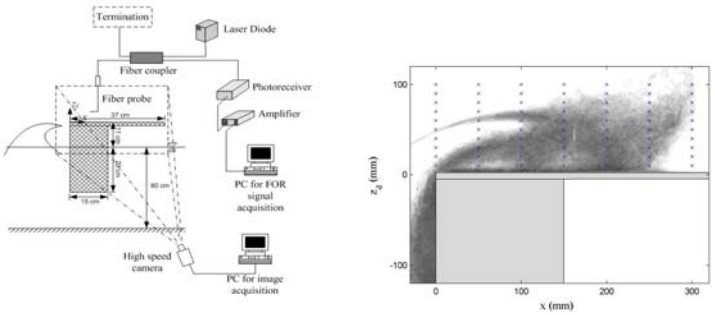

(a) (b)

Figure 1. Experimental setup (a) and measurement points for void fraction (b).

3. Results and Discussion

Void fraction is defined as the ratio of air-phase residence time to the duration of air-water mixture at a point of interest. In the present study, 20 instantaneous measurements of void fraction were taken to calculate the ensemble-averaged void fraction. The time-averaged void fraction is shown in Fig. 6. The time-averaged void fraction is defined as the total period presented by air over the entire duration of the overtopping water at a specific location on the deck. From the figure, it is observed that the void fraction profile changes gradually along the deck from approximately linear increase near the front of the deck to similar to a boundary layer velocity profile near the end of the deck.

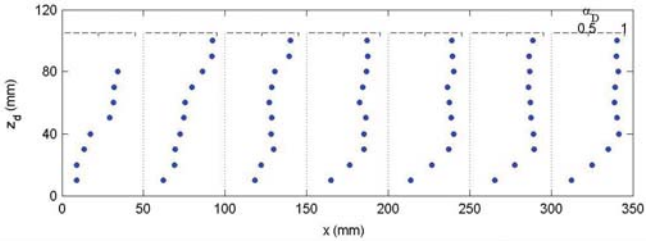

Figure 2. Total void fraction.

Using the measured velocities and void fractions, the time history of volume flow rate of the green water flow can be calculated as shown in Equation [1] and is presented in figure 3.

$$Q = \int_{h_l}^{h} (1-\alpha) U dz_d \qquad [1]$$

At each cross section, the flow rate displays a similar pattern - increasing linearly and rapidly and then, after reaching a maximum, decreasing with a slightly slower pace.

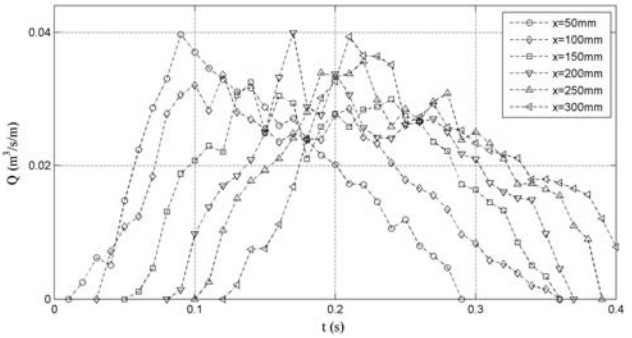

Figure 3. Time history of volume flow rate.

The total volume of the overtopping water, V, was calculated by integrating the flow rate Q with respect to time as follows:

$$V = \int_{T_s}^{T_e} Q dt = \int_{T_s}^{T_e} \int_{h_l}^{h} (1-\alpha) U dz_d dt \ . \qquad [2]$$

The calculated volume using equation [2] is compared with a directly measured water volume. The overtopping water was collected behind the structure using a large container so that the water volume can be directly measured. The directly measured mean water volume per unit width using the container is 5.60×10^{-3} m^3/m that is in good agreement with the corresponding mean water volume per unit width of 6.33×10^{-3} m^3/m obtained using equation [2] as shown in figure 4. The overall comparison confirms that the water volume is conserved and the velocity and void fraction measurements are reliable.

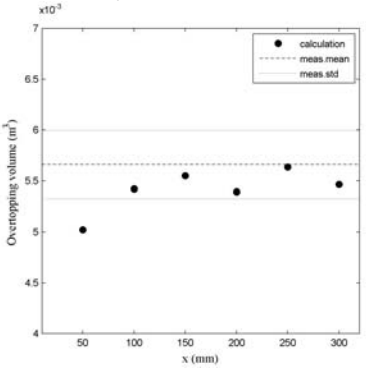

Figure 4. Overtopping water volume.

References

Ryu, Y., Chang, K.-A., and Lim, H.-J. (2005) "Use of bubble image velocimetry for measurement of plunging wave impinging on structure and associated greenwater." Measurement Science and Technology, 16, 1945-1953.

Chang, K. -A., Lim, H. -J., and Su, C. B. (2003) “Fiber optic reflectometer for velocity and fraction ratio measurements in multiphase flows.” Review of Scientific Instruments, 74, 3559-3565.

Wang, D. W., Mitchell, D. A., Teague, W. J., Jarosz, E., and Hulbert, M. S. (2005). “Extreme waves under Hurricane Ivan.” Science, 309, 896.

FREQUENCY OF EXTREME WIND SPEEDS ON THE ADRIATIC AND IONIAN APULIAN COAST: A BAYESIAN APPROACH

Maria Francesca BRUNO[(1)], Leonardo DAMIANI[(2)], Andrea GIOIA[(3)], Vito IACOBELLIS[(4)]

[(1)]*Eng., Research and Experimentation Laboratory for Coastal defense (LIC) - Technical University of Bari,* V. Orabona,4*, Bari, 70125, Italy.* f.bruno@poliba.it

[(2)]*Full Professor, Dipartimento di Ingegneria delle Acque e di Chimica - Technical University of Bari,* V. Orabona,4*, Bari, 70125, Italy.* l.damiani@poliba.it

[(3)]*Eng., Dipartimento di Ingegneria delle Acque e di Chimica - Technical University of Bari,* V. Orabona,4*, Bari, 70125, Italy.* a.gioia@poliba.it

[(4)]*Eng., Dipartimento di Ingegneria delle Acque e di Chimica - Technical University of Bari,* V. Orabona,4*, Bari, 70125, Italy.* v.iacobellis@poliba.it

1. Introduction

The prediction of hydrometeorological variables and their analysis in a regional context is one of the main challenges faced in recent years from the scientific community. these analyses find technical applications in several fields, among those the design of structures, the investigation of climatic change, the mitigation of flood risk, etc.

Interesting studies dealing with the statistical analysis of extreme wind speed, have been developed in the last few years. Sotillo et al., 2006 exploited L-moments to perform extreme wind regional analysis, providing a detailed assessment of Mediterranean offshore high wind areas. Xiao at al., 2006 investigated the probability distribution of extreme wind speed in Hong Kong. They found that Type I extreme value and three-parameter Weibull distributions are more appropriate than the two-parameter Weibull distribution for describing the probability distribution of extreme wind speed data. Leboucher at al., 2008 estimated mean and extreme wind speeds over France at the end of the 21st century. Dougherty et al., 2003 explored the use of mixed distributions for observed wind data and applied a peaks-over-threshold technique. Palutikof et al., 1999 reviewed some methods to calculate extreme wind speeds including 'classical' methods based on the generalized extreme value (GEV) distribution and the generalized Pareto distribution (GPD) and described techniques for calculating the distribution parameters and quantiles for short data sets. Walshaw and Anderson 2000 developed a model for maximum gusts which incorporates data on hourly mean speeds through a distributional relationship between maxima and means.

In this study we focus on the use of a Bayesian methodology aimed to provide an estimation of the probability distribution of extreme wind speed as well as the best set of parameters.

The Bayesian approach provides a valid inference procedure for at-site frequency analysis of hydrometeorological variables. In the past this method has seen limited applications in technical practice because of its numerically intensive implementation when compared with the simpler classical methods of statistic inference. Among pioneers of Bayesian method, applied to flood frequency analysis, were Wood and Rodriguez-Iturbe [1975a,b] and Vincens et al. [1975] which illustrated the principal elements of this theory.

Fawcett and Walshaw, [2006] developed a hierarchical model for hourly gust maximum wind speed data, exploiting the Bayesian framework to obtain predictive return level estimates which incorporate uncertainty estimation.

In this work we present particular sampling experiment based on the three-parameter Generalized Extreme Value (GEV) distribution applied to extreme wind speed data from nine gauged stations belonging to the Adriatic and Ionian Apulian coast. Results show that the parameter evaluation using simple likelihood model gives the most robust parameter estimates. Moreover, a significant improvement in the reduction of the uncertainty of prediction, occurs when parameters are estimated using regional information associated to the third order statistical moment for the definition of prior distribution characteristics.

2. Case study

At present in Italy various institutions are responsible for the systematic wind survey, even if the most reliable data, for acquisition standard and length of the available historical series, are the ones recorded by the Meteorological Service of the Air Force.

We focused on the Apulian coastal stations, extending the analyses to the neighbouring stations in Molise and Calabria. The following table (Tab 1) shows the main features of the analysed stations. The length of data series is variable because some of the stations (e.g. Vieste) were abandoned some years ago.

In a preliminary analysis, the wind data, collected every three hours, were subjected to statistical analysis to get the percentage of occurrence of six class of wind intensity from twelve compass direction (fig. 1) for the available observation periods. The longer the line the higher the occurrence from that direction while the different colour indicate the class force of the wind from that direction.

Table 1. Characteristics of analysed stations

STATION	OBSERVED PERIOD	YEARS OF OBS.	VALID DATA (%)	LAT. N	LONG. E	H [m]
BARI/Palese	1951-2005	55	94.82	41°08'	16°45'	44
BRINDISI	1951-2005	55	99.73	40°38'	17°56'	10
GINOSA MARINA	1968-2005	38	99.64	40°26'	16°53'	12
PALASCIA/Otranto	1951-1978	28	82.20	40°06'	18°31'	86
S. MARIA DI LEUCA	1951-2005	55	99.40	39°42'	18°20'	112
TARANTO	1952-1967	17	97.78	40°28'	17°16'	40
TERMOLI	1965-2006	41	96.89	42°00'	15°00'	44
VIESTE	1965-1977	13	99.42	41°52'	16°10'	66
CROTONE	1961-1995	35	99.74	39°00'	17°04’	161

All the region is characterized by a quite high windiness, in particular, proceeding from North To South it can be observed a wind prevalence from N-NNW on the Adriatic coast, except in Bari may be due to a particular location of the anemometer. In the Southern area it can be seen that the prevailing winds blow from N and S.

On the Ionic versant the observed data show a more complex situation with a N –NNW prevalence in the Gulf of Taranto, while in the Gulf of Crotone wind blowing from N-NNE and SSW show a high frequency. The wind condition is fairly similar to the one discussed in a previous study (CNR, 1981) that discussed the time series recorded in a smaller timeframe.

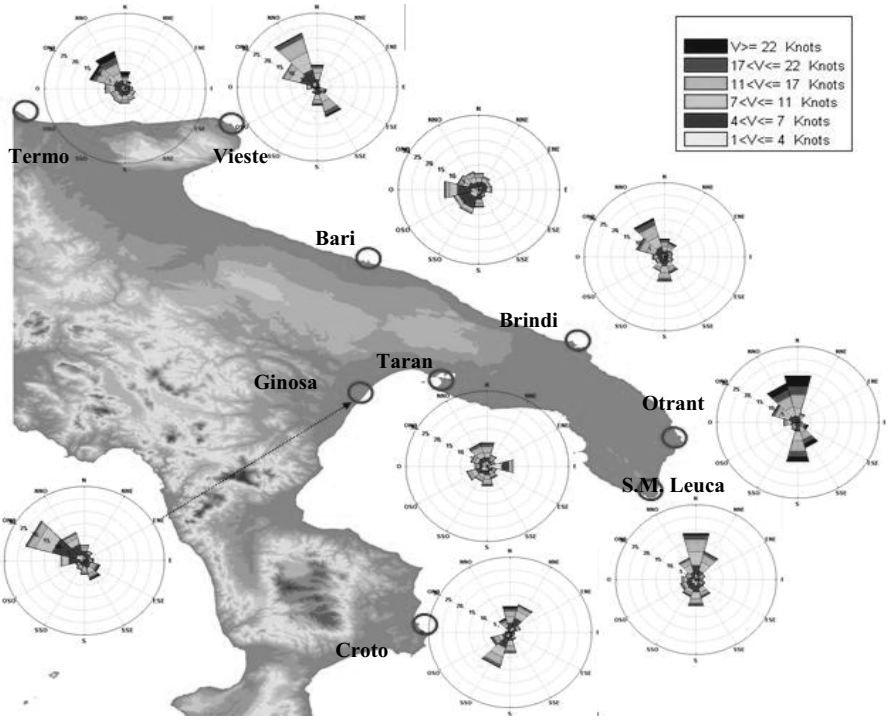

Figure 1. Wind climate along the Adriatic and Ionian coast

For a correct comparison all the data have been referred to the same height, 10m above see level, using in the Pierson formula the expression for friction velocity derived by Smith and Banke, 1975

$$\frac{U_z}{U_{10}} = 1 + \frac{1}{K} C_{10}^{1/2} \ln(z/10) \qquad [1]$$

where:
- Uz wind speed [m/s]at measurement height Z
- U_{10} wind speed at 10m [m/s]
- K Karman constant equal to 0.4
- C_{10} neutral drag coefficient at 10m

3. Methodology and results

In the Bayesian framework a probability distribution can be used to exploit known information about the quantity of interest. The Bayesian inference is fundamentally based on the definition of the conditional probability known as “Bayes' rule" which expresses the posterior probability density of the parameters β given the at-site data D as:

$$\xi(\beta \mid D) \propto f(D \mid \beta)\, \xi(\beta) \qquad [2]$$

where ξ(β), the prior probability density of the parameters, describes what is known about the model parameters prior to analysis of the data D and *f*(D/β) is the sampling distribution of the observed data given a chosen probability model with parameters β and represents the likelihood function of the parameters β given the data D.

β is the true (and unknown) value of the distribution parameters; all that is known about it, given the data D, is summarized by the posterior pdf ξ (β/D), which accounts for the uncertainty associated to each

set of parameters; the pdf $f(w/\beta)$ could be used to estimate the wind speed w_T, which has exceedance probability l/T, with T defined as the return period or average recurrence interval for the wind w_T. The Bayesian distribution of the wind speed annual maxima, w, is obtained by application of the total probability theorem, yielding the pdf:

$$g(w \mid D) = \int_{\beta} f(w \mid \beta)\, \xi(\beta \mid D)\, d\beta \qquad [3]$$

The integral (6) yields the expected pdf of w given the data D. The wind speed w_T with exceedance probability 1/T is defined by

$$P(w > w_T \mid D) = \int_{w_T}^{\infty} g\,(w \mid D)\; dw = \frac{1}{T} \qquad [4]$$

Substituting (3) into (4) and changing the order of integration yields

$$P(w > w_T \mid D) = \int_{\beta}\left(\int_{w_T}^{\infty} f(w \mid \beta)\, dw \right) \xi(\beta \mid D)\, d\beta = \int_{\beta} P(w > w_T \mid \beta)\, \xi(\beta \mid D)\; d\beta \qquad [5]$$

where $P(w > w_T|D)$ is the probability of w exceeding w_T given that β is the true parameter vector. Equation (5) shows that $P(w > w_T|D)$ is the expected exceedance probability for wind speed w_T with the expectation taken over all possible values of β.

We evaluate the expected probability distribution as well as quantile confidence limits for GEV probability model. In the first set of runs we consider "absence" of prior information. In a second set of runs we add prior information, derived from regional analysis, that are easily incorporated into the Bayesian analysis. All the Bayesian procedures previously described are included in a program called FLIKE (proposed by Kuzcera 1999) which is able to perform a full frequency analysis on five distributions: two-parameter lognormal, log-Pearson III, Gumbel, GEV, and generalized Pareto with support for uniform and multinormal priors.

The ability to compute the expected probability distribution and quantile confidence limits for any probability model is made possible by use of importance sampling, which is a general Monte Carlo algorithm for random sampling from the Bayesian posterior distribution. Figure 2 shows the expected probability distribution and the 90% confidence limit without any informative prior knowledge for the SSE direction for Taranto and Vieste stations, which are characterized by short period of observation.

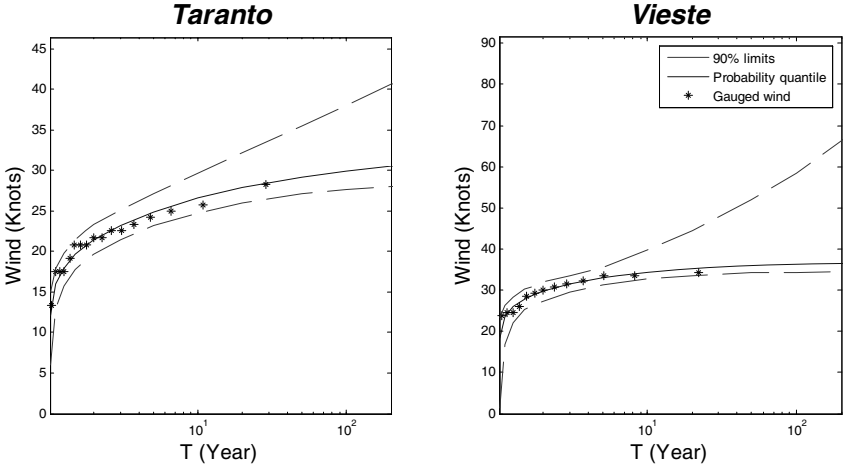

Figure 2. Expected parameter and GEV quantiles and 90% confidence limit for the SSE direction, without any informative prior knowledge.

Table 2 shows the at-site parameters of GEV ("k" is the shape factor, "a" is the scale factor; "u" is the location parameter) distribution evaluated for wind speed data belonging to the SSE direction for all the wind stations investigated.

Table 2 At-site parameters of GEV

	Bari	Brindisi	Crotone	Ginosa Marina	Otranto	S.M.Leuca	Taranto	Termoli	Vieste
u	15.65	26.70	18.09	33.18	29.72	22.34	20.23	19.05	29.10
a	1.50	1.33	1.28	1.67	1.74	1.43	1.30	1.24	1.46
k	0.08	-0.01	0.21	0.49	0.16	0.26	0.36	0.18	0.80

Figure 3 shows the GEV distribution and 90% confidence limit for the same direction. The expected GEV distribution is obtained adopting as prior information the mean and standard deviation of the shape factor derived from its at-site estimates. We use a regional weighted average as in Hosking and Wallis (1993). We observe that the probability distributions obtained exploiting the regional information, provides a meaningful reduction of uncertainty in wind prediction.

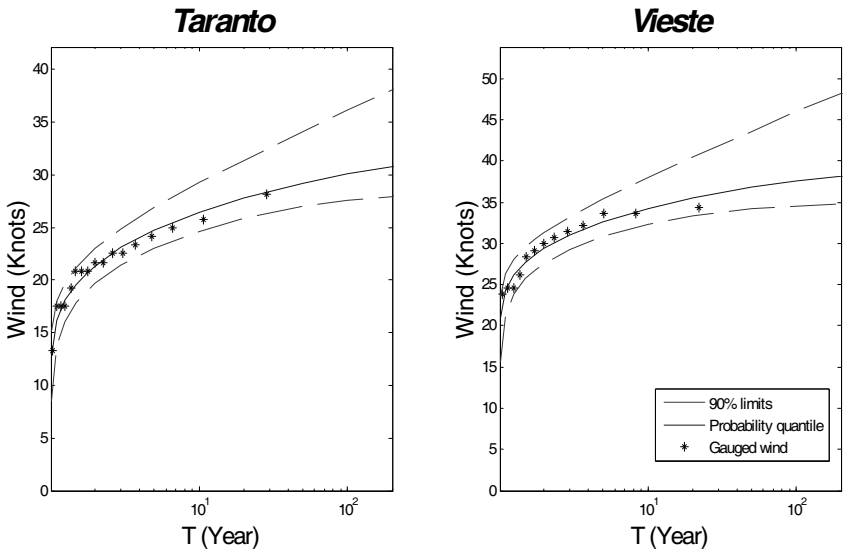

Figure 3. Expected parameter and GEV quantiles and 90% confidence limit for the SSE direction, with regional informative prior knowledge

References

Dougherty A. M., Corotis R. B., F.ASCE and Segurson A.2003., Design Wind Speed Prediction, J. Struct. Engrg., Volume 129, Issue 9, pp. 1268-1274.

Lee Fawcett, David Walshaw (2006) A hierarchical model for extreme wind speeds Journal of the Royal Statistical Society: Series C (Applied Statistics) 55 (5) , 631–646 doi:10.1111/j.1467-9876.2006.00557.x

Hosking J. R. M. and Wallis J. R., 1993, Some statistics useful in Regional Frequency Analysis, Water Resources research, Vol. 29, No. 2, Pages 271-281.

Kuzcera G., 1999, Comprehensive at-site flood frequency analysis using Monte Carlo Bayesian inference, Water Resources research, Vol. 35, No. 5, Pages 1551-1557.

CNR, 1981 Indagine sulle risorse eoliche in Italia; libro bianco sulle elaborazioni statistiche effettuate nell'ambito del Sottoprogetto energia solare del Progetto finalizzato energetica del CNR su i dati eolici disponibili in Italia, Roma, 1981. -- a cura di Alfredo Lavagnini.

Leboucher V., Deltel C. and Laurent-Ottavi C., 2008, Estimation of mean and extreme wind speeds over France at the end of the 21st century for industrial needs, Geophysical Research Abstracts, Vol. 10, EGU2008-A-10049.

Palutikof J. P., Brabson B. B., Lister D. H. and Adcock S. T., 1999, A review of methods to calculate extreme wind speeds, Meteorological Applications, 6: 119-132 Cambridge University Press, doi:10.1017/S1350482799001103

Smith SD, Banke, 1975 Variation of the sea surface drag coefficient with wind speed Quarterly Journal of the Royal Meteorological Society, 1 July 1975, vol. 101, no. 429, pp. 665-673(9).

Sotillo M.G., Aznar R. and Valero F., 2006, Mediterranean offshore extreme wind analysis from the 44-year HIPOCAS database: different approaches towards the estimation of return periods and levels of extreme values, Advances in Geosciences, 7, 275–278, 2006, SRef-ID: 1680-7359/adgeo/2006-7-275

Vicens, G. J., I. Rodriguez-Iturbe, and J. C. Schaake Jr. 1975, A Bayesian framework for the use of regional information in hydrology, Water Resour. Res., 11(3), 405-414.

Walshaw D. and Anderson C. W., 2000, A Model for Extreme Wind Gusts, Applied Statistics, Vol. 49, No. 4 (2000), pp. 499-508.

Wood, E. F., and I. Rodriguez-Iturbe, A, 1975a Bayesian approach to analysing uncertainty among flood frequency models, Water Resour. Res., 11(6), 839-843,.

Wood, E. F., and I. Rodriguez-Iturbe, 1975b, Bayesian inference and decision making for extreme hydrologic events, Water Resour. Res., 11(4), 533-542,.

Xiao Y.Q., Li Q.S., Li Z.N., Chow Y.W. and Li, G.Q., 2006, Probability distributions of extreme wind speed and its occurrence interval, Engineering Structures, Volume 28, Issue 8, Pages 1173-1181.

PRESSURE DISTRIBUTIONS INDUCED BY WAVES AND CURRENTS AROUND A SLENDER CYLINDER LYING ON THE SEA BOTTOM

Francesco ARISTODEMO [(1)] & Paolo VELTRI [(2)]

[(1)] *Post-Doc Researcher, University of Calabria, Dipartimento di Difesa del Suolo, via P. Bucci, Cubo 42B, 87036, Arcavacata di Rende, Italy. aristodemo@dds.unical.it*

[(1)] *Full Professor, University of Calabria, Dipartimento di Difesa del Suolo, via P. Bucci, Cubo 42B, 87036, Arcavacata di Rende, Italy. veltrip@dds.unical.it*

Abstract

The present paper deals with the evaluation of the dynamic pressures around the external surface of a cylinder lying on the sea bottom and induced by periodic and random waves and combined periodic and random waves with a positive current.
A large scale laboratory investigation was carried out at the wave flume of the "Centro Sperimentale per Modelli Idraulici" at Voltabarozzo (Padua, Italy). During the experiments the time variation of the dynamic pressures at 8 transducers mounted at 45° interval and slowly staggered along the longitudinal axis of a smooth and rough iron cylinder were measured (Figure 1). In particular, four pressure transducers PDCR 1830 model by Druck with a pressure range of 0-3.5 mH_20 and an output signal of 0-50 mV and four pressure transducers PTX/160-0241 model by Druck with a pressure range of 0-3.5 mH_20 and an output signal of 4-20 mA at 20 Hz sampling frequency were used. Undisturbed measurements of the horizontal velocity component at the transversal axis of the pipeline were performed using an Acoustic Doppler Velocimeter. Simultaneous measurements of pressures around the cylinder and free stream velocities were made possible by building a longitudinal wall allowing to obtain two separate trenches far from the wave generation area (Aristodemo and Veltri, 2006). The measure of the horizontal velocity has been useful for the determination of the current velocity at the pipeline and as input for the modelling of the horizontal and vertical hydrodynamic forces (Aristodemo et al., 2007).
Adopted values of the Keulegan-Carpenter number, KC, were resulted: $4<KC<13$ for periodic waves, $4<KC<9$ for random waves, $7<KC<11$ for combined periodic waves and current, and $5<KC<7$ for combined random waves and current in the vortex shedding regime. An high number of different wave and current conditions were produced: 39 periodic waves and 20 random waves using a smooth cylinder with k/D (relative roughness) = $4.6*10^{-4}$, 14 periodic waves and 6 random waves using a rough cylinder with k/D = $8.2*10^{-3}$, 11 periodic waves interacting with a positive current and 11 random waves interacting with a positive current using a smooth cylinder. All the time series of the sampled surface elevations, pressures and velocities were smoothed using a bandpass filtering. The screening was used in order to eliminate the lower frequencies due to the wave flume seiching, and the higher frequencies due to the erroneous readings of the instruments.
The values of dynamic pressures at the instants of zerocrossing, maximum and minimum of the time series of the surface elevation for the cases of periodic waves and combined periodic waves and current are shown (Sumer et al., 1991 and 1992). For non periodic tests, the pressure field is analysed in terms of root-mean squares of the entire records of wave and current experimental conditions. The roughness effect on the surface of the cylinder is also investigated with referring to the feature of the dynamic pressures.

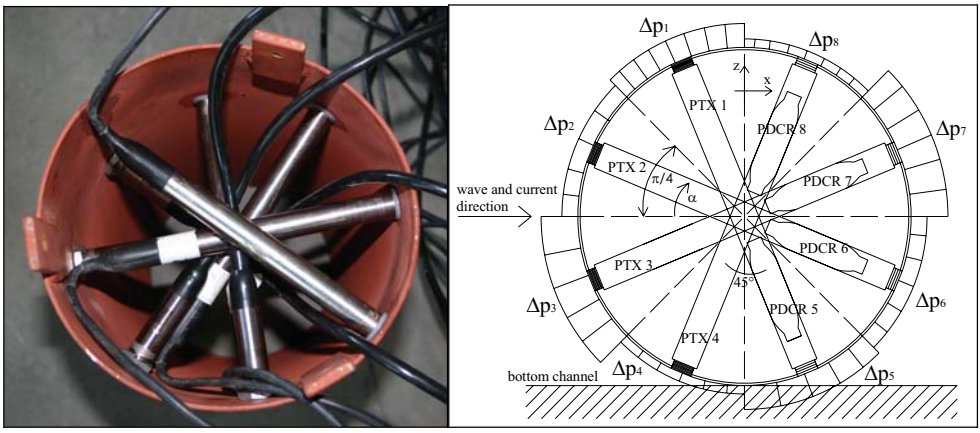

Figure 1. Assembling of the pressure transducers and their influence areas around the cylinder

References

Aristodemo, F., Veltri P., 2006. "On the calibration of Morison force coefficients at submarine pipelines". 2nd Int. Short Course and Workshop on Coastal Processes and Port Engineering, Università della Calabria.

Aristodemo, F., Tomasicchio, G.R., Veltri, P., 2007. "Modelling of combined wave and current forces on smooth slender submarine pipelines". Proc. Int. Conf. Coastal Structure, Venice.

Sumer, B.M., Jensen, B.L., Fredsoe, J., 1991. "Effect of a plane boundary on oscillatory flow around a circular cylinder". J. Fluid Mechanics, No. 225, 271-300 pp.

Sumer, B.M., Jensen, B.L., Fredsoe, J., 1992. "Pressure measurements around a pipeline exposed to combined waves and current". Proc. 11th Int. Conf. on Offshore and Arctic Engineering., Calgary, 113-121 pp.

CIRCULATION OF THE PERSIAN GULF: A PHYSICAL MODEL

Dr. Masoud SADRINASAB

Khorramshahr University of Marine Science and Technology, Khorramshahr, 64199-43175, Iran,
masoud.sadri@gmail.com

Abstract

The Persian Gulf, is an important military, economic and political region owing to its oil and gas resources, and is one of the busiest waterways in the world. Countries bordering the Persian Gulf are Oman, United Arab Emirates, Saudi Arabia, Qatar, Bahrain, Kuwait and Iraq on southern side and Iran alone on the northern side (Fig. 1).

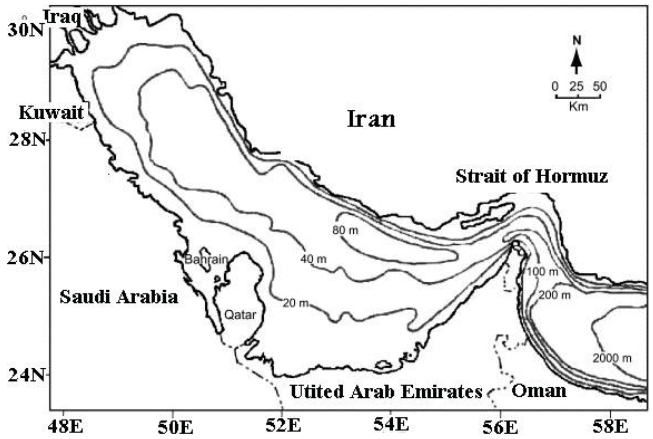

Figure 1. Location and batemetry of the Persian Gulf.

The Persian Gulf is 990 km long and has a maximum width of 370 km. The average depth of the Gulf is 36 m. The Persian Gulf occupies a surface area of 239000km (Emery, 1956). Extensive shallow regions, <20 m deep, are found along the coast of United Arab Emirates, around Bahrain, and at the head of the Gulf. Deeper portions, >40 m deep, are found along the Iranian coast continuing into the Strait of Hormuz, which has a width of 56 km and connects the Persian Gulf via the Gulf of Oman with the northern Indian Ocean. The Persian Gulf is a semi-enclosed, marginal sea that is exposed to arid, subtropical climate. It is located between latitudes 24–30N, and is surrounded by most of the Earth's deserts. The Gulf experiences evaporation rates of approximately 2 m/yr (Ahmad and Sultan, 1990), that exceed by far the net freshwater input by precipitation (0.15 m/yr) (Johns et al., 2003) and river discharge.

Owing to excess evaporation, the Persian Gulf exhibits a reverse estuarine circulation in which, due to geostrophy, the dense bottom outflow follows the coastline of United Arab Emirates, whereas inflow of Indian Ocean Surface Water follows the Iranian coastline (Hunter, 1982; Chao et al., 1992; Reynolds, 1993; Johns et al., 2003). Reynolds (1993) and others (e.g. Hunter, 1982) proposed that the densest water driving this bottom outflow forms in the Southern Shallows.

There are scarcely direct observations of the circulation within the Persian Gulf. The salinity distribution in the Persian Gulf clearly shows the circulation pattern of water in this region. The inflow of Indian Ocean surface water strengthens in late spring and summer and moves further to the head of the Gulf (Reynolds, 1993), (See Figure 2).

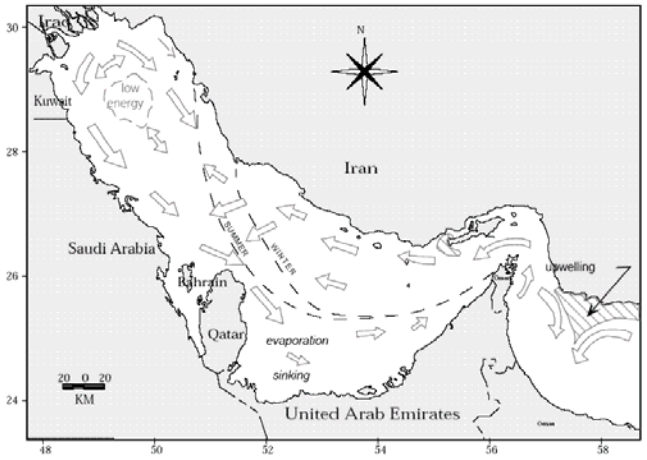

Figure 2. Schamatic of circulation processes
in the Persian Gulf (by Reynolds 1993).

Results from Reynolds (1993) show a general circulation which drives by density differences between Persian Gulf and Gulf of Oman waters. Around the year, fresher water from Gulf of Oman move towards head of the Gulf from surface and saline water from Persian Gulf moves towards Gulf of Oman from bottom layers. In order to simulate this circulation, a physical model is constructed for the first time in history of the Persian Gulf.

An admiralty chart containing Persian Gulf and Gulf of Oman has been used to design the bathymetry of the tank. This tank is on a rotating try which rotates by means of an adjustable motor. The tank has been separated into two parts; Persian Gulf and Gulf of Oman, by a moveable gate at the Strait of Hormuz. Before running the model, each Gulf has been filled up with their respective salinity, i.e., 36 psu and 40 psu for Gulf of Oman and Persian Gulf respectively. To distinguish two parcels of waters, the one in the Gulf of Oman has been colored by potassium permanganate which has no effect on its density. In order to record the movement of water, a camera has been fixed on the top of the rotating system. The model rotates with adjustable revolution until it reaches to its optimum revaluation per second, and then the gate is removed manually. Figure 3 shows movement of the water with 3 seconds time intervals.

As can be seen from these figures the fresher water from Gulf of Oman penetrates from surface into the Persian Gulf along the Iranian side which is in a very good agreement with previous investigations.

In the next experiment potassium permanganate has been applied to Persian saline water, and Water in the Gulf of Oman remains colorless to see the outflow of the saline water from Strait of Hormuz into the Gulf of Oman. In this experiment the camera has been fixed on the eastern side of the system, i.e. on the side of Gulf of Oman, to record the cross sectional movement of the water from Persian Gulf in to the Gulf of Oman.

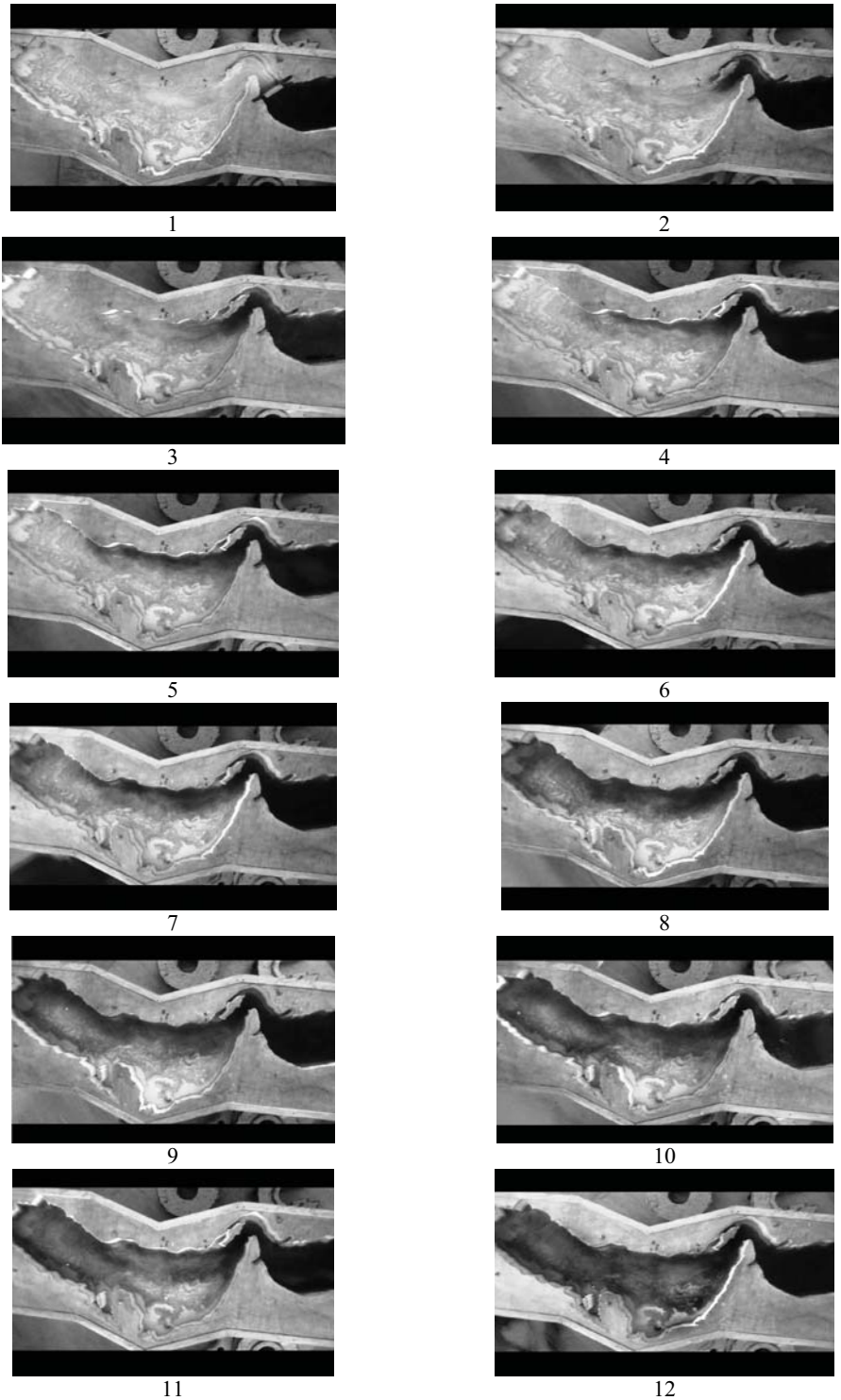

Figure 3. Results of the model showing the circulation pattern in the Persian Gulf.

Figure 4 shows cross sectional movement of water. As illustrated in this figure saline water from Persian Gulf flows out from Strait of Hormuz into the Gulf of Oman from bottom layer which is also in excellent agreement with previous investigations.

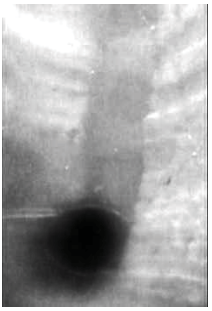

Figure 4. Result of the model showing outflow
of saline water from the Strait of Hormuz.

As this model is the first physical model constructed to describe the circulation of the Persian Gulf, It is clearly shows that the major force to derive the circulation of the Persian Gulf is the thermohaline force which is in agreement with numerical models such as; Hunter (1982), chao et al. (1992), Reynolds (1993), Sadrinasab and Kaempf (2004).

Acknowledgments

This research has been supported financially by Khorramshahr University of Marine Sciences & Technology, Iran.

References

Ahmad and Sultan (1990), 'Mean surface heat fluxes in the Arabian Gulf and the net heat transport through the Strait of Hormuz', Atmos. Ocean., 29, 54–61.

Chao, et al. (1992), 'A numerical investigation of circulation in the Arabian Gulf', J. Geophys. Res. 97, 11,219-11,236.

Emery, K. O. (1956), 'Sediments and water of the Persian Gulf'. AAPG Bull., 40, 2354–2383.

Hunter, J. R. (1982), 'The physical oceanography of the Arabian Gulf'. Proceedings of the First Arabian Gulf Conference on Environment and Pollution, Kuwait, 7-9 Feb 1982, pp. 1-23.

Johns et al (2003), 'Observations of seasonal exchange through the Straits of Hormuz and the inferred heat and freshwater budgets of the Persian Gulf'. Journal of Geophysical Research, VOL. 108, NO. C12, 3391, doi:10.1029 /2003 JC001881.

Reynolds, R. M. (1993), 'Physical oceanography of the Gulf, Strait of Hormuz, and the Gulf of Oman Results from the Mt Mitchell expedition'. Mar. Pollution Bull. 27, 35-59.

Sadrinasab, M., and J. Kämpf (2004). 'Three-dimensional flushing times in the Persian Gulf'. Geophysical Research Letters, VOL. 31, L24301, doi:10.1029/2004GL020425, 2004.

PHYSICAL MODELLING STUDY OF SEA OUTFALL PLUME DISPERSION THE CASE OF BAIXADA SANTISTA, BRAZIL

Emilia ARASAKI [(1)], Paolo ALFREDINI [(2)] & Tiago ZENKER GIRELI [(3)]

[(1)] Professor PhD , Coastal and Harbour Division of Hydraulic Laboratory, University of São Paulo, Fundação Centro Tecnológico de Hidráulica, Av. Prof. Lúcio Martins Rodrigues, 120, São Paulo, 05508-900, Brazil. earasaki@usp.br

[(2)] Associate Professor, Coastal and Harbour Division of Hydraulic Laboratory of Escola Politécnica of Universidade de São Paulo, Full Professor of Escola de Engenharia Mauá of Instituto Mauá de Tecnologia and Engineer VI of Centro Tecnológico de Hidráulica of Departamento de Águas e Energia Elétrica do Estado de São Paulo, Av. Prof. Lúcio Martins Rodrigues, 120, São Paulo, 05508-900, Brazil. alfredin@usp.br; paolo.alfredini@maua.br

[(3)] PhD, Coastal and Harbour Division of Hydraulic Laboratory, University of São Paulo, Fundação Centro Tecnológico de Hidráulica, Av. Prof. Lúcio Martins Rodrigues, 120, São Paulo, 05508-900, Brazil. t_gireli@yahoo.com.br

1. Introduction

Ocean disposal via sea outfall with preliminary treatment of domestic sewage is one of the systems adopted by SABESP - Basic Sanitation Company, in the central area of São Paulo State coastline. The region has four domestic sea outfalls in operation (Santos, Guarujá, Praia Grande -subsystem I and Praia Grande - subsystem II). These outfalls are located in physical fix bed model built in Coastal and Harbour Division of Hydraulic Laboratory, Polytechnic School - University of São Paulo (LHEPUSP), occupying an area of nearly 750 m^2 and representing about 1000 km^2 of Baixada Santista Estuary and Santos Bay, Southeastern Brazil.

The study was initiated as part of a research project support by FEHIDRO (São Paulo State of Water Resource Fund) and Fundação Centro Tecnológico de Hidráulica. The main goal of this survey is to assess sea outfalls performance, considering the development of methodology for sewage dispersion evaluation through physical modelling.

São Paulo coast has seven domestic wastewater submarine outfalls, all of them operated by SABESP (two of them in Praia Grande, one in Santos, one in Guarujá, two in São Sebastião and one in Ilha Bela). According to IBGE (Brazilian Institute of Geography and Statistics), the situation of São Paulo State sanitation is more favourable than the usual Brazilian reality. In particular case of Santos (418288 inhabitants in 2007), in the end of 1960 decade, the sanitary system presented depleted capacity, which provoked the increasing rejection of the city as local of vacation. To change this situation, in 1969 it was created the Managing Plan of Sewage, which recommended the oceanic disposal of the sewage and the construction of the first sea outfall in José Menino Beach with about 4000 m length at 10 m depth.

Other important city is Praia Grande (233806 inhabitants in 2007) with about 44 km of length and mild beach slope. The collecting system, transport, preconditioning and final disposal of the Praia Grande sewage is divided in 2 independent subsystems (I and II), due to the region characteristics.

In Guarujá city (296150 inhabitants in 2007) a modern waste water treatment plant with sea outfall is constructed to attend 2 urban areas. According to computer simulations, this sea outfall presents adequate effluent dilution.

The purpose of this paper is to present the performance of the plume dispersion process for the Santos, Guarujá and Praia Grande I outfalls. Praia Grande II, situated in the physical limit of the model, was not considerate during the simulations.

2. Material and Methods

In 2004, a fixed bed hydraulic physical model has been constructed at the LHEPUSP (see Figure 1), with geometric scale horizontal - 1:1200 and vertical – 1:200; the discharge scale is 1:3394113 and the tidal currents time scale is 1:84.85. The tidal cycle can be simulated in the model, as well as the regular wave regime. The bathymetry and the local shoreline data were obtained from the Brazilian Navy (Nautical Charts 1701 and 1711). The geometric scales used for the construction of the distorted Froude model were: horizontal scale 1:1200 and vertical scale 1:200. The tidal cycle could be representing in the model, as well as the regular wave regime (Alfredini et al., 2008). The tidal cycle was generated by operational software created at the LHEPUSP, where one cycle in the model (8.75 minutes) corresponded to 12.38 hours in the real situation.

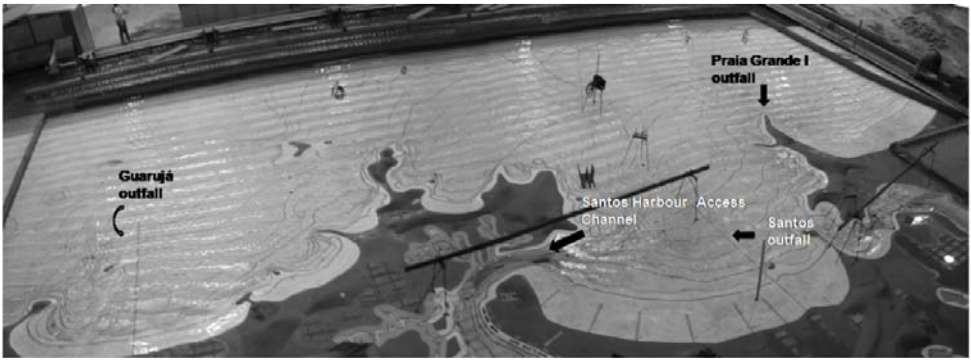

Figure 1 – Panoramic view of the physical model showing the outfalls lines of Guarujá, Santos and Praia Grande I. It is also possible to see the access channel entrance to Santos harbour

The calibration characteristic points were carried out comparing the real estuarine tidal propagation times (values measured and recorded during spring tide) with those of the model. The adjustment was achieved by changing the estuarine bottom roughness with the use of increasing gravel dimensions, thus improving the tidal propagation time regulation. Once achieved an appropriate tidal calibration time, the hydraulic validation was verified comparing local velocities and floating tracks measured in field campaigns. More details about calibration and validation procedures are explained in Alfredini et al., 2008.

To reproduce a constant flow discharged through the outfall, a system composed by Mariotte´s bottle and an energy dissipator cylinder was developed and this system is coupled with a stainless steel tube, representing the outfall, but without the multiple ports system existing in the real condition. The scenarios of dispersion were tested with 0.25 % methylene blue solution, simulating the sewage flow in Santos, Praia Grande I and Guarujá outfalls. The wind influence was carried out in a wind tunnel, simulating SW winds generated during cold fronts. The wind tunnel was constructed in acrylic (total length = 7.5 m and width = 3 m) with a suction fan downwind in the vertex. The system was supported by steel piles used to adjust the tunnel leveling over the water. The suction fan velocity was calibrated according to the numerical modeling results described in Harari and Gordon (2001). This adjustment was achieved by a trial and error procedure, measuring the water velocities corresponding to different suction fan rotations and choosing the one which better fitted to Harari and Gordon (op. cit.) data for a spring tide with storm surge occurrence (50 km/h SW wind).

3. Some simulations results and discussion

Due to the reduced scale, the purpose of physical tests presented in this study is showing only the far field hydrodynamic dispersion process affected by the tidal cycle and wind. The tests were done under conditions of spring tide, which correspond to a higher intensity of tidal current circulation.

More than 50 tests were carried out simulating diverse scenarios like outfall length (Santos case), flow rate (maximum and minimum discharges, mean operation volumetric discharges) in Santos, Guarujá and Praia Grande I outfalls, simulations with mean sea level rise and storm surge condition.

About outfall extension possibilities, tests with different lengths of the Santos outfall (4 and 5 km) and maximum discharge Qmax = 5.3 m^3/s and mean operation volumetric discharge Qmean = 3.34 m^3/s are simulated (see Figures 2a and 2b, respectively). In both cases, the storm surge condition was simulated as wind blowing shoreward.

These tests illustrate that the plume tends to disperse seaward, especially for the scenario with Q = 3.34 m^3/s. Part of the plume returns to the Santos Harbour Access Channel, mainly for Q = 5.3 m^3/s. This result confirms the presence of a larger plume for a larger effluent discharge.

The comparison with the condition 5 km shows that the dispersion tends to move towards deeper waters (minor action of wave transportation currents) due to the pipeline extension, showing a similar trend as to that of the 4 km length, but with minor intensity of shoreward dispersion. Physical modelling results with a wind tunnel showed that the dispersion at the far field in this adverse scenario could be improved by increasing the length of the submarine outfall.

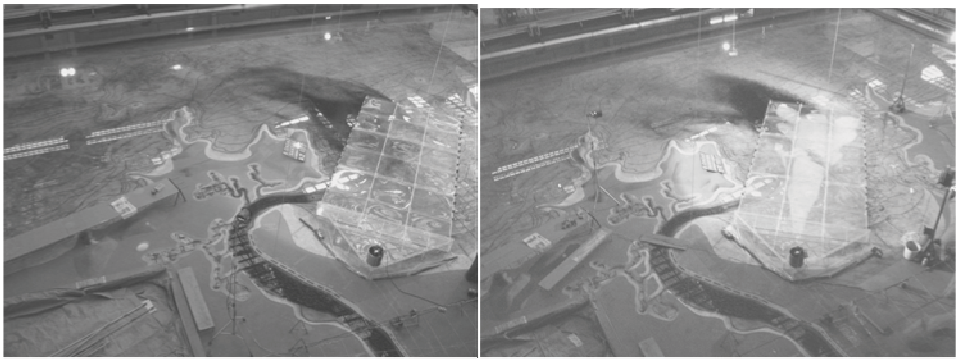

Figure 2a - Plume effluent discharge (Q = 5.3 m^3/s) from Santos outfall with 4 km length (left) and 5 km length (right) after 6 tide cycles. The illustration also shows the wind tunnel located upon outfall area.

Figure 2b - Plume effluent discharge (Q = 3.34 m^3/s) from Santos outfall with 4 km length (left) and 5 km length (right) after 6 tide cycles.

4. Final considerations

In spite of the physical model small vertical scale, the classical principle of Similitude Laws is applicable: the primacy of comparing different projects performances in the same model with the same scale and laboratory effects.

The transition and the far field performance must be evaluated with attention, mainly considering situations when the diffuser system shows problems of operational efficiency caused by structural damage or lack of maintenance.

Physical modelling results with a wind tunnel showed that the dispersion at the far field in the scenario of storm surge could be improved by increasing the length of the submarine outfall.

References

Alfredini, P., Arasaki, E., Amaral, R.F., 2008. Mean sea-level rise impacts on Santos Bay, Southeastern Brazil – Physical modelling study. Enviromental Monitoring and Assessment. (in press). DOI 10.1007/s10661-007-0001-z

Brazilian Navy / Diretoria de Hidrografia e Navegação – Nautical Charts 1701 – Proximidades do Porto de Santos, scale 1:80,000 – and 1711 – Porto de Santos, 2000, scale 1:23,000. Rio de Janeiro.

Harari, J., Gordon, M., 2001. Simulações numéricas da dispersão de substâncias no Porto e Baía de Santos, sob a ação de marés e ventos. Revista Brasileira de Recursos Hídricos, 6(2), 115-131.

STUDY OF OIL SPILL BARRIERS - PHYSICAL MODELLING ON THE UNIVERSITY OF PORTO

H. Guedes LOPES [(1)], F. Taveira PINTO [(2)] F. Veloso GOMES [(3)], G. IGLESIAS [(4)] & A. CASTRO [(5)]

[(1)] PhD Candidate, Faculty of Engineering of the University of Porto, Rua Dr. Roberto Frias s/n, Porto, 4200-465, Portugal, hglopes@fe.up.pt

[(2)] Assoc. Professor, Faculty of Engineering of the University of Porto, Rua Dr. Roberto Frias s/n, Porto, 4200-465, Portugal, fpinto@fe.up.pt

[(3)] Full Professor, Faculty of Engineering of the University of Porto, Rua Dr. Roberto Frias s/n, Porto, 4200-465, Portugal, vgomes@fe.up.pt

[(4)] Assoc. Prof., Dep. Ag. Eng., E.P.S., Univ. of Santiago de Compostela, Campus Univ. s/n, 27002 Lugo, Spain, iglesias@usc.es

[(5)] Assoc. Res., Dep. Ag. Eng., E.P.S., Univ. of Santiago de Compostela, Campus Univ. s/n, 27002 Lugo, Spain, albertecastro@udc.es

Abstract

The project "*Herramientas avanzadas para la protección del litoral de Galicia y la Región Norte de Portugal frente a vertidos de hidrocarburos en alta mar"* (Advanced tools for the protection of Galicia and north of Portugal shorelines towards oil spills in open waters) - acronym PROLIT - was supported by the European programme Interreg III A. The programme promoted the cooperation between Portugal and Spain, involving the University of Santiago de Compostela (Spain), the University of Corunha (Spain) and the Hydraulics and Water Resources Institute of the Faculty of Engineering of the University of Porto (Portugal).

The project had several phases in which the physical modelling of oil spill barriers was included.

In the paper, the results of the physical modelling tests of the barriers, performed in the Faculty of Engineering of the University of Porto, will be presented along with a general description of the PROLIT project.

1. The PROLIT project

The shorelines of Galicia and north of Portugal suffered a dramatic environmental impact with the Prestige oil spill in 2002, Fig.1.

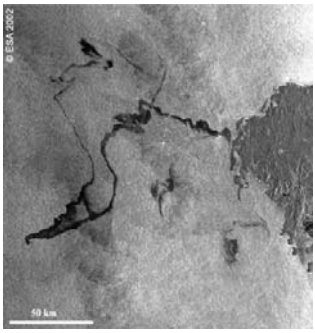

Figure 1. Oil spill - Prestige (source: ESA 2002)

With the continuous grow of the Maritime Transport and despite the efforts to improve security measures - sophisticated systems to control the position and routes of vessels, new traffic corridors for special cargos along the Iberian Peninsula coast, double core bulks, etc., the risk of accidents is real, and though, developing an efficient system to protect and minimize the impacts on shorelines for future oil spills is crucial. The PROLIT project aims to contribute for the development of an efficient barrier system, to protect sensitive shoreline areas of the Galicia and north of Portugal.

The project was divided in 6 different activities: 1 - Inventory and characterization of sensible areas along the shoreline of Galicia and the north of Portugal; 2 - Design of the barriers; 3 - Physical modelling tests in wave channel; 4 - Analysis of the results; 5 - Testing the defence system; 6 - Dissemination of the results.

The paper will focus on the physical modelling tests performed in the wave tank of the Faculty of Engineering of the University of Porto.

2. Laboratory set-up

The physical modelling tests of the barriers were performed on the wave tank of the Hydraulics Laboratory of the Faculty of Engineering of the University of Porto. The wave tank is 28.0 m long, 12.0 m wide and 1.2 m in depth, Fig. 2.

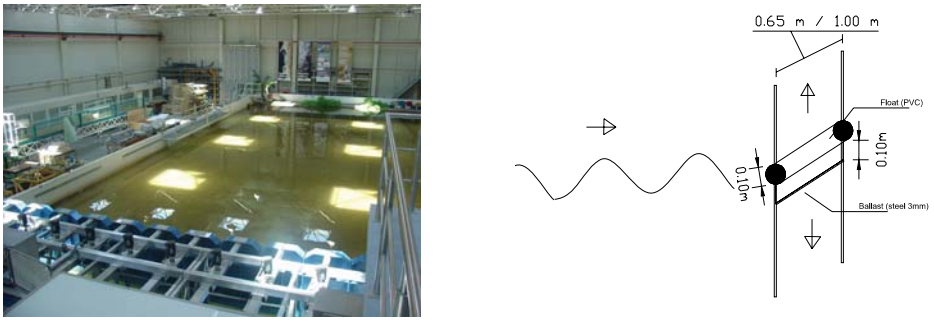

Figure 2. Wave tank of the Hydraulics Laboratory of the Faculty of Engineering of the University of Porto and barriers scheme.

Two different barrier lengths were analysed (0.65 m and 1.0 m), Fig.2, and also different fixing techniques to reduce model effects. In the project was also developed a numerical model that will use the results from the physical modelling tests to calibrate the numerical model and also using artificial vision to analysed the physical modelling tests and evaluate the performance of each solution.

The results obtained on the physical modelling tests with the different barriers, for different test conditions, were analysed and will be discussed in the paper.

References

Hughes, S.A. (1995). “Physical Models and Laboratory Techniques in Coastal Engineering”, Advanced series on Ocean Engineering – Volume 7 , World Scientific, Singapore.

U.S. Army Corps of Engineers. (2003-online). Coastal Engineering Manual. Engineer Manual 1110-2-1100, U.S. Army Corps of Engineers, Washington, D.C. (in 6 volumes). Coastal Engineering Manual.

Iglesias, G. Fraguela, J.A. Castro, Carballo, R. and Taveira Pinto, F.,2006. Oceanic Oil Spill Boom. Design and Laboratoy Tests. Coastlab ’06, Porto (Portugal).

PHYSICAL MODELLING OF MIXING THROUGH COASTAL DEFENSE SUBMERGED BREAKWATERS IN BARCELONA BEACHES

Luis GÓMEZ-DÍEZ-MADROÑERO [(1)], Antonio RUIZ-MATEO [(2)], Ana M. ÁLVAREZ-GARCÍA [(3)] & Marta ESPINÓS-PALENQUE [(4)]

[(1)] *Civil Engineer, CEDEX, Antonio López nº 81, Madrid, 28026, Spain. luis,gomez@cedex.es*

[(2)] *Civil Engineer, CEDEX, Antonio López nº 81, Madrid, 28026, Spain. antonio.ruiz@cedex.es*

[(3)] *Biologist, CEDEX, Antonio López nº 81, Madrid, 28026, Spain. ana.alvarez@cedex.es*

[(4)] *Marine Scientist, SASEMAR, Fruela nº 3, Madrid, 28011, Spain. martaep@sasemar.es*

Abstract

To prevent the need of new nourishments, the Directorate General for Coasts (DGC) designed a set of submerged breakwaters (crested at – 2 m) laid in such a way to form closed cells in plan view with the coastline and the existing groins. These groins support open channel outfalls for rain waters. As this design may have a negative impact on beach water quality, DGC entrusted a research to CEDEX in order to study the possible barrier effect that this project may have on mixing processes between interior and exterior waters.

1. Introduction

In the last years beach nourishment works are having to overcome an increasing number of environmental, administrative and legal troubles mainly related to sand extraction from the sea. So, in January 2006 DGC prepare a new project aimed to stabilization of a set of beaches in Barcelona, those located between Barceloneta and Nova Mar Bella, focused to prevent the need of new nourishments.

The designed measures consist of the construction of submerged breakwaters (crested at – 2 m) laid in such a way to form closed cells in plan view with the coastline and the existing groins. These groins support open channel outfalls for rain waters. The breakwaters have two principal functions: to reduce the wave height at the shore (and so, to reduce sand movements) and to prevent sand losses out of the cells.

However, this design may have a negative impact on beach water quality if contaminated rain waters discharged through the outfalls get into the cell and cannot exit it.

Concerned about this, DGC entrusted a research to CEDEX in order to study the possible barrier effect that this project may have on mixing processes between interior and exterior waters.

For that purpose, CEDEX carried out tests on a physical model scaled 1/54 of a typical cell (that at Bogatell) aimed to estimate, by comparison between the present situation and that after the construction of the breakwaters, not only the possible delay of the output of contaminants previously introduced in the cell (negative impact), but also the possible decrease of the amount of contaminant that enters the cell (positive impact) coming from the incidental discharges of rain waters through the lateral outfalls. This model have been built and operated in a multidirectional wave tank of the Laboratory of Maritime Experimentation, a large facility of CEDEX with a long experience in physical modelling.

Consequently, the tests are of two types: those focused to estimate the renovation rate of the water in the cells and those aimed to study the dispersion of contaminants transported by the rain water discharged through the outfalls that limit the different beaches.

In both cases, tests have been carried out with waves coming from two directions of high probability of occurrence (ENE and S) with two wave heights (non-excedence probabilities of 50% and 90%) and one situation of rather calm waters (waves coming from S with non-excedence probability of 10%), resulting in a total of 20 tests.

2. Tests for renovation rate

To study the present situation, the cell is closed with a metallic screen and the water inside is traced with an homogeneous concentration of Rhodamine WT of about 100 ppb. After that, a crane lifts the screen slowly and carefully to prevent spurious dispersion and then, the multi-segmented piston-type wave maker begins to work. Two pumps with 16 channels each take samples from 32 previously chosen points evenly distributed within the cell. Samples are taken several times until a mean concentration of about 1 ppb is reached. Later on, the amount of tracer that remains within the cell is calculated for each sample time and compared with the amount at the beginning of the test. This test is repeated for each of the planned sea states. Finally, the tests are repeated after the construction of the breakwaters and results are compared.

3. Tests for dispersion of rain waters

These tests are more complex because they were design to take into account the effect of the density difference between dirty rain water and seawater in the prototype.

The approach of heating the discharge water in the test was discarded because the maximum density difference that could be achieved was lower than needed. The actual approach have been the following.

The water in the wave tank is salted (for which, more than eleven tons of salt have been used) and discharges of rain water for the design floods are simulated with traced fresh water (Rhodamine B). After that, dispersion of the tracer is analysed, especially within the cell that encloses the beach, through the spatial and time evolution of tracer concentrations and conductivities. Just like for the previous case, tests are repeated for the planned sea states, with and without the breakwater and results are compared.

4 Results

All the conducted tests produced a great amount of samples, each of them referenced by the exact time at which they were taken and associated to the physical coordinates of the point where they were taken.

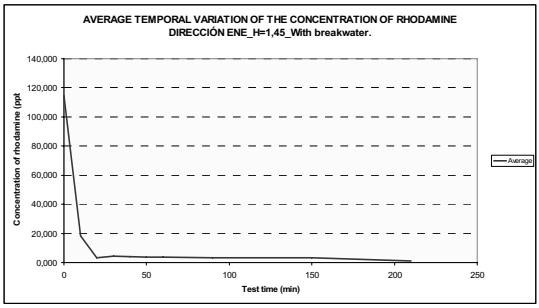

Figure 1 Temporal variation of the concentration of Rhodamine in test

As a result, the obtained distribution is a grid where each of its elements define the average value of the concentration of the tracer in the cell to which its coordenates is associated.

For each test it was obtained as many grid of concentration as instans at en los que se wich samples were taken.

With the purpose of getting for each test a grid in wich it was represented the average of the concentration of the tracer among the water column, the different grids of concentration of rhodamine were associated to the depth of each point.

The value of the mass of rhodamine enclosed in the beach area was obtained integrating the matrix previously generated.

In this way, with the laboratory analysis of the collected samples, the temporal distribution of the concentration of the selected tracer was generated and with the physical cordinates of the points at which the samples were collected, the spacial ditribution of the trace was represented for each time by interpolation.

In order to create this interpolation, the area of study was divided into separated cells of 0,15 x 0,15 m giving rise to a grid of 61 columns by 101 rows.

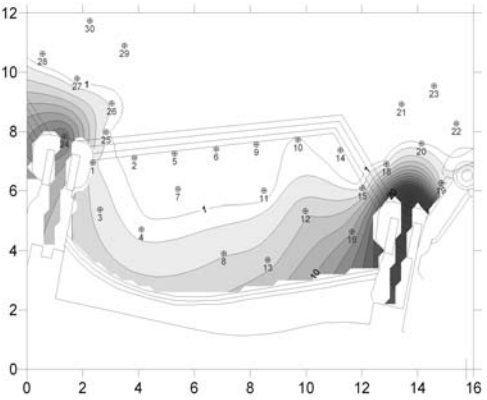

Figure 2 Spatial distribution of the concentration of Rhodamine at the instant of time

$$[1] \quad M(t) = \int c(t) \cdot dv$$

Once all the matrix corresponding to the instans at which the samples were taken were integrated, the temporal variation of the mass of the tracer was represented.

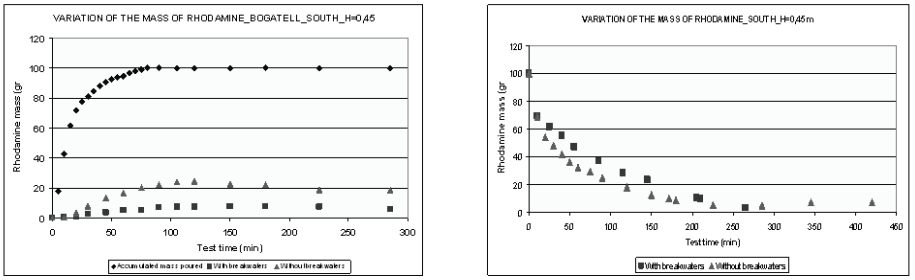

Figure 3: Spatial distribution of the concentration of Rhodamine at the instant of time

The results of both experimental cases; the test of renovation rate and the test for dispersion of brain waters, aimed to compare both the preoperational and the project situation.

The tests conducted to analyse the temporal variation of the renovation of the water system studied, generally showed a bigger renovation rate in the projected than in the preoperational situation, but no more than 24 hours in any case.

In the other hand, from the tests developed to test the impact of the projected structures in the entrance and exit of the contaminants into the studied area, it was concluded that the construction of submerged breakwaters considerably reduced the entrance of contaminants into the beaches studied.

The conclusion of the works carried out, may be completed combining the results from both sorts of experiments, since in most of the cases, despite the time of removal of the area of study is bigger when the structures were present, much less pollution entered the area. Due to this fact, the amount of contaminants inside the beach was bigger without structures than when they were present.

References

Booij, R., (1989). Exchange of mass in harbours. *Proceedings of the 23rd I.A.H.R. Congress*, Delft, Netherlands, pp. D69–D74.

Hattori T. ; Wada A. (1990) 'Prediction of seawater exchange ratios in and outside the bay by hydraulic model' *Proc. Int. Conf. on Physical modelling of transport and dispersion*. Massachusetts Institute of Technology. ASCE, pp 2B.1-6.

Hughes S.A. (1993) 'Physical Models and Laboratory Techniques in Coastal Engineering'. World Scientific. ISBN:981021541X.

Langendoen E.J.; Kranenburg C. ; Booij R. (1994) 'Flow patterns and exchange of matter in tidal harbours'. *J. Hydraulic Research*, vol 32 2, pp. 259-269.

Uitjttewaal W. S. J. ; Lehmann D. ; Van Mazijk A. (2001) 'Exchange processes between a river and its groyne fields: Model experiments'. *J. Hydraulic Engineering*, vol. 127, n°11, pp. 928-936

Tan S. K. (1990) 'Water exchange behind the inlet weir of a semi-enclosed lagoon'. *Proc. Int. Conf. on Physical modelling of transport and dispersion*. Massachusetts Institute of Technology, ASCE, pp 2B.7-12.

CALIBRATION OF A SEA CURRENT NUMERICAL MODEL USING FIELD MEASUREMENTS OFFSHORE TARANTO (ITALY)

M. BEN MEFTAH [(1)], M. MOSSA [(2)], A.F. PETRILLO [(3)] & A. POLLIO [(4)]

[(1)] Research Assistant, Department of Water Engineering and Chemistry, Technical University of Bari, Via E. Orabona n. 4, 70125 Bari, Italy. mbenme@poliba.it

[(2)] Full Professor, Department of Environmental Engineering and Sustainable Development, Technical University of Bari, Via E. Orabona n. 4, 70125 Bari, Italy. mossa@poliba.it

[(3)] Full Professor, Department of Water Engineering and Chemistry, Technical University of Bari, Via E. Orabona n. 4, Bari, 70125, Italy. petrillo@poliba.it

[(4)] Research Assistant, Department of Water Engineering and Chemistry, Technical University of Bari, Via E. Orabona n. 4, 70125 Bari, Italy. a.pollio@poliba.it

Abstract

The goal of the present work is to present some comparisons between current field measurements and numerical simulation results offshore Taranto, a city placed in the South Italy. Field measurements were carried out on 29/12/2006 by means of a Vessel Mounted Acoustic Doppler Current Profiler (VM-ADCP) AWAC manufactured by Nortek. Measurements were acquired at nine stations offshore Taranto into the homonymous gulf. The northern and eastern components of the water velocity were useful in order to describe the horizontal field of motion at various depths. The data so obtained were averaged along the depth and they were compared with the results carried out from a two-dimensional numerical model (MIKE21), using a flexible mesh approach for the domain representation. In order to achieve a good agreement with the measured data and the numerical ones, an adequate model calibration was carried out. It was pointed out that calibration of the seabed roughness and the wind stress factor seem to be sufficient to have a good overlapping between the measurements and the computed data.

1. Introduction

The present work deals with the field measurements and analysis of the sea current and velocity profiles assessed offshore Taranto at the open north-eastern area of the Ionian Sea in Southern Italy (see Figure 1). The analysis of the zone current pattern is a very interesting topic due to the highly extensive pollutant discharges in the same zone because of the presence of extensive industrial activity into the area. Indeed, the city of Taranto is notably known due to the presence of steel, cement and oil treatment plants. As a result, the quantity of undesirable physical, chemical, and biological products, discharged into the coastal areas may affect the local marine ecosystem through advection, diffusion and chemical and biological reactions. This is true especially for coastal ecosystems, which represent a rich and fragile resource (Roberts, 1980; Mossa, 2006; De Serio et al., 2007) that is subject to modifications due to climatic variations and/or human activities.

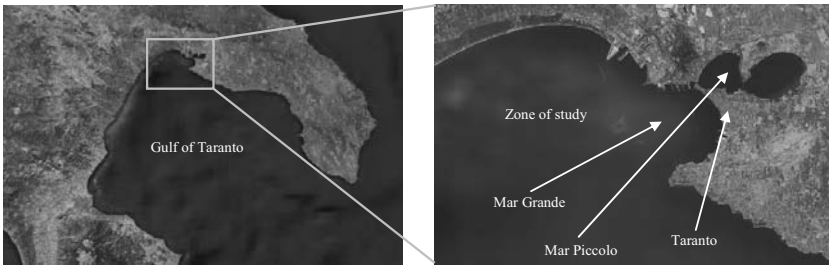

Figure 1. Location of the experimental survey offshore the city of Taranto. The zone of study is the location of almost all the stationing points. However one station was also placed into the Mar Grande (source: Google Map).

Particularly, the advective processes caused by the current pattern may easily carry undesirable chemical and biologic components throughout all the area, thus to endanger the nearby coastal areas and hence all the typical ecological habitat of the same zone. For this reason, a worthwhile study is the analysis of the current circulation in the interested zone, taking into account the main engine forces driving the current patterns, such as tides, winds and salinity and temperature stratifications and gradients.

The main goal of this work is to demonstrate how a numerical model may be useful to describe the current circulation throughout the target area on the basis of a proper model calibration by using measured field data.

2. Measurements facilities and acquired data

A Nortek's AWAC vessel mounted acoustic Doppler velocity profiler allowed the measurements of the three components of the seawater velocity along the water depth at nine chosen stationing points each of which was reached and established by means of a DGPS and a gyrocompass integrated into the profiler that allowed the proper velocity direction with respect the geographical coordinates. The time acquisition of the velocity profiler was longer than 3 minutes. At each station the measures where acquired every one meter, starting from 4 m below the seawater level. The measured of the flow were carried out by using the Nortek AWAC with an acquisition frequency of 0.5 Hz, while the acoustic frequency of its beams is of 600 KHz, thus the obtained data were not useful for turbulence analysis. Figure 2 illustrates the points displacements (see also Figure 1 to overview the site location).

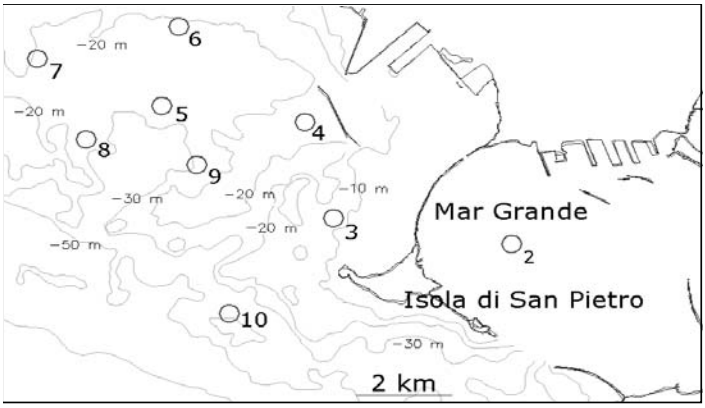

Figure 2. Displacement of the stationing points.

The mean water velocity was calculated by taking the average of the measured velocities over a period of time long enough to eliminate the turbulent fluctuations but sufficiently short to avoid the tidal variability.

The numerical model used was the MIKE21 Flow Model with Flexible Mesh (FM) manufactured by the DHI (Danish Hydraulic Institute). MIKE 21 Flow Model FM is a modelling system based on a flexible mesh approach. The modelling has been developed for applications within oceanographic, coastal and estuarine environments.

Mike 21 allows also a computational domain composed by a series of rectangular cells, and its application is described in Ben Meftah et al. (2007).

Figure 3 shows the computational domain and mesh used in this work for all the simulations.

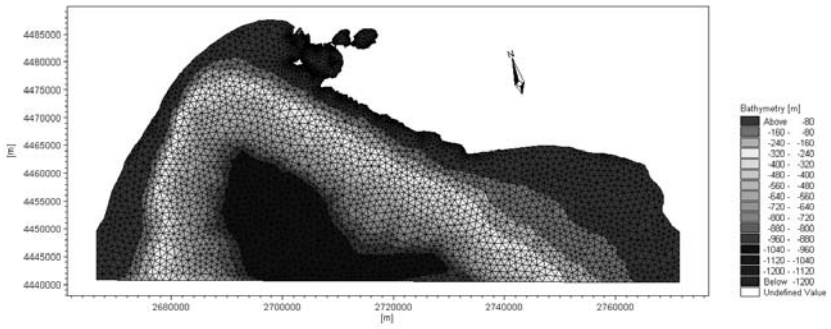

Figure 3. Computational domain and mesh used for the simulations.

In the present study the turbulence was modelled by the classical Smagorinsky subgrid model (Smagorinsky, 1963) with the Smagorinsky coefficient equal to 0.28. A computational time step of 4s was chosen. The test had a total duration of five days since 25/12/2006 at 00:00 to 30/12/2006 at 00:00. The simulation was performed in barotropic condition, with a constant value of water temperature and salinity.
Simplified forcings, such as wind field and tide, were intentionally used in order to highlight the capability of the model to reproduce the real current field. In particular, starting from an initial state of rest, each run was forced by the following selected actions: a spatially homogeneous but time-varying wind field and a time-dependent marine surface level imposed at the open boundary of the domain.
The wind speed and directions and the sea surface elevations were acquired from the oceanographic station of Crotone, a city placed in the Ionian Sea, near the southern open boundary of the computational domain.
In order to validate the model results the wind stress factor and the seabed roughness were varied, in what they may often be chosen as calibration parameters due to the uncertainty about these data.

3. Results

Figure 4 shows the comparison between the measured and computed data first and after the calibration operations. In particular, Figure 4 (a) shows the results obtained by using the model predefined values of the wind stress factor of 0.00125 and the Manning's seabed roughness of $32 m^{1/3}/s$.
On the contrary, the results of Figure 4 (b) represents the numerical values carried out with a wind stress factor of 0.0025 and the Manning's seabed roughness equal to 64 $m^{1/3}/s$. It can be noted that the comparison between the measured data and the numerical ones is in very good agreement in the second case.

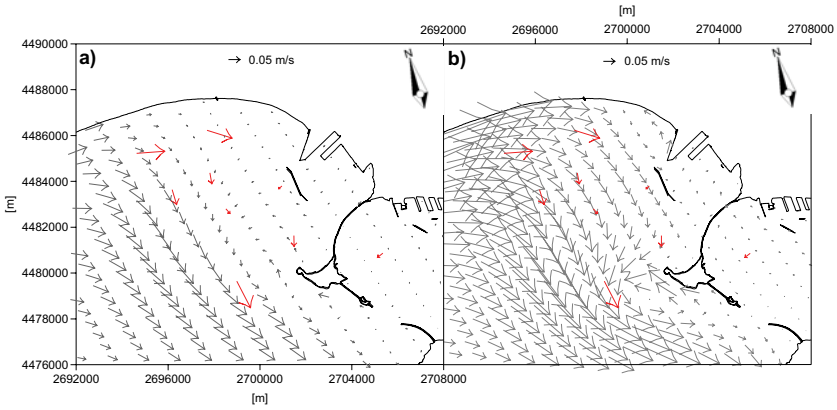

Figure 4. Comparison between the numerical data and the measured ones. a) Wind stress factor=0.00125; Manning coefficient = 32 $m^{1/3}/s$; b) Wind stress factor=0.0024; Manning coefficient = 64 $m^{1/3}/s$.

Moreover, the good quality of the calibration may be confirmed by comparing the surface water

elevation measured at the oceanographic station of Taranto (Figure 5) with the numerical values carried out from the model.

Figure 5. Location of the oceanographic station of Taranto (source: Google Maps).

As Figure 6 and Figure 7 depict, there is a very good overlapping of the numerical seawater elevations near the oceanographic station of Taranto with those measured in situ after the calibration at the same station. Particularly, Figure 6 shows the measured marine surface elevations (blue line) and the simulated ones (red line) at Taranto with the wind stress factor of 0.00125 and the Manning's seabed roughness of $32 m^{1/3}/s$, while Figure 7 the same quantities as obtained after the calibration process with wind stress factor of 0.0025 and the Manning's seabed roughness of 64 $m^{1/3}/s$. The figures also report the sea level as measured at the Crotone station, that is that used for the open boundary condition, which is the same for both the cases.

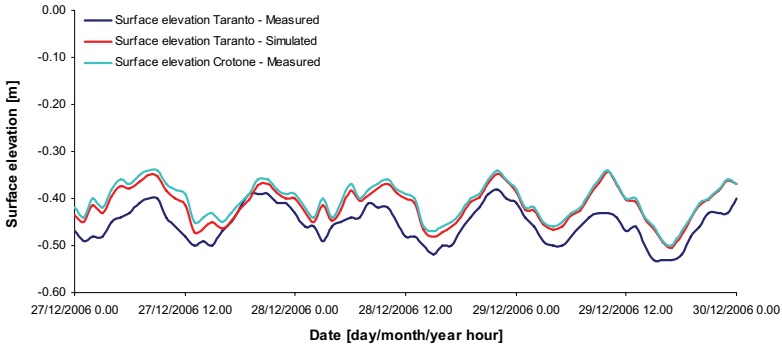

Figure 6. Comparison between sea level as measured at the Taranto's Oceanographic station (blue line) and as obtained from the numerical model (red line).

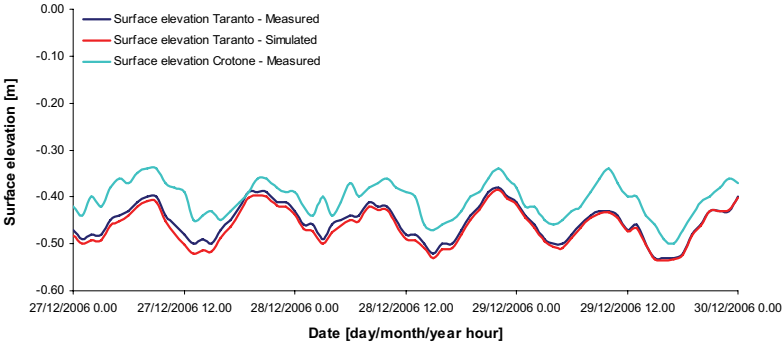

Figure 7. Comparison between sea level as measured at the Taranto's Oceanographic station (blue line) and as obtained from the numerical model (red line) after the calibration process.

As it is possible to see, after the calibration operations (Figure 7), the surface elevations simulated in vicinity of the city of Taranto present a very good agreement with those obtained from the data measured by the oceanographic station of Taranto.

The obtained results show that the present numerical model with a correct calibration may be useful to analyse the marine circulation in the investigated zone and they may be also used as a starting point to further analyses for the pollutants spreading throughout the analysed area.

References

Ben Meftah, M., De Serio, F., Mossa, M., Petrillo, A.F. & Pollio, A., 2007. 'Current circulation in the gulf of Taranto: numeric simulations and experimental data analysis', Flucome 2007, Tallahassee, Florida.

De Serio, F., Malcangio, D., Mossa, M., 2007. 'Circulation in a Southern Italy coastal basin: Modelling and field measurements', Continental Shelf Research, 27, pp.779-797.

Mossa, M., 2006. 'Field measurements and monitoring of wastewater discharge in sea water', Estuarine, Coastal and Shelf Science, 68, pp. 509-514.

Roberts, P.J.W., 1980. 'Ocean outfall dilution: effects of currents', Journal of the Hydraulics Division, ASCE, 48, 769-782.

Smagorinsky, J., 1963. 'General circulation experiment with the primitive equations', Monthly Weather Review, 3, 99-164.

AN ANALYSIS OF THE ARTIFICIAL VISCOSITY IN THE SPH METHOD MODELLING A REGULAR BREAKING WAVE

D. DE PADOVA[(1)], R. A. DALRYMPLE[(2)], M. MOSSA[(1)], A. F. PETRILLO[(3)]

[(1)] *Environmental Engineering and Sustainable Development Department, Technical University of Bari, Via E. Orabona, 4 – 70125 Bari, Italy, e-mail: d.depadova@poliba.it, m.mossa@poliba.it*

[(2)] *Department of Civil Engineering, Johns Hopkins University, 3400N Charles Street, Baltimore, MD 21218, USA, e-mail: rad@jhu.edu*

[(3)] *Water Engineering and Chemistry Department, Technical University of Bari, Via E. Orabona, 4 – 70125 Bari, Italy, e-mail: petrillo@poliba.it*

Abstract

This paper presents free surface modelling by means of the SPH numerical Lagrangian approach, simulating physical model tests on water waves generated in the wave flume of the water Engineering and Chemistry Department laboratory of Bari Technical University (Italy). Smoothed Particle Hydrodynamics (SPH) is a relatively new method for examining the propagation of linear and breaking waves. The development of the JHU SPH model is still ongoing and the numerical model results require further analysis and detailed comparison with other numerical models and experimental data. Comparisons with physical model runs demonstrate the potentialities of SPH like an engineering tool.

The simulations in the present paper used an artificial viscosity, following Monaghan (1992). However, there were some difficulties in establishing the correct value of the fluid viscosity.

The empirical coefficient α, used in artificial viscosity (Monaghan, 1992), is needed for numerical stability in free-surface flows, but in practice it could be too dissipative. Several improvements that we have made in the same numbers of particles with different value of empirical coefficient α are presented here. The study made particular reference to the velocity and free surface elevation distributions with the aim to calibrate the empirical coefficient α, used in the fluid viscosity, in terms of stability and dissipation in the fluid. The final model is shown to be able to model the propagation of regular and breaking waves.

1. Introduction

Smoothed particle hydrodynamics (SPH) is a computational method used for simulating fluid flows. This Lagrangian mesh-free particle model was introduced by Gingold and Monaghan (1977) in astrophysics. Since then, it has been modified for use in solid mechanics (such as impact problems), and fluid mechanics (such as casting in molds). Monaghan (1994) showed that SPH could be used for free surface flows and it had the advantage that no special treatment was need at the free surface; that is, no imposed boundary conditions. Smoothed Particle Hydrodynamics (SPH) can be considered as computing the trajectories of particles of fluid, which interact according to the Navier-Stokes equations.

An alternative view is that the fluid domain is represented by nodal points that are scattered in space with no definable grid structure and move with the fluid. Each of these nodal points carry scalar information, density, pressure, velocity, components, etc. To find the value of a particular quantity at an arbitrary point, x, an interpolation is applied:

$$f(x) = \sum_j f_j W(x - x_j) V_j \qquad [1]$$

Here f_j is the value of f associated with particle j, located at x_j, $W(x-x_j)$ represents a weighting of the contribution of particle j to the value of $f(x)$ at position x, and V_j is the volume of particle j, defined as the mass, m_j, divided by the density of the particle j. The weighting function, $W(x-x_j)$, is called the Kernel and varies with the distance from x. Without viscosity the SPH method is subject to instabilities; one manifestation is that each of the particles begins moving chaotically and this phenomena is called "boiling". Monaghan (1992) introduced an artificial viscosity to simulate a viscosity, dissipative energy within shock fronts, and to prevent particles from interpenetrating other fluid masses.

The term Π_{ij} is empirical and represents the effects of viscosity (Monaghan, 1992):

$$\Pi_{ij} = -\frac{\alpha \mu_{ij} \bar{c}_{ij}}{\bar{\rho}_{ij}} \qquad [2]$$

where α is an empirical coefficient (usually taken as 0.01 - 0.1), $\bar{c}_{ij} = (c_i + c_j)/2$, $\mu_{ij} = h\left(u_i - u_j\right)\cdot\left(x_i - x_j\right)/\left(r_{ij}^2 + 0.01h^2\right)$ and h is the parameter that determines the size of the support for the weighting function, which is a circle of radius $2h$ in 2D and a sphere of the same radius in 3D.

In this paper we analyze the artificial viscosity in SPH, in order to develop a measure of merit for evaluating the empirical coefficient α. The SPH model is applied to the modelling of water waves generated in the wave flume of the Water Engineering and Chemistry Department laboratory of Bari Technical University (Italy).

2. Numerical tests and experimental set-up

The implemented numerical code was first tested using physical experiments on wave motion fields by De Serio and Mossa (2006). The experiments were performed in a wave channel 45 m long and 1 m wide located in the Water Engineering and Chemistry Department laboratory of Bari Technical University (Italy). From the wave paddle to section 73 the flume has a flat bottom, while from section 73 up to the shoreline it has a 1/20 sloped wooden bottom. A sketch of the wave flume is shown in Fig. 1.

Further details about the experimental tests carried out can be found in De Serio and Mossa (2006).

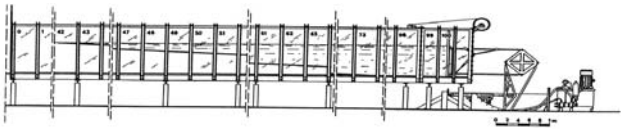

Figure 1. Sketch of the wave flume

The simulations in the present paper used an artificial viscosity, following Monaghan (1992).

In a previous study (De Padova et al., 2008), it was studied that the configuration with 30,000 particles is the best fit to the data. The particle spacing is taken as $\Delta x=\Delta z=0.022$ m and thus approximately 30,000 particles are used. There are a variety of possible weighting functions (see Liu and Liu, 2003), and these SPH calculations using a cubic spline Kernel require neighbors within $2h$ of the selected particle. To calibrate the empirical coefficient α, used in the fluid viscosity, two simulations with different value of this parameter were carried out. Table 2 shows the main characteristics of the SPH simulations. In all two simulations, the water depth, the wave height and the period were equal to 0.70 m, 0.11 m and 2 s, respectively, in section 0.5 m offshore the section 76 (Fig. 2). The experimental and numerical wave profiles at the location of measurement points are shown for both cases (Figure 2). For the sake of brevity only the results of sections 49 will be presented (see Fig. 2). For a defined section, we can study the distribution along the channel of the wave elevation and the horizontal and vertical velocity components for both tests. The velocity measurements were assessed in the vertical sections (Fig. 2) at the intermediate point between the free water surface and the channel bottom.

Test	Coefficient in the artificial viscosity (α)	Particle number
1	0.085	30,000
2	0.045	30,000

Table 1. Characteristics of SPH simulations

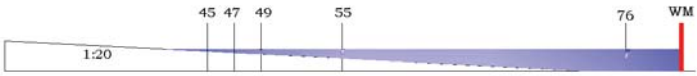

Figure 2. Measurement sections

Figures 3a-3c shows the agreement of numerical data obtained by means of the first SPH model with experimental data. In Figs. 3a-3c it can be seen that in the case with the higher value of α the numerical elevations and the numerical velocities are shown to not be in perfect agreement with the experimental measurements for the strong dissipative effect of viscosity. With a smaller empirical coefficient α (test 2), numerical elevations and the numerical velocities are shown to be in better agreement with the experimental measurements (Figs. 3a-3c). These results show how the empirical coefficient α is needed for numerical stability for free- surface flows, but in practice it is too dissipative. Skewness (Kennedy et al., 2000), a measure of crest-trough shape, is computed and shown in Fig. 4. Test 2 predicts this parameter very well. In fact the trend of wave skewness increases as the wave shoals and breaks, and decreases near the shoreline (section 49). Instead, in the case of Test 1 of Table 1, when the empirical coefficient α is equal to 0.085, the computational results change for the worse and the trend of wave skewness is not well predicted, in particular in sections 47 and 45, where the wave surface profiles are characterized by a rapid change in shape. This result shows how a good efficiency of the computation is not obtained for all values of empirical coefficient α.

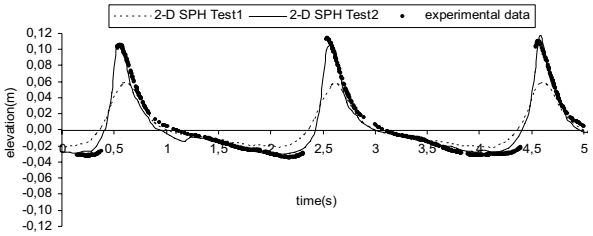

Figure 3a. - Comparison of 2-D SPH with experimental data (section 49)

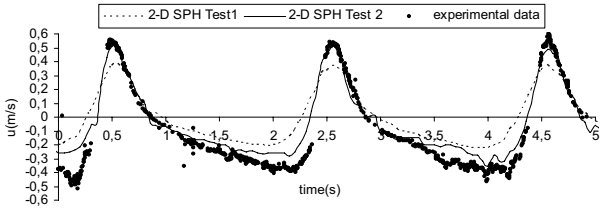

Figure 3b. - Comparison of experimental and numerical horizontal velocity components (section 49, 0.1 m from the bottom)

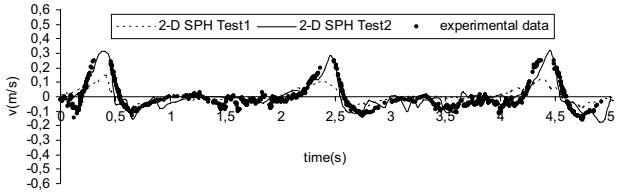

Figure 3c. - Comparison of experimental and numerical vertical velocity components (section 49, 0.1 m from the bottom)

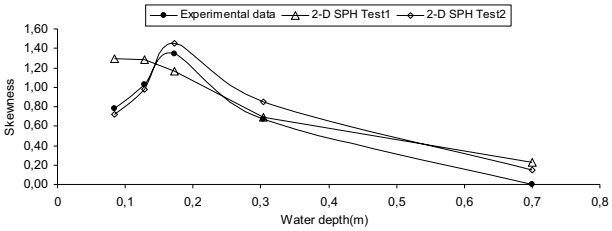

Figure 4. Comparison of experimental and numerical skewness of surface wave elevations

3. Conclusion

Comparisons with physical model runs demonstrate the potentialities of SPH like an engineering tool. However, there have been some difficulties in taking the right value of fluid viscosity. Several improvements that we have made in the same numbers of particles with different value of empirical coefficient α are presented here with the aim to study the effects of fluid viscosity in terms of stability and dissipation in the fluid. The choice of the empirical coefficient α depends on the physical process of the problem and the desired computational accuracy and efficiency. The artificial viscosity term, which depends on the α–parameter, becomes extremely strong with very large numbers of particles. These results show how the empirical coefficient α is needed for numerical stability for free- surface flows, but in practice it is too dissipative. In the runs of the present paper (Table 1), we observed that the case with the higher value of α, the numerical elevations and the numerical velocities were not in good agreement with the experimental ones for the strong dissipative effect of viscosity. With a smaller empirical coefficient α (from 0.085 to 0.045), numerical elevations and the numerical velocities were shown to be in better agreement with the experimental measurements. Therefore, generally speaking, an appropriate and calibrate value of the empirical coefficient α should be used for a settled number of particle in order to obtain good results.

References

De Padova, D., Dalrymple, R. A., Mossa, M. and Petrillo, A. F., Laboratory experiments and SPH modelling of regular breaking waves. *Coastal Technology- Coast, 2008, ISBN: 978-82-92506-61-5 (Book of Abstracts); ISBN:978-82-92506-62-2 (Proceedings CD), Trondheim, Norway.*

De Serio, F., and Mossa, M., 2006 Experimental study on the hydrodynamics of regular breaking waves. *Coastal Engineering*, 53 pp. 53, 99-113.

Gingold, R. A., and Monaghan, J. J., 1977, Smoothed particle hydrodynamics: Theory and application to nonspherical stars. *Mon. Not. R. Astron. Soc*., 181, pp. 375–389.

Kennedy, A. B., Chen, Q., Kirby, J. T., 2000 and Dalrymple, R. A., Boussinesq Modelling of Wave Transformation, Breaking, and Runup. *Journal of Waterway, Port, Coastal, and Ocean Engineering*, 126, pp.39 - 47

Liu, G. and Liu, M., 2003, Smoothed Particle Hydrodynamics: a meshfree particle method. *World Scientific*.

Monaghan, J.J., 1992. Smoothed particle hydrodynamics. Annual Review of Astronomy and Astrophysics 30, 543–574.

Monaghan, J.J., 1994. Simulating free surface flows with SPH. *Journal of Computational Physics* 110, 399–406.

EXPERIMENTAL OBSERVATIONS OF IRREGULAR BREAKING WAVES

Francesca DE SERIO[1] and Michele MOSSA[2]

[1] *Department of Water Engineering and Chemistry, Technical University of Bari, Italy, ph. +39 080 5963557, fax +39 080 5963414, f.deserio@poliba.it*

[2] *Department of Environmental Engineering and Sustainable Development, Technical University of Bari, Italy, ph. +39 080 5963289, fax +39 080 5963414, m.mossa@poliba.it*

Abstract

Since the first pioneering works (e.g. Stive, 1980) to date, the dynamics of regular breaking waves has been widely and successfully investigated, with the exception of the wave crest and the bottom boundary layer (Ting and Kirby, 1994; 1995; 1996). This was also the case of a previous research by the same authors (De Serio and Mossa, 2006) which aimed to describe some principal features of the regular wave dynamics, such as velocity and Reynolds shear stress distributions in the shoaling zone and turbulence in the breaking region. Anyway, many coastal processes, such as undertow currents, sediment transport and action on maritime structures, are strongly due to irregular breaking waves, whose behaviour is not well understood.

The aim of the present research is to analyze the essential physics of a narrow band irregular wave, from deep waters up to the surf zone. The experiments were carried out in the laboratory wave flume of the Coastal Engineering Laboratory (L.I.C.) of the Water Engineering and Chemistry Department at the Technical University of Bari, Italy. The distribution along the channel of some time and phase-averaged wave characteristics was investigated, referring in particular to mean and turbulent horizontal and vertical velocities, Reynolds and turbulent stresses, turbulent kinetic energy. Moreover a comparison with the case of the regular wave was suggested, confirming some vertical trends.

The 2D channel, used in the present experiment, was 50 m long and 2.40 m wide, with a still water level equal to 0.93 m at the wave paddles. Its bottom was rigid and flat in deep waters in the first 35 m m starting from the paddles, while it became sandy onshore, with an average slope of about 1:14 (Figure 1).

The generated wave was characterized by a Jonswap spectrum, with a significative height H_s of 0.10 m and a peak period T_p of 1.6 s.

Both velocities and wave elevations were assessed simultaneously and at the same locations, along the central longitudinal section of the channel. The instantaneous, three-dimensional velocity field was measured, using a 3D Acoustic Doppler Velocimeter by Nortek. In each acquisition, 33000 instantaneous velocity vectors were acquired with a sampling frequency of 25 Hz. The elevations were measured by an ultrasonic gage by UltraLab ULS 2001300 by General Acoustics, characterized by a 0.18 mm resolution and an accuracy of ± 2.00 mm.

Four transversal sections were chosen along the flume, where measurements were carried out. The first was located in deep waters and on the concrete flat bottom, at a distance of 12 m from the wave maker. The other ones were on the sloping bottom, at a distance of 18.50 m, 22.60 m and 24.60 m from the paddles, respectively. For each section, at least 16 measurement points along the vertical were investigated, with a relative distance of 3 ÷ 5 cm, thus covering the whole water column.

It must be underlined that the wave-maker system was properly run in order to reproduce the same irregular wave train after a macro-period of 102 s, therefore the incident wave time series was characterized by twelve equal irregular wave trains, during each measuring operation. This procedure

can be considered rare and therefore innovative, if compared to the experimental approaches used by previous researchers.

In fact, it should be observed that the evaluation of the turbulent components in an irregular wave is more difficult than in the regular one, because the organized wave-induced (ensemble-averaged) components usually change. For example Sultan and Ting (1993) and Ting (2001), in order to apply the ensemble averaging technique, had to generate many times the exact same incident irregular wave. Ting (2002) partitioned the measured instantaneous velocities into a low-pass and a high-pass time series. The ensemble average of the low-pass velocity time series consisted of the undertow and the long-wave velocity. The ensemble average of the high-pass velocity time series was the short-wave velocity. The difference between the high-pass velocity time series and the short-wave velocity was defined as the turbulent velocity fluctuation.

On the contrary, in the present case, each measured instantaneous velocity was separated by ensemble averaging into the organized wave-induced velocity and into the turbulent velocity component, without any interpolation.

As an example, the vertical distributions of the time-averaged horizontal velocities are plotted in Figure 1. Analogous graphs were obtained also referring to vertical velocities and stresses.

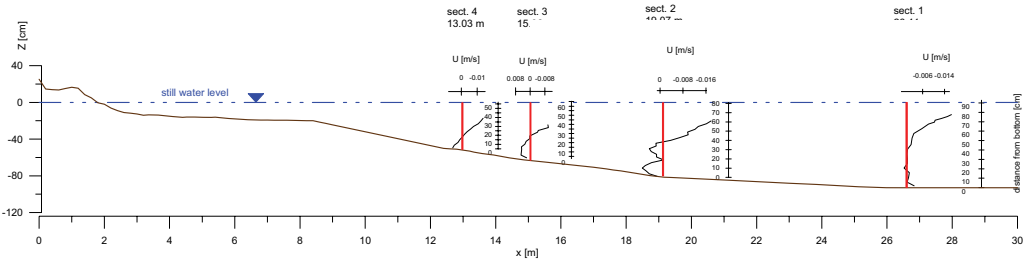

Figure 1. Distribution of the time-averaged horizontal velocities

References

De Serio, F., Mossa, M., 2006. Experimental study on the hydrodynamics of regular breaking waves, Coast. Eng. 53, 99-113.

Stive, M.J.F., 1980. Velocity and pressure field of spilling breakers. Proc. 17th Int. Coastal Eng. Conf., Sydney. ASCE, New York, pp. 547–566.

Ting, F.C.K., 2001. Laboratory study of wave and turbulence velocities in a broad-banded irregular wave surf zone. Coast. Eng. 43, 183– 208.

Ting, F.C.K., 2002. Laboratory study of wave and turbulence velocities in a narrow-banded irregular wave surf zone. Coast. Eng.46, 291-313

Ting, F.C.K., Kirby, J.T., 1994. Observation of undertow and turbulence in a laboratory surf zone. Coast. Eng. 24, 51–80.

Ting, F.C.K., Kirby, J.T., 1995. Dynamics of surf-zone turbulence in a strong plunging breaker. Coast. Eng. 24, 177– 204.

Ting, F.C.K., Kirby, J.T., 1996. Dynamics of surf-zone turbulence in a spilling breaker. Coast. Eng. 27, 131– 160.

Sultan, N.J., Ting, F.C.K., 1993. Experimental study of undertow and turbulence intensity under irregular waves in the surf zone. Proc. 2nd Int. Symposium on Ocean Wave Measurement and Analysis, New Orleans. ASCE, New York, pp. 602– 61.

ANALYSIS ON METEOMARINE CLIMATE AT TREMITI ISLANDS

Maria Francesca BRUNO [(1)], Antonio Felice PETRILLO [(2)]

[(1)] *Eng, Research and Experimentation Laboratory for Coastal Defense (LIC), Technical University of Bari,Via Orabona, 4 Bari , 70125, Italy. f.bruno@poliba.it*

[(1)] *Prof, Research and Experimentation Laboratory for Coastal Defense (LIC), Technical University of Bari,Via Orabona, 4 Bari , 70125, Italy. petrillo@poliba.it*

Introduction

Meteomarine monitoring is one of the main tools for efficient coastal management, but the existing net in Apulia region up to the 2004, was not sufficient to ensure total coverage of the entire territory.

For this purpose, over the past three years the laboratory of Coastal Engineering of the Technical University of Bari has conducted different programs on wave measurements, aimed towards characterising wave conditions along the Apulian coastline. The present paper presents the monitoring programme that was conducted as part of the IMCA research project framework.

Despite their naturalistic importance and the erosive phenomena currently underway, the Tremiti Islands, located about 20km off the northern Apulian coast, were completely lacking in wave measurements and wind data. The mooring of a buoy in the archipelago allowed us to set up wave hindcasting models.

1. Wave data analysis

Since 2005, thanks to an agreement with the Apulia region, a meteo-oceanographic monitoring network, including two directional buoys, has been in operation.

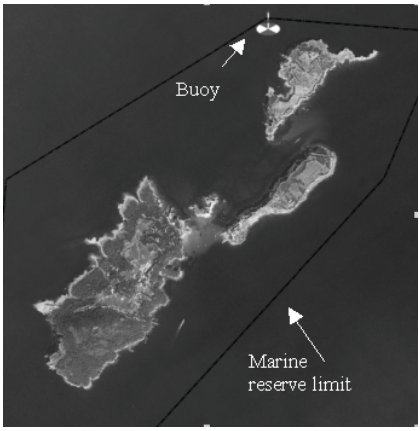

Figure 1- Buoy position

As part of the IMCA research project, another buoy was added to the existing network at the end of 2006. All the data are now available for consultation at the website http://www.puglia-coste.it.

Directional wave measurements are recorded by a Directional Waverider MKIII buoy located offshore the Tremiti Islands. The buoy was moored on 29th December 2006 in the Tremiti Island marine reserve at a location with a water depth of about 94m (figure 1).

The buoy sends its readings to the control centre every 30 minutes via GSM. Here, an application registers the information in a database and updates the website.

The data only refer to one year of observation (2007) and therefore are not sufficient to define the wave climate of the area. Nevertheless, an initial analysis of the data is useful for a discussion about the efficiency of standard methods used for wave hindcasting.

The dataset has been compared with the wave characteristics evaluated by using wave data coming from another buoy, managed by the Italian Environmental Agency, also moored in the Adriatic sea.

Indeed, in the archipelago, wind and wave measurements are not available except for wind data collected by an APAT anemometer in the period between 1993 and 2000. However, the above-mentioned anemometer is prone to measurement errors because of its position near a high cliff.

The wave data normally used for wave hindcasting (De Girolamo, Contini, 2000), are recorded by a buoy moored close to Ortona (less than 100 km north of the Tremiti Islands), which has a fairly similar exposure to wave motion. However, in a previous study (Bruno, De Serio, Petrillo, 2006) it was assumed that the wave climate reliability was poor as it was calculated with a geographical transposition technique using these data. The dataset available was considered as suitable only for the hindcasting of waves coming from the first quadrant, while waves from NNW were considerably underestimated in their intensity and frequency. From a comparison between the Pescara and Tremiti fetch distribution, it is possible to see that, in addition to being fairly similar, the wave sector of Ortona is rotated by about 15° clockwise compared to that of the Tremiti Islands.

An analysis of the series recorded at Tremiti confirms what was previously assumed (figure 2); in the area the most significant sea-storms come from NNO, and are characterized by a high periodicity and high intensity. The Tremiti Islands are, in fact, characterized by extremely intense sea-storms with relatively close frequency. In particular, the buoy registered a sea-storm on January 2nd 2007 which registered a height at its top of 6.29m, one of the highest waves registered in the Adriatic Sea. The events are also characterized by a remarkable duration; this parameter is very important, as waves only develop to the maximum of their potential after a certain period. The wave field direction is notably constant all year round.

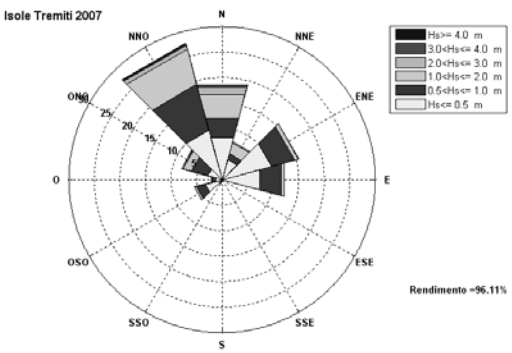

Figure 2- Wave climate at the Tremiti Islands

2. Wave prediction models

From a comparison between recorded and corresponding heights in the period from January to February 2007 (estimated using a geographical transposition model), it is noticeable that this method reproduces the largest part of the sea states examined (Fig. 3 ,4), with a wave height underestimation in the case of waves from NNW (Fig. 5). This is probably caused by the fact that the westerly waves measured at the Tremiti Islands are generated from winds blowing from a wider sector than at Ortona.

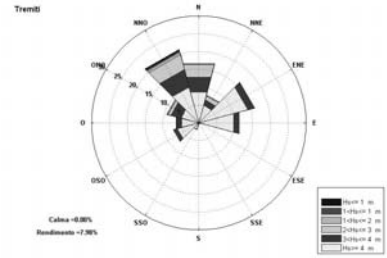

Figure 3-Recorded wave rose

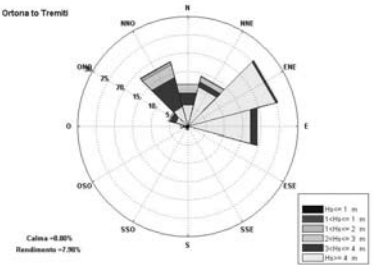

Figure 4- Predicted wave rose

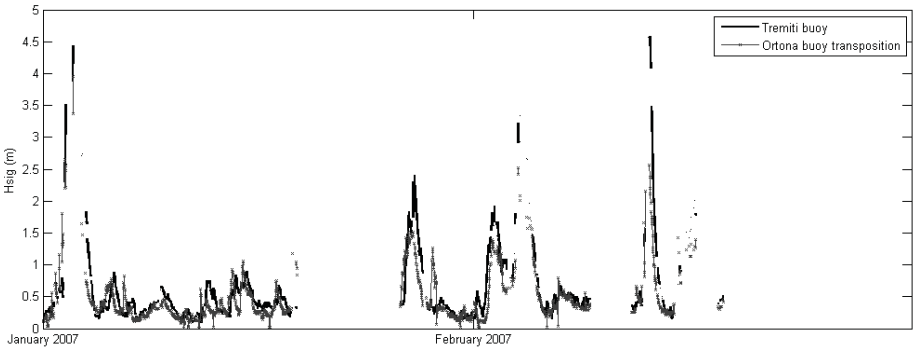

Figure 5- Comparison of recorded and predicted waves from buoy data

The SMB method revised by the Shore Protection Manual was also used to estimate the single sea states recorded in the Tremiti Islands (dashed line in Fig. 6). The wind data used for the hindcasting method came from an anemometer located in Termoli on the Adriatic coast. The technique gives acceptable results in the considering the wind blowing in the wave sector. There is also evidence of a wave height overestimation in the case of waves coming from NNW.

Acknowledgments

This work has been carried out in the framework of the research project "Integrated Monitoring of Coastal Areas (IMCA)", funded by the Italian Ministry of Education, University and Scientific Research.

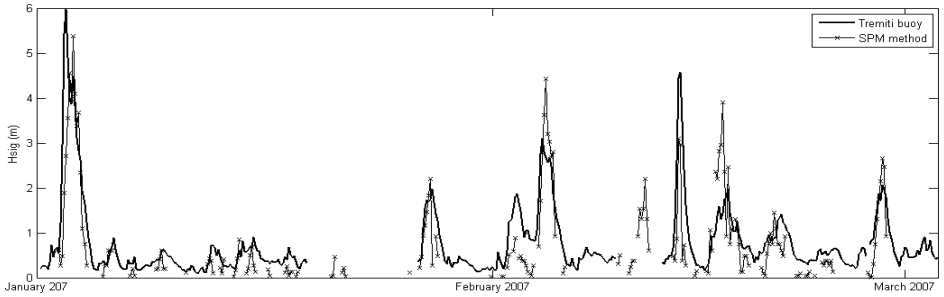

Figure 6 - Comparison of recorded and predicted waves from wind data

References

Bruno M.F., F. De Serio, A.F. Petrillo, 2006 "Analisi delle modifiche dell'idrodinamica costiera di un arcipelago a seguito della realizzazione di opere di difesa e portuali" - *XXX° Convegno Di Idraulica E Costruzioni Idrauliche* -Roma 10-15 Settembre 2006

Coastal Engineering Research Center, 1984 "Shore Protection Manual" Department of the Army- US Army Corps of Engineers

L. Damiani, M.F. Bruno, E. Pagnotta, 2001, "Tecniche per la ricostruzione del clima meteomarino al largo", *22° Corso di Aggiornamento in "Tecniche per la Difesa dall'Inquinamento"*, Guardia Piemontese (CS).

P. De Girolamo, P. Contini, 2000 "Impatto morfologico di opere a mare: casi di studio", RICAMA project,.

K. Hasselmann, 1973 "Measurement of wind wave growth and swell decay during the Joint North Sea Wave Project", *Technical Report*, Deut. Hydr. Inst, Hamburg.

D. Leenknecht, 1992 "Automated Coastal Engineering System: users guide", Coastal Eng. Research Center.

P.Frohle, T. Fittschen, 1999 "Assessment of short term directional wave measurement with resect to long term statistical evaluations", *Copedec V*, Cape Town SA

3D PHYSICAL MODEL TESTING ON NEW EL KALA FISHERY HARBOUR IN ALGERIA

K. RAVEENTHIRAN [(1)], L. V. P. N. JAYAWARDENA [(2)], K. THULASIKOPAN [(3)], M. AMARI [(4)], G. BAY [(5)] & M. MENDIS [(6)]

[(1)] *Senior Research Engineer, Lanka Hydraulic Institute, Moratuwa, Sri Lanka. ravi@lhi.lk*

[(2)] *Research Engineer, Lanka Hydraulic Institute, Moratuwa, Sri Lanka. nilanthi.jayawardena@lhi.lk*

[(3)] *Research Engineer, Lanka Hydraulic Institute, Moratuwa, Sri Lanka. k.thulasikopan@lhi.lk*

[(4)] *Director, Hydro Marine Ingenierie, Kouba Alger, Algeria. hmi.alg@gmail.com*

[(5)] *Project Coordinator, Cooperativa Muratori Cementisti, Ravenna, Italy. guido.bay@cmcra.com*

[(6)] *Chief Executive Officer, Lanka Hydraulic Institute, Moratuwa, Sri Lanka. malith.mendis@lhi.lk*

Abstract

The main breakwater of proposed fishery harbour at El Kala in the eastern Mediterranean coast in Algeria was destructed several times by strong storms during the construction in 1997 - 2004. 3D (basin) physical modelling was conducted to assess the stability of main breakwater in order to avoid any significant destruction of protection during the construction stage for different summer and winter extreme wave conditions. The main breakwater section was redesigned in order to improve the overtopping and the stability of breakwater head.

1. Introduction

Algeria, located on the southern border of the Mediterranean Sea and east of Morocco and west of Tunisia, has a coastline of about 1,200km. The coast has the predominant wave from N-W during winter while weakest appearances from N-E during summer. The tide amplitude is very low in the Mediterranean Sea. The Algerian coastline is diverse going from sandy beaches to rocky cliffs. The littoral drift depends on the orientation and type of the coast. Most of the sandy beach sectors receive waves from NW-NE and induces littoral movement mainly parallel to the coast. The cliff sector receives in general front waves and the littoral drift is quasi insignificant. Algeria's main cities are located along the coastline and more than 50% of the 33 million population lives less than 50km from the coast. Algeria has more than 10 commercial harbours and 35 fishing harbours.

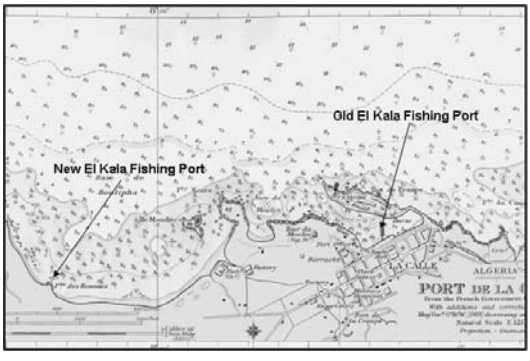

Figure 1: Location Map of Fishing Ports at El Kala

Figure 2: Destructed Breakwater during Construction

The (old) El Kala fishing port is, about 500km east of capital Alger and about 18km west of the Tunisian border, located on point PRESQUILE, a short peninsula enclosing the east side of the harbour. In early 1990, the Government of Algeria planned a new fishing port at El Kala, located 3km west of the old El Kala fishing port (Figure 1). Studies were carried out during early 1990s and the work was lunched in 1996. The main breakwater of the port was destructed several times by strong storms during the construction in 1997-2004 (Figure 2). During the same period complementary hydraulic studies were carried out twice in 1997-1998 and 2002-2003. It was understood the difficulties for the construction of the main breakwater, and 3D (basin) physical modelling was carried out to assess the stability of main breakwater in order to avoid any significant destruction of protection during the construction stage and also the completed stage.

2. Model Setup

The physical model studies were carried out in the LHI wave basin of 35m x 25m on a fixed bed undistorted model 1:60 under the effect of irregular waves. The correct sizes of concrete armour units of ANTIFER of 18T at trunk and 25T at head were used on 1:1.5 slope of 8.3m CD main breakwater to ensure a correct reproduction of hydraulic characteristics of the modelled structures. The placement technique of the armour blocks on the slope toe is especially important as the geometry of the slope toe affects the stability armour (Yagci and Kapdasli 2003). Attention was paid to assure that the semi-cylindrical hole-parts of blocks make contact with the base surface and the adjacent blocks were placed so that the blocks form an angle with each other. After placing the blocks on the slope toe, the remaining part of the first layer as well as the second layer are filled by letting the blocks free fall.

The offshore waves of both summer and winter seasons of 1 - 50yr return periods approaching respectively from N-E and N-W were tested (Table 1). The wave generators used in the model tests were capable of generating irregular wave fields according to the JONSWAP spectrum for specified significant wave heights and periods. The wave heights were measured using conductivity type wave gauges, which comprise two thin, parallel stainless steel electrodes. Prior to construction of model layout, a series of calibration runs were carried out to establish input wave conditions to obtain the required designed wave conditions in front of the wave paddle.

Table 1: Offshore Extreme Wave Conditions at El Kala

Return Period (yr)	NW (315°)		N (0°)		NE (45°)	
	Hs (m)	Tm (s)	Hs (m)	Tm (s)	Hs (m)	Tm (s)
1	6.80	11.5	5.20	10.0	3.80	8.5
2	7.40	12.0	5.60	10.5	4.10	8.5
5	7.80	12.5	6.00	11.0	4.40	9.0
10	8.50	13.0	6.80	11.5	4.70	9.5
20	9.25	14.5	7.30	12.0	5.30	10.0
50	10.00	15.0	8.00	12.5	5.80	10.5

3. Model Results of Original Design

Various sections with different layers such as core, filter, single layer armour, double layer armour without crest wall, etc. of the main breakwater were considered in the modelling in order to avoid any significant destruction of protection during the construction stage and the allowable wave heights were identified. During the model testing it was proposed to remove the layers at the external foot of the main

breakwater in order to avoid the risk of instability of the toe and to reclaim the small rocky bay just west of the proposed harbour in order to reduce the overtopping and damage of armour layer. Based on the tests of completed stage, it was found that the crest of the main breakwater not enough to prevent the overtopping (Figure 3) and the 25T armour units not stable in the head part of the main breakwater (Figure 4).

Figure 3: High Overtopping

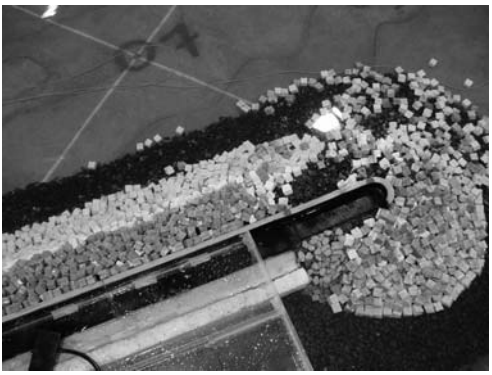

Figure 4: Damaged Breakwater Head

4. Model Results of Revised Design

Following the model tests performed on the original design, a number of alternative solutions were considered and discussed, in order to evaluate the armour blocks' stability and overtopping events in a way that each factor has influence in each other. Hudson's formula (1979) was used to redesign the breakwater armour by selection of appropriate values of stability coefficient of 7 for trunk and 5 for head. The main breakwater was redesigned to 9.7mCD crest and head armour at forward side to 35T and the slope of the section was mild to 1:2. The armour of the breakwater trunk section was kept at 18T and head armour at leeward side at 25T same with the original design. Then the model testing was repeated for the revised design and found that the damage level of both 18T and 35T within the acceptable of 5% for stability (Figure 5). The 25T head armour at leeward side and the secondary breakwater armour were stable for all the model testing and the overtopping was significantly reduced (Figure 6). The wave conditions inside the harbour basin were within the acceptable limit for safe working and mooring conditions.

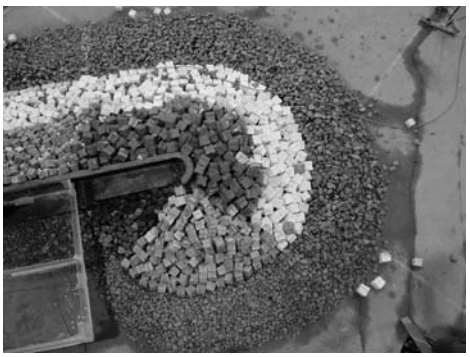

Figure 5: Stable Breakwater Head

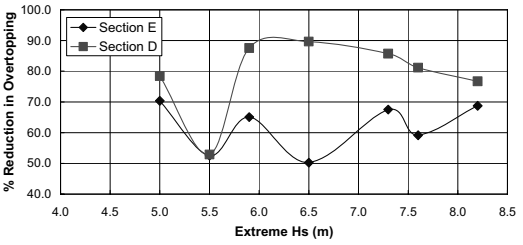

Figure 6: Improved Overtopping

5. Conclusion

The Government of Algeria wanted to find a solution for the frequent failure of construction work of the new El Kala fishing port due to heavy storms. 3D (basin) physical modelling was conducted to assess

the stability of main breakwater in order to avoid any significant destruction of protection during the construction stage for different summer and winter extreme wave conditions. The allowable wave heights were identified for different layers of the breakwater such as core, filter, single and / double layers of ANTIFER armour without crest wall, etc. The damage level of 25T ANTIFER armour near the head and measured overtopping rate are very higher than the standard design criteria, and the main breakwater was redesigned. The wave conditions are within the acceptable limit for safe working conditions at quay as well as safe mooring conditions inside the harbour basin. Construction work has been started based on the revised design (Figure 7).

Figure 7: Harbour Construction Work Underway

References

NIRAS & DHI 2002-2003. 'Hydraulic Studies on New El Kala Fishing Port.

PIANC 1995. 'Criteria for Movements of Moored Ships in Harbours - A Practical Guide', Bulletin 88.

USACE 2006. 'Coastal Engineering Manual: Part VI - Design of Coastal Project Elements', EM 1110-2-1100.

Yagci, O. and Kapdasli, S. 2003. 'Alternative Placement Techniques for ANTIFER Blocks used on Breakwaters', Ocean Engineering, No 30, 1433-1451.

DEVELOPMENT AND CONSOLIDATION OF THE EL KALA PORT IN FISHING AND PLEASURE: PHYSICAL MODELLING INVESTIGATION

A. BASNAYAKA [(1)], N. SUGANDIKA [(2)] , K. RAMACHANDRAN [(3)], K. RAVICHANDREN [(4)], K. RAVEENTHIRAN [(5)], M. AMARI [(6)] & M. MENDIS [(7)]

[(1) (2) (3) (4)] Research Engineer, Lanka Hydraulic Institute, Moratuwa, Sri Lanka. [(1)] ayoma.basnayaka@lhi.lk, [(2)] nimali.sugandika@lhi.lk, [(3)] ramachandran.karunya@lhi.lk, [(4)]k.ravichandren@lhi.lk

[(4)] Senior Research Engineer, Lanka Hydraulic Institute, Moratuwa, Sri Lanka. ravi@lhi.lk

[(5)] Director, Hydro Marine Inginierie, Algiers, Algeria. hmi.alg@gmail.com

[(7)] Chief Executive Officer, Lanka Hydraulic Institute, Moratuwa, Sri Lanka. malith.mendis@lhi.lk

Abstract

This paper describes the 2D stability model of the El Kala Port in order to reduce the overtopping and consolidate the very affected sections of the peninsula and to determine the stability of the proposed main and secondary breakwater structures.

1. Introduction

The El Kala fishing port, about 500km east of capital Algeria and about 18km west of the Tunisian border, constructed in 1975 on point PRESQUILE, a short peninsula enclosing the east side of the harbour (Figure 1). Based on the available wave data information the annual wind distribution is concordant with wave, and NW is the dominant winter wind with 10m wave height and significant wind from NE during summer with 6m wave height of 50yr return period.

The peninsula is quietly narrow near the root and the head, and wider at the middle. Seawall built along the peninsula with the intention of limiting overtopping and its height varies at (5-6)m near the root and the head, and (10-12)m at the middle of the peninsula. Some of the sections of the peninsula severely affected due to the strong storms, and the harbour has been operational difficulties most of the time due to high overtopping and wave penetration.

.

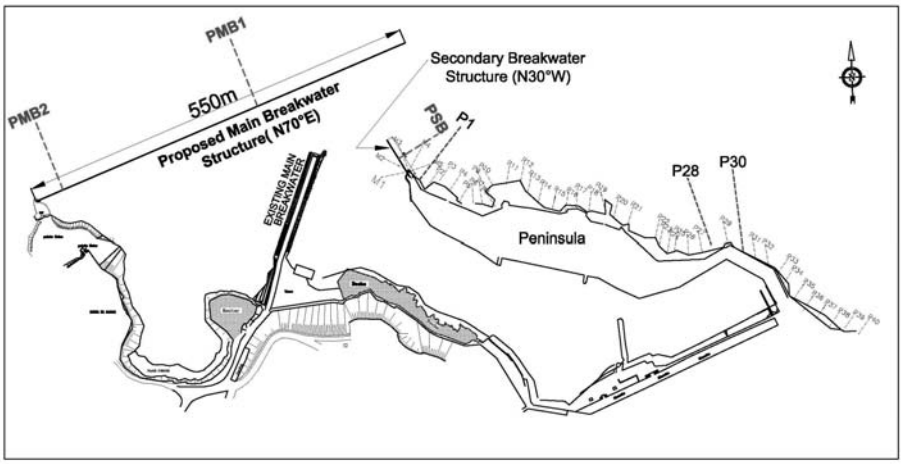

Figure 1: Old El Kala Fishing Port

Further the existing main breakwater, armoured with TETRAPOD units, severely damaged near the head due to storms and the rest of the breakwater protected with additional ANTIFER armour which results high wave disturbance inside the harbour (Figure 2). Therefore a new main breakwater has been proposed from the west side of the port in order to have a protection for the existing port (Figure 1). This will also enable to occupy more space inside the harbour as well as there will be a possibility of develop a marina (pleasure) just west side of the existing port.

Government of Algeria has planned to develop and consolidate the El Kala port in fishing and pleasure and appointed the Hydro Marine Inginierie (HMI) and Lanka Hydraulic Institute Ltd (LHI) for the design and hydraulic studies. The prime objectives of this paper are to reduce the overtopping into the harbour and to consolidate/protect of the very affected sections of the peninsula which requires a protection in foot by assessing the effects of the slope and the water depth at the toe on the wave overtopping as well as to determine the stability of the proposed main and secondary breakwater structure over a range of different storm.

Figure 2: Harbour Entrance during a Storm

2. Model Setup and Tests

The experiments have been carried out in the LHI laboratory wave flume which is 30m long, 0.8m wide and 1.6m deep. Three sections of the peninsula - two near the main harbour basin (P28 and P30) and other near the peninsula head (P01), two sections of the proposed main breakwater - one near the middle (PMB1) and other near the root (PMB2), and one section of the secondary breakwater (PSB1), have been considered for the model testing. The scales for the six different profiles have been selected by considering wave flume dimensions, seabed profile, structure configurations and design wave conditions to represent the actual situation. Gravity and inertia forces have to be same in both prototype and the model. Therefore, it is necessary to use Froude scaling law in order to represent the other parameters correctly in the model and the scale is at 1:40 for P01 and P30, 1:60 for P28 and 1: 54 for PMB1, PMB2 and PSB1. Models have been tested for different storm conditions of return periods 1yr to 50yr for a total duration of tests of 6hr prototype.

Figure 3: Section P28: Existing (Left) and 18T ANTIFER (Right)

Model testing has been first carried out for the profiles of peninsula, the existing stage of each section and alternative options have been then considered to reduce the overtopping into the harbour and to protect the damaged section of the peninsula (Figure 3). Rock and ANTIFER concrete armour units have been used for the proposed sections and the stability has been evaluated by Hudson's formula (1979) which developed for rock armour by extensive hydraulic model testing for seaward armour stability and has been used for random placed concrete armour units including ANTIFER by selection of appropriate values of stability coefficient, and the crest level by the wave run-up along the structure (van der Meer, 1988). Then the model testing has been carried out the section of the Main breakwater, mainly

exposed to N-W waves, and the secondary breakwater, mainly influenced by N-E waves (Figure 4).

Irregular waves in the model have been generated by a hydraulically operated paddle controlled by a PC based Wave Synthesizer, and the communication between the PC based software and Active Wave Absorption Control System (AWACS) established through the wave generator/receiver unit. The AWACS is a digital control system that enables wave makers to simultaneously generate the desired waves and to absorb reflected waves online. Wave conditions have been recorded by wave gauges of conductivity type with twin stainless steel electrodes whilst digital camera and digital video have been employed to monitor wave breaking, wave run-up, overtopping and armour movement. The displacement of the amour units have been quantified using overlay photographs taken from fixed camera positions before and after each test whilst individual wave overtopping has been measured by collecting water that overtops the structure using a tank with a calibrated pump and a water level gauge. The maximum acceptable damage level of 5% has been considered for the design criteria of both rock and ANTIFER concrete armour.

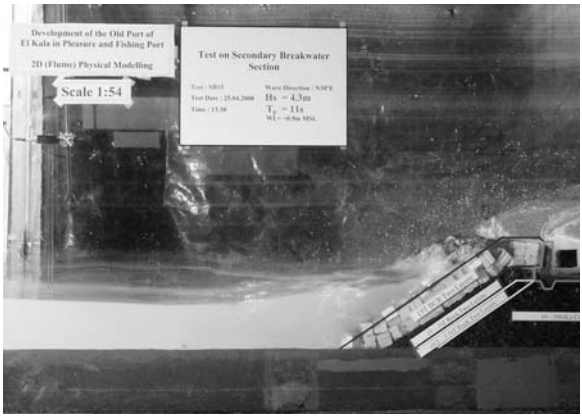

Figure 4: Model Testing on Secondary Breakwater

3. Model Results of Peninsula

The profile 28 near the main harbour basin experiences very severe NW waves and the model testing has been carried out for the higher waves of 50yr and 50yr+20% return period. Basically two alternative options have been proposed one is armour at the toe of the existing seawall and other submerged breakwater at near-shore. By assessing both overtopping rate and damage level of armour units, the armour mound option is more effective and recommended. The armour mound option of 18T ANTIFER reduces overtopping remarkably than other options of armour mound. In addition armour displacements are very less and only little damages recorded for this option. Thus 18T ANTIFER mound is recommended for this particular section.

The profile 1 near the peninsula head experiences significant NE waves and the model testing has been carried out for higher waves of 50yr and 50yr+20% return period. The seawall has been raised to 10m level because the existing section (5m high) experiences very severe overtopping even at 1yr return period wave. Both option of 6T rock armour mound and 10T ANTIFER mound at the toe of the raised 10m seawall are able to reduce overtopping by more than 94%. But stability of structure is better in the option of 10T ANTIFER. Thus 10T ANTIFER for up to 10m of seawall is recommended for this particular profile. The profile 30 near the peninsula root also experiences severe NE waves. Overtopping reduction is similar in both options of 6T rock armour mound and 10T ANTIFER mound and it is around 96% for 50yr+20% return period waves. But the structure stability is better in the option of 10T ANTIFER and it is recommended for this particular section.

4. Model Results of Main Breakwater

The main breakwater has a crest wall with road and quay with buildings on the leeside of the breakwater. Overtopping rate of the profile PMB1 is very high even for 1yr return period waves and it is necessary to increase the crest level in order to reduce it. The main breakwater with 25T ANTIFER gives less overtopping than that of 15T ANTIFER because the later has lesser effective crest than the earlier. The

armour and toe are very stable for both 25T and 15T armoured breakwaters, and 25T is recommended in concerning the overtopping but need to assess in the 3D (basin) modelling.

The overtopping rate of profile PMB2 is very less compare to the profile PMB1 but it is still high when considering the standard criteria (CEM Part VI 2006). It is recommended to increase the crest level in order to reduce the overtopping. The armour displacements are at maximum of 2%, which is in little damage category in standard criteria. As the seabed topography of the main breakwater near the root is rocky and complicated, the breakwater stability can be better assessed in the 3D (basin) modelling than in the 2D (flume) modelling, because lateral variation of the seabed is not considered in the later.

5. Model Results of Secondary Breakwater

The secondary breakwater has a crest wall with road and no quay with buildings on the leeside of the breakwater. The measured overtopped water is very less for 15 T of 50yr return period and within the acceptable limit of standard criteria. The breakwater has been tested for both 18T and 15T armours and no armour displacement has been recorded for both options. Thus it is recommended that 15T BCR is applicable for the secondary breakwater but need to assess in the 3D (basin) modelling.

6. Conclusions

The Government of Algeria has planned to develop and consolidate the El Kala port in fishing and pleasure. 2D (flume) physical modelling has been conducted to consolidate the peninsula and assess the stability of the proposed main breakwater and secondary breakwater.

18T ANTIFER mound is recommended by considering both overtopping and the damage level for the profile 28 since it is experiences in very severe NW waves. The option of 10T ANTIFER is recommended for both P01 and P30. In addition to that, it is recommended to adopt a toe protection to the rock mound for profile P01 and P30 since its seabed profiles are steeper than P28.

Considering the standard criteria, the overtopping rate is within the acceptable limit for the secondary breakwater. As it is high for the main breakwater, it is recommended to raise the crest of the breakwater. The armour displacement for all the options of both main and secondary breakwater is very small. 15T ANTIFER is recommended for the secondary breakwater whilst 25T is for the main breakwater trunk. As the seabed topography at the main breakwater root is rocky and complicated, the breakwater stability can be better assessed in the 3D (basin) modelling than in the 2D (flume) modelling.

References

USACE 2006. ‘Coastal Engineering Manual: Part VI - Design of Coastal Project Elements’, EM 1110-2-1100.

Yagci, O. and Kapdasli, S. 2003. ‘Alternative Placement Techniques for ANTIFER Blocks used on Breakwaters’, Ocean Engineering, No 30, 1433-1451.

CONSTRUCTION OF KRISHNAPATNAM PORT 3D (BASIN) WAVE TRANQUILLITY MODELLING

T.A.N. SUGANDIKA[(1)], L.V.P.N. JAYAWARDENA[(2)], K. THULASIKOPAN [(3)], D.P.L. RANASINGHA [(4)], K. RAVEENTHIRAN [(5)], S. SAMARAWICKRAMA[(6)] , M.A.R. ANASARI [(7)] & M. MENDIS[(8)]

[(1)] *Mrs, Research Engineer, Lanka Hydraulic Institute, Moratuwa, Sri Lank.* nimali.sugandika@lhi.lk , tansugandika@yahoo.com

[(2)] *Mrs, Research Engineer, Lanka Hydraulic Institute, Moratuwa, Sri Lank.* nilanthi.jayawardena@lhi.lk

[(3)] *Mr, Research Engineer, Lanka Hydraulic Institute, Moratuwa, Sri Lank.* k.thulasikopan@lhi.lk

[(4)] *Miss, Research Engineer, Lanka Hydraulic Institute, Moratuwa, Sri Lank.* prasanthi.lanka@lhi.lk

[(5)] *Dr, Senior Research Engineer, Lanka Hydraulic Institute, Moratuwa, Sri Lank.* ravi@lhi.lk

[(6)] *Dr, Senior Lecturer, University of Moratuwa, Moratuwa, Sri Lank.* samans@civil.mrt.ac.lk

[(7)] *Mr, President (Engineering), Krishnapatnam Port Co. Ltd., Hyderabad, India.* mar_a79@rediffmail.com

[(8)] *Mr, Chief Executive / Director, Lanka Hydraulic Institute, Moratuwa, Sri Lank.* malith.mendis@lhi.lk

Abstract

This paper is included wave tranquillity study for construction of Krishnapatnam Port in India from study of 3D basin physical modelling with considering original layout, groyne and wet basin. The main objective of the physical model study is to assess the harbour tranquillity for different incident wave conditions which are expected to prevail at the site during harbour operations. It encompasses to asses the wave disturbance within the harbour basin especially near the quay walls for assuring of safer ship motion.

1. Introduction

The Port of Krishnapatnam, an existing minor port on the Indian east coast, is located in Nellore district of the state of Andhra Pradesh at an approximate distance of 300km from Hyderabad. The port is located in the estuaries of the Khandaleru River, Khandaleru Creek and the Buckingham Canal. A dam is constructed upstream on the Khandaleru River and therefore river silt is negligible. The minor port is to be developed into a modern all-weather deepwater port, capable of handling a large volume of cargo. Presently the roundhead of the South Breakwater and the trunk of the North Breakwater are under construction.

2. Objective

The layout plan of the proposed port development indicates the points of interest for wave tranquillity (Figure 1). The two groynes near zone X and Y shown in the basin at lee side of south and north breakwaters are optional. Similarly a wet basin is also shown as optional duly relocating the zones 11, 12 and 13.

The primary objectives of the 3D physical model study are:

- To study the tranquillity of the harbour basin for both North East and South West Monsoon conditions.
- To fine tune the layout to ensure a minimum of 320 working days in a year by satisfying the different wave conditions required at various berths.

3. Model Set-Up and Testing Procedure

Since model basin is not sufficient enough to construct the full harbour layout, it was decided to use 1:150 scale to cover selected area with considering necessity of the wave disturbance study and sufficient length to propagate deepwater wave to port area.

The head section of the two breakwaters were constructed by using Dolos armor units, the method of placing amour units are random (Figure 2) and it was ensure that prototype packing density was achieved with proper interlocking. As model scale very small in some places of the breakwater Dolos amour units were replaced by similar rock materials with taking into account several factors as layer thickness, model weight and porosity.

The wave generators used in the model tests were capable of producing irregular waves of a pre-determined spectrum and in a particular direction using two or three movable type paddles operating side by side. In the wave generation process, wave parameters Hs and Tp were specified and the JONSWAP-type wave spectrum was used to create input water level time series through inverse Fast Fourier Transformation (FFT).

The wave paddles were calibrated for each wave direction to ensure that the waves are fully developed to the required wave spectrum a short distance away from the wave paddles.

The model testing of the breakwater layouts was carried out at a water level of +0.8m and +2.4m CD (chart datum).

Three wave directions were used for the model testing (60^0, 90^0 & 135^0).

After testing the original layout, it was apparent that the Groynes, Groynes and Wet basin would not give the required tranquility and hence the testing scenarios were changed with the consent of the client.

Finally, following scenarios were tested for different wave conditions.

- Test Series 1: Original Layout
- Test Series 2: Modified South Breakwater
- Test Series 3: Original Layout with Wet Basin at berth 12
- Test Series 4: Open Berths at the Container Terminal (11,12and 13)
- Test Series 5: Open Berths at the Container Terminal (11,12and 13) with a Mound Head at the end of Berth 13
- Test Series 6: Open Berths at the Container Terminal (11-15)

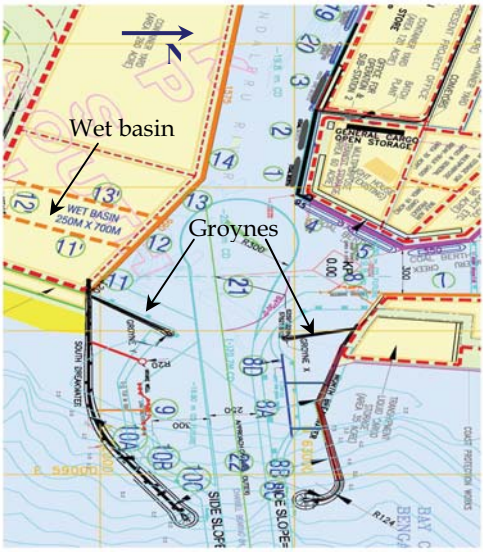

Figure 1 : Layout plan of proposed Krishnapatnam port development

Figure 2 : Dolos arrangement around south breakwater

4. Model Results and Discussion

The existing minor port at Krishnapatnam is to be developed into modern all-weather deepwater port,

which will be capable of handling a large volume of cargo. This study presents the 3D (basin) physical modelling of wave tranquility of the proposed port. The model testing was carried out for the above model configurations:

The model testing of the original layout shows that the berths on the south side of the basin area such as the container berths 12, 13 and 14 are directly exposed to waves from both 90^{o} and 135^{o} directions. Various modifications were done and finally decided to consider the option of open sloped quay (Test series 6) instead of solid vertical quay as in the original layout. It is clear from the model testing of open sloped quay satisfies most of the requirements under wave tranquility.

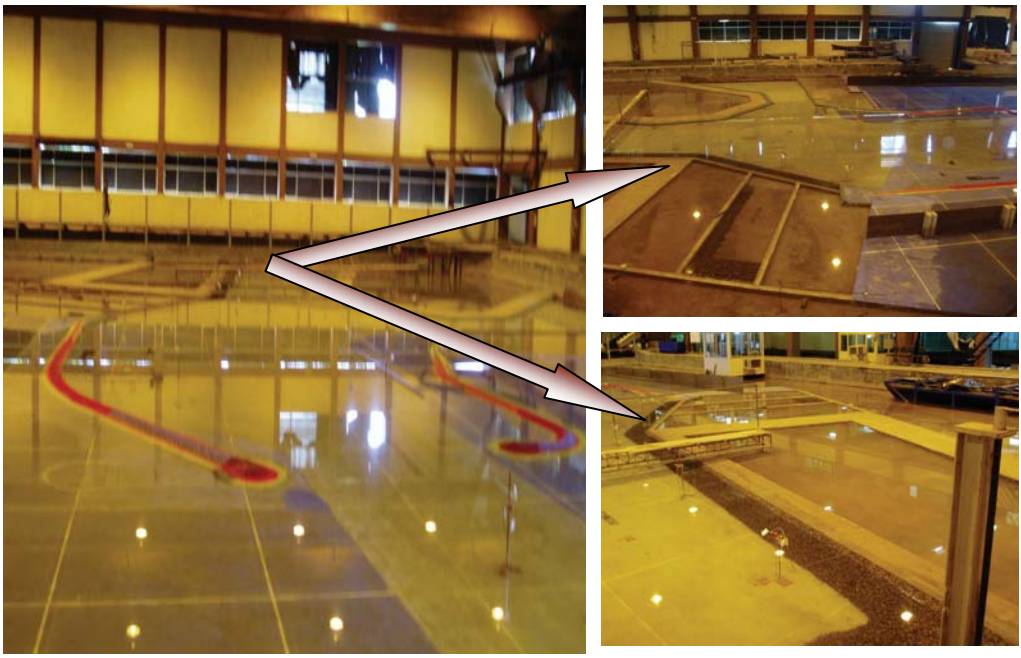

Figure 3 : The open berths at the container terminal (Test Series 6)

(i) Jetty for small craft harbours [8D'& 8D]

Required condition of 0.6m could be achieved in wave directions of 60 and 135. In the case of 90 degree direction, wave condition at the seaward end of the jetty [8D'-0.7m] exceeds the maximum allowable limit. It is recommended to move the jetty slightly towards the harbour side (away from the harbour mouth).

(ii) LNG Jetty [9]

Required wave condition of 0.3m could not be achieved in any of the wave directions. Wave conditions for 90^{0} direction and 135^{0} direction are 0.39m and 0.45m respectively. These conditions are thought to be reasonable, especially wave crests are moving parallel to the Jetty giving mainly surge (translator) and pitch (rotational) movements. Generally stability criteria for surge & pitch movements are low with compared to sway and roll movements. For the 60^{0} direction one year return period wave condition of 0.63m is too high, considering the waves approach at an angle to the jetty. According to the results, the jetty could be used throughout the year apart from certain times of the North East Monsoon Period.

(iii) Liquid Berth [8]

Required wave condition of 0.8m could be achieved throughout the year.

(iv) Bulk Cargo Berths

Required wave condition of 0.8m could be achieved throughout the year.

(v) Container Berths [11 to 15]

Required wave condition of 0.6m could be achieved throughout the year for the berths 11, 12, 14 and 15. In the case of berth 13, wave conditions for 60 and 135 degrees are satisfactory whereas wave conditions for 90 degrees exceed the requirement. It is recommended to use a slope of 1:6 at the back of the open berths 11, 12 and 13, which will increase the energy dissipation. A slope of 1:4 was used for testing.

Gauge Location	H_s (m) for one year return period waves					
	60^0		90^0		135^0	
	T1	T6	T1	T6	T1	T6
1	0.22	0.09	0.64	0.17	0.36	0.13
2	0.09	0.06	0.26	0.13	0.21	0.14
4	0.17	0.06	0.34	0.21	0.18	0.16
5	0.16	0.05	0.35	0.10	0.15	0.08
8	0.16	0.05	0.31	0.08	0.16	0.06
8D	0.2	0.27	0.71	0.58	0.53	0.50
8D'	0.35	0.37	0.74	0.70	0.50	0.61
9	0.71	0.63	0.30	0.39	0.46	0.45
11	0.19	0.21	0.25	0.35	0.21	0.21
11A		0.17		0.25		0.15
12	0.25	0.17	0.49	0.43	0.27	0.16
12A		0.23		0.64		0.24
13	0.43	0.22	0.98	0.74	0.56	0.34
13A		0.16		0.78		0.39
14	0.16	0.14	0.52	0.57	0.27	0.37
14A		0.11		0.49		0.30
14B		0.12		0.55		0.34
15	0.14	0.07	0.37	0.32	0.29	0.18
15A		0.09		0.43		0.28
20	0.07	0.04	0.23	0.09	0.23	0.12
21	0.22	0.13	0.64	0.27	0.45	0.18
22		0.97		1.71		1.05
23		2.16		2.36		0.89
Paddle	2.50	2.50	2.50	2.50	2.00	2.00

Table 1: Comparison of Wave Heights (m) for Test Series 1 and 6

References

Kumuthini S, Dassanayake D.M.D.T.B, 2005. Colombo port efficiency and expansion project, Physical Modelling 3D Stability (Basin) Model, LHI report 1826;

MELBY, J. A. AND TURK, G.F. (1997), Core-Loc concrete armour unites: Technical guidelines, Technical Report, CHL-97-4, US Army Corps of Engineer Research and Development Centre, Vicksburg, MS

BREAKWATER-INDUCED ENVIRONMENTAL EFFECTS AT PESCARA HARBOR: EXPERIMENTAL INVESTIGATIONS

F. LALLI [(1)], S. CORSINI [(1)], F. GUIDUCCI [(1)], I. LISI [(2)], A. BRUSCHI [(1)], L. LIBERTI [(1)], S. MANDRONE [(1)] & V. PESARINO [(1)]

[(1)] *APAT (Italian Agency for Environmental Protection and Technical Service), Via Curtatone, 3, Rome, 00185, Italy.*
francesco.lalli@apat.it
[(2)] *ICRAM (Central Institute for Marine Research) , Via di Casalotti , 300, Rome, 00166, Italy.*

Abstract

In the present work the hydrodynamic field due to the interaction of river run-off with coastal water body is investigated, taking into account the presence of marine structures. The case study is a harbor located in the shallow coastal environment of Pescara river mouth (Adriatic sea, Italy). The river outlet has been recently modified and faced by a large breakwater. The aim of the present analysis is to test, by experimental analysis, some possible improvements of the situation generated at the channel-harbor, by means of suitable modifications of the lay-out. The experimental model set up has been performed taking into account stratification effects. Some harbor configurations have been tested; the results have been discussed and the features of the different solutions were pointed out and specified.

1. Introduction

On entering shallow water environment, river discharge spreads under the effects of marine forcing. Unfortunately, rivers are often considered as very suitable and cheep dumps, and unlimited quantities of pollutants are discharged into fresh waters. Once a pollutant is discharged into the sea, it is transported and dispersed by the flows induced by the typical coastal hydrodynamic forcing, related to barotropic and baroclinic pressure gradients (Fischer et al., 1979).

Pescara river drains into the Adriatic sea the water collected in a mainly mountainous catchments (3200 km^2). In the last tens of kms it runs mainly inside terrigenous sediments crossing a densely developed area, with several towns and industrial settlements exchanging water and pollutants with the river system (Russo, 2003). The river outlet, bounded on both sides by Pescara town, has been recently modified and faced seaward by a 800 m long breakwater. Unfortunately, the harbor configuration gave rise to several, significant environmental effects, concentrating fine sediments and polluted fresh water along the near shore and rapidly changing the sea bottom morphology between the breakwater and the river mouth.

The aim of the present work is to test, by experimental investigations, some possible improvements of the situation generated in the neighborhood of the channel-harbor, by means of suitable modifications of the lay-out. The question to be solved is: how does the polluted river waters spread and how such spreading can be improved, from the point of view of water quality along the shoreline. The problem is complex, due to the interactions of the river flow with marine structures. The presence of waves, wind as well as long-shore streams has been neglected, i.e. the major phenomena are assumed to be the interactions between the flow from the river and the harbor structures. Indeed, from the environmental point of view, the total absence of marine forcing is the worse scenario.

2. Experimental apparatus

The experiments were performed in a horizontal, rectangular water tank (*1500x2000x40* mm). The river inlet is performed by means of a horizontal free surface channel with rectangular (*50x40* mm) cross section, placed perpendicularly in the middle of the tank long side. The channel is connected to a

hydraulic circuit, feeded by a 1.2 kW pump. The outlet section is placed on the whole long side, opposite to the channel mouth: on this side is a wolf-tooth-shaped weir is arranged and the water outflow is almost homogeneously distributed on the whole outlet section of the tank. Next, the water flows into a reservoir which feeds the pump.

The flow through the inlet channel is measured by means of a magnetic induction high precision flow meter, being the accuracy about 0.001 l/s. The flow is visualized by using *Fluorescein sodium salt* ($C_{20}H_{10}Na_2O_5$) and white tempera.

The light from six 120 W incandescent lamps is focused on the investigated region and a standard video camera is used to record the motion of the coloured flow. The camera allows the video record on a PAL standard: frame rate is 25 Hz, image is a 576x720 px RGB array, shutter speed is set to 1/200 s.

The harbour structures have been realized in concrete and the shallow coastal waters river discharge, characterized by the mixing of freshwater with sea water, is simulated using two tanks of the hydraulic circuit. The experiments have been carried out with a flow rate of *0.08 l/s* and average velocity of *10 cm/s*. Reduced gravity Froude (*Fr'*) and Reynolds (*Re*) numbers, defined as $Fr' = U/\sqrt{g'h}$ ($g' = \Delta\rho/\rho_0\, g$, being h uniform water depth, g gravity acceleration, $\Delta\rho$ density difference between river and sea waters, ρ_0 density of sea waters) $Re = Uh/\nu$ (being ν kinematic viscosity) are $Fr'=1.61$ and $Re=2000$.

3. Results and discussion

The river flow is strongly affected by the presence of the breakwater, that diverts the fresh waters stream into two branches (Fig. 1): the former flows through the southern harbour inlet (right side of the images), while the latter flows northward. As a result, due the harbour lay-out, the southern branch flows seaward, whereas the northern branch flows along the coast, which is affected by a progressive degradation of the environment (Lalli et al. 2005).

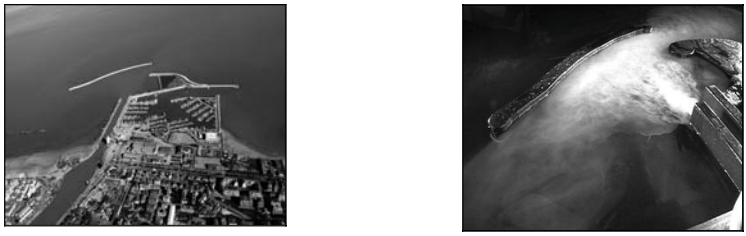

Fig. 1: a) Pescara harbor aerial photo; b) flow visualization at APAT laboratory (1:1000 scale).

In a previous technical report (Lalli et al, 2005) all the carried out experiments were carefully described and all the 11 APAT proposals were specified and discussed. In the present paper, for sake of brevity, only the main features of the activity are outlined, and 8 solutions are described and discussed.

<u>*Solution no. 1*</u>

A floating boom connecting the jetty and the breakwater can prevent the polluted fresh water flow northward. The main features of this solution are:

- efficient protection of the beach;
- cheapness;
- the area between the harbour and the breakwater has an insufficient circulation;
- the northern harbour entrance is blocked off by the boom, so this solution can be used only in the summer time, when tourist fruition needs an efficient improvement of the coastal water quality.

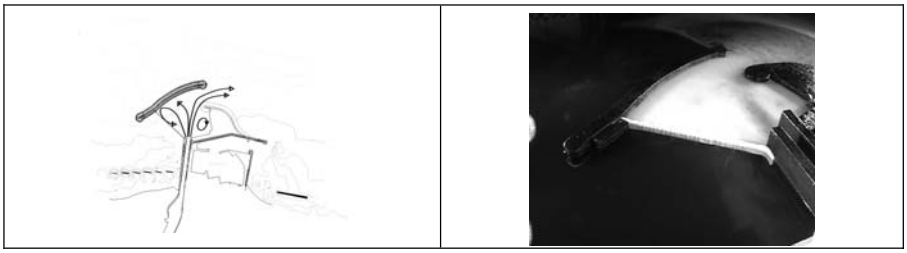

Fig. 2 : floating boom.

Solution no. 2

This solution consists of a gap in the breakwater as well as a flow deflector just downstream (northward) the gap. The features of this solution are:

- part of the river discharge flows through the gap and can spread seaward;
- the deflector does not prevent the fresh water flow to reach the beach, so it could be necessary to use also the boom suggested in the previous case.

Solution no. 3

The previous solution can be coupled with a groin located in the north coast. The features of this solution are:

- very efficient protection of the beach;
- the beach is shortened of the area between the groin and the harbours;

Fig. 3 : gap, deflector and groin.

Solution no. 4

A large gap can be made in the breakwater. The new entrance is protected by two converging breakwaters. The features of this solution are:

- a new, large harbour entrance is available;
- the environmental problem of water quality along the north coast is not solved.

Solution no.5

Also in this case, a large gap in the breakwater is considered; the protection from waves is ensured by a new, larger breakwater. The features of this (very expensive) solution are:

- a new harbour entrance is available;
- only a very small amount of fresh waters can flow toward the beach.

Solution no. 6

Two gaps of the same amplitude are opened in the breakwater. The gaps are provided with permeable protection from waves. The features of this solution are:

- as in the previous case, only a small amount of fresh waters can reach the coast.

Solutions no. 7,8 (fig 4)

Both these solutions consist of the complete separation of the beach from the river mouth and the harbour. This idea ensures the complete solution of the environmental problem related the spreading of fresh waters along the northern coast. The northern entrance is eliminated, and the remaining one needs

to be modified, and made more safe from the navigation point of view.

All the previous solutions, including the 7th, are not able to solve the problem of sedimentation in the harbour, related to the fresh water flow. This feature is very important, in fact the harbour needs frequent, expensive dredging. This problem can be completely solved by the 8th proposed solution. Indeed (Lalli et al, 2005), this solution is suggested by APAT to be the most suitable.

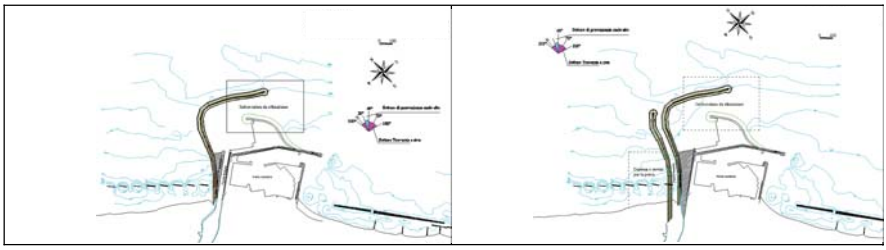

Fig. 4 : solutions no. 7,8 both imply separation between the river mouth and the beach; solution n. 8 suggests also the separation between the harbor and the river mouth.

4. Conclusions

An extensive experimental analysis was carried out at APAT laboratory, concerning Pescara channel harbour. This port, located in the Adriatic Sea, is characterized by environmental, efficiency, and sedimentation problems, mainly due to the interaction between river mouth flow and marine structures. As a result, the experiments show an important feature of baroclinic flows: unlike the barotropic case, significant modifications of the geometry do not give rise to the expected, significant as well, modifications of the flow, which is mainly driven by buoyancy effects. Furthermore, sedimentation problems can be solved only by separating the river mouth from the harbour. These considerations suggest the correct choice for the future development of the harbour, indicated by the solution no. 8.

References

Fischer, H.B., List, J.E., Koh, R.C.Y., Imberger, J., Brooks, N.H., (1979): "Mixing in Inland and Coastal Waters", *Academic Press, Inc.*

Russo M. (2003): "Il fiume Pescara: caratteristiche idrologiche del bacino", Rapporto Tecnico del Servizio Idrografico e Mareografico di Pescara, Regione Abruzzo.

Lalli F, Corsini S, Guiducci F, Cerri C, Falchi M, Lisi I, Morra L, Verrastro E (2005):"Dispersione del deflusso fluviale nell'area portuale di Pescara: proposte preliminari di intervento", *rapporto tecnico APAT.*

MATHEMATICAL MODELLING AS SUPPORT FOR PLANNING DECISIONS

L. DAMIANI[1], D. MALCANGIO[1], M. MOSSA[2], A.F. PETRILLO[1]

1 *Water Engineering and Chemistry Department, Technical University of Bari, Bari, Italy*

2 *Environmental Engineering and Sustainable Development Department, Technical University of Bari, Bari, Italy*

Abstract

The thorough knowledge of the oceanic and coastal circulation pattern is basic for the understanding of several correlated processes, such as the diffusion and dilution processes, as well as for interpreting phenomena linked to the ecosystem activity and forecasting the effects of intervention from outside, through appropriate control policies.

Following an agreement between the city of Bari and the Technical University of Bari, Coastal Engineering Laboratory, the need to focus the study on the interaction between the jet discharged from the outfall coming from the West Bari treatment plant and the surrounding environment arose. It was achieved by means of a 3D hydrodynamic mathematical model, which was tested in previous studies (e.g. Malcangio and Mossa, 2004; De Serio et al., 2005), and further validate in the present study with field measurements. Therefore, a survey was carried out in June 2007 in the area under investigation shown in Figure 1. Collected data were utilized as input by the mathematical model, and its outputs showed a quite good agreement with the field measurements collected during the spring survey. Subsequent to the model calibration, the circulation pattern in the North Bari coast was obtained by several simulations in barotropic conditions (see Table 1), which differed principally in wind field force that are typical of the area (Fig. 2), in order to test (i) the interaction of the real variation in wind direction and intensity on the dilution of the waste water discharge, and mainly (ii) the impact of the last with the coast. The waste water discharge was determined by a salt source distant about 900 m from the coast, that is about the outfall pipe length. Therefore, the salinity was considered as tracer for recognizing the discharge path. The analysis of the salinity diffusion map along the superficial horizontal plane evidences that there is a return of the waste water discharge, identified by the salinity parameter, on the littoral (e.g. see Figure 3a), when the wind comes from the third quadrant.

Further simulations were carried out in order to analyze two project hypotheses about the outfall pipe location that could minimize the impact of the discharge on the surrounding environment, in particular on the littoral that overlooks the waste zone. It must be taken into account that the waste water discharge is situated at 10.5m depth that does not assure an appropriate dilution in the water column over the diffuser as it was observed during the survey, due to the high momentum flux of the jet, especially in overload condition of the treatment plant. In the same zone the sea bed presents a natural rip channel, which less facilitates the jet dilution by the currents. Moreover, the pipe presents several suspended section which could be seat of breaking and the formation of which probably is related to the canyon formation.

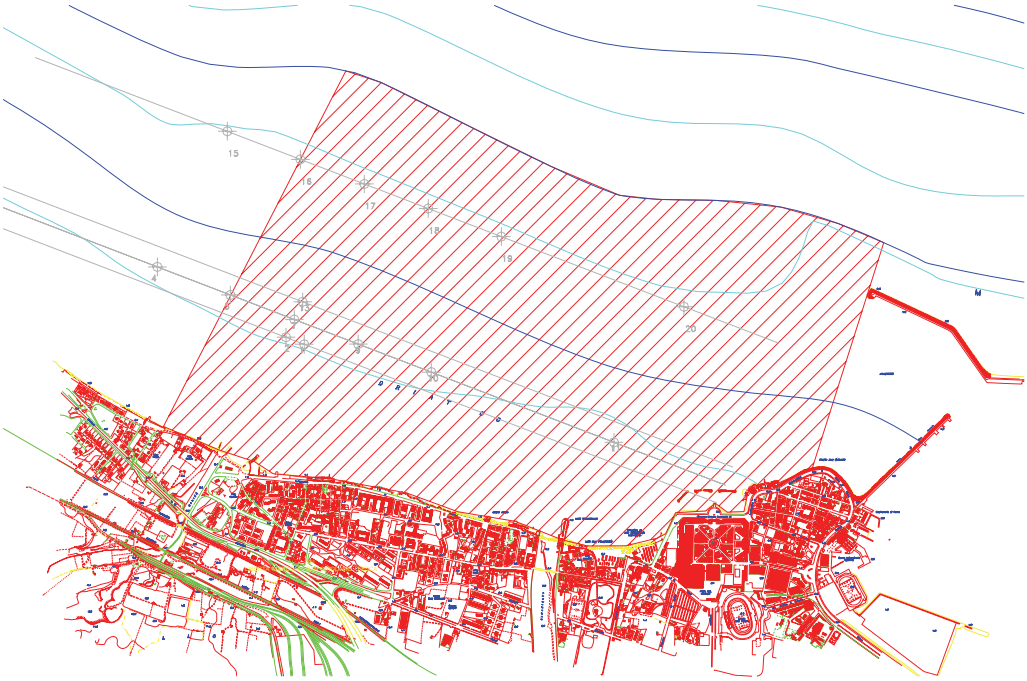

Figure 1. Location of measurement points during the survey.

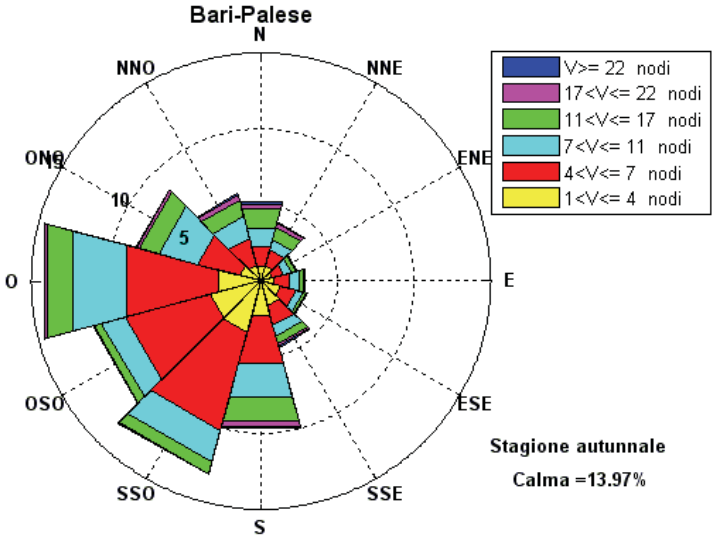

Figure 2. Annual appearance frequency.

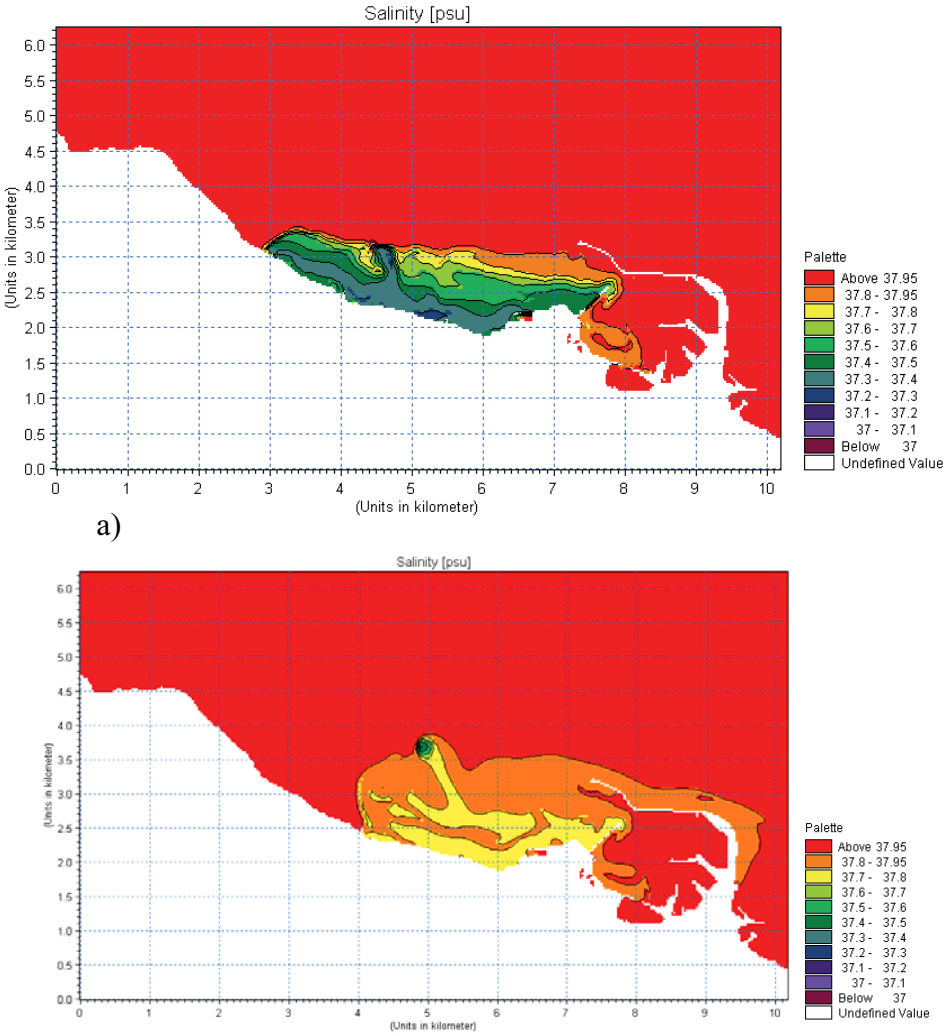

Figure 3. Superficial salinity map for simulations with wind W 2 m/s and discharge point (a) at the current position; (b) outside the natural canyon (second project hypothesis).

Table 1. Main characteristics of runs.

Run	*Wind direction and velocity*	*Outfall configuration*
1	NO: 8 ms^{-1}	present
2	NE: 8 ms^{-1}	present
3	O: 2 ms^{-1}	present
4	SSO: 2 ms^{-1}	present
5	O: 2 ms^{-1}	longer
6	O: 2 ms^{-1}	moved

All the aforementioned considerations led into the analysis of a first project hypothesis that takes into account a removal of the last part of the outfall pipe on the other side of the rip channel, on the understanding of the diffuser geometrical characteristics (length, nozzle number and section, distance between nozzles). The only operative intervention in this case consists in a lengthening of the outfall pipe, which must be renovated anyway. As second hypothesis, the advisability of the outfall pipe full replacement with a new planned route considerably distant from the existing location, and with a longer pipe in order to reach the depth of 15 m, was considered.

Therefore, two further simulations were carried on with the aim of verifying if (i) an increase of the pipe length (about 150 m) and (ii) a different displacement of the waste pipe toward NE but most of all far from the natural canyon, can determine a slight discharge impact on the coast. Both simulations adopted as climatic conditions the less frequent (wind from W with velocity 2 m/s) but the most dangerous, in terms of interaction of the discharge with the coast, among the climatic conditions simulated. The second project hypothesis showed higher salinity values for the diffusion plume and therefore more similar to the background salinity (Fig. 3b), than values obtained by the first project hypothesis, and clearly with less environmental impact than the current situation (Fig. 3a).

References

De Serio, F., Malcangio, D., Mossa, M. and Petrillo, A.F. (2005), *Modelling currents and solid transport offshore Porto Cesareo (Southern Italy)*. Proc. ICS 2005, Island, Höfn 6-8 June 2005.

Malcangio, D. and Mossa, M. (2004), *Tidal Current Computation in the Mar Piccolo (Taranto)*. Shallow Flows, Editors G.H. Jirka & W.S. J. Uijttewaal, The Netherlands, A.A. Balkema, 217-223.

PHYSICAL MODEL ANALYSIS OF FLOATING OIL BOOMS

Alberte CASTRO [(1)], Gregorio IGLESIAS [(2)], José Angel FRAGUELA [(3)],
Rodrigo CARBALLO [(1)], Francisco TAVEIRA-PINTO [(4)] & Hugo LOPES [(5)]

[(1)] *Assoc. Res., Univ. of Santiago de Compostela, Dep. Agr. Eng., Campus Univ., Lugo, 27002, Spain. albertecastro@udc.es, rcarba@usc.es*

[(2)] *Assoc. Prof., Univ. of Santiago de Compostela, Dep. Agr. Eng., Campus Univ., Lugo, 27002, Spain. iglesias@usc.es*

[(3)] *Assoc. Prof., Univ. of A Coruña, Dep. of Naval and Ocean Eng., Campus Esteiro, Ferrol, 15403, Spain. fraguela@udc.es*

[(4)] *Assoc. Prof., Faculty of Engineering of the University of Porto, Rua Dr. Roberto Frias s/n, Porto, 4200-465, Portugal, fpinto@fe.up.pt*

[(5)] *PhD Candidate, Faculty of Engineering of the University of Porto, Rua Dr. Roberto Frias s/n, Porto, 4200-465, Portugal, hglopes@fe.up.pt*

Abstract

Floating oil booms are the fundamental tool to defend the coastlines in the face of an oil slick advancing from deepwater. Their effectiveness depends on a number of factors related to the boom characteristics and the sea state. In this paper, the boom response in terms of its motions is investigated with the aim of analysing the influence of each parameter involved in the process.

1. Introduction

When an accidental oil spill occurs at sea, the oil slick is carried by currents, waves, and winds. In some cases it will be transported towards the shoreline, with the potential to cause extensive environmental damage. Among the available methods to protect the littoral against an oil spill, mechanical floating booms have proved to be the most adequate, and are therefore extensively used (Oebius, 1999). The oil slick contained by the boom is subsequently recovered by means of skimmers either from ships or from the shoreline.

Floating booms have shown a good performance in sheltered waters, such as port basins. However, it is well known that their effectiveness decreases in open waters, where currents and waves are present. The capability of a floating boom to contain an oil slick under these conditions depends greatly on its motions (Iglesias et al., 2005 & 2006) because they modify the hydrodynamic conditions in the retention zone in front of the boom. These motions are a function of several parameters related to the boom characteristics (geometry, buoyancy/weight ratio, mass distribution) and the current speed and wave height and period (Kim et al., 1998).

In this work, several physical models of floating booms were tested in a 2D flume under the action of waves and currents in order to investigate the influence of these parameters on the boom response.

2. Experimental set-up

The physical tests were performed in the wave and current flume of the Escuela Politécnica Superior of the University of Santiago the Compostela. The wave flume is 20 m long and 0.65 m wide with a maximum water depth of 0.8 m. Wave conditions are generated by means of a piston-type paddle

equipped with an Active Wave Absorption System (AWACS) that allows the absorption of reflected waves. At the opposite end, a wave-absorbing artificial beach with a slope ratio of 1:10 was used in order to minimize the effects on the model of the waves reflected at the end of the flume. Current conditions can be also generated by means of a reversible pumping system controlled by a system of valves.

A number of physical boom models (Fig. 1) consisting of a buoyancy cylinder and a vertical skirt were built at a 1:10 scale. Different buoyancy/weight ratios were obtained by attaching steel rods to the bottom of the skirt. The model response (heave and roll motions) was measured with the help of an Artificial Vision System (Ibañez et al., 2007). This system was developed to avoid the distortions of the boom motion that would be produced by conventional measurement procedures (strain gauges). The results obtained in these tests will be presented at the Conference.

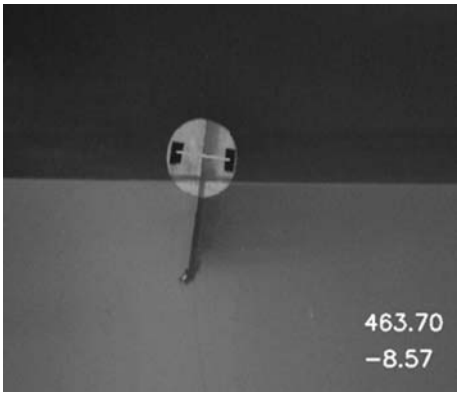

Figure 1. Physical boom model.

References

Oebius. H. U. 1999. Physical properties and processes that influence the clean up of oil spills in the marine environment. Spill Science and Technology Bulletin, Vol 5, No 3/4, pp. 177-289.

Ibáñez O., Rabuñal J., Castro A., Dorado J., Iglesias G, Pazos A., 2007. A framework for measuring waves level in a wave tank with artificial vision techniques. WSEAS Transactions on Signal Processing, Volume 3, Issue 1, pp. 17-24.

Iglesias, G. Fraguela, J.A. Castro, A. Rodríguez,J Nicolás,J.L. Sabín, J.M. Sánchez-Tembleque, F. and Carballo, R., 2005. Diseño y Experimentación en Modelo Físico de una Barrera Oceánica de Contención de Hidrocarburos. VIII Jornadas Españolas de Ingeniería de Costas y Puertos, Sitges (Barcelona)

Iglesias, G. Fraguela, J.A. Castro, Carballo, R. and Taveira Pinto, F.,2006. Oceanic Oil Spill Boom. Design and Laboratoy Tests. Coastlab ’06, Porto (Portugal)

Kim, M.H., Muralidharan, S., Kee, ST, Johnson, RP, Seymour, 1998. 'Seakeeping performance of a containment boom section in random waves and current', Ocean Engineering, Vol 25, 2-3, 143-172.

PHYSICAL MODEL STUDY OF THE BEHAVIOUR OF AN OIL TANKER MOORED AT A JETTY

Paulo ROSA-SANTOS [(1)], Fernando VELOSO-GOMES [(2)], Francisco TAVEIRA-PINTO [(3)], Carlos GUEDES-SOARES [(4)], Nuno FONSECA [(5)], João Alfredo SANTOS [(6)], António PAULO MOREIRA [(7)], Paulo COSTA [(8)] & Emílio BRÓGUEIRA-DIAS [(9)]

[(1)] PhD Candidate, [(2)] Full Professor, [(3)] Associate Professor,
Hydraulics and Water Resources Institute - Faculty of Engineering of the University of Porto,
Rua Dr. Roberto Frias s/n, 4200 465 Porto, Portugal, pjrs@fe.up.pt

[(4)] Full Professor, [(5)] Assistant Professor
Unit of Marine Technology and Engineering, Technical University of Lisbon, Instituto Superior Técnico,
Av. Rovisco Pais, 1049 001 Lisboa, Portugal

[(6)] Research Officer, Hydraulics and Environment Department, LNEC, Av. do Brasil, 101, 1700 066 Lisboa, Portugal

[(7)] [(8)] Assistant Professor, Department of Electrical and Computer Engineering - ISRP, Faculty of Engineering of the University of Porto, Rua Dr. Roberto Frias s/n, 4200 465 Porto, Portugal

[(9)] Member of the Board of Directors, Port Authority of Douro and Leixões, S.A. - APDL, Av. da Liberdade s/n, 4454 851 Leça da Palmeira, Portugal

Abstract

Operational and security conditions in a port terminal are closely related with the behaviour of the moored ships, namely with the ship motions amplitude and the magnitude of the forces in the mooring lines and fenders. In the paper, a physical model study of the behaviour of an oil tanker moored at a jetty will be presented after a brief description of the local environmental conditions and the existing operational conditions at the berth "A" oil terminal. The paper will focus on the comparative analysis of the presently most used mooring layout at the berth "A", with an alternative symmetrical mooring layout.

1. Introduction

The Port of Leixões is located in the northwest of Portugal and handles all the major types of maritime-port traffic. This port has an oil terminal, composed by three berths, operated under concession by *Galp Energia*. Berth "A", located at the harbour entrance, is the most exposed to adverse maritime environmental conditions, despite the protection offered by the Leixões north breakwater, Fig. 1. Alongside this berth the water depth is about -16 m CD, which allows receiving oil tankers of up to 100,000 dwt.

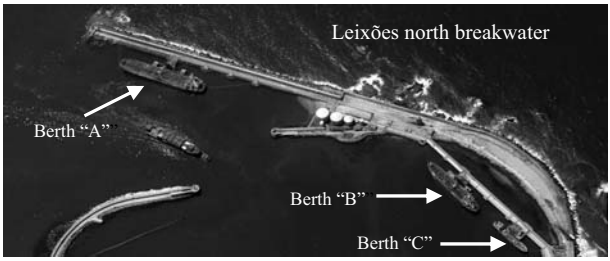

Figure 1 – Leixões Oil Terminal, Porto, Portugal.

Due essentially to its location, berth "A" is affected by hydrodynamic and operational problems. In this berth, breakage of ship mooring lines can occur and excessive motions are sometimes experienced by the moored ships. In some critical situations, the on or off-loading operations are made difficult or even impossible. According to IHRH-FEUP/IST (2005), berth "A" does not assure, in average, the operational and security conditions during about 20% of the time. These facts obviously result in operational costs, as well as, environmental and safety risks, to the port authority, that are important to minimize in order to improve the terminal profitability. To attenuate the problem, a SPM system has been recently installed and is presently in operation offshore the Port of Leixões.

Berth “A” operational conditions are supposed to be influenced by the overtopping of Leixões north breakwater and the wave diffraction around its head, the characteristics of the existing fenders and mooring system, the currents transmission through the breakwater core, and the possible resonance phenomena in the berth “A” area, Veloso-Gomes *et al*. (2005).

A physical model study of the behaviour of an oil tanker moored on the berth “A” is being carried out to clarify the contribution of some of the identified critical issues on berth “A” operational conditions and also to analyse the efficiency of some intervention alternatives proposed in previous studies. This physical model study is part of the *R&D* project DOLPHIN, which also includes numerical simulations and prototype measurements at the berth “A”.

The paper will focus on the results of a simplified physical model of the berth “A” and the surrounding area, built with the aim of analysing the influence of an asymmetrical mooring layout on the behaviour of a moored ship.

2. Experimental set-up

The physical model study is being carried out at the Hydraulics Laboratory of the Hydraulics and Water Resources Division of the Faculty of Engineering of the University of Porto. The existing wave tank is 28 m long, 12 m wide and 1.2 m in depth. The wave generation system, designed by *HR Wallingford, UK*, is of the multi-element type and composed by 16 paddles. The system is equipped with a Dynamic Wave Absorption System. The *3D* motions of the moored oil tanker, in the six degrees of freedom, are measured using a *Qualisys – Motion Capture System*, composed by 3 infrared cameras. With this measuring system ship motions can be measured without direct contact with the model. Forces on the 8 mooring lines and the 2 fenders are measured using specially designed force transducers made by *HR Wallingford, UK.*

The berth “A” jetty structure consists of two breasting dolphins and a loading platform. Each breasting dolphin is equipped with a pneumatic fender and double mooring hooks. The remaining terminal mooring hooks are located on the north breakwater superstructure.

For this stage of the study a simplified physical model of the berth “A” was selected. Bathymetry was considered horizontal and the bottom level near the berth equal to -16 m CD. The breasting and mooring dolphins were reproduced in the physical model; however, there was no need to construct the Leixões north breakwater as the ship model, in this first stage, is only submitted to head waves. Those waves are the ones expected to reach the berth “A” area after diffraction around the head of Leixões north breakwater. The set-up of the physical model in the wave tank is sketched in Fig. 2. One array of four wave probes was installed near the physical model and parallel to the berthing structure, to record the water surface elevations for further reflection analysis, i.e., for the separation of incident and reflected waves, Fig.2. A dissipation beach was created at the end of the wave tank to reduce wave reflections.

The second phase of the study includes the construction of the Leixões north breakwater inside the wave tank on a scale 1/100. The bathymetry will be considered horizontal with waves reaching the berth “A” after diffraction around the north breakwater head.

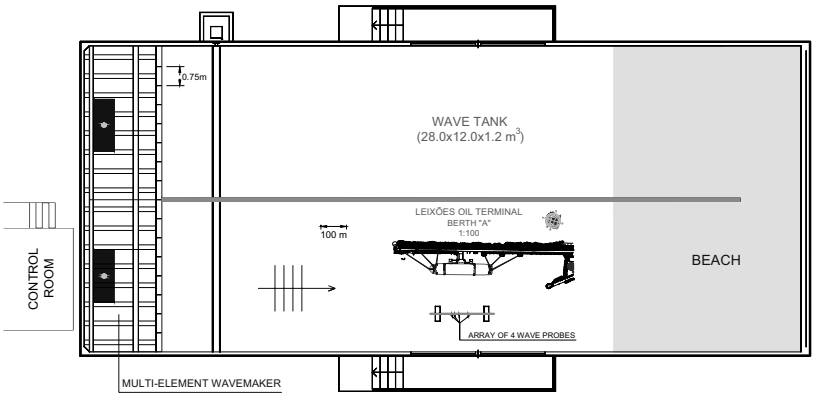

Figure 2 – Physical model set-up on the wave tank.

The ship selected for the study intends to represent the biggest class of oil tankers that regularly demand berth "A". This ship is a 105,000 dwt oil tanker, with 245 m overall length and a maximum draught of 14.1 m. The first ship model was built in fibreglass reinforced plastic on a 1/100 scale, based on the *3D* hull shape definition of a real oil tanker. To analyse scale effects, a ship model constructed at a smaller scale is also foreseen (1/75). Prior to testing, the ship model was ballasted to obtain the required dynamic characteristics of the prototype ship. The calibration allows adjusting the position of the ship centre of gravity and the radius of gyration, as well as its natural periods of oscillation.

The selected mooring layouts are sketched in Fig. 3. The first one is asymmetrical and represents the most usual mooring arrangement for the biggest class of oil tankers that use the berth "A". The second one is nearly symmetrical and takes advantage of the mooring points located near the head of the Leixões north breakwater.

The characteristics of the mooring lines available can differ from ship to ship. The biggest oil tankers that regularly demand the berth "A" are usually moored with steel mooring lines with a synthetic tail (nylon).

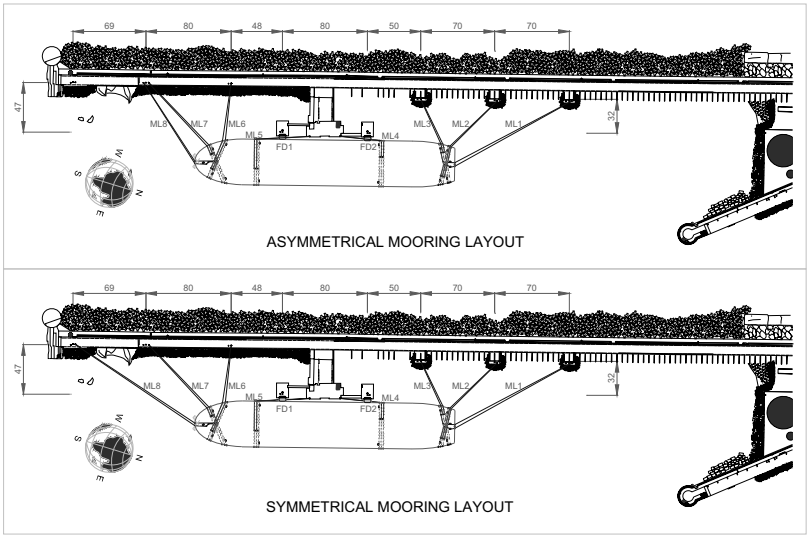

Figure 3 – Asymmetrical and symmetrical mooring layouts considered in the physical model tests.

The load-elongation curves of the mooring lines are simulated using a combination of precision springs, taking also into account the stiffness of the corresponding force transducer. Their non-linear behaviour was linearized. This way the stiffness of each one of the mooring lines (which depends of the mooring line elongation) was substituted by the constant stiffness of an equivalent linear mooring line having the same energy absorption capacity of the non-linear mooring line. The non-linear behaviour of the two pneumatic fenders installed was reproduced in the same way.

3. Preliminary results and discussion

Some preliminary results are summarized on Fig. 4, which presents the maximum loads (prototype) recorded in each one of the mooring lines (ML) and of the fenders (FD), when the ship model is under the action of long crested waves characterized by a significant wave height of 2,0 m and different peak wave periods, during high tide (+4.0m CD). Differences between the two mooring layouts are small, with nearly the same maximum loads recorded on the mooring lines. Loads on the fenders were found to be smaller in the case of the symmetrical mooring layout at intermediate wave periods. Spring lines (ML4 and ML5), as expected, were the most loaded ones due to their lower length and therefore higher stiffness. Maximum loads that the mooring lines and the fenders can withstand (Max Load) are also shown in Fig. 4. Based on the results, spring lines would be the first mooring lines to break.

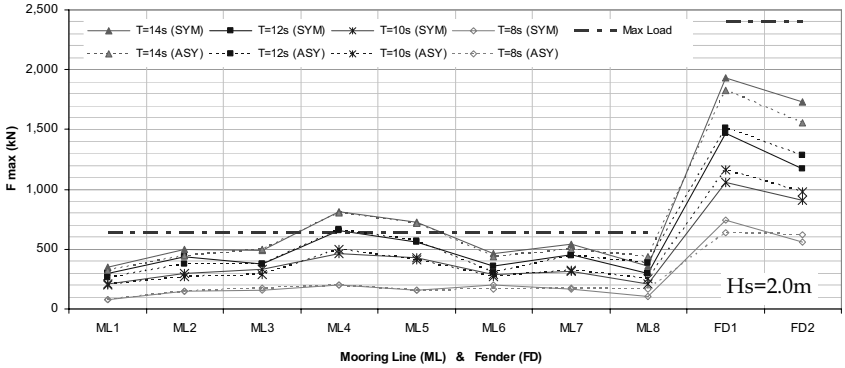

Figure 4 – Preliminary results: asymmetric mooring layout (ASY) versus symmetric mooring layout (SYM).

Acknowledgments

DOLPHIN project (PTDC/ECM/72835/2006) is being funded by the Portuguese Science and Technology Foundation (FCT).

Paulo Jorge Rosa Santos acknowledges FCT for his PhD grant (SFRH/BD/16671/2004). The authors are also indebted to APDL – Port Authority of Douro and Leixões, S.A. for their support to the undergoing study and to INETI-IST for lending the *Qualisys System*.

References

IHRH-FEUP/IST 2005. 'Operational conditions on the oil terminal at Leixões Harbour - Porto - Portugal', Technical Report, 6 Vol. (in Portuguese)

Veloso-Gomes, F., Taveira-Pinto, F., Rosa-Santos, P., Brógueira-Dias, E. & Guedes-Lopes, H. 2005. 'Berthing characteristics and the behaviour of the oil terminal of Leixões Harbour, Portugal', Marine Heritage and Modern Ports, WIT Press, ISBN: 1- 84564-010-1.

ASSESSMENT OF WAVE DISTURBANCE AND SHIP MOTION FOR THE DETAILED DESIGN OF THE HAMBANTOTA SEAPORT

T.D.T.PEMASIRI [(1)], K.RAMACHANDRAN [(2)], K.THULASIKOPAN [(3)], K.RAVEENTHIRAN [(4)], K. PATHIRANA [(5)], J. KURUKULASURIYA [(6)] & M. MENDIS [(7)]

[(1)(2)(3)] *Research Engineer, Lanka Hydraulic Institute, Moratuwa, Sri Lanka.* [(1)] *tharanga.pemasiri@lhi.lk,* [(2)] *ramachandran.karunya@lhi.lk,* [(3)] *k.thulasikopan@lhi.lk*

[(4)] *Senior Research Engineer, Lanka Hydraulic Institute, Moratuwa, Sri Lanka. ravi@lhi.lk*

[(5)] *Senior Lecturer, University of Peradeniya, Peradeniya, Sri Lanka. kpp@pdn.ac.lk*

[(6)] *Chief Engineer, Sri Lanka Ports Authority, Colombo, Sri Lanka. janaka@slpa.lk*

[(7)] *Chief Executive Officer, Lanka Hydraulic Institute, Moratuwa, Sri Lanka. malith.mendis@lhi.lk*

Abstract

This paper describes the 3D physical model for the proposed Hambantota harbour. The main objective of the physical model study is to assess the harbour tranquillity for different incident wave conditions which are expected to prevail at the site during harbour operations. It encompasses the assessment of wave disturbance within the harbour basin especially near the quay walls for assuring of safer ship motion and convenient ship operations and there by, to verify the adequacy and effectiveness of the harbour layout proposed for Hambantota harbour. The proposed harbour layout was subjected to several representative wave conditions in order to examine the wave penetration into the harbour basin and disturbance in front of the quay walls. In addition, movements of fully loaded ships were measured by mooring at various berth locations. Results for wave penetration were checked with mathematical model results. Ship motion results were compared with PIANC criteria. Both wave disturbance and ship motion results were within the acceptable limits.

1. Introduction

Sri Lanka occupies a strategic position along the main shipping route connecting Asia with Europe and America, and needs major seaport to attract the international shipping industry. The Colombo Port even with the impending southward expansion will not be able to cater for the high demand within the region in years to come. Government of Sri Lanka has planned to develop the existing Galle Port as a regional port and identified the Hambantota site as for a major seaport.

Three alternative options for development of a seaport at Hambantota were considered, and an inland port within a part of Karagan Lewaya Lagoon with an entrance from the bay immediately westward of the Hambantota headland (Figure 1) was considered as the best option and the feasibility studies were carried out during 2002 - 2006. In 2006 October, Memorandum of Understanding (MOU)

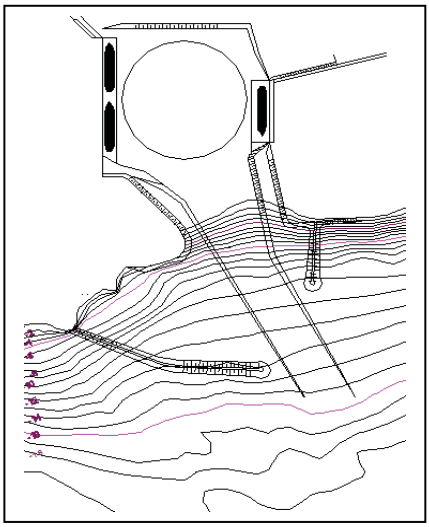

Figure 1. Proposed Harbour Layout

between Sri Lanka Ports Authority (SLPA), and a consortium comprising China Harbour Engineering Company (CHEC) concerning the detailed design studies of Hambantota Seaport Development – Phase I Project was signed. As a sub consultant, Lanka Hydraulic Institute Ltd (LHI) undertook hydraulic studies, which include the field investigations, mathematical modelling and physical modelling to optimise the functional and operational efficiency of the newly developed port layout.

The main facilities to be constructed in the Phase I includes: one way approach channel of 210m wide, turning basin of diameter of 600m, two general berths of 600m long, one oil berth of 310m long and all 16m deep. This paper describes the three dimensional physical model study to verify the adequacy of the proposed harbour layout by testing wave disturbance within the basin area and movements of moored ships at both berth locations and to optimise the layout.

2. Model Setup

A fixed bed undistorted model was constructed at 1:100 scale for the proposed seaport at LHI wave basin of size 35m x 25m (Hughes, 1993). The correct sizes of single layer CHINESEPODE concrete armour units were used for main breakwater and rock armours for lee breakwater to ensure a correct reproduction of hydraulic characteristics of the modelled structures (Figure 2). The wave generators used in the model tests were capable of generating irregular wave fields according to the JONSWAP spectrum for specified significant wave heights and peak wave periods. Wave characteristics for harbour operational condition were derived from detailed mathematical model simulations of wave climate using MIKE 21 NSW model (LHI, 2007). These wave conditions are given in the Table 1.

Two types of vessels were used in the model tests to represent 200m cargo and 230m oil tanker that are expected to use the facility. Ballasting procedures equating for dead weight tonnage, metacentric height and roll period were carried out for both vessels prior to the testing (LHI, 2005). Bridgestone type rubber fenders proposed for the interface between berthing ship and quay wall were accurately represented in the model using pieces of rubber beadings having similar elastic properties as the prototype fenders. The mooring arrangements of both vessels were also reasonably represented in the model using a combination of string – coil spring arrangement for model mooring lines (BS 6349 Part 4, 1985).

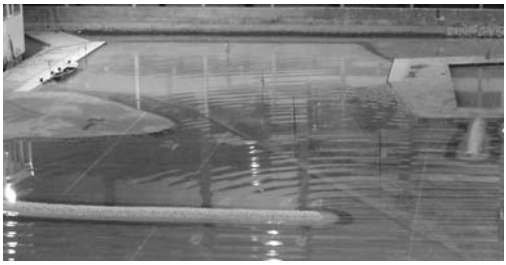

Figure 2. Physical Model Testing

Table 1 - Input Wave Conditions for Model Tests

Wave Direction (in degrees)	Percentage of Exceedence			
	25%		2%	
	Hs (m)	Tp (s)	Hs (m)	Tp (s)
210 swell	1.4	12	2.1	13.5
210 sea	1.1	5.5	1.7	5.5
180 swell	1.5	12	2.1	13.5
180 sea	1	5.5	1.5	5.5
150 swell	1.4	11	1.9	11.5
150 sea	1	5.5	1.5	5.5
120 sea	1	5.5	1.5	5.5

3. Model Tests and Results

The model was subjected to the all wave conditions indicated in Table 1. Each test was run for a period of 25min, which includes 5min of stabilization period and remaining 20min for data acquisition. A 20min running time in the model approximately represents 3.3 hrs in the prototype. For evaluating wave disturbance inside the harbour, waves were generated from four different directions, i.e. 120^o, 150^o, 180^o and 210^o as shown if Figure 3. The wave heights were extracted using wave gauges placed at 16 stations. For each wave condition, the output parameters of Hs and Tp were measured and analysed for all wave gauge stations.

There were three ship berths as shown in Figure 3. Wave conditions in Table 1 were simulated for each berth separately. Movement gauges (Figure 4) were used to measure six particular ship movements, Surge, Sway, Heave, Roll, Pitch and Yaw, according to the PIANC criteria (PIANC, 1995).

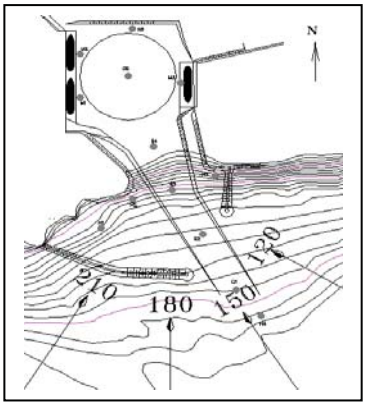

Figure 3 – Wave Directions & Gauge Stations

Figure 4 - Ship Movement Meters

Results for wave disturbance in the harbour basin were compared with the mathematical model predictions using MIKE 21 BW model (Figure 5). The PIANC criteria for acceptable movements of moored ships in harbours for safe working conditions were considered to compare the ship movements.

Reasonably good agreement was observed for wave heights measured in the harbour basin with those predicted by the mathematical model for all wave conditions. High wave penetration into the harbour basin was noted for the offshore waves approaching from 150^o direction compare to the other three directions. Almost all the ship movements were within the recommended values given in the PIANC criteria except several values at general purpose terminal which exceed the limits. The cargo operations at this terminal were affected by the longer period waves due to high sway and yaw movements. Ship movements at the oil terminal were smaller than those at the general purpose terminal for all tested wave conditions, as the oil terminal is almost sheltered for direct wave attack.

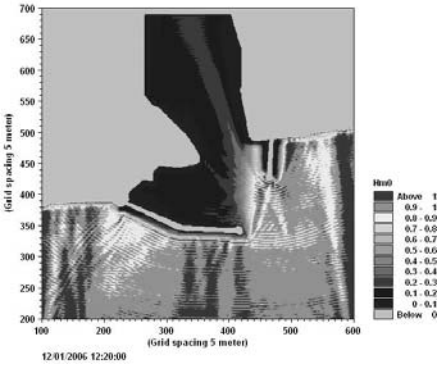

Figure 5 - Mathematical Model Simulation

4. Conclusion

A comprehensive 3D physical model study was carried out in order to assess the wave disturbance and ship motion for the proposed Hambantota port layout. The wave disturbance was compared with the mathematical model predictions and reasonable agreement can be observed. Cargo handling efficiencies of the model ships berthed at each terminal were derived according to the PIANC criteria based on the six components of ship movements measured during the model tests. Ship movements were almost within the recommended limits. Disturbances to cargo handling due to high sway, surge and heave movements observed in few long period wave conditions could be reduced by improving the mooring system. Therefore, few additional cables can be used to moor the ship only during high wave conditions without seriously disrupting cargo operations.

References

BS 6349: Part 1 and 4 (1985), BS Code of Practice for Maritime Structures, ISBN 0-580-14362-7

LHI (2005), 'Colombo Port Efficiency and Expansion Project: 3D (Basin) Wave Disturbance and Ship Motion Model', Report 0404.

LHI (2007), 'Hambantota Sea Port Development - Phase I Project: Mathematical Model Test on Wave Field', Report 0610.

PIANC (1995), Criteria for Movements of Moored Ships in Harbours: A Practical Guide, Bulletin 88

PIANC (1997), Approach Channels: A Guide for Design, Bulletin 95

Robert A. Dalrymple (1985), 'Physical Modelling in Coastal Engineering', A.A.Balkema, Netherlands, ISBN 90-6191-516-3

Steven A.Hughes (1993), 'Physical Models and Laboratory Techniques in Coastal Engineering', World Scientific Publishing Co. Pte. Ltd, Singapore. ISBN 981-02-1540-1

Thoresen, C. A. (1988), 'Port Design: Guidelines and Recommendations', TAPIR, Norway. ISBN 82-519-0839-6

EXPERIMENTAL INVESTIGATION ON THE MOORING FORCES OF A SINGLE PONTOON-TYPE FLOATING BREAKWATER

Fatemeh Aliyari[(1)], Mohsen Soltanpour[(2)] , Payman Aghtouman[(3)] and Feraydon Vafai[(4)]

[(1)] *Hydraulic civil engineer, M.S., SADRA (Iran Marine Industrial Co.), Shafagh Ave., Pounak Khavari Blvd., Shahrak Ghods, 14669 Tehran. I.R. IRAN, P.O.Box 14665-495, f.aliyari@sadra.ir*

[(2)] *Assistant Prof., KNTU university, 322 Mirdamad Ave. West,19697, Tehran, I.R. of IRAN, Post Code 19697 64499 , soltanpour@kntu.ac.ir*

[(3)] *Coastal engineer, M.S., SCWMRI, Shafie st., Asheri st., Karaj Highway, Tehran, I.R. IRAN, P.O.Box 13445-1136, aghtouman_p@scwmri.ac.ir*

[(4)] *Assistant Prof., KNTU university, 322 Mirdamad Ave. West,19697, Tehran, I.R. of IRAN, Post Code 19697 64499, fvafai@kntu.ac.ir*

Abstract

Although using of floating breakwater in comparison with conventional breakwaters is increasing, there is still lack of reliable methods to design them, and employing physical models are necessary. A pontoon floating breakwater is a rectangular structure, fixed to the seabed by mooring system. In this research, the relation between seaward and landward mooring forces of a single pontoon-type floating breakwater and the effects of different draughts on mooring forces are investigated.

1. Laboratory Experiments

To investigate the seaward and landward mooring forces of a single pontoon-type floating breakwater and the effects of different draughts on mooring forces, numerous experimental tests were carried out in the wave flume of the SCWMRI (Soil Conservation and Watershed Management Research Institute). JONSWAP wave energy spectrum was used during the tests on single pontoons with the relative draught of D/d=0.2,0.17,0.13. Wave steepness ranged between 0.01 and 0.08. Incident and transmitted waves were recorded by two wave height meters, located seaward and landward of the model, respectively. Figure 1 shows the intersectional mooring lines and two strain gauges for measuring mooring forces.

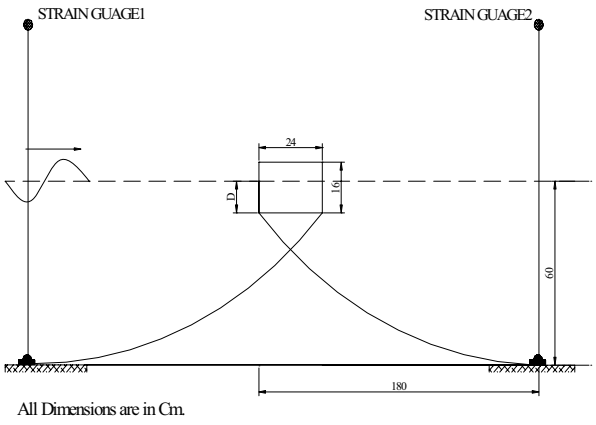

Figure1: details of the model

2. Discussion

The non-dimensional parameters T_0, H_0 and Φ were analyzed which represent wave period, wave height and mooring force, respectively (Eqs. [1] to [3]).

$$T_o = T_m \sqrt{\frac{g}{h_g}} \qquad [1]$$

$$H_o = \frac{H_s}{\Delta h_g} \quad where: \quad \Delta = \frac{\rho_{wood}}{\rho_w} \qquad [2]$$

$$\Phi = \frac{1000 F_s}{\gamma_w B^2 l_{ml}} \qquad [3]$$

Figures 2 to 4 show the landward and seaward mooring forces under JONSWAP wave spectrum. It is observed that for all draughts, the landward mooring forces are less than seaward mooring forces. The difference between two lines can be approximated by

$$\Phi_2 = \Phi_1 - 1/6 \qquad [4]$$

Where, Φ_1 and Φ_2 represent non-dimensional parameters of seaward and landward mooring forces respectively.

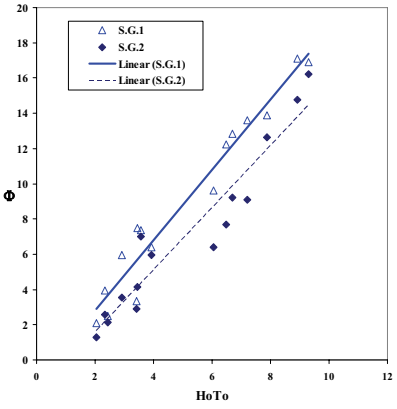

Figure2: Φversus H0T0- D/d=0.17

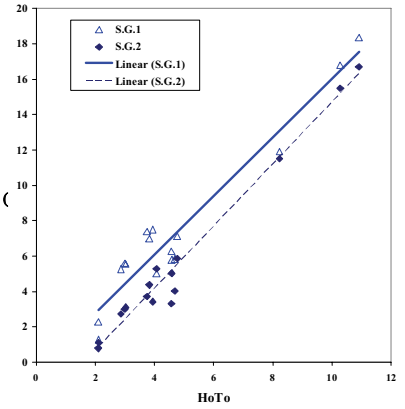

Figure3: Φversus H0T0- D/d=0.13

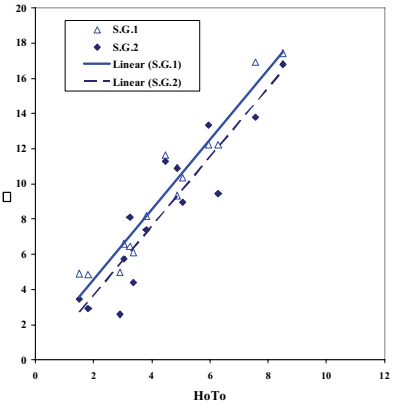

Figure4: Φversus H0T0- D/d=0.2

Figure 5 show the effect of draught on mooring forces. It is observed that draught increasing, results to higher forces in both mooring lines.

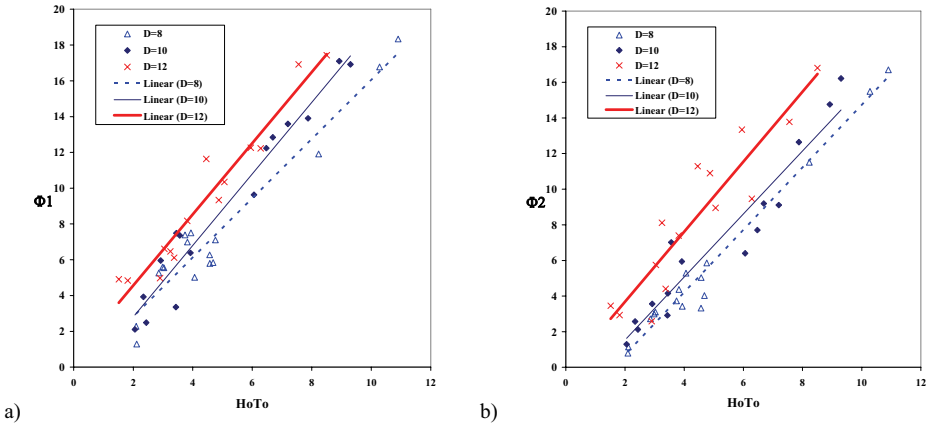

Figure5: Effect of draught on a) seaward & b) landward mooring forces

REFRENCES

Bruce H.Adee, 1979, "Floating breakwater performance", coastal engineering, chapter 159.

Cox R. J., "Floating breakwater model testing for pulpit point, Sydney", 1989, University of NSW, Water Research Laboratory, Technical report NO. 89/03.

"Development of a manual for the design of floating breakwaters ", Ltd. 1981 Western Canada Hydraulic Laboratories, PP. 28-29

Mansard, E.P.D and Funke, E.R. 1980, "The Measurement of Incident and Reflected Spectra using a Least Squares Method" 1980, Proceedings of the 17th Coastal Engineering conference, Vol. 1, pp 154-172

S. A. Sanna Siraj, V. Sunder and R. Sundaravadivelu, 1998, "Mooring forces and motion responses of Pontoon- type floating breakwaters", Elsevier science Ltd. Ocean engineering, Vol. 25. (NO. 1), PP. 27-48.

Steven A. Hughes, August 1993," Physical models and laboratory techniques in coastal engineering", Coastal engineering research center, USA

Experimental study of bottom slamming on point absorbers using drop tests

DE BACKER GRIET [(1)], VANTORRE MARC [(2)], DE ROUCK JULIEN [(3)],
TROCH PETER[(4)], BEELS CHARLOTTE[(5)], VAN SLYCKEN JOOST[(6)], VERLEYSEN PATRICIA[(7)]

[(1)] *Ir., Ghent University, Technologiepark 904, Ghent, 9052, Belgium. Griet.DeBacker@UGent.be*

[(2)] *Prof. Dr. Ir., Ghent University, Technologiepark 904, Ghent, 9052, Belgium. Marc.Vantorre@UGent.be*

[(3)] *Prof. Dr. Ir., Ghent University, Technologiepark 904, Ghent, 9052, Belgium. Julien.DeRouck@UGent.be*

[(4)] *Prof. Dr. Ir., Ghent University, Technologiepark 904, Ghent, 9052, Belgium. Peter.Troch@UGent.be*

[(5)] *Ir., Ghent University, Technologiepark 904, Ghent, 9052, Belgium. Charlotte.Beels@UGent.be*

[(6)] *Ir., Ghent University, Technologiepark 904, Ghent, 9052, Belgium. Joost.VanSlycken@UGent.be*

[(7)] *Prof. Dr. Ir., Ghent University, Technologiepark 904, Ghent, 9052, Belgium. Patricia.Verleysen@UGent.be*

Abstract

Bottom slamming of point absorbers has been studied experimentally by performing free fall drop tests. Rigid axisymmetric bodies are dropped from several heights in a water basin. The pressure time history and deceleration of the body are recorded during impact. A guiding structure is used to increase the accuracy and reproducibility of the tests. The influence of the body shape and impact velocity on the peak pressures is discussed.

1. Introduction

Point absorbers are small (floating) bodies, which oscillate in waves with one or more degrees of freedom. The kinetic energy of the buoys is transferred into electricity by means of a power take-off (PTO) system. Several point absorber systems are currently under development, e.g. FO³ [1], Wave Star [2], Manchester Bobber [3]. The buoys may loose contact with the water surface and be exposed to important impact pressures when re-entering the water. These slamming phenomena occur particularly in case the buoys have a small draft in combination with energetic wave conditions. For design purposes, it is important to know which pressures the bodies experience during impact.

2. Test set-up and instrumentation

The drop tests are performed at Ghent University. The conducted tests are a continuation and improvement of the experimental work that was carried out in [4-5]. A schematic view of the test setup is given in Fig. 1. The guiding structure makes sure that the object falls down vertically, without experiencing small rotations, which causes inaccurate results. Several drop heights are evaluated, up to a maximum of 2.0 m. The tested objects are shown in Fig. 2.

The deceleration during impact was measured by a shock accelerometer with a range of ± 500 g and a resonance frequency of 54 kHz. Two high frequency ICP pressure sensors with a range of ± 2 bar and a natural frequency of 150 kHz have been used to record the pressure time history. The membrane has a small diameter, which is required in order to measure the peak pressure, since it has a very small spatial extent [6]. The position of the pressure sensors is given in Fig. 2. A high speed camera is used to measure the impact velocity during penetration and to produce images of the different stages of water uprise due to impact of the body. The camera delivered images at 5000 up to 18000 frames per second (fps), dependent on the desired pixel resolution. A very high frame rate is necessary, since slamming

phenomena occur in a very short time interval (order of magnitude milliseconds).

Figure 3 gives an example of the measured pressure as a function of time compared with the theoretically predicted pressure based on the classical Wagner theory, for a cone with deadrise angle 20° and drop height 1.0 m at a horizontal distance of 0.04 m from the symmetry axis. In this case the pressure time history was recorded by a high frequency ICP pressure sensor with range up to 3.5 bar and membrane diameter ± 5.5 mm. Piezoelectric pressure sensors are only suited to measure dynamic pressures. Since the generated charge eventually leaks to zero, the measured pressure drops to zero, whereas the Wagner pressure lead to the sum of the stagnation pressure and the pressure due to permanent flow. In the paper, the measurement results will be presented and discussed in more detail.

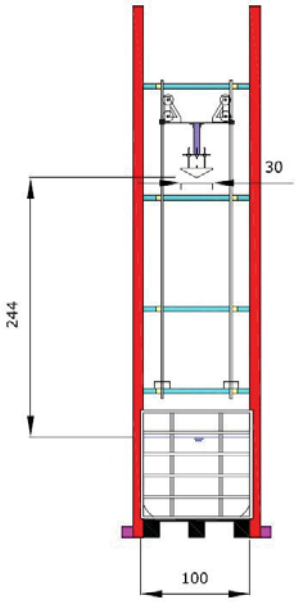

Figure 1. Schematic view of experimental test setup. (dimensions in mm).

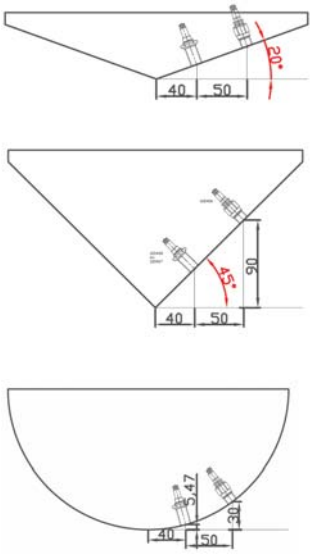

Figure 2. Tested bodies with position of pressure sensors.

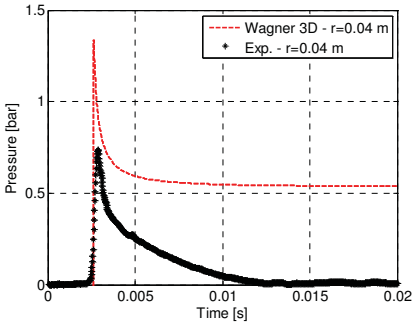

Figure 3. Measured pressure time history and analytically predicted pressure with Wagner theory at r = 0.04 m for a cone with deadrise angle 20° and drop height: 1.00 m.

Figure 4 shows a snapshot of the test objects while entering the water from different drop heights. The penetration depth is 0.02 m for each image. By marker tracking, the impact velocity of the objects is

determined. For the cone shapes the water uprise along the bodies can be clearly seen, whereas for the hemisphere a jet spray can be noticed. In the paper, the impact velocity time history obtained from the high speed camera will be compared with the results from the accelerometer and theoretical results.

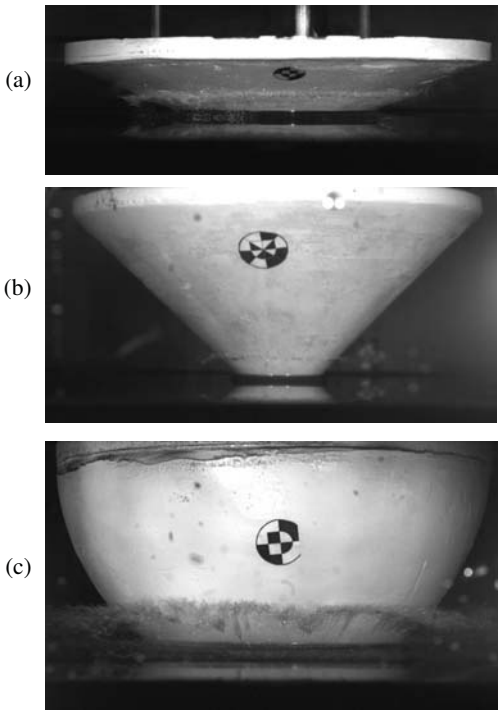

Figure 4. Snapshot of impacting objects at a penetration depth of 0.02 m for different drop heights. (a) Cone 20° - Drop height 1.00 m, (b) Cone 45 ° - Drop height 1.50 m, (c) Hemisphere - Drop height 0.50 m.

Acknowledgements

Research funded by Ph.D. grant of the Promotion of Innovation through Science and Technology in Flanders (IWT-Vlaanderen), Belgium. The research fits into the EU project SEEWEC (Sustainable Economically Efficient Wave Energy Converter – contract n°: SES6-CT2005-019969) within the 6th Framework Programme. The additional support of the European Community is gratefully acknowledged. The authors would like to thank Tom Versluys, Jean De Pré, Herman Van der Elst and Sam Meurez for their contribution in the design and installation of the test setup and measurement equipment and for providing the autoCAD drawings.

References

[1] Website SEEWEC: http://www.seewec.org/
[2] Website Wave Star Energy: http://www.wavestarenergy.com/
[3] Website Manchester Bobber: http://www.manchesterbobber.com
[4] Victor S. (2007): 'Investigation on slamming phenomena on point absorbers: experimental study and literature study', Master thesis, Ghent University, pp. 1-163.
[5] De Backer G., Vantorre M., Victor S. De Rouck J., Beels C. (2008): 'Investigation of vertical slamming on point absorbers', proceedings of OMAE 2008, Portugal.
[6] Faltinsen, O.M., Chezhian, M., 2005: 'A generalized Wagner Method for Three-Dimensional Slamming', Journal of Ship Research, 24 (4), pp. 279-287.

PHYSICAL MODEL TESTS FOR THE NEW SEVILLE PORT LOCK, SPAIN.

Ramon Gutierrez Serret[1];Victor Elviro García[2];Lazaro Redondo Redondo[1];Felipe Jimeno Vazquez[1]
[1]Ports and Coastal Studies Centre.[2]Hydrographic Studies Centre. Studies and Experimentation
Public Works Centre "CEDEX". Ministry of Public Works. C./ Antonio López, 81; Madrid, Spain.
Ramon.M.Gutierrez@cedex.es;Victor.Elviro@cedex.es;Lazaro.Redondo@cedex.es;Felipe.Jimeno@cedex.es

Introduction

The Spanish Government Research Institute: Centre for Studies and Experimentation of Public Works "-CEDEX-", was tasked by State Ports Body and the Seville Port Authority to carry out a series of model tests using a reduced scale physical model to verify the: (i) hydrodynamic and (ii) ship behaviour of the new ship lock design for the Seville port enlargement in the southern of Spain.

The new lock is designed to improve the connection between the port and the Atlantic Ocean by means of the Guadalquivir River, dredging this river from the port until it mouth from 6 to 8 m, in such a way that is expected an important increase of the traffic in the port. Figure 1 shows the present lock and situation of the present and the new and Table 1 the main dimensions of the new.

Table 1. New lock. Characteristics.

Total Length	334 m
Distance between lock gates	253 m
Interior Width	40 m
Floor Elevation	-11 m
Wall Elevation	8 m

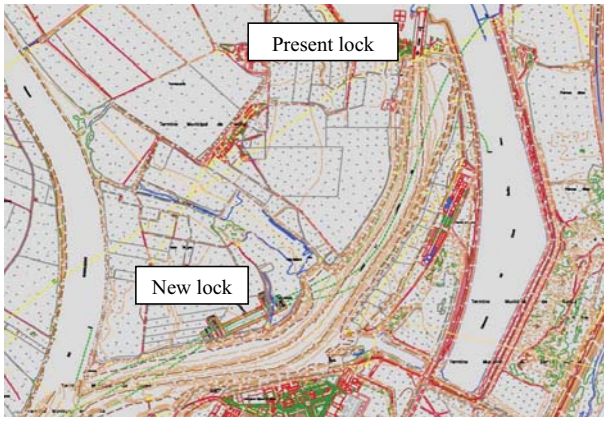

Figure 1. Ship access at present lock and situation of the present and the new lock

The model and the tests

Both aspects of the study -hydrodynamic and ship behaviour- have been carried out with a 3D physical model at a scale of 1:25 using the Froude similarity, constructed in the Maritime Experimental Laboratory of the Port and Coastal Studies Centre at CEDEX (figures 2 and 3).

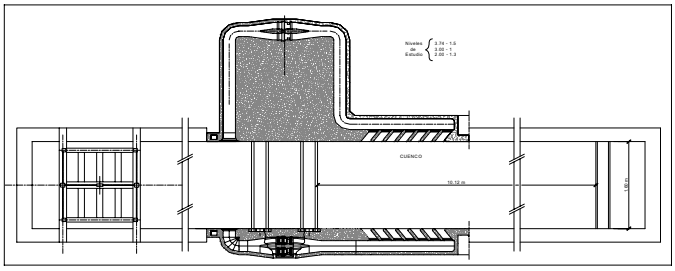

Figure 2. Layout of the physical model

Figure 3. Lock overview model with two vessels (Bulk carrier and LPG tanker)

The purpose of the hydrodynamic study was to analyse and verify the behaviour of the filling and emptying systems (figure 4), as well as flows in the lock chamber, to determine: filling and empting lock times, discharge-time ratio, flow patens in the entrance conduits and in the chamber, pressures in the filling/emptying conduits and slide gates operation.

Figure 4. Filling and emptying system (short and large conduits)

The ship behaviour tests were aimed at studying prospective vessels movement in the lock chamber during the emptying and filling operations, for different water levels combinations in the river and the port basins and with and without ships mooring, taking in account wind action.

Three ship types were studied representing the most important vessels likely to use the port: bulk carrier and LPG tanker (figure 3) and container (figure 5), all reproduced to a model scale of 1:25. Table 2 show the most important characteristics of the ships studied

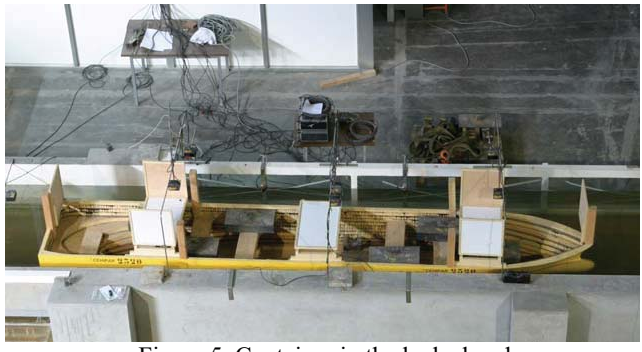

Figure 5. Container in the lock chamber

Vessels	Container	Bulk carrier	LPG Tanker
Total length	140.0 m	230.8 m	160.0 m
Breadth	22 m	34.5 m	20.0 m
Displacement	13.973.8 t	49.729.8 t	16.869.8 t
Draught	6.9 m	7.7 m	7.8 m

Table 2. Ship Characteristics

Each of the vessels was tested for 3 river-harbour level differences and for three wind conditions (table 3). The introduction of wind in the model, which is relatively novel in ship lock tests, was because of the influence which this was expected to have on the behaviour of ships operating in the Seville port, taking into account the ship superstructure (ongoing vessels), especially in the case of the container and the bulkcarrier. Wind effects was reproduced mechanically (figure 6).

Table 3. Tests Performed

Level		Exit (Filled)		Entry (Emptied)	
Harbour (m)	River (m)	Mooring	Wind*	Mooring	Wind*
1.5	3.74	Not moored	Calm	Not moored	Calm
			W-035-S		W-035-S
			E-035-S		E-035-S
		Moored	Calm	Moored	Calm
			W-035-S		W-035-S
			E-035-S		E-035-S
1,00	3,00	Not moored	Calm	Not moored	Calm
			W-035-S		W-035-S
			E-035-S		E-035-S
		Moored	Calm	Moored	Calm
			W-035-S		W-035-S
			E-035-S		E-035-S
1,3	2,00	Not moored	Calm	Not moored	Calm
			W-035-S		W-035-S
			E-035-S		E-035-S
		Moored	Calm	Moored	Calm
			W-035-S		W-035-S
			E-035-S		E-035-S

The wind was v = 20 m/s at 10 m altitude and in the direction coinciding with the prow-stern and port-starboard.

Figure 5. Mechanical system for reproducing wind (cables in red)

The model was monitoring with electric capacitive gauges (4 units along the chamber) for the measurement of the levels and flow disturbance in the lock chamber, sensor pressures in the filling/emptying conduits and in its connexions with the chamber (48 units). To determine the 6 ships movements were used 8 laser sensors placed in the deck and sides of the vessels. The mooring lines were reproduced with inextensible filaments and extensometers and the fenders wits strength cellules. In the figure 6 is shown a detail of a sensor laser, a fender and a level electric gauge.

Figure 6. Monitoring. Details. Sensor laser, strength cellule (fender) and electric level gauge.

Results of the hydrodynamic tests

The tests showed that the filling and emptying times, ranging between 6 min. 30 s and 2 min. 40 s, were in agreement with those foreseen in the design -about 6 minutes-, resulting in a maximum discharge of 200 m^3/s and a maximum velocity of 4 m/s. This velocity reduced for operation at the more frequent level differences to 1 m/s, and the discharge distribution in the filling/emptying conduit mouths were very uniform.

Regarding flow within the lock, the water levels in the chamber were not uniform, so that while initially there was more rapid filling of the zone adjacent to the outside, subsequently a reversal occurred, leading to a sloshing effect. Even though, this oscillation reached only low values, and the transversal velocity distribution was uniform away from the chamber, that which determined the favourable ships behaviour during the filling/emptying operations, as shown in the navigation tests.

Results of the navigation tests

In the lock filling and emptying operations, for the moored case, and the different combinations of port-river water levels, taking into account wind, the resulting maximum movements were found, to be very small, with the exception of surge, and in situations where caused by wind action the boat crossed the lock. In the situation of boat free (i.e. with no mooring) the surge effect was very pronounced in the majority of the tests and for all the boats, leading to, in some situations, an impact of the prow or the stern with the lock gate. In the Table 5 is shown the maximum surge movement in prototype for the three vessels tested.

Table 5. Maximum surge movement. Prototype.

		Access Lock Emptying			Exit Lock Filling		
		Levels: river/port (m)			Levels: river/port (m)		
	Wind	3,74/1.5	3/1	2/1.3	1.5/3.74	1/3	1.3/2
CONTAINER							
Moored	Calm	0.58	0.32	0.07	0.67	0.61	0.21
	W-035-S	1.6	0.94	0.5	Ship cross		
	E-035-S	Ship cross			0.16	0.15	0.05
Not Moored	Calm	16.75	15.75	5.75	16.5	14.75	7.50
	W-035-S	23.00	23.75		15.00	13.00	11.50
	E-035-S	Ship cross			0.25	0.25	0.12
BULK CARRIER							
Moored	Calm		2.85	0.48	3.34	4.61	0.63
	W-035-S	2.82	2.92	0.64		3.09	1.29
	E-035-S	Ship cross			0.41	0.39	0.16
Not Moored	Calm	Door impact			Door impact		7.03
	W-035-S	Door impact			Ship cross		
	E-035-S	Ship cross			0.45	0.42	0.20
LNG TANKER							
Moored	No wind	0.50	0.22	0.06	0.25	0.22	0.06
Not moored	No wind	16.75	15.50	5.50	12.5	12.60	6.30

The reactions measured in the fenders with the boat in the basin without engine, were in all cases very small, always below 4 tonnes.

Acknowledgments

We acknowledge to the Port Authority of Seville and the State Ports Body for the confidence deposited in CEDEX for the development of these test.

SHIPS PORT MANOEUVRING ANALOGICAL SIMULATOR

Paolo ALFREDINI [(1)], Tiago ZENKER GIRELI [(2)] & Emilia ARASAKI [(3)]

[(1)] *Associate Professor, Coastal and Harbour Division of Hydraulic Laboratory of Escola Politécnica of Universidade de São Paulo, Full Professor of Escola de Engenharia Mauá of Instituto Mauá de Tecnologia and Engineer VI of Centro Tecnológico de Hidráulica of Departamento de Águas e Energia Elétrica do Estado de São Paulo, Av. Prof. Lúcio Martins Rodrigues, 120, São Paulo, 05508-900, Brazil. alfredin@usp.br; paolo.alfredini@maua.br*

[(2)] *PhD, Coastal and Harbour Division of Hydraulic Laboratory of Escola Politécnica of Universidade de São Paulo , Av. Prof. Lúcio Martins Rodrigues, 120, São Paulo, 05508-900, Brazil. t_gireli@yahoo.com.br*

[(3)] *PhD Professor, Coastal and Harbour Division of Hydraulic Laboratory of Escola Politécnica of Universidade de São Paulo, Av. Prof. Lúcio Martins Rodrigues, 120, São Paulo, 05508-900, Brazil. earasaki@usp.br*

1. Introduction

Ships Port Manoeuvring Analogical Simulator allows fast time simulation operation with many runs to be carried out in a short time, and this is its major advantage as a port design tool. Indeed, running the simulation repeatedly over a given manoeuvre provides a resulting statistics of the runs. Single runs in various conditions of wind, waves and currents can also be used to judge navigation suitability, based on past experience, and can also provide some handling criteria. These fast time simulations provide a valuable design tool, but it should always be used in combination with judgement and experience. Indeed, all fast time design work should ideally be constructively criticised by mariners with experience of the area or the ship in question.

In 1992 the EPUSP (University of São Paulo Polytechnic School) Hydraulic Laboratory Coastal and Harbour Division, became in Brazil pioneer in radio-controlled interactive fast time simulations with real pilots manoeuvring a calibrated vessel model in a Port physical model basin. In these 16 years, more than 1,300 recorded tests have been performed and the methodology improvement leads to a reliable tool for port operational planning, design and safety navigation, with the joint working of the pilots and port operators in the Ships Port Manoeuvring Analogical Simulator (SIAMA). Different case studies manoeuvring improvements of the SIAMA are presented.

2. Procedure description

The vessel model calibrated parameters are:

- Rudder angle (Turning Circle in loaded and ballast conditions at full and half speed)
- Propeller revolutions and crash stop
- Revolutions of fans mounted inside the hull to reproduce appropriate bollard pull tug forces

The SIAMA fleet is composed by the vessels: Panamax (75,000 DWT), Capesize (150,000 DWT), VLOC (270,000 DWT), ULOC (365,000 DWT) and Large ULOC (575,000 DWT).

The real pilot, from an isolated room, by radio orders, commands the vessel engine, rudder and tugs action to the Laboratory Staff , viewing a similar scenery of the real port facilities from the image of two radio controlled rotating micro cameras in the ship model bridge wings, which may be angular turned by himself (Figure 1). The SIAMA also enables to perform night conditions, reproducing beacons, warning lights and lighthouses.

Based on scores of a questions check list about each manoeuvre answered by the staff involved (pilots, advisors, port operators and Navy officers), it is possible to have objectively the operational and

safety manoeuvre degree, considering: ship attitude, number of engine startings, pilot commands interval, total time, turning difficulties, ship-hydrodynamics interaction, potential risks of vessel failures (risks of groundings, crashes with structures or other ships moored), engine rotations and safe area for the manoeuvre. The manoeuvres are video-recorded from different angles, the vessel velocities are given in real time and strain gauges in the pier platform measure the berthing force.

Figure 1 – Pilot bridge camera room, digital video recordings and Laboratory Staff radio-control room.

3. SIAMA CASE STUDIES

The main case studies of the SIAMA are located at the Maranhão Port Complex, the second in Brazil and Latin America, reaching the rate of 130 millions tons per year, including three port areas located at the east side of São Marcos Bay at São Luís Island, in the northeastern region of Brazil. Figure 2 presents the site location, which includes the Ponta da Madeira Terminal (4 berths receiving from Handy Size to ULOC vessels), Port of Itaqui (4 berths for Handy Size to Large Cape vessels) and Port of ALUMAR (1 berth for Handy Size to Postpanamax vessels). Until 2011 the ports will be ready to operate 4 more berths and the rate will reach 250 million tons per year. The most common vessels operating are Large Capes, but in the next years the ULOC vessels reaching more than 400,000 DWT, class Chinamax, will begin to operate.

Figure 2 – Maranhão Port Complex location, Ponta da Madeira Terminal Pier I and Pier III and Port of ALUMAR.

The physical froudian model (Figure 3) used to study the Port Complex layout characteristics has 1,100 m^2 and the following main scales: geometrical 1:170 (undistorted), time 1:13.04 and forces 1:4,913,000.

Figure 3 – Ponta da Madeira Terminal, Ports of Itaqui and ALUMAR physical model.

The port area is an inner portion of São Marcos Bay and is naturally sheltered from sea storms and the wind regime is moderate. The dominant characteristic of the hydrodynamical pattern are the semidiurnal strong tidal ranges, with average values around 4.5 m and extremes between 6.5 and 7.0 m, generating tidal currents that may reach 7 knots. These currents have a dominant reversal pattern. The complex tidal currents system was reproduced in the model by a proper hydraulic calibration.

In this way important operational savings and improvements on navigation safety were introduced for different sceneries, based on the manoeuvring tests performed by all the pilots of São Marcos Bay Pilots Association and engaging the observations of the real manoeuvring personnel, navigation advisors and hydraulic engineers during the tests. For the Ponta da Madeira Terminal (Figure 4) manoeuvring study was possible to establish, by means of a global quality score, as suggested by the PIANC (1992) for the method of navigator judgment in combination with track analysis, safety berthing distances between vessels and increase the tidal operational windows for combined manoeuvres from 6 to 14 hours per day with an additional tug of 75 tf bollard pull (the others are of 50 tf). These improvements produced an increasing loading rate from 80 to 90 millions of iron ore tons per year. For the Port of ALUMAR, the evaluation of the Access Channel curve and the berthing strategy were performed (Figure 5).

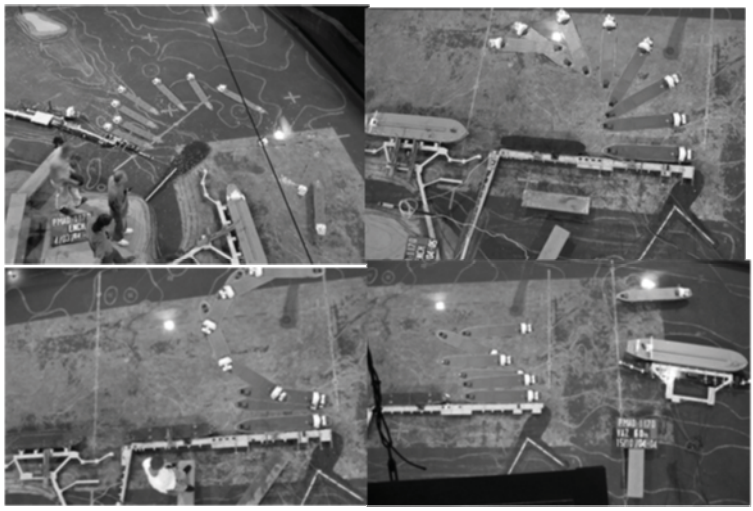

Figure 4 – Ponta da Madeira Terminal berthing and unberthing manoeuvring tests.

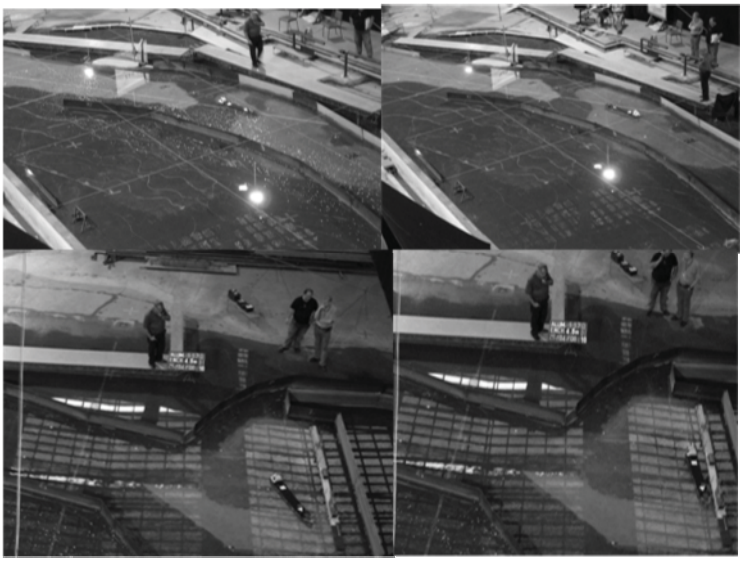

Figura 5 – Port of ALUMAR Access Channel curve manoeuvre and Turning Basin berthing.

4. Critical Analysis

The laboratorial effects simplifications don't invalidate the performed evaluations, because the basic practical purpose of comparison of manoeuvres strategies for identical scenaries was achieved, by a questionnaire answered by the manoeuvring personnel: commands number for the overall manoeuvre procedure; minimum and average time lag from two successive orders; turning difficulties for the full loaded ship; currents action on the ship; risks of grounding and/or collisions with structures or other ships moored; ship and tugs engine power levels; area occupied by the manoeuvre. Indeed, the real manoeuvres procedures validate the hydraulic model verifications.

5. Conclusion

With the Ships Port Manoeuvring Analogical Simulator it is possible to have previous knowledge about the overall manoeuvres dynamics in different sceneries to:

- Establish the best strategy for the design ship manoeuvres
- Decide about tugs number and/or their most convenient bollard pull
- Reduce the empiricism and risks associated in the performance of full scale trials

These conclusions have been verified in real scale for the piers operation in the last years.

References

PIANC / Permanent International Association of Navigation Congresses, 1992. Capacity of ship manoeuvring simulation models for approach channels and fairways in harbours. Supplement of Bulletin nº 77, 49p.

ROWE, R. W., 1996. The Shiphandler´s Guide. The Nautical Institute, 171 p.

ANALYSIS OF FIRST FLUSH WATERS IN THE BARI HARBOUR

G. BALACCO [(1)], M.M. DELL'ANNA [(2)], M. DI MODUGNO [(3)], P. MASTRORILLI [(4)], R. PAOLILLO [(5)], A.F. PICCINNI [(6)]

[(1)] Ph.d., Dep. of Water Eng. and Chemistry, Technical Univ. of Bari, Via Orabona 4, Bari, 70125, Italy, g.balacco@poliba.it

[(2)]Researcher, Dep. of Water Eng. and Chemistry, Technical Univ. of Bari, Via Orabona 4 Bari, 70125, Italy, mm.dellanna @poliba.it

[(3)] Ph.d Student, Dep. of Water Eng. and Chemistry, Technical Univ. of Bari, Via Orabona 4, Bari, 70125, Italy, m.dimodugno@poliba.it

[(4)] Full Professor, Dep. of Water Eng. and Chemistry, Technical Univ. of Bari, Via Orabona 4, Bari, 70125, Italy, p.mastrorilli@poliba.it

[(5)] Ph.d Student, Dep. of Water Eng. and Chemistry, Technical Univ. of Bari, Via Orabona 4, Bari, 70125, Italy,

[(6)] Full Professor, Dep. of Water Eng. and Chemistry, Technical Univ. of Bari, Via Orabona 4, Bari, 70125, Italy, af.piccinni@poliba.it

Abstract

Correct management of first flush waters is one of the most important instruments for the protection of the water bodies; these waters, indeed, are the vehicle through which an elevated polluting load is poured in the water bodies during a meteoric event. In an urban context pollution sources that alter the first flush waters quality can be distinguished in rising spread on the land and rising punctual, such as the external areas of productive sites, in which the typology of polluting load depends on local specific activity.

Besides the productive sites, on the urban coastlines, there are also the harbour areas characterized by big asphalted surfaces on which commercial and tourist activities take part, including move of goods and passengers terminals.

Generally, the rainfall drainage system of harbour areas discharge these waters directly into the sea, without any treatment.

The evaluation of polluting load transported to first flush waters allows, therefore, to individuate the most effective treatments for a proper management.

In this context, in 2007 March, on behalf of the Harbour Authority of Bari, researchers from the Department of Water Engineering and Chemistry of the Technical University of Bari carried out a field survey to determine the nature and to assess the concentration of possible pollutants accumulated on the impermeable surfaces during the dry time between a meteoric event and the following one. The areas object of study were two piers of the Bari Harbour, namely: (i) the East Dock, mainly devoted to handling of goods, and (ii) St. Vito Dock, characterized by a heavy traffic of vehicles (cars and trucks) coming from or getting into ferryboats.

Figure 1. East Dock

Figure 2. St. Vito Dock

This study allows to propose the most suitable treatment for the correct management of these wastewater in line with the indications of the italian regulations and, more specifically, those of Puglia Region.

Analyzing the data recorded during several meteoric events characterized by different intensity and duration, it was found that the pollutant load contained in the first flush waters of the East Dock area is not negligible: in particular, the concentration of COD, TSS, BOD_5, total Nitrogen and total Iron overcome the allowed limits for wastewaters.

Table 1. Pollutants concentrations in East Dock first flush waters

C_{max} Date	TSS (mg/l)	COD (mg/l)	BOD_5 (mg/l)	N (mg/l)	P (mg/l)	Pb (mg/l)	Cu (mg/l)	Fe (mg/l)
30/03/2007	344	355	75	5,6	1,09	0,006	0,011	3,5
04/04/2007	107	209	21	3,9	0,79	0,028	0,013	1,54
26/04/2007	300	506	72	229	3,03	0,015	0,014	8,2
28/05/2007	239	444	76	169	1,08	0,005	0,015	8,17

Table 2. Pollutants concentrations in St. Vito Dock first flush waters

C_{max} Date	TSS (mg/l)	COD (mg/l)	BOD_5 (mg/l)	N (mg/l)	P (mg/l)
26/04/2007	128	880	23	11,8	-
05/06/2007	-	180	23	1,9	0,09

To fulfill the limits imposed by the Regional law it is necessary to collect the first flush waters in a waterproof tank for a suitable treatment before disposal into the sea and, at the same time, to minimize the spreading of powdery materials (e.g. wheat) stored thereby and to avoid that iron stuff (e.g. reinforcment rods) lye on the ground for months.

On the other hand, the samples collected in St. Vito Dock area, where the first flush water is mixed with water used in a refrigerating plant, were characterized by values of TSS and COD both higher than allowed. In particular, TSS amount was slightly higher than the limit set by regional regulations, while COD concentrations were significantly higher.

In the light of these results, a proper management of first flush water should consist in a simple mechanical treatment before its disposal into the sea.

References

Calabrò P., Freni G., La Loggia G., Viviani G., 2003. 'Esperienze e studi sulla qualità delle acque di pioggia', Atti della Giornata di Studio: Acque di Prima Pioggia: Esperienze sul territorio e normativa, Genova, 85-102.

Deletic A.B., Mahsimivic C.T., 1998. 'Evaluation of water quality factors in storm runoff from paved areas', Journal of Environmental Engineering, 124(9), 869-879.

Gnecco I. Berretta C. L.G. Lanza, 2006. 'La qualità delle acque di dilavamento in area portuale e aeroportuale', L'Ambiente, 3, 18-24.

Legislative Decree of 3 April 2006 N 152. 'Norme in materia ambientale'. Ordinary Overflow n 96 of Officia Journal, 14 April 2006, n 88

Sansalone J.J., Koran J.M., Smithson J.A., Buchberger S.G., 1998. 'Particle characteristics of urban roadway solids transported during rain events', Journal of Environmental Engineering, 124(5), 427-440.

Sartor J.D., Boyd G.B., Agardy F.J.,1974. 'Water pollution aspects of street surface contaminants'. Journal Water Pollution Control Federation, 46(3), 458-467.

PHYSICAL MODELLING OF THE SAINT-LOUIS (SENEGAL) SAND SPIT EVOLUTION

M. COUTOS-THEVENOT [1], E. LAGROY DE CROUTTE [2] & V. APPICELLA [3]

[1] *Project Manager, SOGREAH Consultants, 6, rue de Lorraine, Echirolles, 38130, France.*
marie.coutos-thevenot@sogreah.fr

[2] *Project Manager, SOGREAH Consultants, 6, rue de Lorraine, Echirolles, 38130, France.*
eric.lagroydecroutte@sogreah.fr

[3] *Project Manager, SOGREAH Consultants, Immeuble le Condorcet, 18, rue Elie Pelas, Marseille, 13016, France.*
vanessa.appicella@sogreah.fr

Abstract

This paper presents the 3D physical model tests performed at the Laboratory of SOGREAH to examine the morphodynamic evolution of the sand spit closing the estuary of the Saint-Louis river in Senegal. The final aim of the study is to analyse and improve the conditions of navigability in the access channel of the port.

1. Context

The port of Saint-Louis in Senegal currently no longer has any commercial traffic as a result of:

- navigation restrictions on the river owing to a continual drop in its specific flow conditions,
- considerable natural constraints: river flow rate, distance to the river mouth, virtually permanent wave disturbance and a high level of longshore drift, formation of a bar across the river mouth, etc,
- the abandonment of the port of Saint-Louis to the benefit of Dakar.

With a view to injecting a new lease of life into the port and promoting the economic development of Saint-Louis and the surrounding region, the government authorities have decided to take up the challenge of enhancing the layout and accessibility of a port in Saint-Louis.

This project of port of Saint-Louis is one of the key features of a comprehensive programme initiated by the "Organisation pour la Mise en Valeur du fleuve Sénégal" (OMVS), which aims to develop a sustainable navigation on the river, in connection with the international maritime trade: the "Navigation Project".

2. Objectives of the study

The town of Saint-Louis is located at 175 km northward of Dakar (Senegal). The town is separated from the ocean by a sand spit with a fast growth rate measured 500 m/year as the result of intense sediment transport from the North.

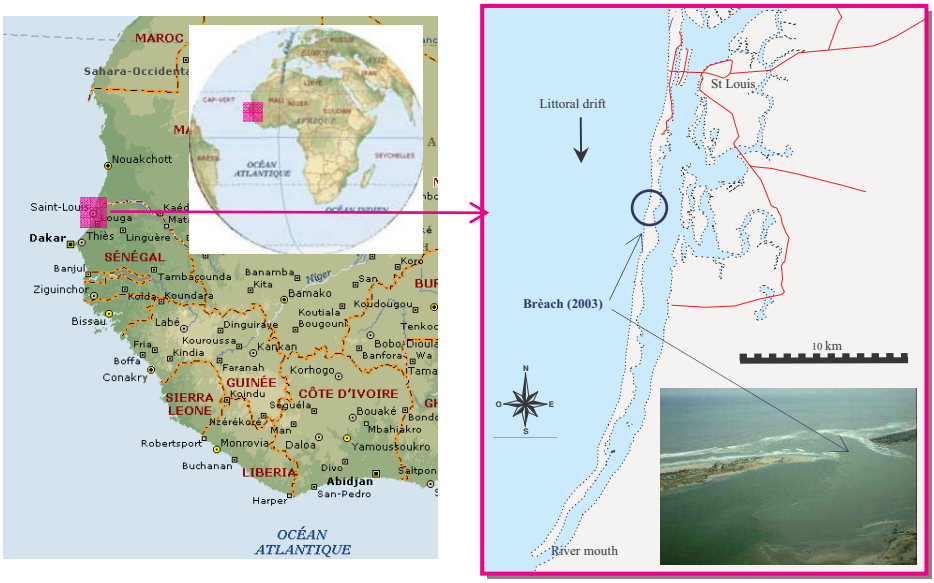

Figure 1: Location of the site

Following a severe flooding of the town in October 2003, the local government made the decision of creating a breach in the sand spit 6 km southward of Saint-Louis as an emergency measure to evacuate the water volumes. The breach also supposed a shorter access to the port than the previous mouth estuary (32 km southward of St-Louis).

The opening, initially 4 m-wide, widened up to 800 m in a few months and was progressively displaced southward, due to very dynamic processes of erosion updrift/accretion downdrift. At the same time, the river mouth closed itself.

In this context, a movable-bed scale model study was carried out to assess the near-future evolution of the breach and to define possible engineering solutions to reduce the impact on the port accessibility and operations.

3. Model tests

A distorted model was defined with a horizontal scale of 1:600 associated with a vertical scale of 1:100 (distortion of 6). The zone in study is a 15 km-long stretch of coast and extends offshore to -20 m CD. The sandy material was reproduced using crushed polymethylmethacrylate (PMMA is a thermo-hardened plastic) with a median grain size of 0.36 mm. A sedimentological timescale of 1:9000 was adopted.

The model was built in a rectangular wave basin measuring 32 m x 20 m and equipped with a 20 m long flap-type wavemaker, a tide generator and an ultrasonic probe system for an automatic survey the movable bed. The designed model reproduces both the tidal fluctuations (mean tidal range 1.2 m) and the river flow (2500 m^3/s as a maximum). The sediment supply from the North was also reproduced (600 000 to 700 000 m^3/year).

The modelling analysis was carried out in two steps. The model was first calibrated and validated. The hydraulic calibration was aimed at adjusting the experimental conditions so that all the natural hydraulic parameters (sea level, wave conditions) were faithfully reproduced.

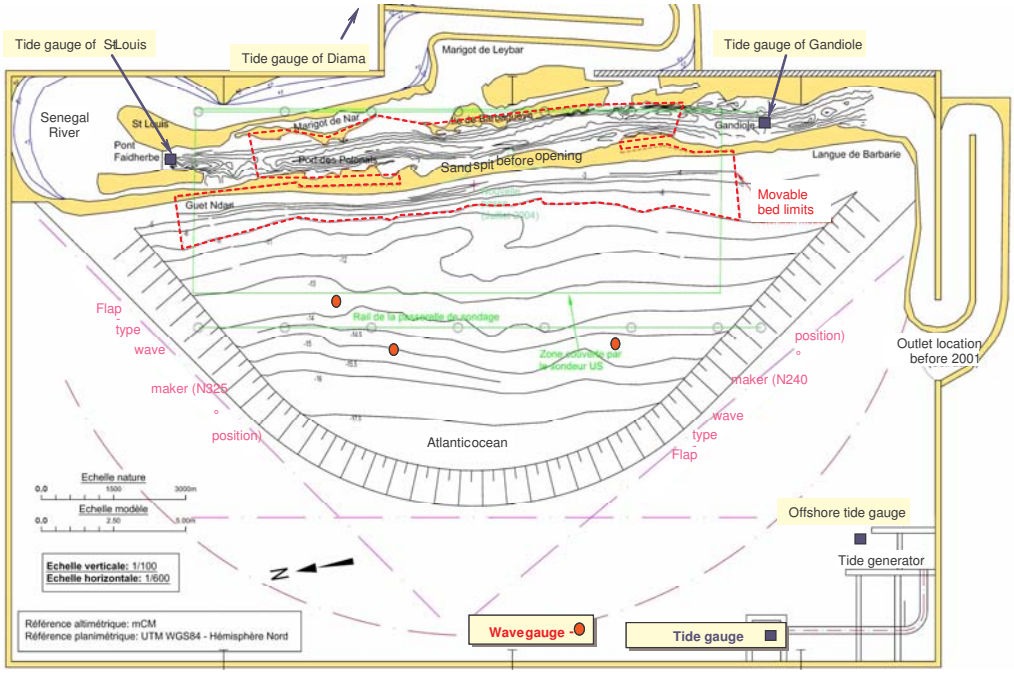

Figure 2: layout of movable-bed scale model

A sedimentological calibration was also performed, to simulate the seabed evolution trends observed in nature as accurately as possible. The model tests were then performed in order to evaluate two configurations of access protection. The morphodynamic evolution of the zone of interest and the impact of the protection groins on the erosion/accretion patterns were assessed for a time period of 25 years. Both solutions include a sand-bypassing that was reproduced on the model.

The final paper will show in detail the results of all the stages of the physical modeling analysis, including the model design, calibration/validation and the final tests.

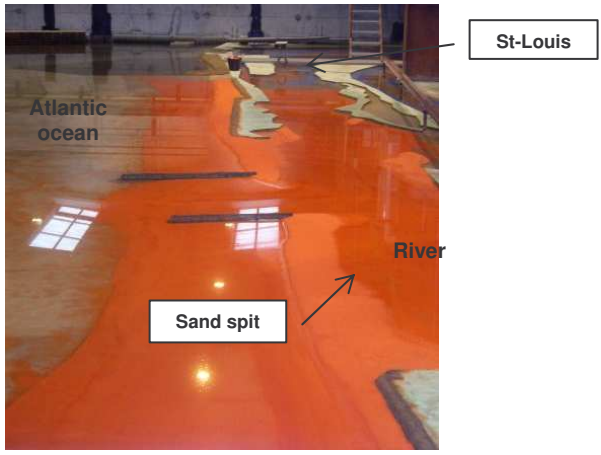

Figure 3: Photo of the model tests

Acknowledgments

This study was carried out on behalf of the OMVS, which is a joint cooperation body founded in 1972 by the states of Mali, Mauritania and Senegal to develop the resources of the Senegal River Basin.

References

Merzoug, M., Abdrabou, M., Camara, B., Moulinier, J-J. and Lagroy de Croutte, E. (2005). « Le projet Navigation sur le fleuve Sénégal ». Journées d'étude consacrées aux secteurs maritime, portuaire et fluvial dans les pays francophones, AIPCN, Paris.

Migniot, C. (1979). Utilisation des modèles réduits sédimentologiques pour prévoir l'influence d'un ouvrage maritime sur l'évolution d'un littoral. La Houille Blanche N°4/5-1979 p 191.

Migniot, C., Orgeron, C. and Biesel, F. (1975). LCHF coastal sediment modelling techniques, Symposium of modelling techniques, ASCE, San Francisco, p 1638.

Gravel nourishments with and without a submerged breakwater as an emergency measure against erosion

CLAUDIA D'ELISO [(1)] AND LORENZO CAPPIETTI [(2)]

[(1)] *Ph.D., Department of Civil and Environmental Engineering, University of Florence, Via S. Marta 3, Florence, 50139, Italy. cldelis@dicea.unifi.it*

[(2)] *Ph.D., Department of Civil and Environmental Engineering, University of Florence, Via S. Marta 3, Florence, 50139, Italy. cappietti@dicea.unifi.it*

1. Introduction, objective and methodology

Coastal erosion is affecting around 42% of the Italian coasts (GNRAC, 2006) and around 15% of the European coasts (EUROSION, 2004). If the erosion is particularly severe, threatening human infrastructures and in case of beach rehabilitation, where conversion from hard to softer protection is required, gravel nourishments seem to be a good coast-benefit solution (Aminti et al., 2000). However, few studies about gravel nourishments in presence of protective structures are available (Coates & Dodd, 1994) and the existing models of the equilibrium profile (Van der Meer, 1988) are normally derived for gravel nourishments in absence of protective detached breakwater. Further physical investigations are therefore necessary. The main objective of the present study is to achieve a better understanding of the cross-shore morphodynamics of gravel nourishments over beaches protected by structures, through a first set of 2D laboratory tests. The results obtained from the tests will be presented in this paper.

2. Laboratory tests on gravel beaches

The laboratory tests have been performed in the wave-current flume of the Civil and Environmental Engineering Department of the University of Florence, which is 50 m long, 0.8 m wide and 0.8 m deep.

A gravel beach profile of 1:5 slope is built in the flume over a natural profile of 1:15 slope (grey line in Fig. 1). The set of laboratory tests is defined combining: (i) 2 mean gravel sizes (D_{50} = 4 mm and D_{50} = 8 mm), (ii) 9 wave attacks combining 3 significant wave heights ($H_{s,0}$ = 6.0/11.0/16.0 cm) and 3 wave steepnesses ($H_{s,0}/L_0$ = 0.02/0.04/0.06), (iii) beach nourishment over a natural beach and over a beach protected by a detached breakwater with crest level submerged by 15 cm.

The tests are lasting 4 hours or at least 6000 waves in order to achieve the equilibrium profile. After each test the beach profile is reshaped at its initial geometry. Measurements during the tests include: (i) water levels at different locations along the wave flume by using 10 common wave gauges, (iii) beach profile over time recorded every 60 s by 4 cameras and (iii) mean water pressure inside the swash zone of the gravel beach by 3 piezometers.

3. Data analysis and preliminary results

The test plan has been successfully set up and analysed in order to investigate: (i) influence of gravel sizes and wave steepness on beach profiles, (ii) differences between gravel beach profiles with and without a structure, (iii) conditions for the formation of an eroding or accreting beach profile (Fig. 1). Data analysis provides: (i) wave height at different location, (ii) reflection coefficient from the beach, (iii) mean water pressure in the beach, (iv) depth of incipient motion of the sediments, (v) evolution of the beach profile over time and (vi) final equilibrium beach profile.

In particular, the evolution of the beach profile over time and at equilibrium has been obtained by analysing the images detected by the cameras, without stopping the tests to take measurements of the profile with a bottom profiler. The images have been processed through rectification and referencing over the wave flume. At a first step, a picture every 10 minutes of the tests have been analysed and the related beach profile has been digitalised. Measurements of the eroding and accreting beach, of the

profile shape and of the berm geometry are taken (Figure 2).

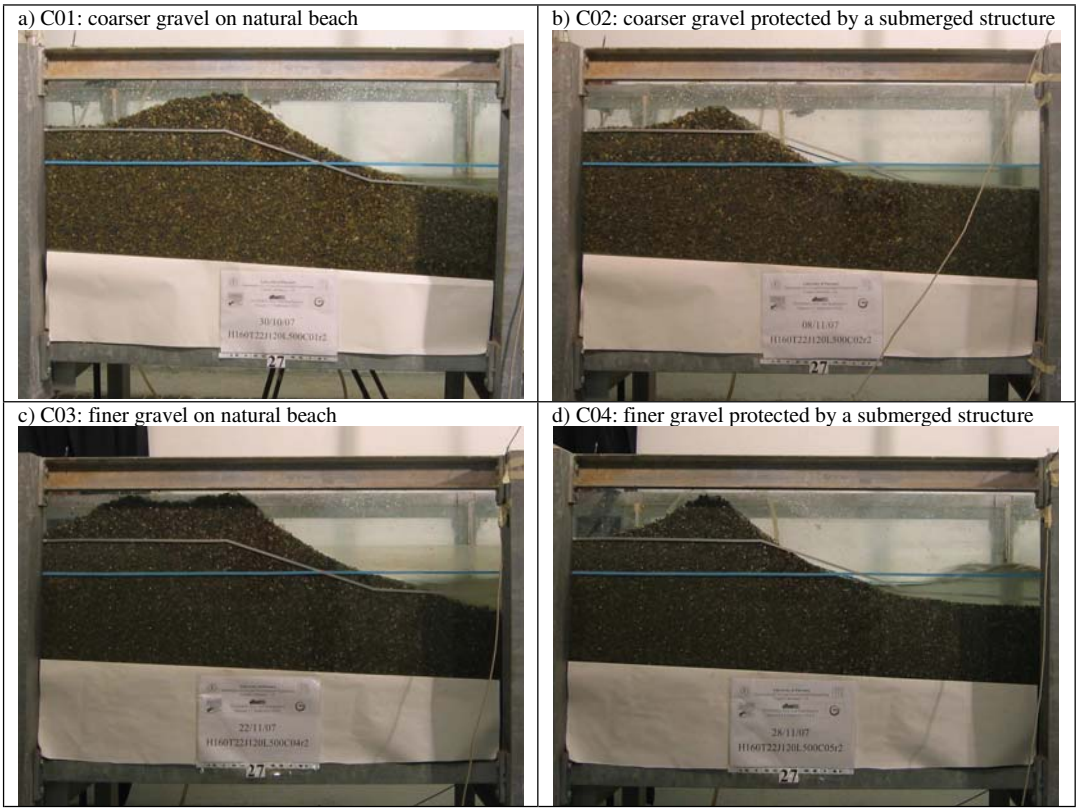

Figure 1. Recorded images of beach profiles at equilibrium (H_s= 16 cm, T_P = 2.2 s)

In Figure 2 and Table 1, the highest wave among the tested, for the four configurations (2 gravel sizes, natural and protected beach) at equilibrium are compared, showing a positive effect of the submerged barrier on the berm. The evolution of the profile for the test case of smaller gravel and protected beach is shown in Figure 3 as an example.

Preliminary analysis of collected data indicates that the performed tests are consistent, realistically reproduces the behaviour of the beach and includes stable beach scenarios under the lower wave attacks.

4. Concluding remarks

Gravel nourishments have been studied through 2D laboratory tests, because of the reduced data set available in the literature. The tests performed provide interesting results on the influence of a submerged structure on the equilibrium profile and on the formation of eroding or accreting equilibrium profiles.

Acknowledgments

The OCR Project BEACHMED-e (2006-2008) is gratefully acknowledged for the financial and scientific support provided for the tests.

References

Aminti, P.L.; Cipriani, L.; Pranzini, E. (2000): "Back to the Beach ": converting seawalls into gravel beaches. Proc. First Int. Conf. On Soft Shore Protection., Partas, October 2000.

Coates, T.T.; Dodd, N. (1994): The response of gravel beaches in the presence of control structures.

Proc. Int. Conf. Coastal Engineering, ASCE, Vol. 2, pp. 1880-1894.
EUROSION (2004): Living with coastal erosion in Europe: Sediment and Space for Sustainability. PART II – Maps and statistics. EUROSION Project Report. Vol. 10, 25 pp.
GNRAC (2006): Lo stato dei litorali italiani. Studi Costieri, Vol. 10, Coastal Engineering research center, Waterways experiment station, Vicksburg, Mississippi, 174 pp.
Van der Meer, J.W. (1988): Rock slopes and gravel beaches under wave attack. Ph.D. thesis, WL Delft Hydraulics, Delft, The Netherlands.

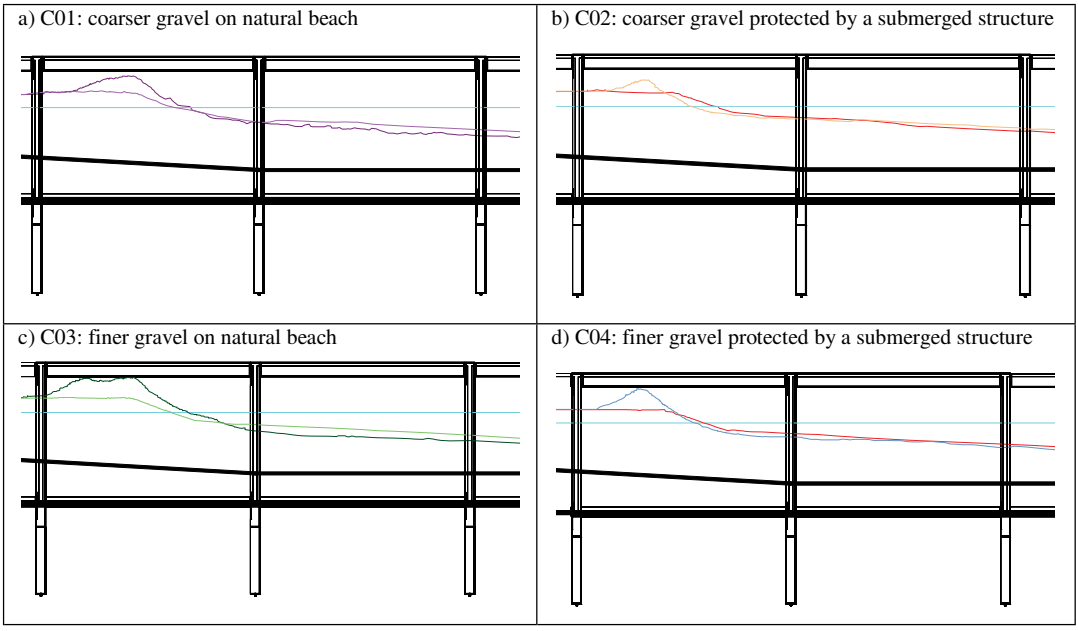

Figure 2. Beach profiles at equilibrium (H_s = 16 cm, T_P = 2.2 s)

Table 1. Measured data at equilibrium (H_s = 16 cm, T_P = 2.2 s)

Configuration	C01	C02	C03	C04
Crest height [cm]	16.12	13.46	19.07	19.24
Accumulation [cm^2]	329.95	114.10	680.69	264.19
Erosion [cm^2]	589.58	176.23	1523.60	616.01

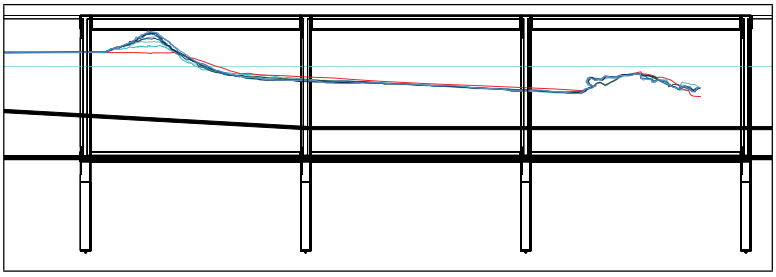

Figure 3. Beach profile evolution (C05, H_s = 16 cm, T_P = 2.2 s)\

APPLICATION OF A CELLULAR MODEL IN A MANAGED REALIGNMENT SITE, PAULL HOLME STRAYS, UK

L.M. TOMAS [(1)], T. COULTHARD, S.J. McLELLAND J. RAMIREZ

Department of Geography, University of Hull, HU6 7RX, UK
[(1)]Corresponding author: Luis M. Tomas; mail: l.tomas@2004.hull.ac.uk

Abstract

Paull Holme Strays was the first site to be opened as part of the Managed Flood Defence Strategy for the Humber Estuary, NE England. The site requires a long-term geomorphological study to determine when the site will be returned to nature and loose its ability as a flood defence scheme. The site has well defined boundaries and being driven by tidal flow, the site would be suitable for the application of 2D Cellular Model, based on spatially distributed version of Manning's Equation.

Introduction

Managed realignment is a process by which existing flood banks protecting coastal land are deliberately breached and flood waters allowed to spread into predefined areas. By allowing flooding in areas where it is acceptable, pressures may diminish in other areas where protection from flooding is of paramount importance, i.e. those where population density is high and/or there is significant industrial investment. This process is gradually finding favour amongst coastal managers as an alternative to, or in combination with, raising flood banks in response to progressive sea level rise (Environment Agency, 2000).

Prior to breaching of the flood banks, numerical modelling is used to predict the impact of this action on the stability of adjacent areas, and particularly associated flood banks, salt marshes and mudflats. Pioneering work now being carried out in the Humber Estuary is one of the first examples of operational use of managed retreat as part of an overall flood mitigation plan. In the summer 2003, the Environment Agency (EA) breached the flood banks at Paull Holme Strays (PHS) and they are planning further breaches in the near future.

A new cellular model has been developed to predict the long-term evolution of the geomorphology at Paull Holme Strays. Cellular modelling (CM) is a rule-based approach, discretizing and simplifying complex differential equations and solving them across a regular spatial domain, for example, using spatially distributed version of Manning's equation instead of the "heavy" physical equations such as the Navier-Stokes equation (Coulthard *et al*, 2000). The basic principles of CM in geomorphology are that an ensemble of cells defines landforms and the interactions between cells, water flow and/or sediment transport, are treated using simple rules based on abstractions of the governing physics. At each iteration, the state and condition of the cell are updated allowing the rules to apply on those new conditions. The same rule is applied to all the cells at the same time, as the CM must be homogeneous. Although the concept of CM is basic, the interaction between the cells can give complex and, sometimes, non-linear behaviour. This capability to replicate complex system behaviour, even with simple rules has enabled them to be applied in many contexts.

One of the main advantages of CM is by using simple rules derived from the basic equations for hydrodynamics, this leads to a substantial reduction in computer time to run a simulation. This reduction can provide extra time to run several simulations with different starting conditions to predict geomorphological evolution in different scenarios. With this type of rule-based algorithm, several rules

can be introduced, as long as they have influence at the local to be replicate. In addition, CM allows running simulations for a long-term prediction necessary for this particular exercise (Coulthard *et al*, 2002). With the reduction of computer time, the forecast range can increase, with usual models, the equations complexity can lead to simulation times longer than the actual forecasting range. Another main advantage is that having a quick solution for the flow field, this allows cells to be raised or lowered corresponding to deposition or erosion and the consequent effects on the flow field to be modelled.

The main disadvantage of CM is on the equation simplification, in some cases this can lead to the loss of certain features, such as some perturbations within the water flow along the slopes or vertical velocity as CM is a 2D model. There has to be a compromise between the equation simplification and feature loss. Increasing the complexity can lead to an increase in computer time, to many simplifications can leave out some important features to obtain a reliable long-term prediction.

Using a Digital Elevation Map (DEM) with a 10 m grid resolution obtained from a low altitude LiDAR survey; this gives the starting grid for the domain where the model will run (Bates and De Roo, 2000). For this case, the domain consists in a lattice of cells with 185 rows and 203 columns, with squares cells of 10 m side (figure 1).

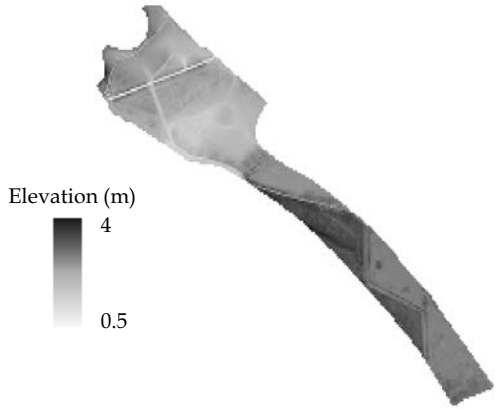

Figure 1: Representation of the DEM for Paull Holme Strays

Implementation

A complication in rectangular grids is that every cell has two different kinds of nearest neighbour, orthogonal, or adjacent, neighbours across its edges, as well as diagonal neighbours at its corners. Orthogonal and diagonal interactions may be expected to differ in strength but can be related. Furthermore, their relative strength will depend on the scaling of the model (Fonstad, 2006). These interactions can be separated into to different approaches: the Van Neumann neighbourhood; meaning that a cell will only interact with its 4 adjacent cells; the Moore neighbourhood meaning that adding to the Van Neumann neighbourhood, a cell will interact also with the 4 cells in a diagonal direction. In this particular case, the Van Neumann neighbouring was used as it gives similar results as using the Moore system and also it takes much less time.

The equation used to implement this CM is the Manning's equation for velocity:

$$v = \frac{1}{n} R_h^{2/3} S^{1/2} \qquad \left(ms^{-1}\right)$$

with n, Manning's roughness coefficient, for this particular case n=0.02, R_h, hydraulic radius and S, the surface water slope. The hydraulic radius is obtained by the following equation

$$R_h = \frac{A}{P} \qquad (m)$$

with A, cross-section area in m^2 and P, the wetted perimeter, in m.

The manning's equation is used to calculate the flow velocity between the cell and its four neighbouring cells, in the orthogonal directions. The programme simply scans the active area and compares the free surface water height with the four neighbouring cells calculating the energy slope to calculate the flow velocity. The discharge is obtained using the following equation:

$$Q = Av \qquad \left(m^3 s^{-1}\right)$$

The model uses a variable time step to control the discharge between cells to control flow velocities to avoid high velocities and consequent error propagation inside the site. The variable time step is controlled by limiting the maximum discharge between cells. In addition, there is a control routine to avoid a discharge greater than the water volume inside the cell.

Results

Model validation

The outputs from the model are validated against data collected from the site, more specifically in terms of sediment deposition/erosion and also velocity flow at the breach. In addition, there is low LIDAR data available from the Environment Agency to compare the model's raster output and the actual geomorphology of PHS. The data was collected during a period of 2 years, 2006-2007, every month, for sediment accretion/erosion and a seasonally survey for velocity flow.

Outputs

The first runs of the model showed a trend for sediment to accumulate in the area close to the breach, as shown in the figure below.

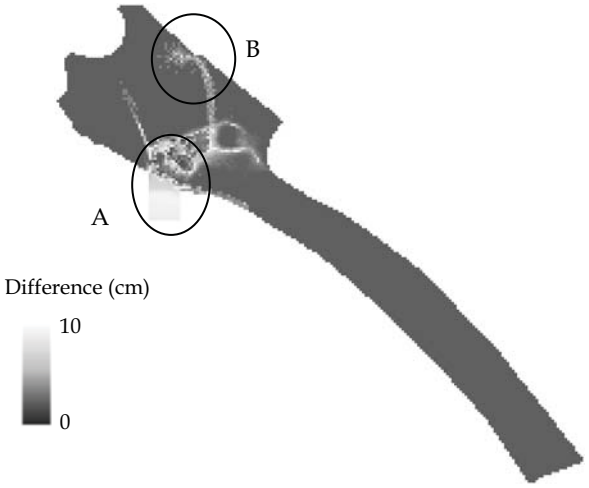

Figure2: Raster map after model runs

In the figure above, we have highlighted the areas, A and B, which are the most active areas inside the site, in terms of sediment accretion. The area A, located close to the breach, is the most active mainly due to its location closest to the main source of sediment. As the flow velocities decrease inside PHS, sediment starts to deposit right after the breach and also due to the water spreading and consequent velocity decrease. In some parts of area A, the average accretion is 1.0 cm/month, which is quite a high value. The area at the back of PHS, area B, is also depositing sediment, although in less quantities than area A. Area B happens due to sediment "warping" as water flows from the breach to back quite rapidly through a channel network which is still active and has been formed after the site was breached.

This raster map is the result for a 1 year range to be used as validation for the model. This test will allow a forecasting range of several years. The suspended sediment concentrations were variable according to the tidal height, varying from 0 to 0.7 kgm^{-3}. The tidal range varies from 2.0 to 8.4m in this particular location and is provided using the tidal predictions from the British Admiralty.

Conclusion

The implementation of a CM to PHS has been successful, particularly due to the well defined boundaries for the site, which facilitate the limits for the raster map. Although the equations are quite simple, the model response, particularly in high time-steps, gives very high velocities.

References

Bates, PD and APJ de Roo, (2000), "A simple raster-based model for flood inundation simulation", *Journal of Hydrology*, 236, 54-77

Chang, Y.H., Scrimshaw, M.D. , McLeod, CL and JN Lester, (2001), "Flood defence in the Blackwater estuary, Essex, UK: the impact of sedimentological and geochemical changes on salt marsh development in the Tollesbury managed realignment site", *Marine Pollution Bulletin*, Vol. 42, No 6, pp 470-481

Coulthard, T.J., Macklin, M.G.and M.J. Kirby, (2002), "A cellular model of Holocene upland river basin and alluvial fan evolution", *Earth surface processes and landform*, 27, 269-288

Environment Agency (2000), The Humber Estuary Shoreline Management Plan

Fonstad, M.A. (2006), "Cellular automata as analysis and synthesis engines at the geomorphology-ecology interface", *Geomorphology*, Vol. 77, Issue 3-4, pp 217-234

Lawler, D.M., (2005), "The importance of high-resolution monitoring in erosion and deposition dynamics studies: examples from estuarine and fluvial systems", *Geomorphology*, 64 (2005) 1-23

Paola, C., (2000), "Quantitative models of sedimentary basin filling", *Sedimentology*, 47 (Suppl. 1), 121-178

DESIGN AND VERIFICATION OF A CONTAMINATED MATERIAL CAPPING STRUCTURE ALONG THE ADRIATIC COAST, IN THE SOUTH OF ITALY

F. D'ALESSANDRO[(1)], G.R. TOMASICCHIO[(2)], R. GENCARELLI[(3)], F. FREGA[(4)]

[(1)] *PhD, University of Salento, via per Monteroni, 73100, Lecce, Italy, dalessandro@dds.unical.it*

[(2)] *Full Professor, University of Salento, via per Monteroni, 73100, Lecce, Italy, roberto.tomasicchio@unile.it*

[(3)] *PhD, University of Calabria, ponte P. Bucci cubo 42B, 87036, Rende, Italy, rgencarelli@dds.unical.it*

[(4)] *Researcher, University of Calabria, ponte P. Bucci cubo 42B, 87036, Rende, Italy, ferdinandofrega@dds.unical.it*

Abstract

The paper presents aspects related to the design of a contaminated material sediment capping in shallow water. The coastline of interest is called "Torre Quetta" and is located just south of the urbanized area of Bari, Puglia region, along the Adriatic coast of Italy. The intervention has been considered in order to allow the reuse of the 2.4 km long coastline for recreational use. For this purpose, the main objective has been to face the aspects related to the challenging problems posed by the design of the capping structure adopted and the consideration of various constraints related to the natural environment.

1. Introduction

Contamination of coastal areas due to industrial activities represents an ongoing threat for the environment. This is very frequent in the case of the industrialized regions of the world; in fact, contaminated spots have been often identified at several locations along industrialized coastlines.
This unique project has been started in order to obtain a recreational area where a contaminated area exists. The end of construction of the new beach is scheduled by the end of spring 2009. The coastal area has been contaminated by the land disposal of asbestos from the residuals of a factory producing concrete pipelines for aqueducts. The factory stopped its activity at the end of seventies. After that time, the consciousness about the presence of pollution at "Torre Quetta" went lost. In fact, the contaminated area was rehabilitated with a nourishment project and officially opened to the recreational use of public in 2002. After an initial use by the inhabitants, the detection of the contaminated material was clear and the area was immediately closed to the public. When the pollution was detected, the area was classified as a site of potential risk to human health and to the environment. In fact, asbestos waste generating pulmonary cancer was found both in the terrestrial and in the near-shore sea environment. Although several asbestos reclamation campaigns have been conducted, the contaminated materials appear along the coastline and at the present swash zone. This because, the 2.4 km long "Torre Quetta" coastline was created through several decades with a continuous seaward advancement made of polluted materials.

2. Design and verification

Following an extensive research program and several design alternatives, the Office for the Environment of the town of Bari has selected the in-situ material capping method together with a beach nourishment intervention in order to remediate the asbestos and to preserve the recreational use of the area.

Preliminary extensive field investigation program and research and design process have been carried out with the purpose of identifying the particularities of the hydrodynamic field and sediment transport for various combinations of incident waves and water levels.

The wave climate has been determined based on the data from the National Sea Wave measurement Network (RON) providing, since 1989, measurements and analysis of wave data in the Italian seas at deep water conditions with excellent results in terms of data acquisition rates, temporal coverage and reliability. The number of RON buoys is continuously increased through the time. The considered buoy is located offshore Monopoli (70 m water depth), 40 km south of Bari. The probability distribution function for the extreme wave climate has been determined based on the Goda's method (Goda, 1988; Goda and Konube, 1990); the Weibull function was selected. For a 25 years lifetime and encounter probability 0.5, the return period results equal to 36 years. The related wave height is H_{36}.

An extensive mathematical and numerical simulation analysis was carried out at University of Salento with the purpose of identifying the characteristics of the hydrodynamic field, considering various combinations of incident waves.

The propagation simulations have been conducted by a steady-state directional wave spectral transformation model for predicting nearshore waves (Rivero and Arcilla, 1993; Rivero et al., 1997; Carci et al. 1997). The model is a half-plane model so that wave can propagate only from the seaward boundary toward the shoreline. With regard to the representation and transformation of the directional wave spectrum (i.e., the distribution of wave energy density in frequency and direction), the model uses a marginal directional spectrum for its wave transformation, which is an integrated directional wave spectrum in the frequency range (Rivero et al. 1997). The model is capable of simulating wave-structure and wave-current interactions. Moreover, it can compute wave reflection, diffraction and wave transmission through and over submerged structures. Bottom friction, wind input, and wave-wave interactions are neglected in the model. The model represents wave diffraction by implementing a formulation of the Eikonal equation (Rivero et al. 1997). It computes forward wave reflection (in the wave propagation direction) from structures. Forward wave reflection is treated as a percentage increase of the local incident wave energy at cells in front of a structure. Wave breaking is based on the method of Battjes and Janssen (1978). The wave action conservation equation is solved with an implicit finite difference method on a rectilinear grid. It also requires a pre specified wave spectrum as input at the offshore boundary.

The design process has also considered the wave induced circulation and morpho-dynamic studies conducted by means of numerical models for different scenarios. In fact, the main goals to be reached have been to ensure water quality characteristics for bathing of human beings and to obtain an acceptable lifetime of the future beach.

The proposed design consists of a capping structure to bury the source of cement asbestos and detached submerged rubble mound breakwater to reduce energy of waves attacking the coastline.

The capping structure will be composed by a calcareous gravel layer 20 cm thick, a reinforced geotextile installed directly on the gravel layer and anchored in a shoreline-located trench. The geotextile will be covered by a layer of 70-300 kg natural stones. The last layer will be composed of well rounded gravel with mean diameter D_{50} = 5 cm and sorting, D_{85}/D_{15}, equal to1.3. Each layer has a different purpose: the geotextile will prevent any further loss of dangerous materials; the natural stones will keep fixed the geotextile and will define in a permanent way the new shoreline position which is seaward advanced of 30 m; the rounded gravel layer, the most expensive, will allow people to enjoy the beach. To facilitate the installation of the geotextile, the bottom will be first cleared of emergent aquatic vegetation and large stones. The detached submerged breakwater will break waves and reduce energy: this will allow the gravel layer at the capping structure to resist the wave attacks and to be dynamically stable.

Fig. 1 shows the approved design with the capping structure determining a shoreline seaward advancement of 30 m, the detached submerged breakwaters with water depth ranging between 2.70 and 3.50 m and with a submergence of 0.40 m respect to the s.w.l. In order to reduce the loss of rounded gravel mate-

rial, the detached breakwaters will have a landward conjunction by means of submerged groynes. In particular, the presence of two groynes at the mouth of channel Valenzano will help to prevent its obstruction. The design was subjected to a preliminary environmental impact study which was made public in December 2006.

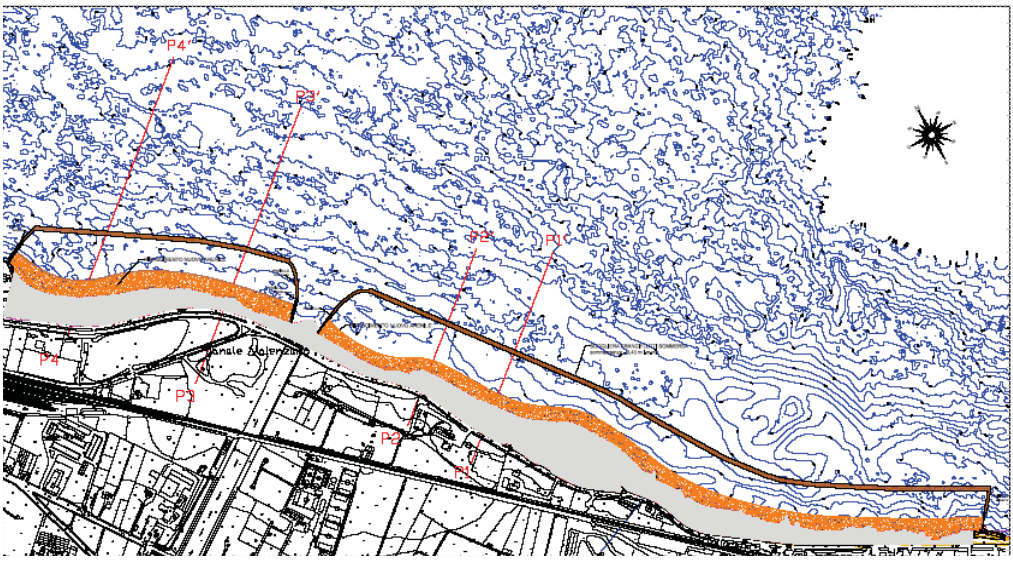

Figure 1: plan view of the approved design

3. Conclusions

The project has been carried for the following aspects: (1) the contaminated materials are located in shallow water - 0 to 3.0 m water depth - along the shoreline, both inside and outside of the surfzone; (2) the project area is subjected to the combined action of waves and currents; (3) given the future use of the area, the capping structure and the beach material must allow the recreational and bathing use to the town inhabitants; (4) the structure of the multi-layer cap has to perfectly seal and prevent the migration of dangerous materials.

The design process has included various armouring options for the upper layer of the composite capping structure, depending on the dominant hydrodynamic forces. The final design includes: (1) a reinforced geotextile installed directly on the contaminated material at the bottom; (2) about 30 cm layer of sand and gravel; (3) a protective rubble mound submerged toe at a water depth of about 2 m; (4) a series of protective submerged detached rubble mound breakwaters to reduce the wave action and to avoid large loss of the new beach material.

The *in situ* capping of dangerous materials at the coastline is a safe, enviromental friendly and viable technology for remediating contaminated areas. Although, contaminated sediment capping interventions have shown its effectiveness in several smaller scale projects in different countries, a project of this size and with the purpose to obtain a recreational area where there was a danger for human health can be considered unique. Remediation of the coastline south of Bari will be performed and will certainly benefit future generations. The paper aims also to represent a source of experience for designers and researchers who will face similar problems in the future.

References

Battjes, J.A., and Janssen, J.P.F.M. (1978). “Energy loss and set-up due to breaking of random waves”. Proc. 16th ICCE, ASCE, Hamburg.

Carci, E., Rivero, F.J., and Sànchez-Arcilla, A. (1997) “Coastal circulation induced by directional waves”(in spanish). Fourth Coastal and Port Engineering Spanish Meeting, Cádiz (Spain).

Goda, Y. (1988). *“*On methodology of selecting the design wave”. Proc. 21st Int. conference on Costal Eng., 899-913, ASCE, Malaga.

Goda, Y., and Konube, K. (1990). “Distribution function fitting for storm wave data”. Proc. 21st Int. Conference on Costal Eng., 18-31, ASCE, Delft.

Rivero, F.J., and Sànchez-Arcilla, A. (1993). “Propagation of linear gravity waves over slowly varying depth and currents”. Waves’93 Symposium, ASCE, New Orleans (USA), pp. 518-532.

Rivero, F.J., Sànchez-Arcilla, A., and Carci, E. (1997). “Analysis of diffraction effects in spectral wave models”. Waves’97 Symposium, Virginia (USA).

Van Deer Meer, J.W. (1992). “Conceptual design of rubble mound breakwaters”. In Proceedings of the Short Course on Design and Reliability of Coastal Structures, ICCE 1992, Venice, 447-511.

AUTHORS

UNIONE EUROPEA
FONDO EUROPEO PER LO SVILUPPO REGIONALE

INTERREG IIIA ITALIA ALBANIA

AUTORITÀ PORTUALE DEL LEVANTE
Porti di Bari, Barletta, Monopoli

P.I.C. INTERREG III A ITALIA-ALBANIA ASSE I - MISURA 1.1 - TRASPORTI E COMUNICAZIONI

PROGETTO JOVE

Parliamo di Porti

Ciclo di incontri tematici sul miglioramento della gestione operativa dei Porti del Levante e del Porto di Durazzo (Albania)

14 MARZO
15 MAGGIO 2008

Biblioteca Santa Teresa dei Maschi (Bari)

REPUBBLICA ITALIANA | REPUBBLICA ALBANESE | REGIONE PUGLIA | AUTORITÀ PORTUALE DI DURAZZO

Il progetto JOVE è finalizzato alla costituzione di una joint-venture tra l'Autorità Portuale di Bari (oggi Autorità Portuale del Levante) e quella di Durazzo allo scopo di fornire assistenza e consulenza per la ristrutturazione operativa, il miglioramento della security e della dotazione infrastrutturale del Porto di Durazzo. Le attività sono svolte in collaborazione le Universitarie baresi e con qualificati esperti nazionali del settore della portualità e della gestione di traffici marittimi.
A tal scopo sono previste attività di formazione ed assistenza a beneficio di circa 60 dipendenti del Porto di Durazzo nelle seguenti materie:
- L'organizzazione dei servizi tecnico-nautici;
- Il miglioramento delle infrastrutture del porto di Durazzo per uno sviluppo del traffico commerciale tra Italia e Albania;
- La gestione dei servizi di interesse generale;
- La qualificazione professionale nell'ambito delle attività operative del porto;
- Il miglioramento della security dell'area portuale di Durazzo.

Inoltre, è già in atto un progetto di ricerca e formazione specialistica post-laurea per n. 8 giovani laureati albanesi in materie giuridiche e/o economiche per l'approfondimento di tematiche connesse all'economia, gestione e organizzazione dei trasporti marittimi e dei porti con particolare riferimento alle problematiche della gestione e valorizzazione economica del demanio marittimo.
I progetti di ricerca sono assistiti da borse di studio che copriranno integralmente i costi della formazione e della permanenza dei partecipanti a Bari per tutto il periodo delle attività.

Calendario Incontri

MARZO 2008

14 VENERDÌ
"Politiche nazionali e comunitarie in temi di servizi tecnico-nautici: aspetti giuridici ed economici"

17 LUNEDÌ
"Lo sviluppo dei trasporti marittimi nel mediterraneo: quale scenario per l'Italia e i paesi vicini"

28 VENERDÌ
"Le politiche di regolamentazione nel settore dei trasporti: aspetti economici e giuridici"

31 LUNEDÌ
"La politica europea per il settore portuale e marittimo: quali implicazioni per l'Italia"

APRILE 2008

4 VENERDÌ
"Politiche nazionali e comunitarie in temi di servizi di interesse generale: aspetti giuridici ed economici"

8 MARTEDÌ
"Il ruolo della logistica nello sviluppo portuale: i distripark e l'integrazione modale"

11 VENERDÌ
"Il ruolo della security nell'organizzazione delle attività portuali"

15 MARTEDÌ
"La governance portuale: quali modelli seguire? Esperienze europee a confronto"

18 VENERDÌ
"Il ruolo delle infrastrutture per lo sviluppo socio-economico di un territorio. Aspetti tecnici, economici e giuridici"

22 MARTEDÌ
"Le reti di trasporto europee e le autostrade del mare"

MAGGIO 2008

15 GIOVEDÌ
"La qualità delle imprese dei servizi e delle risorse umane ai fini del posizionamento competitivo nei porti"

GEOCART

Rilievo con laser scanner, camera digitale e sensori iperspettrali integrati in una piattaforma aviotrasportata

Ispezione aerea di infrastrutture, reti tecnologiche e naturali con acquisizione di immagini e filmati georeferenziati

Elaborazione di dati satellitari con applicazione di tecniche DInSAR per il monitoraggio delle deformazioni del territorio

PRINCIPALI PROGETTI SU RILIEVO E MONITORAGGIO DELLE COSTE

Politecnico di Bari

- Rilievo aereo ed esecuzione del DTM di precisione e restituzione ortofotografica a colori in scala 1:2000 di tratti del litorale pugliese da introdurre nel SIMOC (Sistema Informativo per il Monitoraggio delle Coste)
- Esecuzione di rilievi planobatimetrici e loro restituzione cartografica in alcuni siti della costa pugliese - Ambito 2

Autorità di Bacino della Basilicata

- Produzione di un Modello Digitale del Terreno di precisione ottenuto con tecnologie laser-scanner e di ortofoto della fascia costiera jonica
- Servizio di livellazione, rilievo di sezioni trasversali d'alveo, caratterizzazione della granulometria di fondo alveo dei fiumi Basento e Cavone con produzione del DTM ottenuto da rilievo aereo con tecnologie laser-scanner e realizzazione di ortofoto

Agenzia Spaziale Italiana

- Progetto di ricerca e sviluppo nell'ambito del programma Cosmo/Skymed relativo all'evoluzione dei litorali

Nautilus

- Mappatura delle praterie di Posidonia Oceanica lungo le coste della Sardegna e delle piccole isole circostanti.

MAP ping GEOCART

GEOCART s.r.l.
Viale Del Basento n.120 - Potenza
www.geocart.net - geocart@geocart.net

Geomarine S.r.l.

TERRITORIO & AMBIENTE

www.geomarine.it

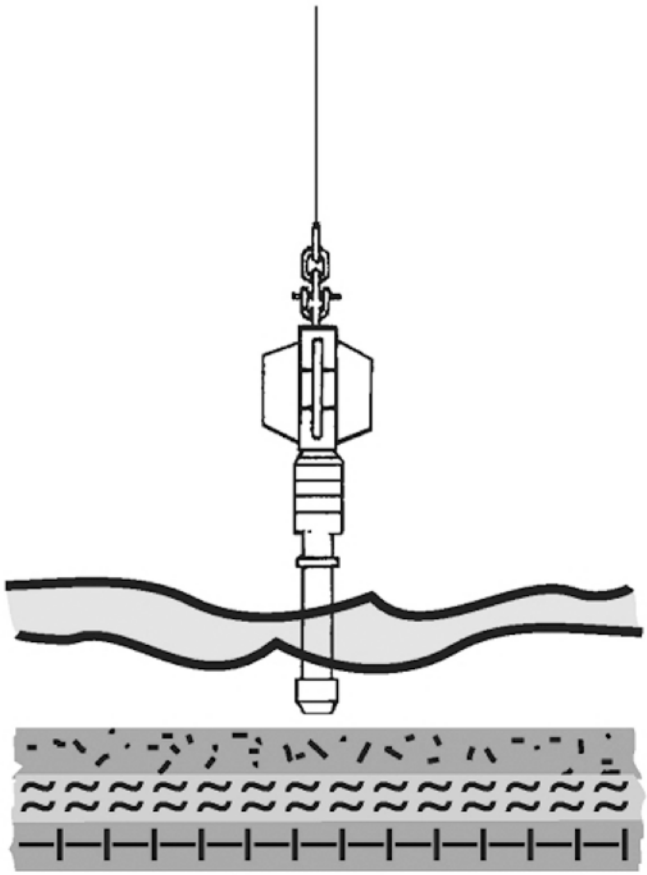

GEOMARINE S.r.l.
Via Guidi, 3/4 | 60019 Senigallia (AN) | t. 071.6608346 | mail info@geomarine.it

TELERILEVAMENTO

il futuro ha una lunga esperienza

SOFTWARE PER

TELERILEVAMENTO E FOTOGRAMMETRIA

- ERDAS IMAGINE
- Estensioni per ERDAS IMAGINE
- ERDAS LPS
- ERDAS ER Mapper Pro
- ERDAS Compressor
- ERDAS LOA
- ERDAS Mosaic Pro
- Estensioni ERDAS per ArcGIS
- ERDAS Radar Mapping Suite

La tipologia di dati geospaziali disponibili sul mercato cresce continuamente. Immagini satellitari, foto aeree e stereocoppie, dati aerofotogrammetrici, Lidar, Radar, multispettrali, Laser scanner, topografici e altri ancora richiedono software specifici per la loro elaborazione. Planetek Italia adotta e commercializza la suite ERDAS che consente in un unico ambiente l'elaborazione di tutti i dati geospaziali. Software affidabili, alta professionalità, esperienza pluriennale e cortesia uniti sapientemente per dare futuro alle tue applicazioni.

Planetek Italia è distributore di:

erdas

PLANETEK ITALIA

www.planetek.it

ELLERRE

CENTRE

EVENT'S ORGANIZATION

www.ellerrecentre.it

Ellerre Centre S.a.s.
Via Salvatore Matarrese, 47/G - 70124 Bari - Italy
T. +39 080 5045353 - mail ellerre@ellerrecentre.it

MARKETINGTECHNOLOGYMULTIMEDIAWEB

01MEDIA
Marketing & Technology

MOLFETTA (BARI) ITALY
piazza Garibaldi 18 - Tel. 080.3353274 - web www.01media.it - mail 01@01media.it

Nuova
EDITORIALE BIOS
ingegneria & scienza

Via Rendano, 25 – 87040 Castrolibero CS
Tel 0984 854149 – fax 0984 854038
www.edibios.it - info@edibios.it